

NASA SP-471

STELLAR ATMOSPHERIC STRUCTURAL PATTERNS

**CASE FILE
COPY**

MONOGRAPH SERIES ON NONTHERMAL PHENOMENA
IN STELLAR ATMOSPHERES



NASA

STELLAR ATMOSPHERIC STRUCTURAL PATTERNS

Richard N. Thomas

Series Organizers

Stuart Jordan, Organizer NASA
Richard Thomas, Organizer CNRS

Senior Advisers

Leo Goldberg, Adviser NASA
Jean-Claude Pecker, Adviser CNRS

MONOGRAPH SERIES ON NONTHERMAL PHENOMENA
IN STELLAR ATMOSPHERES



Centre National de la
Recherche Scientifique
Paris, France

1983



National Aeronautics and
Space Administration
Scientific and Technical
Information Branch
Washington, D.C.

Library of Congress Cataloging in Publication Data

Thomas, Richard Nelson, 1921-
Stellar atmospheric structural patterns.

(Monograph series on nonthermal phenomena in stellar
atmospheres) (NASA SP ; 471)

Bibliography:
Includes index.

1. Stars -- Atmospheres. I. Title. II. Series.

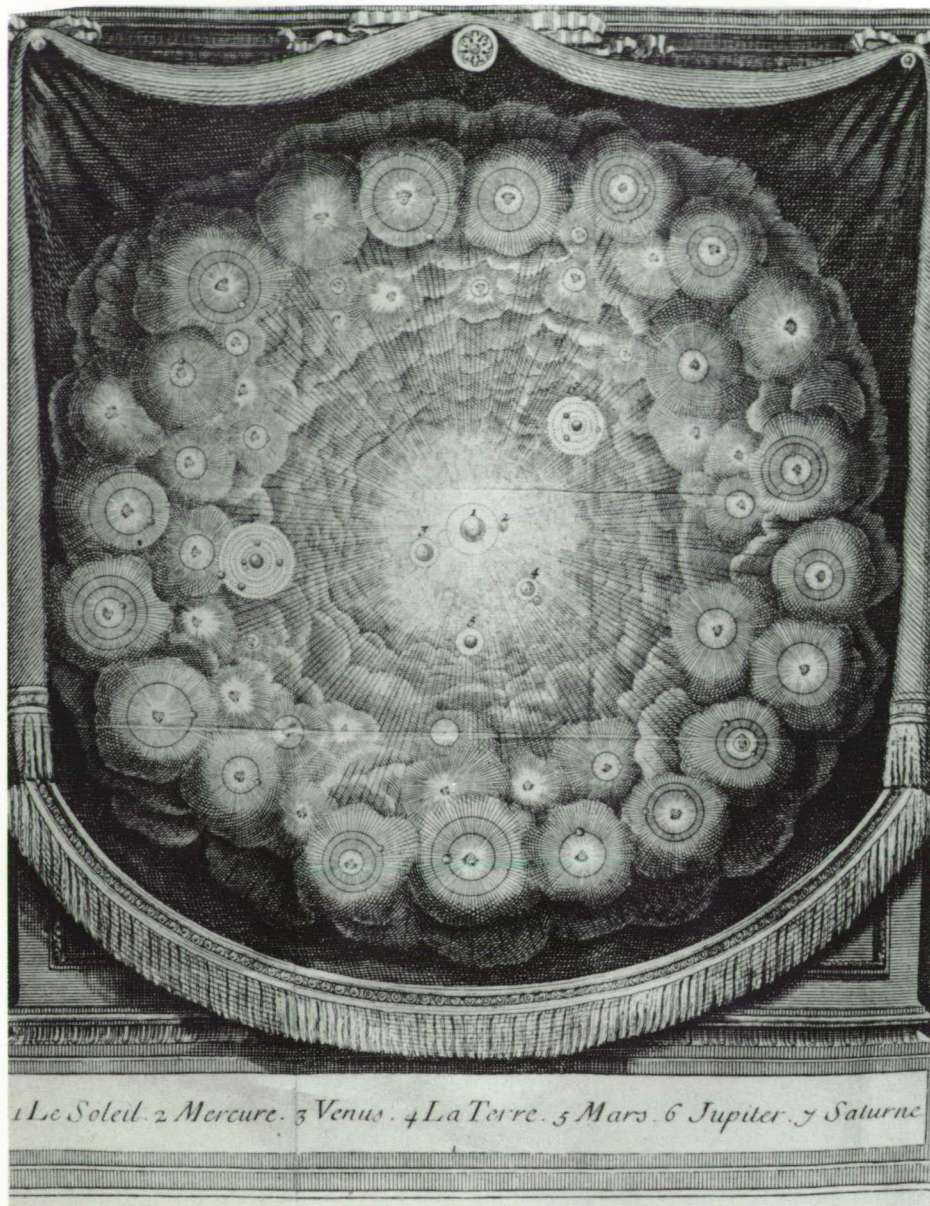
III. Series: NASA SP ; 471.

QB809.T46 1983 523.8 83-20242

STELLAR ATMOSPHERIC STRUCTURAL PATTERNS

Their Forms, Their Implications

the stellar atmosphere as the nonlinear nonEquilibrium transition-zone between the star, as an open nonthermal quasi-Equilibrium concentration of matter and energy, and its symbiotic nonEquilibrium environment.



... Assurons-nous bien du fait, avant que de nous inquiéter de la cause. Il est vrai que cette méthode est bien lente pour la plupart des gens, qui courent naturellement à la cause, et passent par dessus la vérité du fait; mais enfin nous éviterons le ridicule d'avoir trouvé la cause de ce qui n'est point.

...

...

... De grands physiciens ont fort bien trouvé pourquoi les lieux souterrains sont chauds en hiver, et froids en été; de plus grands physiciens ont trouvé depuis peu que cela n'était pas.

—Fontenelle, *Histoire des Oracles*
Chapitre IV, pp. 20 et 23

DEDICATION

in grateful appreciation
we dedicate this series and these volumes

to *Cecilia Payne-Gaposchkin*, who, with Sergei, set the spirit of empirical-theoretical atmospheric modeling by observing:

“All true variable stars have variable atmospheres, but a variable atmosphere is probably the property of all stars, whether obviously variable in brightness or not [as witness the solar envelope]”;

and who, by her intimate knowledge of particular stars, pioneered in the recognition of the fundamental importance of “individuality of stellar atmospheric characteristics.”

to *Daniel Chalonge*, who sought, by ingenious meticulous observations, to make quantitative the features of qualitative classical taxonomy, thereby laying the foundations of showing the inadequacy of its two-dimensional, single-region atmospheric, character;

and who always opposed the spirit of a distinguished theoretical colleague’s remark:

“Don’t show me those new observations of yours; they inhibit the range of my speculations.”

Page intentionally left blank

Page intentionally left blank

PREFACE

About one century has elapsed since the Henry Draper spectral classification scheme was introduced to try to identify physically alike kinds of stars from observational similarities in their visual spectra. The early one-letter classification has evolved into a very complex acronym with numerical subdivisions and symbols defining various kinds of peculiarity in stellar observations. During this time, our understanding of the variety of atmospheric regions which must exist to produce these peculiar spectral features has grown rapidly. The original classification was eventually interpreted in terms of an atmospheric model consisting of blackbody photosphere and a local-thermodynamic-equilibrium (LTE) reversing layer. Today, by analogy with the Sun, we recognize many layers above the photosphere which, although transparent to most visual wavelengths, have significant opacity in the far-UV, the X-ray, the infrared, and the radio spectral regimes. We recognize hot chromospheres, coronae and stellar winds, and even more extended regions such as cool emission envelopes, nebulae, and circumstellar dust clouds. Stellar classification and stellar atmospheric modeling are clearly in a stage of rapid continuing development. In particular, the farther the regions described here are found from the star, the more will their thermodynamic state be affected by nonthermal phenomena, and the less will they be controlled by the gravitational field of the star and by the local thermodynamic equilibrium associated with an extremely opaque medium.

More than two decades ago, the series *Stars and Stellar Systems* was generated under the general editorship of G. P. Kuiper. That series reviewed the status of astronomy and astrophysics at what we might call the beginning of a new era of extensive observations in the nonvisual wavelength regimes, many of them accessible only from space. We are now in the midst of this new era. These more recent observations continue to yield new insights into the outer atmospheric layers of the Sun and other stars. The new insights have forced us to reconsider the adequacy of the older HD system of classification and its classical successors, as well as of the assumptions underlying the classical theories for diagnosis and modeling of stellar atmospheres. All of these were reviewed in the Kuiper series' volume on *Stellar Atmospheres*. The present series will emphasize some of the current attempts to establish a new set of empirically based theoretical guidelines for treating stellar atmospheres. These new guidelines are intended as an elaboration of and also, where appropriate, as a revision of the classical guidelines, to permit a more comprehensive treatment which incorporates the recent new observations in a reasonable way.

To further put the current series, *Nonthermal Phenomena in Stellar Atmospheres*, in perspective in relation to the older series, *Stars and Stellar Systems*, the current series is far less comprehensive, being restricted to stellar atmospheres and, in some cases, subatmospheric boundary conditions. However, the approach is deliberately more critical because the new ideas required to interpret the new data are still in an early and frankly controversial stage of development, while the older

theories on which the Kuiper series focused were relatively "standard" at that time. These new volumes are intended primarily as a stimulus to researchers to probe the unknown, starting with the new data, and not mainly as a compendium of what was known at the inception of the space era. The earlier series served that function well. For this reason the first priority in these volumes will be a review of the highest quality data, particularly the more recent data which exhibit nonthermal phenomena. Observation of the full electromagnetic spectrum exposes to view regions of the atmosphere that are transparent to visible light. The UV spectrum reveals the structures of chromospheres and coronae, the X-ray spectrum is emitted from regions which are very hot, the IR spectrum comes from all layers, hot and cold, which are opaque to IR photons, and the radio spectrum gives evidence of both thermal emission and of energetic nonthermal processes.

In the light of these new extensions of the wavelength regimes covered by stellar spectra, conventional taxonomy provides only a very provisional labeling, useful in classical statistical studies, but insufficient to reflect the intricate nature of physical phenomena and the variety of physical parameters that control the appearance of many stellar spectra. It is also true that theoreticians had long ago generally exhausted the possibilities for modeling stellar atmospheres with only effective temperature and gravity. They have, of course, continued to introduce physical improvements in their models, such as taking account of departures from LTE, or of the ionization in convection zones, etc. But these models, which are barely adequate for unambiguous fitting of the visible spectra, fail completely when confronted by the various new features observed in other spectral regimes. Because of this failure, it is not at all clear that stars which astronomers have called peculiar in the past are, in fact, fundamentally different from stars classified as normal. Until superior models emerge, we cannot be sure that the statistically defined abnormalities are anything more than spectral signatures of large-amplitude nonthermal processes which exist with smaller amplitudes in many stars classified as normal.

In the early days of these recent observational developments, many theorists thought of the new features largely as perturbations modifying the basic classical description. For example, they tried to perturb their models slightly by adding a superficial hot layer labeled "chromosphere," and by representing parametrically the emission features at the centers of such intense spectral lines as $H\alpha$ and $K(\text{Ca II})$. But adding layers ad hoc without considering their possible interactions with the lower regions is physically inconsistent. Whether we talk about shells, winds, or magnetic features, they must be compatible, in the framework of physical laws, with the values of the other parameters characterizing the star. It may well be, for example, that a star of T_{eff} equal to, say, 10^4 K cannot have a dust shell of high opacity; or perhaps it can. However, we cannot blindly accept that such dust shells can occur without full investigation of the processes by which dust grains condense, grow, and are destroyed in a given stellar environment. Nor can we accept them without asking whether the IR and radio excesses they were introduced to produce may not come from chromospheric-coronal emission instead.

Historically, the analysis of stellar spectra may be thought of as proceeding in three sequential stages. The first is based on taxonomy and rough modeling and leads to very approximate estimates of a few basic parameters, such as T_{eff} , g , and chemical composition, while bypassing consideration of any anomalous features in the spectrum. The second is an attempt to explain each anomalous spectral feature in terms of some structural property of the stellar atmosphere, e.g., a circumstellar shell of some temperature and density at a certain distance from the star, a warm chromosphere, or a hot corona. This leads to a provisional, parametric description of the atmosphere of a star which is often physically contradictory: one group of spectral features may require a low density shell, another a high density shell. The red supergiant α Orionis (M2 Iab) offers a good example of the anomalies that are found in this second stage of analysis. For instance, the interferometrically measured diameter is found to decrease with increasing wavelength, which is explained by dust

scattering in the circumstellar shell, but this model requires that the dust be located 1-3 stellar radii from the star, whereas observations of emission at 11μ put the dust no closer than 10 stellar radii. Another example is given by the variability of some B stars, such as γ Cas, which appears at different times in three different guises—as a normal B star, as a Be star, and as a B-type shell star. Still another case is that of Sirius, which has been regarded as a bona fide A0 main-sequence star for years, but which now appears to show some spectral anomalies, possibly linked with metallicity.

The third and ultimate stage of analysis, which is an order of magnitude more difficult than the preliminary ones, aims at models of the atmosphere that will be compatible with all known facts about the star and with the laws of physics. Such models will clearly be neither in LTE nor static, and, therefore, we shall be obliged to take account of all physical processes that may be operating in the star, including some not now recognized as important by astrophysicists.

It is the intent of this series of books to help set the stage for this last step. At the very least, these monographs will try to define some types of observations to be made and some types of models to be constructed before we can approach a full understanding of stellar structure. A good example is the solar case in which we can foresee what new observational and theoretical vistas might emerge from the Solar Maximum Mission and the Solar Polar Mission. Certainly the coming of radioastronomy, infrared astronomy, and space research have made it possible for us to handle the first two steps discussed above.

The principles of classical taxonomy are a necessary starting point for all parts of the HR diagram. In consequence, for each spectral type, the forthcoming volumes of this series will examine thoroughly those phenomena that are not included in the classical description. A typical problem that will be considered is the contrast between stars labeled B and Be, respectively. What parameters or physical processes have been overlooked that might provide a connecting link between these two subclasses of stars? It will be argued that there may be no such thing as a peculiar B star when observed over the whole spectral range. Had we begun the analysis with the far-UV region of the spectrum, our notion of what is normal would have been quite different, and any attempt at one- or two-dimensional classification would have led to a labeling system incompatible with the HD system or its successors.

We hope that readers of these books will sense the emergence of a new point of view in stellar diagnosis and in stellar astrophysics, a global approach which assigns to the whole spectrum and to all its features the same a priori weight as a basis for diagnosis, a physical approach which tries to attract the theoretical astrophysicist to the interpretation of the observed spectra, no matter how elaborate they may be, and an approach which considers each star as a physical object to be understood, by itself, in a coherent way, not simply statistically. Because so many of the data which exhibit nonthermal phenomena have come from observations made from space, we also hope that the delineation of the above trends will be useful in planning observing programs from space in the 1980's, particularly in the UV, farUV, and X-ray regimes, as well as in helping to coordinate these with ground-based observing programs in the visual, IR, and radio regimes. We trust these observations will also stimulate relevant laboratory investigations.

In stressing the role of the principles of classical taxonomy above, it should be recognized that this classical taxonomy rests upon two stages of approximation. It is in these two stages that we find the clue to the distinction between thermal and nonthermal phenomena in the atmospheres of these stars. A first approximation orders the visual spectra of stars in terms of the strengths of absorption lines for any given ion, of line ratios, and essentially of the increasing degree of ionization, as one progresses from cold to hot stars. Essentially this is a temperature sequence. Assuming LTE conditions, one establishes an atmospheric model which represents these trends. Overlying a blackbody-like photosphere whose temperature is fixed by the radiative flux from the star, one has a cooler atmosphere, the reversing layer, which produces the absorption lines. This standard model

underlies classical, first approximation taxonomic diagnostics. A second approximation simply separates the stars into luminosity classes, being essentially an additional classification perpendicular to the first one, according to the gravity. The density in the reversing layer is fixed by the stellar gravity.

A quite different, more profound, difference in degree of approximation then separates all these stars into two groups. That great majority of stars, whose visual spectrum, under low dispersion, can be adequately classified by first-approximation taxonomy are called *normal* stars; the rest are called *peculiar* stars and characterized by a variety of peculiarities, which may differ from star to star within the same class. Most of the visual spectral features of a normal star are represented reasonably well by the standard model. Generally, the peculiar features of peculiar stars are not at all represented by the standard model. For a variety of reasons, summarized and illustrated throughout the series, many of these peculiar features are attributed to nonthermal properties of the stellar atmosphere and of the star as a whole. A knowledge of the effective temperature, the surface gravity, and the chemical composition apparently does not suffice to describe even the visual spectrum of such stars. Hence, the emphasis of this series is to contrast the normal and peculiar stars, to attempt to put into focus the nonthermal properties as contrasted to the thermal ones. The question is then asked, across the series as a whole, whether all stellar types have the same *kind* of nonthermal characteristics, differing only in their *sizes*. To the extent that they do, one can then construct a model which is more encompassing than the standard one.

The first volume in this series was *The Sun as a Star*. The Sun is peculiar only by virtue of its proximity to the Earth, which permits the observation of relatively small size nonthermal phenomena that would otherwise probably escape our attention. The Sun, therefore, puts into focus the kinds of nonthermal phenomena treated in this series. Because most of these peculiarities would not be easily observed if the Sun were at normal stellar distances, the Sun at such distances would undoubtedly be called a normal star.

One of the first stellar peculiarities to be observed in the visual spectrum of some stars was the presence of emission lines in place of some strong absorption lines, especially the Balmer lines of hydrogen, and particularly H α . Such hydrogen emission lines are not confined to one classical spectral type; they are observed all across the HR diagram. It is, thus, essential to understand the implication of their presence and their relation to the occurrence of other peculiarities. The most naive interpretation of the presence of emission lines would demand that the standard model be perturbed by a temperature increasing, rather than decreasing, above the photosphere. However, such a model would demand that emission lines, rather than absorption lines, would be usually, rather than exceptionally, found, which is contrary to fact. Moreover, in hot stars like the B stars, an increase in temperature just above the photosphere decreases the number of neutral hydrogen atoms present, thus negating this simple viewpoint. Such an emission line anomaly was used to define an example of peculiarity in the B star class, namely the Be stars, almost at the same time that solar eclipse observations were giving evidence of the existence of a vastly extended outer atmosphere for the Sun, in about 1860. An interpretation of this B-star emission-line anomaly in terms of the existence of a similar, greatly extended atmosphere for the Be stars seems to be the first approximation to the changed atmospheric structure demanded by this stellar peculiarity. Thus a line-emitting area greater than the continuum-emitting area is required. One is thus faced with the question of why the Be stars have this characteristic and the normal B stars do not. The volume, *B Stars With and Without Emission Lines*, was written to address these kind of issues.

The A-type stars offer a strong contrast to this general picture. Evidence for chromospheric-coronal regions remains difficult to decipher, but it steadily increases. Emission in the X-ray region of the spectrum is seen in some, but by no means all, A-type stars, and the explanation for the range in X-ray fluxes in stars of similar temperature and gravity is not known. There is, however, evidence

that the *photospheric* spectra of A-type stars are *strongly* influenced by nonthermal phenomena. The visible spectra of many, perhaps even a majority, of A-type stars are peculiar in the sense that they cannot be explained in terms of a normal (solar) composition and classical thermal models. The presence, and effect, of magnetic fields seems linked to many phenomena.

The present volume expands the focus on stellar peculiarity much beyond the phenomena of emission-lines, and nonradiative heating. It looks across the HR diagram in such focus on the various aspects of peculiarity, rather than restricting attention to only one class of stars. It tries to put into that same perspective of stellar individuality and variability, which characterized emission-line peculiarity, these other aspects of peculiarity. It tries to use these characteristics of peculiarity to delineate the several exophotospheric regions of the star, which introduce this observational peculiarity, and to link them to the nonthermal fluxes from the star. It puts into focus what now seems to be the primary thermodynamic character of the star: being an (open, nonthermal) system, which evolves from a small concentration occurring in the disorganized ISM into an organized, nonthermally-structured, distinct object.

—Prepared by the Series' Senior Advisers
and the Organizers
Greenbelt, Paris, Tucson, September 1983

Page intentionally left blank

Page intentionally left blank

FOREWORD AND ACKNOWLEDGMENTS

To the lectures at the College de France, 1973–75; and to the evolution of their contents, 1976–83; from which this monograph results.

I am grateful to the College de France for the invitation to lecture there during the academic years 1973–75, in that environment endowed by François I following the insight of Guillaume Bude: of lectures on unfamiliar things not expounded elsewhere, or on familiar things from an unfamiliar viewpoint. In that spirit, I have always been charmed by those qualities of Diane de Poitiers which encouraged such endowment and insight. In essence, while these lectures and this monograph are primarily addressed to an astrophysical audience, they might equally well be addressed to a biological one—if it were equally interested in the nonEquilibrium thermodynamic description of real-world objects, defined as concentrations of matter and energy in some environment with which they interact symbiotically. Globally, one asks if one needs different kinds of nonEquilibrium thermodynamics to study different broad classes of such objects. Is it even necessary to differentiate between the broadest such classes, inanimate and animate objects, between astronomical and biological objects, in constructing a general nonEquilibrium thermodynamic approach to study individual objects? Can we use the same kind of external diagnostics¹ to simply classify which, in a group, are “like” objects—alike in mass, energy, composition, and structure? Given that our observed universe is not static—that it is composed of objects which change in time, at least in their external appearance—a major part of such understanding is to try to distinguish between objects which actually differ intrinsically, and those which appear to differ, simply because they represent different temporal phases of “like” objects.² We need a taxonomy which a priori incorporates, rather than a priori disallows, temporal change in the objects it classifies. And, we need to be able to distinguish between evolutionary and nonevolutionary changes in appearance of like objects with time. Similarly, in progressing from descriptive classification to structural analysis, one needs a thermodynamic description in which change—quasi-cyclic and/or secular—is fundamental, not necessarily simply an infinitesimal perturbation on a quasi-Equilibrium³ state. One requires, a priori, a nonrestricted, nonEquilibrium thermodynamic approach to description, analysis, and synthesis of both object and environment.

Why the above mélange of astronomy and biology/botany in this foreword? For three reasons, aimed at perspective.

¹ As contrasted to subsurface dissection, thus far impossible for stars, and other remote objects.

² For example, the B-normal, Be, and Be-shell phases of “peculiar” Be stars.

³ Refer to Appendix for precise terminology.

1. These are the two great, classical, taxonomic sciences, with the goal of each such taxonomy being to distinguish, observationally/empirically, like kinds of objects, which one might hope to model—in their present, generally time-dependent, structure, and in their evolution, and possibly Evolution,⁴ of structure. There are, after all—if one decides that the microscopic, nuclear/atomic/molecular, “building-blocks” are the same and governed by the same microscopic rules in all environments—just two, basic, parallel “macroscopic” problems: the origin, present structure, evolution and Evolution of (1) nonliving, individual objects and (2) living, individual objects. One has a strong curiosity as to whether the same macroscopic rules for combining microscopic particles into macroscopic structures hold for *all* environments and for *all* kinds of individual structures/objects, of which nonliving and living simply represent the two broadest taxonomic categories. Equally broadly, we categorize the above microscopic rules referring to particles as statistical (evidently quantum-) physics; the macroscopic rules are the province of thermodynamics (evidently, non-Equilibrium). Statistical physics and thermodynamics are degenerately equivalent in the homogeneous Equilibrium configuration where there is no structure and where there are no objects, by conceptual definition, based on extrapolation from observed, quasi-Equilibrium configurations.

2. Recent evolution of observations and thinking in each of astronomy and biology has been away from the Platonic ideal of the existence of some prototype specimen characterizing each taxonomic class of like objects, which can be represented by some “standard model.” One wants to distinguish carefully between two aspects of this changing outlook.

a. On the one hand, *there is an evolution away from the thinking that a taxonomy based on limited observations—such as only in the visual spectrum in astronomy—suffices to define “like” objects*, even when they are observed more broadly across the X-ray, farUV, farIR, and radio spectral regions, simultaneously, with the visual. Such classical stellar taxonomy assumes the star has a quasi-Equilibrium spectrum produced by quasi-Equilibrium atmospheric regions; hence, one can predict what will be observed in one spectral region from a model based only on observations in another. However, observationally, stars judged like or unlike in the visual are not always judged so in, e.g., the farUV. And, over such a broad, pan-spectral, observational baseline, one often finds the observed radiative spectrum to depart strongly from any Equilibrium, or linearly nonEquilibrium spectrum, or even the relatively minor variations from it corresponding to the depth variation in surface layers of temperature and density under the standard model, based on the visual spectrum. Indeed, faced with some apparent conflicts between observations and “standard” modeling, based on visual spectra, astronomers often try to introduce multiple objects instead of the previously-inferred single one. Sometimes such multiplicity is justified; often not; but it is the source of the term “symbiotic stars.” Here, we focus on the alternative resolution in terms of multiple, non-Equilibrium, atmospheric regions of a single star. But in any event, wholly empirically, more parameters enter such a taxonomic classification based on a broader observational range.

One asks whether such an increased number of parameters is also required for structural modeling. Under such a broader description, some like objects may simply constitute a smaller class. But also, some objects “unlike” in only a limited spectral region, observed only statistically at one or a few epochs, may ultimately be recognized as simply reflecting different aspects, or different temporal phases of a larger and broader group of like objects when they are observed individually at various epochs across the full spectral range. The discussion on Be-stars in *B Stars With and Without Emission Lines* (Underhill and Doazan, 1982), puts these alternatives into strong focus. Chapter 3 of the present volume broadens the discussion of “Be-similar” and “solar-similar” stars. Most important, broadening the observational range can change completely the thermodynamic basis for any attempt at “standard” modeling of a taxonomic class. For example, the demonstrated ubiquitous

⁴ evolution is the duration cycle, of its existence as an individual entity, for a particular object; Evolution, if it occurs, is the secular progression of the types of concentration modes for a particular species of object; cosmology is the relation between local and global structure of the universe of objects and environments.

existence of a mass-flux from stars, from the wealth of farUV observations, requires that any standard model be based on the star as an open, nonthermal, thermodynamic system rather than the closed, thermal one of the visual-based, classically standard model. Such change is profound—not only on atmospheric modeling, but also on subatmospheric and stellar evolutionary modeling. Apparently, one cannot characterize the observational manifestations of stellar evolution in terms only of a change in T_{eff} , g , R —or even by allowing a decreasing M . One must also admit the possibility of evolving internal nonthermal storage modes, and these are not necessarily confined to a decrease in rotational velocity and its resulting effect on magnetic storage and energy dissipation.

b. On the other hand, there is an even more profound change in observations and thinking: *one begins to question even the existence of a prototype specimen and of a standard model*, derived from statistical studies of real-world objects. Some biologists have placed the problem in the strongest focus, with what Mayr (1978) terms “population thinking.” Conventionally, members of a class are supposed to differ insignificantly from the statistically idealized prototype, and any Evolution refers to that prototype. Mayr suggests the modern outlook requires, instead, a “population pool,” consisting of individuals differing significantly from any statistical norm, and it is Evolution based on, and from, this diversity which is the correct picture.

In astronomy, modern, pan-spectral, high-resolution observations appear to show that no matter how fine the taxonomic discriminant and no matter what set of “basic” stellar parameters one uses—such as mass, total luminosity, rotation-speed—one observes very significant individual differences in monochromatic radiative, nonradiative-energy and mass fluxes, and in details of regional structure about a broad general pattern. Apparently, such differences reflect individual differences in subatmospheric, nonthermal, structural modes and their amplitudes, and the associated time variations. Possibly in turn, such differences in nonthermal structural modes reflect differing initial conditions in stellar formation, the memory of which has not been lost in stellar evolution. Clearly, one cannot speak of Evolution in the sense of biological species; possibly, if one thinks of recycled material forming the stars, and an evolution of the regions in which stars of a given mass are formed, one can imagine discussing the Evolution of the nonthermal structural modes for a star of given mass and energy. But this is very much in the future, after we really understand whether, and which, subatmospheric nonthermal structural modes are necessary to consider in treating subatmospheric, atmospheric, and local environmental structure.

But however these *evolutionary* and *Evolutionary* problems are resolved, it seems clear that one must incorporate the notions of individuality and variability in both them and in simple questions of structure at a given epoch. Apparently, for many stellar types, and at least in discussing mass-interchange with the local environment, one needs a time history of the mass-flux from a particular star over some nonzero time interval about the considered epoch. Without this knowledge, we will see that it is apparently impossible to model atmospheric and local environmental structure at a given epoch. Hence, it is impossible to answer precisely the definition of “like” objects simply from their external appearance at one epoch. Moreover, until we determine, again observationally, the “range of individuality” permitted among like objects, we have the same problem in specifying “likeness” and modeling these particular like objects.

3. There is much in the literature asserting the need for a fundamental difference in approach when treating living, as contrasted to nonliving, objects. Generally, these assertions accept the universal applicability of the microscopic rules—statistical physics; they ask for basic differences in the macroscopic approach—thermodynamics, even though not always explicitly called such. As examples of this viewpoint, see Elsasser (1966, 1975) from the viewpoint of a physicist and Mayr (1978) from the viewpoint of a biologist. One kind of contrary viewpoint, from a nonEquilibrium thermodynamic approach applied equally to hydrodynamics and biology, is exemplified by the Prigogine school (1965, 1977a, 1977b,). I, myself, hold to the latter, contrary viewpoint, although differing

significantly with it based mainly on empirical astronomical studies (Thomas, 1977). In essence, the Prigogine approach examines fluctuations in an Equilibrium system, which become sufficiently large to produce a quasisteady nonEquilibrium configuration: so evolution is from Equilibrium to nonEquilibrium via nonlinear amplification of Equilibrium fluctuations. On the contrary, I consider that the phenomena of astronomy demonstrate an evolution from the nonEquilibrium configuration of the ISM or IGM to a quasi-Equilibrium⁵ star, galaxy, etc. The Prigogine school retains an unnecessary linearity by retaining an entropy and discussing entropy generation; but this is a detail. *The essential point is whether real-world nonEquilibrium configurations for objects arise from dispersed, strongly nonEquilibrium media and evolve to concentrated objects with less nonEquilibrium in the interior, or the converse.* A priori, and speculatively, we do not know: our experience, hence intuition, with such real-world, nonthermal, nonEquilibrium thermodynamics of open systems is presently very limited but appears to suggest the evolution *from* dispersed nonEquilibrium *to* concentrated quasi-Equilibrium.

My own feeling is that we must therefore proceed *empirically-theoretically*,⁶ in the detailed observational-empirical study of a variety of individual real-world objects, to develop not only a phenomenological understanding of broad classes of real-world phenomena from this nonEquilibrium viewpoint, but then to use this understanding to develop a more axiomatic theoretical formulation of such generalized nonEquilibrium thermodynamics. As in any real-world study, the axioms must ultimately be based on observations, not speculations by Eddington's isolated astronomer on a fog-bound planet. As of this moment we are hardly ready for such a Caratheodory-type approach to the wide variety of nonEquilibrium thermodynamic configurations possible, under nonisolated conditions, as contrasted to the isolated, single, degenerate configuration of Equilibrium thermodynamics.

So, I think that if one asks, *empirically-theoretically*: what, re structure; how, re origin; and where, re evolution and *Evolution* for real objects in the real world; from a general nonEquilibrium thermodynamic viewpoint, any intrinsic distinction between the thermodynamics of living and non-living systems will ultimately vanish. An almost banal example is the apparent paradox presented by the speculative misapplication of the Second Law of Equilibrium thermodynamics to the observed real-world evolution of stars and living objects alike: a speculatively predicted change toward disorganized homogeneity, but an observed change toward organized structure. The apparent paradox vanishes when one simply realizes that the Second Law has nothing to do with nonEquilibrium systems; the origin of the paradox lies in a misunderstanding of the province of Equilibrium Thermodynamics.

So in these lectures and this monograph, I have followed the above spirit applied to the observable nonEquilibrium regions, the atmospheres, of one kind of real-world object, the stars. I have adopted the "familiar things from an unfamiliar viewpoint" approach to summarize and place into context the "familiar" treatment of the "speculative standard model" of the atmosphere of the (closed, thermal) thermodynamic representation of a "statistically normal" star, via the "unfamiliar" language of a linearized nonEquilibrium thermodynamic abstract of the classical, and a nonlinearized nonEquilibrium abstract of the neoclassical, approximation to the model. Then the "unfamiliar things not expounded elsewhere" aspect takes the form of a primary focus—observationally, thermodynamically, and theoretically—on peculiar stars to infer, empirically, what kind of a thermodynamic object any and all real-world stars, normal and peculiar, are. Such focus on peculiar, and generalization to all, rests on the conjecture that peculiarity simply represents a greater amplitude of those nonthermal, nonEquilibrium characteristics and fluxes which are neglected in standard normal star modeling. Consequently, I also focus on nonEquilibrium observational diagnostics of

⁵Refer to Vol. 2 for terminology.

⁶Refer to Chapter 1 for elaboration.

the observed fluxes of matter and energy from stars to delineate, empirically, just what are the structural patterns in, and the role of, the stellar atmosphere and the local stellar environment. These two parts of the star form the directly observable transition region between star and environment—and are also the focus of the distinguishing characteristic of the star as an open thermodynamic system, its mass-flux return to its parent medium. I particularly ask the implications of the observed variability and individuality of these observed fluxes, and of the atmospheric structural patterns and regions, on the questions of origins of the nonthermal fluxes. It appears that atmospheric structural patterns, the local stellar environment, and subatmospheric nonthermal structure are completely interrelated among themselves and to such stellar variability and individuality.

Some of the basic physical background in Part II (Vol. 2) of the book falls into the category of “unfamiliar things not expounded elsewhere”—in the usual astronomical literature. But this is mainly a comment on the usual astronomical literature, not on any great uniqueness of the material presented here, which, apart from the astronomical-nonLTE aspects, I have simply abstracted from developments outside astronomy. Likewise, while many of the suggestions on better empirical-theoretical modeling offered in Part III of the book may appear “unfamiliar, not expounded elsewhere,” this is only partially true. Much of it is gratefully—and I hope completely explicitly—constructed from what I have learned while working with the editors and authors of other volumes in the series and from applying modern data and thermodynamics to the “intuitive-observational” variety of atmospheric patterns suggested by an array of earlier observers, much of whose work has been regrettably set aside. What I abstract here, other volumes in the series treat in much more detail, and probably much more clearly. For certain generalized conclusions, of course, I take full responsibility for any error. What is correct, I again stress, comes from the observational material and the empirical diagnostics, of material from other volumes in the series, from a century of accumulated data on peculiar stars, and from the rapidly expanding panorama opened by observations outside the visual spectrum.

Happily, as the volumes in this NASA-CNRS series appear, those “unfamiliar things” on which I focus become increasingly expounded everywhere, even if not in this nonEquilibrium thermodynamic language. So, hopefully, this volume will become rapidly superseded, or at least followed by more extensive, alternative developments of its empirical-theoretical explorations. For this reason, this volume’s place in the monograph series is not at the beginning, as an introduction, nor at the end, as a summary, but midway, to indicate that its empirical-theoretical discussions and conclusions will, like those of the other volumes, evolve with evolving data. In the same way, I trust that its attempts to use the star and stellar atmosphere as an example of an observational/empirical guide to the development of a completely general nonEquilibrium thermodynamics will be rapidly supplemented, broadened, and improved by other such real-world, not simply speculative, examples.

In collecting and summarizing the observational material presented in the several volumes, many gaps in knowledge have inspired various collaborative programs among the several editors and authors. Most striking among these have been those programs whose fundamental basis rests on making simultaneous observations within and outside the normal visual spectrum. Their results have often been as symbiotic as are the stellar atmospheric regions they study. Too often visual observations analyzed alone suggest one atmospheric model; farUV observations, taken alone, suggest another; adding X-ray and radio observations, again in isolation, remind one of the proverbial six blind men, each studying one region of an elephant. I am grateful to have been admitted as a part of several such collaborative studies.

In the same way, I am deeply grateful for the scientifically wise and organizationally solid collaborative efforts by Stuart Jordan, which began the monograph series with his volume, *The Sun as a Star* (Jordan, 1981), anchored the volumes solidly within the NASA framework, and now brings to the Solar Optical Telescope (SOT) program that same solar-stellar perspective. NASA has been

the rock sustaining the series. Without George Pieper and Jack Brandt taking the initiative at Goddard, and continuously supporting us at Headquarters, the series could never have been started. Without the encouragement and support of Harold Glaser at NASA Headquarters over many years preceding the series, and his off-stage support during the series until his retirement, the series itself, my own commuting and organizing efforts on it spread over Europe and the United States and my own scientific program would have not been possible. I regard his retirement from NASA as most regrettable. Pierre Creyssel, as Codirector of CNRS at the series' inception, gave much initial encouragement and support of the monograph program. His retirement from CNRS was unfortunate. Jean-Claude Pecker and the College de France kindly invited me to a post as Visiting Professor at the College de France during the years 1973–1975, during which some of the scientific background and collaborative organization of the series were brought together. Subsequently, the CNRS gave me a modest post and support, to organize the monographs in Europe. NASA gave me support to work on the series and to continue my scientific program in the United States—and in the persons of Brandt, Glaser, Jordan, Pieper, and Goetz Oertel NASA continuously provided *enormous* moral support. In Boulder, Art Hauler and his right arm, Sue Randolph, of the NBS Boulder Labs provided that warm support characteristic of Hauler's aid to Astro-Boulder since his charter executive efforts with us in embryonic JILA. I am indebted to the Astro-Geophysics Department, and to Charles Barth and LASP, for office space in Boulder, and especially to Jim Warwick and Mahinder Uberoi for continued scientific interaction. I hope it is clear that the monograph series, my own scientific work, and the commuting between scientific centers rest basically on collaborative efforts, abstracted above, and in discussing the science throughout the book; I am deeply grateful.

I am strongly indebted, over the years, to those who have provided such strong and generous collaboration in scientific efforts to broaden the solar-stellar and stellar-solar panorama: Vera Doazan, Dick Dunn, Jack Evans, and Walt Roberts in the observational aspects; Katharine Gebbie, Leo Goldberg, John Jefferies, Stuart Jordan, Jean-Claude Pecker, and Roberto Stalio in the quasi-theoretical.

The perpetual wandering to explore the next frontier, rather than statically filling the details of the last, can be exasperating. For continuous encouragement, and support, over many years, I have been deeply indebted to Jack Evans, Harold Glaser, and especially Gladys Thomas, with whom, at the Ballistic Research Labs, and the snow-bound evenings with the Gaposchkins, much of this started.

CONTENTS

<i>Chapter</i>	<i>Page</i>
Preface	vii
Foreword and Acknowledgments	xiii
Resume	xxiii

VOLUME 1

PART I: THERMODYNAMIC OVERVIEW OF THE STELLAR ATMOSPHERE

1. Introductory Comments on Stellar Atmospheric Structure and Its Modeling.	3
A. Some Comments on A Priori Speculative-Theoretical Modeling of Atmosphere, Star, and Environment.	5
B. General Historical Perspective on Stellar Atmospheric Models.	11
C. Perspective on the Empirical-Theoretical Program of Which This Volume is a Part ..	16
2. Speculative-Theoretical Modeling of the Atmosphere Enveloping a Hypothetical (Closed, Thermal) Star	19
I. Introduction.	19
II. Definition and Representation of Space- and State-Fluxes.	25
A. Definition of Fluxes	25
B. Representation of Space-Flux via Intermediate Parameters	29
C. Translation of Intermediate Parameters to State Parameters	34
III. Predicted Atmospheric Models Under Quasi-Equilibrium.	36
A. Observed Fluxes Expected Under Thermal Models	36
B. Thermal Models	40
1. Overview of Thermal Modeling.	40
2. Classical Thermal Models: Under LTE or LTE-R	50
a. LTE Modeling.	50
b. LTE-R Modeling.	59
i. Gray Models.	59
ii. Multi-Gray Models	65

3. Neoclassical Thermal Models: Thermal nonLTE	71
a. Overall Perspective	71
b. NonLTE Photospheric Models From Continuum Alone	83
i. Photospheres Having Exceptional Collisional Processes: H	85
ii. Photospheres Without Exceptional Collisional Processes	92
c. Multi-nonLTE Continua and Spectral-Line Effects	103
i. Continuous Opacity Only	105
ii. Line Effects	108
3. Empirical-Theoretical Survey of the Varieties of Peculiarities and Anomalies in the Atmospheres Enveloping Actual Stars	115
I. Introduction	115
II. Survey of Stellar Peculiarity	121
A. Stellar Variability	122
1. Classification According to 1938 Gaposchkin Scheme	123
a. Geometric	124
b. Intrinsic	124
i. Pulsational Variability	124
ii. Cataclysmic Variability	134
iii. Spectrum Variability	146
2. 1978 Modification of 1938 Scheme	147
3. Stellar vs. Atmospheric Variability	148
B. Emission-Line Peculiarity	149
1. Prevalence of Such Peculiarity	149
2. General Characteristics of Such Emission Lines	151
3. Varieties of Emission-Line Stars	164
a. The Wolf-Rayet Phenomenon	165
b. Be Stars and Be-Similarity	173
c. Further Be-Similar Stars, Hot and Cold	185
i. The Planetary-Nebulae	186
ii. The T Tauri Stars	190
C. Symbiotic Stars and Symbiotic Phenomena	196
D. Extended-Atmosphere Stars	202
1. General Summary	202
2. Extended-Atmospheres Inferred from Eclipse Observations	207
a. The Sun	207
i. The Low Solar Chromosphere	208
ii. Gross Radial Structure of the Solar Corona	216
iii. Stellar Extrapolation from Solar Configuration	222
b. Eclipse Probing of a Hot-Star Extended Atmosphere	223
c. Eclipse Probing of a Cold-Star Extended Atmosphere	226
E-F. Commentary on Superionization and Superthermic Velocity	230
E. Superionization	232
1. Perspective	232

<i>Chapter</i>	<i>Page</i>
2. Character and Locale of Superionization	235
a. Superexcitation	236
b. Superionization Itself	241
c. X-Ray Emission	245
F. Superthermic Velocity	249
1. Systematic-Flow Velocities	251
2. Quasi-Random Flow Velocities	262

PART II: THERMODYNAMIC AND GAS-DYNAMIC BACKGROUND

VOLUME II

PART III: RADIAL STRUCTURE OF ATMOSPHERE AND LOCAL ENVIRONMENT

Overview of Atmosphere and Local Environment	271
4. Characteristics of Distinctive Regions Comprising Stellar Atmospheres	279
I. Introduction	279
II. Distinctive Atmospheric Regions for Quasi-Thermal Photospheres	283
A. Quasi-Thermal Photosphere	283
B. Chromosphere	285
C. Lower-Corona	287
i. Sub-Thermic Flow in Photosphere and Chromosphere	292
ii. Trans-Thermic Flow in the Lower-Corona	296
D. Upper-Corona	300
E. NonDecelerated Post-Corona	311
F. Decelerated Post-Corona	312
G. H α -Emission Envelope	314
H-I-J ? Remaining Regions of the Local-Stellar-Environment	320
5. Observed Distinctive Radial Sequences of the Distinctive Atmospheric Regions Comprising Stellar Atmospheres	323
I. Perspective from Sequences Whose Variety Includes Quasi-Thermal Photospheres	323
II. Extrapolated Perspective on Those Sequences Including Ejected-Shell and Spherically-Pulsating Photospheres	325
A. Ejected-Shell Photospheres	326
B. Spherically-Pulsating Photospheres	328
III. Abstracted Summary of Gross Distinctive Radial Sequences of Distinctive Atmospheric Regions	330

<i>Chapter</i>	<i>Page</i>
6. Inferences on the Thermodynamic Characteristics of a Star from the Distinctive Radial Sequences of the Distinctive Atmospheric Regions Comprising that Stellar Atmosphere.	333
I. Summary-Perspective	333
II. Taxonomic Considerations	336
A. Classification According to Photospheric Characteristics.	337
B. Classification According to Exophotospheric Characteristics.	338
III. Diagnostic Considerations	338
IV. Modeling Aspects	341
Appendix	345
References.	351
Index.	365
Author's Addresses	369

RESUME

VUE D'ENSEMBLE DE LA STRUCTURE EMPIRIQUE D'UNE ATMOSPHERE STELLAIRE ET DE SON ENVIRONNEMENT LOCAL

A. Perspective Empirique et Théorique des Parties I et II

On peut définir une étoile comme une concentration de matière et d'énergie exothermique, soumise à sa propre gravitation, et qui évolue dans un état de quasi-équilibre au sein du milieu interstellaire qui, lui, est hors de l'équilibre. Du fait qu'elle est soumise à sa propre gravitation, sa structure ne peut être homogène, et à cause de son caractère exothermique, sa structure ne peut être décrite à l'aide de modèles isothermes, ou localement adiabatiques. Enfin, la valeur des flux radiatifs observés dans les étoiles montre que leur caractère exothermique provient de réactions nucléaires et non de l'énergie cédée par contraction gravitationnelle. Le flux rayonné dans le visible ne présente pas de fortes variations pour la plupart des étoiles, pas plus qu'on n'observe de grandes variations de structure. Etant donné que la production d'énergie nucléaire est très sensible à la température et à la densité locales, on représente, en première approximation, la structure interne d'une étoile à l'aide de modèles en équilibre hydrostatique où le champ des vitesses est quasi-thermique. Dans ces conditions, le transport de l'énergie se fait par rayonnement ou par des mouvements de masse quasi-statiques. Cela signifie que toute différence de vitesse non thermique, comme celle qui existerait dans le cas d'une turbulence stationnaire, ou d'une convection laminaire ou turbulente, doit être suffisamment faible pour ne pas perturber l'équilibre hydrostatique, ni dissiper une quantité appréciable d'énergie non radiative. De plus, dans ces modèles, seules de très lentes variations du taux de production d'énergie sont admises comme, par exemple, celles qui accompagnent les phénomènes évolutifs des étoiles. Enfin, notons que ces modèles interdisent toute variation appréciable pendant des intervalles de temps courts comparés aux temps évolutifs.

Dans cette approximation, la structure stellaire, en quasi-équilibre, possède le caractère thermodynamique des systèmes fermés, thermiques. On peut y distinguer trois principales régions: Les régions centrales, où la densité et la température sont suffisamment élevées pour produire des réactions nucléaires, qui, compte tenu des conditions quasi-thermiques imposées, conditionnent la structure. Au-dessus de cette région se trouve l'enveloppe stellaire qui transmet vers l'extérieur l'énergie produite dans la région centrale. La pression, la densité et la température qui définissent les conditions de quasi-équilibre thermodynamique, diminuent en allant vers l'extérieur, depuis de très grandes valeurs dans les régions centrales où l'énergie est produite, jusqu'à des valeurs relativement faibles dans les régions sous-atmosphériques. La limite supérieure de l'enveloppe est définie par la condition qu'aucun rayonnement ne peut s'en échapper directement, en direction du milieu interstellaire. La troisième

region de ce modèle en quasi-équilibre est alors constituée par la couche atmosphérique superficielle d'où le rayonnement peut s'échapper librement vers le milieu interstellaire. Cette région ne sert donc qu'à émettre vers l'extérieur l'énergie produite par l'étoile, et ceci, dans des régions spectrales très différentes de celles où elle a été produite. Comme la gravité s'oppose à la fuite des particules, mais non à celle des photons, ce modèle néglige, de façon explicite, l'énergie transportée par le flux de masse, et interdit l'existence même d'une perte de masse. Le terme "d'écran fluorescent" que nous avons utilisé pour caractériser le rôle de l'enveloppe photosphérique éjectée par les novae, dans le modèle de Pottasch, peut aussi s'appliquer à cette couche atmosphérique superficielle parce que, dans cette première approximation, on s'intéresse seulement aux conditions thermiques imposées aux limites inférieures et supérieures, et non à la cohérence physique de la description de la structure interne. On impose, en outre, que l'interface, entre la limite inférieure de cette région et la limite supérieure de l'enveloppe, soit une région chaude en ETL, dont la température est déterminée par la densité de radiation en cet endroit. La limite supérieure de cette région superficielle peut être plus froide, sa température étant définie par le flux radiatif, dans les conditions de non ETL-R. Les relations structurelles entre le flux et la densité de rayonnement, d'une part, et la température et la densité de la matière, d'autre part, sont obtenues en représentant cette région par une atmosphère gazeuse, dans un certain état thermodynamique, dont les propriétés sont totalement fixées par la gravité et le flux radiatif de l'étoile. Dans cette description, l'atmosphère stellaire et son environnement ne sont couplés que par le flux radiatif. Tant que les hypothèses adoptées sont physiquement cohérentes, et qu'elles ne présentent pas de désaccord notable avec les observations, ce modèle d'atmosphère, constitué d'une seule région, la photosphère standard, permet de déduire des observations des conclusions raisonnables en ce qui concerne la composition chimique, la structure interne et l'évolution de l'étoile.

Tant que cette description en terme d'écran fluorescent reflète entièrement les changements dans les conditions thermodynamiques de l'interface enveloppe/atmosphère, cette méthode peut être utilisée pour interpréter les observations (même en dehors du cadre des modèles entièrement thermiques, en équilibre hydrostatique), pour en déduire les conditions non thermiques de l'interface, et les changements de ces conditions. Dans le Chapitre 3, nous avons montré comment on pouvait faire le diagnostic de quelques observations d'étoiles variables pulsantes, lorsque les pulsations résultent d'instabilités thermiques dans l'enveloppe. On pourrait même faire le diagnostic des premières phases de variation des étoiles cataclysmiques, si ces phases pouvaient être décrites simplement comme l'éjection d'une couche de l'atmosphère, à condition qu'il n'y ait aucun mouvement de compression dû à des vitesses différentielles, et que l'état thermodynamique de l'enveloppe ne subisse aucun changement. En d'autres termes, on pourrait décrire les mouvements de masse dans l'ensemble de l'atmosphère sans que ceux-ci n'entraînent une perte de masse; ou même des mouvements violents conduisant à une éjection de matière—ou des phénomènes d'amplitude intermédiaire—tant que le couplage des mouvements de masse et des flux radiatifs garde son caractère quasi-adiabatique, et qu'il ne dissipe pas de l'énergie. En résumé, on préserverait le caractère de la photosphère standard, constituée d'une seule région atmosphérique, en limitant l'importance des mouvements différentiels.

Dans le Chapitre 2, nous avons, cependant, montré qu'on ne pouvait pas décrire la structure des régions superficielles de l'étoile, à l'aide d'un modèle quelconque en ETL, sans risquer de faire une erreur appréciable sur la détermination de la distribution spectrale du flux radiatif, en fonction de la température et de la structure atmosphérique. Nous avons également montré, dans le Chapitre 3, que des effets de non ER accompagnaient, quelquefois, les effets de non EH, pendant certaines phases de ces mouvements atmosphériques (ER et EH désignent, respectivement, l'équilibre radiatif et hydrostatique). Il faut alors admettre l'éventualité d'une structure non thermique, et hors de l'ETL, pour

ces régions. Cette éventualité est fortement suggérée par les similarités, les différences, et la diversité des conditions atmosphériques observées dans différents types d'étoiles, que nous avons présentés dans le Chapitre 3. La question de la validité de la méthode de détermination de la température des régions exophotosphériques, à partir des conditions d'équilibre radiatif de la photosphère, doit être posée lorsqu'on observe, dans certaines étoiles, des régions atmosphériques beaucoup plus froides que la température limite prédite par les modèles quasi-thermiques, en non ETL. De même, lorsqu'on observe des régions atmosphériques dont les températures sont beaucoup plus élevées que la température effective de l'étoile—et même beaucoup plus élevées que la température au sommet de l'enveloppe—il n'est plus possible de négliger tous les flux, autres que le flux radiatif. Aussi lorsqu'on observe des régions atmosphériques ayant des vitesses supérieures aux valeurs thermiques en un endroit quelconque de l'atmosphère, les conditions imposées par les modèles thermiques ne sont plus respectées, et l'on ne peut plus ignorer les effets de ces champs de vitesses sur la structure atmosphérique. Il est également clair que les étoiles ne peuvent pas être décrites à l'aide de systèmes fermés lorsque les observations montrent qu'elles perdent de la masse continuellement. On réalise aussi que l'atmosphère stellaire est une zone de transition entre l'étoile et le milieu interstellaire, et qu'elle ne constitue pas la limite extérieure de l'étoile, lorsqu'on observe, à différentes distances de la photosphère, la présence d'un environnement local qui résulte des effets d'interaction d'un flux de masse variable. On réalise, aussi, que certaines régions atmosphériques peuvent être affectées par un effet de voile, lorsqu'on observe une émission coronale inversement reliée à l'étendue de l'environnement local. Etant donné les phénomènes de variabilité exhibés continuellement par certaines étoiles, et la variabilité occasionnelle exhibée par un grand nombre d'étoiles, pendant des intervalles de temps très courts comparés aux durées du temps évolutif, on peut se poser la question de l'utilité des modèles thermiques en quasi-équilibre. Enfin, en constatant que des étoiles, ayant un même flux radiatif et une même gravité, possèdent des régions atmosphériques d'importance différente qui peuvent être variables dans le temps, on se pose la question de la validité de tout le fondement thermodynamique de la modélisation—des conditions imposées à la sous-atmosphère, et à l'atmosphère elle-même. Une étoile peut avoir, a priori, n'importe quel caractère thermodynamique que nous devons chercher à reconnaître, pour son atmosphère comme pour sa sous-atmosphère.

La question fondamentale est de savoir si les différents problèmes énumérés, ci-dessus—ceux relevant du caractère thermodynamique, comme ceux posés par l'existence de régions atmosphériques anormales—ont un caractère général, ou s'ils ne concernent que des cas particuliers. On constate que les incohérences d'ordre thermodynamique sont tout a fait générales, du moins en ce qui concerne les modèles thermiques, en non ETL. Ceci conduit alors à rechercher les divers modèles possibles non thermiques, en non ETL. Il faut ensuite voir si les différentes conditions non thermiques et les différentes régions atmosphériques sont de nature différente dans les différentes parties du diagramme HR. Un exemple important est donné par l'existence de régions atmosphériques où les vitesses sont supérieures à la valeur thermique et à la vitesse de libération. Certaines théories supposent, pour les étoiles froides de type solaire, que les vents trouvent leur origine dans une couronne chaude, qui est à son tour chauffée par la dissipation d'une énergie non radiative, liée à la rotation de l'étoile ou à la présence de champs magnétiques. Pour les étoiles cataclysmiques, et sans doute aussi pour les étoiles symbiotiques, certains supposent que le transfert de masse dans un système binaire produit des explosions, dans la sous-atmosphère, suivies d'éjections de matière. Si toutes les étoiles perdaient leur masse dans des conditions aussi particulières, on devrait trouver certaines régions du diagramme HR où ces circonstances n'existeraient pas, et où les observations ne contrediraient pas les prédictions du modèle standard, pour lequel toute perte de masse est interdite. Si, par contre, l'existence de perte

de masse est générale dans le diagramme HR, il faudra changer le caractère thermodynamique fondamental des modèles d'atmosphère classiques, qui est celui des systèmes fermés, thermiques, en celui des systèmes ouverts, non thermiques, et intégrer au système thermodynamique retenu un flux de masse non thermique. Si l'étoile est représentée par un système fermé, thermique, elle doit renvoyer son flux d'énergie radiative dans le milieu interstellaire, et le modèle doit pouvoir rendre compte de la production et de la propagation de ce flux, d'une façon générale. Si l'étoile est représentée par un système ouvert et non thermique, elle doit renvoyer ses flux d'énergie radiative et non radiative, ainsi que son flux de masse dans le milieu interstellaire; et la modélisation de chacun de ces flux doit être faite, également, de façon générale.

Pour décider si les contradictions thermodynamiques proviennent de circonstances particulières dues à l'existence de régions atmosphériques anormales, ou du caractère thermodynamique lui-même, adopté dans la modélisation, il faut appliquer ces modèles dans tout le diagramme HR, aux étoiles normales et anormales. On doit noter qu'il n'existe pas de théorie générale pour décrire les caractères des systèmes thermodynamiques ouverts, non thermiques, et non linéaires. Les caractéristiques des régions distinctes de l'atmosphère stellaire peuvent alors servir de guide dans l'étude des systèmes ouverts, non thermiques. Dans la troisième partie, nous essayons de faire la synthèse des contradictions que comportent les modèles d'atmosphère existants, du point de vue de leur caractère thermodynamique, d'une part, et en ce qui concerne les caractéristiques observées dans les différentes régions de l'atmosphère, et pour différents types d'étoiles, d'autre part. Nous essaierons, ensuite, de déterminer les différentes séquences radiales qu'elles forment, et de déduire les paramètres physiques qui permettraient de décrire les caractéristiques des régions et celles de leurs séquences. Nous pensons que cette approche est nécessaire si l'on veut déterminer un modèle théorique, fondé sur l'observation, qui puisse être applicable à toutes les étoiles, d'une façon générale. De cette façon, il sera capable de représenter les divers schémas de structure atmosphérique que l'étoile peut avoir, en tant que système thermodynamique ouvert. Il pourra aussi, de façon plus précise, décrire une étoile donnée, à une certaine époque donnée, si l'on connaît les valeurs des paramètres nécessaires pour définir un tel système thermodynamique ouvert. Le problème de la relation entre ce schéma atmosphérique, la structure sousatmosphérique de l'enveloppe, et la structure des régions centrales qui produisent l'énergie, est un problème qui sort du cadre de cette Monographie. Il faut souligner que ce schéma de structure atmosphérique, général ou particulier, ainsi que les algorithmes permettant de le définir, sont encore très préliminaires et incomplets. Nous espérons qu'il sera rapidement amélioré et étendu—mais, non en substituant aux problèmes physiques fondamentaux posés par l'observation, la seule rigueur mathématique. Il faut chercher quelles sont les équations qui représentent les observations, et non les quelques observations capables de satisfaire des équations établies d'un point de vue spéculatif, sans s'appuyer sur les données. Nous avons donné, dans le Chapitre 3, l'exemple d'équations qui ont été contractées, à partir de leur forme générale, pour produire une théorie du flux de masse qui ne satisfait pas les observations.

Dans cette troisième Partie, notre approche est la suivante: Le Chapitre 2 est centré sur les diverses approximations de thermodynamique, et sur leurs conséquences en ce qui concerne la structure atmosphérique prédite par les modèles d'atmosphère standards, en ETL et ETL-R, ou thermiques, en non ETL. Ce Chapitre résume aussi la situation, encore incomplète, concernant la prédiction des températures dans les régions supérieures de l'atmosphère. Mais il montre que ce caractère incomplet prend de l'importance lorsqu'on essaie de calculer la quantité d'énergie non radiative qui doit être dissipée pour produire une augmentation appréciable de la température. Dans cette troisième

Partie, on essaie de traduire cet aspect incomplet par une estimation des hauteurs maximales de la base de la chromosphère, pour une valeur donnée du flux de masse, et en utilisant le modèle standard.

Dans le Chapitre 1, nous avons donné les raisons qui nous ont amené à considérer la possibilité de l'existence de régions exophotosphériques non thermiques: C'est, essentiellement, l'observation de différents types de champs de vitesses différentielles et non thermiques, connus de longue date dans les atmosphères stellaires. Certains d'entre eux sont superthermiques. Tous ces types de vitesses sont liés à l'existence de régions plus étendues que ne le prédisent les modèles thermiques. Toutes les expériences et les théories existantes de la dynamique des gaz auraient conclu à l'existence d'une dissipation d'énergie mécanique, en présence de vitesses différentielles superthermiques, qui ne sont pas du type de l'écoulement parfait, en expansion thermique, linéaire. C'est la raison pour laquelle nous considérons les champs de vitesses non thermiques observés, et, plus particulièrement ceux qui sont superthermiques, et nous nous demandons quelles sont, du point de vue thermodynamique, les conséquences de leur existence sur la structure atmosphérique. Les problèmes rencontrés, traditionnellement, dans ce type d'analyse, proviennent, d'une part, du fait que presque toutes les données d'observation étaient faites à faible résolution, dans le domaine visible, et, d'autre part, de ce que le diagnostic de ces observations repose sur l'hypothèse que la méthodologie et les conclusions de ces diagnostics n'étaient perturbés ni par la présence de ces vitesses non thermiques, ni par les phénomènes qui pourraient leur être associés, comme le chauffage non radiatif, et l'extension atmosphérique non thermique.

(1) Le Chapitre 3 a mis en évidence l'importance des étoiles anormales dans l'étude des phénomènes non thermiques—les champs de vitesses, l'extension atmosphérique, la variabilité observée dans une étoile donnée, et l'individualité dans l'amplitude de ces manifestations parmi les étoiles anormales "similaires." Grâce à l'ampleur de leurs manifestations, les étoiles anormales ont permis de détecter et d'étudier les phénomènes non thermiques, même lorsque les observations étaient obtenues avec une faible résolution et qu'elles étaient limitées au seul domaine visible. Ces phénomènes ont pu être ensuite précisés à l'aide de données obtenues avec une grande résolution, et en dehors du domaine visible. Ces observations ont aussi montré, pour les étoiles normales et anormales, l'existence de certaines régions atmosphériques liées aux propriétés non thermiques des étoiles.

(2) Dans la deuxième Partie (qui constitue le deuxième Volume de cette Monographie) on étudie les conséquences d'une représentation non linéaire des fonctions de distribution et des conditions aux limites, sur la structure atmosphérique. Les effets de la non-linéarité interviennent au niveau de la méthodologie du diagnostic et de ses conclusions. La deuxième Partie étudie aussi les conséquences de l'introduction de termes non thermiques dans les équations (thermiques) du modèle standard et dans les conditions qu'il impose. On étudie aussi les effets qui résultent lorsque l'on ne restreint pas les valeurs des termes non thermiques. Cette deuxième Partie, qui constitue maintenant le deuxième Volume, paraîtra après ce premier Volume. Elle exposera certains problèmes d'Aérodynamique, qui sont bien connus maintenant, et des aspects moins courants de Thermodynamique, que nous discuterons du point de vue de l'étude des atmosphères stellaires, et de celui des systèmes thermodynamiques ouverts.

Les données d'observation d'étoiles normales et anormales, obtenues dans le visible et dans d'autres régions spectrales récemment explorées, permettent de déterminer les conditions thermodynamiques qui existent dans les atmosphères stellaires, et de délimiter les différentes régions distinctes, non thermiques de l'atmosphère. En d'autres termes, nous essayons de voir si l'on peut représenter l'ensemble des observations, qui montrent la diversité des conditions physiques qui règnent dans différents types

d'étoiles, par un nombre limité de régions atmosphériques distinctes. Ces différentes régions atmosphériques sont observées dans tout le diagramme HR et non seulement dans un nombre limité de classes d'étoiles. Ces régions, qui présentent toutes des propriétés non thermiques, font partie de la photosphère et de l'exophotosphère. Certaines régions sont plus importantes que d'autres, pour des étoiles de types différents, mais aussi pour des étoiles différentes et de même type spectral, et, également, pour une étoile donnée, en fonction de sa phase de variation. Notre conclusion sur l'existence de ces régions repose sur une analyse des faits d'observation, et non sur des spéculations d'ordre théorique. En dernière analyse, nous cherchons à établir l'ensemble des équations qui permettront de prédire l'existence de ces régions, avec leurs caractéristiques distinctives, en fonction des flux définis par les propriétés de la sous-atmosphère. Ces différentes régions peuvent avoir une importance différente—du point de vue de l'observation et des caractères thermodynamiques—ce qui permet de grouper les étoiles selon une séquence, en fonction de cette importance relative. Ces différentes régions sont décrites dans le Chapitre 4. Dans le Chapitre 5, nous analysons les divers schémas de structure atmosphériques qu'elles semblent former dans une distribution radiale, très générale. On insiste plus particulièrement sur la variabilité de ces schémas parce qu'elle pourrait fournir un moyen d'approche dans l'étude de la structure de la sous-atmosphère.

Enfin, dans le Chapitre 6, on met en perspective les schémas de structure atmosphérique, analysés dans le Chapitre 5. Les schémas sont spécifiés par les changements des paramètres caractérisant l'état thermodynamique à mesure qu'on s'éloigne de l'étoile. On interprète ensuite ces différents schémas en fonction des paramètres suivants: les flux d'énergie et de masse, ainsi que leur dépendance par rapport au temps; la gravité, qui conditionne les valeurs relatives des flux; le caractère thermodynamique du système; et les interactions avec le milieu interstellaire local. Nous espérons que cette étude fournira une meilleure description de l'ensemble formé par l'atmosphère solaire ou stellaire et son environnement local, et que ses conclusions formeront le point de départ de l'étude d'un type de système thermodynamique ouvert, produit par une concentration exothermique, à partir d'un milieu parental, et qui se termine dans une configuration beaucoup plus organisée qu'elle ne l'était lors de sa formation.

Ainsi les discussions des Chapitres 4 à 6 reposent, principalement, sur la variété des conditions atmosphériques observées dans la variété d'étoiles discutées dans le Chapitre 3. Tout essai de synthèse de ces données en un schéma cohérent de propriétés thermodynamiques, et de régions atmosphériques distinctes, doit reposer sur la grande diversité, et quelquefois l'apparente contradiction, des faits observés dans différents objets, de types spectraux différents. Pour ne pas être embarrassés par trop de détails, nous allons esquisser une description générale de l'atmosphère stellaire dans la Section B, avant d'en fournir l'analyse détaillée dans les Chapitres 4 à 6.

B. Résumé, d'un Point de Vue Empirique et Spéculatif, des Différentes Régions Distinctes d'une Atmosphère Stellaire, de l'environnement Local Stellaire et des Schémas de Structure Atmosphérique.

Les Chapitres 2-4 ont permis de poser les jalons nécessaires à la construction d'un modèle empirique et théorique, pour décrire une atmosphère stellaire et son environnement local. Nous avons montré, dans les Chapitres 4-6, que les données d'observation, souvent incomplètes, ne peuvent être interprétées sans ambiguïté, dans bien des cas, et que les conclusions qu'on peut en déduire ne sont pas toujours sûres. Malgré cela, il nous semble que l'on peut déjà esquisser le cadre de la thermodynamique qui devra servir à la construction du modèle, et prédire, dans ses grandes lignes, la structure de l'atmosphère stellaire.

Le problème thermodynamique peut être posé clairement, du moins dans ses aspects essentiels, en constatant, d'une part, les désaccords entre les prédictions du modèle standard d'atmosphère et les observations (cf. première partie), et en réalisant, d'autre part, que le système fermé, thermique retenu par la modélisation classique n'est qu'un choix parmi d'autres possibles et beaucoup plus contraignants (cf. deuxième partie). Nous avons discuté les trois systèmes thermodynamiques qui pourraient être adoptés pour décrire une atmosphère stellaire: à savoir, les systèmes isolés, fermés et ouverts. La présence de flux radiatifs exclut qu'une étoile puisse être représentée par un système isolé. L'évidence grandissante, parmi les étoiles de tous les types spectraux, de la présence quasi-générale d'un flux de masse montre que les étoiles ne peuvent être considérées comme des systèmes fermés. Il ne reste donc plus que les choix suivants: (a) Le flux de masse est si faible qu'il peut être assimilé à une perturbation, et l'étoile peut être décrite de façon satisfaisante par un système fermé, thermique. (b) Les valeurs des flux de masse sont suffisamment élevées pour que leur effet sur la structure de l'atmosphère ne puisse être négligé. Dans ce cas, l'étoile constitue un système ouvert, non thermique. Les faits qui présentent un désaccord avec les prédictions du modèle standard et qui conduisent au choix (b), parcequ'il est le seul compatible avec les observations, sont ensuite analysés.

(1) Tout le long du diagramme HR, on constate, lorsque les observations sont suffisamment discriminatoires, la présence de caractères spectroscopiques qui indiquent l'existence d'une superionisation, ou d'une superexcitation, par rapport au degré d'ionisation, ou d'excitation, prédit par la théorie classique. L'émission observée dans le domaine des rayons X, pour des étoiles appartenant à presque tous les types spectraux du diagramme HR, montre qu'il existe des régions dans l'atmosphère de l'étoile où la température atteint des valeurs de l'ordre de 10^6 K. Les énergies thermiques correspondantes, compte tenu des valeurs des gravités des atmosphères stellaires, impliquent l'existence de perte de masse de l'étoile, c'est-à-dire, une atmosphère non statique. Mais il faut noter que ce phénomène à lui seul nécessite uniquement l'existence d'un flux d'énergie non radiative, ainsi que sa dissipation, il n'implique pas que la perte de masse produise une perturbation majeure de la structure atmosphérique de l'étoile (considérée comme un système fermé, thermique). Par contre, l'existence d'une chromosphère et d'une couronne constitue une perturbation majeure pour toute la catégorie d'atmosphères classiques (d'un système fermé thermique) où seuls des flux d'énergie radiative sont permis. Mais si la perte de masse, due à la présence d'une couronne, provenait seulement d'une évaporation thermique (Chapitre 2) ou d'une expansion linéaire de l'atmosphère, dans les conditions d'un écoulement parfait, elle ne produirait pas une perturbation majeure de la structure en densité des régions facilement observables. La modélisation en terme de faible perturbation est quasi-adéquate, mais ceci seulement, dans le cas limite d'un flux de masse très faible et indépendant du temps. Mais la figure 3-33 du Chapitre 3 montre que les étoiles, qui pourraient être décrites, en première approximation, par ce cas limite, ont des densités si faibles, dans les régions de l'atmosphère où la vitesse du vent stellaire atteint des valeurs très élevées, que ces grandes vitesses ne sont pas détectables par les méthodes spectroscopiques usuelles. Le Soleil fournit un très bon exemple de l'existence de ces vitesses élevées lorsque des techniques particulières (collecteurs) sont utilisées pour les mettre en évidence. Les données solaires indiquent alors que le modèle fondé sur l'hypothèse d'une faible perturbation est inadéquat, même lorsque la perte de masse est faible comme dans le cas du Soleil, où la vitesse maximum du vent ne peut être généralement observée par les méthodes traditionnelles.

(2) La figure 3-33 montre, également, qu'il existe une grande variété d'étoiles, dont certaines sont situées sur la Séquence Principale, pour lesquelles l'utilisation des méthodes usuelles a permis de

l'étoile lorsqu'elle perd sa masse dans le milieu interstellaire dont elle est issue; et la variabilité du taux de perte de masse a pour effet de créer un environnement local plus proche de l'étoile que dans le cas d'une perte de masse constante. Aussi, comme ces régions proches de l'étoile subissent une forte décélération, l'énergie contenue dans le flux de masse ne se transforme pas directement dans l'environnement parental, comme c'est le cas pour les atmosphères étendues discutées en (3), à moins de considérer l'environnement local comme faisant partie du milieu parental. Mais, dans tous les cas, on peut remarquer que la quantité d'énergie émise par l'étoile est sous-estimée (comme on l'a déjà noté en (3)) si on ne considère que le champ de radiation photosphérique, c'est-à-dire, si on l'évalue, d'après les méthodes habituelles, en mesurant l'énergie émise dans le spectre visible et en l'extrapolant aux autres longueurs d'ondes, à l'aide du modèle standard. Nous avons déjà souligné l'erreur qui est faite lorsqu'on se sert seulement de l'énergie rayonnée dans le visible pour déterminer l'énergie produite lors de l'explosion d'une nova. Le même problème se pose, mais à un degré bien moindre, pour cette grande variété d'étoiles qui présentent ce type de structure d'atmosphère étendue, lorsque l'on détermine, de cette façon, l'énergie totale émise par l'étoile, et les contributions respectives des énergies radiatives et du flux de masse. Les étoiles Be nous fournissent, à nouveau, un exemple édifiant: la phase Be est, statistiquement, plus lumineuse, d'une magnitude environ, que la phase B normale, tout en ayant une répartition d'énergie correspondant à une température de couleur plus faible, c'est-à-dire, un rougissement intrinsèque. La phase Be-shell, quant à elle, simule, spectroscopiquement, un type spectral bien plus tardif que la phase B. Pendant les phases de pré-maximum des novae, la luminosité dans le visible augmente, mais l'effet de voile, dû à l'enveloppe qui a été éjectée, produit un type spectral plus froid. Pendant les phases de post-maximum, lorsque l'enveloppe éjectée devient transparente, et que l'effet de voile diminue, le spectre de l'étoile chaude sous-jacente apparaît et photoionise la matière en expansion, comme dans le cas des nébuleuses planétaires. Il est clair que le phénomène d'environnement local—qui n'est pas un phénomène général—constitue une perturbation encore plus grande du modèle fermé, thermique que le phénomène de chromosphère-couronne. Mais, la configuration de l'atmosphère n'est pas du tout celle que certains théoriciens, d'un point de vue spéculatif, tentent de décrire comme une post-couronne: une atmosphère en équilibre radiatif, et en très grande expansion vers le milieu parental. Comme on l'a vu, aucune des deux grandes classes d'atmosphères étendues ne trouve sa place dans cette solution de remplacement du modèle d'atmosphère standard.

(5) Les faits qui permettraient de conclure à l'existence d'un environnement local stellaire ont été résumés dans le Chapitre 3. La grande diversité des types d'étoiles exhibant ce phénomène a été discutée en évoquant un effet de voile possible—pour le continu et pour les raies, quelle que soit la température locale, T_e où $\tau_\lambda = 1$. Nous avons indiqué, dans le Chapitre 3, que l'existence d'un environnement local stellaire peut affecter de différentes façons le diagnostic. Un exemple particulièrement important est fourni par la discussion des observations dans le domaine des rayons X. On a noté que les observations des étoiles T Tauri suggéraient une corrélation inverse entre l'intensité de l'émission X et l'importance de l'environnement local—dont l'émission à $H\alpha$ fournit une mesure. Nous avons, aussi, résumé les observations préliminaires d'étoiles B et Be qui semblaient conduire à la même conclusion: une plus grande intensité d'émission X pour les étoiles B, dépourvues d'environnement local, que pour les étoiles Be. Mais les résultats rassemblés dans la figure 3-33 suggèrent que l'effet de voile peut être encore plus important que l'atténuation de l'émission coronale: la détection des vitesses très élevées, de niveau coronal, $U(\max) > q(\text{couronne})$ est rendue difficile, sinon impossible. Pour les étoiles ayant une atmosphère étendue du premier type, c'est-à-dire résultant d'un flux de masse constant, et lorsque les flux de masse sont aussi faibles que celui du Soleil, il n'est pas possible de

détecter les grandes vitesses parce que la concentration des particules dans ces régions est trop faible. Comme dans le cas solaire, nous ne pourrions pas les détecter par les méthodes spectroscopiques usuelles. Pour les étoiles ayant une atmosphère étendue du deuxième type, c'est-à-dire résultant d'un flux de masse variable, l'environnement local peut masquer l'émission X, aussi bien que les vitesses de niveau coronal. Cette suggestion n'est pas seulement conjecturale, elle repose sur un grand nombre d'observations. On a résumé, dans le Chapitre 3, les observations qui montrent, pour les géantes M0M5, l'existence d'une enveloppe de Ca II, ionisée par le rayonnement chromosphérique et coronal de l'étoile. Les enveloppes de ces géantes M sont fortement variables, de même que les vitesses qui leur sont associées. Nous avons également noté que les vitesses des raies de Ca II sont plus élevées pour les étoiles de type K, et souligné l'existence de vitesses encore plus grandes, dans les enveloppes de Mg II dont les températures sont encore plus élevées, plus proches d'une valeur "coronale" que les enveloppes de Ca II. L'étude des phénomènes produits par l'effet de voile, que l'on observe de façon marginale dans les étoiles froides, est certainement, à l'heure actuelle, parmi les plus importantes à entreprendre, tant du point de vue de l'observation que du point de vue théorique, si l'on veut progresser dans la compréhension de la structure des atmosphères stellaires.

(6) Pour terminer la liste des faits d'observation qui nous conduisent à considérer que le flux de masse est un paramètre indépendant, et que ses effets sur la structure atmosphérique sont de première importance, nous citerons l'exemple le plus frappant: le phénomène de symbiose stellaire, dont les étoiles symbiotiques sont les plus représentatives. En appliquant à ce phénomène sa définition littérale et historique, à savoir, une combinaison de caractères spectraux, dont certains correspondent à de basses températures, et d'autres, à des températures élevées, on doit invoquer, compte tenu du caractère essentiellement homogène de la photosphère standard, soit l'existence de régions exophosphériques multiples, soit la présence de deux étoiles, l'une chaude, l'autre froide. Considérons, à nouveau, les deux types d'atmosphère que nous avons distingués. Le premier, à flux de masse constant (dont le Soleil et les Wolf-Rayet représentent les deux cas extrêmes) peut produire cette classe de symbiose observée dans le Soleil: Une photosphère d'étoile froide, dans le visible, suivie d'une chromosphère et d'une couronne chaudes, dans l'ultraviolet. Mais la symbiose est traditionnellement définie dans le visible: Un spectre froid, de type M, et un spectre chaud, de type B, suivant les phases de variations. Ce sont, précisément, ces phénomènes que nous avons discutés, et qui sont exhibés par les différentes régions distinctes d'une atmosphère étendue, résultant d'un flux de masse variable. Nous pouvons donc décrire, d'un point de vue phénoménologique, les différentes manifestations du phénomène symbiotique—pour les étoiles symbiotiques elles-mêmes et pour celles, non classées comme telles, qui exhibent des phénomènes symbiotiques—si l'on admet que le flux de masse est un paramètre physique qui dépend du temps, et qui est déterminé par la structure non thermique de la sous-atmosphère. Bien entendu, cette conclusion n'élimine, en aucune façon, la possibilité qu'un certain nombre d'étoiles symbiotiques soient binaires. Elle signifie seulement qu'il n'est pas nécessaire qu'une étoile soit binaire pour produire les phénomènes symbiotiques observés. Cela signifie, également, que si l'on admet que le flux de masse est un paramètre indépendant, comme pour les flux d'énergie radiative et non radiative, alors la structure des régions atmosphériques qui en résultera produira, du point de vue observationnel, les phénomènes que l'on appelle symbiotiques. Si l'étoile considérée est binaire, chacune des composantes contribuera à l'aspect symbiotique observé, d'après son type d'atmosphère étendue, et d'après les caractères symbiotiques qui lui sont propres. Si l'une des étoiles est du type "solaire-Wolf-Rayet," et l'autre, une étoile Be, on observera, essentiellement, une variation des caractères symbiotiques provenant de l'étoile Be. Si les deux étoiles ont un flux de masse

variable, elles pourront produire un schéma de structure atmosphérique beaucoup plus riche que celui de chacune des deux étoiles puisque la contribution relative des différentes régions atmosphériques dépendra de la phase des éjections épisodiques de matière.

Nous avons montré quels étaient les développements possibles des différentes régions distinctes d'une atmosphère stellaire, les différents schémas de structure que ces régions pouvaient former, et les paramètres physiques dont dépendaient ces régions et ces schémas. Nous avons reconnu, dans l'atmosphère, une séquence radiale de trois principales régions dont les caractéristiques dépendent des valeurs des flux d'énergie radiative et non radiative, et du flux de masse, ainsi que de leur variation dans le temps. On trouve, en premier lieu, la photosphère, dont le caractère ne doit pas être, nécessairement, celui du modèle standard. Viennent, ensuite, la chromosphère et la couronne, régions dominées par le chauffage non radiatif, et qui semblent exister dans toutes les étoiles, à un certain degré. Vient, enfin, la région post-coronale, dynamiquement étendue, et dont le caractère est fondamentalement lié à celui du flux de masse. Nous avons reconnu deux grandes classes de régions post-coronales; L'une, associée à un flux de masse qui reste constant, pendant de longues périodes. L'autre, associée à un flux de masse continu qui subit de fortes variations épisodiques. C'est dans cette deuxième classe de régions post-coronales que l'on observe, ce que nous avons appelé, un "environnement local" qui peut se trouver à des distances variables suivant les étoiles. Ainsi, cette troisième région se mélange au milieu interstellaire parental. Notons que l'on peut distinguer différentes parties distinctes dans chacune de ces régions. Si la structure de la sous-atmosphère est entièrement thermique, l'étoile ne possède qu'un flux radiatif dont l'énergie représente l'énergie totale produite par l'étoile. Dans ce cas, l'atmosphère stellaire est constituée d'une photosphère seulement. C'est la structure non thermique de la sous-atmosphère qui produit les autres flux dont les effets sont responsables de la formation de régions multiples dans l'atmosphère. Dans cette Monographie, nous ne cherchons pas à savoir ce qu'est la structure non thermique de la sous-atmosphère, ni quelles sont ses différentes structures possibles, ni encore, quelle est leur origine. Nous essayons seulement d'analyser les implications, du point de vue de l'observation, de l'existence d'une telle structure. C'est ce que nous avons présenté dans la Première Partie.

Nous avons vu que le principal problème était de caractériser, du point de vue cinématique, les différentes régions distinctes de l'atmosphère. Ensuite, il faudra déterminer les équations et les différents termes à introduire pour traiter le problème cinématique. C'est seulement après, que la question de la relation entre ces termes et la structure non thermique devra être posée. Notre analyse ne permet pas encore de progresser sur le troisième point, et elle n'apporte qu'une contribution marginale sur le deuxième. Il nous semble, par contre, que sur le premier point, la description des régions et des schémas de structure atmosphérique que nous proposons, en première approximation, devrait permettre de progresser dans l'étude des atmosphères stellaires et de leur environnement. Nous avons posé les trois problèmes que nous avons mentionnés, et nous avons essayé de les mettre en perspective en considérant l'étoile comme un système thermodynamique ouvert, non thermique. De ce point de vue, notre analyse diffère de celle qui est généralement adoptée, et qui traite le problème théorique, d'un point de vue spéculatif.

Part I
Thermodynamic Overview
of the Stellar Atmosphere

Page intentionally left blank

Page intentionally left blank

1

INTRODUCTORY COMMENTS ON STELLAR ATMOSPHERIC STRUCTURE AND ITS MODELING

At our epoch, the conventional approach to astrophysical investigations proceeds under the implicit assumption that we know the kind of thermodynamics governing stellar structure and evolution, hence, that we can correctly write the equations describing it. We may not know how to evaluate some of the terms entering these equations, but we assume that the equations are correct in the sense of including all the terms which the assumed type of thermodynamics tells us are necessary. So, a book like this would begin with an exposition of the assumed thermodynamics—usually speculative;¹ develop the necessary equations from that thermodynamics; introduce certain conditions under which the equations are to be solved—such as the kinds of velocity fields and degree of time variability permitted by “gross” stellar observations; then proceed to discuss solutions. The major focus, at our epoch, lies on obtaining solutions that are sufficiently precise to allow the observations to be diagnosed, using these solutions, in terms of “cosmological parameters” such as present-epoch chemical abundances. That is, the solutions are sufficiently precise to model those fluxes of energy and matter from the star—and the stellar atmosphere which is their immediate source—which the star would produce *if* the actual thermodynamics by which it lives agrees with those which we speculatively assign to it. Paraphrasing Louis Malle (1982), the speculative-theoretician is born into the world to verify what he already knew.

There is an alternative approach to studying the observed fluxes of matter and energy, to studying the atmosphere which is their immediate source, and to studying the star which the atmosphere envelopes. We ask, not tell, the star what is the thermodynamics by which it lives. We ask the star to collaborate with us in exhibiting the kind of thermodynamics by which a concentration exists and evolves in a nonEquilibrium, parental medium. We ask it, and our instrumental-oriented colleagues, to provide a sufficient variety of fluxes that these can be translated into the range of atmospheric conditions necessary to produce the whole spectrum of energy and matter ejected/returned by the star to its parental environment. We ask whether this inferred range of atmospheric conditions can be translated into a set of distinct atmospheric regions, distinct in the sense of having distinctly different thermodynamic properties, not just a different numerical value of a parameter. We ask whether this set of regions is sequential, in the sense that its spatial evolution outward from the subatmosphere corresponds to the spatial evolution of some set of thermodynamic parameters, from the bottom of the atmosphere outward. We ask whether this same variety of regions characterizes all stars, or whether it differs for stars having large differences in their thermodynamic fluxes, or other parameters. We ask whether the sequences of regions, if indeed we find—*empirically*—that they exist are also universal, or if different sequences occur only among different varieties of stars. We ask whether we can find some, hopefully limited, set of thermodynamic parameters, whose spatial and temporal variation suffices to model the spatial and temporal variation of such regions and sequences of regions, in the variety of stars. We ask whether we can establish a set of equations which describes such spatial and temporal variation of these parameters as a function of “input” from the thermodynamic state of the star as a whole. Finally, we ask whether all this information gives us a good

¹Usually quasi-Equilibrium; cf Appendix and Vol. 2.

characterization of the star as a particular thermodynamic system: which precisely describes what it really is—a concentration of matter and energy in a nonEquilibrium parental medium.

In caricature, the first approach, which I call speculative-theoretical, is a conjectured variety of thermodynamics plus a set of equations looking for an application. The second approach, empirical-theoretical, is a set of observed energy and mass fluxes looking for an atmosphere capable of producing them, a set of equations capable of describing the atmosphere, and a variety of thermodynamics capable of embracing them all. In equal caricature, standard thermal atmospheric modeling is an asymptotic approximation to a thermally stable, time-independent, evaporative-diffusive mass-loss star. Observationally, it appears that such stars do not exist in the real world. We are curious as to what kinds of stars do exist, what they tell us about astronomy, and what they tell us about thermodynamics. The stellar atmosphere is what we observe, so we had best understand it. Once we admit that it is not a blackbody surface, and that we really have yet no profound knowledge of general nonEquilibrium thermodynamics, the empirical-theoretical approach seems to me the most efficient. In any event, it is the way most observational/experimental science develops when one is not absolutely certain he knows what is the thermodynamics and what are the complete forms of the descriptive equations. So, in a strong sense, any conflict between speculative-theoretical and empirical-theoretical approaches, today, is not simply a matter of personal taste between data analysis and model computing. Rather, it is a difference of opinion on the degree to which one thinks one knows the kind of thermodynamics which is applicable, and the completeness of the equations adopted. Three quotations seem illustrative.

Greenstein (1960) described very well the situation in his editorial preface to the *Stellar Atmospheres* volume of the Kuiper series:

The normal star can be treated by the elaborate apparatus of modern theoretical astrophysics, insofar as its continuous and absorption-line spectrum are concerned—it is interesting to note the rarity of equations in the later chapters dealing with observational problems in stellar spectra. That part of solar astrophysics concerned with the chromosphere, the corona, and deviations from LTE is not discussed.

In the same volume Böhm was more explicit:

Only recently has it become evident that there are numerous difficulties in the present form of the theory—part of the difficulty arises from the fact that it is very hard to get a real self-consistent picture of the thermodynamic and hydrodynamic state of a stellar atmosphere (and the determination of the thermodynamic state of the atmosphere cannot be separated from the theory of line-formation).

Mihalas was more optimistic 14 years later in the printed version of his Warner Prize Lecture:

It is clear that the interpretation of stellar spectra is a mature field, one which is hardly at the frontiers of astrophysics today—there are likely to be few startling discoveries to be made here—the availability of large-capacity, high-speed computers made it possible actually to solve the complicated mathematical systems describing stellar spectrum formation.

It is very clear that Greenstein's normal star, Böhm's theory, and Mihalas' spectroscopic diagnostics refer to the *speculative-star*—for which the thermodynamics and equations underlying the standard thermal model of the photosphere are simply assumed, a priori. On the contrary, Greenstein's comments on *observed* spectra refer to real stars and point out the uncertainty among observing astronomers on what equations can be used to describe them. Mihalas has kindly allowed me to abstract parts of his original verbal presentation which were editorially censored from the printed version as being "unscientific": "There is a tendency, when much effort has been expended to develop a theoretical framework, to want to stop there and make it work, ignoring the danger signals that we are not fitting the data. *We become enmeshed in a theory that becomes orthodox, replete with dogma.*" Modern, high-resolution spectra in the

visual, spectra of all levels of resolution in the farUV and X-ray, and modern farIR and radio observations reemphasize Greenstein's bemused comment on real-star spectra, and on the real-star atmospheric regions and nonEquilibrium thermodynamics omitted from speculative standard modeling. They reinforce Mihalas' worry that speculative-star models continue to be applied from a mixture of inertia and dogma. These modern data simply tell us that nonradiative heating, and nonevaporative mass-loss are so ubiquitous and large that the basic thermodynamic character of contemporary speculative modeling is basically wrong. Stars are (open, nonthermal) systems, not (closed, thermal). And, in the same star's atmosphere, one finds regions of very low subthermic, and regions of ultrahigh superthermic flow, regions of $\sim 10^3$ K and regions of $\sim 10^6$ – 10^7 K electron temperature, and regions of particle concentrations of 10^{15} – 10^{17} , and regions of 10^3 – 10^5 . What approximations to what equations, even what terms to include and which to ignore, are not at all clear, a priori.

This mélange of modern observations, modern nonEquilibrium thermodynamics, and modern awareness of the necessity of equations-before-solutions makes one point very strongly. The interpretation of stellar spectra and the modeling of stellar atmospheres—for real stars—is not a mature field; it is at the frontiers of astrophysics today; and it is indeed likely to produce many surprises in the years to come. But this is hardly a modern conclusion—I refer to the quotation from Struve which opens Chapter 3.

Then my own viewpoint remains as stated some years ago in the series of papers *Superthermic Phenomena in Stellar Atmospheres* (1948 et seq.): “We start from certain observed features, anomalous under the equilibrium (i.e., standard atmospheric) theory, and inquire what consequences can be deduced from the simple fact of the existence of these phenomena.” Fundamentally, the phenomena centered around superthermic velocity fields, energy dissipation by them, and the associated nonEquilibrium-thermodynamic effects. The basic observational change since then has been the enormous accumulation of data on the prevalence of such velocities, nonradiative energy dissipation, and nonEquilibrium-thermodynamic effects somewhere in the atmospheres of all stars. The basic empirical-theoretical change has been the recognition of the variety of regions and sequences of regions found in stellar atmospheres: some cousin of the standard-model photosphere is an essential, but not the only, part of the atmosphere; not all observed photospheres satisfy the standard model. The basic thermodynamic change has been the recognition of the open-system character of stars. The present volume summarizes where we stand in many of these aspects. This chapter gives some general perspective on stellar atmospheres. Part I contrasts the speculative, standard, thermal model (Chapter 2) to those phenomena observed in actual stellar atmospheres (Chapter 3) which strongly contradict the standard model. Part III (Chapters 4, 5, and 6) is a cautious, empirical-theoretical attempt to collect these Chapter 3 implications into distinctive atmospheric regions, then sequences of regions, then algorithms for modeling sequences of regions in terms of subatmospheric energy and mass fluxes. Initially, I had hoped to insert a Part II after Chapter 3, detailing the thermodynamic background necessary for choosing, empirically-theoretically, the thermodynamic character of star and atmosphere on the basis of the observations. The volume became too long; Part II is pushed to a separate volume. It is still called Part II, because one really should have a working familiarity with its contents to properly appreciate what the observational material of Chapter 3 imposes on the synthesis attempted in Part III. So, I abstract and insert portions of Part II (now Vol. 2) when it seems useful, in these Parts I and III.

Because the book follows an empirical-theoretical approach, I first abstract a speculative-theoretical approach which views the star as an (open, nonthermal) concentration in a nonEquilibrium medium, to which it returns nonthermal fluxes of energy and matter as it evolves. This puts the difficulty of such speculative-theory into focus.

A. SOME COMMENTS ON A PRIORI SPECULATIVE-THEORETICAL MODELING OF ATMOSPHERE, STAR, AND ENVIRONMENT

Throughout the book, I stress the interrelation between atmosphere and environment when one tries to diagnose the observations to obtain, empirically, real-world atmospheric characteristics. I also stress the interrelation between atmosphere and subatmosphere, or star-proper, when one tries to ask the origin, or “cause,” of the several observed fluxes of matter and energy, which both determine the atmospheric structure and provide a basis for its observational

diagnostics. So, if one prefers to replace an observational-empirical approach by a wholly a priori, speculative-theoretical study of stars, their atmospheres, and their environments, he really has three alternative starting points: a preoccupation with the star as the concentration of matter and energy which actually produces the fluxes; or a preoccupation with the atmosphere as the immediate origin of the observed fluxes; or a preoccupation with the environment as the region which originally produced the star and, reciprocally, is now modified by the star. Since star, atmosphere, and environment are intimately interrelated, any complete theory must ultimately embrace all three, but one can start a theoretical approach with any of the three, depending upon where his intuition feels most secure, so long as ultimately the cycle of the three is closed self-consistently. The first self-consistency requirement is that of the theory with itself; the second self-consistency must be between the "physics" of these theoretical models, and the observations of the real-world star, atmosphere, environment. Here, and in Chapter 2, I simply make a few remarks on the first self-consistency requirement; the rest of the book focuses on the second, as did the preceding introduction to this chapter.

Any theoretical modeling, which is not simply a mathematical-philosophical exercise, must be attached to some observed phenomenon. So, observationally, we distinguish a star as a region in the sky from which the various observed fluxes exceed those from surrounding regions. The observed properties of the flux excess imply that the main body of the star is opaque against those contributions to the transport quantities—whose flux we measure—which originate behind the star relative to the observer. And we simply define the stellar atmosphere as that part of the star which is the place of immediate origin—in the sense we have already used it—of those observed fluxes which identify the star. A priori, of course, we have no idea of the extent of the atmosphere; it depends on the opacity of stellar material to these fluxes. If we include the neutrino, the atmosphere apparently extends throughout the star; so, at least here, we exclude the neutrino from our discussion. This does *not* mean we consider it unimportant, simply, that it is unimportant in determining the properties of the atmosphere defined in terms of fluxes other than neutrinos. Since our definitions are based on fluxes, and fluxes depend on concentrations of matter and energy, we simply define the star as a concentration of matter and energy and ask what should be the properties of such concentrations. Here, the essential aspect is that there be non-zero fluxes of matter and energy *from* the concentration *to* the environment.

This simple fact of non-zero fluxes characterizes, in thermodynamic language, the star as a *nonisolated* concentration of matter and energy, by contrast to the idealized *isolated* concentration, the Equilibrium concentration (Vol. 2), having zero flux exchange with its environment. Again thermodynamically, there are two broad classes of concentrations of matter and energy, depending simply upon the kinds of fluxes they produce: a *closed* system has *only* fluxes of energy, not of matter; an *open* system has fluxes of both. If one restricts the kinds of models he studies to *closed* systems, his model must incorporate a boundary-condition which inhibits mass fluxes. Clearly, one has a choice between a rigorous inhibition or one which permits mass fluxes only of such small size that they have neither structural nor observational consequences on the theoretical models considered. Which, if either, of these prohibitions to introduce, a priori, is the choice of the theoretician—the only "check" is self-consistency of model, and ultimately of consistency with observations. In a priori, speculative-theoretical modeling one must be very explicit on *what is assumed*.

In the same way, any nonEquilibrium object must, in all generality, be allowed to evolve, to change with time systematically as well as only by fluctuations. If the theoretician wishes, he can restrict such evolution to a type which does not involve accretion or excretion to the environment in either the *isolated* system or *closed* system sense. In the same sense, one must characterize the environment: either it is restricted to being a time-independent system or it is permitted not to be. Since current opinion is that stars are produced by condensation of the interstellar medium (ISM) (no matter how), and since one discusses such concentrations in terms of instabilities in the ISM, one must characterize the environment as inherently unstable and inherently nonEquilibrium. Furthermore, current opinion considers stars to evolve more or less unidirectionally, so the ISM must be both unstable and in such a state that concentrations, at least of a certain amplitude, spontaneously evolve unidirectionally.

Thus, in any a priori, speculative-theoretical approach, one must put well into focus this three-point theme: (1) observational-operational definition of a stellar atmosphere; (2) structural characterization of a star and of what kind of thermodynamic system it is permitted—or restricted—to be; (3) the stability characteristics of the state of

the ISM and of fluctuations about that state producing a systematic evolution of concentrations arising in it. Any of these considerations can provide a starting point of theoretical modeling. We consider them, very briefly.

Aspect 1: If we adopt the above observational-operational definition of the stellar atmosphere as the place of immediate origin of fluxes from the star, and if structurally we describe the star in terms of: (i) its *global type of concentration* of matter and energy (either *isolated*—no fluxes, or *closed*—only energy fluxes, or *open*—energy and matter fluxes); (ii) *local kinds of storage modes* (*thermal*, or *nonthermal* of various kinds; cf Vol. 2); (iii) *local degree of nonEquilibrium* (linear, or various kinds of nonlinear; cf Vol. 2); then we can understand the role of the atmosphere in the structure of the star. It is the *transition-zone* between stellar and interstellar *states* of matter and energy, with this spatial evolution of states being conditioned by the spatial evolution of kinds of storage modes and degrees of nonEquilibrium, as well as by the change in values of those parameters required to specify a given storage mode and degree of nonEquilibrium for particular type of concentration in particular environment.

This understanding places in focus the first broad question to be clarified: What is the *pattern of this spatial evolution* in the kinds of storage modes and degrees of nonEquilibrium as we pass from the unobservable central regions of the star, through the directly observed regions that are the atmosphere to the faintly observable regions of the ISM?

In any theoretical investigation from this Aspect 1—the atmosphere as a starting point—we focus on the atmospheric storage modes. Then we are particularly interested in any sequential pattern of distinct regions within the atmosphere, which reflect such evolution-transition in storage modes. In addition to whatever *theoretical* guide this concept of a transition-zone carries, we have as an *observational* guide the first broad *empirical* characterization of star and atmosphere: the “inferred” geometry and physical structure of the atmosphere differ according to the particular flux studied (Chapter 3 and Part III). The problem, of course, is the significance to be attached to “inferred”; it is the *diagnostic problem*. In abstract, the diagnostic problem is that the diagnostic method applied to analyze a particular configuration must be consistent with that configuration; unfortunately, it is not always the case. One often assumes the diagnostic method to be independent of configuration, which leads to erroneous “empirical” results, which can lead to erroneous confirmation or rejection of theoretical models.

Historically, until the introduction of the nonLTE approach to diagnostics and to atmospheric structure, the thermodynamic representations of the states of interior and atmosphere were presumed to be the same, and to be quasi-Equilibrium. By contrast, the state of the ISM was admitted as nonEquilibrium. The stellar atmosphere was modeled as a single region: the static, thermal photosphere. The earliest model of a “blackbody surface” producing the continuum, surmounted by a “reversing-layer,” producing the absorption lines, was quickly replaced by an ensemble of various opacity subregions. These opacity subregions are the pattern of classical, speculative-theoretical, standard atmospheric structure: the distribution of T_e and density were modeled under the “speculation” that radiative and hydrostatic equilibria existed. Those many structures, now identified as atmospheric, alluded to in the above, were considered as part of the ISM, or vaguely described as “extended atmospheres,” whose states were treated “differently”—i.e., by ad hoc approaches which in no way demanded physical consistency. It is hardly surprising that the first perturbation of the quasi-Equilibrium interior and atmosphere was introduced in those regions considered as part of the phenomena of the ISM—the planetary-nebulae (PN)—or in the “outer-atmospheric regions.” The essential point to emphasize, is that the thermodynamic necessity for some kind of transition-zone between the *restricted* quasi-Equilibrium interior and atmosphere and the *nonrestricted* nonEquilibrium ISM was not recognized—still today is often ignored in practice—in these speculative-theoretical models. The reason, of course, is clear. Equilibrium thermodynamics, and its small-amplitude perturbations, has for several hundred years been a well-established discipline, indeed, since Caratheodory, held up as the model of axiomatic theory. Hence, it is straightforward to apply, theoretically. If, by contrast, one does not impose the structures of Equilibrium thermodynamics, he is uncertain with what to replace them; wholly from speculation, the range of possibilities is too great to explore, sans observational guidance.

However, given the necessity for the existence of a transition-zone between stellar and interstellar thermodynamic states of matter and energy—because of the *speculative imposition* of quasi-Equilibrium for the star, and nonEquilibrium for the ISM—the problems of defining the thermodynamic states of the transition-zone are clear. Primarily, we ask in what lies the transition? And does any sequence of exophotospheric regions simply reflect this transition, or something different? That is, should we expect to be able to predict the existence and characteristics of a

sequence of atmospheric regions simply by replacing the “quasi-adiabatic wall” necessary to retain the quasi-isolation of a quasi-Equilibrium ensemble by “no-wall,” and asking what results? Instead of *imposing* quasi-Equilibrium, or linear (local) thermodynamic-equilibrium we simply *admit* nonLTE. In short, we explore what is the possible range of nonEquilibrium configurations in this transition-zone which is the stellar atmosphere. NonLTE implies *range* of possibilities, *not* a specific configuration; it permits *any* nonEquilibrium configuration. Speculatively-theoretically, we must impose *which* nonLTE configuration. Empirically-theoretically, we let the data decide which is the configuration; we don’t impose, a priori, any theoretical model, or any theoretical diagnostics. Rather, we iterate—between diagnostics and thermodynamics; nonEquilibrium thermodynamics generally, not a particular brand of it. The basic theoretical problem in nonEquilibrium vs. Equilibrium thermodynamics is that the latter has *only one* configuration, while the former has many; our basic theoretical knowledge and intuition in completely nonrestricted nonEquilibrium thermodynamics is woefully inadequate. These kinds of astrophysical investigations will probably contribute as much to developing this basic insight into nonEquilibrium thermodynamics as they draw from it, in describing stars.

So finally, in a more limited view of the nonEquilibrium problems of stellar atmospheres, we return to ask in what lies the transition? Are the physical states of interior, atmosphere, and environment described by the same set of parameters which differ only in numerical value from place to place? Or does the much greater concentration of material and energy in the interior than in the environment and atmosphere introduce significant difference in description? And does such a possible difference in description result *only* from the increased concentration of mass and energy; for example, introducing a change in the set of internal energy states, from many-body effects? Or does the change in description possibly relate to the occurrence of some kind of “induced” boundary for the concentration, through effects of, e.g., closed magnetic fields, or gravitational anisotropy, on transport quantities? And then, is the change in description abrupt, beginning at the outermost observable part of the star, or possibly at the innermost observable part of the star—at the top or the bottom of the atmosphere—or is the change in description a gradual thing, possibly unfolding across the whole range from bottom to top of the observable range of material across the whole atmosphere? Is, indeed, this “unfolding” the structural discriminant for the several regions comprising the transition-zone, which is the atmosphere? Thus, we must recognize that the transition is a composite. It includes transition in *values* of any particular parameter—e.g., the electron kinetic-temperature, T_e , *if* it exists—and a transition in *description*—e.g., from a situation where the population of some energy level of the atoms at some particular place and time is fixed by collisions (so that the local value of T_e is important), to a situation where it is fixed only by the radiation field (so that T_e has only minor, if any, importance), to a situation where it is simply fixed by diffusion or more general motions. It also includes transition in description of macroscopic parameters: e.g., from a situation where macroscopic kinetic energy may (mostly) be stored quasi-adiabatically (small “leakage”) in a standing pulsation wave, to a situation where it propagates quasi-adiabatically (small mechanical dissipation) in a nearly-acoustic progressive wave, to a situation where it propagates as a shock-wave with large mechanical dissipation. From this last example, we recognize that the overall aspect of the transition is that from a *mainly-storage* configuration at the base of the atmosphere to a gradual unfolding of more and more nonstorage aspects higher in the atmosphere.

Clearly, if some speculative-theoretical approach to modeling *the* atmosphere forbids any of the just-mentioned interactions or evolution in storage modes it risks eliminating some atmospheric region. For example, beginning at the photosphere, if one ignores the difference between collision-dominated and photoionization-dominated source-function, he risks error in discussing line-blanketing, hence, in the photospheric boundary-temperature (Chapter 2). If he forbids a nonradiative energy-flux, he loses a chromosphere-corona. If he forbids a mass-flux, he loses the exocoronal regions. If he imposes that thermal point and escape point coincide, he loses the distinction between upper and lower corona. If he forbids variability, he loses the extended H α emission regions in Be stars—possibly in others; and in some stars he imposes the existence of an asymptotic velocity equal to its value from radiative acceleration alone. One hardly needs the most modern computing machine—indeed, no machine at all—to foresee the consequences of most of the “speculative hypotheses” in wholly-theoretical atmospheric modeling.

So, let us be precise as to what would be an acceptable *wholly-theoretical* approach to modeling a stellar atmosphere, given that its role is that of a transition-zone between the interior (nonobservable) regions of the star, considered as a concentration of matter and energy, and the ISM, considered as a nonEquilibrium, unstable environment

whose concentration produced the star. Clearly, the first decision is whether to model the star itself as an *isolated*, or as a *closed*, or as an *open* thermodynamic system. This decision determines what kinds of fluxes must be admitted at the lower boundary of the atmosphere: no fluxes, only energy fluxes, energy and mass fluxes, respectively. Because we see the star, an *isolated* system is excluded, although this was the basis for Emden's original (1907) modeling of stars. A *closed* system, with the energy fluxes being restricted to radiative fluxes, underlies the standard, classical atmospheric model which we summarize in Chapter 2. For some of us, such stars as the novae, Wolf-Rayet (WR), and a few others have long shown that mass fluxes—now popularly called winds—must be admitted, so the star must be an *open* system. To most astronomers, these stars were peculiar and exceptional, so they could provide no guidance or basis for general modeling of stars. However, today, farUV observations confirm that all stars, when observed sufficiently accurately, show such mass fluxes (cf the abstracted discussions in Chapter 3, and the more detailed discussions in the various volumes in the monograph series); hence, all stars must be *open* systems, and the atmospheres must be modeled accordingly.

At the moment, the chief controversy between some theoreticians and those empirical-theoreticians who focus on data is whether *any* stars—and principally the Sun as the only cool, main-sequence “garden-variety of star” observed in detail—can be considered to be *thermal* open systems. That is, in essence, one asks whether the mass-flux must be considered to be something more than simple evaporation from the outer layers of a stellar corona—the thermal expansion of a passively heated corona, as Parker (1981) poses the question. And here, if one wants to do a priori, speculative, theoretical modeling—he must decide whether, *a priori and speculatively, he restricts himself* to such thermal expansion of a passively heated corona. Such restriction is of course permissible, in such speculative-theoretical modeling; one constructs/computes such a model, then asks if it agrees with reality. We consider this last point in Chapter 3.

Such a priori theoretical restrictions are even stronger, in those varieties of open-system modeling which, while they do not restrict the winds to being thermal evaporation, do restrict the star, and atmosphere, to not having any nonradiative energy-fluxes which do not transport mass, *and* they prohibit the mass-fluxes themselves from dissipating mechanical energy. Thus, a priori, they prohibit the existence of chromospheres-coronae. One would think the spatial data of the last decade—even if the theoreticians do not take seriously the prespatial observations of “peculiar” stars—would make uninteresting such models; but speculative-theoreticians continue to compute them, and insist that they accord with certain kinds of data. We consider these data in Chapter 3.

Here, I would only note that either of the preceding variety of speculative-theoretical atmospheric models cannot really be called atmospheric models which are capable of representing a transition-zone between a nonEquilibrium, unstable ISM and a concentration of matter and energy in it whose only thermodynamic specification is that it is an open system. Generally, one must leave open the possibility that such an open thermodynamic system can have nonthermal as well as thermal storage models. Observationally, stellar mass-fluxes seem too large to be thermally produced (cf Chapter 3). So, in constructing, a priori, theoretical atmospheric models, even if one does not understand what kind of subatmospheric configuration could produce such observed mass-fluxes, one cannot, in formulating the boundary conditions for the theory, exclude such nonthermal conditions in the subatmosphere. If one wants to make a wholly-theoretical model, he must use boundary conditions at the base of the atmosphere which permit thermal and nonthermal storage modes in the subatmosphere—with such nonthermal modes being wholly unspecified. One simply gives lower boundary values to all the thermodynamic parameters—nonEquilibrium parameters, as well as the classic quasi-Equilibrium ones, then asks the atmospheric model. Clearly, the possible range is very large; for this reason, I myself think wholly-theoretical atmospheric models are, at our stage of knowledge, uninteresting; better to try to develop these lower boundary conditions empirically, then proceed to construct empirical-theoretical atmospheric models. The alternative is to try to construct wholly-theoretical models of the star itself; then, the boundary conditions at the base of the atmosphere are automatically defined by the fluxes produced by the stellar model.

Aspect 2: If we adopt the preceding structural characterization of a star as a quasi-Equilibrium concentration of matter and energy in the ISM, and if in terms of stability we describe the ISM by (i) the degree of nonEquilibrium characterizing it, and (ii) the direction of fluxes between it and stellar concentrations, then we can understand the role of the star in any local structure and evolution of the medium. It is an accreting, ejecting, or no mass flux, local

concentration which progresses unidirectionally toward a more-Equilibrium configuration. In the process, it may produce fluxes of matter and energy to and from the environment. The capacity for such flux production is the reason the ISM is unstable against forming such concentrations which evolve unidirectionally toward greater Equilibrium.

This understanding places in focus the second broad question to be clarified, following the first one on what are the storage modes for matter and energy. What is the *temporal evolution* in these storage modes and in the kind and degree of nonEquilibrium for (a) the several structural regions of a given star, and for (b) a given structural region across the variety of stellar types? Here, of course, we refer to stellar *internal* structural regions. Any theoretical atmospheric structural regions and their evolution, must be compatible with this theoretical internal structure. (We define a stellar type in terms of the properties of the quality and quantity of matter and energy which formed the original condensation.) In terms of how to approach this problem of storage modes, we are particularly interested to know whether, at each phase in the life of a given star, at least some of the structural regions of the star can be considered to be in a steady state, even though nonEquilibrium, and just what this implies. In addition to whatever theoretical guidance results from this notion of a local concentration, which is more equilibrium than its environment, we have as an empirical guide the variety of stellar configurations which actually exist. The problem, in such empirical guidance, of course, is to distinguish between the configurations at successive phases of the life of a given star and the configurations corresponding to the same phase in the life of different types of stars. Again, it is a diagnostic problem, but indirect rather than direct. In practice, we would need to infer from the sequence of atmospheric regions just what are the possible storage modes, and associated fluxes which can produce such a sequence. Resting on a wholly-theoretical approach, one would need to investigate all possible nonthermal storage modes.

It is not at all obvious that all such nonthermal modes can be found simply by a stability analysis of thermal storage modes. As an example, one notes that the existence, source, and amplitudes of the nonradiative energy-fluxes responsible for stellar chromosphere were never predicted before their necessary existence was shown observationally. Indeed, many astronomers argued, long after the characteristics of the solar chromosphere had been observationally shown, that chromospheres could not exist in stars lying in certain regions of the HR diagram—those hotter than about F2—because the *speculated* cause of the solar nonradiative fluxes could not arise in the stars in these regions. The discussion in Jordan (1981) shows well the present great uncertainty in the origin of the solar nonradiative energy-fluxes responsible for the production of the solar chromosphere. Observations (cf Chapter 3 and the series' volumes on the hot stars) show well the existence of chromospheres and coronae in these “theoretically excluded” stars: “theoretically excluded” on the basis of stability analysis of the thermal models of these stars.

Thus, while a wholly-theoretical approach to stellar structure is certainly possible, it is difficult. For this reason, only thermal—i.e., static—storage modes have been treated, in general, in the literature. Pulsating stars, such as cepheids, have been treated (for the most recent summary, cf Cox, 1980). However, the full range of nonradiative fluxes and mass-fluxes, chromospheres-coronae, etc. have not yet been included in such treatments. I do not consider, in this volume, any of the thermal models or pulsating models. I only summarize the considerations in Part III which suggest such theoretical models are inadequate to represent the subatmospheric regions of the kind of stellar atmospheres that modern observations and nonEquilibrium thermodynamics require.

Such a situation certainly renders difficult any approach to the third broad question which must be answered. What are the kinds and the sizes of the fluxes produced by the possible variety of storage modes—thermal and non-thermal—in the variety of stars? Clearly, any adequate theoretical models must produce radiative energy, nonradiative energy, and mass fluxes. But they should also delineate what other fluxes are possible, e.g., magnetic. They should delineate those cases in which all these fluxes are independent and those cases in which their values are so linked that one can predict the value of some particular flux from the values of certain others. Clearly, the corollary question is how these fluxes condition the production of a pattern of atmospheric structure which is physically self-consistent with the theoretical model of the interior. Thus, this Aspect 2 closes on Aspect 1.

Aspect 3: If we adopt the above stability characterization of the stellar environment as a completely non-Equilibrium medium that is unstable against the formation of concentrations, and if we describe the Universe (i) structurally, in terms of concentrations and interconcentration media, and (ii) temporally, in terms of local behavior with respect to the formation of concentrations and large-scale behavior with respect to yet-to-be-specified criteria,

then we can understand the role of concentration and interconcentration medium in the *local* behavior of the Universe. The interconcentration medium is the source of the matter and energy whose local and transient concentration forms the objects whose structure and temporal change reflect the *local* structure and change in the state of the Universe. Here, we study that type of concentration that forms single stars, i.e., that type which, after some initial phase, follows a sequence of phases without accretion, which returns a continuous flux of matter and energy to the environment, up to some final phase.

This understanding places in focus the fourth broad question to be clarified: What is the detailed *local* sequence of temporal states for the Universe? That is, what is the sequence of temporal phases for the development of a particular concentration—overall and with respect to each of its structural regions? And, is there an end point to this sequence of phases such that the concentration becomes essentially an isolated, Equilibrium object, after returning a certain amount of matter and energy to the interconcentration medium? Or is there some ultimate cyclic, although unidirectional behavior of a particular concentration such that its last phase is dispersal, no longer a concentration? (How would such a phase be reached, energetically?) And of course, we are especially interested in how such temporal behavior is reflected in atmospheric structure for two interrelated reasons: *Diagnostically*, we ask whether this directly observed part of the star may, through its general or particular structure, give information on the sequence, and phase, of temporal states. *Theoretically*, we emphasize the extent to which all these considerations depend upon nonEquilibrium considerations, upon the evolution to a quasi-Equilibrium concentration in a nonEquilibrium medium, instead of the reverse. Again, in approaching this problem of temporal change in a particular concentration, we have both the observational guide of the variety of stellar types, and the theoretical guide centered on the two aspects of the atmosphere as a transition-zone *and* the star as a quasi-Equilibrium concentration in completely nonEquilibrium environment. I stress the empirical guidance of *all* varieties of stars to delineate what is the possible range of temporal states, thermal and nonthermal, for a specified concentration in a specified environment, before asking the evolution of temporal states of only one kind—thermal.

The Fontenelle frontispiece for the monograph series is indeed very appropriate for stellar atmospheres. One paraphrases it as: be certain of the existence, properties, and location of some atmospheric region before you try to explain and model it. A proper, physically self-consistent, diagnostics of the various fluxes from the atmosphere—and environments—is basic to any structural, compositional, or evolutionary interpretations. The same must be emphasized for any application of concepts from other disciplines to interpret and model stellar atmospheric and environmental phenomena. I would stress that such outlook is not inspired just by the modern X-ray, farUV, farIR, and radio data; but observations in the visual spectrum, even crude and at low resolution, have long demanded it. It is useful to place the demand in perspective: empirical-thermodynamic, not just speculative-theoretical.

B. GENERAL HISTORICAL PERSPECTIVE ON STELLAR ATMOSPHERIC MODELS

In the decade of the 1860's, long before the standard-star idea and speculative theory of atmospheric structure were conceived, Secchi, Wolf, and Rayet described some of the observational bases for inferring the real-world existence of three types of stellar "peculiarity." Although, not knowing standard atmospheric theory, these authors did not realize the "degree of peculiarity." (i) At solar eclipse, Secchi observed an outer atmosphere extending several radii; the outer-photospheric density distribution of a solar-type standard star is roughly exponential, with a scale-height of some 0.0002 radii. (ii) He also discovered Be stars, characterized by emission lines replacing some of the strong hydrogen absorption lines observed in most stars and required for the "standard" star. Ad hoc, empirical interpretations of the presence of the emission lines demanded, again, outer atmospheres extending to many radii. (iii) Still in the same decade, Wolf and Rayet identified the emission-line stars bearing their name, most of the lines being very, very broad and some having displaced absorption components, implying highly superthermic velocities. Early in this century, the lines were identified as coming from very highly ionized species, requiring temperatures much larger than their total luminosities would suggest, under standard modeling.

In the 1930's and early 1940's, long after the ideas of radiative equilibrium (RE) and hydrodynamic equilibrium (HE) and the standard model were well introduced, Struve and Beals separately and complementarily remarked

the apparent existence of a sequence of emission-line stars, exhibiting a range of peculiarities—relative to standard star characteristics—of widely differing amplitudes: between stars, between epochs of the same star. Most of these are hot stars, but Struve proposed to model these peculiarities via the characteristics of two, broad, outer-atmospheric regions patterned after those observed for the cool-star Sun. Just above the photosphere—the only atmospheric region compatible with the standard star—lay the chromosphere, cool and quasi-static, but very extended relative to thermal support. “Turbulence” was the obvious interpretation for the support mechanism. Above the chromosphere lay the corona, dynamic in character and support, but still too cool to be the boundary region of the standard photosphere. The Be stars were central in this empirical modeling scheme; they are a crossroad of the observational characteristics defining the emission-line sequence. Fe II, in their Be-shell cousins, demanded cool outer atmospheres. McLaughlin added depth to Struve’s pattern by remarking the similarity of Be stars to “little PN.” The quasi-static, radiative-equilibrium density distribution of the standard atmosphere, with scale-heights 0.0001–0.001 radii, must be expanded to produce subionized regions extending, in some cases, to 10^6 photospheric radii. The several sequences were bounded on one end by the WR stars, the extreme of the emission-line sequence, having a “dynamic” atmosphere, and by P Cyg, with its prototype expanding-atmosphere profile. The sequences were bounded on the other end by the A sg, α Cyg, with its sharp, deep, absorption lines of Fe II linking to the Be-shell spectrum. Recalling that P Cyg, the star after which those prototype expanding atmosphere profiles were named, was once a nova, the novae were brought into the sequence. Noting that the archtypical symbiotic star, Z And, was equally once a nova, the symbiotic stars also entered. Noting the sequential similarity between dwarf and recurrent novae and the Bp stars we return again to the crossroads of “peculiar real-world stars,” defined by their peculiarities relative to the statistical, standard model of a speculation.

Separately, with regrettably little contact with the preceding, but contemporary in this 1930–40 epoch, the Harvard group around the Gaposchkins and Menzel-Aller-Baker-Goldberg stressed stellar variability; the nonLTE similarities between the PN and the outer solar atmosphere, with all thinking focused on the “cool” outer atmospheres in the 10^4 K range, that of the Be-shell, again a crossroads; and symbiotic phenomena. The efforts were refocused with Edlen’s identification of the solar coronal lines as demanding a 10^6 K corona; the symbiotic combination of cool photosphere and hot outer atmosphere flourished. Observations of coronal lines in novae and symbiotic stars, since the early 1930’s, again demonstrated the similarities among exophotospheric regions—prohibited by the standard model—across the HR diagram. Edlen’s identification of the coronal lines as superionized species, relative to photospheric T_e , simply showed that the “anomaly” of such exophotospheric regions included super- as well as sub-ionized regions.

With this identification of the solar corona as “hot,” and the same identification of “hot” solar chromosphere, starting with Redman’s 1942 eclipse demonstration that chromospheric line widths varied with atomic mass, Struve’s outer-atmospheric structural pattern was also required to embrace both hot and cold regions. This “symbiotic” problem led to it, the Struve-Beals sequences, and McLaughlin’s “the Be stars resemble little PN,” falling into limbo, then vanishing, for most astronomers, and certainly for the speculative-theoreticians. Most “reliable” speculative-theoreticians realized that while a thermal convective instability might, for the Sun, produce a mechanical heating of the outer atmosphere for solar-like stars, such was forbidden for the hot stars, even the peculiar hot stars upon which Struve, Beals, and McLaughlin had focused in their “observational empirical modeling.” And finally, if one includes the Sun as being “peculiar” in that it is too close to ignore small-amplitude and low-luminosity anomalies, all the above remarks on discrepancies with standard models refer to peculiar stars, not “normal stars.” One defines “normal stars” as those from which standard taxonomy, which gave birth to standard modeling, sprang. A typical attitude among speculative-theoreticians toward the close of this era was that we are not interested in special objects—like WR stars—we are interested in normal, hot, main-sequence stars in these questions of the universal existence of hot chromospheres. Unfortunately, too many astronomers overlooked Struve’s summary remark:

Some of the peculiar phenomena generally ascribed to a few freaks in the stellar population are probably characteristic, in a small degree, of the majority of stars in certain stages of their evolution—upon the answers to these questions will depend the degree of confidence which we are prepared to bestow upon discussions of “normal” reversing layers, built up according to the standard procedure.

So, for well over a century it has been clear from observations in just the visual spectrum that broad classes of phenomena exist in stellar atmospheres which are totally alien to the concepts of standard modeling or standard taxonomy. Each decade, new observations and new empirical models appear to support this conclusion. It was clear that they are associated with a dynamic, not static, state of stellar atmospheres; that the atmosphere consists of various kinds of regions, with various kinds or degrees of nonthermal effects and that they are both hotter and colder than wholly RE would permit. It was also clear that even the most static regions of stellar atmospheres, at low particle concentrations and large thermodynamic gradients, could no longer be described by the *local* Thermodynamic Equilibrium—or linear nonEquilibrium thermodynamic—methods developed for the high-density, radiatively quasi-isotropic regions of subatmosphere and interior. From these atmospheric observations, it was equally apparent that even static, nonlinear nonEquilibrium thermodynamic methods would be inadequate. In short, it was clear that neither the empirical-modeling implications, nor structural consequences for atmosphere and subatmosphere, of a century of observations of peculiar stars—like the Sun, WR, Be, and symbiotic—had been, or were being, properly exploited. They had been set aside by the speculative-theoreticians in favor of the easy-to-compute—with large modern machines—variety of standard models. It was equally clear that the mathematically tractable aspects of thermal, linearized, nonEquilibrium thermodynamics held the focus over the nonthermal, nonlinear variety—for progress in the latter of which we badly need empirical/observational guidance.

It was also clear that the attempts by astronomers to introduce various aerodynamic concepts into ad hoc modeling of various nonstatic, even dynamic, effects required by the observations—but without changing the fundamental idea of thermal, radiative control—were more “folkloric” than physically sound. The classic, outstanding example is the variety of attempts to introduce various kinds of “turbulence”—or quasi-random motions, having a range of geometrical scales—which involved superthermic velocities, but which were forbidden to dissipate energy, thus forbidden to couple to thermal degrees of freedom. At most, one permitted a reversible quasi-adiabatic coupling between macroscopic velocity and compression; but an irreversible energy dissipation was prohibited. No strong deviations from RE were permitted. All the phenomena of these “extended atmospheres” were required to be radiatively controlled, no matter the size of the velocities introduced, ad hoc.

At that epoch of the late 1940’s and early 1950’s, one was strongly reminded of the situation during the preceding 2 decades in modern aerodynamics proper, which had been preceded by 200 years of divergence between “theoretical,” and engineering or “empirical,” fluid mechanics. The long-term evolution had centered on d’Alembert’s paradox: for a “perfect,” inviscid fluid, a moving symmetrical body should experience no deceleration. The resolution of the conflict with the observed “air-resistance” to the motion of all kinds of bodies came with Prandtl’s observational/experimental recognition of the importance of the neglected, very small, viscous terms in those regions immediately near the moving body—the boundary layer. There, the large velocity gradients needed, microscopically, to bring the fluid to rest at the body surface gave the viscous terms a major importance. The thermal-viscous dissipation of the macroscopic velocity, as the flow followed around the body contour, induced a separation of the flow from the surface toward the rear; there developed a “turbulent” wake and an underpressure at the base. The body decelerates; the lost energy goes into turbulence, ultimately into thermal energy, irreversibly. For years, the aerodynamic focus was on such viscosity-induced phenomena; the Reynolds’ number—the ratio of inertial to viscous forces—was the descriptive parameter. A “folklore” grew up on “the” value of the “critical” Reynolds’ number at which “turbulence” appeared. In astronomical “adaptations” of these phenomena, the laboratory/aerodynamic studies of the effect of curvature, compressibility, etc., on the value of this critical Reynolds’ number were ignored: theoretical, not laboratory, results are easily borrowed.

In the aerodynamics laboratories of the 1920’s, 1930’s, and 1940’s, the focus on viscosity and turbulence gave way to one on the compressibility effects associated with higher velocity flow: first, just large enough that the incompressible approximation failed; then the transonic flow associated with the creation of supersonic wind tunnels; then the supersonic flow itself; at our epoch, the hypersonic flow associated with meteor and satellite re-entry problems. The mission of the aerodynamics/ballistics/astroballistics laboratories of these earlier, and the present, epochs has been to exhibit, experimentally, just what are the basic phenomena occurring at such supersonic, hypersonic, and astroballistic velocities; then, to model them, at least empirically-theoretically; hopefully, eventually,

axiomatically-theoretically. At the epoch of the 1930's and 1940's, a popular guiding phrase to give focus to such efforts, glued on many of the laboratory doors, was: "Behold the bumblebee; according to the best aerodynamic theory, it cannot fly; but the bumblebee, not knowing any aerodynamic theory, proceeds to fly." In astronomy, one might paraphrase this as: "behold the peculiar stars; according to the best standard-atmospheric theory, they cannot have extended, hot and cold, quasi-HE and moving, atmospheres; but the peculiar stars, not knowing standard atmospheric theory, continue to produce extended, hot and cold, quasi-HE and moving, atmospheric regions." And, like the bumblebee, peculiar stars come in an impressive variety of forms—but also like the bumblebee, they are basically similar in the essential contradictions to standard theory. And finally, there are the more conventional "honey-bees"—who also fly, "normal stars," who also have chromospheres-coronae, and winds.

Figures 4-1 to 4-6 reproduce a series of shadow photographs, exposure time of a few microseconds, of the gas-flow around a sphere; the sphere was launched at a series of velocities from Mach number about 0.3 to about 4; taken by Alex Charters and myself (1945). Viscosity-induced separation of the flow from the body occurs very early, at the lowest, essentially incompressible, velocities; the turbulent wake is pronounced and the air resistance is controlled by this phenomenon. As the initial speed increases, one observes the evolution of two phenomena: the separation point moves farther to the rear; and a system of acoustic waves, then shock-waves, gradually develops, then predominates in the flow pattern. Using the distance from the "nose" of the sphere to the separation point as the distance scale, one finds that at these highly supersonic flows, the critical Reynolds' number is about 10^6 instead of the folkloric value of some 10^3 . Fig. 4-7 shows the behavior of the "drag" coefficient, $K_D = \text{resistance} / d^2 V^2 \rho$, with increasing velocity, or Mach-number. d is the sphere-diameter, V , the velocity, and ρ the atmospheric density. The abrupt rise near $M \sim 1$ corresponds to the onset of "wave-drag," corresponding to dissipation of energy into the system of acoustic, then shock, waves. One notes the appearance of the acoustic waves already at a free-stream Mach number of 0.7–0.8. If one recognizes that the sphere represents a "constriction" of the flow—first converging, then diverging—one sees that one also obtains some insight into nozzle flow from studying these photographs. One can construct a "flying wind-tunnel" by hollowing out the axis of a projectile. Vol. 2 shows photographs of several such. In Vol. 2 of the monograph, where we discuss real-world, empirical-theoretical astrophysical aerodynamics, we return to such laboratory observations/experiments. Chapter 4 continues this discussion.

I stressed, above, that already, for over a century, the peculiar stars had demonstrated, observationally, the inadequacy of standard modeling, even before it was invented, progressively as better observations of real stars, and more detailed computations of "standard" stars appeared. The advent of farUV, spatial observations in the late 1960's, 1970's, and 1980's destroyed the last illusions that standard models were other than only first approximations to just stellar photospheres, completely incapable of representing the exophotospheric regions that these farUV—and modern farIR, radio, and X-ray—observations show to exist for all stars, not just "peculiar" ones.

Normal and peculiar stars, observed in the farUV and the X-ray, are far more similar than they are different, relative to the really basic departures of both, in the same sense, from the predictions of the standard model. The phenomena of chromospheres-coronae, and of stellar winds, differ in degree and in time-dependence, not in their existence, between peculiar and normal stars. For example, a WR-type *atmosphere*—I carefully do not say WR-type *star*—differs from a solar-type, or other dwarf main sequence-type, or other type of giant and supergiant atmosphere, mainly in the large size of its mass-flux, which, observationally, translates into a strong opacity of chromospheric-coronal regions. So even in the visual, the WR atmospheres are directly observed as showing very strong "exophotospheric chromosphere-corona." This contrasts to various degrees of exophotospheric opacity, in lines and continuum, only partially "veiling" the visual spectrum, in "more normal" stars, by their chromospheres-coronae. But after all, at eclipses, and with the coronagraph, one does see coronal lines in the visual, for the peculiarly close, but otherwise normal, Sun. And, one of the first successes of modern-day eclipse studies was the demonstration of just how widespread is chromospheric influence on the visual disk spectrum (1952 HAO eclipse expedition; Thomas and Athay, 1961). But this last came by self-consistent, meticulous, nonLTE diagnostics of the eclipse spectrum. In the farUV, the farIR, and the radio spectra, chromospheric and coronal influence are so outstanding as to be obvious in much less sophisticated diagnostics.

In the farIR and radio, again both normal and peculiar stars differ greatly from predictions of the standard model; but peculiar stars differ from normal as much as normal stars differ from standard—indeed, much more. And again, the difference is associated with the mass-flux, but with its variability as much as with its size. For example, a Be-type atmosphere differs from a B-type atmosphere in the size of its exophotospheric extent, not in its existence. Today, we think the structural pattern of this differential size results from difference in variability of the mass-flux as well as simple difference in its size. The variability produces the several phases of the Be stars (Be, Be-shell, B-normal), and the differential extent of the post-coronal, subionized regions (cf Underhill and Doazan, 1982, and Chapter 3 and Part III). We think the relative sizes and time scales of this mass-flux variability contribute strongly to the similarities producing the “Be-similar” sequences—especially to McLaughlin’s Be, planetary-nebular linkage, also to the Bep, symbiotic linkage, and to the progression to dwarf and recurrent novae (cf the Cataclysmic-star volume; and Chapter 3 and Part III). This mass-flux, which extends the stellar atmosphere, also contributes to providing the matter comprising the local environment of the star—from the above, it may induce its variability. This area of study just begins to have a solid observational basis.

So, observationally/empirically, real-world stellar atmospheres differ profoundly from that envisioned by the assumptions, hence, physical characteristics, of the “standard stellar atmosphere.” Consequently, stellar atmospheric studies have developed an interesting three-way schizophrania. One personality represents the heirs of the “traditionalists,” who x years ago would be analyzing data or computing models based on the “classical” model (cf Chapter 2). They demand simply a definite model, the least complicated in terms of physics that is not obviously wrong, in terms of which numbers can be produced by either observational analysis or computing speculative-theoretical models. A second personality represents a combined group of skeptics and converted traditionalists, who demand investigation of everything from first principles, and the suspension of all diagnostics and models until the basic physics is inescapably proven correct. These two personalities have developed a *détente*—neither takes seriously what the other does as being impractical in the real world. The third personality represents a pragmatic realization that in any event, every observation will be analyzed in some way and that most kinds of possible models will be explored numerically—for curiosity or as busy work, no matter, and that the basic physics will never be understood except as the result of a successive, joint, iterative approximation to observations and theory. So it asks that analysis of data, and exploration of models, and development of physical understanding be done simultaneously, but with any results to be taken seriously only to some consciously explored limit, based on the degree to which a *mélange* of all three are self-consistent. It asks that overall, the aim be the establishment of just what is required in the way of the above-mentioned general structure, so that any specific model—observational or theoretical—which violates the general structure can be placed into focus: either as a counter-example to the general structure or as a pedagogic example.

Obviously, this book follows the third personality. Unqualifiedly, it rests on observations, on observational diagnostics, and on empirical-theoretical modeling; after the Chapter 2 summary of the standard model, it focuses not at all on any a priori, or speculative, theoretical models. Its basic approach to obtaining a physical picture of atmospheres, local environments, and subatmospheres is by contrasting-comparison: global properties of real-world stars contrasted to those of the standard model; observational characteristics of a representative variety of peculiar stars contrasted to those of normal stars; visual spectral characteristics contrasted to nonvisual spectral characteristics, especially those in the farUV but also those in the IR; the detail of small-amplitude features revealed by solar proximity contrasted to the variety of too-often unresolved but large amplitude stellar features exhibited by the wide range of stellar peculiarity; the physical characteristics of (closed, thermal) thermodynamic systems contrasted to the much greater variety of characteristics permitted in (open, nonthermal) systems. Given these contrasts of real-world stars and thermodynamic systems to visual-spectral-based (closed, thermal), standard models—even to low-amplitude nonthermal solar models—one tries to infer (open, nonthermal) stellar models with fluxes of arbitrary amplitude relative to those produced by classical, thermal, storage modes.

Consider this book a status assessment of a long-term program of delineating, empirically-theoretically: stellar atmospheric structural patterns, some properties of the local stellar environment, and some necessary characteristics

of subatmospheric structure—all inferred from the observations of nonthermal fluxes and phenomena, and thermodynamic self-consistency. This program was originally inspired by the pre-spatial contrast between the predictions of the standard thermal models, visual spectral observations of the Sun and certain kinds of stars, and the thermodynamically obvious inconsistencies of then-current observational diagnostic methodology. I give a quick abstract of what that program has tried to do, which puts into perspective the approach and contents of this monograph.

C. PERSPECTIVE ON THE EMPIRICAL-THEORETICAL PROGRAM OF WHICH THIS VOLUME IS A PART

From the quick historical perspective of Section B, we see that just at the disruptive epoch of WWII, observational-empirical modeling of real-world stellar atmospheres faced two major climactic developments: (1) Gradually accumulated evidence on the anomalously large extent of a wide variety of stellar atmospheres, and of anomalously large breadths of many spectral lines in a variety of stars, led observers to recognize the impossibility of confining stellar atmospheres within the thermal and geometrical limits placed by thermal HE at an RE-determined T_e . One illustrative response was Struve's (1942) modeling of hot-star exophotospheres by the cool-Sun example—static-extended chromosphere, dynamic-extended corona. A second illustration was the (1938 Paris Colloquium) combination of WR, P Cyg, and novae envelopes into a dynamic-extended “supercorona,” with a corollary emphasis on the “(planetary) nebular phase of novae spectra.” (2) A gradually enlarging variety of identification of “coronal” lines, and anomalous excitation/ionization, in a variety of stars, climaxed in Edlen's (1942) identification of the coronal lines as highly superionized species, requiring environments of some 10^6 K. The result was a requirement that any solar-coronal model have a $T_e \sim 10^6$ K, and produce the dynamic structure, ranging from jet-like spicules to almost hemispheric spectacular eruptions, observed with Lyot's coronagraph.

At the same epoch, the major problems impeding successful completion of speculative-theoretical standard thermal atmospheric models were also twofold: (1) How to make accurate line-blanketing calculations to obtain a more precise boundary, minimum, temperature for the photosphere; (2) How to better represent a convective transport of energy, which might well be turbulent, in those subatmospheric and atmospheric regions that were unstable against a wholly radiative energy transport. The above-mentioned observational problems were assigned to exceptional stars, or to exceptional atmospheric regions; and they were generally considered, among theoreticians, as of not much interest in the major atmospheric modeling preoccupation of abundance determination. A possible common intersection of observational and theoretical problems lay in the common phenomenon of “turbulence,” because of its effect on the diagnostics of the total absorption in lines, which measures abundance. Theoreticians and observers largely went their separate ways, as exemplified by Greenstein's comment on the structure of the Kuiper Stellar Atmospheres volume.

In the post-WWII epoch, astronomers returned with new techniques and new laboratory knowledge gained outside astronomy. Radar produced radio astronomy. Nuclear-fission programs produced support for laboratory-fusion studies. Rocket-missiles produced laboratory meteor ablation studies, and solar-stellar observations from space. A variety of supersonic and hypersonic studies produced laboratory knowledge quite beyond thermal convection, laminar or turbulent.

The present program began with an attempt to exploit the last two developments/experience cited. We attempted to devise a diagnostic technique which works equally well to measure the “temperature” of an ablating meteor surface, of the hydrostatic-but-extended solar chromosphere, and of the dynamic-extended and hot “corona” of WR stars. Then we ask how to model each domain of application, from the data obtained via such diagnostics. In all these cases, the problem is to distinguish between thermal—but hotter-than-expected—and nonthermal effects; their description; and their modeling application. A discussion of the meteor-ablation problem is irrelevant here, except to note that it provides a good example of the breakdown of those linear nonEquilibrium thermodynamic transport relations discussed in Vol. 2 and briefly here, in Chapter 2, in the radiation transfer formalism.

Then note that the common focus of the real-world atmospheric modeling of the observing astronomers lies on those contradictions, to speculative-theoretical standard thermal models, which are associated with superthermal motions, of whatever variety; their relation to the local kinetic-temperature; and also associated superionization and superexcitation. The visual-spectral data range from the 5000 km/s novae-ejections, the 3500 km/s WR phenomena, the 1000 km/s solar outbursts; to the solar-coronal lines of Fe X, etc. observed alike, in Sun, novae, symbiotic stars, O VI observed in WR and PN, $\lambda 10830$ observed widely,—and to emission lines generally. And also, these contradictions focused on atmospheric extent, and its equivalent of low atmospheric density gradient, in the upper and outer stellar atmospheres of, again, a wide variety of stars. So, as earlier noted in the chapter's beginning, the program has focused on studies of what were diagnosed, observationally from the visual spectrum, as *Superthermic Phenomena in Stellar Atmospheres* (Thomas, 1948, et seq). We have asked if they are really all superthermic; and, if so, what does their existence imply on stellar atmospheric structure, and on the properties of those mass and energy fluxes necessary to produce such structure. Ultimately, of course, one wants to understand the circumstances of origin of such fluxes since thermal models only produce radiative energy fluxes from such stars. But, as the Fontenelle frontispiece cautions, we had first be sure what we must explain.

So, we have tried to distinguish between hydrostatic chromosphere models produced jointly by a T_e higher than RE permits, and the effects of random motions—sometimes called “turbulence.” Studies of the problem in the solar atmosphere via eclipse data (Thomas and Athay, 1961) showed that in such stars, a thermal-hydrostatic—but at higher-than-RE T_e (r)—chromosphere, without superthermic turbulence, does indeed suffice. Unfortunately, these results, and their successors, have too often been interpreted solely in terms of a particular T_e -range defining a chromosphere; rather than as reflecting the joint properties of outward-decreasing density gradient associated with this outward-increasing T_e . Clearly, as the photospheric T_e becomes hotter, we must—to produce the kind of solar guidance of stellar atmospheres invoked by Struve and others—admit an increasing T_e -level in such a chromosphere. To accomplish the above objective, we needed to develop better diagnostic methods—necessarily nonLTE to apply to this strongly nonLTE configuration (Thomas, 1965; Jefferies, 1968). We also tried to investigate more dynamic chromospheres, embracing random superthermic macroscopic motions and their dissipation to produce the necessary T_e , by reopening the WR problem, after its post-1938 hiatus, from this standpoint of it being an atmospheric phenomenon, possibly common to a variety of stars, rather than uniquely referred to one (M,L,R) kind of star (Gebbie and Thomas, 1968). In parallel with these studies, we tried to bring together existing astronomical data on such aerodynamics of stellar atmospheres—a blend of superthermal motions and nonradiative energy production and transport—and astrophysical/aerodynamical collaboration toward putting the real problems into focus. Refer to the Proceedings of the 3rd (Burgers and Thomas, 1957), 4th-5th (Thomas, 1961, 1967), and 6th (Habing, 1970) Workshops-Symposia on Cosmical Gas Dynamics.

Out of these Workshops, it became clear that the common focus on mass loss—of the Nova, WR, and P Cyg Paris Colloquium of 1938, and of Struve's hot-star, solar-model, dynamic corona, and of Parker + Biermann's solar-wind studies, and of Deutsch's identification of low-velocity mass-loss from cool supergiants—was at least associated with all those other exophotospheric phenomena demanding a revision of standard atmospheric modeling. It was only not clear whether this mass-loss was caused by, was a causer of, or was simply associated with, these other phenomena of anomalous atmospheric extent, superthermic velocities, superexcitation and ionization, emission lines of high and low ionization, etc. It was only clear that one required a basic change in thermodynamic character of the star, in trying to model it; from a closed thermal system without mass-loss to an open nonthermal system with very significant mass-loss.

It was also clear that further empirical studies should expand the focus on those stars which have historically been called peculiar because of just the fact that they exhibit, more strongly, these phenomena characterizing the star as an open thermodynamic system. So, in continuing, as above, to exploit the Sun as a guide to stellar atmospheric structure, one should also shift, profoundly, to using *all* peculiar stars, of whatever kind, as a guide to both solar and normal star atmospheric structure. Most of those nonthermal phenomena which are observed in the peculiar stars because of their large amplitude, and in the Sun because of its proximity, are probably present in all stars, to some degree, at all evolutionary stages. Contrast my comparison of these two approaches to the solar-stellar

connection at the 1976 MAJORANA summer Workshop on the subject (Thomas, 1976, in Caccin and Rigutti, 1977), with the popular focus on the Sun alone as exhibiting and defining the universal characteristics of all chromospheres at the Goddard 1972 Colloquium on stellar chromospheres (Jordan and Avrett, 1973): "If an atmospheric region is not a solar-like chromosphere, it is not a chromosphere; a WR-phenomenon example is excluded, as being too peculiar." Such a narrow viewpoint is myopic.

So we have organized (1976-198?) a collaborative effort to bring together existing information on nonthermal phenomena in stellar atmospheres; contrasting peculiar to normal stars of a given MK type; emphasizing the changed empirical-theoretical outlook accompanying the addition of spatial observations of the outer atmospheres (the NASA-USA, CNRS-France monograph series; organizers-coordinators, Jordan and Thomas; advisers, Goldberg and Pecker). Each volume focuses upon a particular MK spectral type: normal, peculiar; standard model vs. empirical-theoretical modeling changes demanded. The present volume is the exception; it walks across the HR diagram, comparing, against the background of the nonLTE standard thermal model, the variety of peculiar stars, searching the variety of atmospheric patterns their peculiarities demand. We have also organized a series of yearly Workshops (CRS-Italy, NASA-USA sponsored), to compare results across the HR diagram, from the several volumes on particular types of stars, on specific kinds of common nonthermal phenomena (Trieste Observatory, Stalio; SacPeak-AURA, Zirker). The first (Trieste, 1982) focused on those velocity fields associated with the mass-flux (Stalio, 1983); the second will focus on the effect of variable mass-flux in producing a local environment in some stars (Trieste, 1983).

So, the present volume reports on its above-stated objective: what can we learn, from this focus on peculiar stars and the Sun, about the variety of atmospheric structural patterns existing in real-world stars. And, what can we infer from such patterns about the characteristics of those fluxes of energy and matter producing them. Obviously, any conclusions are tentative to the extent that they can be modified by new or improved observations. I would, however, stress that point with which I opened this Chapter 1: we ask, not tell, the stars what is their thermodynamic characterization, and what patterns of atmospheric structural regions does it produce. Our focus is not first on what some assumed set of equations produces; rather, it is on asking what equations are adequate to represent what we infer from observations, diagnosed self-consistently with the thermodynamic character of the star. We collaborate with the real-world stars, not sleep with their a priori speculative, computer-simulated, images (paraphrasing Emma Goldman, 1936).

2

SPECULATIVE-THEORETICAL MODELING OF THE ATMOSPHERE ENVELOPING A HYPOTHETICAL (CLOSED, THERMAL) STAR

—It may be as you say, that my stellar atmospheric models do not agree with real stars. But, aesthetically, they please me so much, that I will continue computing them, in the hope that one day, some observing astronomer will find a real star that agrees with them—

—refrain of a Platonic computer, 1970—

I. INTRODUCTION

In this Chapter 2, which represents the speculative-theoretical aspect of this thermodynamic overview that is Part I, I summarize the predictions of theoretical stellar atmospheric structural modeling, and the theoretical picture of the local stellar environment, from the speculation that stars are (closed, thermal) thermodynamic systems. This speculation underlies those deductive models which impose the thermal configuration of radiative and hydrostatic equilibria. Such a hypothetical star should have only a single-region atmosphere, the photosphere. The transition-zone aspect of the atmosphere is exhibited only in the transition from linearly (LTE) to nonlinearly (nonLTE) non-Equilibrium forms for the distribution functions of populations of the thermal energy states of photons and atomic particles. The “classical” forms of such “standard” thermal models of “normal” stellar atmospheres permit such a transition to nonLTE only for photon distribution functions; we call this kind of nonLTE, LTE-R. LTE is imposed everywhere for the populations of atomic energy levels. The “neoclassical” forms of such standard thermal stellar atmospheric models allow a transition to nonLTE distribution functions for both photons and atoms. So long as the local environment is also in a wholly thermal, although nonlinearly nonEquilibrium, configuration, such a neoclassical model atmosphere can indeed provide a transition to it; otherwise, the neoclassical model is insufficient. Furthermore, once it has formed by condensation from the ISM, the only contribution such a (closed, thermal) star makes to its local environment is (electromagnetic) radiative ionization and excitation. There is no mass interchange with the local ISM, to provide a local environment by stellar mass-loss—such is forbidden *by definition* of a closed thermodynamic system, to which this hypothetical star is restricted. Any perturbation on such a restriction that comes only from thermal evaporation from the outer atmospheric regions is trivial, for the atmospheric conditions predicted by these models, and under the observed radiative energy-fluxes (cf Section III). The single-region atmosphere of this star, the photosphere, has a temperature distribution whose maximum, in the outer photosphere, nowhere exceeds the equivalent blackbody temperature of its integrated radiation field. The density distribution in the outer atmospheric layers is the isothermal, exponential one, with a scale-height not exceeding that fixed by this equivalent blackbody temperature and photospheric gravity. Such an atmosphere is miniscule in size, relative to the stellar radius, and of interest mainly as a fluorescing-screen exhibition of the composition of the star. An upper limit to that wholly radiative influence on the local environment, to which this stellar model is restricted, is set by this equivalent blackbody temperature, the *effective* temperature of the star.

Historically-conceptually, such a model is based on low-resolution photometric and spectroscopic observations of stars, in the visual spectral region, which suggested that by far most of the stars are quiet, steady-state, sources of radiation to the environment and observer. To a first, crude, taxonomic approximation, it appeared that the stars could be distinguished by the *quality* and *quantity* of this radiation; so modeling based on these parameters might be adequate. Its crudest observational background rests on an empirical sequence of stellar colors, “red” through “white” through “blue,” and a comparison of the associated spectral distributions of the radiation to laboratory sources. Very roughly, the energy distribution follows the general pattern of a blackbody, even though for the “bluer” stars, a wavelength of maximum intensity is not reached before a terrestrial atmospheric cutoff. So one “speculated” that the conditions in the deepest and densest atmospheric regions, where the continuous spectrum arises, reflect, locally, blackbody or Equilibrium conditions whose temperature is T_C , the *color* temperature of the star in the visual spectral region. In the earliest days of insensitive instruments, the Sun provided by far the most precise spectrophotometric data; and indeed, its energy distribution was well represented by such a blackbody distribution (Fig. 2-1). The several curves show how this T_C decreases from the center to the edge of the Sun. This was readily understandable under the recognition that the Sun’s surface is not solid, but consists of a gas, so that one sees deeper at the center of the disk than at the edges, and apparently there is a temperature gradient, T_C increasing inward in the solar—and generally stellar—atmosphere. This recognition introduced the first realization that the stellar atmosphere is the province of non-Equilibrium thermodynamics: conditions are not those of the homogeneous blackbody. Confirmation came from discovering, in the visual spectral regions, that most stars exhibit absorption lines crossing the continuum, such as Kirchoff’s classic laboratory experiments showed a cool gas to produce, when it lies between observer and a hotter source of a continuum. Within the visual spectrum from a single star, the range of ionization of the atoms producing such absorption lines is, generally, relatively small. But as one traverses the sequence of stars from red to blue—from cooler to hotter stars, under the above blackbody interpretation of the continuous spectrum—the “mean” degree of ionization within the spectrum of a single star increases. With Saha’s application of Equilibrium statistical thermodynamics

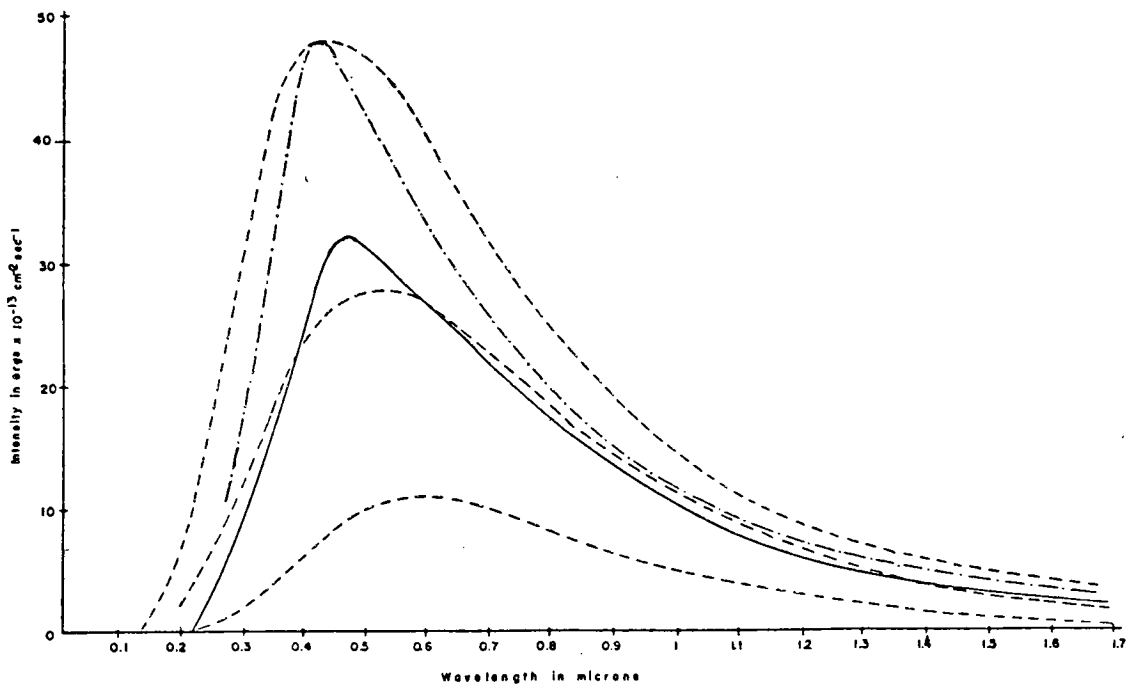


Fig. 2-1. Spectral distribution of solar radiation: The solid line shows the intensity of the whole disk; the dash-and-dot line shows the intensity of the center of the disk; and the dash lines show the intensity of a black body at temperatures of 6500° , 5800° , and 4880° K.

to the local ionization states of stellar atmospheric gases, the observed increase in ionization states of the gases producing the absorption lines, as one moved from redder to bluer stars—from the lower T_C to higher T_C —became completely coherent. One could classify stars either according to their color temperature, T_C , from the distribution of continuous radiation, or according to their ionization temperature as inferred from the strongest absorption lines in their spectra; the results should be the same. Because the T_C refers to deeper layers of the atmosphere where the continuum is formed, it should be somewhat larger than the ionization temperature, T_i , referring to the absorption lines formed in the upper atmospheric regions; and, roughly, it was. In the same way, one should observe a range of T_i in the atmosphere, if the temperature gradients are sufficiently large; and one does observe such a range.

If all stars were the same size, and if indeed the above picture of nearly Equilibrium—linearly nonEquilibrium in the sense of always LTE but just “gentle” gradients in an Equilibrium temperature parameter—were correct, then the total radiative flux—the *quantity* of radiation per unit area—should increase with T_C . The Kirchoff-Boltzmann law gives a wavelength-integrated flux proportional to T_C^4 . So, if one could infer the absolute flux—the flux at the star, not at the observer—it should be monotonically related to the T_C determined from the colors or absorption spectrum. For some stars close enough to measure distances by triangulation about the positions of the Earth in its orbit about the Sun, and eventually by other methods, one could indeed measure total luminosity of the star—but not flux. One could not measure stellar sizes, except for the Sun, the only star for which the surface could be directly resolved. So one had direct measures of the absolute *visual* luminosity of some stars—the λ -integrated flux in the visual spectrum multiplied by the surface area projected on the line of sight. One expressed these observations in terms of the visual magnitude—either the *apparent*, as directly measured, m_V magnitude, or that corrected for distance, M_V , the *absolute* magnitude when referred to a standard distance of 10 psc, or some 30 light-years, related to the distance, r , measured in psc, by

$$M_V = m_V + 5 - 5 \log r(\text{psc}). \quad (2.1)$$

One also expressed this total luminosity in terms of the blackbody concept by defining the *effective* temperature, T_{eff} , as the equivalent blackbody temperature to produce the same total flux as the actual star, not just the visual flux. Thus, from Kirchoff-Boltzmann (Vol. 2):

$$\sigma T_{\text{eff}}^4 R^2 \pi = \int F_\nu d\nu R^2 \pi = \text{bolometric luminosity}. \quad (2.2)$$

One knows M_V ; one does not know the total luminosity, the so-called bolometric magnitude, M_{bol} . One makes a preliminary estimate of it, by using the Planck law and T_C to compute the radiative flux from the unobserved spectral regions. For the Sun, this is not serious; for very hot stars, it is fundamental: so, for them, M_{bol} is completely “model-dependent.” But in any event, whether one used M_V or M_{bol} , when one plotted “quality” vs. “quantity”— T_C vs. either of M_V or M_{bol} —one obtained the famous Hertzsprung-Russell (HR) diagram (Fig. 2-2). One did indeed find the “speculated” monotonic relation between T_C and luminosity for the majority of the observed stars; but, in addition to some scatter, one also found two other relations—the so-called “giant” and “supergiant” branches—which represented the most luminous stars. The interpretation was quick: not all stars have the same size/radius; the giant and supergiant stars have, respectively, increasingly greater radii. The results were systematically confirmed as observations and studies of eclipsing binary systems, especially of visually eclipsing, not just spectroscopically-inferred, systems, increased. There is a very wide range in stellar radii; factors of 10^4 —as observed in the visual spectrum. So, the situation seemed clear: there is a necessary second parameter, in addition to the temperature—the radius. Stellar taxonomy cannot be 1-dimensional; it is *at least* 2-dimensional. A good first approximation to classify stars may be temperature and radius of an equivalent blackbody. But the observational result is that not all values of temperature and radius seem found; otherwise, one would simply have a scatter diagram in the HR plane. Obviously one needs to ask why, and this must relate to general stellar structure. For atmospheric modeling, one does not need to ask so profoundly; it suffices to ask how to incorporate size into such modeling. But even here, the resolution is not a priori obvious.

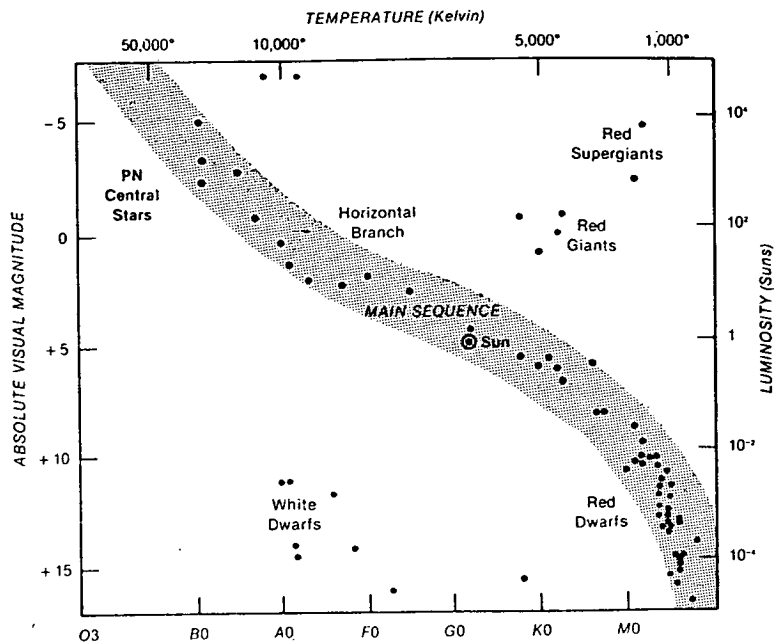


Figure 2-2. Schematic HR diagram from Kwok (1982b), which also locates some particular types of stars useful in Chapter 3 discussions.

So long as one retains the LTE assumption, it is easy to describe the *quality* of a radiation field: how it is produced by, and how it interacts with, atmospheric material. Specifying the local temperature fixes the local relative populations of thermal energy levels; specifying a value of the local particle concentration—or mass-density, usually simply called density—suffices to give local relative ionization; specifying the local chemical concentration adds the last necessary parameter. But to specify the *quantity* of the radiation from a star requires a nonlocal quantity: the local geometry of the star. If one permits all kinds of arbitrary dynamical states for the star, the geometry can be quite complex, and it complicates the specification of that density required, with LTE, to give quality of radiation; it raises complicated questions of energy transfer; it may violate the closed restriction of no mass-flux. With the stellar gravities required by those masses inferred from planetary and binary motions, and with approximate radii, there is just one “simple” configuration: the static thermal one. Under such a configuration, the atmospheric regions of the star are very, very small relative to the stellar radius—a plane-parallel structure of atmospheric layers suffices. For example, under solar gravity and solar T , the static (thermal) density scale-height in the atmosphere is some 200 km; the solar radius is some 10^6 km; the atmospheric density falls by a factor of 10^{17} —to reach ISM values—in some 40 scale-heights or some 0.01 solar radii. *The plane-parallel approximation should largely suffice; under the speculation that the star, and stellar atmosphere, are in thermal configurations.* Under such a configuration, specifying the quantity of radiation per unit area—the total radiative flux—is identical in simplicity to specifying the quality of radiation; indeed, they are the same problem. Then, to specify total radiation from the star, it suffices to specify the atmospheric radius, which is the same as the stellar radius. If we know the mass of the star, specifying the radius is equivalent to specifying the gravity.

Thus, the gross approach to specifying the supposed-static atmosphere of the star, considered as a thin layer enveloping the star, often called the *reversing-layer* where the absorption lines were supposed formed, the equivalent of Kirchoff’s experimental laboratory blackbody source surrounded by a gaseous mantle, does indeed give a 2-dimensional model. Observationally, the two parameters are quality and quantity of radiation; for the speculative-theoretical standard model, the two parameters are T_C (or T_{eff}) and radius (or gravity). The structure of the atmosphere is

ignored; it is characterized by mean values. The speculative aspects of the model are twofold: that the quality of the radiation can be interpreted in terms of one parameter, *the* temperature, under the LTE assumption; and that the ratio between quality and quantity of radiation, evaluated under this LTE assumption, can be interpreted in terms of a single parameter, the stellar radius. If one assumes he knows the stellar mass, the radius parameter is equivalent to introducing the gravity as a parameter. Most of the early, and fundamental, investigations of chemical abundances in stellar atmospheres were carried out under this gross, average, model.

For a more refined model, one needs distributions of temperature and density with height in this thin, plane-parallel, atmospheric model. As already used above, the static assumption alone suffices to give a rough distribution of density—the exponentially decreasing outward one—assuming that the temperature variation is not *too* large. One can obtain an equally rough estimate of the temperature gradient, under the same conditions. Following the definition of the effective temperature, one simply defines the actual thermodynamic temperature at each point in the same way; it is the equivalent blackbody temperature corresponding to the local energy density of the radiation field. Then, from conditions in the deep atmosphere where the radiation field is essentially isotropic, to conditions in the upper atmosphere, where the radiation field comes exclusively from the stellar hemisphere, the radiative energy density decreases by about a factor 2. Since blackbody energy density varies as T^4 , the drop in T from the deepest region we see to the boundary is about $2^{1/4}$, or some 20 percent. We will see that such a result is quite good for those atmospheric models where the opacity is essentially independent of frequency, but gives larger change when opacity varies strongly with frequency. However, it gives us a good idea of the kind of temperature and density distributions possible under this standard, thermal modeling: temperature can never exceed the effective temperature; density decreases exponentially outward, under a scale-height fixed by the boundary-temperature. Relative to the discrepancy between actual, and standard-model, stars, we will see that the modifications of this simple result that are introduced by more sophisticated computations are quite small. They are essential for representing the stellar photospheric spectrum, but are minor for seeing the panorama of complete atmospheric structure, and representing high-resolution observations, and those outside the visual spectral regions.

The above discussion buries any considerations of what other factors than the energy density of the radiation field might influence the local value of the temperature. Primarily, this burial is a consequence of the historical identification of the stellar radiation field with that of a blackbody, hence the presumption that conditions in the atmosphere mimic those in an actual blackbody cavity, in an Equilibrium environment. The essential aspect of such an environment (cf Vol. 2) is that detailed processes are irrelevant: all processes reach an energy equilibrium; the principle of detailed balance holds—all processes destroying the Equilibrium are precisely balanced by their inverse processes. It is irrelevant what “storage mode” for energy one “samples”—one obtains the same value for the equipartitioning parameter, the temperature. The only essential is that the “leak” of energy be negligible relative to its storage: the observation cannot perturb the state of the system. This condition underlies the concept of Equilibrium; its imposition in the stellar atmosphere standard model delineates the range of reliability of the model. To the extent that energy leak—the flux by which one diagnoses the atmosphere—significantly modifies the LTE state, to that extent, the LTE imposition is invalidated. We have already violated this condition in our way of estimating the boundary-temperature above: the radiative energy-flux at the boundary is comparable with the radiative energy density; the LTE configuration is, physically, nullified. However, the mathematical conditions of the standard model continue to impose it.

The condition is enforced by a third basic axiom, in addition to those of LTE and hydrostatic equilibrium: the condition of radiative equilibrium—the value of *the* temperature is fixed by the local radiation density—implicitly applied above. In defining the temperature, one drops any notion of an equipartitioning parameter; one imposes the notion only that it measures the equivalent blackbody energy of the radiation field. Under the RE definition, all the energy could be confined to a single, very limited, frequency interval. It is only the addition of the LTE condition that introduces the Equilibrium-thermodynamic notion of the same energy density residing in the thermal energy of the photons and in that kinetic energy of the atoms which specifies the gas pressure defining the hydrostatic equilibrium. Initially, we stated that if temperature were specified, then the density distribution of the atmosphere followed;

but this is the kinetic temperature of the atoms, not the energy content of the radiation field. We require the equipartitioning assumption of LTE to link the two. Since coupling between the energy of the photons and that of the kinetic energy of the atoms occurs via photoionization, and elastic and inelastic collisions between electrons and atoms, the balance of the rates of the various processes must be carefully considered in evaluating the self-consistency of the conditions of RE and LTE, and their application to HE. Clearly, it depends upon atomic structure as well as the local values of radiation field, kinetic temperatures of ions and electrons, and density.

So, this Chapter exhibits the consequences of strictly applying the speculations and deductive restrictions underlying the standard model, in either its classical or neoclassical forms. I make no attempt to summarize those extensive computations of either variety of the standard model which are already in the literature, nor even to summarize in any detail their particular approximations of computational schemes. I simply summarize the structural basis of these standard models from the nonEquilibrium standpoint and language, and try to clarify two questions: (1) What are the essential physical and numerical features of the standard models? (2) Have these physical and numerical features been sufficiently developed, in the literature, that we can use such computations of standard models as some of the lower-boundary conditions for exophotospheric empirical-theoretical models—at least, for those stars where such a lower-boundary condition, expressed in terms of observations specifying the properties of a quasi-thermal photosphere, does not in itself conflict with other observations of that star? In asking such questions we must, as above, also ask the self-consistency of the framework under which we answer them. For example, are the various LTE assumptions consistent with the atmospheric models we produce from them? But there is a second aspect of self-consistency, other than the physics; the mathematical approximations used to get numerical results. And here, we must always ask how precisely do we need numerical values, in terms of how much they will change under a better physical approximation, but equally approximate mathematics. For example, if a derived boundary temperature changes by 5 percent due to more elaborate mathematics in an LTE transport equation, but by 30 percent—or maybe a factor 2—with a nonLTE transport equation, a focus on the LTE mathematics and neglect of the nonLTE physics is hardly productive.

My viewpoint here is that we know standard modeling is quite inadequate to match modern observations, for *all* stars, not just a few peculiar ones. The question is, how useful is it for describing these lower atmospheric conditions; for describing regions which might be used as the lower-boundary conditions on empirical modeling of upper regions; and how must such models be modified to avoid their imposing false conditions on the outer regions. There are already sufficient discussions of standard atmospheric modeling in the literature, if our only purpose were to describe how to compute them. In Nebraskan *franglais*: once you have seen one standard atmospheric model—which is incapable of representing the lower part of a more extended atmosphere that includes chromospheres, coronae, superionized superthermic-velocity winds, subionized H α and Fe II envelopes, the transition-shock between them, and circumstellar environments produced by the star itself—then you have seen all such standard models. Modern inadequacies in standard modeling which still exist, within their own reference frame, are probably still amusing to remedy—but only that; unless in the remedying, one delineates something significant in their use as lower-boundary regions for the complete stellar atmosphere. Had Mihalas replaced the term “stellar atmospheres” by the term “standard models of stellar atmospheres,” then his above-quoted remarks, and mine here, would be saying the same thing. However, by such change in terminology, the impression given to someone seeking to enter the field, and asking what are the outstanding problems, would be quite different. The same applies, but stronger, to the remarks by Böhm and by Greenstein. The important problems in modeling appear quite differently to a theoretician and to an observer. Finally, a more realistic viewpoint toward standard modeling is that by Struve, with which I open Chapter 3. Note that it is the viewpoint of a keenly perceptive observer, and moreover an observer who doubts whether “peculiar stars” are really all that peculiar, in the broad context of asking the significance of exophotospheric atmospheric regions as well as photospheric, and wondering why solar considerations must be divorced from those on hot stars. In the current rush to distinguish between solar-like stars and “the others,” one recalls Martin Schwarzschild’s impromptu remark, to the effect that most theoreticians seem to get their observational data from other theoreticians. He might have been anticipating Harwit’s (1981) recent invitation to physicists to come dance with astronomers—but not the head-reeling kind of dance inspired by Cecilia Gaposchkin’s contrasting of wide varieties of stellar characteristics without recourse to notes. Apparently preferable are the simplistic, speculative models of several theoreticians of the modern English

school, not that older one in which Cecilia Payne was raised, where the taxonomic empiricisms of astrophysics and biology are often, and usefully, confused. One notes that the spirit of that older school has apparently evolved into just that preoccupation with biological and stellar individuality which appears to give an empirical basis for developing an exo-Caratheodory type of thermodynamics. Elegant and simple as the Caratheodory approach to Equilibrium configurations is, it, like the standard atmospheric modeling based on it, is incapable of representing the wide diversity of real-world objects and conditions. One hopes that a similar axiomatic approach might eventually be developed for the general nonEquilibrium configuration.

II. DEFINITION AND REPRESENTATION OF THE SPACE- AND STATE-FLUXES WITHIN AND FROM THE ATMOSPHERE

In all the foregoing, I have stressed the definition of the thermodynamic character of a star in terms of the fluxes of energy and matter from it; clearly, they can be positive or negative. These fluxes measure the kind of interaction between star and environment. An isolated star has no fluxes and is unobservable except for its gravitational effect. A closed star has only fluxes of energy; any nonradiative energy-flux can propagate away from the star, hence exist, only in an environment of sufficiently large density; the prohibition of a mass-flux ensures that the mass of the star will change, during its evolution, only by that amount converted into energy by nuclear reactions; after its initial formation, such a star can no longer couple to its environment, by either accretion or mass ejection. An open star has fluxes of both energy, nonradiative as well as radiative, and matter. The star can continually deplete, or build, its local environment.

In general, the total fluxes are fixed by the star itself, not simply by their immediate place of origin, the atmosphere, which simply conditions their spectral distribution over whatever is the characterizing parameter: frequency for radiative energy-flux, and velocity for mass-flux. For example, the total energy flux is ultimately fixed by the stellar nuclear reactions—with transient, or maybe longer, fluctuations from filling and voiding various energy storage modes. While it is customarily assumed that—except transiently for novae, and other “superejections”—the energy-flux from the star is overwhelmingly radiative, this is not obviously true, as we shall discuss in Chapter 3 and Part III. So in addition to a spectral distribution of radiative energy-flux, one has a “spectral” distribution of that energy which is generated in the stellar interior, into various kinds of time-dependent storage modes, and into various kinds of fluxes which transport energy—including the mass-flux. But one wants to carefully distinguish between the mass in the mass-flux and the energy in it. One can add or subtract energy locally—for example, in the atmosphere—to a mass-flux whose mass content is fixed by conditions far below the atmosphere. It is only in those circumstances corresponding to the third approximation to the atmospheric structure surrounding a closed star—a consideration of energy and mass fluxes arising in the instability of a closed star—that we envision a mass-flux produced by the atmosphere itself—the thermal evaporation of a quasi-statically heated corona. Usually, we expect a mass-flux linked to some subatmospheric storage mode; we discriminate by the size of the mass-flux, as discussed in Chapter 3 and Part III.

But now, because of this emphasis on the fluxes as determining the thermodynamic kind of star, and atmosphere—either by diagnosing the observed fluxes from the star, or constructing a model which produces the fluxes—we begin the modeling by considering the various fluxes into, within, and from the stellar atmosphere. When we speak of the flux from the star, we mean that actually leaving, or entering, the star, a net flux, redundantly. Within the atmosphere, there can be, locally, a flux, of some quantity, which does not actually persist throughout the atmosphere and escape from the star. Physically, a flux is communication between different storage modes: it is that quantity which negates an adiabatic isolation of some storage mode of stellar material—microscopic or macroscopic. We proceed to formulate all this algebraically.

A. Definition of Flux

The relation between the *concept* of fluxes of matter and energy between a star and its environment, and the *observational usage* of these fluxes to diagnose the structure of the star as an inhomogeneous concentration of matter

and energy, develops in three steps: first, *observational*; second, *idealized-theoretical* (speculative-theoretical); and third, *real-world theoretical* (empirical-theoretical).

Observational: Our identification of a star as a distinct object in some environment proceeds from: (i) Our collector registering an excess in photons and/or matter-particles arriving, over those leaving, in the direction of the star; we call these excesses *fluxes*, between observed region and collector, of photons, etc.; (ii) These fluxes differing between star and adjacent regions on the sky; (iii) Our asserting that such fluxes, and flux differences, exist because the (undefined) thermodynamic states of star, environment, collector differ; and these three “ensembles” of matter and energy are not mutually isolated. We propose to “diagnose” the fluxes to infer that difference in thermodynamic state.

Idealized-Theoretical: The definition of thermodynamic state (cf Vol. 2) evolves from the idealized-theoretical concept of a Thermodynamic Equilibrium (TE) ensemble, defined as a *definite quantity of matter, M , and energy, E , concentrated and stored, isolatedly and homogeneously and time independently, in a specified volume, V . We call this a TE ensemble, or sometimes TE system, of matter and energy*. The thermodynamic state of this TE ensemble is defined to be specified by M , E , V alone; thus “state” refers to storage of matter and energy. Similarly, the “flux” between two TE ensembles is defined as that interchange of matter and energy which results when the mutual isolation of the two ensembles is removed for some transient period. Thus *a nonzero flux exists because of a nonzero difference in storage of matter and energy*.

But note that by definition of a TE system as isolated, neither the thermodynamic states of each of the two components of this idealized, interacting model of an exchange of matter and energy, nor the fluxes, can be directly observed or measured. Again idealistically, one approximates such a measurement of thermodynamic state by cutting a very small hole in the box that isolates the system, measures the microscopic flow outward of the particles comprising the system, and *assumes* that this flow is the same as it would be in the interior of the box if there were no hole. Then, clearly, the microscopic distribution function of these particles—atoms or photons—must be fixed by the thermodynamic state parameters (Vol. 2); and so we determine, from the measures, these latter, of course, after “correcting” for the state of the collector. We note that this “idealized” measure of state is what was used in practice to establish, experimentally, the distribution functions of Equilibrium thermodynamics, under the quasi-Equilibrium conditions of terrestrial laboratories.

Correspondingly, the “idealized” flux between the two components of the interacting TE ensemble mentioned above is simply defined as the difference between the two “flows” from the two components when the boundary between them is removed. The “size” of the boundary that is removed conditions the various kinds of “thermal contact” discussed in Vol. 2, and the kind of quasi-Equilibrium in the vicinity of the boundary, thus the degree of “real-world” configuration.

Thus, relative to diagnostics, it is the “single-system” flux between observed and observer that is relevant in this idealized approach. The simplest conceptual “idealized-world” system to study is the homogeneous object. Relative to modeling, it is the “two-system” flux between adjacent systems that is relevant. The simplest conceptual “idealized-world” system to study is composed of a sequence of adiabatically-isolated, internally-homogeneous, adjacent, thermodynamic systems. We formulate this in more detail in Vol. 2.

Real-World Theoretical: The “real-world” situation of inhomogeneous, nonisolated, time-dependent storage and fluxes, in configurations which may be far from TE, is that which we actually need to study, and attempt to diagnose and model from the observed fluxes. Thus, while we need definition of fluxes in terms of definition of storage configurations and their differences, these definitions must be broad enough to cover any real-world, not only idealized TE, or quasi-TE, situations. We develop such definitions rigorously in Vol. 2; here, in Chapter 2, we proceed “loosely,” following classical quasi-Equilibrium thermodynamics, models, and diagnostics, to develop an understanding of why such rigor is necessary, empirically as well as conceptually.

Such a “clear but loose” approach does *not* come from beginning with the idealized TE thermodynamic ensemble, and then trying to guess, intuitively, what is the kind of “whole-system” nonEquilibrium thermodynamics applicable to the particular, observed kind of real-world concentration of matter, energy, and environment. We have no intuition on which to base such a guess; so we need to begin with the completely general approach of Vol. 2, and then

simplify it, to show explicitly what restrictions we impose when we focus on these classical models. Here we do this “loosely” and in abstract, leaving the details to Vol. 2.

Then we note that even in the idealized-theoretical approach to the TE ensemble—whose state is defined by a set of macroscopic thermodynamic parameters (M, E, V)—one measures the *local* state-parameters (T, ρ) in order to diagnose/infer the state of the ensemble. And, one measures these local parameters by observing the “flow” of particles fixed by these local statistical distribution functions, the flux of particles between system and observer under some assumption on the perturbation of the thermodynamic state by such “flow.” By contrast, if one adopts the classical-idealized approach of measuring thermodynamic state by displacements of the walls enclosing the system, thus not perturbing the isolation, one is restricted to diagnostics based only on measures at an imposed boundary. There is no possibility of a diagnostics in depth, for such a bounded system, nor is there any possibility of such diagnostics for an unbounded system.

In quick, oversimplified illustration, we take the example of measure only of asymptotic velocity of a mass-flux from a star, divorced from measure of it and its ionization-excitation state in depth into the atmosphere. One decouples thermodynamic and microscopic state-parameter diagnostics, by such an approach, *unless* one is sure he has a complete theory, whose particular solution is specified by this single asymptotic value of one thermodynamic parameter—or even of two, if a way could be found to measure the asymptotic density value. The TE system is degenerate in this distinction between thermodynamic-macroscopic, and statistical-microscopic, state-parameters; knowledge of one set is equivalent to knowledge of the other.¹ But in the general case, and particularly the example cited, one needs in-depth measures of both thermodynamic (e.g., macroscopic-velocity) and statistical (e.g., microscopic-velocity, or kinetic-temperature, particle concentration) state-parameters. The Be stars (Chapter 3) illustrate the danger of depending only upon a measured asymptotic velocity.

Thus to consider any nonEquilibrium situation, one profits from the quasi-TE diagnostic example to realize that even there, diagnostic focus must begin on microscopic-statistical, local, distribution functions, and then expand to consider their relation to macroscopic thermodynamic parameters. In essence, one reduces the problem to consideration of a set of *thermal* state-parameters, which specify such microscopic distribution functions, and a set of non-thermal state-parameters, whose distribution is linked by mutual interactions to that of the thermal. The *classical* stellar atmospheric models are those which assume there is no need for any nonthermal parameters to describe the distribution of thermal parameters; the classical “anomalies” are that the observations assert that there are such non-thermal parameters, which are linked to the thermal. The modeling problem consists of deciding how significant are these nonthermal parameters in changing the distribution, and significance, of the thermal parameters, and how to develop the analytical basis for describing all this.

¹We discuss this degeneracy in detail in Vol. 2. Here, its nature is intuitively clear from the above emphasis on thermodynamic state as basically referring to storage of matter and energy, expressed as concentration of matter and energy in terms of the macroscopic thermodynamic state-parameters. Generally, the whole system is not homogeneous; so the total storage is some kind of sum of local concentrations over whatever we consider to be the system—which generally we cannot isolate from its environment, and the kind of nonisolation is described by boundary conditions. So, the macroscopic state-parameters are not homogeneous, neither in kind nor in value; and their kinds and values are expressed by a set of storage/transport equations whose solution is subject to these same boundary conditions. Because local concentration must be expressed, at least in part, in terms of statistical distributions over the micro-particles composing the system, we must be able to determine such statistical distributions from the macroscopic state-parameters—but not necessarily their local values, possibly their distributed values, in combination with the storage/transport equations. And, in turn, unless we have locally the degenerate condition of detailed balance in all microscopic reactions, these statistical distribution functions must enter these storage/transport equations. In the degenerate, thermal, TE configuration, there is one set of macroscopic *thermal* state-parameters (temperature, density); for *all* TE ensembles, each parameter having one value homogeneously over the system, for a given state; and the functional form of the statistical distribution functions is the same for all TE states, with statistical values fixed by the particular values of the macroscopic state-parameters. But, the boundary conditions on the system are isolation from its exterior environment and homogeneity in its interior. So, micro- and macro-descriptions are degenerately equivalent, instead of being independently necessary and supplementary, in describing the system. In restricting, a priori and ad hoc, consideration to thermal systems, we risk an uncritical imposition of this degenerate equivalence, and a neglect of the importance of proper boundary conditions because of an oversimplification of storage/transport equations.

Thus we begin with the Boltzmann equation, which describes the space-time variation of the concentration—hence storage—of various quantities q , whose totality suffices to characterize, locally, the statistical, microscopic state of an ensemble of microparticles. The Boltzmann equation is (cf Vol. 2 for greater discussion; here, we simply use results which are derived there):

$$\frac{\partial f_q(v_i)}{\partial t} + v_j \frac{\partial f_q(v_i)}{\partial x_j} + a_j \frac{\partial f_q(v_i)}{\partial v_j} = \sum_{\alpha, q, v'_i} \{P_\alpha(q, v_i \rightarrow q', v'_i) - R_\alpha(q', v'_i \rightarrow q, v_i)\} \quad (2.3)$$

repeated index above means sum over it:

$f_q(v_j, x_i, t)$ is the concentration of q , in terms of the numbers of particles, at (x_j, t) and with velocity components v_i , that have property q .

a_j is the acceleration acting on a particle of velocity v_j at (t, x_i) .

P_α is a process changing, at (x_i, t) , particles having property q and velocity v_i into particles having property q' and velocity v'_i . R_α is the inverse process: q', v'_i into q, v_i .

The Boltzmann equation, and others derived from it by considering averages of various quantities instead of f_q , are often referred to as *transport* equations, because some of its terms represent fluxes. But in a broader sense, the equation is precisely what was stated above: a description of the change in state of an ensemble in space and time by detailed microscopic description of concentrations; thus, it describes the change in local storage of matter and energy. If there is no change in local state, in time or from one point to another, there are no fluxes, so no transport: so change in (storage, transport) go hand-in-hand. It is often implicitly assumed that change in state simply means change in numerical values of a fixed set of state-parameters, especially when the Boltzmann equation with right-hand side (RHS) zero is considered. But it must be emphasized that this case is exceptional, especially in the problems of interest to us here. The Boltzmann equation is quite adequate to describe change-in-state when the kind of state-parameters, as well as their value, change. And it is this aspect which describes the “transition-zone” aspect of the stellar atmosphere. Such questions become paramount in Vol. 2; here, we lay only the formal descriptive background, so that we can be precise on the simplification introduced in this chapter.

Then we can specify precisely the idea of fluxes. That combination of terms which changes f_q only because of the motion of particles is the space-flux, $F_{qi}(S)$, across the surface element dS of the surface S surrounding some infinitesimal volume of the concentration:

$$F_{qi}(S) dS = dS \int_{\Omega} \int_{v_i} f_q(v_i) v_i \mu_i dv_i d\Omega, \quad (2.4)$$

where Ω is the solid angle and where $\cos^{-1} \mu_i$ is the angle between v_i and the normal to dS . The change in concentration resulting from the space-fluxes alone is then the integral of F_{qi} over the whole surface enveloping the small volume, or the integral of the divergence of F_{qi} over the volume: effectively, the volume integral of the second term on the left-hand side of eq. (2.3) after regrouping some terms (cf Vol. 2). We can also speak of the monochromatic space-flux of $f_q(v_i)$, for particles of given velocity, by omitting the velocity integral in eq. (2.4).

Restricting attention to this space-flux of q obviously suffices for the usual description of the observing process as a measurement of the increase in f_q at the collector resulting from a stream of particles arriving from some source, and being completely absorbed by the collector. Slightly differently, we say the observing process corresponds to measuring the difference between numbers of particles incident on the front surface of the collector and those emitted by all its surfaces. If the collector is a solid which is not ablating, but has only thermal emission, there

is a strong difference in physical—as well as chemical—states for the material contributing to $f_q (v_i > 0)$ and to $f_q (v_i < 0)$; essentially, there is a discontinuity—a true boundary, in the usual sense. If we imagine the source to be also a discontinuous surface, and there to be no medium between source and collector, then we can take the integral in eq. (2.4) over the two surfaces at the opposite ends of the volume separating collector and source, with $f_q (v_i > 0)$, $f_q (v_i < 0)$ being (characteristic of source, zero) and (zero, characteristic of receiver) respectively. The solid angle is that subtended by receiver and source, respectively, in eq. (2.4). In effect, this approach was the “earliest-antique” approach to diagnosing fluxes from stars—introduced at a time when, actually, one considered the stellar surface to be a solid blackbody, and the ISM to be empty.

If the collector—or the source—is a solid object, but ablating because of its motion through a gaseous atmosphere, the “discontinuous boundary” becomes blurred. If the collector is itself a radiating gaseous ensemble, the distinction between $f_q (v_i > 0)$ and $f_q (v_i < 0)$ becomes less sharp—except possibly for the chemical composition of the particles, arriving and emitted; but these can consist of both material particles and of photons. $f_q (v_i > 0)$ consists of a melange—arriving material and “ambient” material. The difference between $f_q (v_i > 0)$ and $f_q (v_i < 0)$ becomes further blurred; each is specified by the “state” of the arriving, ambient, and emitted particles. And, because of the medium lying between source and collector, the question of the “origin” of the “arriving” particles becomes blurred.

Indeed, the last situation becomes essentially that *within* the stellar atmosphere. The size of the volume element over which one performs the integration in eq. (2.4) becomes smaller; in the limit, infinitesimal. We think of the element dS as a combination of source and collector—whether it lies in the stellar atmosphere or at the observer. So, in essence, the flux represents the interchange between something and its environment, with “something” and “environment” being completely relative and interchangeable. So, we completely reconcile the two aspects—flux as a diagnostic tool and flux as an interchange mechanism—by recognizing, again, that it is the ensemble of (concentration + environment) that must be treated as an ensemble. Only in certain extreme cases can an “isolation” simplification be introduced. In essence, the space-flux is simply an interchange of storage quantities between two storage regions: it represents the departure from isolation of the two regions.

We introduce the idea of *state-flux* by contrast to this last interpretation of space-flux. The *state-flux represents an interchange between two storage modes which coexist at (x_i, t)* . Such modes can be microscopic internal energy states—as the electronic energy levels of a hydrogen atom—or they can be two macroscopic storage modes, as convection and rotation. That is, we call the *microscopic state-flux* that combination of terms which changes f_q because of a change in the energy- or mass-states of the particle. These terms represent the RHS of the Boltzmann eq. (2.3). Any pair of terms— (P_α, R_α) —which vanishes, has zero microscopic state-flux in that process α . For the summation of the RHS equal to zero, we have zero total microscopic state-flux relative to storage-quantity q . The extension to macroscopic storage modes is not as specifically easy to exhibit here; but citing the example of interchange between convective and rotational macroscopic velocity fields makes the concept clear.

Dimensionally, the RHS of eq. (2.3) is df_q/dt ; or is dimensionally the same as the divergence of the space-flux; viz, it represents the time rate of change of concentration of the quantity q , at a fixed point. This is of course what interests us in time-evolution. For space-evolution, this state-flux will play a strong role in our discussion of the atmosphere as a transition-zone, because it is in essence the successive unfolding from zero of a set of state-fluxes which characterizes the “transition” across the atmosphere. We elaborate on this in Vol. 2. In the rest of the present chapter, we focus on space-flux.

B. Macroscopic Representation of Space-Flux in Terms of Intermediate Parameters

From the foregoing, it is clear that the only “simple” diagnostic situation is that where source and collector are each discontinuous surfaces, separated by a vacuum, and with entirely different f_q . Even in this situation, we need to know the relation between f_q (source) and those physical quantities—the state-parameters—which we need to describe the source. The more common, less simple, situation requires that we admit the possibility that both source and collector are “extended,” if only in the sense that the source itself has many regions contributing to the flux, and also the environmental medium between source and collector contributes to the flux. Then, the first point

to clarify is the meaning of our definition of the atmosphere as the “place of immediate origin” of the fluxes from the star and the relation of the atmospheric state-parameters to fluxes. In the present chapter, we adopt a macroscopic approach to a first-approximation diagnostic analysis, in order to make clear the diagnostic-analytic problem, at the same time that we present a rough summary of the problem of interpreting the atmosphere as a transition-zone by exhibiting those anomalies that result from considering it as a boundary.

Fluxes of something from the star must of course represent a transport phenomenon that extends throughout the star. But we recognize that the photon, or particle, impinging on our receiving apparatus came directly from the last place that it interacted with material other than the detector. So we distinguish two kinds of “last place of interaction,” accordingly as the “particle” can be treated individually or must be treated collectively. In the first instance, we consider that the particle experiences its last collision, or some other kind of deflecting interaction, before that with the detector, somewhere in the star or medium between star and collector. In the second instance, we consider that the particle belonged to a moving stream within which there is a continuous interaction among particles, the stream itself having escaped from the star. A general application of the Boltzmann eq. (2.3) covers both alternatives, and demonstrates which is the more nearly correct. But here, we want a pictorial overview, for which the oversimplified distinction between the two descriptions is convenient. We denote them, respectively, as “single-particle” and “particle-stream” descriptions, again emphasizing the oversimplification implied by use of the terms. “Single-particle” is used for both photons and matter-particles, “particle-stream” for matter-particles.

1. Single-Particle Description

Phenomenologically, we represent the situation in terms of the specific intensity of a beam of particles, or of photons, which is increased or decreased only by emission from, or absorption by, material along the propagation path from observer to emitting-absorbing region. Call I_{qi} the *specific intensity* of the number, or energy, or whatever is a convenient statistical description of the transport quantity crossing unit surface perpendicular to the given direction per unit time and per unit range in q , per unit solid angle. Then in terms of f_q :

$$I_{qi} = v_i f_q / 4\pi \quad (2.5a)$$

So I_{qi} is a monochromatic quantity. And then, phenomenologically, we can write the steady-state condition for the variation of I_q along the direction x , as (Ω denotes the solid angle, and r the position):

$$dI_q dx dt d\Omega dq = -k_q(\Omega, r) I_q dx dt d\Omega dq + E_q(\Omega, r) dx dt d\Omega dq, \quad (2.5b)$$

where we have assumed only that the “decrease” of I_q by interaction with the material is proportional to the value of I_q rather than some other form. And of course, even that assumption can be removed by incorporating a dependence of k_q on I_q . We have introduced no assumption as to what E_q depends upon. We repeat, this is simply a phenomenological description, and by itself tells us nothing. The physics lies in the behavior of k_q —the absorption coefficient—and of E_q —the emission coefficient. For the moment, we are interested in the steady-state condition, assuming that any time-dependent phenomena occur slowly relative to the relaxation times of the stellar atmosphere.

We introduce the generalized “opacity” variable, τ_q , and the “source-function,” S_q , which we call the *intermediate* local state-parameters.

$$d\tau_q = -k_q dx \quad (2.6)$$

$$S_q = E_q / k_q. \quad (2.7)$$

Then we can write eq. (2.5) in the familiar transfer form:

$$\frac{dI_q}{d\tau_q} = I_q - S_q \quad (2.8)$$

which, to the extent that our assumption on the I_q -dependence of the absorption process is correct, can be integrated in the form:

$$I_q(0) = I_q(T_q) e^{-T_q} + \int_0^{T_q} S_q(\tau_q) e^{-\tau_q} d\tau_q. \quad (2.9)$$

T_q is the maximum value of τ_q along the given direction. We recognize that τ_q , S_q , and I_q generally depend upon direction and position.

If we introduce the further assumption that k_q depends only upon the radial coordinate r , we can introduce τ_q as measured along the radius, with $dx = \cos(x, r) dr$, and so eq. (2.9) takes the form, setting $\mu = \cos(x, r)$

$$I_q(0, \mu) = I_q(T_q, \mu) e^{-T_q/\mu} + \int_0^{T_q} S_q(\tau_q, \mu) e^{-\tau_q/\mu} d\tau_q/\mu. \quad (2.10)$$

Then the flux corresponding to $I_q(\tau_q)$ is—note that it is a *monochromatic* flux:

$$F_q(\tau_q) = \oint I_q(\mu, \tau_q) \mu d\Omega. \quad (2.11)$$

If I_q does not increase with τ_q faster than $\exp(+\tau_q)$, we can drop the first term on the RHS of eq. (2.10) for a star, for which T_q is arbitrarily large, and set the upper limit of the integral as infinity. And, the emergent flux, measured by the detector, is the combination of eqs. (2.10) and (2.11):

$$F_q(0) = \oint \mu d\Omega \int_0^{\infty} S_q(\tau_q, \mu) e^{-\tau_q/\mu} d\tau_q/\mu. \quad (2.12)$$

We can interpret eq. (2.12) to say that the specific intensity along a given direction arises from a source, S_q , of particles, photons—whatever—per unit opacity-distance, at each point along the line of sight. Of the quantity emitted by the source, only the fraction $\exp(-\tau_q)$ reaches the observer. The rest is either “scattered,” without change in its character except for direction, or absorbed and reemitted in several directions with a “different” character—corresponding to the terms on the RHS of eq. (2.3) and the last term on the RHS of eq. (2.5b). The details of the physical processes represented by these terms are what specify the way in which the state of the matter at that point τ_q relates to the contribution to I_q , and thus to F_q .

Thus each small volume of the atmosphere and enveloping medium contributes $S_q \exp(-\tau_q/\mu) d\tau_q/\mu$ to the observed intensity, and a corresponding quantity to the observed flux. Again, unless S_q increases inward toward the

center of the stars as fast as $\exp(+\tau_q)$, only the outermost parts of the star contribute to the particles, photons, whatever—thus, these outermost regions form the immediate place of origin of the observed flux.

Writing

$$S_q \exp(-\tau_q/\mu) d\tau_q/\mu = S_q \times (\tau_q/\mu) \exp(-\tau_q/\mu) d\ln(\tau_q/\mu) \quad (2.13)$$

we see that if S_q varies slowly, this quantity reaches a maximum at about $\tau_q = \mu$. So, we have the rough approximation that in eq. (2.10) with the first term dropped, $I_q(0)$ is about $S_q(\tau_q = \mu)$. F_q is the weighted value of S_q over $\tau_q = \mu$. If we consider eq. (2.10) we see that the regions at the extreme edge of the star begin to diminish their contribution as τ_q in the upper limit of the integral drops below the value 1. Roughly, we have $F_q(0)$ is about $S_q(\tau_q = 2/3)$, and

$$I_q(0, \text{limb of star}) = S_q(\text{outer layers}) \cdot (1 - e^{-\tau'_q}) \quad (2.14)$$

with τ'_q being the value of τ_q along the line-of-sight tangential to the edge of the star, so that we have a very rapid drop of I_q at the edge of the star. The details of the drop depend upon the detailed height-variation of τ_q , but an exponential drop simply follows directly from the “optical” geometry. When τ'_q is very small, the RHS of eq. (2.14) becomes $S_q \times \tau'_q$.

This last result lets us see directly the effect of the environment on the observations. Unless $S_q \times \tau_q$ for the medium between star and collector is significant relative to S_q (atmosphere), the medium does not contribute significantly to the observed flux. If $S_q \times \tau_q$ (medium) is large enough, of course—then, by definition, what we thought was medium is indeed an atmospheric region. Of course we reach an ambiguity in our definition when another star, or some nonstellar condensation, lies between us and the observed star. Then, we have an eclipse situation (Section 5). So it is the physical conditions in these outer regions of the star, where S_q is significant, which we define as the atmosphere—these regions are the “immediate origin” of the observed fluxes. And it is these physical conditions which determine the form and the value of S_q and τ_q ; and these, in turn, fix the observed I_q and F_q .

Thus we define the atmosphere in terms of its emissive and absorptive properties for those quantities comprising the particular flux observed. The extent of the atmosphere, for a given kind of flux, depends upon a combination of the q -dependence of τ_q and the τ_q -dependence of S_q . Moreover, the functional dependence of S_q upon whatever quantities specify the state of the atmosphere may change with position, as may these quantities themselves. (Indeed, it is to this type of change that we referred earlier when discussing the unfolding of the state-parameters of the atmosphere.) Thus, the “atmosphere” defined by one type of flux may be quite different, in extent, location, and physical characteristics from that defined by another kind of flux.² All these considerations enter, when we begin to specify “atmospheric regions.” The conceptual history of the development of the picture of a stellar atmosphere, which we sketch in the following, reflects these questions of the form and variation of S_q and τ_q as well as the variety of fluxes considered.

2. Stream Description

Here, we admit a continuous interaction among the “particles” comprising the flux in such a way that we directly measure the flux only by the arrival of the entire stream at the detector (we return below to indirect detection). In this case, we need a broader representation than the simple phenomenological one of eq. (2.5), and must go to the Boltzmann-type representation in terms of the local distribution function $f_q(r, v)$ for number of particles of

² For this reason, we set aside the neutrino problem.

type q at point r having velocity component v . Then $v_s f_q(v_s, r)$ is the quantity I_q discussed in eq. (2.5b) for transport in the direction s , and the steady-state equation is then, rearranging terms in eq. (2.3) under the condition $\partial/\partial t = 0$:

$$\frac{d}{dx_s} (v_s f_q) = - \frac{a_s}{dv_s} \frac{df_q}{dx_s} - f_q \frac{dv_s}{dx_s} - f_q k(v_s, r) + E(v_s, r) \quad (2.15)$$

where a_s represents the acceleration from either collective or external effects. Equation (2.15) differs from eq. (2.5) in the presence of the first two terms on the right-hand side, each depending on a collective motion and acceleration. Because what the detector will measure is the arrival of the stream, at some velocity averaged over the individual particles, we cannot integrate eq. (2.15) as we did in eq. (2.5), but must first average it over the set of particles. Then, we obtain a set of macroscopic aerodynamic equations to describe the flux (cf Vol. 2), and we cannot, as we did from eqs. (2.10) and (2.12), attribute an “immediate region of origin” to the flux provided by the stream. The most that we can do is to trace backward—observationally or theoretically—the stream from the detector to the star, and ask where the kinetic energy in the stream flow first exceeds that necessary to “escape” from the gravitational field of the star. We can identify the particles in the stream at that point as those comprising the mass-flux from the star. If no such point exists, for the streaming velocity, the mass-flux from the star cannot be carried by such a stream, but it must consist of single-particle loss by thermal evaporation from the atmosphere. In such a thermal distribution of velocities, there always exist some particles with energy exceeding the escape energy, of course. The questions are how many are there of such particles, and where is the region of “immediate origin” of such escape, in terms of opacity, as in Section 1. The problem, of course, is how to trace the stream flow backward. Observationally, we require the above-mentioned indirect diagnostics.

3. Indirect Diagnostics of Streams

Diagnostics of single particles and streams differ, according to the above picture. We analyze single-particle flow in terms of a source-function, S_q , at a region of origin, specified by opacity, τ_q , by postulating no interactions between single particles in the region between origin and detector. We analyze stream flow in terms of flux at the detector, plus an extrapolation process, by admitting interactions within the stream everywhere. Observationally, we accomplish the extrapolation by analyzing a single-particle photon sampling of the mass flow. This process requires that we have diagnostic theory for S_q and τ_q in terms of the flow characteristics of a stream as well as of whatever properties would characterize the material if we ignored the flow. This requires a careful discriminant in the theory between random velocities, of whatever sort—thermal, nonthermal—and systematic velocities. If the whole atmosphere is not to be characterized by the unstable situation of the systematic velocity being everywhere greater than the escape velocity, we see that a strong characteristic of any systematic velocity field, in a star with nonthermal mass-flux, must be a gradient in systematic velocity. We shall see that a major diagnostic problem lies in a discrimination between random velocities and gradients in systematic velocity.

We see that this process of indirect diagnostics of the stream producing a mass-flux requires two things for the diagnosis to be possible from a wholly observational standpoint. First, it requires that S_q and τ_q for the radiation be coupled to the systematic velocity of the particle stream. Second, it requires that we have some method of inferring the particle concentration in the same regions where we infer the velocity. We shall see that this is not usually possible, except by constructing a self-consistent atmospheric model out to and including the regions where the velocities are inferred. Thus, at best, this indirect diagnostic process is iterative.

4. Time- and Space-Variability of Fluxes

In Section 1, we assumed that any temporal variation occurs slowly with respect to the relaxation time of stellar material and radiation fields. Such an assumption is not necessarily true, but cannot be checked until we actually

compare computed relaxation times to observed times of something that varies. But in summarizing those a priori conditions on what we mean by the atmosphere as the region of origin of fluxes, the fact that stellar variability in radiative flux is observed means that we must admit the same possibility in mass-flux. And, indeed, contemporary observations in the farUV demonstrate such variability. In turn, this also implies that we must admit the possibility of material moving both inward and outward, and ultimately that we must admit the possibility of different regions of the atmosphere having velocities of different signs at the same time. This implies that a satisfactory observational study of fluxes requires surface resolution of the star, which is usually impossible. Exceptional circumstances occur for the Sun and under such conditions as stellar eclipses, but these cannot in general be depended on. So one must develop this diagnosis in such a way as to include this inherent ambiguity from observing different regions having different velocities across the line of sight as well as along it.

5. Flux Source Eclipsed by a Star

In addition to the situations envisaged, we have that in which the star eclipses some other object. Then the flux from the other object produces the I_q on the RHS in eqs. (2.9) and (2.10); the contribution of the eclipsing region provides S_q and τ_q . Again, only the atmospheric regions permit any significant transmission of I_q from the flux source; so such eclipse studies permit another type of investigation of atmospheric structure. Also, since the “tangential” opacity is larger than the “radial,” at the same radial “depth” in the atmosphere, such eclipse studies permit probing more extended atmospheric regions than do the noneclipse studies. But again, the physics of the analysis is contained in the relation between τ_q , S_q , and the physical properties of the atmosphere. (Cf Chapter 3, II.D.2.)

Again, if the flux consists of the “streaming motion” of Section 2 rather than the single-particle approach of Section 1, we have the same kind of problem in eclipse as in noneclipse studies.

C. Translation of Observed-Inferred Values of Intermediate Parameters into Macroscopic Parameters Characterizing the Atmosphere

From Section B, we see that diagnostics of the observed flux give us, at most, information about the intermediate parameters S_q and τ_q . Specifically, since stellar fluxes are either photons or matter-particles, q is ν for photons, and v or kinetic-energy, E_k , for matter-particles. In a rough way, we saw that for objects whose disk we could resolve, and with S_q a function of radius only, we obtain $I_\nu(\nu, \mu)$ (at observer, $\tau_\nu = 0$) $\sim S_\nu(\tau_\nu \sim \mu)$; and for objects whose disk we cannot resolve: $F_\nu(\nu, \bar{\mu})$ (at observer, $\tau_\nu = 0$) $\sim S_\nu(\bar{\tau}_\nu \sim \bar{\mu})$. For the Sun, in the most favorable spectral regions and best observing conditions, we can observe over the range: $1 \geq \mu \geq 0.05$. Thus, numerically, we can possibly get an empirical estimate of S_ν over the range: $2-3 > \tau_\nu \geq 0.01$, with increasing inaccuracy at the extremes of the range. If we know nothing about the relative ν -dependence of either S_ν or I_ν , we have simply this set of data with which to work. If we have some knowledge of the ν -dependence of S_ν , we can use observational data for different ν to determine, empirically, the ν -dependence of τ_ν and to extend the τ_ν -range of $S_\nu(\tau_\nu)$. Conversely, if we have some knowledge of the ν -dependence of τ_ν , we can use these empirical data to infer ν -dependence of S_ν . The same kind of remarks can be made for the particles. There is then the problem of inferring, by combined empirical behavior plus some physical model of what quantities fix S_q and τ_q , the depth distribution in the atmosphere of these physical quantities.

The best example is a blackbody, under the assumption that cutting a very small hole in its surface does not change its properties, even in the neighborhood of the hole. We observe the flux of photons, and of particles, from the small hole with some kind of spectrum (ν , v) analyzer; hopefully, the ν - and v -dependences of these fluxes will give us, respectively, a Planck distribution for $I(\nu)$ and a Maxwellian distribution for $I(v)$ (cf Vol. 2); and from these distributions, we infer—from each—a temperature, T , which characterizes the blackbody. From the absolute value of either flux, we can also obtain a temperature, for the photons, and a combined temperature and particle concentration, for the matter-particles. So, under the assumption of a true blackbody—a homogeneous “storage-pot” of matter and photons—we obtain three measures of temperature and one of particle concentration. Hopefully, the three

measures agree; if they do not, we must investigate what departure from the assumed blackbody character of the storage-pot could produce the observed discrepancy.

The simplest “perturbation,” of course, is departure from blackbody conditions only, in the neighborhood of the hole. The departure can be simple—only a departure from the homogeneity condition, caused by flow of gas from the small hole, hence a gradient in temperature and density. The departure can be complex—also a departure from the basic condition of thermodynamic equilibrium distribution functions for photons and particles, again caused by the nonhomogeneity introduced by the small hole. The question is the extent to which either, or a combination, of these two departures from the assumed blackbody conditions suffice to match the actual observations, after we have constructed a “model” of this “perturbed” blackbody. The whole question centers, of course, on the definition of “neighborhood” of the small hole. Either we can investigate the “perturbation” wholly empirically, “reluctantly” admitting, in a step-by-step process, increasing complexity, or size of “neighborhood,” or we can start with the complete geometry of (container + hole), and a knowledge of what and how much matter and energy is stored, and investigate the “configuration” theoretically. From either direction, we will believe the results only when theory and observations coincide, and then, only to the extent that several different theories do not predict the observational uncertainty-ambiguity. So, in abstract, we have the problem of the study of stellar atmospheres generally, and the problem of converting S_q and τ_q to some set of macroscopic parameters, in terms of which we “model” the atmosphere, particularly. First step: preliminary physical model of the atmosphere. Second step: identification of the macroscopic parameters which suffice to describe such model. Third step: “estimate,” in some way, the distribution of such parameters, either theoretically, or by inversion of the measured I_q and/or F_q . Fourth step: “consistency” check on several independent measures of same macroscopic parameter, or, if the observations are not complete enough for that empirical comparison, then a comparison between the several parameters’ empirical values to ask if they are “physically consistent.” Fifth step: searching for the simplest possible way to resolve the ever-present anomalies, then iterating the procedure again, with this new set of parameters—new in value, possibly new kinds of members of the set of parameters.

Caution: especially given the “incomplete” character of astrophysics that was stressed in Chapter 1, particular attention needs to be paid to ambiguity in choice of model, and physical consistency of results derived from observation. And, we must be particularly careful that “physical consistency” is not based on insight derived from incomplete physics. So it is that we must recognize the obvious—but unfortunately often-ignored—two parts of the above step-by-step procedure: the *diagnostic* part, and the *model* part, and their complete interrelation as regards their application to a particular object. In the above example, we assumed that the concentration of matter and energy could be structurally modeled as a blackbody, even in the neighborhood of the “diagnostic hole,” and that it could be “diagnosed” via blackbody relations for the fluxes. As a first approximation to reconcile “discordant” measures of “temperature,” we might be willing to modify a blackbody structure, but only in terms of admitting gradients in blackbody parameters—temperature and density—but not to ask whether, indeed, these were the adequate structural parameters. The same, re diagnostics: admit gradients in blackbody parameters, but do not sacrifice these parameters as such. Actually, of course, we must be prepared to introduce other structural parameters, and diagnostics parameters, and ask the extent to which the necessity for change in structural parameter requires change in diagnostic parameter.

So, in Section III, a summary of the standard model atmospheres, we discuss several approximations to diagnostics for intermediate parameters. First, in Section III.B.2 we assume that S_q and τ_q can be expressed in terms of blackbody parameters. Although the first taxonomic study of stellar spectra “ordered” stars according to a blackbody characterization of “color” of continuum, which was said to originate in a quasi-homogeneous “photosphere,” the presence of spectral lines implies nonhomogeneity in temperature distribution through the atmosphere as a whole. So in the “classical” model of an atmosphere, one adopts a diagnostics based on S_ν being given by the Planck function: *locally* the ratio of emissivity to absorptivity of radiation is given by *local* blackbody = thermodynamic equilibrium parameters. For a given chemical composition, the ν -dependence of τ_ν is fixed by that composition of atmospheric gases coupled with *local* blackbody occupation numbers of energy levels of a given ionization stage, *local* blackbody occupation numbers for different ion stages, and atomic physics of static diffuse gases to fix absorption coefficients. Physically, as we summarize in Vol. 2 such assumption requires particle-particle collisional processes to fix such energetic distribution functions to the exclusion of any radiative excitation, de-excitation, ionization. This

places a lower limit on the concentration of particles in the regions under study; thus, it limits the atmosphere to just such concentrations. *Any fluxes originating in regions having lower particle concentrations are, by definition, non-atmospheric.* Such definition-limitation is not in obvious accord with our earlier definition of star and atmosphere; so we are prepared for "anomaly" in diagnostic result if significant fluxes are produced outside these limiting particle concentrations. In a sense, this diagnostic limitation defines any departure from local blackbody conditions to occur in the interstellar medium, not in the stellar atmosphere. So this *classical atmospheric model, adopted as a first approximation for diagnostics of observed fluxes, defines those regions which can be called atmospheric,* and so limits those regions which can be considered from the structural first approximation. The question is whether this limited model provides any kind of satisfactory representation-synthesis of the observations.

Second, in Section III.B.3, we remove the restriction that S_q and τ_q must be expressed in terms of blackbody parameters. They are free to assume whatever form the physical state of the atmosphere dictates, but consistently with a thermal structure of the atmosphere. Possibly, but not necessarily, they can be expressed in terms of blackbody parameters. But they cannot be expressed in terms of any nonthermal parameters, such as nonthermal velocities or magnetic fields, which are postulated/restricted not to exist. Rather, S_q and τ_q can depend upon the radiation fields at various ν , in addition to their dependence upon T_e and density, and composition. Thus, the inversion problem to infer T_e and density from a diagnosed set of values of S_q and τ_q is not so direct. In the same way, because of their dependence upon the radiation field, the condition of RE—which relates the S_q and the J_ν —gives a different distribution of T_e than in the LTE situation. Thus, even if the standard atmospheric model is of interest only as a lower-boundary condition for an actual atmospheric model, which includes exophotospheric regions, this lower-boundary region differs between classical and neoclassical models. And finally, because there is no restriction on the densities of photospheric regions that can be treated by this nonLTE approach, there is no restriction on the densities of atmospheric phenomena that can be included in this neoclassical model if the phenomena satisfy the thermal restrictions of RE and HE. In practice, this requires that the actual atmosphere have no nonthermal velocities exceeding about one-third the 1-dimensional thermal velocity, if the neoclassical model is to give a reasonable representation of its temperature and density structure. It also requires that any phenomena which satisfy this restriction on size of any nonthermal velocities, but which have the capacity to dissipate nonradiative energy, such as wave-motion of various kinds, do not dissipate such energy, to invalidate the condition of RE. We proceed to consider these problems, and the resulting atmospheric structure.

III. PREDICTED ATMOSPHERIC MODEL UNDER THE quasi-EQUILIBRIUM ASSUMPTIONS

Abstract: The model's restriction to thermal fluxes; the relation between thermal fluxes and atmospheric state-parameters; predicted sizes of thermal matter-flux for observed stars, and its implied unimportance; distribution of state-parameters throughout the atmosphere under the condition of only photon fluxes and linear nonEquilibrium; the same, removing the linearity condition for photon storage and fluxes; resulting physical internal inconsistency of the simple model re linearity; the model when the linearity condition on internal atomic degrees of freedom is removed.

A. Kinds of Observed Fluxes to be Expected Under Thermal Models and Their Sizes

Obviously, we expect only thermal fluxes; but the questions are their expected size, relative to our observing capability, and upon what this size depends.

An upper limit to the flux size is fixed by using the size of the corresponding storage quantity, the f_q , at some quasi-Equilibrium interior point to compute the flux at the boundary. Consider, for reference, the above-mentioned blackbody cavity whose walls are surrounded by a vacuum. The fluxes from an infinitesimal hole are given by eq. (2.4), where we use Equilibrium distribution functions (cf Vol. 2) for $f_q(\nu_i)$ because it is a blackbody cavity:

photons;
$$f_q = \frac{4\pi}{c} B_\nu = \frac{8\pi h \nu^3}{c^3} (e^{h\nu/kT} - 1)^{-1} \quad (2.16)$$

particles;
$$f_q = F_0(\nu) = \frac{4n}{\sqrt{\pi}} \left(\frac{m}{2kT} \right)^{3/2} \nu^2 \exp\left(-\frac{m\nu^2}{2kT}\right). \quad (2.17)$$

We recognize that the specific intensities, the I_{qi} , are isotropic over the outward part of the integral but zero over the inward part. Thus such fluxes would depend only upon the values of the two Equilibrium state, or storage, parameters: temperature, T , and density, ρ (or particle concentration, $n = \rho/m$, where m is the particle mass), whose (homogeneous) values characterize the blackbody cavity. If we replace the vacuum-environment by a "thin atmosphere," the inward integral in eq. (2.4) is not zero, and the flux is decreased below the value given simply by the blackbody values. In nonEquilibrium configurations for the "cavity," storage parameters are inhomogeneously distributed, and intermediate parameters measure only a lower limit on them when the nonlinearity is included. One obtains the emergent I_ν and F_ν , specific intensities and fluxes, by integrating the transfer eq. (2.8) into one of the forms of eqs. (2.9) – (2.12), using the local values of the intermediate parameters τ_q and S_q , defined by the local values of the state-parameters.

We implicitly assume that fluxes are very small relative to storage quantities when we use the linear nonEquilibrium forms of eqs. (2.16) and (2.17) for the storage quantities. As discussed later in this chapter, and in Vol. 2, such use implies that the forms and values of the storage quantities (i.e., the distribution functions), and of the intermediate parameters τ_q and S_q appearing in eq. (2.8), are independent of the fluxes; that their functional forms are the universal Equilibrium ones; and that their values are fixed by the local values of the thermal, quasi-Equilibrium state-parameters. Moreover, such strict linear nonEquilibrium implies that any flux associated with this distribution of state-parameters can be expressed as the first derivative of some function only of these state-parameters (cf eq. (2.91 et seq.). But even in such a linear nonEquilibrium, even if the f_q in eqs. (2.4) – (2.12) are blackbody, it is not generally true that either of the emergent I_q or F_q will have the blackbody, eqs. (2.16) and (2.17), forms. So, neither their total integrated value, nor their monochromatic values, will give, directly and unambiguously, a set of values for T and density, characterizing the "cavity-atmosphere," that can be used to verify the self-consistency of these thermal models. It is only when we adopt the "effective-temperature" approximation of setting I_ν , and F_ν , approximately equal to $B_\nu(T)$ at $\tau_\nu \sim 1$, as discussed following eq. (2.13), that we "derive" numerical values for T and density, which can be used only to the stated degree of approximation.

Given these cautions, and this approach to estimation of fluxes from (thermal) storage quantities (distribution functions)—or, conversely, diagnosing observed fluxes to infer storage quantities—we make such approximate estimates for the two thermal models considered: (1) the classical one of LTE; and (2) the neoclassical one of (thermal) non-LTE.

1. *The classical standard model* assumes that we can use, *locally*, Equilibrium distribution-functions, specified by the local values of the Equilibrium state-parameters. Then we compute the surface-values of radiative intensity, I_ν , and radiative flux, F_ν , from eqs. (2.10) and (2.11), using the LTE forms of eqs. (2.6) and (2.7) for the intermediate parameters, τ_ν and S_ν :

$$d\tau_{\nu a} = -n_a \alpha_\nu dx, \quad (2.18)$$

$$S_\nu = B_\nu(T). \quad (2.19)$$

The quantity n_a is the number of particles in some energy state a which are capable of absorbing radiation at frequency ν . We compute n_a from the density and temperature, using the Equilibrium formulae of Vol. 2. Thus, given

$T(\tau_a)$, which we call the *model* of a thermal-storage atmosphere, we immediately obtain radiative fluxes from eqs. (2.10) – (2.12). Thus, *if we observe a star by a photon flux, there is no question—under this imposed thermal model—that its thermal photon flux is large enough for our observing capability to measure*, by the definition of a star, and by assumption on the model of its atmosphere. Then, eq. (2.13) and the discussion at the beginning of Section II.C, give us a value of T near $\tau_v = 1$; a value of α_v gives us, from the integral of eq. (2.18), a value of n_a ; and n_a gives us, by LTE statistical physics, a value of total n , or ρ . With these, we can ask whether a thermal particle flux—essentially, a thermal evaporation—from the outer atmospheric layers would be detectable, for these thermal models, and whether its local size, and possibly its velocity spectrum, could be used to verify the self-consistency of the state-parameters inferred from the photon flux, as we discussed earlier for a blackbody cavity.

One can consult the literature on exospheric mass-escape, ranging from Spitzer's (1949) survey of classical work, through van de Hulst's (1953) survey of considerations on the pre-solar-wind thinking on the solar corona, to that by Jockers (1970) just prior to the flood of data on stellar mass-flux from spatial observations in the farUV. One can also read the surveys of the relation of such thermal evaporation to Parkers's (1958, 1963) work on thermal modeling of the solar wind (cf Chamberlain, 1960; Brandt, 1970; Jordan, 1981; Parker, 1981), to which "stream-description" we return in Chapter 3 and Part III. Here, we simply put such thermal "particle" flux into the same perspective as thermal photon flux, especially in its blackbody, and departures from blackbody, diagnostics of conditions in the atmospheres of such models. The thermal photon flux is *by definition* observable because we use the observed flux to define the thermal state of the atmosphere in these standard thermal models. As stressed above, an observed mass-flux could be used to test the self-consistency of such thermal models. So, here, in summarizing these models, we ask order-of-magnitude predictions by thermal models of those phenomena not used in constructing the models, for comparison with the observational material in Chapter 3.

Then we note the first complication relative to the blackbody cavity: a gravitational inhibition of such particle flux over that of the photon flux: no particles having a velocity less than that of escape can leave the star, and be observed. Any mass-flux has a cutoff at the gravitational escape velocity, which is perturbed by the effect of the local electric field on any charged particles. The latter simply reduces, for a proton, the effective escape velocity by a factor $2^{1/2}$ over that for a neutral hydrogen atom (cf the above references). So, if we proceed in parallel to the corresponding treatment of a fluid/wind, adopting the mean molecular weight as $1/2$ for an ionized gas, 1 for a neutral gas, the correct value of w_{esc}^2/q^2 automatically follows the transition from neutral to ionized gas, and we need consider only the gravitational inhibition. Because the above photon diagnostics assign temperatures $\lesssim 5 \times 10^4$ K to normal stars, and because gravitational escape velocities of some 100–1000 km/s characterize such stars and models, $w_{\text{escape}}^2/q_{\text{thermal}}^2$ ranges over some 250–5000; and so we obtain only the extreme tail of the thermal velocity spectrum to form a mass-flux. We emphasize, and return to, this point.

The second complication is that already stressed: for such estimates we impose the f_q of eq. (2.17). Such an f_q requires strong collisional interaction among the particles. Those particles which escape, by definition, suffer no collisions, so the mass-flux, estimated from the evaporation of individual particles—not from a hydrodynamic stream-flow where collisions can be arbitrarily frequent—is already strongly nonLTE. Similar problems, for photons, require, at least, the neoclassical model rather than classical, to treat the upper photosphere.

Nonetheless, we adopt the formalism of eqs. (2.5) – (2.12), as for the photon flux. We have, correspondingly:

$$\int d\tau (\text{particle}) = \int Q n_{\text{abs}} dx \longrightarrow \tau \sim Q n_{\text{abs}} \times (\text{density scale-height}), \quad (2.20)$$

$$E (\text{particle}) = \frac{v}{4\pi} f_{\text{part}} Q n_{\text{abs}}, \quad (2.21)$$

$$S(\text{particle}) = \frac{v}{4\pi} f_{\text{part}}; \quad (2.22)$$

and so for the flux of particles with $v > w_{\text{esc}}$:

$$F_{\Sigma}(\text{particle}) = \int_{w_{\text{esc}}} S_{\text{part}}(\tau_{\text{part}} = 2/3) dv; \quad n_{\text{abs}} Q \frac{kT_e}{\mu g} = 2/3 \quad (2.23)$$

$$F_{\Sigma} = \frac{n_{\text{part}}}{n_{\text{abs}}} \frac{\mu}{m} \frac{qR}{Q} \frac{\sqrt{2}}{3\pi\sqrt{\pi}} \left[\frac{w_g^2}{2q_p^2} \right] \left[\frac{w_{\text{esc}}^2}{2q_p^2} + 1 \right] \exp \left[\frac{-w_{\text{esc}}^2}{2q_p^2} \right], \quad (2.24a)$$

where n_{part} and n_{abs} are, respectively, the concentrations of evaporating particles and those with which they collide; R is the photospheric radius; w_g is the gravitational escape velocity and w_{esc} the actual escape velocity; q_p is the particle 1-dimensional thermal velocity, $(kT/m)^{1/2}$, in distinction to q_f , that of the mean atmospheric atom, with mean mass μ . Q is the (elastic) collisional cross-section. For neutral particles, $Q \sim 10^{-16}$ suffices; for ionized particles there is a v^{-4} dependence, and Q is a factor 10^4 – 10^5 larger (cf the references cited above). By considering only neutral atmospheres, we set an upper limit on the particle concentration at $\tau = 1$; and in this case, $w_g = w_{\text{esc}}$. By considering an ionized atmosphere, n_{abs} at $\tau = 1$ decreases by a factor 10^4 – 10^5 ; but $w_{\text{esc}}^2 = 0.5 w_g^2$, which is a much stronger effect because it occurs in the exponent. So, to set upper limits, we set $Q = 10^{-12}$ and $w_{\text{esc}}^2 = 0.5 w_g^2$. Then we obtain for the total mass loss, $4\pi R^2 F_{\Sigma} m$, considering only protons and so $n_{\text{part}}/n_{\text{abs}} = 1$, $m = m_{\text{H}}$, $\mu = 0.5m_{\text{H}}$.

$$\frac{dM_{\text{star}}}{dt} = 7 \times 10^{-18} y (y + 1) e^{-y} \left(\frac{R}{R_{\odot}} \right) \left(\frac{T}{6000} \right) \text{ solar masses/yr.} \quad (2.24b)$$

$$y = 1.91 \times 10^3 \left(\frac{6000}{T} \right) \left(\frac{M}{M_{\odot}} \right) \left(\frac{R_{\odot}}{R} \right)$$

Had we treated neutral particles, the coefficient in eq. (2.24) would have been twice larger; but the value of y would double. Clearly, it is not important, such changes in the coefficient; what counts is the exponent; and its value for T and g attributed to normal stars, under this model, implies completely negligible mass-fluxes from stars. Some $\exp(-2000)$ solar masses per year is predicted for the solar mass-loss; other main-sequence stars are predicted to have comparable values; WR stars can increase to $\exp(-400)$, and MO super-giants to $\exp(-250)$.

To change this result significantly, under thermal modeling, one must either increase q^2 —or T —by a factor 100–1000, or decrease w^2 —or increase the radius of the regions of mass-loss—by that factor. So either one should not observe any evidence for mass-loss, or atmospheric temperatures of some 10^6 K, or atmospheric radii of some 100–1000 times the photospheric values would be required for such thermal models. But even such drastic changes in thermal models—even accompanied by the 10^4 – 10^5 decrease in Q when going to a neutral atmosphere, which is hardly compatible with a T of 10^6 K—would not suffice to give those observed values of mass-loss to be discussed in Chapter 3. These range upward from the 10^{-14} solar masses per year observed in the Sun, to 10^{-4} in the WR stars. The observed solar value only approaches, but still exceeds, that upper limit permitted by eq. (2.24), even with more favorable Q .

Clearly, what is wrong with this thermal-evaporation approach is its treatment of mass-loss as precisely a thermal evaporation: a diffusion process, wherein a very small fraction of the particles in a given atmospheric region participate in the mass escape, diffusing through the great mass of quasi-static atmospheric material. This is in contrast to a picture, made graphic by those modern observations summarized in Chapter 3, of the mass-flux being an outward motion of the atmosphere as a whole, accelerating outward from very small velocities in the photosphere to super-thermic in the coronal regions. So the basic picture, in the thermal-evaporation model, of the atoms providing the mass-flux being a very small fraction of those at a given atmospheric level, the fraction being given by the thermal f_q —this picture is simply wrong. Unfortunately, this concept of a quasi-static atmosphere, pervaded by a mass-flux diffusing outward, has engendered erroneous pictures of the mass flow. Far too often one reads descriptions of “a mass-flux, or a wind, moving *through* the stellar atmosphere”: wrong, because the mass-flux, the wind, *is* the atmosphere, from the base of the atmosphere to its local environment; its velocity is simply highly variable, in position. We will also see that it is often highly variable in time. After summarizing the observational material which demands this non-thermal origin and description of stellar mass-flux in Chapter 3, we return to the above point, in Part III of this volume, to develop a better physical picture than such thermal evaporation or origin.

2. *The neoclassical, thermal, standard model* does not change the essentials of the above picture of radiative and mass-fluxes. It removes the LTE restriction on internal degrees of freedom of the particles. It removes neither the thermal restrictions of HE and RE, nor the restriction of velocities to thermal, given by the LTE expression of eq. (2.17).

The neoclassical change in modeling and diagnostics of the radiative flux is significant, but minor relative to its exophotospheric inadequacies. Thermal taxonomy or diagnostics or modeling, classical or neoclassical, rests on the hypothesis that all these are 2-dimensional, specified by the total radiative flux, or effective temperature, and the gravity. One can dispute the details of the T -distribution, especially in the outer photosphere, and the relation between diagnostics from the line-spectrum and from the continuum, hence the relative location of their regions of origin, and the physical conditions there, and the precise values of the inferred chemical abundances—as one changes from LTE to nonLTE analysis. But under all such models, $T(\text{max})$ cannot exceed $T(\text{effective})$; the outer atmospheric density gradient exceeds that computed for an isothermal atmosphere at $T(\text{effective})$; and macroscopic velocities are restricted to be strongly subthermal; so, as in (1) preceding, any mass-fluxes are, in consequence, absolutely negligible.

This result on the negligibility of thermal evaporative matter-fluxes implies that energy transport by matter can only be significant via a thermal conduction or convection that gives no matter flux: thus, which is stationary. We will see that under the T_e -gradients resulting from thermal models, thermal conduction is completely negligible in stellar atmospheres, and thermal convection occurs only in deep photospheric subregions. Thus, in Section B, *we consider the situation where the state-parameters are those specified above, and where energy transport is only by photons. This is the configuration of Radiative Equilibrium, RE.* Under it, and for this thermal storage, the star can be in a quasi-steady-state only if all the energy produced in the interior is ejected from the stellar surface by a photon flux.

B. Thermal Models: Radiative and Hydrostatic Equilibria: Space-Distribution of State and Intermediate Parameters, and ν -Distribution of Emergent Photon Fluxes, Under Classical and Neoclassical Assumptions

1. Overview of Thermal Modeling: Elaboration on Introduction

In Section A, we showed the insignificance of thermal matter-fluxes, and borrowed a result (yet to be shown) on the insignificance of thermal conduction, and of thermal convection except in deep photospheric layers, to conclude that thermal, standard stellar atmospheric models can be constructed to sufficient accuracy by imposing radiative equilibrium. Furthermore, since thermal models imply only thermal motions, we impose hydrostatic equilibrium. So, such thermal models have two characteristics: the integrated radiation-flux essentially gives the atmospheric temperature distribution, without much complexity; gravity essentially gives the density distribution, again without much complexity.

This first thermal-model characteristic rests on the use of the observed ν -integrated photon flux, F , and its equivalent, the effective-temperature T_{eff} , defined by:

$$F (\text{observed}) = 2\pi \int_0^\infty \int_0^1 B_\nu (T_{\text{eff}}) \mu d\mu d\nu = \sigma T_{\text{eff}}^4 \quad (2.25)$$

as one of the a priori specified state-parameters whose observed value alone suffices to give boundary-value and depth-distribution of T_e in the atmosphere, once chemical composition and gravity of the star are specified. In the simple, often used (if only for reference, or first-approximation diagnostics) case of a gray opacity (photon absorption independent of ν), even gravity and composition are unimportant: the absolute value and distribution of T_e are fixed by F alone. Then, because we observe monochromatic fluxes, not total flux, and there are many of them, we can, in principle, verify the validity of the computed $T_e(\tau)$ —of course, using a diagnostic which rests on the same assumptions underlying the model. For example, we can try to invert the relations (2.9), (2.10), (2.12), using the observed I_ν and F_ν , to obtain an empirical $T_e(\tau_\nu)$ under the stated diagnostic assumptions (LTE, plane-parallel atmosphere, etc.). We obtain, using the approximate results implied by the discussion following eq. (2.13):

$$\begin{aligned} I_\nu(0) &\sim B_\nu(\tau_\nu = \mu) \\ F_\nu(0) &\sim B_\nu(\tau_\nu = \mu \sim 2/3). \end{aligned} \quad (2.26)$$

At best, we might find that the data are not inconsistent with thermal model + thermal diagnostics: at worst, we might find internal contradiction—such as hydrogen Balmer lines in emission rather than absorption. In the latter case, we might try an ad hoc resolution: “normal” atmosphere producing the continuum, with the lines resulting from an extended atmosphere or a shell that is produced by “turbulence” or by “winds,” distinctly nonthermal, but postulated to be in RE, and “diagnosed” for T_e via “thermal” diagnostics. Such an approach is “playing” because the speculative-theoretical basis is no longer either coherently axiomatic or physically self-consistent.

The greatest uncertainty in the above approach, when applying it to an actual star, lies in choosing T_{eff} . Historically, one observed the integrated visual flux, and applied a “bolometric correction” for the unobserved regions—essentially based on an extrapolation using a Planckian, blackbody relation. For the farUV regions, one could use a boundary-temperature instead of T_{eff} for such extrapolations, iterating for consistency. The problem is not serious for the cool stars; it is critical for the hot stars. Equally serious for all stars are those farIR and radio excesses attributed to “dust shells,” to which we return in Chapter 3. A good example of the problems one faces comes from comparing the mutually contradictory discussion by Underhill (1982) and by Conti (1982) for a variety of hot stars. In computing theoretical models, of course, there is no problem: one simply *chooses* T_{eff} , or integrated radiative flux, and computes the visual spectrum. If one believes the computations, one compares the computed visual spectra, for a variety of models, to the actual star, obtaining T_{eff} (and gravity) for it, from the comparison. The resulting anomalies are those discussed in Chapter 3.

The second of the two thermal-model characteristics is linked to the first. Often, one calls the distribution $T_e(\tau)$, *the* model of an atmosphere. The underlying logic has two parts: (i) as above, RE fixes $T_e(\tau)$, given gravity; (ii) then, the “rest” of the atmospheric structure follows from this $T_e(\tau)$, given gravity. This is not a situation to be expected, a priori. Generally, one expects a model to be a tabulated distribution of a number of quantities: temperature, density, ionization, excitation, nonthermal motions, etc. which follow from a general set of equations and boundary conditions describing the particular thermodynamic system. However, (i) and (ii) say life is easier for these thermal models. In the rest of this overview, I outline *why* it is easier under this thermal restriction, and just what such an easier approach requires, thermodynamically, the star to be. Whether the stars are happy with this requirement, we consider in the “anomalies” in Chapter 3.

There are two choices in approach: wholly descriptive, or an attempt to put the thermal model in focus, quickly, relative to an approach which assumes much less. I follow the latter, beginning with the general descriptive equations developed in Vol. 2 of the monograph before the restrictions to closed system (no matter-flux), thermal storage modes, either LTE or thermal nonLTE for the internal (microscopic) energy states have been imposed, in order to see clearly just what these restrictions involve. Then, quickly, I show how the thermal assumptions reduce the equations, and their solution to the results (i) and (ii) above, without any details on the solutions. Then, in the following sections we consider the details of thermal modeling, as a function of the degree of nonEquilibrium assumed (or permitted).

In Vol. 2 we derive three macroscopic equations from the infinite set of Boltzmann microscopic equations for the particles, eq. (2.3). The Boltzmann microscopic equations represent the storage of a combination of thermal (microscopic) plus nonthermal (macroscopic) energy, as well as matter; so we obtain a smaller number of macroscopic equations by averaging the microscopic equations over matter, thermal kinetic energy, and thermal internal energy. We obtain a representation of (i) storage and transport of matter; (ii) storage and transport of thermal energy; and (iii) storage and transport of nonthermal energy. These three macroscopic equations then partially describe the space-time evolution of the local thermodynamic state of the system. To complete the description, we also need the complementary photon equations. Sometimes we introduce such equations in their microscopic form, directly as a Boltzmann equation, sometimes, in an integrated form. Finally, we need a proper set of boundary conditions, which we consider later.

As discussed in Vol. 2, even the following equations contain limitations on the degree of generality of nonEquilibrium effects permitted. We assume that we can separate particle velocities into a systematic flow, on which there is superposed a thermal distribution of velocities. What remains, can be called "turbulence," for which a good description has not yet been developed, in either laboratory aerodynamics or astrophysics. It is very clear that the wealth of material from observational astrophysics can greatly expand the phenomenological scope of aerodynamics; we hope it can be synthesized into solid theory, not be dispersed into disjointed pieces, because some can be treated analytically.

The general forms of these particle equations are: C_i is the systematic velocity component in direction i ; v_i the thermal component, $\bar{v}_i = 0$. Thus all quantities are expressed relative to a local reference frame moving at C_i relative to an observer

$$\left\{ \frac{\partial \rho}{\partial t} \right\}_1 + \left\{ \sum_j \frac{\partial (C_j \rho)}{\partial x_j} \right\}_2 + \{0\}_3 = \text{RHS (2.27)}$$

$$\left\{ \frac{\partial \epsilon}{\partial t} \right\}_1 + \left\{ \sum_j \frac{\partial (C_j \epsilon)}{\partial x_j} \right\}_2 + \left\{ \sum_j \frac{\partial h_j}{\partial x_j} + \sum_j \left[p \frac{\partial C_j}{\partial x_j} + \sum_i p'_{ij} \frac{\partial C_j}{\partial x_i} \right] \right\}_3 = \text{RHS (2.28)}$$

$$\left\{ \frac{\partial}{\partial t} \left(\rho \frac{C^2}{2} - \rho \phi \right) \right\}_1 + \left\{ \sum_j \frac{\partial}{\partial x_j} \left(C_j \left[\rho \frac{C^2}{2} - \rho \phi \right] \right) \right\}_2$$

$$+ \left\{ \sum_j \frac{\partial}{\partial x_j} \left[C_j p + \sum_i C_i p'_{ij} \right] - \sum_j \left[p \frac{\partial C_j}{\partial x_j} + \sum_i p'_{ij} \frac{\partial C_j}{\partial x_i} \right] \right\}_3 = \text{RHS (2.29)}$$

The RHS of the equations, under various approximations on nonEquilibrium, are listed in Table 2-1.

Table 2-1
RHS of Eqs. (2.27)–(2.29)

Eq.	TE	LTE	nonLTE
RHS (2.27)	0	0	0
RHS (2.28)	0	0	$4\pi \int_0^{\infty} (J_\nu - S_\nu) \frac{d\tau_\nu}{ds} d\nu$
RHS (2.29)	0	$-\sum_j \frac{C_j}{c} \int F_\nu \frac{d\tau_\nu}{ds} d\nu$	same as LTE

The symbols not already defined are, using n_j to denote concentration of particles in energy state j :

$$\langle nQ \rangle = \int QF \pi d\nu_j, \quad (2.30)$$

$$\epsilon = \sum_j n_j \epsilon_j \quad (2.31)$$

$$\rho = m \sum_j n_j \quad (2.32)$$

$$p_{ij} = m n \langle v_i v_j \rangle = p \delta_{ij} + p'_{ij}, \quad (2.33)$$

$$p = \sum_i p_{ii}/3, \quad (2.34)$$

kinetic temperature:

$$T_k = p (nk)^{-1}, \quad (2.35)$$

$$h_i = n m \sum_j \langle v_j v_j v_i \rangle / 2 \quad (2.36)$$

If we apply the LTE, Chapman-Cowling small-perturbation approach (cf Vol. 2) to the TE velocity-distribution function eq. (2.17) (i.e., assume particle-particle collisions to be very rapid), thus use

$$F = F_0 \left[1 + \sum_i A_i v_i + \sum_{i,j} B_{ij} v_i v_j \right] \quad (2.37)$$

we obtain the more explicit—but more restricted—forms for h_i and p'_{ij} , which we call, respectively, *thermal heat conduction* and *thermal viscosity*:

$$\text{thermal viscosity: } p'_{ij} = -\eta \left[\left(\frac{\partial C_i}{\partial \chi_j} + \frac{\partial C_j}{\partial \chi_i} \right) - \frac{2}{3} \delta_{ij} \sum_R \frac{\partial C_R}{\partial \chi_R} \right]; \eta = \rho \theta (T_k, \rho), \quad (2.38)$$

$$\text{thermal heat-conduction: } h_i = -\lambda \frac{\partial T}{\partial \chi_i}; \quad \lambda = \rho \psi (T_k, \rho) \quad (2.39)$$

The forms (2.27) – (2.29) of the particle equations exhibit clearly their dual role of describing the evolution of the storage quantities and the transport of the fluxes, with the relation between them. Braces with subscript 1 describe temporal evolution of storage quantity; those with subscript 2, spatial evolution, which is measured by the nonthermal spatial flux

$$j\text{-component of nonthermal flux of } Q \text{ is: } F_j(Q) = C_j Q; \quad (2.40)$$

subscript 3 designates terms describing “interaction” between adjacent volume elements; the RHS terms represent interactions within a given volume element, the divergences of the *state* fluxes. Continuing our assumption that particle collisional terms satisfy LTE, there remain only radiative terms on the RHS which can be represented tabularly as in Table 2-1 (assuming S_ν is independent of μ). We see how the radiation-interaction terms, which depend on particle-photon interaction cross-sections through $d\tau_\nu/ds$, occur on the RHS.

For our present purposes, the most convenient general form of the photon equation is (Simon, 1963)

$$\left(\frac{1}{c} \frac{\partial I_\nu}{\partial t} + \sum_i \mu_i \frac{\partial I_\nu}{\partial \chi_i} \right) (1 + 3\tilde{C}_I) + \left(\frac{1}{c} \frac{\partial \tilde{C}_I}{\partial t} + \sum_i \mu_i \frac{\partial \tilde{C}_I}{\partial \chi_i} \right) \left(3I_\nu - \nu \frac{\partial I_\nu}{\partial \nu} \right) \quad (2.41)$$

$$+ \sum_i \left(\frac{1}{c} \frac{\partial \tilde{C}_j}{\partial t} + \sum_i \mu_i \frac{\partial \tilde{C}_j}{\partial \chi_i} \right) \frac{\partial I_\nu}{\partial \mu_j} \left| + \sum_i \tilde{C}_i \frac{\partial I_\nu}{\partial \chi_i} = (I_\nu - S_\nu) \frac{d\tau_\nu}{ds} \right.$$

$$I_\nu = c \frac{h\nu}{4\pi} f_\nu; \quad \tilde{C}_I = C_{I/c} = \sum_i \mu_i C_i/c; \quad (2.42)$$

$$\frac{d\tau_\nu}{ds} = - \left[\sum_i n_j dv_j + n_s \sigma_\nu \right] h\nu/4\pi; \quad (2.43)$$

$$S_\nu = [S_{th} + n_s \sigma_\nu J_\nu] / \left[\frac{4\pi}{h\nu} \frac{d\tau_\nu}{ds} \right]. \quad (2.44)$$

$$p_{vij} = 4\pi \langle \mu_i \mu_j I_\nu / c \rangle \quad ; \quad p_\nu = p_{vij} \delta_{ij} \quad (2.45)$$

S_{th} represents that familiar part of the source function coming from absorption-emission processes as contrasted to the purely scattering, $\sigma_\nu J_\nu$ part. Since C_i are the components of C , and since $\mu_i I_\nu$ are components of I_ν , C_i is the component of C along I_ν . We have the following relation between quantities in local rest-frame system (unprimed) and observer's system (primed):

$$\nu' = \nu (1 + \tilde{C}'_I), \quad (2.46)$$

$$I'_\nu = I_\nu (1 + 3\tilde{C}'_I),$$

$$\mu'_i = \mu_i + \tilde{C}'_i$$

Again, we obtain the Boltzmann photon equation in the observer's rest frame by setting C_i and its derivatives equal to zero on the left-hand side of eq. (2.41), but rewriting $d\tau_\nu$ and S_ν in terms of velocity-dependent quantities. For static systems, eq. (2.41) reduces to the photon equation already introduced (2.8). We can obtain a set of equations like (2.27) – (2.29) by multiplying eq. (2.41) by 1, μ_i and μ_i^2 and integrating over ν and μ , but in this chapter, eq. (2.41) alone, and simplifications on it, suffice, except to express RHS (2.29) by p_r . (Cf Cannon and Thomas, 1977.)

Generally, we use equations very much simpler than eqs. (2.27) – (2.41). The chief purpose in writing these here is to emphasize just how much simplification is introduced in “theoretical” discussions. One must hesitate, in saying “theory predicts.”

We will return to eqs. (2.27) – (2.29) and (2.41) in defining, and exploring, the classical (Section 2) and neo-classical (Section 3) models, below. But first, we consider the essentials of the process of stellar modeling from the 1-dimensional, plane-parallel, time-independent form of these equations. This form is:

$$\text{matter:} \quad \frac{d(\rho U)}{dX} = 0 \quad (2.27a)$$

$$\text{microscopic-energy:} \quad \frac{d}{dX} (U\epsilon + h) + (p + p') \frac{dU}{dX} - 4\pi \int (J_\nu - S_\nu) \frac{d\tau_\nu}{dX} d\nu = 0 \quad (2.28a)$$

$$\text{macroscopic-energy:} \quad \frac{d}{dX} (\rho U^2 + p + p' + p_r) + \rho g = 0 \quad (2.29a)$$

We also have:

$$p' = -\theta(T_e) \frac{dU}{dX} \rho \quad (2.38a)$$

$$p_r = \int p_\nu d\nu = \frac{4\pi}{c} \int I_\nu \mu^2 \frac{d\Omega}{4\pi} d\nu \quad (2.45a)$$

$$h = -\psi(T_e) \frac{dT_e}{dX} \rho \quad (2.39a)$$

provided the gradients in T_e , ρ , U are not too large.

photons:
$$\frac{\mu \partial I_\nu}{\partial \tau_\nu} + \left[3I_\nu - \frac{\nu \partial I_\nu}{\partial \nu} \right] \frac{dU}{d\tau_\nu} \frac{\mu^2}{c} = I_\nu - S_\nu \quad (2.41a)$$

provided U/c is not too large. In practice, this condition on U/c to reduce eq. (2.41) to (2.41a) requires, for its violation, much larger U than would be admissible under the restrictions permitting eqs. (2.27a) – (2.29a) to be used instead of eqs. (2.27) – (2.29).

Then consider, by subordinating mathematical detail to essential physics, the overall pattern of model building under this speculative-theoretical approach, in steps (a) to (c).

a. Temperature-Distribution: $T_e(\tau)$. If U is less than about 20 percent of the 1-dimensional thermal velocity, q , where

$$q^2 = kT_e/m \quad (2.47)$$

laboratory aerodynamics shows that we can neglect its effect in the microscopic energy eq. (2.28); the same for dU/dX . So to start the modeling, we assume that U , while not necessarily zero, is small: quasi-thermal model. We borrow from Vol. 2 the result

$$\psi(T_e) \sim 2 \times 10^{-6} T_e^{5/2}. \quad (2.48)$$

For comparison of the heat-conduction and radiative-flux terms, we consider LTE-R and that quasi-gray case where the only opacity is the negative hydrogen ion, H^- . So we write eq. (2.28a), without terms in U , and using

$$d\tau = -\alpha_{H^-} n_{H^-} dX \quad (2.49)$$

$$\alpha_{H^-} n_{H^-} = 3 \times 10^{-17} (10^{-22} n_e n_H) (10^{-4} T_e)^{-3/2} \exp(0.87/10^{-4} T_e),$$

as:

$$J - B = 1.2 \times 10^{-18} \left[(10^{-22} n_e n_H) (10^{-4} T_e) \exp(0.87/10^{-4} T_e) \right]^{-1} \left[\frac{dT_e}{dX} \right]^2 B n_H \quad (2.50)$$

or
$$= 0.7 \times 10^{-43} \left[(10^{-22} n_e n_H) (10^{-4} T_e)^{-2} \exp(0.87/10^{-4} T_e) \right] \left[\frac{d \ln T_e}{d\tau} \right]^2 B n_H$$

H^- is the dominant continuous opacity in F–G stars; in the visible atmosphere, reasonable values for T_e measured by T_{eff} from these spectral classes are $T_e = 5 - 10 \times 10^3$ K, $n_e = 10^{12}$, $n_H = 10^{15}$. So for the thermal heat conduction to introduce an effect of $10^{-2} B$ into J–B, the RHS of eq. (2.50), we must have:

$$dT_e/dX > 10^3; \quad \text{or,} \quad d \ln T_e/d\tau > 10^{-10}. \quad (2.51)$$

The first condition would require T_e to halve its value in 10 cm; the second, the same change in $\Delta\tau \sim 10^{-10}$. From eclipse observations of the Sun in the visual continuum or from speculative, RE models developed below, such values are many orders of magnitude too large. Hence, *in these thermal models*, we ignore the effect of thermal conduction. So, proceeding under the quasi-thermal approximation— U is restricted to be small, but not zero—eq. (2.28a) becomes, under this condition of *radiative-equilibrium*, RE:

$$\int J_\nu \kappa_\nu \rho d\nu = \int S_\nu \kappa_\nu \rho d\nu \quad (2.28b)$$

That is, effectively, all energy is transported by radiation, and the total radiation absorbed in some small volume is also emitted by that volume. Under the gray, LTE-R situation, eq. (2.28b) becomes

$$J = B = \sigma T_e^4/\pi = 1.8 \cdot 10^{-5} T_e^4 \text{ erg cm}^{-2} \text{ sec}^{-1} \text{ deg}^{-4} \text{ sterad}^{-1} \quad (2.52)$$

and the radiative-transfer equation, (2.41a), under this restriction to small U , and integrated over ν becomes:

$$\mu \frac{dI}{d\tau} = I - B = I - J \quad (2.53)$$

$$J = \frac{1}{2} \int I d\mu. \quad (2.54)$$

Noting

$$F = 2\pi \int I \mu d\mu \quad (2.55)$$

we can, as already mentioned, use the observed F (emergent) as boundary value, and solve eq. (2.53) to obtain $J(\tau)$, thence $B(T_e[\tau])$ and so $T_e(\tau)$. For the moment, the mathematical details of the solution (cf Section 2) are irrelevant. The essential point is that for this gray, LTE-R case, we obtain directly $T_e(\tau)$ without reference to any other of the eqs. (2.29a) or (2.27a). Thus we obtain the distribution of microscopic thermal energy per particle (or, per unit mass) directly, as a function only of the boundary state-parameter, F (emergent), cf Section 2a, 2b following.

b. Density-Distribution: $\rho(\tau)$. With this $T_e(\tau)$, we proceed to eq. (2.29a). Under the same approximation as above on the size of U , we drop the U terms. Ignore, for the moment, the radiation pressure, eq. (2.45a), p_r . Then eq. (2.29a) becomes:

$$\frac{d}{dX} [\rho k T_e(\tau)/m] + \rho g(X) = 0. \quad (2.29b)$$

This equation can be considered as a relation between gravitational (nonthermal) energy and thermal energy, with specified distribution of thermal energy per particle and specified distribution of gravitational energy per particle. No matter that the two are specified differently—by τ and X , respectively—because we have eq. (2.32) and

$$d\tau = -\rho \kappa dX \quad (2.56)$$

to relate τ and X . So, we solve eqs. (2.29b) and (2.56) simultaneously to obtain $\rho(\tau)$. (And, of course, $\tau[X]$.) The boundary condition is again fixed by specifying the value of a state-parameter; in this case, the value ρ_0 , at $\tau = 1$, which comes from integrating, simultaneously, eqs. (2.56) and (2.29b) between 0 and 1 in τ . We see this, approximately, by noting, as already mentioned, that the solution $T_e(\tau)$ gives an asymptotic-outward, boundary value for T_e , which we label T_0 . Assuming—incorrectly in detail, but useful for illustration—that $T_e = T_0$ for all $1 > \tau > 0$, eq. (2.29b) gives:

$$\rho = \rho_0 \exp(-[X - X_0]/H) \quad (2.57)$$

$$H = kT_e/mg, \text{ the isothermal scale-height.} \quad (2.58)$$

Integrating eq. (2.56) with $\rho = \rho_0$ at $\tau = 1$:

$$\rho_0 = (\kappa H)^{-1} = \frac{mg}{\kappa k T_e} \quad (2.59)$$

if we measure height from $\tau = 1$ at $X_0 = 0$. Thus gravity and ρ_0 are equivalent state-parameters, as already noted. Lifting the restriction that $T_e = T_0$ for $1 > \tau > 0$, to introduce the actual $T_e(\tau)$, does not change the argument, except in mathematical detail, because of this asymptotic behavior of T_e . So we have obtained $\rho(\tau)$, and introduced one more state-parameter, g .

Now, going to the nongray, and nonLTE cases, and including radiation pressure, p_r , changes only the computational details of the above. One is no longer able to obtain $T_e(\tau)$ from just eq. (2.28b) and a modified eq. (2.41a), divorced from eq. (2.29b), and with the sole boundary condition (or state-parameter on the boundary) being the value of F (emergent). Rather, one must combine eq. (2.28b), eq. (2.29b), and a modified eq. (2.41a) and solve them simultaneously, with the boundary state-parameters F , g , and, usually, chemical composition to determine $\alpha_\nu(\nu)$. Again, we consider the details in Sections 2 and 3. Here, our point is that no matter whether one has the first-summarized, simple, situation of independent solutions of eqs. (2.28b) and (2.29b), or one requires their joint solution, one ends up with the same general kind of form for $T_e(\tau_i)$ and $\rho(\tau_i)$, based on the stated boundary parameters, under the two limitations: ($L - 1$) the quasi-thermal limitation that U and dU/dx remain small enough that radiative-equilibrium and hydrostatic-equilibrium are satisfied; and ($L - 2$) the LTE-R limitation that $S_\nu = B_\nu(T_e)$, which usually requires collisional excitation to predominate over radiative³, thus only T_e and ρ —not radiation field—to fix populations of particle energy levels, kinetic and internal. ($L - 2$) requires that we consider no atmospheric regions where ρ drops below some minimal value fixed by those atomic collisional and radiative processes of interest. We now show that ($L - 1$) also depends on ρ not dropping too low, by considering how $U(\tau)$ varies from its lower boundary value.

c. Velocity-Distribution: $U(\tau)$. We obtained the distribution of thermal energy per particle, $T_e(\tau)$, from eq. (2.28b) alone, and of the particle distribution, $\rho(\tau)$, from eq. (2.29b) alone, using the results of eq. (2.28b). Consider the use of eq. (2.27a) to obtain $U(\tau)$. It integrates to give:

$$\rho U = (\rho U)_0 = \text{matter-flux.} \quad (2.60)$$

Since we know $\rho(\tau)$, we can compute $U(\tau)$, given some lower boundary value of U , U_0 . Lower, because from eq. (2.57), ρ becomes arbitrarily small, hence U becomes arbitrarily large, with increasing X . (In the spherically-symmetric,

³ But see Section 3 for discussion of this point.

nonplane-parallel situation at large distances from the star, ρ approaches an asymptotic lower limit; but this is so small that its correction to our developments here is irrelevant—cf Part III). But we recognize that ρ decreases very strongly from the bottom of the observable atmosphere, the photosphere, to its top: from some 10^{18} particles/cc to some 10^{10} —indeed to some 10^4 , if one admits “extended atmospheres,” and “shells,” and “nebulae” to “explain” some of the discrepancies in strictly thermal models (Chapter 3). Thus, if we allow subphotospheric outward velocities, U_0 , as large as 10^{-8} thermal values—some 10^{-2} cm/sec— U will amplify to reach q , and we will violate the conditions earlier imposed on U and dU/dX , well within the “normal” atmosphere, not to mention the “nebular shells,” for which *subphotospheric velocities of 10^{-8} cm/sec will introduce violations of these conditions*. Thus, because of the large density decrease outward through the atmosphere, and in order to maintain strictly thermal models (radiative and hydrostatic equilibria), we must strictly impose a zero— 0 —value for U_0 in eq. (2.60). Whether the “real” star, in whatever is its subatmospheric structure—possibly quiescent, possibly rotating, convecting, pulsating—can actually exist with this limitation imposed by a “speculative-theoretical” modeling can only be decided by the observations.

The alternative to “imposing” $U = 0$, is to define the (closed, thermal) atmosphere as only existing in regions whose particle density exceeds some value, chosen such that whatever U_0 is observed or postulated, U cannot exceed the thermal-modeling limits in the admitted atmosphere. Indeed, this is also the only way to retain LTE-R (Section 2b) in such model atmospheres: the minimal density is chosen such that for *all* atomic transitions of interest, collision processes exceed radiative. Under this alternative, all phenomena where the decrease in atmospheric density amplifies U , so that radiative and hydrostatic equilibria fail, or amplifies radiative relative to collisional processes, so that LTE-R fails, would be termed “exo-atmospheric”—outside the lower, “normal,” atmosphere, which satisfies the (closed, thermal) model. Historically, the term “outer-atmosphere” was more often used, with the photosphere (where the visual continuum arises) and the reversing-layer (where the normal absorption spectrum arises) being the “normal” (closed, thermal) atmosphere. For example, the planetary-nebulae were originally included in the International Astronomical Union (IAU) commission structures as part of the ISM.

Thermodynamically, either of the above alternatives is clearly artificial and unjustified. But, for the moment, the above suffices as a quick summary of the speculative-theoretical modeling process based on *imposing* the RE, HE, LTE-R conditions, not asking, a priori, whether these exclude, a priori, some of the observed atmospheric phenomena. Further, the several refinements over the crude thermal modeling just summarized—nongray, nonLTE, etc.—do not change the basic thermal character just stressed: monotonic gross outward decrease in T_e , with possibly a minor recovery-increase in the low-density, outer regions coming from nongray and nonLTE effects, to an asymptotic boundary value; monotonic outward decrease in ρ , exponential near the boundary. The still-thermal refinements now discussed introduce changes of much less than a factor 2 in T_e and in density gradient. In Chapter 3, we will see that real stellar atmospheres differ by factors of 100 or more in T_e from these predictions, and give density gradients resembling more nearly r^{-2} than something exponential in either r or height. The former effect comes from a nonradiative heating; the second, from a radial aerodynamic flow, rather than static atmosphere, fixing density distribution. What distinguishes one star from another, even among stars of the same classical taxonomic variety, is where such nonradiative heating, and such nonexponential density gradients, start, and how they change the transition between star and ISM. So the remainder of this chapter, especially those sections following the gray-body models (LTE and LTE-R), is more or less a detail in the overall physical problem of what, thermodynamically, fixes stellar structure, and how it differs from the “speculative-theoretical” thermal models.

We now proceed to summarize these “differences in detail” of the various approximations to thermal modeling. The basic equations for the modeling are then the macroscopic equations (2.28b) and (2.29b), and the microscopic equation (2.41a) in which all terms in U are set equal to zero. Whenever we can integrate (2.41a) over ν and reduce S_ν to an expression involving only macroscopic state-parameters, such as in the simplification (2.53), eq. (2.41a) also becomes macroscopic. So we have the working equations:

$$\int (J_\nu - S_\nu) \frac{d\tau_\nu}{dX} d\nu = 0 \quad (2.28b)$$

$$\frac{d}{dX} (p + p_r) + \rho g = 0 \quad (2.29b)$$

$$\mu \frac{dI_\nu}{d\tau_\nu} = I_\nu - S_\nu \quad (2.41b)$$

to which we adjoin eqs. (2.43) and (2.44), together with some definition of S_{th} and some means for computing the n_k . The particular definition and computing algorithm—which introduces microscopic equations—distinguish between the cases of “classical” and “neoclassical” models. We consider them in turn.

2. The “Classical” Speculative-Theoretical Atmospheric Model:

Besides the restriction to thermal energy storage and propagation, *what characterizes the “classical” model is its restriction to local thermodynamic equilibrium, LTE, for all thermal, microscopic, energy storage modes.* However, there are two degrees of such restriction: LTE proper, which is imposed both on particles (equally to kinetic and internal energy) and on photons, and LTE-R, which applies such restriction only on particles, leaving photon distribution functions to be as arbitrary as possible consistently with the LTE restriction on particles. In Section a, we consider LTE, in Section b, LTE-R.

a. Thermal, LTE Storage Modes: For the particles, the LTE restriction imposes a Maxwellian distribution function on kinetic modes,

$$x\text{-component: } F_x(u) du = \left(\frac{m}{2\pi kT_e} \right)^{1/2} n \exp(-mu^2/2kT_e) du \quad (2.61)$$

$$\text{total velocity: } F_x(U) dU = \text{eq. (2.17);}$$

a Boltzmann distribution on internal energy modes,

$$n_k/n_j = (g_k/g_j) \exp[(e_k - e_j)/kT_e], \quad (2.62)$$

where internal energy e_j is measured down from the ionized level of particle in energy state j , and g_j is the statistical weight of level j ; and a Saha distribution between ionization states $i, i + 1$

$${}^i n_{/i+1} n = n_e (G_i G_e / G_{i+1}) \left(\frac{h^2}{2\pi m_e kT_e} \right)^{3/2} \exp(x_i/kT_e), \quad (2.63)$$

where the G_g are the partition-functions of ion i , ion $(i + 1)$ and electron, defined in Vol. 2. For the photons, the LTE restriction imposes a Planck distribution

$$J_\nu = (c/4\pi) U_\nu = (2h\nu^3/c^2) [\exp(h\nu/kT_e) - 1]^{-1}, \quad (2.64)$$

where U_ν is (energy) concentration of photons.

Strictly, in LTE, J_ν is also I_ν ; and these particle and photon distribution functions give zero fluxes: no transport; only storage; strict adiabatic isolation of each infinitesimal volume element. To obtain fluxes, one admits $I_\nu \neq J_\nu = B(T_e)$, for the photons— I_ν depending on direction—and admits particle distribution functions (2.37) which give nonzero values to the heat conduction and viscosity terms discussed earlier. We consider all this in detail in Vol. 2, mentioning it here only for clarity. Here, we wish only to make very clear what a priori limitations on predicted fluxes these speculative models impose. We have already seen one such limitation—no significant particle fluxes. Now we are considering the photon fluxes. We have seen—eqs. (2.9) – (2.12)—that F_ν and I_ν represent weighted integrals of S_ν over the atmosphere. We shall see in detail in Vol. 2 that eqs. (2.61) – (2.64) imply

$$S_\nu = B_\nu(T_e). \quad (2.65)$$

Thus we see that eqs. (2.64) and (2.65) imply the strong condition of *monochromatic* radiative equilibrium, $(RE)_\nu$,

$$J_\nu = S_\nu, \quad (2.66)$$

which of course also implies the weaker condition of integrated RE, given by eq. (2.28b). But we see that $(RE)_\nu$ follows wholly from conditions imposed on degree of nonEquilibrium, not at all from conditions imposed on kind of energy transport, from which followed eq. (2.28b). Indeed, this LTE rests on two conditions: (i) that energy transport, and fluxes, be so small that they do not perturb TE distribution functions, which are fixed by local energy density only; (ii) equipartition is so complete that photon energy density, measured by the radiation field, and particle internal energy density, measured by T_e , are in complete equipartition. Thus we can determine the local photon energy density from the radiative transport problem and use it to fix particle energy density—monochromatically.

Because of these limitations, strict LTE is mainly of historic, not current, interest in atmospheric modeling. Its present application is restricted to the subatmosphere. But it is useful to see just what the strict LTE model predicts; and for this purpose, we consider first a caricature—a thin, columnar gray atmosphere—which will also be useful later in considering simple nonthermal models. Then, we examine how the “thinness” and the “boundary” place explicit limitations on this strict LTE model, hence restrict its application to the subatmosphere.

i. Thin, Columnar, Gray Atmosphere. We represent the angular dependence of I by just two “streams” of photons: one moving outward, I^+ ; and one moving inward, I^- . Then we have

$$J = (I^+ + I^-)/2 \quad (2.67)$$

and we introduce a “flux-quantity,” F' , in parallel with J

$$F' = (I^+ - I^-)/2 \quad (2.68)$$

which is half the actual flux

$$F = (I^+ - I^-) = 2F' . \quad (2.69)$$

Then the transfer eq. (2.53) becomes, noting that μ has only the values ± 1 ,

$$\frac{dI^+}{d\tau} = I^+ - B \quad (2.70a)$$

$$-\frac{dI^-}{d\tau} = I^- - B \quad (2.70b)$$

subject to the RE condition

$$J = B \quad (2.71)$$

and the outer-boundary conditons: (1) no incident photons on the atmosphere

$$I^-(\tau=0) = 0; \quad (2.72)$$

and (2) the outward photon stream at the “boundary” is the emergent (observed) flux

$$I^+(\tau=0) = F(\text{emergent}) = 2F'(\text{emergent}) = 2J(\tau=0) \quad (2.73)$$

From eqs. (2.73) and (2.71) we see immediately that T_e has an asymptotic, “boundary,” value, T_0 , given by

$$\left(\frac{\sigma}{\pi}\right) T_0^4 = B(\tau=0) = F'(\text{emergent}), \quad (2.74)$$

which relates to the effective temperature, T_{eff} , defined by eq. (2.25) as modified in our “columnar,” rather than that plane-parallel, model, hence

$$F(\text{emergent}) = \left(\frac{\sigma}{\pi}\right) T_{\text{eff}}^4, \quad (2.75)$$

so that:

$$T_{\text{eff}}^4 = 2 T_0^4. \quad (2.76)$$

We obtain $T_e(\tau)$, and see the significance of the relation (2.73), by integrating eqs. (2.69) and (2.70)—by adding and subtracting them to obtain

$$\frac{dF'}{d\tau} = J - B = 0 \rightarrow F' = \text{constant} \quad (2.77)$$

$$\frac{dJ}{d\tau} = F' \rightarrow J = F'\tau + J(\tau=0) \quad (2.78)$$

$$= F'(\tau + 1)$$

using eq. (2.73). Then eq. (2.78) combines with eqs. (2.71) and (2.73)–(2.76) to give

$$T_e^4(\tau) = T_0^4(\tau + 1) = 0.5 T_{\text{eff}}^4(\tau + 1), \quad (2.79)$$

while eqs. (2.78), (2.66), (2.67), and (2.74) give:

$$I^+(\tau) = T_0^4(\tau + 2) \left(\frac{\sigma}{\pi} \right), \quad (2.80)$$

$$I^-(\tau) = T_0^4 \tau \left(\frac{\sigma}{\pi} \right). \quad (2.81)$$

Diagnostically, we interpret the observed T_{eff} as simply T_e at $\tau = 1$, the effective point to which we “see” and at which the flux “originates,” in accordance with our earlier discussion, eq. (2.13), where we noted that

$$I_\nu(\mu = 1, \tau_\nu = 0) \simeq S_\nu(\tau_\nu = 1) \quad (2.82)$$

if S does not vary too rapidly with τ_ν . Because T_e increases inward, under this LTE assumption, no matter what the details of $T_e(\tau)$, there will always be *some* τ at which $T_e = T_{\text{eff}}$: so this result $T_{\text{eff}} = T_e(\tau = 1)$ does not tell us much. We see that the factor 2 difference between T_0 and T_{eff} simply reflects the presence of two photon streams in the interior, and only one in the “surface,” when the two streams each increase inward in the same proportion to τ , as in eqs. (2.80) and (2.81).

In terms of a model, we have two results. First, there is an asymptotic lower limit to the energy storage, per particle, in the atmospheric boundary region, measured by T_0 , which is directly proportional to the observed T_{eff} , so that it cannot be zero. The model tells us nothing about the relation of this “boundary” region to the “environmental” region, because *by assumption we have isolated star from environment in the modeling process*. Second, the energy storage, as measured by T_e^4 , increases linearly inward. Again, this is hardly an informative result: we have imposed it. To see this clearly, multiply eq. (2.53) by μ and integrate over it, using $\mu = \pm 1$. J is isotropic, so $\int J \mu d\mu$ vanishes and we obtain:

$$\frac{d}{d\tau} \int \mu^2 I d\mu = 2 \frac{dJ}{d\tau} = \int \mu I d\mu = F = 2F', \quad (2.83)$$

or, using eqs. (2.71) and (2.74)

$$\frac{d}{d\tau} \left[\left(\frac{\sigma}{\pi} \right) T_e^4 \right] = \frac{dB}{d\tau} = F'. \quad (2.84)$$

Equation (2.84) is identical with eq. (2.78); we simply reached it in a different way; in essence, we asked, upon what depends the flux? The answer is that *the flux depends linearly upon the gradient of an energy-storage quantity, or what is called a generalized potential, in thermodynamics*. When, as here, the flux is constant, the generalized potential, or energy-storage quantity, here T_e^4 , also integrates to vary linearly with whatever is the independent variable in forming the gradient, here τ . But *the important point is this linearity between flux and gradient of a potential. The existence of this relation defines what is called linear nonEquilibrium thermodynamics: each flux is linear in the gradient of some potential*. Thus, we see that the relations (2.78) – (2.84) are simply the consequence of applying the condition—

or assumption—of LTE, which as we shall see below, is completely equivalent to assuming linear nonEquilibrium thermodynamics.

We return now to the normal stellar atmosphere, under the plane-parallel assumption, to see precisely the above, which we have seen here in caricature.

ii. Condition that the Stellar Atmosphere be Modeled as a Linear NonEquilibrium System: We begin with the photon storage/transfer equation (2.41b) under the condition of LTE, eq. (2.65). Multiply by μ and integrate over Ω , as above: we obtain

$$\frac{d}{d\tau_\nu} \int \mu^2 I_\nu d\Omega = F_\nu. \quad (2.85)$$

One often introduces the *Eddington-approximation*

$$(4\pi)^{-1} \int \mu^2 I_\nu d\Omega \sim J_\nu \int \mu^2 d\mu = \frac{1}{3} J_\nu, \quad (2.86)$$

which, with eq. (2.66)—monochromatic RE—reduces eq. (2.85) to

$$\frac{1}{3} \frac{dB_\nu(T_e)}{d\tau_\nu} = \frac{F_\nu}{4\pi}, \quad (2.87a)$$

and, in the gray case—imposing only RE—reduces to

$$\frac{4\sigma}{3} \frac{dT_e^4}{d\tau} = F. \quad (2.87b)$$

Writing eq. (2.87b) in the form:

$$-\left(\frac{16\sigma T^3}{3\rho\kappa}\right) \frac{dT_e}{dX} = F, \quad (2.88)$$

shows its similarity to the particle, thermal, energy-storage/transfer—or heat-conduction—eq. (2.39). Equations (2.87) are called the *diffusion-equation* for radiative transfer. Like the particle eqs. (2.39), they are applicable to determine the T_e -distribution only under some variety of LTE. We assert that their use imposes the condition of linear nonEquilibrium—and conversely—and we proceed to show this, and also the perturbation on such use by any “boundary-region.” We do not present such demonstration in this chapter simply for general culture, but, rather, to show precisely the “imposed simplicity” upon which these classical and neoclassical models rest, and how equally simple are the thermodynamic consistency arguments, and the empirical diagnostics, which show the inadequacy of such models.

Linear nonEquilibrium (linear nonE) requires that all fluxes be the gradient of some potential, with the potential being a function of the local values of the Equilibrium state-parameters. That is, there must exist at each point in the atmosphere a function Q_ν for each flux F_ν , such that

$$F_\nu = dQ_\nu(T, p, \rho, \text{etc.})/dX. \quad (2.89)$$

We can see the condition that eq. (2.89) is satisfied, by comparing it to eq. (2.85) which we write as

$$F_\nu = - \left\{ \frac{d}{dX} \left(\int \mu^2 I_\nu d\Omega \right) \right\} (n_a a_\nu)^{-1} \quad (2.90)$$

Thus eq. (2.89) is satisfied *if* we can show that the quantity

$$Q'_\nu \doteq \int \mu^2 I_\nu d\Omega \quad (2.91)$$

depends *only* on the local values of the thermodynamic state-parameters T, p, ρ , etc.

Toward that purpose, consider the value $I_\nu(\tau_\nu, \mu)$ at the point τ_ν in the direction μ . Using $S_\nu = B_\nu$, eq. (2.10) gives

$$I_\nu(\tau_\nu, \mu) = I_\nu(t_\nu) e^{-(t_\nu - \tau_\nu)/\mu} + \int_{\tau_\nu}^{t_\nu} B_\nu(t_\nu) e^{-(t_\nu - \tau_\nu)/\mu} dt_\nu/\mu \quad (2.92)$$

where t_ν is infinite in the interior direction, and 0 in the exterior direction. Corresponding to these two directions, μ is > 0 or < 0 . Now, because the atmosphere is assumed to be spherically-symmetric, B_ν depends on t_ν only: so we write, quite generally:

$$B_\nu(t_\nu) = \sum_r (d^r B_\nu/dt_\nu^r)_{t_\nu} (t_\nu - \tau_\nu)^r/r! = \sum_r D_r (t_\nu - \tau_\nu)^r/r! \quad (2.93)$$

Inserting eq. (2.93) into eq. (2.92) and performing the integration, we obtain:

$$\begin{aligned} I_\nu(\tau_\nu, \mu) &= I_\nu(t_\nu) e^{-(t_\nu - \tau_\nu)/\mu} + B_\nu(\tau_\nu) \left[1 - e^{-(t_\nu - \tau_\nu)/\mu} \right] \\ &+ D_1 \left[-(t_\nu - \tau_\nu) e^{-(t_\nu - \tau_\nu)/\mu} + \mu \left(1 - e^{-(t_\nu - \tau_\nu)/\mu} \right) \right] \\ &+ D_2 \left[-(t_\nu - \tau_\nu)^2 e^{-(t_\nu - \tau_\nu)/\mu} - (t_\nu - \tau_\nu) e^{-(t_\nu - \tau_\nu)/\mu} + \mu^2 \left(1 - e^{-(t_\nu - \tau_\nu)/\mu} \right) \right] \\ &+ D_3 \text{ etc.} \end{aligned} \quad (2.94)$$

If we impose the condition that the point τ_ν is sufficiently far from any boundaries that the t_ν -dependence of eq. (2.94) is negligible, which means

$$\exp [-(t_\nu - \tau_\nu)/\mu] \ll 1 \quad (2.95)$$

$$(t_\nu - \tau_\nu)^r (r!)^{-1} \exp [-(t_\nu - \tau_\nu)/\mu] \ll 1,$$

we obtain

$$I_\nu(\tau_\nu, \mu) = B_\nu(\tau_\nu) + \sum_r D_r \mu^r. \quad (2.96)$$

Using eq. (2.96) to evaluate the integral in eq. (2.90) we obtain:

$$F(\tau_\nu) = \frac{-4\pi}{n_a \alpha_\nu} \frac{d}{dx} (B_\nu/3 + D_2/5 + D_4/7 \dots). \quad (2.97)$$

Because the D_r depend upon derivatives of the thermodynamic state-parameters, the condition eq. (2.89) can only be satisfied if D_2 et seq. are small enough to be negligible: B_ν must vary linearly with $(t_\nu - \tau_\nu)$ in eq. (2.93), thus I_ν linearly with $(t_\nu - \tau_\nu)$ and with μ , in eq. (2.96). Thus $J_\nu = B_\nu$ and we have $(RE)_\nu$.

Thus the condition of linear nonEquilibrium imposes two strong conditions on the model of the atmospheric region considered.

(L-nE: 1) The region considered must be sufficiently far from any boundary regions that eq. (2.95) is satisfied!

The lower boundary, $t_\nu \rightarrow$ very large, offers no problem; it is only the outer region $t_\nu \sim 0$ that is relevant; and that region, for the inward-directed beam, $\mu < 0$. So this condition is:

$$\left. \begin{array}{l} \exp(\tau_\nu/\mu) \ll 1 \\ \tau_\nu^r (r!)^{-1} \exp(\tau_\nu/\mu) \ll 1 \end{array} \right\} \text{for } \mu < 0 \quad (2.95a)$$

$$(L - nE: 2) B_\nu(\tau_\nu) \text{ must be linear, for all } \tau_\nu. \quad (2.98)$$

Note that we reached this linearity in τ , in the simple situation of (i) preceding, only by imposing the additional condition of constant flux, or RE. But, here, we see that the linearity in τ_ν is a consequence of imposing the linear nonE condition, not a consequence of imposing RE. As earlier remarked, RE then follows from this consequence—from this linearity in τ_ν : $(RE)_\nu$ is a consequence of linear nonE—eq. (2.96) integrated over μ gives eq. (2.66).

These two conditions, $(L - nE: 1)$ and $(L - nE: 2)$, are so strong as to make LTE not very interesting for the observed part of stellar atmospheres, although it is sometimes useful in the subatmospheres. In particular, the restriction $(L - nE: 1)$, that these linear conditions can only apply far from the boundary, makes it impossible to apply the boundary-conditions used for the columnar model, eqs. (2.72) and (2.73), to relate radiative flux to T_e -distribution near the boundary. We see this explicitly by applying to the LTE expressions for $B_\nu(\tau_\nu)$ and $I_\nu(\mu, \tau_\nu)$, eqs. (2.93) and (2.96), the linearity condition (2.98); viz

$$D_k(\tau_\nu) = d^k B_\nu(\tau_\nu)/d\tau_\nu^k = 0 \text{ for } k > 1 \quad (2.99)$$

Thus we have, under this linear-nonE LTE (noting that $D_1 = dB_\nu/d\tau_\nu$ at $\tau_\nu = 0$, $T_e = T_{e0}$)

$$B_\nu(\tau_\nu) = B_\nu(\tau_\nu = 0) + \tau_\nu D_1 \quad (2.93a)$$

$$I_\nu(\mu, \tau_\nu) = B_\nu(\tau_\nu = 0) + (\mu + \tau_\nu) D_1 \quad (2.96a)$$

To apply this to the atmosphere, we must satisfy the outer-boundary conditions equivalent, here, to eqs. (2.72) and (2.73) for the columnar model; viz,

$$I_\nu(\mu < 0, \tau_\nu = 0) = 0 \text{ for all } \mu < 0 \quad (2.100)$$

of no photons incident from outside on the atmosphere, and

$$F_\nu(\tau_\nu = 0) = 2\pi \int_0^1 \mu I_\nu(\mu > 0, \tau_\nu = 0) d\mu = \text{observed monochromatic flux} \quad (2.101)$$

Clearly, there is no way that eq. (2.96a) can satisfy eq. (2.100); there is a continuous range of $0 \leq \mu \leq 1$, but only one value for $B_\nu(T_{e0})/D_1$. Equally clearly, using eq. (2.96a) alone to compute eq. (2.101) does not allow a T_{eff} , defined by the observed flux, to be related to a T_{e0} , because eq. (2.96a), substituted into eq. (2.101), gives

$$F_\nu(\tau_\nu = 0) = \pi \left[B_\nu(T_{e0}) + \frac{2}{3} D_1 \right] \quad (2.101a)$$

So a single numerical quantity, the flux, involves *both* T_{e0} and $dT_e/d\tau|_0$. The ‘‘historical’’ definition of T_{eff} rested upon a blackbody equivalent, where there is no T_e -gradient, so involving only a T .

But here the linearity condition (2.85), and its present equivalent eqs. (2.97) + (2.99) resolve the problem, by giving a relation between $B_\nu(T_{e0})$ and $dT_e/d\tau|_0$. From eqs. (2.97), (2.99), and (2.101a) we have:

$$\frac{4}{3} D_1 = B_\nu(T_{e0}) + \frac{2}{3} D_1 \rightarrow \quad (2.102)$$

$$D_1 = \frac{3}{2} B_\nu(T_{e0})$$

Thus, *for the linear case, as well as for the blackbody case, the effective temperature, defined by the integrated flux, also defines the thermal structure of the atmosphere*: the boundary-temperature as well as the (constant) temperature gradient. We have, from eqs. (2.101a) and (2.25), and using eq. (2.102):

$$F(\tau = 0) = \pi B(T_{\text{eff}}) = \pi B_\nu(T_{e0})(1 + 1) \quad (2.103)$$

$$\text{or } T_{\text{eff}}^4 = 2 T_{e0}^4. \quad (2.104)$$

Note that this result is quite independent of whatever replacement one introduces for the second outer-boundary condition (2.100). It is wholly a consequence of the linearity condition. Its derivation is more explicit, in showing upon what it depends, than was the columnar model. In place of eqs. (2.80) and (2.81) for I^+ and I^- , one has, using eqs. (2.102) and (2.96a)

$$I_\nu(\mu, \tau_\nu) = B_\nu(T_{e0}) [1 + 1.5(\mu + \tau_\nu)] \quad (2.105)$$

Correspondingly, using eqs. (2.102) and (2.93a), one has

$$B_\nu(T_e) = B_\nu(T_{e0}) (1 + 1.5\tau_\nu) \quad (2.106)$$

We have already stressed that the linear result (2.96a) cannot satisfy the condition (2.100) no matter what is the relation between B_ν and $dB_\nu/d\tau_\nu = D_1$. Historically, in the literature, authors have applied a pseudolinear result to the boundary regions by replacing eq. (2.100) by

$$I_\nu(\mu < 0, 0) = J_\nu(\mu < 0, 0) = 0 \quad (2.107)$$

which gives, when applied to eq. (2.96a),

$$D_1 = 2B_\nu(T_{e0}) \quad (2.108)$$

instead of the result (2.102), which can be reached by replacing eq. (2.100) by the condition that the inward component of the radiative flux is zero.

Finally, we see directly the inconsistency of imposing this linearity on $B_\nu(T_e)$, relative to outer-boundary conditions, simply by applying eq. (2.93a) to eq. (2.92), then integrating the result over angle to obtain J_ν , then comparing J_ν to the assumed B_ν . We obtain, taking the lower boundary as $t_\nu = \infty$, and the upper as $t_\nu = 0$:

$$I_\nu(\tau_\nu, \mu > 0) = B_\nu(T_0) + (\tau_\nu + \mu)D_1, \quad (2.109)$$

$$I_\nu(\tau_\nu, \mu < 0) = B_\nu(T_0) \left[1 - e^{-\tau_\nu/\mu} \right] + \left[\tau_\nu + \mu \left(1 - e^{-\tau_\nu/\mu} \right) \right] D_1, \quad (2.110)$$

whence integrating over μ to form J_ν

$$J_\nu(\tau_\nu) = B_\nu(T_0) \left[1 - 0.5 \int_0^1 e^{-\tau_\nu/\mu} d\mu \right] + \left[\tau_\nu + 0.5 \int_0^1 \mu e^{-\tau_\nu/\mu} d\mu \right] D_1. \quad (2.111)$$

So J_ν and B_ν differ, at small τ_ν , thus near the boundary $\tau_\nu = 0$, if one applies literally the LTE relations. These are simply internally inconsistent, when applied near the boundary. Such lack of internal self-consistency is of course already evident from the result that we must impose constancy on $D_1 = dB_\nu/d\tau_\nu$, while we obtain the result that T_e^4 varies by a factor 2 between $\tau = 1$ and $\tau = 0$, in the gray case. So, for all these reasons one cannot apply the LTE,

linear nonE, approximation in the region $\tau_\nu \lesssim 1$ —the interesting region when discussing atmospheric, spectral phenomena. We note, however, that often in stellar spectroscopic diagnostics, one adopts as a first approximation the linear relation (2.106). In any situation where the T_e -gradient rather than simply a mean value is important, this approximation is unreliable. One might as well use an isothermal atmosphere, unless all that is important is the *sign* of the T_e -gradient.

So, because of this failure of the LTE models to be either applicable or self-consistent in the boundary regions, we consider the LTE-R models.

b. Thermal, LTE-R Storage Modes: For the particles, the LTE-R restrictions remain the same as for LTE: eqs. (2.61) – (2.63). Actually, in practice, one usually admits implicitly that *if* heat-conduction and viscosity must be considered—which is usually not the case—one admits the distributions of eq. (2.37) instead of eq. (2.61). And, especially in discussing “anomalies” in LTE-R models, one introduces a variety of “temperatures” other than T_e , each being defined by requiring the validity, but not the mutual consistency, of eqs. (2.62) and (2.63). Thus one often finds “excitation-temperature,” T_{ex} , and “ionization-temperature,” T_{ion} , discussed, and differing for different excitation states and ionization levels at the same point in the atmosphere. The introduction of nonLTE-R models has diminished, but not curtailed, this practice. But, here in Section 2.b, we ignore all “exceptions” to the imposed validity of eqs. (2.61) – (2.64).

For the photons, eq. (2.64) is removed; J_ν and I_ν are allowed whatever values the combination of the boundary conditions (2.72) and (2.73), applied in monochromatic form, permit under the particle restrictions (2.61) – (2.63). The most direct consequence of the latter is the imposition of eq. (2.65) on S_ν , in the photon storage/transfer equation (2.41b). As we shall see, this is a severe restriction.

However, because only LTE, not LTE-R, is equivalent to strict linear nonE, neither the condition of RE, nor of (RE) $_\nu$ is implied by LTE-R. Thus, imposing either of these conditions is a separate “axiom” for the LTE-R modeling. One applies the weaker of the two, RE, and rationalizes its application by the earlier discussion of the small influence of thermal heat-conduction under the T_e -models given by the LTE-R configuration. So, we simply make reference to these earlier arguments, centering on eqs. (2.48) – (2.51).

Then, the equations giving the distribution $T_e(\tau_i)$ are the modified eq. (2.28b) for particle thermal storage,

$$\int [J_\nu - B_\nu(T_e)] n_a \alpha_{a\nu} d\nu = 0; \quad (2.28c)$$

the photon storage/transport equation, the modified (2.41b)

$$\mu \frac{dI_\nu}{d\tau_\nu} = I_\nu - B_\nu(T_e) \quad (2.41c)$$

the several eqs. (2.61) – (2.63), which give the concentrations of those particles n_a which absorb at ν ; and the profile of the absorption coefficient, $\alpha_{a\nu}$. For the latter, we need equations, which depend upon the “species” absorbing, and which we introduce when necessary, in their thermal LTE-R forms. The nonthermal, nonLTE forms of these equations, of S_ν , and of $\alpha_{a\nu}$, differ considerably from the thermal, LTE forms adopted here. We consider the nonLTE forms in Section 3 of this chapter; the nonthermal forms, in Vol. 2.

i. Gray Atmosphere: Single Subregion Photosphere: Again, for the following reasons, it is useful to consider first the gray atmosphere, for which eq. (2.28c) again becomes eq. (2.52), and eq. (2.41c) again becomes eq. (2.53). Basically, we wish to find solutions for $T_e(\tau)$, which depart from the linear solution and are capable of better representing

conditions in the upper photosphere. As seen above, in discussing the boundary condition (2.100), this requires a better representation of the angular dependence of $I_\nu(\tau, \mu)$, in order to satisfy $I_\nu(0, \mu < 0)$ for each μ . By first considering the gray case, we see how to obtain such a better angular representation.

However, as we also saw above, we must also expect such departure from linearity at small τ . When we consider the nongray case, small τ_ν at one ν may be large τ_ν at another; and we want to know how this affects the solution. So, after considering the gray case, we go to the next simpler one of an atmosphere which is gray, with one absorption coefficient, over one part of the spectrum; and also gray, but with another absorption coefficient, over the rest of the spectrum.

We abstract the situation schematically, as above, for this "two-gray" atmosphere; but use the computations for a variety of solar models by Dumont and Heidmann to exhibit specific details for the illustrative case of a gray atmosphere becoming nongray as density decreases in the upper photosphere and changes the species responsible for the opacity. This is important, as we will see in Chapter 3, for the transition to exophotospheric regions.

These results illustrate the behavior of T_e in the outermost photosphere, showing it can increase as well as decrease, while remaining within the condition $T_e \lesssim T_{\text{eff}}$. The results also show how the relation between J_ν and B_ν —the departure from monochromatic RE—is affected. In turn, this lets us see how to include the effects of spectral lines, under LTE-R, and it gives us some insight into the relation between S_ν and J_ν in the nonLTE-R situation. Taken altogether, these results paint a picture of an atmosphere, having only thermal storage modes, as a sequence of opacity subregions, within each subregion the opacity evolving from "subatmospheric" to "outer-atmospheric," from quasi-detailed-balance in radiative transition [LTE, or linear nonE, or (RE) $_\nu$], to large departures from this condition. Such a picture of opacity subregions, and its utility in visualizing the physics of the T_e -distribution, has been emphasized by Rudkjoning (1947). Even in the presently considered LTE-R configuration, but especially in the nonLTE configuration of Section 3 following, we see how this evolution of the opacities controlling the T_e -distribution (under RE) brings the state of the "stellar material" to that of the "interstellar material." Thus, we stress the role of the atmosphere as a transition-region, not as a boundary-region. In Part III, where nonthermal atmospheric models, with a mass-flux, are considered, so that the distinction between stellar and local-environmental material fades, we appreciate even more the transition, rather than boundary, character.

If we attempt to solve eq. (2.53) under some kind of angle-averaging approximation, such as we adopted in Section 2.a, in order to obtain directly $J(\tau) = B[T_e(\tau)]$, then $I(\tau, \mu)$ from eq. (2.92), we must focus on

$$\frac{d}{d\tau} \overline{(\mu^2 I)} = F \rightarrow \overline{(\mu^2 I)}_{\tau=0} - \overline{(\mu^2 I)}_{\tau=0} = F\tau. \quad (2.112)$$

Equation (2.112) does *not* satisfy the linearity condition of flux being the gradient of some potential that is a function only of the thermodynamic parameters, because the above angle-average depends upon location relative to the boundary—upon τ . If we did assume the average was independent of τ , that the $\overline{\mu^2 I}$ could be replaced by some constant times J , then we would recover the linear solutions discussed in considering LTE rather than LTE-R. And, we would again find difficulty in representing correctly the boundary. Consequently, to introduce a boundary effect, we must consider some method of solution which considers explicitly the $I(\mu)$ dependence.

For this purpose, any quadrature method which decomposes J in eq. (2.53) in terms of its components $I_i(\mu_i)$, instead of integrating over I to obtain J , will give some insight. The "best" approach is simply that which gives the most accuracy in this boundary representation. However, as we shall see in Section 3, deviations from LTE-R also depend upon the boundary; and we have already noted that any velocity effects amplify exponentially (with decrease in ρ) toward the boundary. Thus it is pointless to insist on a mathematical sophistication that obtains an arithmetic accuracy unwarranted by the physical effects yet to be included, in an actual star. So those existing solutions (Chandrasekhar, 1950; Kourganoff, 1952; Krook, 1955) based on a Gaussian quadrature for the weights a_j in the representation

$$\mu_i \frac{dI_i}{d\tau} = I_i - \frac{1}{2} \sum_{-n}^n a_j I_j \quad (2.113)$$

provide sufficient insight into how to represent boundary effects in this gray atmosphere. Chandrasekhar's further developments in the nongray RE and gray nonRE cases also provide sufficient insight into those variations on this gray RE case. The approach is also useful in Section 3, in treating nonLTE, ν -dependent, line-transfer; so we give details here.

We see that a particular solution of eq. (2.113) is, again, the linear expression

$$I_i = b(Q + \tau + \mu_i), \quad (2.114)$$

where b and Q are arbitrary constants. It is inadequate, alone, at outer boundary for the reasons discussed above. Further, we see from our earlier discussion that eq. (2.113) has several exact solutions involving exponential terms in the optical depth. Such a solution is of course the usual expectation in a set of linear first-order differential equations such as eq. (2.113). Thus we look for a solution of the form:

$$I_i = g_i e^{-k\tau}, \quad (2.115)$$

where the g_i and k are constants, to adjoin to eq. (2.114). Substituting eq. (2.115) into eq. (2.113), we obtain:

$$g_i (1 + \mu_i k) = \frac{1}{2} \sum a_j g_j = \text{constant}, \quad (2.116)$$

whence:

$$g_j = \frac{\text{constant}}{1 + \mu_j k} \quad (2.117)$$

Substituting eq. (2.117) into eq. (2.116)

$$1 = \frac{1}{2} \sum_{-n}^n \frac{a_j}{1 + \mu_j k} \quad (2.118)$$

and using the relations: $a_i = a_{-i}$; $\mu_i = -\mu_{-i}$

$$1 = \sum_1^n \frac{a_j}{1 - \mu_j^2 k^2} \quad (2.119)$$

an equation of degree n in k^2 . We note that the Gaussian quadrature is exact for an arbitrary polynomial of degree $4n - 1$; hence

$$\sum_{j=1}^n a_j \mu_j^m = \int_0^1 \mu^m d\mu = \frac{1}{m+1} \quad (2.120)$$

whence:

$$\sum_1^n a_j = 1 \quad (2.121)$$

and we see that eq. (2.119) is satisfied by $k^2 = 0$. Further, we see that since eq. (2.119) is a polynomial in k^2 , the roots for k appear in pairs $\pm k_\alpha$. We can not allow negative roots for k , for I cannot increase downward exponentially with τ if we require a constant flux of radiative energy through the atmosphere. Thus we have $(n-1)$ roots of eq. (2.119) giving positive values k_α , and the general solution is a superposition of these values and the linear part of the solution (2.114). We thus have:

$$I_i = b \left\{ \sum_{\alpha=1}^{n-1} \frac{L_\alpha e^{-k_\alpha \tau}}{1 + \mu_i k_\alpha} + \mu_i + \tau + Q_i \right\}; i = \pm 1 \dots \pm n. \quad (2.122)$$

The L_α, b, Q are constants to be determined by the boundary conditions. We have already used one boundary condition to eliminate the positive-exponent terms; the second boundary condition is the one that we could not fulfill in our earlier approximate treatment, namely:

$$I_{-i} = 0 \quad \text{at} \quad \tau = 0 \quad \text{for} \quad i = 1, \dots, n. \quad (2.123)$$

Now, however, we see that the conditions are uniquely satisfied—by using them to fix the value of the $(n-1) L_\alpha$ and the value of Q . We have the conditions:

$$\sum_{\alpha=1}^{n-1} \frac{L_\alpha}{1 - \mu_i k_\alpha} + Q = \mu_i \quad i = 1, \dots, n \quad (2.124)$$

For the value of b , we have again the condition on the net flux:

$$F = 2\pi \int_{-1}^1 I \mu d\mu. \quad (2.125)$$

Thus, using again the Gaussian quadrature formula and eq. (2.122):

$$F = 2\pi b \left\{ \sum_{\alpha=1}^{n-1} L_\alpha e^{-k_\alpha \tau} \sum_i \frac{a_i \mu_i}{1 + \mu_i k_\alpha} + \sum a_i \mu_i^2 + (Q + \tau) \sum a_i \mu_i \right\}. \quad (2.126)$$

The second and third members have the value $2/3$ and 0 , respectively, by eq. (2.120) and the conditions on a_i, μ_i , respectively. Also:

$$\sum_{-n}^n \frac{a_i \mu_i}{1 + \mu_i k_\alpha} = \frac{1}{k_\alpha} \sum_{-n}^n a_i \left(1 - \frac{1}{1 + \mu_i k_\alpha} \right) = \frac{1}{k_\alpha} \left(2 - \sum_{-n}^n \frac{a_i}{1 + \mu_i k_\alpha} \right), \quad (2.127)$$

by eq. (2.121). But then by eq. (2.118) the bracket vanishes. Thus:

$$b = \frac{3F}{4\pi} \quad (2.128)$$

the same relation obtained in our LTE approximation.
Then we have

$$\begin{aligned} B = J &= \frac{1}{2} \int_{-1}^1 I d\mu = \frac{1}{2} \sum a_i I_i \\ &= \frac{b}{2} \left\{ \sum_1^{n-1} I_\alpha e^{-k_\alpha \tau} \sum_i \frac{a_i}{1 + \mu_i k_\alpha} + \sum_i a_i \mu_i + (Q + \tau) \sum a_i \right\} \\ &= \frac{3F}{4\pi} \left\{ \tau + Q + \sum_{\alpha=1}^{n-1} L_\alpha e^{-k_\alpha \tau} \right\} \end{aligned} \quad (2.129)$$

or writing:

$$q(\tau) = Q + \sum_{\alpha=1}^{n-1} L_\alpha e^{-k_\alpha \tau} \quad (2.130)$$

$$\frac{\sigma T^4}{\pi} = B = \frac{3F}{4\pi} [\tau + q(\tau)] \text{ or } T^4 = \frac{3}{4} T_{\text{eff}}^4 [\tau + q(\tau)]. \quad (2.131)$$

The function $q(\tau)$ gives the nonlinear contribution to $B(\tau)$, thence to $I(\tau, \mu)$, which permits the boundary conditions (2.123) to be satisfied. One obtains the exact relation

$$q(0) = \frac{1}{\sqrt{3}} \quad (2.132)$$

for the boundary value. So we have

$$\frac{\sigma T_0^4}{\pi} = B(0) = \frac{\sqrt{3}}{4\pi} F. \quad (2.133)$$

So: in place of eq. (2.104) for the linear solution, we have

$$T_0^4 = T_{\text{eff}}^4 \frac{\sqrt{3}}{4}, \quad (2.134)$$

which is some 15 percent less, in T_0^4 —or some 4 percent less in T_0 —than the result from the linear solution: for the Sun, this is about 250° . As we shall see, this effect is significantly less than the effect of nongrayness coming from both the effect of another continuum and from the presence of spectral lines, under RE and LTE-R; and considerably less than nonLTE-R or mechanical heating effects. Also note, from eq. (2.131), that $T \sim T_{\text{eff}}$ at $\tau = 2/3$.

Also, we obtain the relation between $I(0)$ and μ in the form:

$$I(0, \mu) = \frac{3F}{4} \left(\mu + Q + \sum_{\alpha=1}^{n-1} \frac{L_\alpha}{1 + k_\alpha \mu} \right). \quad (2.135)$$

Thus we see that I departs from a simple linear dependence on μ , reflecting the “surface terms,” $\exp(-k_\alpha \tau)$, entering the depth-dependence of the temperature. The linear μ term reflects the general outward flow of the radiation, and is not primarily a surface effect, as seen by its independence of the k_α . Recalling our discussion of the relation between $I(0, \mu)$ and $B(\tau)$, centering on eqs. (2.12) and (2.26), we see that it is precisely the nonlinear, surface terms (L_α, k_α) that introduce departure from the linear model, LTE, and the linear diagnostic relations (2.26).

In the LTE, linear, case, we stressed that it is its linear nonEquilibrium thermodynamic character that permits us to translate the observed integrated flux into the temperature distribution, not just a boundary temperature. That is, the linear nonEquilibrium condition (2.89), which relates flux to gradients of thermodynamic state-parameters, via the linearity condition (2.99) acting on eq. (2.97), establishes a relation (2.102), between T_{e0} and $(dT/d\tau)_{\tau=0}$. Consequently, the value of one parameter alone, the integrated flux, specified these two quantities. That is, this imposed condition of linearity replaces the physical boundary condition of no incident radiation, at any angle, falling on the atmosphere—which the linear LTE case cannot satisfy, as we saw. One does not know, a priori, in any particular case whether this linear condition (2.89) is satisfied; it is wholly an a priori speculative definition of a mathematical configuration, which one must then ask if it can be satisfied. Here, the answer is “no,” because it cannot satisfy the physical condition (2.123). But we see that the less-restrictive, nonlinear, LTE-R case removes the need to impose such linearity (2.89). Then it, also, specifies both boundary temperature and temperature gradient—again in a form where the gradient is a function independent of the particular flux or boundary-temperature except for a scale-factor—for this particular case of a ν -independent opacity. This imposed “grayness” is again a thermodynamic constraint; so we continue our evolution toward asking effect on T_e -distribution as we remove more and more such constraints.

The LTE-R model describes better the upper atmosphere than does the LTE, by removing an imposed linearity. The result is to introduce a steeper T_e -gradient and a lower T_{e0} . Numerically, the result is small, for the Sun: T_{e0} changes from 4850 K for the linear case, to 4650 for the nonlinear. We place this change in numerical perspective by noting that observationally, one finds values for T_{e0} , in the solar atmosphere, in the range 4000–4200 K, so that the further decrease required to model T_0 is some two to three times the above correction for nonlinearity. We further note that eclipse observations in the visual continuum at the solar limb show rises in T_e up to values exceeding some $10,000 \text{ K}^4$. So if we are to explain such results by LTE-R modeling, we can only hope to do so in terms of nongray opacity effects, in the continuum and in the spectral lines, and these must give first, a decrease, then a rise, of T_e .

⁴As we shall see in Chapter 3, the line spectrum of the solar outer layers show that this rise continues up to some 10^6 K ; so the problem is even greater. But here, I mean only to stress that a correct thermodynamic modeling must show both a further decrease, followed by a rise, over the gray atmosphere result, even for this star where that part of the continuum carrying by far most of the energy is indeed essentially gray. The goal is to put into focus that thermodynamic character of the atmosphere which can introduce these effects.

outward, relative to the gray case. Apart from this, there remains only the alternative of nonLTE effects, if we are to explain such behavior in terms of thermal modeling.

Strictly in terms of LTE-R modeling, we see that observations are both encouraging and discouraging toward explanations in terms of nongray effects. Under LTE-R, the central intensities of spectral lines should have the value of $B_\nu(T_e)$ at $\tau_\nu = 1$ in the line-center. Then, in the lines, one sees effectively to much more superficial layers; hence by eq. (2.93) or its equivalent, the line-flux should correspond to much smaller T_e than does the adjacent continuum. Roughly, the “gray” visual continuum corresponds to $T_e \cong T_{\text{eff}} \cong 5800$ K for the Sun. In a rough way, the strong hydrogen lines have central intensities some 15 percent of the continuum; but for the strong Ca II and Na I lines these are only some few percent. Near the center of the solar disk, the hydrogen Balmer H α observations correspond to some 4100 K, which is near the T_0 quoted above as inferred from the continuum. However, as one observes toward the limb, thus higher in the atmosphere, such inferred T_e values from the lines drop to some 3500 K. The same low values characterize the Ca II and Na I lines. Either the estimates from the continuum are much too high, and we must look for much greater nongray opacity effects on T_0 , or the use of the lines under this LTE-R assumption is invalid, and leads to erroneous models. We ask first what nongray effects in the continuum would predict.

As in all the preceding, we wish an approach which emphasizes the physics and does not get lost in computational details. The above comments on differences in regions of origin for different opacities, and our earlier discussions of linear and nonlinear, LTE and LTE-R regimes suggest just such an approach. To discuss a ν -dependent opacity, we must consider eq. (2.87a), instead of eq. (2.87b), which we used in treating the gray opacity. One can consider eq. (2.87a) either as an equation that specifies F_ν for given $T_e(\tau_\nu)$, or as an equation specifying $B_\nu(T_e)$, in terms of given $F_\nu(\tau_\nu)$ and some boundary value of T_e , at some atmospheric point. The first alternative gives F_ν , but what we want is T_e . The second alternative is useless, in discussing individual ν , because we have neither observational knowledge of $F_\nu(\tau_\nu)$, which would permit numerical integration to obtain $T_e(\tau_\nu)$, nor can we assume a constant F_ν , a relation which holds only in the linear atmospheric regions, to obtain $T_e(\tau_\nu)$ piece-wise. In the gray case, we resolved the problem by working only with integrated, total flux, which is constant in this classical atmosphere, and using the nonlinear approach only in the surface regions where T_e changes strongly with depth, as τ_ν goes from about 1 to very small, and also F_ν changes significantly with depth. If, now, the opacity can be represented as having, roughly, two values: one, which is roughly constant, in each of two spectral regions, and these two opacity values differ strongly, we can introduce a 2-gray approximation, which profits from this linearity, nonlinearity contrast and exhibits the effect of nongrayness. In those “lower” atmospheric regions where the small-opacity spectral region has τ_ν varying from about 1 to small values, τ_ν in the large-opacity spectral regions remains very large. So the large-opacity spectral region is essentially linear, in this lower atmospheric region; $dB_\nu/d\tau_\nu$ is small; $J_\nu \sim B_\nu$ and F_ν varies only slowly. In effect, in this spectral region, we have the first alternative on the use of eq. (2.87a); T_e determines F_ν , by B_ν determining J_ν . The flux is determined, in this spectral region, not used. By contrast, in the low-opacity spectral region, conditions are nonlinear; we can now use the second alternative on the use of eq. (2.87a); $T_e(\tau_\nu)$ is determined from the fluxes. Again, as in the gray case, we use these relations in integrated form, but integrated only over a limited spectral region. Thus, in this atmospheric region, the T_e -distribution is obtained by using only that flux to which the region becomes transparent, in passing from the bottom of the region to the top. Eventually, in the upper atmosphere, conditions become nonlinear in the large-opacity spectral region, and we repeat the procedure, noting that the flux in the low-opacity spectral region is constant here, because the opacity is too small for interaction with the material to change the flux. This is the basic physics; we proceed to the algebra. Again, I emphasize that the objective is to show what physical-thermodynamic features of “theory” correspond to what kind of observational features, so that from the observational summary-abstract in Chapter 3, and the detailed observational summaries of the other monographs, we can see which physical-thermodynamic features must form the basis of modeling.

ii. **Two-Gray Atmosphere: Two-Subregion Photosphere.** We consider the situation where the opacity is given by:

$$\left. \begin{array}{l} 0 < \nu < \nu_1 \quad d\tau_1 = -n_1 \alpha_1 dx \\ \nu_1 < \nu < \infty \quad d\tau_2 = -n_2 \alpha_2 dx \end{array} \right\} \alpha_1, \alpha_2 \text{ are gray} \quad (2.136)$$

$$n_1 \alpha_1 \ll n_2 \alpha_2, \quad (2.137)$$

and we write eq. (2.28c) as

$$\int_0^{\nu_1} [J_\nu - B_\nu(T_e)] n_1 \alpha_1 d\nu + \int_{\nu_1}^{\infty} [J_\nu - B_\nu(T_e)] n_2 \alpha_2 d\nu = 0, \quad (2.28d)$$

or:

$$n_1 \alpha_1 (J_1 - B_1) + n_2 \alpha_2 (J_2 - B_2) = 0, \quad (2.138)$$

where

$$\begin{aligned} J_1 &= \int_0^{\nu_1} J_\nu d\nu & B_1 &= \int_0^{\nu_1} B_\nu d\nu & J_{\nu_1} &= J_\nu (\nu < \nu_1) \text{ etc.} \\ J_2 &= \int_{\nu_1}^{\infty} J_\nu d\nu & B_2 &= \int_{\nu_1}^{\infty} B_\nu d\nu & J_{\nu_2} &= J_\nu (\nu > \nu_1). \end{aligned} \quad (2.139)$$

Then we distinguish the two subregions of this thermal, two-gray atmospheric model:

Lower photosphere:

$$\nu > \nu_1: J_\nu = B_\nu(T_e) \quad \text{because of LTE} \quad (2.140a)$$

$$\nu < \nu_1: J_1 = B_1(T_e) \quad \text{because of RE, eqs. (2.140a) and (2.28d).} \quad (2.140b)$$

That is, in this subregion, J_ν is fixed by $B_\nu(T_e)$ from eq. (2.140a), while $T_e(\tau)$ is fixed by the transfer equation in I_1 —hence, in J_1 —under the RE condition (2.140b). As we emphasized in Section a, the condition (2.140a), which is often called “monochromatic radiative-equilibrium,” comes not by imposing radiative-equilibrium, only from linearity of model—i.e., degree of nonisotropy of I .

Upper photosphere:

$$\nu < \nu_1: I_\nu, \text{ hence, } J_\nu, \text{ is fixed because } \tau_1 \ll 1. \quad (2.141a)$$

$$\nu > \nu_1: J_2 = B_2(T_e) + (n_1 \alpha_1 / n_2 \alpha_2) [B_1(T_e) - J_1 \text{ (fixed)}] \quad (2.141b)$$

and in the subatmosphere: the solution follows LTE.

Thus, we proceed to obtain the photospheric distribution $T_e(\tau)$ in two steps: first, a solution in the lower photosphere, following eq. (2.140); second, a solution in the upper photosphere, following eq. (2.141). The photosphere solution relates to the subatmospheric solution via the flux through the linearity condition (2.87). We have already

remarked that we cannot satisfy the correct transition to the ISM under any variety of LTE approximation, so we simply apply the outer-boundary conditions (2.100) and (2.101), which effectively correspond to isolating the star from the ISM, to the photosphere.

Lower photosphere: region 1:

If we integrate eq. (2.41c) over the range of $0 < \nu < \nu_1$, and apply eq. (2.140b), we obtain:

$$\mu \frac{dI_1}{d\tau_1} = I_1 - B_1(T_e) = I_1 - J_1 \quad (2.142)$$

instead of the same equation without the subscript 1, which we solved in the 1-gray, single subregion photosphere of Section i above. Following the 1-gray approach, the same Gaussian quadrature representation gives, similar to eq. (2.113), simply understanding I_i to be I_{1i} ,

$$\mu \frac{dI_i}{d\tau_1} = I_i - \frac{1}{2} \sum_{-n}^n a_j I_j. \quad (2.143)$$

We follow the same approach to the solution of eq. (2.143) as we did in solving eq. (2.113), via eqs. (2.114) – (2.124). Because we require the linear condition to be satisfied by $\nu > \nu_1$, we see from eq. (2.87a) that fluxes $F_{\nu 2}$ are individually constant, so that F_2 is constant; thus for RE and constant local flux F , we have also that the flux F_1 is constant. So, we apply eqs. (2.125) – (2.130) again, using, however, F_1 and B_1 with J_1 instead of F and B with J as in i . Thus, instead of a relation in T^4 , as in eq. (2.131) et seq., we obtain these relations in terms of

$$B_1(T_e) = T_e^4 \left[\frac{2h}{c^2} \left(\frac{k}{h} \right)^4 \right] \sum_1^{\infty} \frac{6}{n^4} - \sum_1^{\infty} \frac{e^{-nX}}{n} \left[X^3 + \frac{3X^2}{n} + \frac{6X^2}{n^2} + \frac{6}{n^3} \right] = T_e^4 \frac{15\sigma}{\pi^5} f_1(X_1), \quad (2.144)$$

where

$$f_1(X) = \sum_1^{\infty} \frac{6}{n^4} - \sum_1^{\infty} \frac{e^{-nX}}{n} \left(X^3 + \frac{3X^2}{n} + \frac{6X^2}{n^2} + \frac{6}{n^3} \right) \quad (2.145)$$

$$X_i = h\nu_i/kT_e.$$

So we would have, in place of eq. (2.131)

$$B_1(T_e) = (3F_1/4\pi) [\tau_1 + q(\tau_1)], \quad (2.146)$$

where F_1 is the flux in the band $0 < \nu < \nu_1$. Then an observed or proscribed F_1 fixes the T_e -distribution, especially T_{01} , the value of T_e in the region where τ_1 is small but τ_2 is still large, the “boundary-value” for the lowest photospheric subregion. Normally, F_1 would correspond to the flux observed in the visual spectral region.

If, now, F_ν in this region 1 could be represented by a blackbody distribution, or very near such corresponding to gray atmosphere and small T -gradient, so that F_1 could be represented as $T_{R1}^4 f_1(Y_{11})$, $Y_{11} = h\nu_1/kT_{R1}$, and if X_1, Y_{11} were large enough that $f_1(X_1)$ and $f_1(Y_{11})$ were essentially the same, then—since one obtains bolometric-corrections by extrapolating the visual continuum, to this approximation—eq. (2.146) would essentially reduce to

eq. (2.131). We would have essentially the relation (2.134) between T_{01} and T_{R1} . The subsequent T_e -drop across region 2 would give the 2-gray cooling, relative to the 1-gray.

Upper photosphere: region 2:

If the opacity ratio is very large, so that the second term in eq. (2.141b) is minor—e.g., corresponds to $\lesssim 50 - 100$ K change in $B_2(T_e)$ —then we have again the gray-body solution, in this region 2. Except, in place of eq. (2.144), we would have

$$B_2(T_e) = T_e^4 \frac{15\sigma}{\pi^5} \left\{ \sum_1^{\infty} \frac{6}{n^4} - f_1(X_1) \right\}, \quad (2.147)$$

and, since F_2 , the total flux minus F_1 , is constant in this region 2, we have, following the same procedure as above:

$$B_2(T_e) = (3 F_2/4\pi) [\tau_2 + q(\tau_2)]. \quad (2.148)$$

Again, if F_2 could be represented as $T_{R2}^4 f_2(Y_{12})$, $Y_{12} = h\nu_1/T_{R2}$, and if the bracket on the RHS of eq. (2.147) were essentially the same for X_1 and Y_{12} , then we would again have the relation (2.134) between T_{02} and T_{R2} . Furthermore, while T_{R1} corresponds to the visual flux, so does T_{R2} correspond to the flux in the high-opacity region, so T_{R2} is essentially T_{01} .

Thus, subject to the very strong approximations made:

$$\text{region 1: } T_e^4 = \frac{3}{4} T_{R1}^4 [\tau_1 + q(\tau_1)] \quad (2.149a)$$

$$T_{01}^4 = \frac{\sqrt{3}}{4} T_{R1}^4;$$

$$\text{region 2: } T_e^4 = \frac{3}{4} T_{01}^4 [\tau_2 + q(\tau_2)] \quad (2.149b)$$

$$T_{02}^4 = \frac{\sqrt{3}}{4} T_{01}^4 = \frac{3}{16} T_{R1}^4.$$

So, crudely, and in a very lower limit, the boundary-temperature in this 2-gray approximation is about 0.66, or 2/3 the "color-temperature" of the visual continuum, in contrast to the 0.81, or 5/6, in the 1-gray case.

It is clear that these crude values for the LTE-R case are lower limits on T_{02} for this 2-gray case, for two reasons:

First: Because T_e decreases outward, and because T_{Ri} is effectively T_e at a lower atmospheric level than that considered, $X_1 > Y_{11}$, Y_{12} . Thus numerically:

The RHS of eq. (2.149a) will be multiplied by a factor less than 1, but the correction is not large for $X_1 > 1$. If we take ν_1 at the head of the Balmer continuum, $X_1 = 7$ for the Sun; 2.5, for $T_{\text{eff}} \sim 15,000$ and about unity for a B0 star, where the correction to f_1 will be some 10 percent.

On the contrary, the RHS of eq. (2.149b) will be multiplied by a factor significantly greater than 1: essentially $[Y_{12}^3 \exp(-Y_{12})]/[X_1^3 \exp(-X_1)]$. So, the actual T_{02} will be higher than the estimates from eq. (2.149b); but T_{01} will be lower than the estimates from eq. (2.149a).

Second: From the complete form of the RE condition in this 2-gray case, eq. (2.28d), we see the consequence of our above neglect of the term $(n_1 \alpha_1 / n_2 \alpha_2) [J_1 (\text{fixed}) - B_1 (T_e)]$ in applying eq. (2.141b) to obtain the equivalent of eq. (2.142) in region 2. As T_e decreases upward, this neglected term will make a positive numerical contribution to eq. (2.28d), requiring T_e to rise, above the solution without the term. We can see this easily by rewriting eq. (2.138) as:

$$B_i (T_e) = J_i (\text{fixed primarily by lower regions}) + [n_k \alpha_k / n_i \alpha_i] [J_k - B_k (T_e)]. \quad (2.138a)$$

i) If we consider $i = 1, k = 2$, then we obtained the results (2.149a) by ignoring the correction term in eq. (2.138a) by virtue of $J_2 = B_2$ from the locally opaque condition. As one moves upward in the atmosphere, between regions 1 and 2, the local opacity condition begins to fail. Also, as is the case when the opacity in region 1 is H^- but Balmer bound-free in region 2, $n_2 \alpha_2 / n_1 \alpha_1$ increases, because $n_1 \sim n_H n_e$ while $n_2 \sim n_H$, thus the ratio increases outward as $(\text{density})^{-1}$. Thus, the correction term is positive because $J_k > B_k$ as T_e decreases outward, and its size increases outward. So, B_i and T_e can, under the correct combination of circumstances, increase outward.

ii) If we consider $i = 2, k = 1$; then we obtained the results (2.149b) by ignoring the correction term in eq. (2.138a) from the condition that $(n_1 \alpha_1 / n_2 \alpha_2) \ll 1$. Because T_e decreases outward, the term $(J_1 - B_1)$ becomes increasingly positive; its presence slows the rate of outward decrease in B_2 and T_e ; under the correct circumstances, it can even cause T_e to increase outward, *locally*.

Clearly, such a 2-gray extension of the 1-gray case can be further extended to n -gray models, approximating non-gray situations by a series of opacity plateaus, to make simple but rough estimates of conditions in the outer photospheric subregions of these classical models. As already mentioned, our interests in such rough estimates are essentially two: (1) What, actually, is the T_e -minimum which such models can produce. For peculiar hot stars, like the Be and the WR, can T_e decrease significantly from photospheric values to produce significant hydrogen $H\alpha$ in the outer photosphere? For the cool stars, can T_e decrease significantly to produce farIR excess, and dust? (2) How large a T_e -rise above this minimum can these models produce? For the solar-type stars like the T Tauri, we ask if T_e can increase significantly, to produce emission $H\alpha$ without an extended atmosphere. For the hotter stars, and some intermediate ones, we ask whether such apparently superionized ions like C IV can be produced in thermal standard models. And with this range of T_{e0} values, we ask whether the atmospheric density gradient can be reduced sufficiently to produce atmospheres of sufficient extent to produce the observed hydrogen Balmer emission lines, for both hot and cold stars, across the HR diagram. We recall that under thermal LTE modeling and taxonomy, the hydrogen lines reach maximum strength near spectral type A0, $T_{\text{eff}} \sim 10,000$ K. We return to these questions in Chapter 3, using the results from this Chapter 2.

So we reach the very crude estimates, for the several opacity subregions of this classical, LTE-R photosphere, of the limits on T_{0k} , in the upper photosphere:

$$T_{\text{eff}}^4 (\text{or } T_{\text{Rvis}}^4) > T_{0k}^4 > (\sqrt{3}/4)^k T_{\text{Rvis}}^4. \quad (2.150)$$

For perspective, such limits can be compared with the modern calculations of such classical atmospheres by Auer and Mihalas (1969b) for a $T_{\text{eff}} = 15,000$ K, $\log g = 4$, mid-B star model composed only of hydrogen, and with only continuous opacity. Table 2-2 exhibits four values of T_e : T_{R1} or T_{eff} ; T_{01} (Paschen continuum non-opaque); T_{02} (BaC non-opaque); T_{03} (LyC non-opaque).

Table 2-2
Limits on T_{e0} in Hydrogen Opacity Subregions

	Lower Limit: Eq. (2.150)	Auer-Mihalas (1969a)
T_{R1}	15,000 K	15,000 K
T_{01} (PaC)	$< 12,200$ K	11,300 K
T_{02} (BaC)	$> 9,900$ K	10,400 K
T_{03} (LyC)	$> 8,000$ K	9,400 K

Clearly, from this crude approach, a sufficiently extensive set of independent, and differing, opacities would give a correspondingly extensive set of opacity subregions, and an almost arbitrarily low drop in T_{e0} (min), until those processes mentioned above, which produce an inversion of dT_e/dh , are effective. As an example of such extension of opacity subregions, we could combine all spectral lines whose $n_i\alpha_i$ values were roughly the same, and add their effect to that of the continuum, to obtain a "line-blanketing" depression of the boundary-temperature. Essentially, this was the method of the "picket-fence" perturbation, by lines, of the gray-atmosphere continuum model by Chandrasekhar and Munch (1946). It also embraces the attempt by Böhm-Vitense (1954) to match the apparent, under LTE diagnostics of the hydrogen Balmer lines, drop in the solar T_e (min) to something below 3500 K. The above-cited LTE-R computations of Auer and Mihalas illustrate very well the approach. For this case (15,000 K, $\log g = 4$), by including only the hydrogen H α line, they obtain a drop to T_e (min) = 7800 K. The actual illegitimacy in such use of the hydrogen lines, in either diagnostics or modeling, lies in nonLTE effects (Thomas, 1949, 1957, 1961, 1965; Jefferies and Thomas, 1958; Pottasch and Thomas, 1960; Jefferies, 1968; Gebbie and Thomas, 1971; Auer and Mihalas, 1969 a, b, c, d, 1970; Mihalas, 1970, 1978; Gebbie and Steinitz, 1974; Vernazza, Avrett, and Loeser, 1981). The basic "halt" to such a monotonic outward decrease in T_{e0} with added number of opacity subregions, in such LTE-R atmospheric models, comes from the processes mentioned. In Section 3 and Chapter 3, we explore whether this kind of rise in T_e , or a nonLTE rise, or a nonthermal mechanical heating, or all three are what represent the observations.

The present kinds of T_e -rise have been demonstrated in LTE-R model calculations by Feutrier (1968), Hill (1972), and others; but they are most usefully illustrated here by the results of Dumont and Heidmann (1973). They consider atmospheres with only H and He contributing to the opacity, but with representative metals contributing to n_e ; with $5000 \text{ K} < T_{\text{eff}} < 15,000 \text{ K}$; and $2 < \log g < 5$. They obtain such an LTE-R rise in T_e only for $T_{\text{eff}} \lesssim 8000 \text{ K}$; for in such atmospheres, the deepest photospheric subregions are effectively gray, H $^-$ dominating, with the outward density decrease eventually producing subregions where hydrogen bound-free opacity dominates. In the 15,000 K atmosphere, no significant H $^-$ appears, and the several opacity subregions corresponding to Paschen (PaC), Balmer (BaC) and Lyman (LyC) continua do not suffice to produce such a T_e -rise in this LTE-R atmosphere. These results are supplemented by those of Auer and Mihalas, in the cited references for the hotter-star models: $T_{\text{eff}} = 12,500 \text{ K}$ and 15,000 K, $\log g$ ranging from 2.5 to 4. The addition of hydrogen lines gives only a further drop in T_{e0} (min), no outward rise in T_e , in any subregion. Their extension of these results to the even hotter O stars again shows no T_e -rise, under LTE-R models, in the outer photosphere; nonLTE effects are required. We consider these, in the following Section 3.

This summary of the LTE-R standard modeling exhibits the pattern I follow here. I try to abstract the thermodynamic essentials, of the approximation, then establish limits, which depend on these thermodynamic essentials, which require trivial computational sophistication, but which suffice to exhibit the presence and gross size of the observational anomalies of Chapter 3, to answer the question of the physical adequacy of such standard thermal modeling. Obviously, for any great precision on the detailed structure of such standard models, one turns to modern investigations which, using modern computing facilities and software, have provided exhaustive results. One need make none of the above simplifying assumptions on angular and frequency dependence. The amount of information on

atomic properties one incorporates—to treat line-blanketing, for example—simply depends on machine storage capacity. The comment earlier quoted from Mihalas summarizes the situation, regarding LTE-R thermal modeling, very well. One should consult his reference texts (1970, 1978) for the approach and techniques. Such detailed programs as ATLAS, for treating line-blanketing LTE-R models (Kurucz, 1970) are available to learn and to use. There are extensive tables of results in the literature, including those by Auer and Mihalas (loc cit); Mihalas (1972); Klinglesmith (1971); Kurucz, Peytremann, and Avrett (1973); Kurucz (1979).

3. The “Neoclassical” Speculative-Theoretical Atmospheric Models

a. Overall Perspective and Physical Picture. Like the varieties of classical models, these neoclassical ones impose the thermodynamic conditions of HE and RE to determine the distribution throughout the atmosphere of a wholly thermal mass and energy storage. Models differ in the proscribed microscopic partition of such mass and energy. *The classical plus neoclassical sequence of varieties of models is based on allowing successively greater departures from the degeneracy of the TE, and strict LTE, configurations* under which the thermodynamic and statistical-mechanical descriptions are equivalent for describing this microscopic partition of the local energy and mass storage. As we continuously stress, *such degeneracy is exhibited by the ability to define local distribution functions for microscopic quantities wholly in terms of local values of a set of macroscopic, LTE, state-parameters.* Such approximation may suffice far from boundaries. But an atmosphere, which is the transition-zone replacement of a boundary, requires sequential approximations, permitting successively increasing dependence of such local microscopic distribution functions on the distribution over this transition-zone of such macroscopic state-parameters, as one goes farther into the regions. Essentially, such a dependence of local energy populations on distant regions is introduced by a dependence on local radiation field. Self-consistency then requires whole-atmosphere coupling between radiation field and populations. This is the heart of nonLTE modeling. One function of this thermal atmosphere is to transmit a fixed flux of radiative energy, imposed from the subatmosphere. We ask how the degree to which the local energy partition depends upon the radiation field affects the structure of an atmosphere having such a function. We give a physical picture, then details.

In the TE (and strict LTE) configurations, such degeneracy arises from two things: the spatial homogeneity (and near-homogeneity) in values of thermodynamic parameters; and the condition of detailed balance (and near-detailed balance) of all microscopic reactions. Homogeneity permits no *space-fluxes* of matter or energy; detailed balance ensures no *state-fluxes*, as we earlier defined these. Strict LTE corresponds to infinitesimal, rather than zero, spatial inhomogeneity and departure from detailed balance. Such inhomogeneities, and departures in radiative microscopic reactions, are the only ways, respectively, to sustain the space-fluxes of matter and energy from the star to the ISM and ourselves, and to produce any change in the spectral energy distribution of the radiation field as it traverses the atmosphere. So, the sequence of models successively increases the possibility for spatial inhomogeneity, hence space-fluxes, and for departures from detailed balance, hence state-fluxes, to increase the influence on microscopic distribution functions of the distribution of state-parameters. Given a population dependence upon radiation field, inhomogeneities and nondetailed balance arise naturally near boundaries.

In Section 2, we saw that the varieties of classical models focused on increasing generality for photon distribution function, corresponding to admitting the effect of space-fluxes and departure from detailed balance in radiative processes. Local T_e and density sufficed to describe local states of matter, but not of radiation. In this Section 3, the varieties of neoclassical models focus on increasing generality for distribution functions over particle internal energy states, corresponding to admitting, also, departure from detailed balance in collisional process. Local T_e and density do not suffice to describe the local states of either matter or radiation.

Then, we note two “degeneracy” features that are retained, in all these thermal models, which greatly simplify the theoretical specification of microscopic mass and energy states. First, in the low-density and low-energy environment of stellar atmospheres, and especially in these wholly thermal models, occupation numbers of mass states are fixed: these are the relative chemical abundances for a given total quantity of matter. Density and energy are “low” relative to conditions in the interior, where nuclear reactions take place and, over evolutionary times, change such

relative abundances within a given star. (There are some theoretical proposals of nuclear reactions in nearly atmospheric regions, resulting from mass-exchange in binaries and accreting disks, to initiate novae, other cataclysmic, and symbiotic phenomena, cf Chapter 3 and Part III. This would change the simple situation of frozen-in mass-states considered here.) So, here, a local thermodynamic mass parameter, the density—for given chemical composition—unambiguously characterizes all models. In the same way, all these classical and neoclassical models impose TE distribution functions for all microscopic particle velocities, eq. (2.61). Further, they impose that the same kinetic-temperature parameter characterizes all kinds of particles; we take it as the electron kinetic-temperature, T_e . So the local value of a single thermodynamic parameter, T_e , describes both the local kinetic energy storage, and thermodynamic pressure, eq. (2.35), per particle. How broadly useful, and sufficient is the local value of T_e , in combination with that of the density, to describe the local populations of the other particle and photon energy-storage modes, distinguishes the successive approximations in the sequence of models.

Then, we recall that the LTE classical model proscribed that the local values of T_e and density suffice to specify the local populations of energy states for photons, by imposing $J_\nu = B_\nu(T_e)$, and of internal energy states for particles, by imposing eqs. (2.62) and (2.63). Such a configuration is less restrictive than TE only in the freedom given I_ν to be anisotropic in place of its TE isotropy, where I_ν , rather than only J_ν , equals $B_\nu(T_e)$. So, in contrast to the homogeneous TE, where the fluxes are zero, LTE permits nonzero values of the fluxes, because I_ν is permitted to be anisotropic. By contrast, particle motions are imposed isotropic, locally; no thermal particle fluxes are permitted. An LTE atmosphere can transmit the energy produced by the star *only radiatively, and only because of a T_e -gradient*. But LTE is unnecessarily strong for the RE proscription; it permits the individual F_ν to be constant, not just the integrated F_ν . So to restrict the atmospheric distribution of T_e to that which produces constant F_ν for all ν demands too much. We note that it would require the star to impose, at the bottom of the atmosphere, precisely those fluxes, F_ν , sent to the ISM and the observer. We discussed the implication of such specification in Section 2.a. Here, we simply put into focus what such a “scattering” character of the radiative transfer problem— $S_\nu = J_\nu$ —in this LTE atmosphere implies. What means this derived character, resulting because each of S_ν and J_ν is proscribed equal to $B_\nu(T_e)$? Physically, scattering simply means there is no thermal energy transfer when photon and particle interact. *Either there is zero coupling between thermal states of photons and particles, so no possibility of energy interchange; or there is complete coupling, and zero interchange means they are in the same thermal state.* And physically, we imposed the latter, by proscribing that all populations, and all rate-controlling radiative fields—angle-averaged radiative intensity and isotropic collision velocities—have their TE forms, and are fixed by a common TE parameter, T_e . The energies of all these storage modes are absolutely coupled, as in TE. Formally expressed, we have, locally, detailed balance in all microscopic processes; there are no state-fluxes, radiative or collisional. *So we see that imposing the condition of no local state-fluxes, requires that there be no local change in space-flux. A space-flux imposed by the interior does not change, is only transmitted, by “scattering.”* It does not affect the local thermal state because it is imposed to be completely coupled to it; and the partition process is TE, thus independent of details of capacity of storage mode. We have already used this, implicitly, in discussing the two-gray atmospheric region approximation, in Section 2.b. We will use it continuously, enlarged beyond the restriction to TE storage modes, in comparing the influence of space- and state-fluxes in producing various spectral features. Here, we see that a space-flux in J_ν , in this LTE model, requires a space-gradient in S_ν , hence directly in T_e ; but the particular space-flux, and the particular space-gradient are too greatly restricted by prohibiting the possibility of a state-flux in microscopic interactions. This last prohibition is implicit, resulting from prescribing a too-local dependence of the microscopic distribution function for photons upon macroscopic state-parameters.

The LTE-R classical model removes the proscription that the local photon distribution function be specified by the local value of a macroscopic state-parameter, but retains it for particle internal energy states. Thus, it permits state-fluxes in radiative processes, but prohibits them in collisional processes. Again, it obtains space-fluxes in J_ν , hence nonzero values of F_ν , by permitting space-gradients in J_ν . But it contrasts to the LTE model, where the condition $J_\nu = B_\nu(T_e)$ requires that local energy storage in photons and particles be described by the same single temperature parameter, hence that space-gradients in J_ν and $B_\nu(T_e)$ be precisely the same; hence a space-gradient in J_ν requires one in $B_\nu(T_e)$, hence that a nonzero F_ν implies a nonzero gradient in T_e . The LTE-R models differ. It is not

imposed that local energy storage in photons and particles be described by the same local temperature-parameter. There can be a space-gradient in photon storage without one in particle energy storage—simply because of the presence of the open boundary. I_ν from the outer hemisphere falls below that from the inner, directly because of the lesser optical thickness of the outer hemisphere, even for constant S_ν ; in consequence, J_ν decreases outward. So if some processes, not depending upon the radiation field, can maintain S_ν constant, we can see the extreme example of this contrast to the LTE situation: *a space-gradient in J_ν does not always require one in S_ν . There can be a radiative flux without a temperature gradient*, in LTE-R. We have, for such constant S_ν :

$$J_\nu(\tau) = \oint \frac{d\Omega}{4\pi} \int_0^{\tau(\mu)} S_\nu(\tau_\nu) \exp[-(t_\nu - \tau_\nu)/\mu] dt/\mu = W_\nu(\tau) S_\nu(\text{constant}), \quad (2.151)$$

$$W(\tau) = 1 - 0.5 [e^{-1} - \tau E_1(\tau)]. \quad (2.152)$$

So, under LTE-R, in such an iso- S_ν atmosphere, there is no space-gradient in T_e nor in particle-energy storage; there is, in photon energy storage.

As the considered point, at τ , goes progressively deeper into the atmosphere, J_ν increases, traverses LTE, and finally reaches the homogeneity of TE. State-fluxes approach zero, at interior points; they are nonzero only in the outer, LTE-R, part of the atmosphere, approaching the boundary. So there is a gradient in space-flux, in the LTE-R region, which demands nonzero radiative state-fluxes. There is a departure from detailed balance in microscopic radiative processes, because J_ν departs from B_ν ; but there is no such departure from detailed balance in microscopic collisional processes, because S_ν is proscribed equal to $B_\nu(T_e)$. We emphasize—*the departure from detailed balance in radiative processes, the admission of state-fluxes in radiative processes, comes from that space-gradient in J_ν which is produced simply by the presence of a boundary, in even an isothermal atmosphere, when one removes the proscription of an LTE form $J_\nu = B_\nu(T_e)$ on the photon distribution function*. The presence of the boundary “naturally” introduces this space-gradient in J_ν , as τ decreases outward. So, an imposition of LTE in this region, demanded by the boundary to be LTE-R, would be physically illegitimate and diagnostically misleading. If we did impose LTE, and an LTE diagnostics, and had some way to measure J_ν at each depth τ , then we would follow the illegitimate and erroneous diagnostic sequence: (1) Define a T_{rad} by $J_\nu(\tau) = B_\nu[T_{\text{rad}}(\tau)]$; (2) Infer $T_e(\tau) = T_{\text{rad}}(\tau)$; (3) Conclude, erroneously, that T_e increases inward, from these measured J_ν , which would follow eq. (2.151). We could “cure” this inconsistency by discarding LTE. We continue this query on physical and diagnostic self-consistency to the transition from LTE-R to nonLTE, but first make two remarks on this proscribed iso- S_ν situation that we used for illustration.

(1) The essential aspect of the proscribed situation is that “something” maintain a constant S_ν —i.e., a constant T_e under LTE-R—in some way that it is independent of J . Clearly it is not the condition RE; under this, J and S are related by $\int \alpha_\nu J_\nu d\nu = \int \alpha_\nu S_\nu d\nu$.

Moreover, the iso- T_e configuration is incompatible with a constant radiative flux, imposed in the subatmosphere. This iso- T_e atmosphere only “cools” at the surface, radiatively; something other than radiation transports any energy from the subatmosphere to balance such surface radiative emission. The “pure-scattering” imposed by LTE—corresponding to monochromatic RE—cannot be responsible for maintaining S_ν constant and independent of J_ν . Under it, J_ν and S_ν are, thermally, either completely coupled, $J_\nu = B_\nu(T_e)$, or completely uncoupled, $S_\nu \neq B_\nu(T_e)$; but locally $S_\nu = J_\nu$. Under such thermally-uncoupled scattering, there would be a further outward decrease in J_ν , unrelated to a T_e decrease, corresponding to the coupled τ -dependence of S_ν , in eq. (2.151). So, under such scattering, and again applying the illegitimate LTE configuration and diagnostics, we would incorrectly infer an even greater outward decrease in T_e . So in the general, noniso- S_ν , situation we must be sure that whatever the mathematical formulation of it that is adopted, the two sources of a J_ν -gradient can be distinguished: boundary, and “intrinsic” variation of S_ν —i.e., that not coming simply from a coupling to J .

(2) In this proscribed situation, the local radiation field has no effect on local populations of energy states of the particles. S_ν is proscribed to be $B_\nu(T_e)$, and S_ν is proscribed to be independent of J_ν . However, the distribution of relative populations of particle energy states over the atmosphere has a primary effect on the local photon partition through the factor S_ν ; and the boundary—or transition-zone to the ISM—has an effect through the τ -dependence of the factor W_ν in eq. (2.151). Pragmatically, as shown by the particular example, the preceding shows that in this LTE-R model—as contrasted to the LTE—the local radiation field is indeed affected by distant regions of the atmosphere, via the effect of the τ -distribution of T_e . But for the same reason it is also affected by the presence of the transition-zone, independently of the T_e -distribution in the other hemisphere. However, the local particle energy states are affected only by the local value of T_e , no matter how T_e is determined, and are independent of the distribution of the material, i.e., of any boundary. If the value of T_e is independent of the boundary—so also will that of S_ν , and conversely. There is not permitted, under LTE-R, any wholly boundary effect on S_ν that is independent of the value of T_e . No J_ν , by itself, because of some microscopic reaction involving J_ν , is permitted to affect the value of S_ν . If, as under RE, the local T_e is fixed by the local integrated radiation field, then there is an influence of J on S_ν —but only in this indirect way. Photon partition can change drastically near the boundary—i.e., in the transition-region established by the decrease of τ , even if it is an isothermal region. S_ν cannot change drastically at a boundary, or a transition-zone, established by the decrease of density, of an isothermal region, *by proscription, not by investigation*.

So this discussion of the transition from an LTE to LTE-R model of an isothermal atmospheric region near a boundary puts into focus the essential reason for exploring nonLTE models: to permit a better description of the boundary, or transition-zone, regions of the star by removing an arbitrary proscription of populations of particle energy states. Also, eq. (2.151) shows that the term “transition-zone” is a better one than boundary. In this particular isothermal situation considered, where T_e is maintained constant by something other than the radiation field, $W_\nu(\tau_\nu)$ measures the extent of the transition-zone—which we note can be of different geometrical extent at different ν , if the absorption coefficient is nongray. In more general situations, where there is a T_e -gradient—especially one maintained by RE—the effect of the “opacity” transition from quasi-isotropic to nonisotropic I is mixed with that of space-gradient in S_ν , hence in T_e under LTE-R.

This suggests that we explore the necessity for, and the region of, a possible transition from LTE-R description to a nonLTE description by continuing to look at an isothermal atmospheric region, and asking the behavior of S_ν near the boundary—or a transition-region formed by decrease in density, or opacity, or etc. But of course such a region is just that in the upper parts of the photosphere, where all the standard models give an asymptotic T_{e0} , and exponential density decrease. The preceding also suggests that if indeed there is a boundary effect on S_ν , then a diagnostic based on applying LTE-R diagnostics to an actual nonLTE atmospheric region should give an erroneous T_e -distribution, as in the above-discussed case of falsely applying an LTE diagnostics to an LTE-R situation. Here, however, such an empirical test is much easier, because it focuses on I_ν rather than J_ν . That is, eqs. (2.10) to (2.14) give that $I_\nu(\tau=0) = S_\nu(\tau_\nu \sim 1)$. So we only need compare the intensity at some observed ν to the S_ν predicted by the model, and ask whether they are consistent. And, we have a wide range of observational conditions, from the continuum to the centers of the strongest lines, in a variety of stars, especially the Sun. Thus, we have an *empirical-theoretical* approach to the necessity and utility of nonLTE atmospheric modeling. Empirically, we can compare observed radiative intensities to model predictions. Theoretically, we can compute the various microscopic rates which determine populations of particle energy levels, and compare the results to the LTE-R demand of overwhelming dominance by collisions. Then we can combine the two to develop a self-consistent nonLTE approach, which, empirically, gives a correct distribution of T_e , and which, theoretically, gives an interpretation of such T_e -distribution in terms of its thermodynamic significance.

Just as the LTE to LTE-R transition marked the influence of a boundary on photon distribution function via the opacity-gradient effect, so we might expect the LTE-R to nonLTE transition to mark the influence of a boundary on particle distribution function via the density-gradient effect on collisions. The validity of LTE-R, classically, depends upon strong domination by collisional over radiative processes. However, the development of contemporary atmospheric modeling and diagnostics under thermal nonLTE follows this logic only for exceptional ions. For most ions, it is again the opacity effect at the boundary which gives the LTE-R to nonLTE transition; collisional-dominance

of the source-function disappears well below the region where LTE-R continues to be a reasonable approximation. The radiation field in the transition dominates. The problem is, what are the microscopic processes that fix the value of this radiation field? Again, we give first a physical picture, based on considering the line source-function, for which such nonLTE was first considered. Then we treat specific examples, contrasting the exceptional case of continuous opacity from H^- with that from hydrogen, then with the lines, and finally with line-blanketing.

i. Historical Dilemma on LTE-R to NonLTE Evolution. Pannekoek pointed out in 1930 that inelastic collision rates are too small, relative to radiative, to permit LTE-R in at least the upper parts of stellar photospheres. Oversimplified forms for the source-function of an atom having two discrete levels and a continuum showed that none of the three processes—radiative transitions at ν , collisional processes at ν , photo-ionizations and recombinations involving the two levels separated by ν —could generally be neglected (Milne, 1930; Stromgren, 1935). There was a long hiatus in self-consistent, thermodynamic investigations of the source-function in “normal” stellar atmospheres. Instead, spectral diagnostics were made on the basis of ad hoc forms for the line source-function, and LTE-R for modeling atmospheric structure and solving radiative-transfer equations in the continuum to obtain T_e -distribution under RE. The resonance lines were considered to be formed in pure-scattering; only the radiative transition in the line was retained in the source-function. Various authors argued that the scattering should be noncoherent—radiation absorbed and emitted at different ν within the line—rather than coherent, as proposed by Milne. Other astronomers took a linear combination of scattering and collisional terms—sometimes including the photo-ionization terms—to use a hybrid source-function, characterized by the weights assigned the several terms, which were all treated as mutually-independent. A variety of temperature parameters were introduced to represent thermodynamically inconsistent results obtained from these LTE-R diagnostics. The schools developed by Unsold at Kiel and Minnaert at Utrecht argued that two-level atoms were oversimplified, and that when all microscopic processes were taken into account—at least for nonresonance lines— S_ν reduces to its LTE-R form (Unsold, 1952; Bohm, 1960; a perspective on the errors in these attempts to preserve LTE-R is given by Thomas, 1961, 1965). Mainly, however, these combined ad hoc and LTE-R models were used to interpret the observed total intensities in spectral lines, to derive abundances and these several kinds of temperatures. The models were mainly applied, not investigated for self-consistent thermodynamic validity (cf Unsold, 1938, 1955; and Aller, 1953, 1963).

ii. Resolution of Dilemma on LTE-R to NonLTE Evolution. This study of the evolution from LTE-R to nonLTE in the lowest atmospheric region, the photosphere—presumably as the result of diminishing collisional dominance of the source-function—was placed back in perspective by nonLTE studies of the farthest outer-atmospheric region, whose existence is not compatible with the thermodynamic basis of standard atmospheric models—the planetary nebular region (cf Chapter 3). There, for years, the nonLTE studies by Rosseland, Cillie, Menzel, Aller, Baker, Goldberg focused on complete radiative control of particle populations and source-functions. The exception was the introduction by Bowen of a prototype kind of “line-blanketing effect”—a collision-dominated one—the impurity cooling by forbidden lines of oxygen and nitrogen. The effect was to reduce the nebular RE temperature predicted from such wholly radiative control, from $\approx 10^5$ K to $0.5\text{--}2 \cdot 10^4$ K, by the effect of collisions. Attempts were made to extend, downward, these nebular nonLTE studies to the atmospheric region just above the photosphere, the chromosphere. Wholly radiatively-controlled nonLTE configurations were discussed by Menzel and Cillie (1935, 1937). Continuing this work of the Harvard group, the problem was re-examined from nonEquilibrium thermodynamic first principles, not imposing, a priori, any restriction on radiative or collisional control, by myself and a number of colleagues (Thomas, Jefferies, Matsushima, Athay, Whitney, Zirker, Pottasch, Orrall) with application to the Sun, WR, novae, cepheid, and other stars. Because the approach was empirical-theoretical, we tried to tie it solidly to good data, and a practical application, which we were able to do by virtue of the superb design and execution of observations of the 1952 solar eclipse by a High Altitude Observatory group led by Evans and Roberts. These continued into complimentary $H\alpha$ solar limb studies at the Sacramento Peak Observatory by Dunn, and eventually E.vP. and H. Smith, who also linked such studies to the WR phenomena. These empirical-theoretical results on the jointly-developed modern nonLTE approach, and on a model of the lower solar chromosphere based on them, are summarized by Thomas and Athay (1961), and the

references given there, with elaborations on the nonLTE methodology by Thomas (1965) and Jefferies (1968), again with the references given there. From these developments of the nonLTE approach downward from wholly radiatively-controlled regions, in the far outer-atmosphere, adding collisions to the nonLTE equations of thermal equilibrium and asking how their effect appears, we can resolve the problem outlined above when discussing the evolution from LTE-R to nonLTE regions as we approach a boundary. We put the thermodynamics in focus by considering first those spectral regions in which we see farthest out in the atmosphere: the central regions of strong lines from abundant elements.

For simplicity of discussion, I simply reproduce here what has become, since its introduction (Thomas, 1957, 1965) the standard form for the ν -independent line source-function of an atom with two discrete levels and a continuum. It serves to put these earlier, ad hoc, representations of S_ν into perspective. The derivation is in Vol. 2.

$$S_\nu = \frac{\int \Phi_\nu J_\nu d\nu + \text{source-term}}{1 + \text{sink-term}} = \frac{\bar{J}_\nu + \text{source-term}}{1 + \text{sink-term}} \quad (2.153a)$$

$$S_\nu = \frac{S_{C\nu} + r_\nu S_\nu}{1 + r_\nu} \quad (2.153b)$$

$$\text{source-term} = \epsilon B_\nu(T_e) + \eta B^*, \quad (2.154a)$$

$$\text{sink-term} = \epsilon + \eta, \quad (2.154b)$$

$$r_\nu = d\tau_\nu/d\tau_C. \quad (2.155)$$

To treat model atoms with more than 2 discrete levels, one uses the "equivalent 2-level atom" (Thomas, 1965), in which all other interchange processes with these two levels are expressed as net rates, and combined into the source-sink terms because they are processes competing with these, not with the scattering term in the line, J_ν . The corresponding particle energy-level populations have, since Rosseland, customarily been expressed in terms of their ratio, b_k , to what they would be, in TE, at the specified T_e and n_e . Absolutely no restriction is placed, a priori, on the size of the b_k . Thus:

$$n_k^* = (h^2/2\pi m_e kT_e)^{3/2} (G_k/G_i G_e) n_i n_e \exp(E_k/kT_e) \quad (2.156)$$

$$n_k = b_k n_k^*. \quad (2.157)$$

ϵ is the ratio of collisional de-excitation rate to spontaneous transition rate, from upper to lower levels, whose energy difference is $h\nu_0$. ηB^* is the same ratio for photoionization rate from the lower level to the continuum; η , photoionization rate from upper level. Φ_ν is the normalized line-absorption coefficient. Coherent scattering simply corresponds to setting Φ_ν to be $\delta(\nu, \nu_0)$. The parameterized combinations of "pure-scattering," retaining only the J_ν term, and "pure-absorption," setting $\epsilon \rightarrow \infty$, correspond to taking ϵ as a parameter, independent of its physical significance. A solution of the line-transfer equation under pure absorption—i.e., LTE-R—gives a central intensity of $B_\nu(T_{e0})$ for a strong line. A solution under pure-scattering gives a line of zero central intensity. The essential aspect of all this pre-modern nonLTE was the treating as independent each of the terms in eq. (2.153a): scattering, pure-absorption, photoionization. One discussed scattering-dominated, collision-dominated, photoionization-dominated source-function. Below, and in Vol. 2, we see that *in stellar atmospheres the source-function is almost always scattering-dominated*, in

this sense; to be correct, one must discuss what dominates the source- and sink-terms (Thomas, 1957, 1965; Jefferies and Thomas, 1958, et seq.; Jefferies, 1968).

We see these physical-descriptive results algebraically and numerically, by considering the case underlying LTE-R—collisions dominating source-sink terms—and rewriting eq. (2.153a) as:

$$(S_{\bar{\nu}} - \bar{J}_{\bar{\nu}}) = \epsilon [B_{\nu}(T_e) - S_{\bar{\nu}}]. \quad (2.158)$$

We use the Burgess, Seaton, van Regemorter (1961) approximation for collision rates between upper, U , and lower, L , levels of some permitted line transition.

$$C_{LU} = 1.25 \times 10^{-4} n_e T_e^{-1/2} (\chi_H/h\nu) \bar{g} f_{LU} e^{-X_{\nu}} \quad (2.159)$$

with

$$C_{UL} = C_{LU} (G_L/G_U) e^{X_{\nu}} \quad (2.160)$$

$$A_{UL} = (8\pi^2 e^2 \nu^2 / mc^3) f_{LU} G_L / G_U, \quad (2.161)$$

where f_{UL} is the oscillator strength, and g is a dimensionless parameter for which $\bar{g} \sim 0.2$ suffices here. χ_H is the ionization energy of hydrogen. Then

$$C_{UL}/A_{UL} = \epsilon = 21\lambda^3 n_e T_e^{-1/2} \bar{g} \lesssim 10^{-2}. \quad (2.162)$$

For this example, we considered the upper solar photosphere, with $n_e < 10^{12}$, $T_e \sim 4\text{--}6000$ K, and any permitted line in the visual spectrum. One can increase n_e by a factor 10, while increasing T_e by a factor 5, in considering a hot star, but the result is always the same, in the visual and especially the UV and farUV spectral regions: $\epsilon \ll 1$. As mentioned, the result is classic; Pannekoek showed it in 1930. Simply stated, eq. (2.158) says that $S_{\bar{\nu}}$ lies 100 times closer to $J_{\bar{\nu}}$ than to B_{ν} : the line source-function is dominated by the “scattering” term, not by the “pure-absorption,” LTE-R, term. But this is true not just for resonance lines, but for all lines satisfying the above expression for ϵ .

The same result holds if we choose the photoionization-dominated terms rather than the collisional. We have from Vol. 2, abstracted from Thomas (1965):

$$\eta B^* = (2h\nu^3/c^2) (e^{Y_{L-Y_U}} - 1)^{-1} \quad (2.163)$$

$$\eta = \frac{32}{3\pi\sqrt{3}} \frac{kL}{k_L + k_U} \frac{R^2}{g_L f_{LU} \nu_{LU}^2} \frac{W_{kL}}{k_L^3 Z^2} \left(e^{Y_{L-Y_U}} - 1 \right), \quad (2.164)$$

where we have represented the radiation fields in the continua arising from levels U and L as:

$$J_{\nu} = W_j (2h\nu^3/c^2) (e^Y - 1)^{-1} \quad (2.165)$$

$$Y = h\nu/kT_{\text{rad},k}, \quad (2.166)$$

i.e., as a dilution-factor times a Planck function as in eqs. (2.151) and (2.152). k is the principal quantum number of level k ; R is the Rydberg constant; Z is the ionic charge. For hydrogen Balmer α , in the upper solar photosphere, $\eta \sim 0.004$. So, again S_ρ lies closer to the scattering-term than to the photoionization source-term; so a choice between them would demand keeping J_ρ .

In both these examples, a literal choice of scattering-term alone for S_ρ would introduce all the problems earlier discussed of no coupling between J_ν , hence S_ν , and thermal state of the atmosphere. There would be no coupling with the local state, arising from the collision-term, or with the distant state, arising from the photoionization-term. So, as abstracted below, and in Vol. 2, one retains both scattering and source-sink terms; the scattering is a function of the distribution of the source-sink terms. One seeks solutions of the radiative-transfer problem which keeps $(S_\rho - J_\nu)$ equal to $\epsilon(B_\nu - S_\rho)$. Either $T_e(\tau)$ is prescribed, or sought under the condition of RE, or something replacing RE. The only choice lies in which source-sink terms one retains, and their distribution. One discusses which processes dominate the source-function, S_ρ , in terms of which processes dominate the source-sink terms. Ignoring this functional dependence of J_ν on the distribution of source-sink terms has led to physically incorrect results in the literature which are still quoted and used. Among these, is the belief in the possibility of zero central line-intensities, based on the belief that a pure scattering in the line is possible, and the belief that emission lines can be produced in a normally-extended, standard atmosphere by pure-absorption in the line, combined with absorption plus scattering in the continuum. This contrasts to absorption lines produced by only pure-absorption, or LTE-R, processes in both line and continuum. In Vol. 2, I abstract our work showing the nonvalidity of such conclusions, and what replaces them. Here, to continue our discussion of the evolution from LTE-R to nonLTE, it suffices to consider the same isothermal atmospheric region that we used in discussing the LTE to LTE-R transition. Although ϵ decreases outward as n_e —thus exponentially—it suffices here to take a constant value of ϵ , hence n_e . We also note that in such an atmosphere, because of the large difference between line opacity and continuous opacity, the quantities η and ηB^* will also be constant in such an atmospheric region. So, in contrast to the LTE to LTE-R transition, where we imposed constant S_ν , we consider the LTE-R to nonLTE transition by imposing constant source-sink terms. This difference exhibits the heart of the non-LTE configuration: a focus on specifying source-sink distribution, not S_ρ distribution. Thus, instead of directly integrating the radiative-transfer equation with constant S_ν to obtain eq. (2.151), we perform such integration with only a constant source-sink term in the variable, J_ρ -dependent, S_ν given by eqs. (2.153) – (2.155). Because we want a J_ν to compare with eq. (2.151), we integrate the Eddington approximation, eqs. (2.85) – (2.86), applied to the transfer equation. We also ignore the continuum, for the moment. Thus

$$\frac{1}{3} \frac{d^2 J_\nu}{d\tau_\rho^2} = J_\nu - (\bar{J}_\rho + sB)/(1+s), \quad (2.167a)$$

or

$$\frac{d^2 J_\nu}{d\tau_0^2} = x_\nu^2 \left(J_\nu - \delta \int J_\nu \Phi_\nu d\nu - \gamma B \right) \quad (2.167b)$$

$$B = \text{source-term/sink-term}; s = \text{sink-term}; \gamma = s/(1+s) \quad (2.168)$$

$$d\tau_\rho = \phi_\nu d\tau_0; x_\nu^2 = 3\phi_\nu^2; \delta = 1 - \gamma.$$

We solve eq. (2.167) subject to the usual boundary conditions that J_ν not increase exponentially inward, and that there is no radiation incident from outside the star. Under the Eddington approximation, this last condition is:

$$\text{at } \tau_0 = 0: J_\nu = x_\nu^{-1} dJ_\nu/d\tau_0. \quad (2.169)$$

The ν -integral in eq. (2.167b) resembles the μ -integral in eqs. (2.53), (2.41b), and (2.113), whose solution gives $J(\tau)$, hence $T_e(\tau)$, under LTE-R and RE for a gray body. Carrying the integral—i.e., approximating it in some way such as the Gaussian quadrature scheme used in solving eq. (2.113)—instead of replacing it by some single J —e.g., $J(\nu_0)$, corresponding to the point farthest out in the atmosphere—simply means a better representation of $J_\nu(\tau_0)$. This is a critical point, to which we return. But first, we exhibit the essential thermodynamics of the LTE-R to nonLTE transition by comparing the two simplest approximations of replacing J_ν by J_ν and $J(\nu_0)$. We obtain:

$\bar{J}_\nu = J_\nu$: *coherent scattering + source-sink terms*:

$$d^2 J_\nu / d\tau_\nu^2 = 3\gamma (J_\nu - B) \quad (2.170a)$$

$$J_\nu = B [1 - (1 + \gamma^{1/2})^{-1} \exp(-\sqrt{3\gamma} \tau_\nu)] \quad (2.171a)$$

$$S_\nu = B [1 - (1 - \gamma^{1/2}) \exp(-\sqrt{3\gamma} \tau_\nu)]; \quad (2.172a)$$

$\bar{J}_\nu = J(\nu_0) = J_0$: *noncoherent scattering + source-sink terms*:

$$d^2 J_\nu / d\tau_0^2 = 3 (J_\nu - \delta J_0 - \gamma B) \quad (2.170b)$$

$$J_\nu = B [1 - (1 + \gamma^{1/2})^{-1} \exp(-\sqrt{3\gamma} \tau_0)] \quad (2.171b)$$

$$S_\nu = B [1 - (1 - \gamma^{1/2}) \exp(-\sqrt{3\gamma} \tau_0)]. \quad (2.172b)$$

The solutions are the same, in showing an outward decrease in S_ν to an asymptotic value of $\gamma^{1/2} B \sim s^{1/2} B$ from a “saturated” value of B deep in the atmosphere. The solutions differ only in the “depth to saturation.” For coherent scattering, it is $\tau_\nu \sim (3s)^{-1/2}$; for noncoherent scattering, it is the same depth in τ_0 . If we again consider the case underlying LTE-R, we see that these solutions correspond to LTE-R being reached at this depth: $B = B_\nu(T_e)$, $\epsilon = s$.

So we see that, contrary to our original expectations, the transition from LTE-R to nonLTE—in the case of collision-dominated source-sink terms—has nothing to do with passage from collisional domination of the source-function to its radiative domination. That transition involving collisions occurred deep in the LTE-R region. It did not affect the form of the source-function, because the local homogeneity maintained by high local radiative opacity kept the source-function in its LTE-R form. The LTE-R to nonLTE transition is that from the “Locally-Opaque-Situation,” LOS, where S_ν saturates at $S_\nu = \text{source-term/sink-term}$, *whatever* that is, to an outward decrease toward the surface. From eq. (2.172), we can write

$$J_\nu = W_1(\tau_0) S_\nu(\text{LOS}), \quad (2.173a)$$

$$S_\nu = W_2(\tau_0) S_\nu(\text{LOS}), \quad (2.173b)$$

$$W(\tau_0 = 0) = (\text{sink-term})^{1/2} \quad (2.174)$$

The boundary value eq. (2.174) holds only when source-term/sink-term are constant in this region. Otherwise, we must do a transfer solution in which the τ -dependence of source and sink terms is specified.

Clearly, these results, and physical picture, are not changed if one uses a more adequate treatment of \bar{J}_ν ; such as the Gaussian quadrature scheme. One simply obtains a W of the form (cf Vol. 2, or Thomas, 1965):

$$W_\nu(\tau_0) = 1 + \delta \sum_j L_j (1 - k_j^2/x_\nu^2) e^{-k_j \tau_0}, \quad (2.175)$$

where the k_j and L_j come, respectively, from the equations

$$-1 + \delta \sum_i \alpha_i (1 - k_i^2/x_i^2) = 0 \quad \text{and} \quad (2.176)$$

$$1 + \delta \sum_j L_j (1 - k_j/x_j)^{-1} = 0. \quad (2.177)$$

The values of (α_i, x_i) come from choice of the Gaussian quadrature points. Clearly, any other scheme of representing \bar{J}_ν could be equally well adopted. Using eq. (2.175) instead of the coefficient of B in eqs. (2.172) simply gives a different depth at which S reaches sufficiently close to S_ν (LOS). Jefferies has called such distance-scales "thermalization-depths," in particular application to this LTE-R problem: these are the depths to reach LTE-R, as stressed. I have used the term "diffusion-scale" as being more neutral, to cover also the case where S_ν saturates, but not at its LTE-R value. For example, in the photoionization-dominated source-sink terms, S_L (LOS) saturates at B^* . Then, to ask when B^* takes on an LTE-R value, one must discuss a transfer solution in that photoionization continuum. We consider that problem in Section b following in which we consider several examples, applying the above.

But from the foregoing, the analogy between the LTE to LTE-R, and LTE-R to nonLTE transitions is clear. And, in the quasi-isothermal boundary regions of the standard models, the representation of the types of eqs. (2.151) and (2.173) are quite instructive and useful, in separating the influence of the boundary and the effect of variation in source-sink terms. We exploit this approach, in Section c, in discussing the utility of what we have called the "temperature-control-bracket."

With this understanding of the passage from LTE-R to nonLTE, of the change in S_ν coming simply from the effect of a boundary and not from a T_e -gradient, and of the difference in type of line source-functions depending on the source-sink terms, we can return to comment succinctly on the error involved in applying LTE-R diagnostics to a nonLTE situation. I focus on determining T_e from LTE-R diagnostics of line-intensity. Originally Pecker (1958, et seq.), then Mihalas (1970, 1978), have stressed the confusion on structural and evolutionary questions, coming from erroneous abundances derived by misapplying LTE-R models to diagnose observations. I ignore abundance problems in this monograph.

Throughout the era of LTE-R theoretical investigations, the observed line-profiles were sometimes used to compare with predictions, but more usually to derive the values of the atmospheric parameters upon which the particular theory made the profiles depend—in addition to the above-mentioned abundance determinations. Because of difficulties with matching observed spectral line widths, one often added a "turbulence" to the parameters used to compute line-profiles, which made difficult any belief that one was testing the adequacy of the LTE-R condition. An especially sensitive point was the very small central intensities found in a number of spectral lines for which the LTE-R, not scattering, model was retained. In the Sun, under LTE-R diagnostics, the central intensities of the Balmer lines demanded T_{e0} as low as 3400 K; the Mg II and Na I lines demanded T_{e0} drop to some 2800 K. The contrast of these

values with the LTE and LTE-R theoretical models—where $T_{e0} \gtrsim 4600\text{--}4800\text{ K}$, as we saw in Section 2—led to production of “improved” theories of LTE-R line-blanketing, which indeed produced such low T_{e0} . Apparently, LTE-R theory and diagnostics of observations concurred, in giving strong decreases in T_{e0} in the outer solar atmosphere. The same kinds of “empirical-theoretical” LTE-R approach were extended to other stars, with the same results. Unfortunately, these results were simply a case of such an empirical-theoretical approach applied without at the same time demanding thermodynamic self-consistency, which would have required reconciling this speculative-imposed, LTE-R macroscopic formalism with the nonLTE thermodynamic-microscopic detailed approach, centered on eqs. (2.153), et seq., and their application. The problem, and its resolution, were discussed critically by Thomas (1961, Thomas and Athay, Chapter 9; 1965); Fig. 2-3 succinctly summarizes the result. It shows the empirical values of T_{rad} , which under LTE-R would be T_e , at the centers of the hydrogen Balmer lines; the simple theoretical prediction of this quantity under a 2-level atom computation of $S_\nu(\tau)$ for $H\alpha$ and the assumption that it could be used for the other Balmer lines also; and T_e determined empirically from the continuum at solar eclipse. Clearly, the scattering-decrease of S_ν to the boundary, not the behavior of T_e , is what controls the source-function for this photoionization-dominated line. The behavior is precisely as outlined above: an illusory drop in T_e to the boundary, resulting simply from scattering in the presence of the boundary. For this photoionization-dominated line, there is no competition from the effect of a rising source-term toward the boundary, as is found for a collision-dominated line, such as the H and K lines of Ca II or Mg II, which are formed in the regions of that chromospheric rise in T_e indicated in Fig. 2-3. For these lines, the outward rise in $\epsilon B_\nu(T_e)$ gives an emission core. The scattering effect toward the boundary gives the self-reversed center. Figure 3-27 illustrates this collision-dominated case (Jefferies and Thomas, 1958). Even for such lines, no $I_\nu(\tau = 0)$ gives directly $B_\nu(T_e)$, in regions outside LOS.

Three things should be stressed from the above development, and the specific example of diagnostics of observed line-intensities to infer T_e . First, of course, is the same kind of error in applying LTE diagnostics to an LTE-R situation; the outward, large, decrease in J_ν and I_ν reflects simply a scattering transfer effect near a boundary, not a decrease in T_e . Second, the inward terminus of this boundary-scattering effect is a “modified LTE,” not an LTE-R

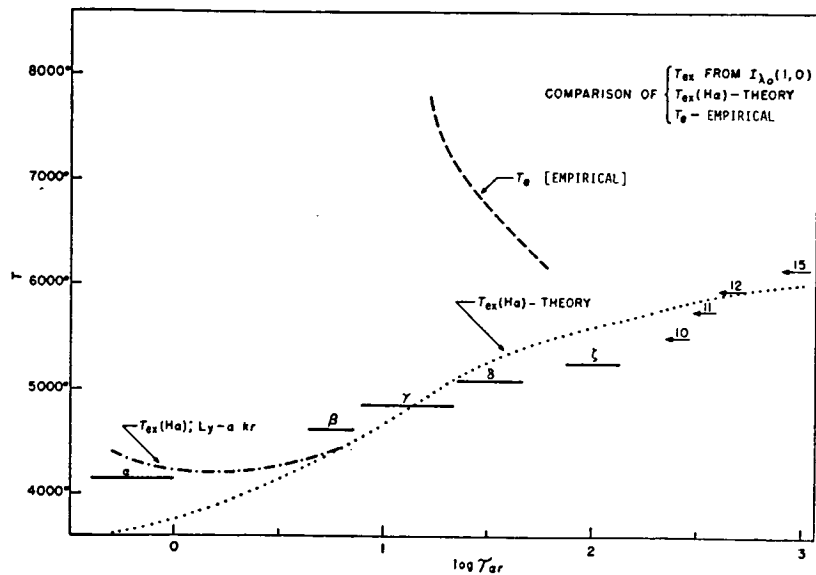


Figure 2-3. Comparison of $T_{\text{ex}}[\text{H}\alpha]$ theoretical with empirical T_{ex} for early Balmer lines (Thomas and Athay, 1961).

configuration. Eqs. (2.172) and (2.175) show that the inward evolution of S_ν “saturates” at $S_\nu = B = J_\nu$. *This was the general operational consequence of LTE: complete coupling between radiation field and internal energy states of the particle, expressed by $S_\nu = J_\nu$.* We reached this, under LTE, by separately imposing $S_\nu = B_\nu(T_e)$ and $J_\nu = B_\nu(T_e)$, and requiring that J_ν be maintained by essentially isotropic I_ν , not affected by some inhomogeneity like a boundary. And above, we reach $S_\nu = J_\nu$, in an imposed situation of homogeneity from constant source-sink terms, by the separate results $S_\nu = B, J_\nu = B$, under LOS, far from the inhomogeneity of the boundary. But, third, we have not imposed $B = B_\nu(T_e)$. Rather, microscopic computation shows that while some lines—like Ca II H and K, etc.—do indeed satisfy $B = B_\nu(T_e)$, under that LOS reached by moving downward from the boundary and strong nonLTE, other lines, like the hydrogen H α , do not. For them, LOS is not LTE. $B \neq B_\nu(T_e)$; it does not measure T_e in this isothermal region, but B^* , whose value is fixed by conditions in another atmospheric region. But in both cases—Ca H and K, H α —the configuration is one where J_ν dominates S_ν , collisions do not. In moving upward from the LTE configuration to the LTE-R to the nonLTE, the transition is completely one in opacity—not in collisions, for lines with collision-dominated source-sink terms. But for lines with photoionization-dominated source-sink terms, there is an intermediate step—the behavior of B^* , which is a melange of the two photoionization continua of this 2-level atom. We must investigate its evolution through the atmosphere. This brings us to consideration of the continuum—for itself, as an observed and to-be-diagnosed quantity; for its use in fixing line source-functions, as above; and for its use in fixing $T_e(\tau)$ under RE. So we consider it, in the following Section b. But first, two things are incomplete in this abstract of the outward evolution of the effect of lines on internal energy partition in particles: a comment on thermal coupling of atmosphere to J_ν , and on the overall height-evolution of S_ν . The last is best considered after considering the continuum source-function, in Section b.

We stressed that a J_ν formed in pure-scattering has no coupling to the thermal state of the atmosphere. This is clear from eqs. (2.171). Setting $B = 0$ in S_ν , retaining only J_ν in whatever form, gives $S_\nu = 0$. Only the incident radiation in eq. (2.10) gives a nonzero term in J_ν . If τ_ν is sufficiently large, we have the classical scattering result of zero line-intensity. This results from zero coupling to the thermal state of the atmosphere, which is provided by source-sink terms. Then we see that a collision-dominated source-sink term provides coupling to thermal states of both local and nonlocal atmospheric regions. The photoionization source-sink terms generally provide coupling to distant regions of the atmosphere—because the line opacity generally greatly exceeds the continuous opacity. This distinction is very important in two problems. One is in the effect of line-blanketing on T_e -distribution, which we consider in Section c below. The other is in diagnosing emission from lines and continua to assess nonradiative energy-dissipation. Neglect of the distinction has led to significant errors in both problems, in both the standard photospheric models discussed in this Chapter 2, and in those exophotospheric regions considered in Chapter 3 and Part III. Finally, when the thermal coupling by both these collisional and photoionization terms is too small, we can no longer neglect that from the continuum at those ν within the line. We modify the source-sink terms in eqs. (2.167) et seq. by:

$$\text{add to source-term:} \quad r_\nu^{-1} S_c, \quad (2.178a)$$

$$\text{add to sink-term:} \quad r_\nu^{-1}. \quad (2.178b)$$

The total opacity becomes, replacing that in eq. (2.168)

$$d\tau_\nu = d\tau_\nu (1 + r_\nu^{-1}). \quad (2.178c)$$

The solution remains as before; one simply uses the ν -dependence of the added terms in the quadrature weights, and adjoins the correct form for S_c , which we proceed to discuss. So, even if the thermal coupling in line processes is very small, that from the continuum, at the ν in the line, provides such coupling.

b. The NonLTE Continuum, and Photospheric Models Based on the Continuum Alone. To put the foregoing discussion of nonLTE effects on lines into general perspective, we note that the microscopic form of the radiative-transfer equation is:

$$\mu \frac{dI_\nu}{dx} = -I_\nu (n_C \alpha_C + n_L \phi_\nu h\nu B_{LU}/4\pi - n_U \phi_\nu h\nu B_{UL}/4\pi) + n_C^* \alpha_C^* B_\nu(T_e) + n_U \phi_\nu h\nu A_{UL}/4\pi, \quad (2.179a)$$

where we have assumed the same ν -profile for all processes in the line, as underlies eq. (2.153). We have combined induced emissions into the continuous absorption coefficient, α_C . As in eq. (2.157) an “*” indicates LTE populations at specified n_e and T_e . Then eq. (2.179) can be written in the standard form.

$$\mu dI_\nu/d\tau_\nu = I_\nu - S_\nu \quad (2.179b)$$

under the definitions, added to those of eqs. (2.153) et seq., in the standard form.

$$d\tau_C = -n_C \alpha_C \quad ; \quad d\tau_\varrho = -n_L B_{LU} \phi_\nu h\nu (1 - b_U e^{-X_{LU}}/b_L) \quad (2.180a)$$

$$S_C = b_C^{-1} (\alpha_C^*/\alpha_C) B_\nu(T_e) \quad ; \quad d\tau_\nu = d\tau_\varrho + d\tau_C \quad (2.180b)$$

$$S_\varrho = (2h\nu^3/c^2) (b_L e^{X_{LU}}/b_U - 1)^{-1}. \quad (2.180c)$$

Then, the discussion of S_ϱ in Section a focused on its transition from LOS to nonLTE, wholly due to scattering effects near an open boundary, because we considered an isothermal upper photosphere such as any variety of the standard model predicts to exist. Because, in such case, X_{LU} in eq. (2.180) is constant, the evolution in S_ϱ wholly reflects the evolution in b_L/b_U . In the case of collision-dominated source-sink terms, b_L/b_U approaches 1, under LOS; thus, S_ϱ approaches its LTE-R value. This does not mean each of b_L and b_U individually approaches 1, only their ratio. And, for photoionization-dominated source-sink terms, b_L/b_U approaches—from eqs. (2.163) and (2.164).

$$b_L/b_U = (e^{Y_L} e^{-Y_U}) e^{-X_{LU}}, \quad (2.181)$$

where Y_k is defined by a radiation temperature in the n_k continuum, via eq. (2.166). This value of b_L/b_U in eq. (2.181) is 1 only if the radiation temperatures in the individual ionization continua each equal T_e —which is the LTE condition. Thus, in the photoionization-dominated case, the transition is never really nonLTE \leftrightarrow (LOS) \leftrightarrow LTE-R \leftrightarrow LTE, as it is in the collision-dominated case; rather, it is nonLTE \leftrightarrow (LOS) \leftrightarrow LTE. The point is possibly subtle, but important. It really focuses on the behavior of the individual b_k , not just their ratios. If $b_k \rightarrow 1$, we have indeed LTE-R; but if its reaching 1 requires such homogeneity of radiation field—of J_ν —that we require LTE to have LTE-R, then we have a much wider atmospheric range where nonLTE, not LTE-R, holds. So, to settle the point, we require discussion of solution of the radiative-transfer/scattering problems of b_k alone. Since those terms in which b_k alone, not as a ratio, appears are those involving the continuum, we must discuss the continuum. We see why, of course, such a situation holds. By imposing LTE in the electron velocity distribution, we impose the b 's, which could be introduced to represent electron velocity states under a broader nonLTE, to have value 1. (Some discussions of this broader situation do exist, e.g., Oxenius, 1970 and Shoub, 1977. It is not essential that we consider them here.)

Then to maintain thermodynamic perspective, we see that we required a radiative-transfer solution, even in this isothermal atmosphere, to specify J_ν , S_ϱ , and so b_U/b_L via eqs. (2.171) – (2.175) and (2.181) rather than a simple

integration, as in the LTE-R situation, which gave eq. (2.151). Likewise, it is generally the case that we require a radiative-transfer solution to obtain the individual b_k . Effectively, one determines a b_c —referring to eqs. (2.179)–(2.180)—by a transfer solution in its photoionization continuum under the condition of LOS—i.e., detailed balance in radiative transitions—for those lines of which n_c is the upper level. That is, one effectively suppresses the levels below n_c , by such detailed balance, in discussing the evolution of the photoionization continuum from n_c . When one reaches, moving upward, the atmospheric regions which are optically thin in that continuum, so that I_ν (outward) has become constant, then b_c either remains at its boundary value in that solution—if it is indeed a ground level of the atom—or it further evolves in value, being fixed by a transfer solution in a line for which it is the upper level. In turn, the lower level of that transition has its b_L fixed by a transfer solution in the continuum from that level. This simplified situation is particularly marked in hydrogen, and was demonstrated in the nonLTE diagnostics of the solar chromosphere, using the 1952 eclipse data (Thomas and Athay, 1961, chapters 6 and 9). It was for algebraic discussion in such terms that the “equivalent two-level atom” was introduced (Thomas, 1965). It has been adopted, variously, and applied for machine computations as a convenient iterative approach (Mihalas, 1970, 1978).

There is departure from these generalities in two extreme situations: (1) *optically-thin nonLTE region*. Here, when $\Delta\tau < 1$, S_ν has the local value (source-term)/(1+sink-term). The situation is interesting when a particular ion exists only in a limited atmospheric region, or when ν_0 for the considered line changes strongly over the region in which the ion exists, such as can arise in an accelerated velocity field. (2) *low-threshold transition*. An example is an ion with a low ionization value, near local thermal energies. Then LTE-R can be a good approximation, depending upon how it is used. We illustrate this with the H^- continuum, in the following.

So we proceed to use these characteristics of nonLTE atmospheric regions to make explicit the evolution of thermodynamic state across the upper photosphere. As emphasized, this evolution does not simply reflect the decreasing importance of collision rates in fixing the populations of particle energy states. Instead, it is the evolution toward optically-thin atmospheric regions of a J_ν -controlled S_ν , and a source-sink term controlled J_ν . That is, the evolution is that accompanying an outward decrease in the quantity of radiation—crudely, our earlier-discussed factor-2 change because one hemisphere of radiating source replaces two. But this is too gross. The example of the photoelectric control of T_e in a photoionized gas shows the problem: T_e is fixed by quality, not quantity of the radiation field. The number of electrons is fixed by quantity of photons absorbed; the energy of the electrons is fixed by the quality of the photons absorbed. When we go to the extreme outer atmospheric region, that of the planetary nebulae, we see that classically, the degree of ionization is fixed by quality of the radiation field from the central star, even though the local T_e is fixed by the energy input from that same quality of radiation, perturbed by inelastic collisional energy-loss to such an extent that it is lower, by a large factor, than would correspond to that observed degree of ionization. I say “classically,” because we will see in Chapter 3, that modern farUV data on the PN show the region between them and the central star to be filled with an ultravelocity gas, so that collisional effects on heating, as well as cooling, must be considered. Although, in this Chapter 2, we focus on the standard photosphere, we should try to put all non-classical effects into clear focus, for use when considering those exophotospheric regions, in succeeding chapters, which are of major interest in discussing nonthermal atmospheric phenomena.

As we saw in Section 2, a first approximation to models is based on the continuum alone and considers the continuum piecewise, in terms of spectral regions of increasing opacity. Thus one considered the gray, then the 2-gray, then gray plus line-blanketing as being a multi-gray, etc. sequence of increasingly better representation of an LTE-R atmosphere by dividing it into a sequence of opacity subregions. The lower the ionization energy of the level producing the continuous absorption, in the deepest atmospheric region, the larger the spectral region covered by the opacity from that level. Also, possibly, the closer the ionization energy to thermal values, the greater the chance that the LTE-R to non-LTE transition can indeed be one between collisional and radiative dominance of the source-function. Otherwise, we have the more usual transition between the LOS and transparent situations for a J_ν -dominated source-function, under a source-sink term dominated J_ν . Finally, the lower the abundance of the ion providing the opacity, and the smaller the continuous absorption coefficient, the deeper in the atmosphere lies the photospheric region to which the model applies. The continuous absorption from other energy states enter as corrections to this first approximation: in extending the spectral range, in extending the atmospheric height range, and in introducing

the effects of spectral lines. We give two examples: one with a continuum from an ionization level comparable to atmospheric thermal energies; the other, where ionization energy is strongly superthermal.

i. H^- Photosphere: Exceptional Collisional Processes. If one can identify an ion that is: (1) sufficiently abundant to provide the continuous opacity, yet not so abundant that we see only the upper photosphere; (2) has sufficiently-small absorption coefficient for the same latter purpose; and (3) has sufficiently-small ionization energy that it both covers a large spectral region and can be ionized by thermal velocities so that collisions are effective in maintaining ionization balance, then LTE-R may be a reasonable approximation. Effectively, one would have decreased the complication which invalidated LTE-R partition over particle internal energy states by reducing such states to one, which is populated by thermal collisions at the high densities of the lower atmosphere, so it is coupled directly to the kinetic energy storage. Moving upward in the atmosphere brings lower densities; radiative processes compete with collisional; nonLTE replaces LTE-R. Exhibiting the height-evolution of collisional processes compared with radiative for such an ion places this conventional type of evolution of LTE-R into nonLTE into good perspective.

For the Sun, and cool stars like it, H^- is such an ion as described (Wildt, 1939). Its ionization potential is 0.747 eV, which equals the thermal kinetic energy per particle, $3kT_e/2$, for $T_e = 5750$ K, which is very near T_{eff} for the Sun, some 5800 K. At $n_e = 10^{12}$, and $T_e = 5750$ K, eq. (2.64) gives $n_{H^-}/n_H \sim 10^{-8}$. Finally, its absorption coefficient is indeed nearly gray (Chandrasekhar, 1946), with $\alpha_\nu \sim 10^{-17} \text{ cm}^{-2}$. Its ionization equilibrium is maintained more by associative detachment by (H^- , H) reactions rather than by electron collisional ionization, and this literal problem has been discussed from our present viewpoint by Gebbie and Thomas (1970) in a way that is particularly useful in considering more complicated ions, and also the effects of departure from RE. We simply abstract the details of that discussion.

We assume an atmosphere in which H^- is the only atom capable of absorbing and emitting radiation and that its absorption coefficient is gray for radiation beyond the ionization limit, $\nu > \nu_i$, and zero for $\nu < \nu_i$. The radiative processes can then be expressed in terms of the following integrals:

$$E(J, \nu_i) = \int_{\nu}^{\infty} J_{\nu} d\nu, \quad E(B, \nu_i) = \int_{\nu}^{\infty} B_{\nu}(T_e) d\nu, \quad (2.182)$$

$$N_J(J, \nu_i) = \int_{\nu}^{\infty} (J_{\nu}/h\nu) d\nu, \quad N_B(B, \nu_i) = \int_{\nu}^{\infty} [B(T_e)/h\nu] d\nu, \quad (2.183)$$

where $E(J, O)$ is the total energy and $N(J, O)$ the total number of photons in the radiative field.

The two important collisional-ionization reactions are:



The question is whether the ionization equilibrium of (H , H^-) can be regarded as the only important nonLTE process. Lambert and Pagel (1968) discuss nonLTE effects in H^- and H_2 for given atmospheric models; for the statistical equilibrium of H_2 , they conclude that the reaction



is the only one that need be considered in addition to reaction (2.185). We write the net rates for collisional processes as:

$$\text{for eq. (2.185)} \quad n_{\text{H}^-} n_{\text{H}} D_{\text{H}^-, \text{H}} (1 - b_{\text{H}_2} / b_{\text{H}^-}) = n_{\text{H}^-} n_{\text{H}} D_{\text{H}^-, \text{H}} (\text{NCB})_{\text{H}^-, \text{H}_2} \quad (2.187)$$

$$\text{for eq. (2.186)} \quad n_{\text{H}}^3 D_{3\text{H}} (1 - b_{\text{H}_2}) = n_{\text{H}}^3 D_{3\text{H}} (\text{NCB})_{3\text{H}} \quad (2.188)$$

$$\text{for eq. (2.184)} \quad n_{\text{H}^-} n_{\text{e}} D_{\text{H}^-, \text{e}} (1 - 1/b_{\text{H}^-}) = n_{\text{H}^-} n_{\text{e}} D_{\text{H}^-, \text{e}} (\text{NCB})_{\text{H}^-, \text{e}} \quad (2.189)$$

We take the actual values of n_{H} , n_{e} , T_{e} as given. Thus $b_{\text{H}} = 1$. For the radiative reactions, we include stimulated emission in the absorption coefficient in this example. It is not quite legitimate: the correction factor is $[1 - \exp(-h\nu/kT_{\text{e}})]$ for recombinations, and $[1 - b_{\text{H}^-} \exp(-h\nu/kT_{\text{rad}})]$ for photoionization; but it suffices for our objective here. Then since recombinations can be treated as photoionization with $J_{\nu} = B_{\nu}(T_{\text{e}})$, we have for the H^- photoionization, recombination balance:

$$4\pi \alpha_{\text{H}^-} \left\{ n_{\text{H}^-}^* N(B, \nu_i) - n_{\text{H}^-} N(J, \nu_i) \right\} = 4\pi \alpha_{\text{H}^-} n_{\text{H}^-}^* N_{\text{B}} (\text{NRB})_{\text{H}^-} \quad (2.190)$$

where we represent net rates in terms of the Net-Radiative-Bracket (NRB) and Net-Collisional-Bracket (NCB) defined as in the equations and discussed in detail in Vol. 2. Then the equations of statistical equilibrium are, assuming that no radiative dissociation of H_2 occurs.

$$4\pi \alpha_{\text{H}^-} n_{\text{H}} N_{\text{B}} (\text{NRB})_{\text{H}^-} = n_{\text{H}^-} n_{\text{e}} D_{\text{H}^-, \text{e}} (\text{NCB})_{\text{H}^-, \text{e}} + n_{\text{H}^-} n_{\text{H}} D_{\text{H}^-, \text{H}} (\text{NCB})_{\text{H}^-, \text{H}} \quad (2.191)$$

$$0 = n_{\text{H}}^3 D_{3\text{H}} (\text{NCB})_{3\text{H}} + n_{\text{H}^-} n_{\text{H}} D_{\text{H}^-, \text{H}} (\text{NCB})_{\text{H}^-, \text{H}} \quad (2.192)$$

the conservation of energy in the electron continuum is given by:

$$0 = 4\pi \alpha_{\text{H}^-} [n_{\text{H}^-}^* E(B, \nu_i) - n_{\text{H}^-} E(J, \nu_i)] - \Delta e, \quad (2.193)$$

where we have added a nonradiative energy input, Δe , for use in the following.

To relate this configuration to the 2-level atom earlier discussed, note that ignoring stimulated emission gives

$$S_{\text{Q}} = B_{\nu}(T_{\text{e}}) \times b_{\text{U}}/b_{\text{L}} \quad (2.194)$$

while, quite generally,

$$(\text{NRB})_{\text{UL}} = 1 - \int J_{\nu} \phi_{\nu} d\nu / S_{\text{Q}} \quad (2.195)$$

Thus, by algebra, eq. (2.158) can be written:

$$(\text{NRB})_{\text{UL}} = \epsilon (\text{NCB})_{\text{LU}} (B_{\nu}/S_{\text{Q}}) < \epsilon^{1/2} (\text{NCB})_{\text{LU}} \quad (2.196)$$

We have used the boundary value, $\epsilon^{1/2}$, for $S_{\nu}/B_{\nu} = b_U/b_L$ in an isothermal atmosphere (cf Vol. 2). Note that S_{ν}/B_{ν} decreases monotonically outward simply from the scattering, so the limit is correct if T_e is correct. So our earlier remarks could be rephrased to say that the departure of S_{ν} from being numerically equal to the scattering term is $\epsilon^{1/2}$ times the departure from equality of the b_j . Thus the $\epsilon < 10^{-2}$ found there ensures the J_{ν} -dominance of S_{ν} . Then we see that analogously to this line situation, we can, from eq. (2.162), define two ϵ , corresponding to the electron-collisional and associative-detachment processes. (Note that the photorecombination rate, $\alpha_H^- N_B$, plays a role corresponding to the downward transition probability, A_{UL} , for discrete transitions):

$$\epsilon_e b_{H^-}^{-1} = n_e D_{e,H^-} (4\pi\alpha_H^- N_B)^{-1}, \quad (2.197)$$

$$\epsilon_H b_{H^-}^{-1} = n_H D_{H^-,H} (4\pi\alpha_H^- N_B)^{-1}, \quad (2.198)$$

From the empirical data in Table 2-3, which is table 6-4 of Thomas and Athay (1961), we find $\epsilon_e b_{H^-}^{-1} \lesssim 10^{-2}$, but $\epsilon_H b_{H^-}^{-1} \sim 10$, at an upper-photospheric level of $\tau_5 = 0.02$, $n_e \sim 10^{12}$, $n_H \sim 10^{16}$, and $T_e \sim 4700$ K. In the lower photosphere, $\tau = 0.4$, $n_e \sim 10^{13}$, $n_H \sim 10^{17}$, $T_e \sim 5800$ K, the ϵ become, respectively, 0.03 and 20. Thus, if the only collisional terms were those involving electrons, we would expect H^- also, even in the photosphere, to show the non-LTE effects coming from the scattering term in the source-function. This scattering term, $N(J)$, would dominate the source-function, and we would need to solve a transfer equation to obtain S_C and b_{H^-} . However, given the exceptional presence of associative-detachment, for this exceptional, almost-gray ion, H^- , we would expect that collisions indeed drive the system to LTE-R in the H^- continuum. The b_{H^-} comes from solving eq. (2.191), using the quantities in Table 2-3 plus $J_{\nu} \simeq 0.5 \times B_{\nu}$ (5800 K) to evaluate N_j .

Table 2-3
Estimate of b_{H^-}

τ_5	0.01	0.05	0.1	0.2	0.375	1.0
T_e	4400°	4900°	5200°	5450°	5800°	6470°
$\log n_e$	12.32	12.57	12.84	12.99	13.28	13.87
$\log n_H$	16.24	16.61	16.75	16.89	17.01	17.11
$n_e D_{e,H^-}$	3.2×10^3	6.8×10^3	1.4×10^4	2.1×10^4	4.5×10^4	2.0×10^5
$n_H D_{H^-,H}$	0.6×10^7	1.3×10^7	1.8×10^7	2.5×10^7	3.3×10^7	4.1×10^7
$4\pi \int \alpha_{H^-}^* \times B_{\nu}(T_e) dv/h\nu$	0.9×10^6	1.2×10^6	1.5×10^6	1.7×10^6	1.9×10^6	2.5×10^6
b_{H^-}	0.99	1.02	1.02	1.02	1.01	1.00
b_{H^-} (with $D_{H^-,H}/4$)	0.98	1.04	1.07	1.06	1.04	1.01

We can show this explicitly by solving eq. (2.191) and (2.192) for b_{H^-} , then obtain an explicit expression for S_C (H^-) similar to that of eq. (2.153a) for S_{ν} , by using the analog of eq. (2.194) with $b_L = b_{H^-}$ and $b_U = 1$, in order to show very explicitly the parallelism and the difference. To do this, I follow the algebraic scheme developed with Gebbie (1970, 1971), in order to facilitate later discussion of the line-blanketing. We carry out the discussion in terms of the mean energy per photorecombining electron: $f(T_e) = E_B/N_B$. So, defining

$$\Delta = \frac{\Delta e}{4\pi\alpha_{\text{H}^-} n_{\text{H}^-} N(J, \nu_i)} ; \quad \Delta_2 = \frac{n_e D_{\text{H}^-, e}}{4\pi\alpha_{\text{H}^-} N(J, \nu_i)} ; \quad \Delta_3 = \frac{n_{\text{H}^-} D_{\text{H}^-, \text{H}}}{4\pi\alpha_{\text{H}^-} N(J, \nu_i)} \quad (2.199)$$

$$f(T_e) = \frac{E(B, \nu_i)}{N(B, \nu_i)} ; \quad r = \frac{N(B, \nu_i)}{N(J, \nu_i)} ; \quad \beta = \frac{n_{\text{H}_2} D_{3\text{H}}}{n_{\text{H}^-} D_{\text{H}^-, \text{H}}}$$

we solve eqs. (2.191) – (2.193) simultaneously to obtain:

$$f(T_e) = \left[\frac{E(J, \nu_i)}{N(J, \nu_i)} + \Delta \right] \left[1 + r^{-1} (1-r) \frac{\Delta_2 + \beta\Delta_3/(1+\beta)}{1 + \Delta_2 + \beta\Delta_3/(1+\beta)} \right] \quad (2.200)$$

$$b_{\text{H}^-} = 1 - \frac{1-r}{1 + \Delta_2 + \beta\Delta_3/(1+\beta)} \quad (2.201)$$

$$b_{\text{H}_2} = 1 - \frac{1-r}{\beta(1 + \Delta_2 + \Delta_3) + 1 + \Delta_2} \quad (2.202)$$

Note that this particular algebraic solution is more succinctly expressed in terms of the $\Delta_i = \epsilon_i r$ than always writing $\epsilon_i r$; but that Δ_i increases outward toward the boundary in an isothermal, constant-density atmosphere because of the decrease in J giving an increase in r . Note also the algebraic forms for $E(T, \nu_i)$, $N(T, \nu_i)$, $f(T)$ and $r(T, J)$: $\nu_i \neq 0$. Taking $\alpha(\text{H}^-)$ to be ν -independent and $J_\nu = B_\nu(T_c)$, we have

$$E(T, \nu_i) = K (kT)^4 \sum \frac{e^{-nX_i}}{n} (X_i^3 + 3X_i^2/n + 6X_i/n^2 + 6/n^3), \quad (2.203)$$

$$N(T, \nu_i) = K (kT)^3 \sum \frac{e^{-nX_i}}{n} (X_i^2 + 2X_i/n + 2/n^2) \quad (2.204)$$

$$X_i = \chi(\text{H}^-)/kT.$$

For $\nu_i = 0$, we had $E/N = 2.70 kT$; for $\nu_i \neq 0$, E/N depends on T through X_i . Since we are interested in the range $4600 \text{ K} < T < 5600 \text{ K}$, neglect of all terms $n > 1$ will introduce errors of less than 2 percent. Then, with subscripts c and e referring to T_c and T_e ,

$$E(T, X_i)/N(T, X_i) = kT \frac{(X_i + 1) [(X_i + 1)^2 + 3] + 2}{(X_i + 1)^2 + 1} \quad (2.205)$$

$$r = W^{-1} (T_e/T_c)^3 \frac{(X_{ie} + 1)^2 + 1}{(X_{ic} + 1)^2 + 1} \exp(X_{ic} - X_{ie}). \quad (2.206)$$

Then except when otherwise stated, we use $E(T)/N(T) = 2.7 kT$ and $r = (T_e/T_c)^3 W^{-1}$ —the limiting case of $\nu_i = 0$ —to exhibit the essential features of this exceptional ion, H^- , as contrasted to the free-bound continuum of atomic hydrogen considered afterward, in Section b.β.

Then in discussing the nonLTE effects in the continuum, we have three kinds of questions: (C-1) What is the size of the nonLTE effects, as a function of the J_ν (equivalently, T_e and W_ν) evolving from its LOS value to its boundary value in a situation of specified T_e and density? (C-2) If b_C differs significantly from 1, does the evolution of its value come mainly from a density or J_ν effect, i.e., from nonLTE to LTE-R, or to LOS? (C-3) How is the $T_e(\tau)$, determined under the condition of RE, affected by (C-1) and (C-2)? That is, under LTE-R, the radiative flux, which is fixed by the J_ν -gradient, reflects only a T_e -gradient, but under the kind of nonLTE in stellar atmospheres—one governed strongly by a radiation field—a strong part of the J_ν -gradient is fixed by the boundary, independent of T_e -gradient. We consider these in order.

High-density limit: We have $b_{H^-} = 1 = b_{H_2}$, independently of the value of J_ν . Note that $r \gtrsim 1$; so $\Delta \gtrsim \epsilon$. So, from the values already quoted, one reaches this high-density limit already in the upper photosphere, certainly for $\tau_5 \gtrsim 10^{-3}$. Table 2-3 shows, explicitly that $(b_{H^-} - 1) < 3$ percent at this and lower heights. (We give details on self-consistency of the table, below.) $(b_{H_2} - 1) < 5$ percent for $\tau_5 \gtrsim 10^{-4}$. Thus questions (C-1) and (C-2) are answered: nonLTE effects on the H^- continuum are negligible; collisions maintain LTE-R out to $\tau_5 \gtrsim 10^{-3}$; the configuration is indeed LTE-R, not just LOS. We can forget radiative-transfer effects on the continuum source-function. Correspondingly, in this high-density limit, the second bracket on the RHS of eq. (2.200) reduces to r^{-1} , so the equation reduces to

$$E_B = E_J + \Delta e / 4\pi \alpha_{H^-} n_{H^-}^* N_B. \quad (2.207)$$

If we impose no nonradiative heating, $\Delta e = 0$, this RE condition gives the standard condition under which we solved the LTE-R transfer equation. The decrease in J resulting from the presence of a boundary causes also the LTE-R decrease in T_e^4 . Roughly, we obtain the factor-2 decrease in T_e^4 caused by the factor-2 decrease in J , corresponding to the hemispheric anisotropy. The collisional dissociation maintains the n_{H^-}/n_H relative population; the radiation field does not perturb it.

Low-density configuration: In the limit, when $\Delta_i \ll 1$, we have $b_{H^-} = b_{H_2} = r = N_B/N_J$, thus strongly dependent on the value of J , for specified T_e , but completely independent of density. Thus, generally, we would need a solution of the transfer equation in this continuum, with the nonLTE source-function $b_C^{-1} B_\nu(T_e)$ —to the extent we neglect stimulated emissions, otherwise S_C is $(2h\nu^3/c^2)(b_C \exp X_\nu - 1)^{-1}$ —in order to specify both b_C and J_ν self-consistently. But in this exceptional case of the solar atmosphere and H^- , we have LTE-R valid until some $\tau_5 \gtrsim 10^{-3}$; J_ν (outward) is fixed, and it is the $W_\nu(\tau_\nu)$ in eq. (2.165) for J_ν which varies. Indeed, in this possible nonLTE region of $\tau_5 \gtrsim (10^{-2}, 10^{-3})$, even W_ν , hence J_ν , are constant, with $W_\nu = 0.5$. (This is true until one departs from the photosphere, and enters the extended atmosphere, where an r^{-2} factor enters W_ν .) So, for given T_e , b_{H^-} , hence S_C , is specified. Thus, questions (C-1) and (C-2) are answered in this other extreme region.

In this region, with the $\Delta_i \ll 1$, the second bracket on the RHS of eq. (2.200) reduces to 1, so we have

$$E_B/N_B = E_J/N_J + \Delta e / 4\pi \alpha_{H^-} n_{H^-}^* N_B. \quad (2.208)$$

The second factor on the RHS—the nonRE term—is the same for the high-density, eq. (2.207), case as here, because $b_{H^-} N_J = N_B$, as above. With no nonradiative heating, RE, and using $E/N = 2.7 T$ as above, we see that T_e is the same for the local gas as the mean energy per photoionized electron. That is, T_e is imposed by the quality of the radiation field; not by its quantity, as in the “collisionally-dominated, dense” case of eq. (2.207). This is literally Einstein’s classic photoelectric effect. It is Eddington’s symbiotic ISM configuration: hot gas, by this nonLTE, E/N , temperature; cold dust, by classical LTE energy balance. It is the classical result for the classical planetary-nebular model (Baker and Menzel, 1938)—i.e., PN without Bowen’s impurity cooling by the low-lying metastable lines of C, N, O. Cayrel (1963) emphasized the importance of the effect for the Sun. It appears in Feautrier’s solar models (1968). The main question is the choice of T_C . At the Earth, $F_\nu(\text{Sun}) \sim B_\nu(5800 \text{ K})$, cf Fig. 2-1. But in these upper-photospheric regions, J_ν lies closer to $B_\nu(5600 \text{ K})$. So by using a $J_\nu = 0.5 B_\nu(5600 \text{ K})$, we have a reasonable estimate of J_ν in the

upper-photosphere, low-chromosphere. Using $J_\nu = 0.5B_\nu$ (5800 K) would give a better estimate far from the star, as well as the best estimate of a gray, LTE-R value for T_0 —4700 K.

Atmospheric Model: Since these computations show that LTE-R is valid out to some $\tau_5 \sim 10^{-2}$, we should expect the gray-body, LTE-R solution of Section 2 to give a good value for T_0 , the asymptotic boundary value of T_e , up to the region where nonLTE effects enter. Then, far enough out in the atmosphere that collisional effects disappear, we have the solution of eq. (2.208). Thus, for the neoclassical, nonLTE, region of the Sun, so long as only H^- is the opacity source, we have:

$$4700 \text{ K} \lesssim T_e (\text{nonLTE, Sun, } H^-) \lesssim 5600 \text{ K (near)} - 5800 \text{ K (far)}. \quad (2.209)$$

This result exhibits what we said earlier, on several occasions: the difference in the several approximations for T_0 in the LTE and LTE-R cases all introduce uncertainties much smaller than the change in the boundary regions from non-LTE effects. We recall that the former uncertainty came from use of the factor 2, rather than $4/\sqrt{3}$ for T_{eff}^4/T_0^4 . In our present language, this difference reflects including or not including the T_e -gradient in computing W_ν .

We can exhibit the detailed behavior of T_e and the b 's across this nonLTE region from eqs. (2.200) – (2.202). We use the values:

$$D_{H^-, H} = 1.3 \times 10^{-9} \text{ cm}^3 \text{ sec}^{-1} \text{ (Schmeltekopf, Fehsenfeld, and Ferguson, 1967);}$$

$$D_{3H} = 10^{-32} \theta \text{ cm}^6 \text{ sec}^{-1} \text{ (Lambert and Pagel, 1968);}$$

$$4\pi\alpha_{H^-} N(J, O) = 1.0 \times 10^6 \text{ sec}^{-1} \text{ (Thomas and Athay, 1961);}$$

(2.210)

$$\alpha_{H^-} = 3.0 \times 10^{-17} \text{ (Geltman, 1962);}$$

$$\Delta_3 = 1.3 \times 10^{-15} n_H ; \quad \beta = 2.7 \times 10^{-2} (n_H/n_e) \theta^{-1/2} \exp(-1.739 \theta)$$

$$\theta = 5040/T_e ; \quad \gamma = z/(1+z); \quad z = \beta \Delta_3/(1+\beta).$$

I reproduce two tables showing the results of such computations, from Gebbie and Thomas (1970). Table 2-4 represents computations with $h\nu_i = 0$; Table 2-5 uses the actual H^- value of 0.74 eV, corresponding to a cutoff of the continuum at $\lambda 16,500\text{\AA}$. These are tables 1 and 4, respectively; from Gebbie and Thomas. Clearly, the ν_i effect is trivial; so one makes good estimates, easily, with $h\nu_i = 0$. Tables 2-4 and 2-5 cover the region $\tau_5 < 10^{-2}$. Table 2-3, from Thomas and Athay (1961), covers the region $\tau_5 > 10^{-2}$; but $b_{H_2} = 1$ was imposed, and T_e was taken from observations; the objective was to evaluate b_{H^-} . In this table I used $J_\nu = 0.5(1 + 1.5\tau_5) B_\nu$ (5800 K). Then from these results, one can make several kinds of comments, on wholly continuum models of the photosphere for the Sun, and for stars like it in having H^- as the predominant continuous opacity source.

First, the nonLTE effect is perceptible, but barely, at $\tau_5 = 10^{-2}$; it gives a $\Delta T_e \sim +300$ K at $\tau_5 = 10^{-4}$; and +800 K at $\tau_5 = 10^{-5}$. It has, however, not yet reached its asymptotic value of 5600 K in the near atmosphere at that τ , by some 100 K. Nonetheless, these nonLTE ΔT are very large compared with the ± 200 K in T_0 between approximate and rigorous gray-body solutions. The nonLTE rise is also large compared with that coming from adding the atomic hydrogen as an absorber, in the LTE models of Dumont and Heidmann. There, the LTE-R rise corresponding to this nongray effect is only some 100 K at $\tau = 10^{-5}$, and some 400 K at its maximum, at $\tau = 10^{-7.5}$. Clearly, as

Table 2-4
Gray-Body Solution: No Mechanical Heating

Variable	τ_5			
	10^{-2}	10^{-3}	10^{-4}	10^{-5}
n_H (cm ⁻³)	1.7×10^{16}	3.8×10^{15}	4.7×10^{14}	7.0×10^{13}
n_e (cm ⁻³)	2.1×10^{12}	6.4×10^{11}	4.6×10^{11}	4.7×10^{11}
Δ_3	22.1	4.94	0.611	0.091
β	32.6	24.4	4.75	0.842
γ	0.956	0.826	0.336	0.0399
τ	1.197	1.220	1.442	1.890
T_e (° K)	4720	4755	5025	5495
b_{H^-}	1.0088	1.0383	1.295	1.854
b_{H_2}	1.00026	1.0015	1.0510	1.465

Table 2-5
Table 2-4 With $\nu_i \neq 0$ Correction

Variable	τ_5			
	10^{-2}	10^{-3}	10^{-4}	10^{-5}
β	33.2	24.5	4.62	0.829
γ	0.956	0.826	0.335	0.0396
T_e (° K)	4765	4785	4970	5460
τ	1.120	1.138	1.309	1.830
b_{H^-}	1.0053	1.0240	1.206	1.797
b_{H_2}	1.00016	1.00094	1.0366	1.436

earlier said, the nonLTE effect heavily outweighs these other effects, although none of them become appreciable until τ reaches the range $10^{-4} - 10^{-5}$.

Second, the nonLTE effect is only about half the chromospheric-heating effect at $\tau = 10^{-5}$. Table 3-4 gives the empirical models found in Thomas and Athay (1961), cautioning that the values for $\tau_5 \gtrsim 10^{-5}$ are only approximate, being upper limits. Current estimates locate T_e (min) in the range $10^{-3} > \tau_5 (T_e \text{ min}) > 10^{-4}$, with a value $4000 \text{ K} < T_e \text{ (min)} < 4500 \text{ K}$. Thus, the significant nonLTE rise in T_e occurs just in that height-range where the observed rise in T_e becomes significant, but, as emphasized, the observed rise is about double the nonLTE one.

Third, the above considerations do not include the effect of the lines. We return to this, below, after considering the situation where the continuous opacity arises from an ion where the exceptional kind of collisional effect, that of associative detachment, does not exist.

Fourth, in summary, this simple approach to modeling this H^- atmosphere consists of—exclusive of the line effects discussed later:

- (1) a gray-body, LTE-R, distribution $T_e(\tau)$, out to about $\tau_5 \sim 10^{-2}$; and
- (2) use of eqs. (2.200) – (2.202) out to where the influence of a nonradiative energy dissipation occurs.

This should be a reasonable approximation for all “stars like the Sun” in having an H^- -dominated opacity. “Reasonable,” of course, depends on use. Our use is aimed at the photosphere as the lowest in a sequence of atmospheric regions, for whose modeling some estimate of T_e and density distributions are essential. I cite two examples of such use. One is in estimating where a given size mass-flux reaches the local thermal velocity; as we see in Part III, this depends on density and temperature distributions. Another is the question of what “untraps” the energy stored in the oscillatory modes of the photosphere (cf Leibacher, in the solar volume of the series, Jordan, 1981). If such untrapping occurs in the region where T_e begins its rise, it is possible that this nonLTE rise will suffice to “trigger” the nonradiative dissipation.

Finally, for comparison, Fig. 2-4 gives examples of these several models discussed: the gray-body model, the above nonLTE rise, the LTE-R models of Dumont and Heidmann showing the effect of additional absorbers, a theoretical LTE-R model by Kurucz, the Thomas-Athay 1961 empirical model of the T_e -rise in the low chromosphere, a current chromospheric model by Vernazza, Avrett, and Loeser.

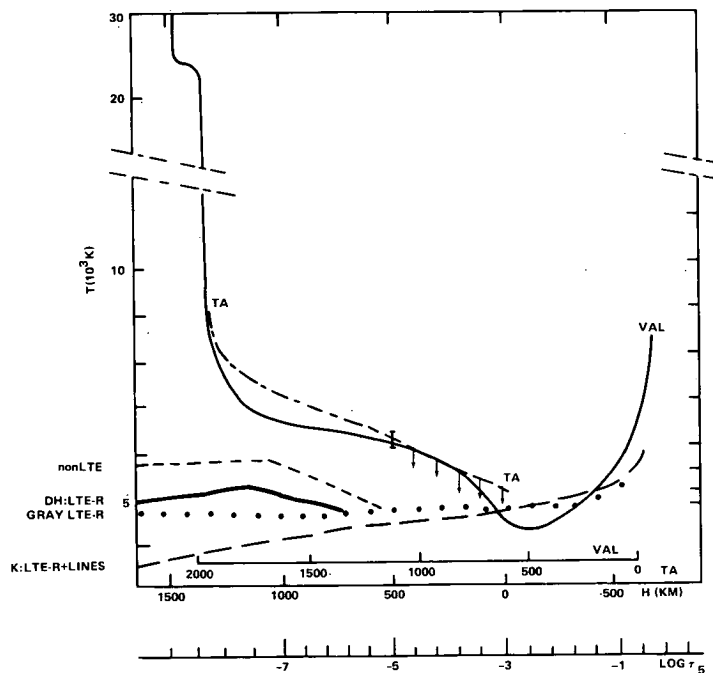


Figure 2-4. Various empirical and theoretical models of $T_e[h, \tau]$ in the solar atmosphere; explanation in text.

ii. 1-Level-Atom NonLTE Photosphere; No Exceptional Collisional Processes. The H^- photosphere maintains LTE-R out to very small $\tau - \tau_5 \gtrsim 10^{-3}$ —before significant nonLTE effects on T_e occur. Here the LTE-R, nonLTE transition is indeed via the diminishing role of collisions, but collisions of a particular character: thermal, atom-atom collisions at local thermal energies. In the LTE-R, reasonably high density, region the quantity of radiation absorbed, E_j , fixes T_e by its equality to the quantity of radiation emitted in photo-recombinations, E_B —via eq. (2.207). Consequently, the decrease in size of E_j to the boundary is accompanied by a corresponding decrease in T_e . In the nonLTE, low-density region, the quality of radiation absorbed, E_j/N_j —the mean energy absorbed per photoionization—fixes T_e by

its equality to the mean energy emitted per photo-recombination, E_B/N_B . Consequently, the decrease in size of E_J to the boundary, accompanying that of J_ν , is compensated by the same decrease to the boundary of N_J , and so T_e stays constant, after rising from its depression caused by the radiation-quantity-dependence in the LTE-R regime.

When we pass to an atmospheric configuration that does not have such exceptional, thermal, collisional partition of energy among kinetic, internal, and radiative degrees of freedom, we expect a nonLTE configuration to begin deeper in the atmosphere. That is, we expect the same decrease in J_ν to the boundary. Artificially imposing LTE-R would result in an apparent T_e decrease following this J_ν -decrease, just as in the situation already discussed for the lines. The nonLTE effect, as measured by the b_K , must enter to maintain T_e at its quality-controlled, rather than quantity-controlled, value. The small size of the ϵ introduces a spatial lag, before the boundary effects damp out, and T_r approaches T_e —and can be used as a diagnostic measure of it. We make these remarks explicit, by simply considering again a 1-level atom; but one without an exceptional collisional interaction with the kinetic energy storage measured by T_e .

As before, we consider only the continuum, so we have the radiative-transfer eq. (2.179a) with no line-terms, which reduces to eq. (2.179b), for the continuum S_C and $d\tau_C$ of eqs. (2.180). We can modify the definitions of E and N , eqs. (2.182) and (2.183), to place a ν -dependent α_ν under the integral. The only difference it makes to the following is in the ease of evaluating E/N . So, because our focus does not lie on these details, but rather on the effect of only very small collisional terms, we continue to consider the gray atmosphere without stimulated emission. Especially in the case of setting $\nu_i \rightarrow 0$ for algebraic and numerical simplicity, the numerical results will change, but not the principal point of contrast with the H^- case. Then in place of eq. (2.191), statistical-equilibrium gives:

$$4\pi\alpha_C (n_C N_J - n_C^* N_B) + (n_C C_{C\kappa} - n_C^* C_{C\kappa}) = 0, \quad (2.211)$$

defining:
$$\epsilon_C = C_{C\kappa}/\alpha_C^* N_B 4\pi \quad (2.212)$$

we obtain, using eqs. (2.182) and (2.211):

$$b_C^{-1} = \frac{(N_J/N_B + \epsilon_C)}{1 + \epsilon_C} \quad (2.213)$$

We note the basic condition that ϵ_C is small. We have typical values for the several hydrogen continua:

$$\epsilon \text{ (Paschen)} = 4 \times 10^{-7} (X+2) X_1 (10^{-11} n_e) (10^{-4} T_e)^{3/2} \quad (2.214a)$$

$$\epsilon \text{ (Balmer)} = 8 \times 10^{-8} (X_2+2) X_1 (10^{-11} n_e) (10^{-4} T_e)^{3/2} \quad (2.214b)$$

$$\epsilon \text{ (Lyman)} = 5 \times 10^{-9} (X_1+2) X_1 (10^{-11} n_e) (10^{-4} T_e)^{3/2} \quad (2.214c)$$

Then to obtain N_J , b_C , and J_ν we must solve the transfer equation (2.179b) in the continuum. The question is the conditions under which we solve it: for prescribed $T_e(\tau)$, or under RE to determine $T_e(\tau)$? In the first alternative, we ask what radiative flux is produced in this continuum for a given atmospheric model. In the second alternative, we proscribe the radiative flux imposed on the atmosphere from the subatmosphere, and ask what atmospheric $T_e(\tau)$ it produces.

a. Solution Under Specified $T_e(\tau)$. First, compare the situation to that of a spectral line, which we have already discussed. If the integrals for E , N were over $\Delta\nu$ as small as a line-width, the ν -factor, which distinguishes N from E , would be constant over $\Delta\nu$, and we would have $N \sim E/h\nu \sim \Delta\nu (J_\nu \text{ or } B_\nu)/h\nu$. So, S_C would reduce to the form of

S_{ν} in eq. (2.153) – (2.154). So the difference between line and continuum lies in the ν -range over which one integrates, and that we must consider ν -integrated rates as well as ν -integrated energies. For the continuum, one can think of the scattering terms as entering with a variable weight, B_{ν}/N_B , at each ν -point, which preserves the same relative importance of photoionization and collisional ionization at each ν . That is, radiation field and collisions always enter the equation for I_{ν} , at each ν , with the same weight, B_{ν}/N_B .

Second, the monochromatic transfer equation is then

$$\mu dI_{\nu}/d\tau_{\nu} = I_{\nu} - S_{\nu} = I_{\nu} - \delta \cdot N_J (B_{\nu}/N_B) - \gamma B_{\nu}, \quad (2.215)$$

using:

$$\delta = (1 + \epsilon)^{-1} \quad ; \quad \gamma = \epsilon/(1 + \epsilon) = 1 - \delta \quad (2.216)$$

To solve it, it is best to convert it into two equations, in N_J and E_J , with N_B and E_B considered as specified by specifying $T_e(\tau)$. Here, to illustrate the physics, we use the Eddington approximation, eq. (2.167a) in the continuum. We integrate it over $d\nu$ to obtain the E_J equation, and over $d\nu/h\nu$ to obtain the N_J equation. We focus on showing how the interaction of E and N , not the value of E , determine T_e , in this nonLTE situation of small ϵ . So, we first treat the imposed isothermal, and the gray, cases as the simplest illustration. If necessary, one can include an $\alpha_{C\nu}$ in the N and E integrals, but that is a numerical, not physical, detail. We can always consider 1-gray, etc., regions, as before.

The isothermal proscribed T_e -distribution lets us introduce, since E_B and N_B are constant:

$$R_N = N_J/N_B \quad ; \quad R_E = E_J/E_B. \quad (2.217)$$

We obtain

$$\frac{d^2 R_N}{d\tau^2} = 3 (R_N - \delta R_N - \gamma) = 3\gamma (R_N - 1) \quad (2.218a)$$

$$\frac{d^2 R_E}{d\tau^2} = 3 (R_E - \delta R_N - \gamma) . \quad (2.218b)$$

So clearly the equations have the same solution, which is, applying the same boundary-conditions as those on J_{ν} , eqs. (2.169) (and note eqs. 2.170)

$$E_J/E_B = N_J/N_B = 1 - (1 + \mathcal{J}\gamma)^{-1} \exp(-\sqrt{3\gamma}\tau) \cong b_C^{-1} \quad (2.219)$$

The boundary values are:

$$\text{in depth: } E_J \rightarrow E_B \quad ; \quad N_J \rightarrow N_B \quad (2.220a)$$

$$\text{at } \tau = 0: E_J/E_B = N_J/N_B = b_C^{-1} = \mathcal{J}\gamma/(1 + \mathcal{J}\gamma) \quad (2.220b)$$

Applying these results for b_C , we see that we do indeed, as depth increases, reach LTE-R: $b_C \rightarrow 1$, at $\tau \gtrsim (3\gamma)^{-1/2}$. But this LTE-R arrives because of LOS, not because collisions predominate over photoionization or photo-recombination. In this isothermal atmosphere, the boundary value of E_J is small—just as was the boundary value for J_{ν} , and J_{ν}

in the line. But we would make the same erroneous diagnostics if we interpreted these E_J to imply an outward decrease in T_e . It is the ratio $E_J/N_J = E_B/N_E$ which measures T_e , and as shown by eq. (2.219), that ratio remains constant, as it should, in proper, nonLTE, diagnostics of this isothermal atmosphere.

We want to apply this result to models—empirical and theoretical—of both upper photosphere and lower exo-photosphere, so it is useful to know what such nonLTE implies on energy loss and cooling.

$$\begin{aligned}
 \text{net-radiative-energy-loss} &= 4\pi\alpha_C (n_C^* E_B - n_C E_J) \\
 &= 4\pi\alpha_C n_C^* E_B (1 - b_C E_J/E_B) \\
 &= 4\pi\alpha_C n_C^* E_B \epsilon (N_B/N_J - 1)/[1 + (\epsilon N_B/N_J)] \\
 &= 4\pi\alpha_C n_C^* E_B \epsilon e^{-k\tau} [(1 - e^{-k\tau}) + (\epsilon + \sqrt{3}\gamma)]^{-1}; k = \sqrt{3\gamma}.
 \end{aligned} \tag{2.221}$$

From the boundary values in eq. (2.220b) above, we see that there is energy balance—no radiative energy-loss—at great depth—corresponding to the LOS configuration. At the boundary, the loss is proportional to $\epsilon^{1/2}$. So, again, one must be careful in diagnosing energy loss from observed intensities. It is much less under nonLTE than under LTE, for the same collisional rates. We have the limits:

$$0 \leftarrow \epsilon e^{-k\tau} < \frac{\Delta e \text{ (rad)}}{4\pi\alpha_C n_C^* E_B} < \sqrt{\epsilon}/(1 + \sqrt{3}\tau). \tag{2.222}$$

So the radiative flux produced by this isothermal atmosphere is highly variable. Essentially, it is “surface cooling,” as we have earlier called it. LOS, not collisions, maintains quasi-homogeneity in the interior. At the surface, radiative-cooling compensates for the integrated, not local, collisional excitation, but not in simple proportion to the radiative rate. If, in place of $n_C^* E_B$, the recombination energy, we use $n_C E_J$, the radiative-absorption energy, in eq. (2.222), we obtain the same result, because of the value of b_C from eqs. (2.213) and (2.219). Again, in all this, continuum and line results are completely parallel: *diagnostics of only the energy, in line or continuum, leads to misleading result*—an underestimate of T_e . One needs adjoin to such diagnostics of observed radiation in line or continuum a value of b_C —or its equivalent N_B/N_J —obtained either empirically or theoretically. When we do not know $T_e(\tau)$, a priori, in a non-isothermal atmosphere, any diagnostics must be done iteratively.

We see the diagnostic situation in a nonisothermal atmosphere by rewriting eqs. (2.218) in their general forms:

$$\frac{d^2 N_J}{d\tau^2} = 3(N_J - \delta N_J - \gamma N_B) = 3\gamma(N_J - N_B) \tag{2.223a}$$

$$\frac{d^2 E_J}{d\tau^2} = 3(E_J - \delta N_J [E_B/N_B] - \gamma E_B). \tag{2.223b}$$

E_J and N_J do not have the same solution, so E_J/N_J and T_e vary. So, specifying $N_B(\tau)$ gives $N_J(\tau)$ from eq. (2.223a); then this solution, plus $E_B(\tau)$, gives $E_J(\tau)$ from eq. (2.223b). In this simple gray case, N_B and E_B are given by eqs. (2.203) and (2.204) in terms of T_e ; so specifying $T_e(\tau)$ gives the required N_B and E_B . Observations of $E_J(\tau)$, compared with those predicted from $T_e(\tau)$ and eq. (2.223) then provide, iteratively, an eventual $T_e(\tau)$, as a function of

the parameter ϵ . For the gray case, of course, we have no observational probe of $E_J(\tau)$ except at the limb of stars—most effectively, by eclipse measures of emission as a function of height above the limb, as τ decreases. So in the solar case, we can actually observe those limb regions where strong nonLTE effects in the continuum occur, not only in the value of b_H —discussed in the preceding Section α , as collision effects decrease and H^- opacity gives place to neutral hydrogen opacity, but also in the value of b_1 for the ground-level of neutral hydrogen. There, it is the height evolution of departure from LOS which evolves b_1 . In eqs. (2.156), (2.157) written for H^- , n_i is n_H , which is effectively n_1 (hydrogen). So it, in turn, has a b_1 factor determining its value. These solar limb regions are transparent in the H^- and Balmer continua, and it is the opacity of the Lyman continuum which evolves, decreasing outward. At the lowest heights, where it is LOS in the Lyman continuum, $b_1 = b_2$ and is fixed by the boundary value of the BaC radiation field. At intermediate heights, it is the evolution of the LyC from LOS to optical thinness which fixes the value of b_1 , according to the above transfer problem, for the actual $T_e(\tau)$. A priori, in the upper-photosphere, lower-chromosphere, $T_e(\tau)$ is unknown, and is to be determined; its empirical behavior fixes, empirically, where the photosphere ends. So we have precisely the above problem of observing/infering E_J , and converting this to an E_B —hence, T_e , by the stated iteration.

A good example is provided by our first diagnostics of the outer-photosphere, lower-chromosphere (Athay et al., 1955) where we ignored the nonLTE effect on the ground-level of hydrogen, in computing H^- opacities, to diagnose the observed Paschen continuum at eclipse. These diagnostic results severely underestimated the chromospheric rise of T_e . Subsequent work by Zirker (1956, 1958) on the hydrogen-ionization, by Pottasch and Thomas (1959, 1960) and Thomas (1961) on the above-type coupling to the LyC transfer problem, and by Thomas and Zirker (1961a, b, c) on He II, resolved, and applied, the diagnostic problem to the lower solar chromosphere. To my knowledge, it was the first application of this combination of observed energy, and computed b_C (or N_J/N_B), to: (1) exhibit the wide divergence between LTE-R and nonLTE diagnostics, in the empirical determination of a T_e -distribution; (2) apply this T_e -distribution, with proper nonLTE correction, to predict the emission in the LyC. Result (1) gave a factor-2 difference in T_e at 1500 km eclipse height—(6000 K vs. 10,000 K). Result (2) gave a value $0.5\text{--}2.3 \times 10^{10}$ for $b_1 \exp(h\nu_{\text{LyC}}/kT_e)$; Morton and Widing's (1961) NRL rocket observations gave an observational value of this quantity—which is $\exp(h\nu_{\text{LyC}}/kT_{\text{ex}})$ —as $0.8 \times 10^{10} \pm$ a factor 2. The corresponding LTE-R diagnostics would interpret T_{ex} literally as T_e , and obtain 6900 K instead of the actual 8000–8500 K in the region of LyC origin. As we have seen, photospheric models give a T_{e0} between 4000–4500 K. Because of the large $h\nu_{\text{LyC}}/kT_e$ value, this difference between 4000 K and 6900 K represents a factor 10^7 in LyC emission at the $\lambda 910$ series head. If one used $T_e = 8500$ K, without the b_1 correction, he would overestimate the LyC emission by about a factor 100, corresponding to the converse of diagnosing the 6900 K as the actual T_e . Thus, we see that these nonLTE effects are significant, but can be empirically-theoretically determined to within factors of about 2 uncertainty rather than the factors $10^2 - 10^7$ resulting from their ignorance. In Chapter 3, we summarize our knowledge of a wide variety of stars exhibiting profound exospheric structure. The use of standard, LTE-R photospheric models, or nonLTE models where the only effects are, as for H^- , collisional—not these photoionization and opacity-induced ones—can lead to bad estimates of upper-photospheric boundary conditions for the exospheric regions. So we want physically-correct, even if mathematically-crude, approaches based on the preceding, which distinguish between J -variation and B -variation. The RE condition, as remarked, illustrates the problem well, supplementary to the isothermal; so we consider it. As before, we consider 1-gray, then multi-gray continua, then line-blanketing.

β . *Solution Under the RE Configuration*: Alternatively to specifying T_e , empirically or otherwise, we ask the result when a T_e -distribution is imposed by the combined conditions of only a radiative flux, but under nonLTE. Then the RE condition

$$\int J_\nu \alpha_{C\nu} d\nu = \int S_\nu \alpha_{C\nu} d\nu, \quad (2.224a)$$

or in this gray case

$$E_J = J = S = b_c^{-1} B = b_c^{-1} E_B, \quad (2.224b)$$

reduces the monochromatic radiative-transfer equation (2.215) to the same ν -integrated form of eqs. (2.53) or (2.113) to determine $J(\tau)$,

$$\mu dI/d\tau = I - E_J = I - J, \quad (2.225)$$

whether the configuration is LTE-R or nonLTE. The difference lies in the relation between J and $B(T_e)$, between E_J and E_B , and in the value of τ for given (n_e, T_e) . Under nonLTE, RE no longer gives $J = B$; instead, it gives the relations (2.224b). Then the statistically-steady-state condition gives the expression (2.213) for b_c , in terms of N_J/N_B . And, finally, some equation equivalent to eq. (2.223a) gives N_J/N_B . Noting that the condition $J = b_c^{-1} B$ gives

$$E_J/E_B = b_c^{-1} = (N_J/N_B + \epsilon)/(1 + \epsilon); \quad (2.226)$$

we see that substituting it into eq. (2.223b) gives the RHS of that equation to be zero. That is, solving that equation for E_J —i.e., J —gives only the linear terms. Instead, we solve the gray-atmosphere equation (2.225) as before, obtaining eq. (2.131) for J , not for B , emphasizing that flux-constancy depends primarily on J , not B , space-gradient.

$$E_J(\tau) = J(\tau) = \frac{3F}{4\pi} [\tau + q(\tau)] \quad (2.131a)$$

where, as before, F is the radiative flux. To translate this into $E_B(\tau) = B[T_e(\tau)]$, we either solve eq. (2.223a), or by defining

$$N_I = \int (I_\nu/h\nu) d\nu; \quad (2.227)$$

we can write the equivalent of the radiation-energy equation (2.225), for the radiation-rates:

$$\mu dN_I/d\tau = N_I - N_J - \epsilon(1 - b_c^{-1})N_B. \quad (2.228)$$

Apart from the term in ϵ , eq. (2.228) in (N_I, N_J) is the same as eq. (2.225) in (I, J) ; J and N_J are the μ -integral of I and N_I , and the boundary conditions (2.123), (2.124) on I would be the same for N_I . So, were $\epsilon = 0$, the solution (2.131a) for $J(\tau)$ would be precisely the same for $N_J(\tau)$, except for the coefficient, which is F in eq. (2.131a), the constant flux in I . Considering this case $\epsilon = 0$ shows the parallel to the case of electron scattering in classical atmospheric modeling, so it is useful, for perspective. I emphasize: in both cases, $\epsilon = 0$ corresponds to forbidding creation-destruction of photons; an original radiative input at the base of the atmosphere is transmitted by simply being scattered. From eq. (2.222), we see that an atmosphere with $\epsilon = 0$ does not “cool” by transferring collisional excitation into radiation; it simply “leaks” the radiation put into the atmosphere at its base.

So, we consider the configuration: $\epsilon = 0$. The solution of eq. (2.228) is, corresponding to eq. (2.131a) being the solution of eq. (2.225),

$$N_J(\tau) = \frac{3K}{4\pi} [\tau + q(\tau)], \quad (2.229)$$

where K is some constant, to be determined. Then eq. (2.226) gives

$$f(T_e; \nu_i) = E_B/N_B = E_J/N_J = F/K = \text{constant.} \quad (2.230)$$

We appreciate the significance of the result (2.230), which says that this RE atmosphere with $\epsilon = 0$ must be isothermal, by combining eqs. (2.224b), (2.213), and (2.229) to convert E_J into E_B :

$$E_B = b_c E_J \cong N_B (E_J/N_J) = N_B (F/K) = N_B (\sigma T_{\text{eff}}^4/K) \quad (2.231)$$

from the definition of T_{eff} . That is, if we define

$$K = N_B (T_{\text{eff}}) \quad (2.232)$$

eq. (2.230) becomes:

$$f(T_e; \nu_i) = E_B(T_e)/N_B(T_e) = E_B(T_{\text{eff}})/N_B(T_{\text{eff}}). \quad (2.230a)$$

Since $f(T_e; \nu_i)$ is a single-valued function of T_e —with value $2.7 kT_e$ for $\nu_i = 0$ —the atmosphere is simply isothermal at T_{eff} , for $\epsilon = 0$.

Thermodynamically, this solution—which gives E_J and N_J increasing inward without limit, b_c decreasing inward without limit—is of course nonsense, at large depth. The solution (2.131a) for $J(\tau)$ is correct, independent of the value of ϵ ; it simply gives the behavior of a J which preserves a constant radiative flux. But it is the product of a $B(T)$ and a “boundary effect,” a parameter $[b_c(\tau=0)/b_c(\tau)]^{-1} W$ in the representation and discussion of eq. (2.151). So, while eq. (2.131a) can indeed represent $T_e(\tau)$ far from the boundary it cannot, by itself alone, near the boundary, and we must have the correct $N_J(\tau)$ to go with it, to make the boundary correction. The representation (2.229) does make such a correction, but its accuracy is the less correct, the farther one goes from the boundary-region $0 \lesssim \tau \lesssim 1$, because of the neglect of the source-sink terms, ϵB and ϵ , in the source-function—the last two terms—of its correct transfer equation (2.228). We also kept only an approximation, N_J , to its scattering term, whose correct value is $N_J \delta$.

We can reduce this problem to a familiar one, by comparing it to the classical Milne-Schuster problem of an atmosphere where the most abundant absorber only scatters, coherently, and there is a minor constituent which absorbs and re-emits according to LTE-R. (We can update this problem to a modern nonLTE treatment of the impurity by writing a scattering + source-sink representation for its source-function; cf Gebbie and Thomas, 1968; but it adds nothing to our point here, just elaborates it. And we consider this complete example later, in discussing the Temperature-Control-Bracket.) Then we have eq. (2.179b), but with

$$S_\nu = J_\nu \delta + B_\nu \gamma, \quad (2.233)$$

$S_C = J_\nu; S_\nu = B_\nu; d\tau_\nu/d\tau_c = s; \gamma, \delta$ from eq. (2.216) using s , not ϵ . Setting $s = 0$ corresponds to $\epsilon = 0$ in the above, and eq. (2.179b) becomes:

$$\mu dI_\nu/d\tau_\nu = I_\nu - J_\nu \quad (2.234)$$

the equation already discussed with $S_\nu = J_\nu$: pure monochromatic scattering, which implies the strong condition of monochromatic-RE, rather than integrated-RE. The solution of eq. (2.234) is eq. (2.131a) with F_ν , rather than F , being constant, with a value imposed at the bottom of the atmosphere. Then the ν -dependence of the observed F_ν and I_ν is whatever is imposed at the bottom of the atmosphere, independent of the atmospheric T_e . Again, as in the

above nonLTE example, this example treats a given amount of radiation put into the bottom of the atmosphere, and emerging at the top, without thermal interaction with the matter in the atmosphere—as measured by the terms in ϵ and s . Such processes are not useful in either controlling the thermodynamic state of the atmosphere, or permitting its diagnosis.

So we return to the complete transfer equation for N_J , eq. (2.228), which it is more convenient to write as:

$$\text{either} \quad \mu dN_I/d\tau = N_I - N_J + \gamma(N_J - N_B), \quad (2.235a)$$

$$\text{or} \quad = N_I - N_J \delta - \gamma N_B. \quad (2.235b)$$

Since, a priori, we do not know that $T_e(\tau)$ which permits a flux-constancy under this gray-body, RE, configuration, the combined solutions of eqs. (2.131a) and (2.235) must be iterative, with iterative parameter being either N_B or $(N_J - N_B)$, the coefficient of each, in the equations, being $\epsilon \ll 1$. Then we note that the small size of ϵ , and the relations (2.220), suggest that we can retain the relations

$$E_B/N_B = E_J/N_J \quad \text{everywhere}, \quad (2.236)$$

imposing $E \rightarrow E_B$, $N_J \rightarrow N_B$ for large τ . Then we begin the iteration from eq. (2.235b), assuming N_B linear in τ ,

$$N_B = x + y\tau, \quad (2.237)$$

and use a discrete-ordinate representation of N_J , obtaining instead of eq. (2.113)

$$\mu_i dN_{Ii}/d\tau = N_{Ii} - 0.5\delta \sum_{-n}^n a_j N_{Ij} - \gamma(x + y\tau). \quad (2.238)$$

We follow precisely the solution pattern of eqs. (2.114) et seq., and so obtain the expressions corresponding to eqs. (2.122) and (2.129):

$$N_{Ii} = y \left\{ \sum_{\alpha=1}^{n-1} \frac{L_\alpha e^{-k_\alpha \tau}}{1 + \mu_i k_\alpha} + \frac{L_0 e^{-k_0 \tau}}{1 + \mu_i k_0} + z + \tau + \mu_i \right\}, \quad (2.239)$$

$$N_J = y \left\{ \sum_{\alpha=1}^{n-1} L_\alpha e^{-k_\alpha \tau} + L_0 e^{-k_0 \tau} + z + \tau \right\}. \quad (2.240)$$

The k_α and L_α are to be determined from the expressions corresponding to eqs. (2.119), (2.124):

$$\sum_1^n a_j / (1 - \mu^2 k^2) - (1 + \epsilon) = 0, \quad (2.241)$$

$$\sum_{\alpha=1}^{n-1} \frac{L_\alpha}{1 - \mu_i k_\alpha} + \frac{L_0}{1 - \mu_i k_0} + z - \mu_i = 0. \quad (2.242)$$

Then we note several differences between this solution for N_{I_i} and N_{J_j} , relative to that for I_i and J_j , because $\epsilon \neq 0$. First, we note that the linear terms in τ and μ_i , in eq. (2.239) arise only from a τ -dependence of N_B . If we began the iteration with constant N_B , the particular, nonconstant, solution corresponding to eq. (2.114) would not exist in eq. (2.238) because $\delta \neq 1$, $\epsilon \neq 0$. Second, eq. (2.119) has only $n-1$ roots k_α^2 , because one root is $k^2 = 0$. With $\epsilon \neq 0$, this degeneracy is removed, and there are n roots k_α^2 , of which the smallest—which we designate by k_0^2 —is proportional to ϵ . The other k_α are essentially independent of ϵ , for these $\epsilon \ll 1$, and these k_α ($\alpha > 0$) > 1 . For example, we compare algebraic solutions for the first two approximations (taking a_i, μ_i from Chandrasekhar, 1960):

$$\text{First approximation:} \quad \mu_1 = 0.577 \quad ; \quad a_1 = 1 \quad (2.243a)$$

$$\text{for } E_J : k_0^2 = 0 \quad ; \quad \text{for } N_J : k_0^2 = \epsilon(\mu_1^2 + \epsilon \mu_1^2)^{-1} \cong 3\epsilon$$

$$\text{Second approximation:} \quad (2.243b)$$

$$\mu_1 = 0.340 \quad ; \quad a_1 = 0.652$$

$$\mu_2 = 0.861 \quad ; \quad a_2 = 0.348$$

$$\text{for } E_J : k_0^2 = 0 \quad ; \quad \text{for } N_J : k_0^2 = \epsilon \left\{ (\mu_1^2 a_1 + \mu_2^2 a_2) + \epsilon (\mu_1^2 + \mu_2^2) \right\}^{-1} \\ \cong 3\epsilon$$

$$E k_1^2 = \frac{\mu_1^2 a_1 + \mu_2^2 a_2}{\mu_1^2 \mu_2^2} \quad ; \quad N k_1^2 = E k_1^2 + \epsilon \left\{ \frac{a_1 \mu_1^4 + a_2 \mu_2^4}{\mu_1^2 \mu_2^2 (a_1 \mu_1^2 + a_2 \mu_2^2)} \right\} \\ = 3.88 \quad \cong 3.88 + 7.1\epsilon .$$

Following Chandrasekhar (1960), or Jefferies (1968), or Thomas (1965) one readily shows that the division points, μ_i , and roots k_α of eq. (2.241) satisfy

$$\prod_1^n \mu_j \prod_0^{n-1} k_\alpha = \epsilon, \quad (2.244a)$$

so, using $k_0^2 = 3\epsilon$, we obtain the usual

$$\prod_1^n \mu_j \prod_1^{n-1} k_\alpha = 3^{-1/2} \quad (2.244b)$$

Then, because we do not, a priori, know $N_B(\tau)$, hence, neither y nor z , we have $n+1$ unknowns in eq. (2.242) and just n equations. But for sufficiently-small ϵ , the term $[z + L_0/(1 - \mu_i k_0)]$ does not vary significantly with μ_i , so this combined term can be considered the equivalent of Q in eq. (2.124), and we have, corresponding to eq. (2.244b), and eq. (2.132)

$$\sum_1^{n-1} L_\alpha + (L_0 + z) = q(0) = 3^{-1/2}. \quad (2.245)$$

So, to these approximations, which rest on $\epsilon \ll 1$, we can distinguish three regions in this RE, nonLTE photosphere:

The nonLTE boundary region: $0 < \tau < k_1^{-1} < 1$:

$$2.7 kT_0 \sim E_B(T_0)/N_B(T_0) = E_J[\tau]/N_J[\tau] \cong [3F/4\pi]/y. \quad (2.246)$$

In this region, the solution corresponds to the isothermal solution of eq. (2.230). The essential approximations in defining the region are two: (1) that the k_α, L_α for $\alpha > 0$ are the same for E_J and N_J ; (2) that the term in L_0 remains constant, because ϵ —hence k_0 —is so small. Then we have an isothermal boundary-region, over this range in τ , where

$$T_0 > T_e [1 \lesssim \tau \lesssim (3\epsilon)^{-1/2}]. \quad (2.247)$$

The parallel decreases of E_J and N_J toward small τ are simply the boundary effect on anisotropy of I_i and N_{I_i} . Because the boundary effect on diffusion has so much greater a scale, corresponding to the small ϵ , these two boundary effects are uncoupled. So the change in E_J and N_J is compensating; the region remains isothermal, at the temperature at its base, $\tau \sim 1$, which is measured by the quality of the radiation.

The nonLTE diffusion, or thermalization, region.

LOS builds up across the region, as the opacity becomes great enough to contain the photon scattering-diffusion. This does not affect J , whose gradient is fixed by RE, but which still differs from B ; so no terms in ϵ enter. It does affect N_J , with the major differentiating change from $E_J(\tau)$ being just the L_0 term. So,

$$2.7kT_e \cong E_B(T_e)/N_B(T_e) \cong E_J(\tau)/N_J(\tau) \sim (3F/4\pi)y^{-1}(\tau + Q) \left\{ \tau + z - (z - Q)e^{-k_0\tau} \right\}^{-1}. \quad (2.248)$$

That is, N_J increases inward more rapidly than E_J , so T_e decreases inward, more rapidly at first, then leveling off, as the L_0 -effect vanishes.

The LOS region, $E_J = E_B$.

The above first-iteration approximation, N_B linear in τ , becomes increasingly inadequate as one approaches this region where E_J, N_J become E_B, N_B ; because E_B varies as T^4 and N_B as T^3 ; so a linear variation in τ for both is impossible. One abandons the algebraic approach, if he wants other than schematic accuracy.

But for our present purposes—here, in the multi-gray region that follows, and in discussing line-blanketing—the above suffices. Because, it tells us that what we see—the radiation originating near $\tau \sim 1$ —measures T_e by its quality, not its quantity. It tells us that we should estimate T_e from E_J/N_J , at the top of each atmospheric opacity region. Then we use this T_e as the quasi-isothermal T_e in the overlying opacity subregion, until that region, in turn, becomes optically-thin enough to depart from LOS in its opacity. Then we repeat the above procedure in this region.

We proceed to abstract this approach, initially applied in the above-mentioned analysis of the LyC region of the solar atmosphere, then developed in *the so-called Temperature-Control-Bracket*, TCB, by Gebbie and Thomas (1970, 1971), which exploits just this shift from quantity to quality of T_e by the radiation field in the continuum. It is of interest in not only the upper photosphere, and the LOS to nonLTE transition, but also in the exo-photospheric

regions, So, it provides a transition between Chapters 2 and 3, in giving a physical picture of what controls the T_e -structure. But first we complete the discussion of this 1-level-atom photosphere by treating that photosphere which also includes a purely scattering constituent, like electrons.

γ . *The RE configuration with electron-scattering.* The monochromatic transfer eq. (2.179a) is modified by using a source-function essentially like eq. (2.233)—i.e., adding an opacity term, $-\sigma_e n_e dx$ to $d\tau_\nu$, and an emission term, $\sigma_e n_e J_\nu$, and dropping the line terms. So the $n_c \alpha_c$ retained in the opacity is nonLTE, but the emission term retained, $\alpha_c^* n_c^* B_\nu(T_e)$ is LTE. Thus, the s defined just after eq. (2.233) is nonLTE; so the γ and δ are hybrid and independent. So we slightly modify definitions to obtain

$$d\tau_\nu = d\tau_s + d\tau_c = -(\sigma_e n_e + n_c \alpha_c) dx = (1+s)d\tau_s, \quad (2.249)$$

$$S_\nu = J_\nu (1+s)^{-1} + B_\nu (s b_c^{-1}) (1+s)^{-1} = J_\nu \Delta + B_\nu b_c^{-1} \Gamma \quad (2.250)$$

$$s = n_c \alpha_c / \sigma_e n_e \quad ; \quad \Delta = (1+s)^{-1} \quad ; \quad \Gamma = 1 - \Delta. \quad (2.251)$$

The preceding cases (α) and (β) correspond to $s \gg 1$; an opacity dominated by electron-scattering corresponds to $s \ll 1$. Then using eq. (2.213) for b_c , we can make exactly the same kind of discussion as we did in (α)–(β). The last term in eq. (2.250) divides into terms in J_ν and B_ν . Effectively, for small s , we obtain solutions in terms of the parameter $(s + \epsilon)$ instead of only ϵ . As above, the condition of RE reduces the equation in J , or E_J , into eq. (2.225)—which holds independently of the form of S_ν . As before, we have the same relation $E_B = b_c E_J$ to apply to the solution $E_J(\tau)$ to obtain $E_B(\tau)$; so we need $N_J(\tau)$. Instead of eq. (2.235), we obtain, by the same procedure, with S_ν from eq. (2.250):

$$\mu dN_I/d\tau = N_I - N_J (\Delta + \Gamma\delta) - N_B \gamma \Gamma. \quad (2.252)$$

Again, we use a discrete ordinate representation for N_J , and a linear representation for $N_B(\tau)$, eq. (2.237), as first iteration. Instead of eq. (2.238) we obtain:

$$\mu_i dN_{Ii}/d\tau = N_{Ii} - 0.5 (\Delta + \Gamma\delta) \sum_j a_j N_{Ij} - \Gamma\gamma (x + y\tau), \quad (2.253)$$

and again the essential quantities are the roots k_j which, instead of from eq. (2.119) for E_J , or eq. (2.241) for the case with no scattering, we have the determining equation:

$$a_j / (1 - \mu_j^2 k^2) - (1 + \epsilon + s + \epsilon s) / (1 + \epsilon + s) = 0. \quad (2.254)$$

The fact that $\epsilon, s \neq 0$ again removes the degeneracy of $k_0^2 = 0$. But we see that to first order, $k_0^2 \sim \epsilon s$; so it will be smaller in this scattering case. Thus, relative to the three regions discussed in eqs. (2.246)–(2.248), we see that the nonLTE isothermal boundary-region will not be strongly changed. However, the extent of the nonLTE diffusion-thermalization region will be larger. We do not go into details here. To our accuracy, they have been sufficiently discussed in the preceding sections, one must simply take into account the change in k_0 , primarily.

c. **Multi-NonLTE Continua, Spectral Lines, and Their Combined Effects on Upper-Photospheric Models.** The discussion in Section b parallels our LTE-R discussion of the 1-gray continuum. It shows that, except for cases of exceptionally large collisional processes, $T_e(r)$ is best determined in terms of the ratio E_B/N_B , which we compute by computing the depth-variation of E_j/N_j , and relating the two ratios via the energy equation. So, rather than paralleling our discussion of the multi-continuum atmosphere in the LTE-R case via the multi-gray approximation, then introducing the lines, it is easiest to consider directly E/N in the general case. We can in this way exhibit most clearly both the effect of several continua, and of the differing effects of photoionization- and collision-dominated lines. We abstract the approach of Gebbie and Thomas (1971), and extend it to the lines. Detailed solutions do not exist; but we can show clearly the inadequacy of existing nonLTE line-blanketing computations. And, the results suffice for our present purposes of exhibiting the reliability of using existing photospheric models as a lower boundary condition on modeling the exophotospheric regions.

We obtained an expression for the ratio $E_B/N_B = f(T_e)$ in the case of an H^- dominated continuum by combining the equations of statistical equilibrium, (2.191) and (2.192), with the energy equation for the electron continuum, (2.193), to obtain eq. (2.200). We obtain a generalized form of eq. (2.200), when several continua—free-free and bound-free—and several lines are present, by writing the corresponding generalized form of eq. (2.193)

$$4\pi n_c \int_0^\infty \alpha_{\text{ff}}^* (J_\nu - B_\nu) d\nu + 4\pi \Sigma \left(n_j \int_{\nu_i}^\infty \alpha_{jc} J_\nu d\nu - n_j^* \int_{\nu_i}^\infty \alpha_{jc}^* B_\nu d\nu \right) - \Sigma_i n_{U_i} A_{ULi} h\nu_i [\text{NRB}]_i + e_m = 0 \quad (2.255)$$

where n_c is the effective concentration of particles absorbing in the free-free continuum, α_{ff} is the free-free absorption coefficient, α_{jc} is the bound-free absorption coefficient from energy level j with occupation number n_j , $(\text{NRB})_i$ is the net-radiative-bracket for the line i in transition $U \rightarrow L$, e_m is any nonradiative energy supply, and an asterisk denotes the LTE population. The absorption coefficients α_{ff} and α_{jc} include the stimulated emissions, treated in the usual way as negative absorptions. (A more detailed form of this equation, cf Gebbie and Thomas (1970) eq. 15, would show explicitly its dependence on the various microscopic processes; in the above form, this dependence is implicit in the ratio $b_i = n_j/n_j^*$.) Following our preceding approach, we set

$$\begin{aligned} E_J &= \int_0^\infty \alpha_{\text{ff}}^* J_\nu d\nu, & E_{Jj} &= \int_{\nu_i}^\infty \alpha_{jc} J_\nu d\nu, & N_{Jj} &= \int_{\nu_j}^\infty \alpha_{jc} J_\nu d\nu/h\nu, \\ E_B &= \int_0^\infty \alpha_{\text{ff}}^* B_\nu d\nu, & E_{Bj} &= \int_{\nu_i}^\infty \alpha_{jc}^* B_\nu d\nu, & N_{Bj} &= \int_{\nu_i}^\infty \alpha_{jc}^* B_\nu d\nu/h\nu, \end{aligned} \quad (2.256)$$

$$\Delta = (e_m - e_j)/(4\pi \Sigma_j n_j N_{Jj}), \quad e_i = \Sigma_i n_{U_i} A_{ULi} h\nu_i (\text{NRB})_i,$$

$$P_j = n_j^* N_{Bj} / (\Sigma_j n_j^* N_{Bj}), \quad P_{\text{ff}} = n_c / (\Sigma_j n_j^* N_{Bj}).$$

The weight P_j is the ratio of the rate of photo-recombinations in the j th continuum to the total rate of photo-recombinations. Eq. (2.255) can be rewritten

$$\sum_j \frac{E_{Bj}}{N_{Bj}} P_j + E_{\text{B}} P_{\text{ff}} = \sum_j \left(\frac{E_{Jj}}{N_{Jj}} + \Delta \right) \left(b_j \frac{N_{Jj}}{N_{Bj}} \right) P_j + E_{\text{J}} P_{\text{ff}}. \quad (2.257)$$

When the free-free contribution is negligible relative to the bound-free contribution, and when the bound-free transitions come from only one energy level, eq. (2.257) reduces to the form discussed in Section b, preceding.

$$E_{\text{B}}/N_{\text{B}} = (E_{\text{J}}/N_{\text{J}} + \Delta) (bN_{\text{J}}/N_{\text{B}}). \quad (2.258)$$

The factor $(E_{\text{J}}/N_{\text{J}} + \Delta)$ is then the rate at which energy is supplied to the system divided by the rate of photoionization. It includes radiation, mechanical heating, and the direct effect of line-blanketing. Any change in T_{e} due to a change in these quantities, we call a transfer effect. The factor $(bN_{\text{J}}/N_{\text{B}})$ is the rate of photoionization divided by the rate of photo-recombination, or the (TCB). Any change in T_{e} due to a change in the (TCB), we call a population effect. We call the (TCB) the Temperature-Control-Bracket for the reasons now to be outlined. We recognize that in our above discussion of a single continuum, with radiative and collisional effects on source-function and bound-state population, eq. (2.213) gives the TCB of that continuum to be unity, for vanishingly-small ϵ , hence eq. (2.258) reduces, under RE, to eq. (2.236). Its generalization, via multi-TCB, is eq. (2.257).

Consider the physical significance of eq. (2.257), and of what we call transfer and population effects in controlling T_{e} , in the general situation. The discussion carries over to more general atmospheric regions than simply photospheric. Then the coupled equations describing the structure of a stellar atmosphere can be divided into two categories: population equations and transfer equations. The population equations determine the populations of all the energy states in terms of a set of state parameters, which by definition suffice to fix the rates of the microscopic interactions. The transfer equations, together with the conservation conditions, determine the values of these state-parameters in terms of interactions between the populations and such transfer quantities as mass, momentum, energy, and radiation. Changes in the values of the state-parameters arising directly from changes in the transfer quantities we call transfer effects. Changes in the state-parameters due to changes in the populations, without a change in the associated transfer quantity, we call population effects. Such changes in population arise from changes in the relative importance of the net rates of the microscopic processes in the population equations, as a function of particle concentration and opacity. Thus, the population effects are indirectly coupled to the transfer quantities because the latter determine the density distribution. It is, however, convenient to make a first-order division into population and transfer effects.

In the degenerate state of Thermodynamic Equilibrium, the homogeneity of the system precludes transfer effects, and the state-parameters are determined directly by the transfer quantities, which in this case are constant. Likewise, the condition of detailed balance precludes population effects, and the populations are determined directly by the state-parameters, independent of the microscopic processes. In strict LTE the system is still in detailed balance, so there are no population effects; but because it is no longer homogeneous, there are transfer effects. In LTE-R, departures from radiative detailed balance are allowed, and it is possible to have hybrid population effects.

In these terms, we see the population effect of the TCB reflecting the various nonLTE effects we have discussed, in controlling the dependence of T_{e} on a given radiation field. In LTE-R, $b_{\text{c}} = 1$, so $\text{TCB} = N_{\text{J}}/N_{\text{B}}$. For a single continuum, and ignoring the nonradiative heating and line terms so that $\Delta = 0$, $E_{\text{B}} = E_{\text{J}}$: T_{e} depends upon the *quantity* of the radiation field. At the opposite extreme, a nonLTE maintained wholly by radiative processes, photoionizations are balanced by photo-recombinations, and $\text{TCB} = 1$. Then, $E_{\text{B}}/N_{\text{B}} = E_{\text{J}}/N_{\text{J}}$, and we have the solution we have discussed with the various transfer solutions for E_{J} and N_{J} , in Section b. T_{e} is fixed by the *quality* of the radiation field. A classical example lies in the original RE model of a PN (Baker, Menzel, and Aller, 1938). A shift from LTE-R in the immediate atmosphere of the central star, to radiative control in the nebula, predicted a T_{e} near the color temperature of the star, at the nebula, rather than the LTE-R boundary $T_{\text{e}0}$. Because the free-free terms are in LTE-R, their effect is to hold T_{e} closer to the LTE-R value than would be the case without them. This is reflected in table 1 of the cited reference, where T_{e} drops progressively below T_{c} as the importance of the free-free terms increases with

increasing T_c . But when we introduce the effect of impurity cooling via metastable levels in the low-density nebula, a transfer effect via Δ_q , T_e drops from $0.3\text{--}1.5 \times 10^5$ to $0.5\text{--}2 \times 10^4$ K. This impurity cooling arises from ions not producing the continuous opacity, so it does not affect the TCB. When, however, the line-effects occur in ions producing the continuous opacity, the TCB are affected. Such a situation arises in diagnostics of the solar chromosphere, to be discussed in Chapter 3, Section D. There, the relative populations n_1 and n_2 of hydrogen change, under a shift in the relative importance of the radiative transitions in the Balmer and Lyman continua and the contribution of H α . We return to the line-effect on TCB, below.

The small rise in T_e , under LTE-R, found by Dumont and Heidmann (1973) exhibits the effects of multi-continua, as we have already said in Section 2.b. It is a transfer effect; resulting from a shift in dominating opacity from H $^-$ to atomic hydrogen, under LTE-R, all $b_i = 1$. We can crudely illustrate the corresponding behavior of multi-continua, in the extreme radiative-dominated case, by adopting the caricatured version of the variation of J_ν already discussed, in eqs. (2.151) and (2.165): $J_\nu = W(\tau_\nu) B(T_c)$. T_c is held constant, so the J -variation is represented by the W -variation. In the LTE-R region, the outward decrease in W gives an outward decrease in T_e . On entering the non-LTE region, T_e increases outward to reach T_c . We measure it by $E_J/N_J = E_B/N_B$ —either via the transfer solution in each of E_J and E_N already discussed, or by some approximate representation of the variation of N_J corresponding to the above on $J (= E_J)$. Essentially, we obtain the 1-continuum results already discussed. Generalizing the approach to the multi-continuum case, via eq. (2.257), we must describe each of the E_{Jj} and N_{Jj} . Because of the ν -dependence of the opacity and source-function, there will not, in general, be a single T_c for which $WB_\nu(T_c)$ is a reasonable approximation over the entire spectrum. Suppose, however, that within each continuum j , $J_{\nu j}$ could be represented by a T_{c_j} that is constant for $\tau_j \lesssim 1$ and W_j decreasing outward. Then the value of T_e as given by the left-hand side of eq. (2.257) would be a weighted average of the T_{c_j} as given by the ratios E_{Jj}/N_{Jj} on the right-hand side. The weighting factors would be the (TCB) $_j$ and the P_j . But whereas for the single-continuum model the number of photoionizations equals the number of photo-recombinations at the low-density limit, (TCB) = 1, this will not in general be true for the multi-continuum model because of radiative transitions in the lines. Thus while we would expect an outward increase in T_e above the boundary of the LTE regions, its detailed behavior will depend on the particular population processes that fix the (TCB) $_j$. In the same regions, because of the ν -dependence of τ_j , there will also be transfer effects.

The Δ -term contains the heating effect e_m of nonradiative energy sources and the cooling effect e_q of the lines. For e_q we distinguish two classes of lines. The first class arises from ions that contribute significantly to the continuous opacity—for example, hydrogen lines in a hydrogen atmosphere. These will have both population and transfer effects. The second class of lines arises from ions that are not involved in the continuous opacity—for example, metal lines in an H $^-$ atmosphere. These will have only transfer effects. Consider, in order, the multiregion T_e -distribution without lines, then with lines.

i. Continuous Opacity Only. In Section 2.b.ii we considered the LTE-R T_e -distribution by treating two opacity regions: $\nu > \nu_i$, having large opacity; $\nu < \nu_i$, small. Our discussion revolved around the relation between J_ν and $B_\nu(T_e)$. For large opacity, $J_\nu = B_\nu(T_e)$ because of LTE-LOS. In the small opacity region, the integrated $J =$ integrated B because of RE, and comes from a gray transfer solution, in the lower atmosphere. In the upper atmosphere, J_ν ($\nu < \nu_i$) is constant, because $\tau(\nu < \nu_i) \ll 1$. The integrated $J(\nu > \nu_i)$ comes from a gray transfer solution.

In the present nonLTE region, we consider the radiative-dominated situation which, with lines absent or in detailed balance, gives

$$(\text{TCB})_j = 1 \quad , \quad b_j = F_{c_j}/F_{j_c}, \quad (2.259)$$

where F_{c_j} and F_{j_c} are photo-recombination and photoionization rates. Effectively, they replace, respectively, N_{Bj} and N_{Jj} . The N 's enter the rate equations expressed in terms of the n_j ; the F 's, in terms of the b_j .⁶ Eq. (2.259)

⁶ All these rate-coefficients, the F 's and the N 's, are given in Appendix A for this Chapter 2.

corresponds to detailed balance in the j th continuum, independent of the continuous opacity. However, the opacity determines which are dependent and which independent quantities, just as it determined whether J determined T_e , or conversely, in the LTE-R discussion of Section 2.

In the layers transparent in continuum j , eq. (2.259) fixes b_j in terms of F_{c_j} and F_{j_c} , where F_{c_j} is fixed by T_e and F_{j_c} is fixed by a transfer solution in the underlying layers. From the approximation of J_ν by $WB_\nu(T_c)$, and eq. (2.259), $b_j \sim W_j^{-1}$. As an approximation to b_j in the radiation-dominated case, it is analogous to the approximation $b_c = 1$ in the collision-dominated case. It implies that T_e is fixed only by the quality of the radiation field, W_j affecting only the number of photoionizations. It carries over into the most distant atmosphere, like the PN, with the consequences mentioned above. In the layers that are locally opaque in continuum j , eq. (2.259) determines F_{j_c} in terms of b_j and F_{c_j} , analogously to the determination of J_ν from T_e in LTE-R and LOS.

We can give simple illustrations of the utility of this simple approach to estimating outer-photospheric conditions, taken from the discussion by Gebbie and Thomas (1971). Eq. (2.257) can be rewritten

$$T_e = T_e \frac{E_J}{E_B} + \Delta' + \frac{2hR}{kg_{III}} \left\{ \sum_{k+1}^{\infty} g_{III} j^{-3} \left(\frac{E_{Jj}}{E_{Bj}} - 1 \right) + \sum_1^k g_{III} j^{-3} \left[\left(\frac{E_{Jj} N_{Jj}}{E_{Bj} N_{Bj}} \right) (\text{TCB})_j - 1 \right] \right\}. \quad (2.260)$$

The last term on the right represents those continua treated as nonLTE; the next to-last are those continua treated as LTE-R.

Strict enforcement of radiative detailed balance in the locally opaque configuration would lead to zero radiative flux in the deeper layers of the atmosphere. In these layers, therefore, one uses the "diffusion approximation" to obtain a nonzero flux that comes wholly from a T_e gradient in an LTE configuration. In the surface layers, however, the radiative flux has two distinct origins: (1) the anisotropy in optical path, caused by the presence of the boundary, and (2) the inhomogeneity in source-function, due to the nonLTE effects of the boundary combined with the effect of the T_e gradient. Our procedure for computing $T_e(\tau)$ in the atmosphere consists of neglecting the energy transferred by the diffusion approximation relative to that by the boundary effects. That is, in any region that is locally opaque in a given continuum, we set the flux in that continuum equal to zero. The decision on which continua are opaque, together with the method for evaluating E_{Jj} and N_{Jj} , constitute our computing procedure.

For a complete calculation, we must evaluate J_ν , hence E_{Jj} and N_{Jj} , by solving eq. (2.260) simultaneously with the appropriate (nonLTE) transfer equations, as in Section b preceding, in the several continua. The procedure is iterative, but by writing eq. (2.260) in terms of net rates and by beginning in regions where the lines are in detailed balance so that $(\text{TCB})_j = 1$, we have canceled out the large terms common to both emission and absorption, retaining only the critical difference terms. A simplified treatment of the relevant transfer problems, including the coupling between line and continuum, has been presented for $H\alpha$ and the Lyman continuum in the solar work cited above.

Here, however, we adopt an extreme caricature that appears to reproduce many of those details of the height variation of T_e that exhibit its dependence upon population effects. We assume that the net energy exchange in the j th free-bound continuum is zero for $\tau_j \gtrsim 1$, and that for $\tau_j < 1$ its value follows from the terms in eq. (2.260) with appropriate values of W_j and T_{c_j} . Physically, it corresponds to representing the anisotropic effects of the boundary by the parameter W_j and representing the effect of an inhomogeneous source-function by the combined effects of a T_e gradient and a nonLTE departure of T_{c_j} from the value T_e ($\tau_j \simeq 1$). We use eq. (2.152) for W_j . Thus, relative to our treatment of the transfer of E_J and N_J in Section b above, W_j describes the common boundary ($0 < \tau_j < 1$) behavior of E_J and N_J in the isothermal region of their common outward decrease; but it does not represent that differential behavior of E_J and N_J , interior to the outer boundary, which describes the nonLTE outward rise in T_e to T_{c_j} , after an initial LTE-R decrease. This is not so serious in the multi-continuum problem, because LTE-R holds

across the spectrum only in the lowest atmospheric region; so it is here that any initial outward LTE-R drop in T_e occurs, from the continuum alone, not from a line effect.

We compare the results from this rough algorithm for estimating upper-photospheric conditions to our earlier, LTE-R ones, in Section 2.b, Table 2-2. We consider both LTE-R, $b_c = 1$, $(TCB)_j = N_{Jj}/N_{Bj}$; and nonLTE, $(TCB)_j = 1$. We consider a hydrogen atmosphere, with only the lowest three levels treated as nonLTE, when appropriate. We consider the $T_{\text{eff}} = 15,000$ K, which is then T_e in the Paschen continuum near $\tau_3 \sim 1$, the beginning point of our outward computation.

α . *An LTE-R model without lines.* Here the bound-free terms $j \leq 3$ have the same form as those for $j \geq 4$. We start at the lowest observed level, $\tau_3^+ \sim 1$, with a T_e sufficiently small that (a) the Balmer and Lyman continua are in detailed balance and (b) electron scattering may be ignored so that the observed T_{c3} is the starting value of T_e .

We start with $T_{c3} = T_{\text{eff}} = T_e(\tau_3^+ = 1)$ and compute $T_e(\tau^+)$ as $W_3(\tau_3^+) = W_{\text{ff}}$ decreases from 1 to its limiting value of 0.5. T_e then remains constant until $\tau_2 = 1$, where the cycle repeats for $j = 2$. Thus $T_e(\tau_j)$ consists of a series of plateaus, each extending from $\tau_j \sim 10^{-2}$ to $\tau_{j-1} = 1$, with T_e decreasing as τ_j decreases from 1 to 10^{-2} between each plateau. For $T_{c3} = 15,000$ K, we obtain the following LTE-R model.

$$T_e(\tau_3^+ \lesssim 0.01, W_3 = 0.5; \text{Balmer and Lyman continua in detailed balance}) = 10,800 \text{ K} = T_{c2};$$

$$T_e(\tau_2 \lesssim 0.01, W_2 = W_3 = 0.5; \text{Lyman continuum in detailed balance}) = 9800 \text{ K} = T_{c1};$$

$$T_e(\tau_1 \lesssim 0.01, W_1 = W_2 = W_3 = 0.5) = 9400 \text{ K} = T_0, \text{ the boundary temperature.}$$

The results are an improvement over those of Table 2-2 in the sense of showing closer agreement with the precise calculations of Auer and Mihalas quoted there; but of course are not those of the real, nonLTE, atmosphere.

β . *A Radiation-dominated nonLTE model without lines.* We need expressions for the E_{Jj}/N_{Jj} to use in eq. (2.260). We continue to neglect stimulated emissions, and so obtain (cf preceding sections, or Vol. 2, or Gebbie and Thomas, 1971, for details) from eqs. (2.259) and (2.256)

$$b_j = \frac{(W_j^{-1} - 1) E_1(X_j) + \sum_1^{\infty} E_1[(m + \Delta T/T_e) Y_j]}{\sum_1^{\infty} E_1(m Y_j)} \quad (2.261)$$

In the limit where $W_j = 0.5$, and setting $\Delta T = T_{c_j} - T_e$,

$$\frac{E_{Jj}/N_{Jj}}{E_{Bj}/N_{Bj}} = \left[\frac{X_j \exp(X_j) E_1(X_j)}{Y_j} \right] \left[\frac{\sum_1 \exp(-m Y_j)/m}{\sum_1 E_1(m Y_j)} \right] \left\{ 1 + \frac{\sum_2 E_1[(m + \Delta T/T_e) Y_j]}{2E_1(X_j)} \right\} \quad (2.262)$$

$$- \frac{X_j \exp(Y_j)}{2Y_j} \sum_1 \left[\frac{\exp(-m Y_j)}{m} \frac{m}{m + \Delta T/T_e} \right].$$

To solve this, we require values of the T_{c_j} . These may either be chosen observationally or computed as part of a model. The former approach was applied to the Sun by Pottasch and Thomas (1960) and by Thomas and Athay (1961), who introduce T_{c2} and T_{c3} from observations in the visible spectrum. Noyes and Kalkofen (1971) have shown that a T_{c1} can be obtained from the solar rocket ultraviolet. This same observational approach could be applied to any particular star. Here, however, we specify T_{c3} and obtain T_{c2} and T_{c1} from a step-by-step calculation analogous to that of the LTE-plateau model. Holding the Lyman and Balmer continua in detailed balance, we use the

specified T_{c3} to compute T_e ($[\tau_3] \sim 10^{-2}$). Eq. (2.261) gives b_3 at $\tau_3 \sim 10^{-2}$, $W_3 = 0.5$. We enter the region where the Balmer opacity decreases to small values. If we can estimate b_2 , we can obtain T_{c2} , at the base of the Balmer region, from eq. (2.259).

In the layers that are locally opaque in continuum j , eq. (2.259) gives F_{jc} in terms of b_j and F_{cj} . Here the behavior of b_j reflects the presence of the boundary only through its coupling with b_{j+1} . We suggest that in the collision-free case this coupling may take the following approximate form. Local opacity in the line implies that S_ν (line + continuum) = J_ν at the frequency ν of the line, and detailed balance suggests that J_ν is fixed by the transfer problem in continuum j alone, i.e., that J_ν (line $j, j+1$) = J_ν (continuum $j+1$). Thus, this equality of source-function in line and continuum at $\nu(j, j+1)$ requires

$$(b_j/b_{j+1}) \exp(h\nu_{j,j+1}/kT_e) = \exp(h\nu_{j,j+1}/kT_{c,j+1}). \quad (2.263)$$

This suffices to specify b_j in terms of b_{j+1} , $T_{c,j+1}$, T_e . Eq. (2.259) then gives T_{c2} ; and the cycle repeats for the Lyman continuum. Again taking $T_{c3} = T_{\text{eff}} = 15,000$ K, we obtain the nonLTE plateau model:

$$T_e([\tau_3] \sim 10^{-2}, W_3 = 0.5; \text{Balmer and Lyman continua in detailed balance}) = 10,600 \text{ K:}$$

$$b_3 = 0.88, b_2 = 0.48, T_{c2} = 12,500 \text{ K;}$$

$$T_e([\tau_2] \sim 10^{-2}, W_2 = W_3 = 0.5; \text{Lyman continuum in detailed balance}) = 10,750 \text{ K:}$$

$$b_2 = 1.05, b_1 = 0.22, T_{c1} = 11,900 \text{ K;}$$

$$T_e([\tau_1] \sim 10^{-2}, W_1 = W_2 = W_3 = 0.5) = 10,400 \text{ K} = T_0, \text{ the boundary temperature:}$$

$$b_3 = 1.46, b_2 = 1.18, b_1 = 0.70.$$

The Auer and Mihalas more precise nonLTE calculations for this 3-level hydrogen atom give T_e ($\tau_2 \lesssim 10^{-2}$) = 10,150 K, and $T_0 = 10,530$ K. So, our simplified approximations give reasonable results, under the point continually stressed of using an upper-photospheric model as a beginning point for adding the exophotosphere, and gives a clear physical picture of the several effects operating to produce the T_e -variation.

ii. Effects of the Lines. In most of the literature (cf, e.g., Athay and Skumanich, 1969; Athay, 1972), the physical picture of the effect of lines is divided into just two parts: backwarming and thermal cooling; i.e., the blocking effect of the lines, and a net energy transfer because the line source-function differs from J_ν . Basically, this is a carryover from an LTE-R treatment of line-formation, and represents what we called transfer effects. Such treatments completely ignore what we called population effects, and especially the distinction between the effects of the different types of lines—notably collisional- and photoionizational-dominated—on both population and thermal-cooling. Hereafter, we use the term “impurity-cooling” in place of thermal-cooling, the effect having been first recognized in the PN under that designation. Then we note that the backwarming effect, upon which early work focused, is actually minor, in the outer layers where the line-effects are the most important. The effects of population cooling and heating can be major (Pottasch and Thomas, 1959; Thomas and Athay, 1961; Auer and Mihalas, 1969a, b, c; Gebbie and Thomas, 1971). The difference between impurity cooling by a collision-dominated line and by a photoionization-dominated line is very significant; it can differ in sign; the former depends on density, while the latter does not. A clear physical picture comparing the operation of all these effects exists nowhere in the literature. Invariably, when line-effects—usually called line-blanketing—are calculated, only one or two of the above effects are included; so that the results cannot really be compared. For example, the cited Athay-Skumanich, and Athay, calculations include only backwarming and impurity-cooling by collision-dominated lines, ignoring both photoionization-dominated lines, and population cooling and heating. But the Auer and Mihalas calculations focus on the population effects of photoionization-dominated lines, and ignore impurity cooling, by considering only a pure hydrogen atmosphere. So, in this section, we try to put all these effects into focus, especially toward our objective of understanding conditions in the upper photosphere, and its transition to the exophotosphere.

α . *Impurity-Cooling put into focus*: definition of the line-effects.

(ℓ -1) *Back-warming*: The effect on J (continuum) coming from the change in radiation flux introduced by the presence of the lines. It raises J outside the lines, corresponding to the amount the lines are in absorption; its effect is minor. Athay and Skumanich (1965) and Mihalas and Luebke (1971) discuss it adequately.

(ℓ -2) *Population-cooling*—which can also be heating: Those effects on T_e which come from changes in n_j , hence, in photoionization, which accompany a change in relative opacity of the several lines and continua, or change in relative importance of collisional and radiative processes. In eqs. (2.257) and (2.260), the $(TCB)_j$ measure, and represent, these population effects. They are what introduce the dependence of T_e upon the quality, rather than only quantity, of the radiation field.

(ℓ -3) *Impurity-cooling*: That change in T_e arising from a departure from detailed balance in the lines; a departure from zero of the quantity $(\int J_\nu \phi_\nu d\nu - S_{ik})$. This last is S_{ik} (NRB) $_{ik}$ (cf eq. 2.195). It is measured by ϵ_Q , in eqs. (2.257) and (2.260); thus, it is a transfer effect. There are two essential points to keep in mind, in discussing such impurity cooling.

1. First is LTE-R vs. nonLTE impurity cooling. Practically all so-called line-blanketed models in the literature are the LTE-R variety. Such an approach neglects the scattering in the line source-function, which neglect is the same as that one leading to using the central line-intensities to measure T_e . It leads to strong error if the ϵ and η are small, which is the case for those strong lines giving major effects. From eq. (2.222) we see the expression for the value of this impurity cooling term, in the case of a continuum. The line results of eqs. (2.171b) and (2.172b), applied to the expression for the NRB of eq. (2.195), show the same result: the LTE impurity cooling is decreased by a factor between ϵ and $\epsilon^{1/2}$, as detailed by eq. (2.222). The situation is most simply seen (Thomas, 1965) by rewriting eq. (2.179a), using eq. (2.153a), and K_c, K for opacity, e.g.,

$$K_Q = n_L \phi_\nu B_{UL} h\nu/4\pi = K_L \phi_\nu \quad (2.264)$$

$$\mu \frac{dI_\nu}{dx} = - (K_C + K_I + \sigma_C) J_\nu + K_C B_\nu (T_e) + \sigma_C J_\nu + K_I \left(\frac{\int J_\nu \phi_\nu d\nu + sB}{1+s} \right), \quad (2.265)$$

so that radiative equilibrium leads to the temperature distribution

$$\int K_C B_\nu (T_e) d\nu = \int K_C J_\nu d\nu - \sum_j K_j \left(B - \int J_\nu \phi_\nu d\nu \right) \frac{s}{1+s}. \quad (2.266)$$

The LTE-R situation corresponds to large s ; the pure-scattering, to $s = 0$. NonLTE depends on the size of s ; which, as continuously emphasized for the significant lines, gives $s \ll 1$. The line-free T_e -distribution corresponds to using only the K_C terms in eq. (2.266). The change in J_ν with and without the other terms is, as remarked re ($\ell - 1$) above, small. So, the differential perturbation, between LTE-R and nonLTE, on the line-free T_e is simply proportional to s , multiplied by the details of the bracket. We see these, from eq. (2.171b); and so note that, as from eq. (2.222), the line-effects are important only in the upper-photosphere, small τ_0 (line).

This differential effect between LTE-R and nonLTE was re-emphasized by Mihalas (1970), together with that coupling to the continuum we discuss below. It has been again discovered by Kalkoven (1982). However, Athay challenges this simple picture on the basis that n_Q increases with decreasing s ; so that the product n_Q (*bracket*) s shows little change between LTE-R and nonLTE cases (1970, 1982). We see the error of his conclusions from 3 aspects. First, for resonance lines, n_Q is fixed by the local density, not any excitation. Second, if n_Q does increase, so also does the line-opacity, entering the several cited solutions, eqs. (2.171b) and (2.222). So, the region where the line-effects occur simply moves outward in the atmosphere; but there reaches the s -dependence cited. Third, we have the situation emphasized throughout this nonLTE section. If we make the pictorial approximation of constant flux in the

line, and $F_\ell = I_\nu^+$ ($\tau_\ell = 0$) $\sim S_{jk}$ ($\tau_\ell = 1$), we have: LTE case, $F_\ell \cong B_\nu(T_e)$; nonLTE case, $F_\ell \cong \epsilon^{1/2} B_\nu(T_e)$, independently of where in the atmosphere $\tau_\ell = 1$. So, the “boundary-temperature” required to match a given flux in the line is higher for nonLTE than for LTE-R. Indeed, we note the well-known result that a very strong line (continuum-opacity/line-opacity = $\tau_0^{-1} \sim 0$) in which the residual flux is $\epsilon^{1/2}$ that in the continuum, and small ϵ , gives effectively no change in boundary-temperature from line-effects. The cited Luebke-Mihalas computations show the result in detail; lines with $\epsilon \lesssim \tau_0^{-1}$ leave the boundary-temperature essentially unchanged.

So, looking at the form (2.260) for determining T_e , we see that there is a very significant difference between the nonLTE and the LTE-R perturbation on that T_e determined with detailed balance in the lines. Eq. (2.266) shows that the difference between E_B and E_J under RE is just the sum of $K_\ell (B - \int J_\nu \phi_\nu d\nu)$ over the various lines, for LTE-R. For nonLTE, the contribution of each line is decreased by s . So, the primary problem is to compute the s_i for all lines included in any line-blanketing computation. All this is translated from a difference in E_B and E_J into one in T_e , via the formulation of eq. (2.260). This kind of impurity cooling, where only the line’s effect on Δ is considered, is then a pure transfer effect, felt in a dependence of T_e on quantity, not quality, of the radiation field, as “corrected” by the line-cooling.

2. The second important point in impurity cooling is to recognize that the effect of some lines is felt beyond the Δ term; they change the value of the TCB. A necessary condition for such lines is that they be photoionization dominated. If, however, the photoionization continuum controlling the line is not produced by the ion whence comes the line, the condition is insufficient. The line has no feedback on its continuum. The H α line in an atmosphere whose continuous opacity comes from atomic hydrogen provides a good example of this kind of line whose effect is felt on the TCB as well as the Δ . An Fe I line, even though photoionization dominated, does not fall in this class. So, in discussing the effects of lines in this class, one must consider their total effect, resulting from the combination of Δ and TCB effects. As mentioned, Athay’s discussion of line-blanketing (1972) ignores both population effects and photoionization-dominated lines, so is incomplete in this important aspect. Moreover, his treatment of radiative cooling by the Balmer lines (1976) is incomplete for the same reason. The Auer and Mihalas discussions of pure hydrogen atmospheres include both these effects; but they make no attempt to put into focus a distinction between them; only their combined effects are discussed, scrambled in the computing routine. The clearest way to put their separate effects into focus is algebraically, via the TCB.

β . *Effect of a single photoionization-dominated line, whose parent ion is the continuous opacity source.* In Section (i), we illustrated the TCB approach when there was only continuous opacity: case (α), under LTE-R with $b_c = 1$, so $\text{TCB} = N_J/N_B$; and case (β), in a radiation-dominated nonLTE configuration, $\text{TCB} = 1$. In each case, we used eq. (2.260) with $\Delta' = 0$: which corresponds to neither spectral-lines nor nonradiative heating being present. If, now, we were to introduce a line, which belongs to no ion that contributes significantly to the continuous-opacity, we see from the algebraic expression for Δ , in eq. (2.256), that it would enter the RHS of eq. (2.260) as a negative quantity. The NRB is always positive, in this situation: and Δ and Δ' differ only by a positive numerical factor. So the net effect would be to reduce the value of T_e : because all other terms in the equation remain unchanged. The minor effect of the line on the value of J is, as already remarked, negligible. So we would have a literal impurity cooling; a transfer effect, the value of NRB being fixed by a transfer solution in the line, under the $T_e(r)$ fixed by the solution of eq. (2.260). So these two solutions are coupled, but only through the Δ . This is the usual nonLTE, line-blanketing approach—with the line collision-dominated.

If, on the contrary, we consider a line whose parent ion contributes to the continuous opacity; and which is itself photoionization-dominated; then in addition to the net radiative emission in the line—measured by the NRB—appearing as a cooling term via Δ , it also appears in the continuum TCB. And there, by contrast to the negligible contribution of the spectral line to J , the line-effect can be strong. It is this effect which produces the nonLTE line-heating exhibited in the cited calculations by Auer and Mihalas (1969, et seq.). It is also the H α correction term which appeared in our (Thomas and Athay, 1961) treatment of the perturbation of H α on the empirical diagnostics of eclipse data for T_e (height), via the LyC transfer solution which fixes b_1 . It is also what makes the observed emission in H α —and in the other Balmer lines—useless as a measure of the nonradiative energy dissipation in the solar chromosphere:

this emission reflects photoionization, not collisional, effects. In the 3-level atom configuration, the NRB of the Balmer continuum is negative, just balancing the positive value of the NRB for H α : cf table and associated discussion, p. 140 of Thomas and Athay (1961). Averett, et al. (1982) have recently re-discovered this coupling between BaC and H α , re diagnostics of nonradiative heating. The same effects hold, of course, for any other photoionization-dominated line, when the continuum of its parent ion is significant in the energy-balance.

Gebbie and Thomas (1971) exhibited how the effect of such a photoionization-dominated line enters an energy equation such as eq. (2.260). If one considers a 3-level hydrogen atom, in the radiative-dominated situation—i.e., collisions ignored, the usual algebraic solution for the statistically-steady-state equations give:

$$(\text{TCB})_1 = b_1 \frac{F_{1c}}{F_{c1}} = \left\{ 1 + \frac{\delta_{21}}{\delta_{21} + F_{2c}} \frac{F_{c2}}{F_{c1}} \left[1 + \frac{\delta_{32}}{\delta_{32} + \delta_{31} + F_{3c}} \frac{F_{c3}}{F_{c2}} \left(1 + \frac{\delta_{31}}{\delta_{32}} \frac{\delta_{21} + F_{2c}}{\delta_{21}} \right) \right] \right\} \quad (2.267)$$

$$(\text{TCB})_2 = b_2 \frac{F_{2c}}{F_{c2}} = \left(1 - \frac{\delta_{21}}{\delta_{21} + F_{2c}} \right) \left(1 + \frac{\delta_{32}}{\delta_{32} + \delta_{31} + F_{3c}} \frac{F_{c3}}{F_{c2}} \right) \quad (2.268)$$

$$(\text{TCB})_3 = b_3 \frac{F_{3c}}{F_{c3}} = \left(1 - \frac{\delta_{32} + \delta_{31}}{\delta_{32} + \delta_{31} + F_{3c}} \right) \quad (2.269)$$

where

$$\delta_{ij} = g_j f_{ji} \nu_{ij}^2 \exp(X_i) (\text{NRB})_{ij}. \quad (2.270)$$

To consider the simple case of a single line present, we consider that atmospheric region that is opaque in the Lyman lines. Then the δ_{i1} vanish: $(\text{TCB})_1 = 1$; and $(\text{TCB})_2$ and $(\text{TCB})_3$ depend only on δ_{32} —i.e., H α . Inserting these expressions into eq. (2.260) we obtain just that equation solved under alternative case (i- β) above, with the exception of the added term

$$\frac{\delta_{32}}{\delta_{32} + F_{3c}} \frac{E_1(X_3) \exp(X_3)}{27kT_e} \left\{ \frac{E_{J2}}{N_{J2}} - \frac{E_{J3}}{N_{J3}} - h\nu_{23} \right\}.$$

The first and second—population—terms in the bracket come, respectively, from the TCB terms in the last term on the RHS of eq. (2.260). The third—transfer—term, $h\nu_{32}$, comes from the Δ' term, in the expression (2.256) for which there occurs a b_3 ; and we have evaluated it from eq. (2.269). Thus, the common coefficient, outside the bracket, of these 3 terms is clear. In the event that the Y_k entering the J_k are large enough for the asymptotic expression— $E_1(Y) \sim Y^{-1} \exp(-Y)$ —to be valid; and if we can continue to neglect the induced emissions terms in E_{Jk} and N_{Jk} ; then from the expressions for these in the appendix of this chapter, $E_{Jk}/N_{Jk} \sim h\nu_k$. In this asymptotic case, the bracket has the value $(h\nu_2 - h\nu_3 - h\nu_{23}) = 0$. That is, the population terms in the continuum, expressed by the TCB, exactly compensate for the transfer term in Δ' ; a population “heating” has precisely compensated for a transfer “impurity-cooling.” “Impurity” is hardly an appropriate term, here, since the ion involved provides the continuous opacity. But the physical point is clear. In this asymptotic case, the net effect of H α on an RE-determined T_e is zero.

This asymptotic case is not generally useful. For example, we used the fact that for very small X_k —zero, in the limit— $E/N \sim 3kT$ to develop our method for fixing T_e , in preceding sections. In this event, the bracket becomes $[3k(T_{c2} - T_{c3}) - h\nu_{23}]$ and its value depends upon how precisely one can determine the T_{ck} —and how seriously one considers the significance of their differences.

As an explicit algebraic exhibition of the difference between population and transfer effects, the above is useful. It illustrates that one can hardly discuss line-blanketing in terms which treat photoionization-dominated and collision-dominated lines in the same way; in a first approximation, we see indeed that line-blanketing disappears. But to decide, generally, between heating or cooling, one needs the more precise numerical, not just algebraic, approach as have done Auer and Mihalas for the stellar case, and Avrett, Loeser, and Vernazza for the solar chromosphere. It would simply be useful if such numerical discussions exhibited the several physical effects underlying them. At our epoch, there is too great a tendency to believe that effects of nonLTE, nonRE, nonHE, etc., are so complicated that only exhaustive numerical calculations can exhibit them. This is hardly true, and simple approximations that focus on the basic physics are necessary to delineate both upper photospheric and exophotospheric conditions.

Appendix 2-A

Rate Coefficients

$$N_{Bj} = \left(\frac{2\alpha_{0j}}{c^2} \right) E_1(X_j) \qquad \alpha_\nu [f-b] = \alpha_{0j} \nu^{-3} [1 - \exp(-h\nu/kT_e)]$$

$$E_{Bj} = \left(\frac{2\alpha_{0j}}{c^2} \right) (kT_e) e^{-X_j} \qquad \alpha_{0j} = 2.813 \times 10^{29} g_{IIj} j^{-5}$$

$$N_{Jj} = \left(\frac{2\alpha_{0j}}{c^2} \right) \left[\sum_1^\infty E_1(mY_j) - b_j^{-1} \sum_1^\infty E_1\left(mY_j \left[1 + \frac{T_c}{mT_e}\right]\right) \right] \times W_j$$

$$E_{Jj} = \left(\frac{2\alpha_{0j}}{c^2} \right) (kT_{cj}) \left[\sum_1^\infty \frac{e^{-mY_j}}{m} - (b_j e^{X_j})^{-1} \sum_1^\infty \frac{e^{-mY_j}}{m \left(1 + \frac{T_c}{mT_e}\right)} \right] \times W_j$$

$$F_{cj} = \frac{2.11 \times 10^{31}}{j^3} E_1(X_j) e^{X_j}$$

$$F_{jc}/F_{cj} = W_j \left[\frac{E_1(Y_j) + \sum_2^\infty \left\{ E_1(mY_j) - b_j^{-1} E_1\left(\left[m + \frac{T_c - T_e}{T_e}\right] Y_j\right) \right\}}{E_1(X_j)} \right]$$

$$C_{12} = \frac{3.8 \times 10^6 n_e T_e^{3/2} (X_{12} + 1) e^{X_2}}{1 + 0.34 \times 10^{-4} T_e} ; \qquad C_{13} = \frac{6.1 \times 10^5 n_e T_e^{3/2} (X_{13} + 1) e^{X_3}}{1 + 0.34 \times 10^{-4} T_e}$$

$$C_{23} = \frac{1.26 \times 10^8 n_e T_e^{3/2} (X_{23} + 1) e^{X_2}}{1 + 0.34 \times 10^{-4} T_e} ; \qquad C_3 = 2.7 \times 10^7 n_e T_e^{3/2} (X_3 + 2)$$

$$C_1 = 1.0 \times 10^6 n_e T_e^{3/2} (X_1 + 2); \qquad C_2 = 8.0 \times 10^6 n_e T_e^{3/2} (X_3 + 2)$$

$$E_{B} P_{ff} = \frac{k^2 T_e^2}{2hR} g_{III} \left(\sum j^{-3} g_{IIj} e^{X_j} E_1[X_j] \right)^{-1}$$

Note: Refer to Menzel (1937) and Pottasch and Thomas (1959) for derivations.

Page intentionally left blank

Page intentionally left blank

3

EMPIRICAL-THEORETICAL SURVEY OF THE VARIETY OF PECULIARITIES AND ANOMALIES IN THE ATMOSPHERES ENVELOPING ACTUAL STARS

. . . Some of the peculiar phenomena generally ascribed to a tenuous outer atmosphere in some early-type stars are not confined to a few freaks in the stellar population, but are probably characteristic, in a small degree, of the majority of stars in certain stages of their evolution . . .

—observation by Otto Struve, 1942

I. INTRODUCTION

In Chapter 2, we summarized the essential characteristics of the atmosphere of a star that can be modeled as a (closed, thermal) thermodynamic system. There are three characteristics *imposed*, a priori, by the (closed, thermal) restrictions: (C-1) only radiative flux from the star, so radiative-equilibrium, RE, holds; (C-2) *zero* nonthermal systematic velocity fields anywhere in the atmosphere, so hydrostatic-equilibrium, HE, holds; (C-3) no atmospheric, or stellar variations except over stellar-evolutionary times, corresponding to secular changes in stellar energy generation, so time-independence of atmospheric structure effectively holds. (C-1)–(C-3) predict a single region atmosphere, effectively linearly nonEquilibrium in T_e and density, having three characteristics: (C-4) A limiting boundary value, T_0 , for T_e whose ratio to the effective temperature does not exceed $(\sqrt{3}/4)^{1/4}$ in the LTE and LTE-R configurations, and 1 in the nonLTE, with a monotonic outward decrease of T_e except in the very outer atmosphere, where a rise is possible, but not exceeding the cited T_0 . (C-5) An exponential outward decrease in density in the boundary region, with a scale-height of $kT_0/\mu g$ in the plane-parallel region, and a corresponding expression in $\Delta R/R$ if curvature must be included. (C-6) A mass-flux from the star, by thermal diffusion-evaporation of those particles whose energy exceeds that of gravitational escape, so that there is a negligibly small, *diffusive mass-flow through the outer atmosphere, not a flow of the atmosphere as a whole*.

Because this first-approximation modeling was suggested by the visual spectral region, two-parameter, empirical, taxonomy of (i) total luminosity, and (ii) rough spectral distribution in absorption lines and continua for most stars, we expect such a model to give, in first approximation, rough agreement with observations in this visual spectral region. And, indeed, such is the case. The spectral energy distribution in the visual continuum is in *reasonably* good agreement with predictions from the models; and the relative importance of various ions in producing the strongest absorption lines in various spectral classes is *reasonably* well predicted, again in the visual spectrum. Also, in a *rough* way, absorption lines in the visual spectral region are broader in the main-sequence stars than in the giant and supergiant branches, corresponding to the higher gravities and atmospheric densities assigned to the former. For details of such comparisons, refer to each of the other volumes in the series.

However, again in an overall kind of way, there are distinctly observable discrepancies between actual stars and model predictions. These appear in a kind of four-stage, or four-aspect, sequence of maturation of doubt on the adequacy of this (closed, thermal) modeling. I abstract these stages, in this Introduction, then summarize some of them, in detail, in the rest of the chapter. Hopefully, a really detailed account of these discrepancies in each spectral class will come in the individual volumes. After examining this sequence of doubt, one asks whether a fundamental change in the basis of such modeling, or only some modest "patching-up," is needed, for all stars. Myself, after looking at the sequence from all aspects, I think the evidence is strong that one may be able to model all kinds of stars, and atmospheres, from the same general thermodynamic representation of star and structural pattern of atmosphere, but as an (open, nonthermal) rather than a (closed, thermal) system. So, this is a fundamental change in the thermodynamic basis of the modeling, not just a "patching-up." Such a change is reflected, observationally, in the existence of additional, exophotospheric, nonlinearly nonEquilibrium, variable and highly individual atmospheric and local environmental regions. Thermodynamically, such regions demand a variety of time-dependent, nonthermal structure for the subatmosphere.

The sequence of evidence demanding such regions is the following.

First, there are *gross* differences between the characteristics of *some* stars as observed *only* in the visual spectrum and *some* of the basic characteristics (C-1)–(C-6); modern extension of spectral coverage and resolution shows, in these stars, conflict with all these characteristics. *Gross* means that difference between observation and model is so striking that one needs no, or only trivial, computation to recognize their incompatibility; visual inspection of spectral tracings usually suffices, e.g., an observed emission line where an absorption line is predicted by the model. These differences are so fundamental that they were detected in the first epochs of stellar spectroscopic observation, wholly in the visual spectrum; and they led to a division of all stars into two kinds: *normal*, for which such gross differences were not apparent, and *peculiar*, for which such gross differences, of one or several types, were apparent. Astronomers abandoned early all hopes of modeling peculiar stars and atmospheres by the "standard" (closed, thermal) approach, and simply set them aside, as different kinds of species from normal stars, to which, from time to time, one applies various ad hoc models, simply to represent observations more concisely and coherently than by a numerical table. The primary examples of peculiarity are, listed in the order in which they are apparent in low spectral-resolution observations: (A) an *intrinsic variability* in various features including, but not restricted to, luminosity; (B) the presence of strong *emission lines* from abundant ions; (C) a *symbiotic* appearance of the spectrum of some single stars, consisting of the appearance of spectral features corresponding to those in both *high- T_{eff}* and *low- T_{eff}* standard models, sometimes simultaneously, sometimes at different epochs; (D) a *strongly-extended atmosphere*, directly and indirectly observed/inferred; (E) lines corresponding to both *super-* and *sub-ionized species*, relative to the ionization range expected in a standard-atmosphere corresponding to the T_{eff} and g assigned to that star; (F) *nonthermal velocity fields*, ranging from *sub-* to *trans-* to *super-*thermal values, some definitely systematic outward and inward flow, some apparently quasi-random, or "turbulent," all demonstrating strongly differential motions within the atmosphere.

Thus, there are a variety of stars, classically and historically labeled peculiar because of the presence of one or more of the above peculiarities in their spectrum. We summarize some of these, which most clearly exhibit these features; this is the main focus of this Chapter 3. But we also note that, over the years, the Sun itself satisfies more and more the above definition of *peculiar star*, because of its proximity, which lets us observe features that would be undetectable at normal stellar distances. This suggests what also becomes increasingly obvious as observational resolution increases: the class of peculiar stars continues to expand rapidly, with such improvement in observations. So we include the Sun in this category of peculiar stars, as a particularly striking, illustrative, and thought-provoking member. What will we observe, when spatial observations, made far from the Earth, bring other stars to that solar proximity, especially those labeled peculiar from their visual spectrum even at normal distances?

Second, historically, there are more refined differences, not readily detectable at low resolution, which usually come into focus when one tries to represent, *literally*, higher-resolution observations of normal stars, via the standard (closed, thermal) models, and finds anomaly of some kind. We have already mentioned the solar case, as the most striking example. But other "normal" stars, even at "normal" distances, exhibit such low-amplitude anomalies.

These consist of: inferred thermodynamic parameters lying outside the range permitted by the model, as measured by absorption lines too deep, or the presence of too great ionization stage; or atmospheres apparently too extended, as inferred from absorption lines too narrow or arising from levels too metastable to correspond to normal atmospheric densities; or the apparent necessity to introduce some other thermodynamic parameters than those presumably adequate under the (closed, thermal) model, as inferred from absorption lines being too broad and strong—or displaced and/or asymmetric—to be represented by thermal effects alone. When one considers phenomena like *superionization* and *line-displacements*, there is no strong distinction between *peculiarity* and *anomaly*, particularly as one observes an increasing number of stars showing the same behavior. The real distinction is how astronomers have historically treated these discordant phenomena. *Peculiarity* was simply acknowledged as such and set aside, off the mainstream of stellar atmospheric analysis of “normal-type” stellar objects, until those epochs when a “peculiar” model for such objects could be found. But, *rather than using these anomalies in normal stars to question the basis of (closed, thermal) modeling, one hoped to find a way to “patch up” the usual models, while still retaining their two essential qualities of radiative-equilibrium and hydrostatic-equilibrium*, which give characteristics (C-4) and (C-5) above. Thus, the problems of multivalued “temperature,” remarked in Chapter 1, were eased by admitting *thermal* nonLTE modifications. One tried to resolve line-width and density problems by introducing a “turbulence,” interpreted fictitiously as rising and falling thermal convective elements, or interpreted literally as a real turbulence arising from such convection at very large Reynolds’ numbers (see Vol. 2). Alternatively, one hoped that a stellar rotation could be introduced in such a way as to simply reduce equatorial gravity a bit, without changing a vertical hydrostatic-equilibrium, and without modifying radiative-equilibrium. Such rotation is also thought to produce a turbulence, as from thermal convection, at these large Reynolds’ numbers. So the essential characteristic of *anomaly in normal stars*, under visual, medium-resolution observations, was the hope that (closed, thermal) models could be “patched up,” retaining the essential characteristics (C-1)–(C-6). Although historically, these “anomalies” in the spectra of normal stars were observed and discussed long before the nonvisual data of the third point following, we defer their discussion, and subordinate it, to these nonvisual spectra in both peculiar and normal stars, because its evidence for departure from standard models is so much more striking. Also, presumably all these anomalies, in the various stellar classes, will be discussed in detail in the several monographs of the series. In abstracting departures from the predictions of standard models, across the HR plane, it is clearest to focus on the most outstanding, immediately diagnosable, features. Finally, much of this material on visual-spectral anomalies, especially relative to nonthermal velocity fields, was collected and presented during the 1960’s in the Proceedings of the several symposia on Cosmical Gas Dynamics, as noted in Chapter 1. So, any discussion of anomaly in normal stars is blended with that of the discussion of stellar peculiarity in the visual, and anomaly plus peculiarity in the nonvisual.

So, third, we come to those really gross differences between the predictions of standard models and what one actually observes in those spectral regions outside the visual, for peculiar and normal stars alike. Observations in the farUV and X-ray regions are the most striking. All the evidence, accumulated in a century of observations of peculiar stars, for the existence of dynamically-extended, hot and cold relative to the photosphere, exophotospheric regions is reinforced multifold. The interpretation of the immediate cause of these exophotospheric regions in terms of non-thermal fluxes in addition to the radiative–nonradiative energy, mass, hydromagnetic—is equally solidified. But also, observations in the farIR and radio regions give much more detail on the very extended atmospheric regions, and their cooling and decelerating, when this occurs. These also provide a link to the properties of the local environment created by such mass-fluxes. But probably because they relate to the farthest-out regions, the material from the farIR and radio studies is much less extensive than that from the farUV. In *all* types of stars we see evidence for the lower regions of the exophotosphere: the chromosphere and lower corona. In many fewer stars, even among such peculiar stars having extended atmospheres as the Be stars, do we have extensive data from the farIR and radio. So, in these spectral regions lies much work for future studies. But for all these, while the broad panorama of the exophotosphere begins to become clear, we have only just begun that empirical-theoretical modeling needed to make precise what future, wholly-theoretical, atmospheric models must provide, and what subatmospheric modeling must encompass.

To summarize the material provided by nonvisual spectral observations supplementary to those peculiarities, and to those exophotospheric atmospheric regions, demanded by visual data, we have two alternatives. One is to first summarize these several aspects of peculiarity and exophotospheric regions, wholly from the visual data on which the definitions were historically based, for the whole variety of peculiar stars; then to retrace in the nonvisual spectral regions the same path. The second approach is to survey visual plus nonvisual data contiguously, using the visual data to select which stars and stellar classes to focus on, but trying to construct the enlarged panorama of exophotospheric regions from all the data as a whole. I adopt the second alternative, recognizing that at our epoch, with new observing techniques, spectral ranges, observational results, and empirical syntheses changing almost monthly, one needs an open-ended data bank of material and atmospheric regions. This is particularly true, when one tries to discuss sequences of peculiarities and peculiar-stars, along which the amplitude of some peculiarity may change, or some atmospheric regions may become more predominant in the spectrum. So, one should regard this Chapter 3 as one in which new observations may make obsolete many of its conclusions on what atmospheric regions may be predominant, at our observing epoch, for some particular star or kind of star; what is the complete set of exophotospheric regions that exist, and what are their several patterns of coexistence; and what this may imply on the characteristics of nonthermal fluxes and their origins. Thus, I blend these first three stages of “sequence of doubt” as to adequacy, and just where lie the major inadequacies of standard models, in Section II following.

By this blending of the first three stages of doubt, I do not mean to underemphasize the amalgam of visual-spectral anomalies in normal stars, and their clarifying-supplement by modern nonvisual data, especially in the farUV and X-ray. Rather, I try to put these into perspective. Particularly, using that perspective on the Sun as a normal star which appears peculiar because of its peculiar location giving detail on low-amplitude nonthermal phenomena, one tries to put the statistical normal star into perspective. That is, one regards it simply as a star in which, for whatever reason, nonthermal phenomena are present, but simply show low amplitudes. The challenging question, of course—which we try to clarify empirically-theoretically—is why the nonthermal amplitudes are small. A priori, our viewpoint is simple; the observational fact is that they are small; and that makes the standard thermal model only a gross, first-approximation, quasi-adequate representation of the visual spectra of statistically-defined normal stars. *It is not that normal stars are (closed, thermal) systems; it is that the departures from such are observationally small in their effects, especially in the visual spectrum. Low-amplitude, not necessarily zero, nonthermal fluxes define a normal star, just as higher-amplitude, nonthermal fluxes define a peculiar star.* Clearly, the observational phenomenon/characteristic of *gradualness*, in degree of peculiarity—i.e., there exists a range of degree of peculiarity in most peculiar stars, from zero to large—which we will continually emphasize, but which has been put into strong focus for the Be stars by Doazan, and for the T Tauri stars by Kuhl, simply states that *the classes of peculiar and normal stars are hardly isolated—they blend gradually into each other, from a variety of aspects.*

Fourth, there is that category of phenomena labeled “activity,” in which the “magnetic” phenomena observed on the Sun have, historically, inspired the conceptual developments. Possibly “activity,” or simply magnetic or hydromagnetic phenomena, should better be taken as a seventh class of stellar peculiarity in that first aspect of non-standard phenomena mentioned above. But the study of “activity” has, until recent years, been mainly confined to the Sun, and to late-type stars, such as the dMe, and to magnetic variability in the Ap and Bp stars. It is certainly true that “activity” has more than made up for its late start in stellar astronomical consciousness, having become today a major focus in defining “solar-type” stars, among late-type stars. Its presence in early-type stars is more conjectural than otherwise, at the moment. Nonetheless, it is a major aspect of study, when one discusses evidence for departure from standard modeling. Again, I under-summarize it, in this volume, from lack of competence, and from its major emphasis elsewhere in the series (the A-star, M-star, and Solar volumes). Such underemphasis also results in an underemphasis on the presence and effect of lateral inhomogeneities, in favor of my major focus here: to establish the range of patterns in radial distribution of atmospheric regions. When one recognizes that the extent of radial patterns of observed atmospheric structure now extends to some 10^2 , 10^4 , 10^6 , 10^8 photospheric radii and even beyond—depending on the kind of star, and even the phase of a particular star (cf the Be stars, for example)—I think this first-approximation focus on radial structure is warranted.

So, overall, in this Chapter 3, one hopes to combine observations of peculiarity with observations of anomaly, in a way that can be summarized: Look for common phenomena, which are contradictory with (closed, thermal) modeling and which are:

1. prominent, in so-called peculiar stars, even though these are distant, because of the large inherent amplitudes of the underlying phenomenological cause;
2. observable, although of small amplitude, in the Sun because of its proximity;
3. observable, only in limited aspects in limited spectral regions, in *most* normal stars, because of the “normally small” amplitudes in “normally observed” spectral regions of “normal” stars; and
4. the physical consequences of whose existence are profound and basic on stellar atmospheric structure.

The most striking examples of such phenomena that are common to (1)–(4) are:

- a. A nonradiative energy-flux, which produces chromosphere and corona; hence, superionization, excitation, and quasi-static atmospheric extension.
- b. A mass-flux, which produces: (i) upper height-limits on where the chromosphere and corona begin; (ii) a very large atmospheric extension, by changing an HE exponential decrease of density to the $(r^2v)^{-1}$ decrease of an expanding atmosphere; (iii) a local-environment for some stars—at some epochs and some phases—by a self-interaction within a variable mass-flux, and possibly with the local ISM, for them at some phases. This apparently builds up a “balloon-storage” around, and very near to, some stars (of particularly Be and T Tauri stars); but for other stars, it occurs very far away (e.g., planetary-nebular objects). Apparently, all these effects can be highly variable within a given star, and highly individual, differing from star to star, even among “like” stars.
- c. Energy storage in a magnetic field, which is either primeval, or produced by dynamo interaction between other nonthermal storage modes, such as rotation and convection. Such a field can catalyze the dissipation of such non-thermal energy locally, in space and time, and “guide” the flow of ionized gases.

Only in such “peculiar” stars as Wolf-Rayet, novae, planetary-nebulae, symbiotic, Sun are superionization phenomena of chromospheres-coronae observed in the visual spectrum. The only star for which we can directly measure a particle flux, hence, directly measure a mass-flux, is the Sun. For other stars, the only direct measure on the mass-flux is its velocity, from line-displacements; inferences of the associated density and distance from the star are model-dependent. But the mass-flux from the Sun is so small that its induced departure from an exponential atmospheric density gradient occurs so far out from the photosphere as to leave ambiguous an observational decision between alternative theories for its origin. And, finally, the size of magnetically-induced energy discharges must, apparently, be much greater than in the Sun to be generally visible: except in the “peculiar” emission-line stars of the dMe variety. *Possibly*, in the “peculiar” Ap stars, magnetic guiding/sorting is observed. Otherwise, inferences from the visual spectrum are indirect.

We proceed to summarize in more detail the empirical basis for this four-stage evolution of doubt on the adequacy of the (closed, thermal) modeling. The full set of observational details for all stellar types across the HR diagram is provided by the several volumes of the series; and one must read them to really have a firm basis for understanding why we must move to another kind of modeling. Nonetheless, there is some advantage in trying to look, in abstract, across the whole range of the HR diagram to tie together this evidence from a variety of spectral classes. This is particularly important if one thinks, as I do, that there is no intrinsic difference between hot, warm, cool, and cold stars relative to the kind of thermodynamic model, of star, and of atmosphere, needed. And also, if one thinks that *thermodynamically all stars are “like the Sun,” not just some types are like the Sun*, the same logic of the utility of a “global look across the HR diagram,”¹ in comparing solar and stellar phenomena, holds. It is clear from the literature that such an outlook of “no essential difference between hot through cold stars, and all are like the Sun, in thermodynamic structure” is not generally held, particularly among speculative-theoreticians. Witness the

long disbelief in the prevalence of chromospheres-coronae because this would imply universal nonradiative energy-fluxes, and "theoretically," one saw no way to produce such nonradiative energy fluxes in the hot stars. The situation is the same, for the universality of nonradiatively-heated mass-fluxes. Some believe that some stars must choose between fast winds or hot coronae. One continues to find the divisions into "solar-type" and "nonsolar-type" stars: originally on the basis of the existence or not of chromospheres-coronae; more recently on the basis of "activity." Here, I emphasize only that while I have been explicit, above, on what I think the data demand, neither our empirical knowledge of stars, nor our theoretical knowledge of nonEquilibrium thermodynamical concentrations of matter and energy are sufficiently complete to permit certainty in any of these conclusions and models. So, while hoping they are possible, as making possible a panoramic outlook, one wants to maintain a strong skepticism toward all generalizations.

Having said this, we proceed to such a "generalization-oriented" survey across the HR diagram, *from each of the stages of doubt on the (closed, thermal) modeling just abstracted, to introduce stages of belief in the possibilities of (open, nonthermal) modeling*. I repeat: I do not try to survey all phenomena in each stage; I try simply to give a broad, overall picture of the existence of such phenomena, in each such stage, across the HR diagram. In choosing what material to include, and from what orientation to discuss it, I try to put into broad thermodynamic perspective the utility of each feature of peculiarity and anomaly in guiding us toward a satisfactory atmospheric modeling. That is:

The "standard-star" is (closed, thermal). It has a static thermal structure, with energy produced by thermal-nuclear reactions that are highly sensitive to local temperature and density. The energy produced diffuses quietly (thermally) to the surface, where it is quietly (thermally) radiated away to the environment. No changes should occur in structure, energy-generation, energy-transfer, energy-ejection except over evolutionary times. All stellar mass-loss comes from nuclear conversion to energy. Peculiarity and anomaly imply departure from this standard model; and we ask in what way, grossly, for each.

Variability is a many-sided perturbation. Variable luminosity can arise in: nuclear generation rate accompanying nonthermal change in local conditions; supplement from nonnuclear source; activation of nonthermal storage mode, hence, phase-lags in transport and release; conversion from thermal transport and ejection into nonthermal. Variable mass-flux can arise in each of the above, given some mechanism to produce it. Variable atmospheric structure can result from, and cause, each of the preceding. We particularly ask the significance of a "catastrophic" variability, which apparently leaves the star unchanged, and capable of repeating it, in nonevolutionary times—particularly, relative to the general question of origin of mass-loss.

Emission-lines require either or both of: a strong outward-increase in T_e , hence, nonradiative energy and dissipation; line-producing atmospheric regions that are greatly extended relative to those producing the visual continuum. The presence of both sub- and super-ionized emission lines requires both alternatives to exist. So also does the presence of both photoionization-dominated and collision-dominated emission lines. The basic questions are then the source of nonradiative heating, and greatly extended atmospheres.

Extended atmospheres themselves require either static or dynamic extension or both. The observed extent is too great for only the former, either thermal or turbulent, so primary focus lies on the origin of the required super-thermal mass-flow. The a priori theoretical choice lies between: thermal evaporative diffusion, not tenable for any observed T_e ; simple thermal, outer-atmospheric expansion of the hot-coronal type, which produces too-small mass-fluxes and too-small particle concentrations far from the star to be generally useful; low-velocity subatmospheric injection; cataclysmic subatmospheric ejection. Apparently both the latter kinds exist, among different stars, and among different epochs of the same star. A primary question is the acceleration mechanisms, once the mass-flow starts.

Symbiotic stars put into strong focus that observational ambiguity between multi-regioned atmospheric structure and multiple components of an observed, but unresolved, system. Their strong, graduated, variable, observational linkage in these symbiotic aspects to a variety of other kinds of peculiar stars gives a tantalizing potential to the use of them, and their symbiotic features, for the delineation of distinctive atmospheric regions.

Super- and sub-ionized species are the stellar-atmospheric, contemporary, counterpart of Eddington's original hot-gas and cold-dust symbiotic structure of the ISM. Diagnostically, the problem is to choose between radial and horizontal components as best representing the observations; at least for the Sun, both exist. The major problem is to link the hot–cold spatial evolution to that of the large density spatial evolution already cited; and to the spatial evolution of nonthermal velocities covered in the next point.

Sub-, Trans-, Super-, and Ultra-thermal velocities, which vary enormously in space and in time, are the most directly observable features of the mass-flux, and of any other mass-transport in the stellar atmosphere. Controversy exists as to their observational properties; no theory has yet succeeded in representing their distribution over the atmosphere, and its time-variation, for any single star. The above comments on extended-atmospheres put the most immediate problems on the velocity fields into focus.

These questions are what we hoped to clarify, in looking at stellar peculiarities. When one adjoins the farUV observations of normal stars to the visual, they are also the questions one raises in asking how we should change normal-star atmospheric modeling, so that the models can represent all these observations. So, hopefully, the material in the chapter will make clear the basis for understanding why the open, nonthermal, nonlinearly-nonEquilibrium focii of Parts II and III are necessary, even though we do not yet understand how to develop, properly, the analytical structure that must accompany the gross thermodynamic picture.

II. SURVEY OF STELLAR PECULIARITY: DEFINED BY STARS IN THE VISUAL, ELABORATED AND EXHIBITED BY ALL STARS IN THE farUV, CHARACTERIZING EXOPHOTOSPHERIC, AND LOCAL-ENVIRONMENTAL REGIONS.

It is simply an empirical fact that the broader the spectral range covered, and the higher the (spectral, temporal, spatial) resolution, the greater the number and variety of stars showing, from even gross but thermodynamically-consistent analysis, strong discord with the features of (closed, thermal) modeling. So, according to our definition in the introduction to this chapter, all such stars should be classified *peculiar*; all such obviously-discordant features, *peculiarities*; and the number and variety of stars, and atmospheric phenomena, for which thermal modeling must be undisputably excluded, apparently grows continually. Then we see that any star which is admitted to be peculiar only under more numerous observations, broader spectral range, or higher resolution spectroscopy has either: (1) the same kind of peculiarities as exhibited by other, less-extensively studied, stars under lower spectral range and resolution; (2) some totally new kind of peculiarity, which is observable only under a novel, higher resolution or in hitherto unstudied, nonvisual spectral regions; or (3) we have elevated some feature from *anomalous* to *peculiar*, deciding that it is indeed fundamentally, not just marginally, in contradiction with (closed, thermal) models. As stated, in the following we establish classes of peculiarity from visual, low-resolution observations—then elaborate their features by extending spectral range and resolution. But it is nonetheless a fact that, historically, as even low-resolution visual observations simply expanded in number, the membership in any particular class of peculiarity also expanded, simply from the assignment of previously known, “normal” stars to it. Either the peculiarity characteristics were variable, or a better telescope was used, or etc. But in any event, as already mentioned, a primary characteristic of peculiarity stands out: *GRADUALNESS*, a range from very small to very large size, of any observed aspect of peculiarity. For example, “standard” stars have no H α emission; neither do most real stars; but some stars show faint emission H α ; and some, very strong; while some show *all* these aspects—only absorption, weak emission, strong emission—at differing times. Any improvement on standard modeling, to permit the occurrence of an H α emission line, must permit such gradualness in its size—and variability.

It is an equally empirical fact that “identical” stars, in the HR identification by (T_{eff}, g), can differ completely in some aspect of peculiarity. Not all stars in the cepheid-gap pulsate. Not all B stars showing the largest values of $V \sin i$ show H α emission, even over historic times. Not all close binaries are symbiotic or cataclysmic. Such *INDIVIDUALITY* among stars of the same MK class, even enlarged to include other properties, like $V \sin i$, even peculiarities of one type but not another, is a second primary characteristic of peculiarity. It is not sufficient to just introduce some phenomenon that produces a particular peculiarity in ad hoc extension of standard modeling; we

must also allow a "classically-similar" star *not* to have that peculiarity: we must explain absence as well as presence. Possibly absence can simply be interpreted as presence with vanishingly small amplitude; but then the new theory must explain, carefully, what fixes the amplitude—not just why the phenomenon exists. The theory must be non-linear, not just linear. This is an important aspect, in deciding whether the standard, (closed, thermal) model can be patched up, simply by investigating and including all thermal instabilities, or whether a basically different thermodynamic model must be introduced. It is equally an important problem in internal structure and evolution questions, if one would attribute peculiarity, in some aspect, to some evolutionary stage of the star.

I have chosen the third general characteristic of most types of peculiarity, *VARIABILITY*, as the first specific type of peculiarity. Historically, the oldest discord to the "unchanging stars," its presence, today, in some aspects of all stars is routine. I put the choice in focus, not only in Section A following, but also in the other sections.

Finally, a fourth general characteristic comes increasingly into prominence, even though our knowledge is rudimentary. Apparently, for at least some kinds of stars, we cannot model the atmosphere at any particular epoch without knowing the *TIME-HISTORY of a VARIABLE MASS-FLUX* over some preceding period, which is characteristic of the particular star. Currently available data show the effect to be most observationally striking in Be stars. It also appears to be very important in understanding the planetary-nebulae and other kinds of stars intermediate to them and Be stars—Bep, symbiotic stars, recurrent novae. It seems to be of lesser importance in modeling the atmospheres of the Sun and those WR stars not occurring in PN—but this last is tautology, because there is as yet no theory, only observational characteristics, to be discussed.

Our translation of peculiarities into characteristics of exophotospheric regions must include these four. We proceed to the details.

A. STELLAR VARIABILITY

Clearly, the following abstract of variability as one type of peculiarity can only be superficial, even if we tried to cover only its visual, low-resolution characteristics, especially because of its evolution toward *all* stars showing it in some one or more of its increasingly numerous variety of aspects. However, we need not be encyclopedic to comment on the impact of its simple, multi-aspect, *existence* on the adequacy of (closed, thermal) modeling. Basically, we want to interpret such multiple variability to guide our revised modeling—of atmosphere and subatmosphere—among three gross alternatives: (1) Does such variability simply reflect multiple thermal instabilities of (closed, thermal) models, with the thermonuclear energy input from the star remaining essentially constant, the energy being only redistributed in (energy, mass) fluxes, possibly with phase-lags arising from quasi-thermal storage mechanisms? (2) Does such variability also reflect the existence of nonthermal energy production and mass-ejection, which negates the (closed, thermal) models in favor of (open, nonthermal)? (3) Are some aspects of such variability only illusory, such as eclipses of one object by another? So one has the classic first division of variability into: *intrinsic*, arising in the atmospheric and subatmospheric behavior of a single star; and *geometric*, coming either from literally geometric obscuration effects in a binary system, or some variety of dynamically interacting multiple structure, ranging from Struve's historic model of Be stars as reflecting ejection of a planetesimal-like equatorial ring, to contemporary models of degenerate companions and accretion disks to explain cataclysmic and symbiotic stars. At our epoch, the increasing evidence for the ubiquitous nature of widely-differing physical kinds of exophotospheric regions in a single star—chromospheres-coronae, cool H α envelopes and shells; ultravelocity and very low-velocity winds; X-ray emitting regions and dust-shells; isolated-star mass-fluxes of sizes differing by dex (10)—removes much of the historical incentive to require binarity to explain symbiotic appearance because of the single-region characteristic of the standard-model atmosphere. Nonetheless, the distinction between intrinsic and geometric variability remains, even today, as a primary point for clarification. In the same way, a decision whether the important contribution of stellar rotation to atmospheric modeling, static and variable, may be as a nonthermal energy source, rather than simply as an agent to reduce equatorial gravity, remains critical, in discussing the way one must change standard modeling. But the essential thing to remember, in summarizing variability today rather than a decade or two ago, is that the existence of many atmospheric regions beyond the photosphere is a fact, independently of

whether we can explain them. And we must take their multiple existence into account, in inferring which atmospheric region is varying, in what way, and by how much, to produce the observed variation of the given size, in the particular spectral range, in the several fluxes from the star. Again from the standpoint of the Sun as a continued reference, and certainly one for which there is no question of the existence of a companion or an accretion disk, it is extremely interesting to note: (i) the symbiotic nature of the solar spectrum and atmospheric structure; (ii) the strong variability in surface features with *apparently* only small variability in integrated energy output; and (iii) the rapid expansion of studies of solar variability (cf the Proceedings of the NASA Workshop, *Variations of the Solar Constant*, Sofia, 1980. It is misleadingly labeled, because the range of variable quantities covered is much broader than just the total radiative output).

Having said all this, we obtain a still excellent perspective, and overall picture, by considering the 1938 classification scheme for characteristics and sources of visual-radiation variability in the classic book, *Variable Stars*, by Gaposchkin and Payne-Gaposchkin; their suggested revision of some classes in 1978; and their succinct contrast of *stellar* and *atmospheric* variability. However, because their focus on variability as a peculiarity rests mainly on classical, low-resolution, visual data, I adjoin several comments on the Gaposchkins' picture (especially the latter of the three aspects), which are based on better temporal coverage for some representative stars, on high-resolution data at different epochs, and on data outside the visual-spectral region. I do this to put into better focus the eventual transition from this Chapter 3 to Part III. I compare the 1938 and 1978 summaries as reflecting an evolution of data and thinking toward higher resolution and broader spectral range, but not reflecting the farUV and multi-region atmospheres; and their stellar vs. atmospheric contrast as an early sharp focus on the fundamental problem of *origin* of nonradiative fluxes which discriminate between *closed* and *open* thermodynamic characteristics. The increased and higher resolution data illustrate the difference in conclusion from low-resolution statistical, and high-resolution individual, data; and the nonvisual data extend atmospheric-region, and spectral-region, coverage to the exophotosphere.

1. Gaposchkin 1938 Classification Scheme According to Broad Mechanism of Variability in Luminosity

The basic, easiest, hence historically-first measure of stellar variability was that of stellar *luminosity*; one needs only a light collector, not a spectral disperser. The limitation is that, historically, we consider only *visual* luminosity. For Part III, atmospheric structural patterns, we see that distinctions between *visual* and *total* luminosity, and between *total* luminosity and *total* energy flux, are critical in discussing mechanisms of variability. Yet on the basis of only this limited kind of measure, one can introduce a first broad division into types of variability: *gradual, and usually small, vs. abrupt and usually large*. Most stars exhibit the former; some, the latter; the significant thing is that with *very* few exceptions, the stars in both categories eventually regain their quiet state, showing that such variability is not unidirectional, evolutionary change. Indeed, the essential characteristic of stellar variability, the reason for considering its presence of such great importance in the search for a general stellar nonthermal modeling, is just this recurrent character; not necessarily periodic, nor even with any well-defined pattern in many cases. Only in some exceptional cases is variability *apparently* a "one-time" occurrence. Clearly, we do not imply that the exceptional "apparent one-time" occurrences are, any more than are "peculiar" stars, to be set aside from consideration. We simply want to know whether to associate variability with nonthermal structure or with evolution of thermal structure. Overall, present evidence implies the former.

I take a slight liberty with the Gaposchkins' classification scheme, while guarding its essentials, to fit it into the thermodynamic approximation scheme of this book. Then to the same first-approximation used for modeling in previous chapters, broad mechanisms are delineated by treating the "stellar surface" as a blackbody characterized by surface temperature and area, and asking what a particular kind of variation of luminosity implies for variation of these two surface characteristics. In higher approximation, we adjoin nonvisual luminosity and exophotospheric, multi-regional, atmospheric structure.

a. Geometric Variability corresponds to either of:

i. An eclipsing binary source of luminosity: two opaque disks, revolving in mutual orbit, unchanged in their intrinsic characteristics by such binarity, produce luminosity change *wholly* by either partial or total eclipses. Such eclipse-induced variability, or even variations coming from tidal distortion of the disk, have little interest to us here. Our only concern is that the variability does indeed arise in such binarity. In 1938, this was the focus on binarity.

ii. A mass-transfer between two components of a very close binary, resulting in an impact of the transferred mass on the atmosphere of one component, producing nonthermal atmospheric velocity fields, heating, luminosity, etc. Or, one can replace the second component of the binary by an equatorial disk, produced by a rotationally induced instability and mass ejection. Or, one can have companion *and* disk. This aspect was the prominent one in 1978.

Variability configurations (i) and (ii) differ drastically, but each does not depend upon any intrinsic, non-thermal subatmospheric or atmospheric structure of the star, the sources toward which we look in discussing intrinsic variability. True, a rotational velocity which exceeds that of gravitational instability is hardly thermal, but that is another matter. Such has been suggested as the cause underlying the Be phenomenon; but modern data do not support this suggestion, as we comment later in discussing the “Be peculiarity,” associated with emission-line peculiarity. So an observed variability, originating in either of these two geometrical alternatives, would contribute nothing toward resolving our attempt to decide whether the (closed, thermal) or (open, nonthermal) character of stars in general is the correct one. *If* the mass-transfer arises wholly within one star, not primarily from the presence of the companion, then, of course, alternative (ii) attests to nonthermal phenomena arising intrinsically in the primary.

b. Intrinsic Variability corresponds to a single star, which changes in either or both of surface area and temperature: the alternative cases correspond to modeling *how* and *why* surface area and temperature change. The 1938 summary set up three main divisions: pulsational, cataclysmic, and spectral. The first two were primarily, but not exclusively, based on luminosity variability; the third, on low-resolution spectral change.

i. Pulsational Variability. This variety, at the 1938 epoch, was pictured as one where the mechanism is a periodic rise and fall of the photosphere—hence, primarily a compression-expansion of surface layers—but not basically an ejection of mass, although this is not excluded except by any speculative boundary conditions imposed in modeling. In any event, unless ejected material has nova-like amplitude, it will have sufficiently low opacity *in the visual spectrum* that the pulsational, periodic expansion-contraction effects—rather than those of any systematic velocity of ejection—dominate in that spectral region. The variation is gradual, and the atmospheric and stellar configurations definitely repeat themselves, without apparent secular change in structure. This is a *kinematic* characterization. A *dynamic* description must include the relation between surface-layer behavior, and subatmospheric/internal structure and variation; so it is a model. The observations must guide such, to avoid the imposition of improper boundary conditions such as no mass-flux from the system. We survey the kinematic situation, then turn to the dynamic, and the question of modeling. Both have evolved considerably since the 1938 epoch; and the division between pulsating and cataclysmic variables—the next category considered here—has evolved in an interesting manner. Shapley “rescued” Cepheids from binarity by substituting simple photospheric oscillations for single-spectrum orbital motion. Binarity is returning to the cepheids, especially to explain some “symbiotic” observations in the farUV. Such binarity, from such motivation, becomes increasingly favored for the cataclysmic variables; even in the Gaposchkin 1978 summary. My viewpoint in this book is quite the contrary.

One finds such *apparently*-pulsational changes all across the HR diagram; Shapley (1914) identified them from B through M types; i.e., the β Cephei through long-period variable types. Fig. 3-1, from J. Cox (1965) shows current ideas on their locations. They are most easily observed among the giants and supergiants because of their greater brightness, but Cox (1980) suggests that the most recent observations imply that pulsating white-dwarfs of the ZZ

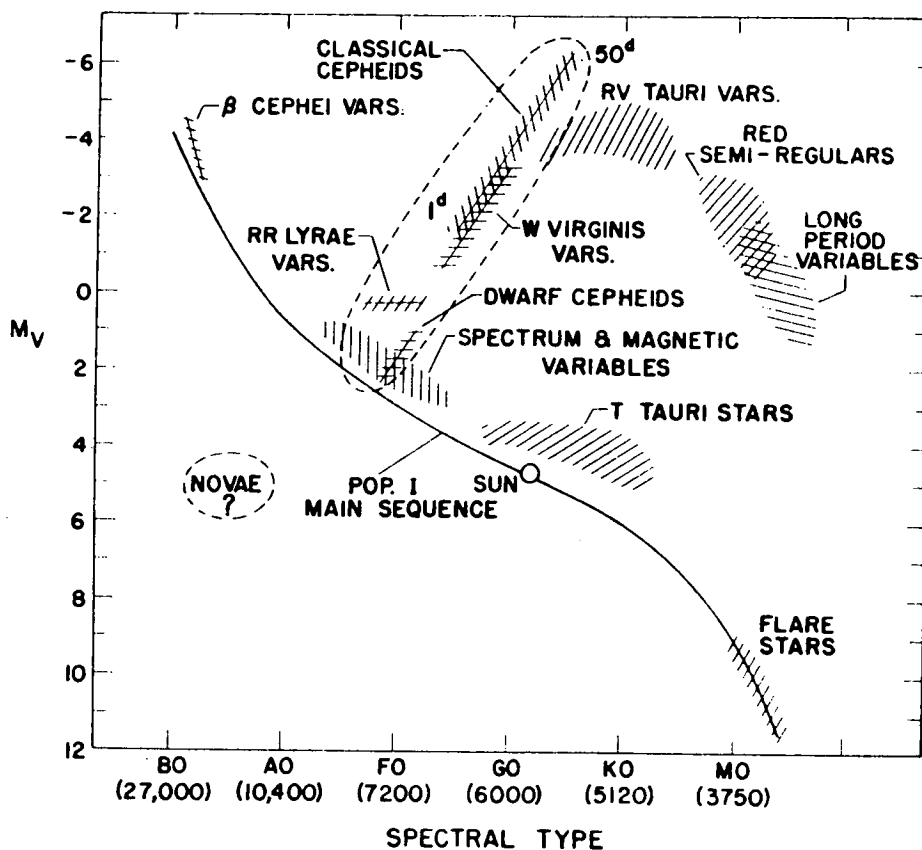


Fig. 3-1. Location of various types of intrinsic variables on the Hertzsprung-Russell diagram (from J. P. Cox, 1965).

Ceti type may be the most abundant such apparently-pulsating stars. Possibly such suggestion is correct, if one considers only stars in which pulsation is the *only* nonthermal phenomenon; for one notes current discussion of pulsation aspects even in the Sun (Jordan, 1981).

I stress *apparently*, because in the early days of the discovery of repetitive spectral-line displacements associated with repetitive luminosity-changes, one subordinated the latter to the former to interpret the changes as caused by eclipsing binarity, *even though always only one spectrum was observed*. Shapley gave a thorough discussion of the cepheids and RR Lyrae stars, based on the low-resolution material of that time, to show the inadequacy of the binary interpretation. Mainly the objections focused on the universal absence of the second spectrum, and the fact that the derived orbits showed the hypothesized companion to lie within the atmosphere of the primary star, and to have only a fraction of its mass. Accompanying evidence against binarity were irregular variations in the photometric period, continually changing forms of the light-curves, and periodic change in type of the observed spectrum. Attempts to avoid such "internal-structural" origin of these luminosity and velocity changes included models of rotating, spotted, stars, and compression effects of the enveloping interstellar medium during the binary motion. Shapley's discussion of the then-available data consisted mainly in showing the untenability of the binary speculation, and the greater consistency of attributing the variability to an oscillatory (nonthermal) internal structure of a single star. The main *kinetic* features of the pulsating model were then presented by Eddington (1918, 1926) with explanation of the source and maintenance of the pulsation following some years later (J. Cox, Whitney, and Zhevakin during 1950's). Detailed study of the differences between different types of pulsating stars and phenomena are still current, including nonradial pulsations, in stars ranging from hot B stars through the Sun and to cold M stars; main-sequence and supergiants—and subdwarfs. Finally, we note that although there appear to be regions in the HR

diagram where pulsating variables are concentrated, modern data show that *not all stars* in these regions of concentration show this pulsational variability—at least not to the same “strongly-apparent” amplitude. Again, we see stellar individuality; any complete model must include it, and be based on more than mass, luminosity, and “radius.”

I stress these details of the historically suggested alternatives to such pulsation, because we will see, in the rest of this chapter and in Part III, how continually re-occurring are these same kinds of attempted substitutes that retain an internal thermal, or pseudothermal, structure—especially binarity and rotation of “surface-inhomogeneity”—in place of some nonthermal internal structural origin. We note that *single* stars, whose spectral lines show variable line-displacements, are very often listed in catalogs as “spectroscopic binary ?.” Too often, especially these days of looking for neutron-star or black-hole companions to interpret such things as X-ray fluxes, the speculative-theoretician forgets the “?” in the catalog. We continually return to this point.

For our present survey, the important fact is this occurrence of pulsation across the HR diagram: periods range from an hour to several years, although the lower limit, especially in “localized” phenomena, continues to decrease with better resolution. Equally important, the shorter the period, the smaller the luminosity change, and conversely—as *observed in the visual spectrum*. Thus, the β Cephei (B-type) stars have periods of a few hours and amplitudes less than some 0.1 mag; the dwarf cepheids (types A–F4), periods 0.1–0.5 days, amplitudes 0.1–0.25 mag; RR Lyr (A-type), less than a day, and 0.5–1.0 mag; classical cepheids (G-type), 5–100 days, 2–3 mag; long-period (M-type) variables, 100–1000 days, 5–10 mag. This small luminosity change for small period was the logic for beginning the summary of intrinsic variability with pulsational variability, interpreted as originating in a thermal instability which preserved the thermal model: a gradual and gentle, rise and fall, of a photosphere; the variability coming mainly from a change in T_{eff} , not from a major change in radius. But if we assume that size of change in visual luminosity also characterizes size of change in bolometric luminosity, then pulsational variability is no longer small. The 5–10 visual magnitude change in the Mira stars approaches that observed in novae—with the exception of the time-scale in change. However, we also note that as period and amplitude increase, T_{eff} decreases, from some 25,000 K to some 2000 K along the sequence listed. So, the range in peak blackbody emission is, correspondingly, from some 1000 Å to some 15,000 Å. Only for the classical cepheids, spectral type mid-F at maximum, ranging to KO at minimum, thus nearly like the Sun, does maximum blackbody emissivity lie in the visual. We have already noted that the *theory* of simple pulsation finds the major luminosity variation coming from T_{eff} -variation, not change in area. So, on this blackbody approximation, visual measures of variability amplitude should underestimate the bolometric, for the hot, low-amplitude stars; and it should overestimate the bolometric, for the cool, large amplitude stars. And, indeed, modern measures in the 10–20,000 Å range for the cool Mira stars find only a variability of 1–2 magnitudes there. Thus, restricting attention to the visual continuum, one is reasonably content with a thermal instability that retains thermal photospheric models. We except stars hotter than late A, early F, where the hydrogen-helium instability does not, theoretically, apply, but where the stars appear to be satisfied with pulsation interpretations.

I do not want to imply by the above that this first-approximation, homogeneous single-layer, blackbody representation actually represents well the spectral distribution in the several continua, especially in the cold stars for which we used it to resolve the apparent dilemma of amplitudes. Nor, even that T_{eff} and radius changes, independent of opacity changes, suffice to represent the amplitudes (cf Smak, 1966; Wing, 1980; and the M-star volume in this series, ed. Quercis and Johnson). The above simply says, that the bolometric luminosity amplitudes cannot be used, in first-order approximation, to argue against thermal photospheric models, in the thermally unstable, simple pulsation, case. In the same way, I do not want to imply that all *apparently*-pulsational variability is simply represented as above. The Gaposchkin 1938 summary exhibits the wide variety of visual light-curves found, which modern data augment and detail. Ledoux and Walraven (1958) and Cox (1980) discuss the observational and theoretical elaboration of the simple model. For us, here, it suffices to note that one observes, even in the visual, both symmetric and asymmetric light variations: some being asymmetric with rapid rises in luminosity; others, asymmetric with rapid drops. And, in examining the variety of stars assigned to the cataclysmic class, one sees that some of them, like the pulsating stars cited, form an observational transition between the two categories, even in visual, low-resolution data. The transition varieties of stars are usually, but not always, those which are quasi-regular in variability, but differ according to whether the phenomena are strictly periodic or only statistically so, and according to the degree of

“abruptness” in onset of a rise, or fall. In the cataclysmic sense, “abrupt” usually implies “unpredictably sudden”—i.e., without pattern, and often, but not always, large. Then when we pass to the category the Gaposchkins called *spectrum-variability*—with which kind of variability, at that epoch, luminosity-variability was not required—we will also find abrupt, unpredictable, changes, sometimes, using modern data, also showing luminosity changes. And we will also see that a major interpretive problem for all these stars is the nonvisual contribution. And like a more detailed discussion of the Mira variables requires (Wing, 1980), such nonvisual variability is strongly linked to multi-regional structure, instead of the simple single-region blackbody. The basic contrast of such “abrupt” changes is with those where some strong rise in luminosity—or spectral change—is preceded by a long interval of gradual increase in “something.” In caricature, pulsational-variability has a precursor; the conceptual-ideal of the cataclysmic variable does not.

Given this viewpoint that pulsational variability is that set of phenomena accompanying a quasi-periodic rise and fall of the photosphere, one can caricature it by replacing the subphotosphere by an oscillating piston; then one asks two kinds of questions. The first kind focuses on cause of the piston motion; the second, its consequences. We highly abstract the first, as background; our interest lies in the second, for atmospheric structure, and origin of non-thermal fluxes.

α *PULSATION CAUSE*: Contemporary pulsational theory, and linear nonEquilibrium diagnostics of visual observations, agree in placing the origin of most pulsational variability in thermal instability of (closed, thermal) models. (cf Cox, 1980; Fischel, Lesh, and Sparks, 1980, NASA 1978 Pulsation Symposium; for current theory. Kraft, Oke, Whitney, for visual observations and diagnostics, with Cox and Christy summarizing the associated linear and non-linear theory, Nice, Atmospheric Aerodynamics Symposium, Thomas, 1965). For stars cooler than about spectral class F2, the origin of thermal pulsational instability lies in the large thermal heat capacity of subatmospheric hydrogen and helium ionization zones. (Classical pulsation and convection, both depending on hydrogen ionization, have this same, near F2–F5, cutoff toward hot stars.) Under these conditions, a compression simply increases the density; thermal energy of compression goes into ionization, leaving ΔT_e small. So opacity increases during compression; a volume element retains more energy; it amplifies, rather than damps, any compressive perturbation. So long as the pulsation retains a standing-wave character, the photosphere simply rises and falls as a whole; there are no differential motions to mechanically-dissipate energy and destroy RE. Radiative flux and effective gravity are fixed by the phase of the pulsation. Whitney (1965) summarizes such an “instantaneous photospheric” representation of the visual continuum by showing that atmospheric disturbances whose characteristic time is comparable with the pulsation period will nearly mimic RE, because of the much shorter radiative relaxation times. Phenomena whose time-scales are fixed mainly by such radiative-energy exchange will, essentially by definition, be optically thin in the visual continuum, so unobservable in it. Thus, variability in the optical continuum is insufficient as a guide to consider—theoretically or observationally—a spatial evolution of this standing-wave, instantaneous photosphere, into running-waves, which can steepen into shocks and dissipate mechanical energy (Schwarzschild, 1938; Whitney, 1955 et seq.; Kraft, 1965; Hill, 1972 et seq.; Willson, 1976 et seq.; Wood, 1980); or into a shell-ejection associated with maximum luminosity (Pannekoek, 1946); or generally, this (thermally-unstable, closed) system evolving into a (nonthermal, open) one. Such evolution can arise because of changed conditions imposed at the upper boundary in the model, or in a system of exophotospheric regions arising from a combination of the pulsation and other nonthermal fluxes. Then to the accuracy of our crude interpretation in terms of blackbody temperature and area, the observed pulsation phenomena are dominated by the compression effect on temperature: T_{eff} varies by some 25 percent for a classical cepheid; the photospheric radius by some 5–10 percent; integrated luminosity varies as $T^4 r^2$; “blue” luminosity as $r^2 \exp(-h\nu/kT)$; “red” luminosity as $r^2 T$. Refer to the several 1-zone representations of the pulsation (Cox, 1980), which give the internal structure of the equivalent piston caricature—its lower boundary is fixed in mass-depth; its upper boundary oscillates, with spatial homogeneity between the boundaries; its structure can introduce phase-lags between compression and luminosity.

Clearly, the outstanding dynamical problem is to locate the mechanisms which produce pulsational variability—either radial or nonradial—in those stars for which the H-He thermal valve is insufficient. Interest lies in these stars for themselves, but also as adding some physics overlooked in the H-He ionization-zone explanation. The obvious extension is to thermal ionization of the next-most-abundant elements. This means a particular focus on the stars hotter than the mid-F; the same focus in seeking sources for nonradiative energy-fluxes across the HR diagram; but also on the very cool giants and supergiants, again for pulsational and nonradiative-energy sources. And, of course, again one asks the effect of adding rotational instability, and coupling, to the nonrotating configuration. One notes the peaking of stellar rotation velocities in the B-star class. Again, the summaries in Fischel, Lesh, Sparks (1980) and G. E. V. O. N. and Sterken (1981) should be read. Here, our focus does not lie on this dynamic problem, except insofar as it places the origin of exospheric, nonthermal, atmospheric structure in subatmospheric rather than atmospheric cause: in variable radiative, and both quasi-steady and variable nonradiative, energy and mass fluxes originating in subatmospheric nonthermal configurations and phenomena. Again in caricature, one asks how broad a representation of subatmospheric input to atmospheric structure can be obtained by a dynamically-driven piston—either quasi-periodic or stochastic—representation of the subatmospheric boundary-condition on the atmosphere. This is particularly important in formulating the boundary-condition on the mass-flux. The piston configuration is by contrast, for example, with either of two other extremes. One is a radiatively-driven mass-flux, with amplitude fixed by this mechanism. In this case, any variability in size of mass-flux should be associated with the variability in radiation associated with the preceding pulsations, not with their own mass-flow. The other extreme is an outer-envelope nuclear burning, triggered by binary mass-exchange.

As stressed in the cited references, the best guide to resolving all these problems lies in comparing expected observable consequences to actual observation: atmospheric structure, and its variability. We continue that path.

β . PULSATION CONSEQUENCES: An idealized pulsation in which the photosphere simply rises and falls, with neither differential expansion nor compression, nor differential velocities, nor nonradiative energy dissipation, nor mass-ejection, has, today, as little interest as it has physical reality. Aerodynamically, representing a pulsation as a standing wave (Eddington, 1926), and a standing wave as the superposition of outward and inward progressive waves (Schwarzschild, 1938), breaks down in two ways: (1) a nonlinear steepening of the outward moving expansion wave, which ultimately becomes a shock if the atmosphere is extended enough, and in any event the inward-moving compression wave forms a shock under gravitational acceleration; (2) if the piston period is short enough, the waves from successive oscillations interact, and the eventual state of the atmosphere will not be that of one which has time to completely relax between oscillations. Atmospheric distension, heating, and mass-loss can result. Some variety of these consequences should be expected in the atmospheres of any or all of pulsating-variable stars. The question is whether the consequences are significant, in actual stars: in their observational consequences, in whatever spectral region, preferably that giving information on most exterior regions; in their effect on atmospheric structure, via non-radiative-energy generation, mass-flux, and the resulting effect on atmospheric heating and distension; in their effect on stellar structure and evolution—e.g., via mass-loss.

Historically, one observed emission lines and line-doubling in the visual-spectral regions. In RR Lyrae and W Virg stars, Balmer and Ca II doubling occur between minimum and maximum luminosity (which coincides with maximum outward velocity). For classical cepheids, Balmer emission begins at luminosity-minimum. Ca II emission occurs only for periods ≥ 4 days; it begins just after luminosity minimum, and lasts longer, the longer the period. In the Miras, hydrogen Balmer, Paschen, Brackett emission lines occur from just before maximum until just before minimum. Presumably, all these imply persistence, in the atmosphere, of the effects of one oscillation into the epochs of another, and/or the presence of shock-waves, and certainly of some nonradiative heating. Visually-historically, one found a good representation of cepheid atmospheric structure by modeling it at each phase as being a normal supergiant photosphere with “effective” radiative flux and gravity fixed by the pulsation, as in the above Oke-Whitney summary. Also historically, there were few visual measures that were sufficiently sensitive to infer atmospheric extension and heating. After all, even nonpulsating supergiants are strongly anomalous, in many respects, relative to standard models. Examples are the widespread occurrence of emission lines, and the introduction

of large “turbulent” velocities in spectral diagnostics. In the last several decades, parallel to the strong advances in theoretical studies of the subatmospheric cause of pulsation, there have been increasingly detailed theoretical studies of the consequences of pulsation. Over the same epoch, spatial observations in the farUV have appeared. In consequence, we have a clearer picture of the impact of pulsation on atmospheric structure; that is, on the departure of such structure from what it would be if, indeed, the standing-wave photosphere were an adequate model. This clarity has come from the theoretical aspects as from the observational, although the theoretical modeling has been strongly guided by the mentioned presence of line-doubling and emission lines. The impact of farUV observations has not yet been as large and varied as for other stellar types, apparently because the photospheres of cepheids and Mira types are cool, hence, have low farUV luminosity. There is, however, a complication of presumed binarity in some of these stars for which there do exist prominent spectra in the farUV, to which we return below. So I abstract inferences on nonstandard atmospheric structure for three types of pulsating variables: cepheids and Miras, cool-stars, and an illustrative, farUV study of one β Cephei, hot-star.

Then these studies of atmospheric consequences of pulsation have focused on the piston model: a specification of luminosity and velocity at some specified atmospheric layer, as a function of time. Representative studies are those by Whitney of cepheids, particularly of W Virg-type (1955, 1956); Hill, of RR Lyrae-type (1972); Willson (1976), Willson and Hill (1979), and Wood (1978) of Mira-type. Whitney exhibited how the progression in type of velocity-curve from quasi-sinusoidal to discontinuous might be pictured in terms of the two parametric ratios: (pulsation-acceleration/gravity), (atmospheric-extent/pulsation-“wavelength”). The sequence of quasi-cepheids, RR Lyr, W Virg, RV Tauri exhibit increasing values of both these parameters; and increasing discontinuity of velocity-curve. The implication is that the more extended the atmosphere, relative to the acceleration of the wave, the greater the chance for shock-discontinuous velocities to develop, and phenomena from one pulsation-phase to persist into the following ones. All these models exhibit a steady increase in atmospheric extension, once the piston is “turned on,” and phases of shock heating. Particularly the Wood, and Willson-Hill, calculations exhibit how a mass-loss can be produced: mainly episodic; but also as a continuous flow, depending upon characteristics of atmosphere and piston, as the far-out material, trying to fall back, is continually reflected by the latest oscillation. Wood exhibits the dependence of mass-flow on assumed energy description of the material, ranging from adiabatic to isothermal. Willson and Hill suggest that the flow is isothermal in the low atmosphere, but adiabatic in the upper, reflecting the lower rate of radiative cooling by recombination.

From our present standpoint, the most essential aspect of their suggestions is their equivalence to saying that *the size of the mass-loss is ultimately fixed by a self-consistent formulation of whatever fixes the amplitude of pulsation-ejection in the lower outer-atmospheric regions*—both a statistically-steady flow, and an episodic enhancement—and that any subsequent acceleration affects the velocity, not size, of the mass-loss. We return to this point in Section F, of this chapter, and Part III of the monograph, relative to the general problem of what fixes the size of the mass-loss from a given star. Here, if the Wood and Willson-Hill physical picture is correct, we have a specific example of a subphotospheric mechanism that fixes the size of the mass-loss. The details of the acceleration of the atmosphere, as a function of height (radius) are determined by atmospheric factors, such as converting atmospheric thermal energy into expansion, and taking directly energy and momentum from the radiation field. As in all mass-flow problems, once the *differential flow velocity becomes near thermal, the energy balance is critical, between that accelerating the flow, that dissipated by the flow, and the coupling to the radiation field*. Clearly, as discussed in Chapter 2, a proper treatment of the radiation field resolves the energetic question of adiabatic vs. isothermal vs. intermediate flow. And, finally, the initial piston conditions must incorporate the mass-flow, which must be replenished from the subatmosphere. Nonetheless, these preliminary investigations provide a very promising link between the impulsive mass-input of the cataclysmic variables next summarized, and that from the sequence of less obviously subatmospheric controlled mass-flux from the sequence of stars continuing from cataclysmic, into symbiotic, into Be-similar, et seq. All the above models give relatively-low mass-flow: ≈ 10 km/s for the Mira-type; $\lesssim 50$ km/s for the W Virg. The T_e rises are also modest, lying below some 1×10^4 K. None of the models suggests the kind of T_e values which would produce the superionization (Si IV, C IV, N V), and velocities (up to ≈ 100 km/s), associated with main-sequence cool stars, some G and K giants, and some G supergiants as observed in the farUV.

Before commenting on farUV observations of such cool stars, which—like many other objects we will survey—are currently clouded by arguments as to the prevalence of binarity, it is useful to abstract IUE observations, and suggestions on model, of two β Cephei (hot) pulsating variables by Burger and de Jager (1980, 1981). These detailed observations, using Si IV and C IV lines, confirm inferences by Lesh and Karp (1977) on three other such stars, from less-detailed Copernicus material (using Si III lines), on the probable presence of significant mass-loss from such stars. In essence, Burger and de Jager find, observationally, superionized atmospheres, with velocity amplitudes and atmospheric distension in such lines (Si IV, C IV) much larger than in photospheric lines. Zero outward pulsation velocity, for both photospheric and superionized lines, occur simultaneously, essentially at luminosity maximum—greatest photospheric compression. Thereafter, the expansion persists longer in the superionized lines, even after the photospheric lines indicate the photosphere is compressing. They suggest, from the blue edge of the superionized lines, an ultimate outward velocity of some 500 km/s. Also, at the end of the contraction phase, the photospheric Si III lines become double: one component infalling, the other static for some time, then abruptly accelerating upward. They summarize the picture of this atmospheric oscillation as:

- a. a phase of photospheric rest;
- b. a sudden upward acceleration of, progressively, photosphere and upper, superionized, atmosphere;
- c. eventual descent of the whole atmosphere, *except* for that escape of matter corresponding to the 500 km/s component;
- d. this pulsation-induced mass-ejection is some $10^{-9} M_{\odot}/y$, and small compared with a value of some $10^{-7} M_{\odot}/y$, inferred from an empirical formula by Lamers (1981), involving only (mass, radius, luminosity).

We will survey mass-loss rates across the HR diagram in Section F; and we will see there that the strong variability in mass-loss rates from a given star, and the individuality between two stars of the same (M, R, L), preclude taking seriously Lamers' formula to predict any observed mass-flux for any given star. The simplest example is the Be stars, whose extended atmosphere arises from the mass-flux, and is highly variable. If Lamers were correct, all B stars should be Be, and there should exist no variability in the Be character. Indeed, there should exist no variability for any star, in mass-flux; but such variability is common. So the Burger and de Jager specific argument for the second component of mass-flux cannot be accepted until they have established it observationally, for those stars. However, there is considerable observational evidence for the *general* kind of suggestion they make: i.e., a quasi-steady mass-flow, perturbed by episodic enhanced mass-flow. Refer to the Section B.3.b discussion of Be stars, which are classically similar to the β Cephei. And, indeed, we note the Willson-Hill theoretical suggestion that pulsation, itself, can produce both a background steady-flow, corresponding to the cumulative effects of many pulsations, plus the episodic effect of the particular pulsation of that epoch. The striking importance of the Burger and de Jager result is that they have established, observationally, the connection to the pulsation of just such episodic enhancement of the mass-flow. Additionally, one has their suggestion that this "pulsation" has the characteristics (a)–(c), rather than a more standing-wave like, simple oscillation. Fig. 3-2 reproduces their schematic representation of the pulsation, not because it is obviously correct in detail, but because of the "kind of piston" behavior suggested by the observations. As we progress to the cataclysmic, then symbiotic, then Be-similar, then PN-type stars, we will see the evolution of such representations. Finally, I stress again that many of the "background" stars—i.e., those *apparently* not pulsationally-variable—of similar spectral-type but ranging in luminosity-type from supergiant through giant through main-sequence—present that superionized, ultravelocity, exophotospheric structure in the *direction* of which these pulsational effects push the atmosphere. A single phase apparently adds to, but does not provide the whole of, this exophotosphere. The similarity to the Willson-Hill proposed model and physical interpretation for cool pulsating variables is clear, but it does not, of course, prove that their proposal is either correct or unique—only highly interesting, and instructive, as the current level of understanding of the effect of a cumulative history of episodes on the atmosphere.

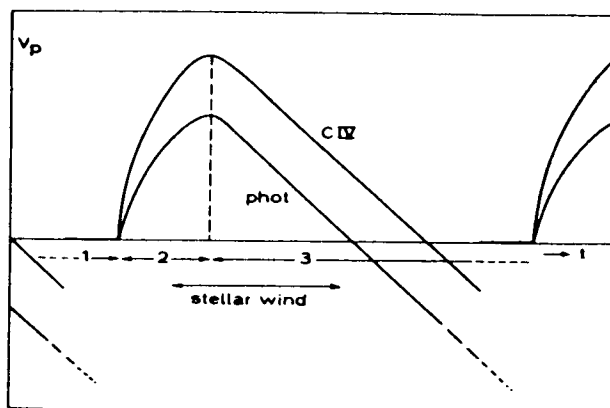


Fig. 3-2. Schematic representation of the pulsational cycle of BW Vul (from Burger and de Jager, 1980).

Now we turn to the farUV material on the cooler pulsating stars. As for the hot stars, our focus lies on what perturbation on the classical model of a standing-wave photosphere the actual pulsation makes, as exhibited by any atmospheric heating and differential atmospheric distension. Also as for the hot stars, given the observed existence of heating and extended atmospheres among nonpulsating cool stars, we ask what effects, different from these, cool pulsating variables show in the farUV. And, in terms of theoretical modeling, we ask the evidence for cumulative-episodic, as well as individual-episode, effects, and how to tie them to theoretical representations. Then the situation is observationally complicated by several things, which we try to make very clear here, because we will continuously return to them in following sections on other peculiarities and anomalies. (1) Because cepheids and Miras are cooler, their short-wavelength farUV spectrum is weak. (2) There are apparently at least two distinct types of such farUV spectra of cepheids, especially at luminosity minimum—one with a “blue-star component,” one without—which some astronomers interpret as indicating, respectively, the presence and absence of a companion, probably a B star. (3) Some astronomers propose that there is a relatively-abrupt change in exophotospheric structure between that kind of cool star including the main-sequence and yellow giant, which have chromospheres-coronae and have small mass-loss, and that kind of star including red giants plus supergiants, whose exophotospheric T_e do not exceed some $1-2 \times 10^4$ K, but which show large mass-loss. The presumed dividing line is set at about KO III. (4) In the process of arguing for this last distinction, some astronomers *define chromospheres* as only those atmospheric regions lying within the solar-chromospheric range of $T_e \lesssim 1-2 \times 10^4$ K, with *transition-regions* being those covering the super-ionized range found in the IUE limits of N V, C IV, Si IV. Coronal regions are called those which either show solar-coronal ions, and/or X-rays, since such coronal ions lie outside the IUE range. I find such definitions semantical rather than physical, since they a priori exclude hot stars, with photospheric $T_e > 1-2 \times 10^4$ K, from having chromosphere. They are also misleading, because they inspire such nonsense-statements as “it also appears that chromospheres do not exist in supergiants earlier than late F,” when discussing the controversial point (3) above. We return to a systematic, physical-operational definition of atmospheric regions in Chapter 4, valid throughout the HR diagram; here, we only try to put into focus the farUV spectra of cepheids, relative to their nonpulsating neighbors.

Then three papers are particularly useful to place the farUV cepheid spectra in focus, at the time of this writing: Parsons (1980), Schmidt and Parsons (1982), and Eichendorf, et al. (1982). The first two are based on low-dispersion observations; the latter has a few high-dispersion observations. Then there are three essential points; but for each, one must recognize the phenomenon stressed in this chapter’s Introduction—strong individuality among stars. Then: (i) Mg II emission occurs over many more phases than the Ca II, especially in longer period stars. This accords with the generally stronger Mg emission than Ca, in nonpulsating stars, presumably reflecting the greater Mg abundance, hence, occurrence higher in the increasingly-outward-heated atmosphere. (ii) Emission lines are generally strongest after minimum, en route to maximum. Granted the scantiness of material, one should note the strong

Finally, from these farUV, cepheid, data obtained thus far, it is interesting that pulsation appears to diminish, rather than intensify, the steady existence of *some* “hot” regions. That is, apparently, *all* stars “similar” to cepheid, pulsating or not, have a nonradiative heating mechanism. But, in addition, pulsation introduces also a cooling mechanism, operative in some lower parts of the atmosphere, and only in some phases, beginning after maximum luminosity, and extending to near minimum. Such phases are those of outward expansion, before the photosphere begins to contract, and before any regions just above it fall back.

Before combining this picture with the above from β Cephei, we comment on the few available Mira farUV observations; e.g., Casetella et al. (1980a, 1980b) and the Quercis (1979, 1982). The single star, χ Cyg, shows emission Fe II near maximum luminosity (phase 0.04), but, only absorption Mg II. At phases 0.18 and 0.22, Mg II is in emission. The authors suggest shock heating of the low photosphere gives emission Fe II at phase 0.04, while a cold envelope gives absorption Mg II. When the shock reaches the higher layers, emission Mg II appears. They invoke the Willson-Hill model. In the first paper, on Mirá Ceti itself, a blue farUV contribution is attributed to a white-dwarf companion which, by contrast to the cepheid companion, produces an emission-line spectrum. All these emission lines, N V, C IV, through Mg II are assigned to an accretion disk surrounding the companion.

Summarizing, we can ask whether, empirically-theoretically from the above examples, we can distinguish some common atmospheric behavior associated with such pulsation, for hot and cold stars alike. As continuously emphasized, any nonthermal velocity fields can produce, to some degree, nonradiative heating, atmospheric distension, and a nonthermal mass-loss. Ubiquitously, we observe all three phenomena, to some degree, in all types of stars across the HR diagram; but we have very incomplete understanding of their causes. We survey such general characteristics in Sections D–F. Here, we ask pulsational contributions to them. We note that there is as yet no basis for an a priori assumption that a pulsating star simply superposes its episodic, or cumulative, effect on a general nonthermal level of the above three phenomena, which may or may not characterize nonpulsating stars of the same classical spectral type. The situation is still unclear, and remains for study. Then we note the following pulsational-characteristics. (PC-1) Just as the increase in luminosity is associated primarily with a rise in photospheric T_e rather than increase in surface area, so the presence of emission lines, *in this case, apparently* corresponds to a nonradiative heating rather than being an extended-atmosphere effect. For example, H α emission occurs just before maximum luminosity in all Mira stars, and varies from star to star only in the fraction of time near minimum luminosity—maximum atmospheric extent—that it is absent. Superionized lines are in emission in the cool stars, in absorption in the β Cephei. Thus, in contrast, e.g., to the Be stars of Section B, *observable* pulsational-variability effects arise relatively near the star. (PC-2) The longer the period, the greater the fraction of the cycle over which such nonradiative-heating effects as Ca II and Mg II emission are observed, in the cool pulsating stars. The superionized C IV and N V are observed throughout the cycle, in the hot, short-period β Cephei. All these suggest a background nonradiative heating which individual pulses perturb. (PC-3) There is a variety of evidence for superposition of longer period cycles of non-thermal effects, of some variety, on the general pulsation (β Cephei, some 6 days, Lesh, 1981; RR Lyr, some 40 days, Preston et al., 1965). (PC-4) In a rough way, the data suggest that the pulsation can result—near and following minimum-luminosity = maximum photospheric distension—in a division of the atmosphere, at some phases. The photosphere and low chromosphere descend. Expansion in these outer-atmospheric regions, where expansion velocity has reached escape values, continue, unaffected. Those atmospheric regions which have superthermal, or thermal, velocities have a motion determined by whatever is the accelerating mechanism plus the effect of the rarification wave propagating upward from the photospheric descent. One “loses” an intermediate atmospheric region, until the next cycle.

Then the problems arising in a broad application of some wholly-pulsational model, such as the Willson-Hill type, to explain all the nonthermal phenomena, and exophotospheric structure, in stars which exhibit pulsational variability of the above types, appear to be three: (i) How does one maintain the superthermic, superescape velocity region of the atmosphere, whose existence is necessary to provide a continuous mass-loss? One either needs pulsations of sufficiently-short period that the atmospheric “void” in (PC-4) above does not develop, or one needs an additional steady flow which retains a net outward velocity in all phases of the photospheric pulsation, or one finds only episodic mass-loss. The last does not appear to be the case, but observations are far from sufficiently-complete

to be definitive. One should compare the variation in dM/dt in Burgers et al., with the uncertainty in its derivation; but the variation in line-profiles from which it was derived, and the similar variations in Lesh's work, can hardly be ignored. Refer, also, to following sections in this chapter, for the same kind of variations. (ii) How does one maintain the range of nonradiative heating demanded by Ca II, Mg II in the cool, and N V, C IV in the hot, stars (also, how to resolve the C IV problem in the cool stars, for those showing C IV emission and those showing absorption). (iii) How does one produce the general nonradiative heating, atmospheric extension, and mass-loss in nonpulsating neighbors of the pulsating stars. In Section B, we will see that the problem is aggravated, between B—including β Cephei types—and Be stars, where the differential atmospheric extension is *apparently* much greater, while the differential heating is apparently minor.

The basic question in pulsation is simple. If we could produce all these phenomena of heating, atmospheric extension, mass-loss by only a Willson-Hill type model, then we would have shown that for these pulsating-variable stars, we need only consider thermal models of the interior. Pulsation is simply an instability on such models. Then so long as the mass-loss, and associated energy loss to the mass-loss and enhanced radiative-energy loss from the non-radiative energy-flux not transporting mass are sufficiently small, we would need no basic change in modeling. All this remains to be explored.

ii. Cataclysmic Variability. This type—terminology introduced by the Gaposchkins—was, at the 1938 epoch, characterized by its prototype, the nova, which in turn had the historic pictorial caricature—“star swells up and bursts.” Caricature: because while a first-order approximation for the novae—contrasted to the pulsating-variables—is indeed a large increase in photospheric surface-area and lesser surface-temperature effect, they share the outstanding characteristic of nearly all stellar variability; the star returns, effectively unchanged, to an earlier “quiet” configuration. In simply comparing observed luminosity change, not interpreting it, I already stressed that pulsation shows a precursor of change: cataclysmic change does not: in the extreme, it is defined as unpredictable and abrupt change in luminosity. Such abruptness is not restricted to a one-time classical-nova size of change, which is some 9–17 visual magnitudes. The historic dwarf-novae, the SS Cyg type, rest at minimum luminosity for intervals, depending on the star, of 20–150 days, abruptly rise by 2–5 visual magnitudes, rest a few days, descend, less abruptly— but all unpredictably, except statistically, for a given star.

As for the pulsating variables, we try to put three things into perspective, relative to atmospheric structure—photospheric and exophotospheric. One is the classical variety of such cataclysmic types, based on luminosity variation. A second is the “kinematic” relation of this to photospheric and atmospheric structure. A third is the implication on nonthermal properties: nonradiative heating, atmospheric extension, mass-flux. The major evolution in our empirical picture, as for the pulsating-variables, comes from the farUV observations showing that the mass-flow which produces the atmospheric extension is not confined to those epochs of “outbursts,” which produce the abrupt and unpredictable luminosity increases accompanying a photospheric “swelling.” Rather, there is a steady background of very high-velocity mass-flow—a steady, not just episodic, mass-flux. Again, I stress that this theme will follow us throughout these discussions of stellar peculiarity. The details, for different stellar types and individual stars, of the particular combination of steady mass-flow, broken by episodes of changing mass-flow, give the basic material for atmospheric modeling. The observational fact that atmospheric structure depends so heavily on these details of variability and individuality weighs heavily against putting much confidence in theories of mass-flux which a priori exclude them.

A final overall remark, again in parallel to one aspect of the pulsating variables, is on the competition between binarity and multi-region atmosphere, to represent observations, in both of which there has been a strong evolution from 1938 to the present. In 1950, Schatzman proposed that the nova outburst was thermonuclear in origin. Kraft (1952, 1953) identified several dwarf novae, then several classical novae, as members of binary systems. That identification was taken to imply that the nova outburst originates in the binary character, via a mass-transfer. So, the several cataclysmic—and more recently even the symbiotic—stars are often hypothesized to represent the result of such mass-transfer, from a late-type component to an earlier, degenerate or at least evolved, component, possibly with an accretion disk enveloping the latter. For a few magnitude outburst, the liberation of the gravitational energy

of transferred matter is said to suffice. For stronger outburst, Schatzman's suggestion is incorporated in the form of the mass-transfer resulting in a near-surface nuclear reaction, which blows off the nova, or nova-like, ejected shell. A very considerable amount of radiative energy is liberated at the same time. Payne-Gaposchkin (1977) summarizes the model as a low-luminosity red star, a low-luminosity hot star, surrounded by an accretion disk, which has a hot spot where the transferred material arrives.

In several versions of these binary mass-interchange models, the observed mass-flux from the systems comes from the accretion disk. This ejected mass from the system is supposed to be orders of magnitude smaller in size than that ejected from the cooler, later-spectral-type component onto the hotter, earlier-spectral-type, late-evolutionary-stage, even degenerate, other component—possibly via an accretion disk around this second component. Thus, the mass-flow from the system as a whole, which produces the *observed* part of the cataclysmic event, has no direct relation to the atmospheric structure of either of the two component stars, in those versions where it flows out from the accretion disk. So this binary plus accretion-disk model is basically and fundamentally different from our model of the cataclysmic mass-flow as simply being one kind of photosphere of a single star, that of “cataclysmic” stars, which spatially evolves into one variety of pattern of extended atmospheric structure. According to the approach adopted in this monograph, the basic difference between Sun, WR, Be, novae, etc. atmospheres lies in the thermodynamics of subatmospheric structure, which fixes the several nonthermal fluxes, which—with gravity—fix the atmospheric structure. But this is a working hypothesis only, based on the accumulated evidence of more than a hundred years of atmospheric observations, which we try to synthesize, tentatively, in a unified way, in this monograph—to ask, empirically-theoretically, what are actually the various patterns of atmospheric structure. If, on the contrary, cataclysmic variability corresponds to the “atmosphere” of an accreting disk, one should equally be able to demonstrate it, observationally. The regrettable aspect of current binary mass-transfer theories of the origin of cataclysmic stars, and their discussion of observations, lies in their considering these as the only possible models (cf Gallagher and Starrfield, 1976, 1978; Robinson, 1976 for summaries). They give little attention to the historical and contemporary evolution of extended atmospheric structure for single stars. In the following, I try to make a comparison between the two alternatives, whenever possible, because it is not only in discussing cataclysmic variables that binarity is offered as a panacea for “stellar peculiarity” of one form or another. One is too habituated to “standard” atmospheric structure.

Then, to put such comparisons into perspective, we note five things which give the strength and weakness of the current, popular focus on binarity to interpret cataclysmic and symbiotic stars and phenomena. First, there was Kraft's identification of *some* novae, among the several varieties of novae, as binary. Second, there is the progressive phenomenological elucidation of the original combination of (hot, cold) standard-star photospheres required to interpret symbiotic stars. FarUV observations of symbiotic stars themselves provide one example; the solar photosphere-chromosphere-corona is another; so is the Be-star combination of slow-moving, cool H α envelope and hot, underlying O VI–N V–C IV ultravelocity region. Third, there are the conflicting observations of the quiet minimum state of various kinds of novae: most often, a hot blue dwarf for ordinary novae; but usually an M-type star for recurrent novae. Fourth, there is the theoretical speculation—today, almost dignified as gospel—that the only way to produce “eruptive” phenomena of the observed energy level is by mass-transfer to an evolved, degenerate, blue component of a binary. Such mass-transfer produces the nuclear instability hypothesized by Schatzman. Prior to the spatial observations of the last decade, one required a close binary: one star as the mass-source, because it filled its Roche lobe; the other star as a potential nuclear-unstable environment. But, fifth, today, with observations of essentially ubiquitous mass-loss from even single stars, these requirements seem to be evolving: I quote three passages from Gallagher and Starrfield (1978): “. . . It is now commonly accepted that the nova outburst occurs on one component of a close binary system—the star is a compact object, most likely a white dwarf . . .” “. . . The basis for the usual assumption that the compact components in novae are white-dwarfs is derived from model-fitting to the observed pulsational characteristics—such pulsations are, with the possible exception of DQ Herc, not seen in classical novae . . .” “. . . This does not imply that all novae must be close binaries—thus there is no necessity to invoke a mass-exchange binary—for single stars, accretion from the interstellar medium might suffice to produce a thermonuclear runaway, and novae from isolated white dwarfs must be considered theoretically feasible, if rare.” So, I

trust the reader will regard the binary mass-exchange model as a speculation to be investigated, not as a fact to be simply applied. And try to regard, globally, the coherence of cataclysmic variability within the varieties of stellar variability.

In the 1977 article cited above, Payne-Gaposchkin describes the strong impact of nova Pers 1901. Prior to it, one had only observed the emission-line spectrum of the late stages of the nova outburst. Nova Pers, plus its successors, exhibited the sequence of spectra displayed by a nova outburst during its evolution. Table 3-1 summarizes McLaughlin's (1960) compilation of this sequence of spectral phases, supplemented from Payne-Gaposchkin, as seen in the visual. The components of each spectral phase are identified by a common radial velocity. Different spectra may coexist. It is small wonder that Z And, now considered to be the prototype symbiotic star, was originally classified as a nova. Its classification was changed largely because the amplitude of its outburst was only some 5 magnitudes, contrasted to the 9-17 magnitude range for more typical novae. The Gaposchkins' 1938 description of Z And was: a late-type star; an emission-line, early-type star; and a nebula—each exhibited at some nova phase. So, among all stars, I focus on a variety of photospheres, then the variety of exophotospheric regions, and patterns of these regions. Even though many of them were clear from visual spectra alone—including 1901 nov Pers, Z And, the WR stars, the Be stars, and the Sun—the farUV has added many more details. And, these must be applied to both components of any presumed binary. It is interesting to note that SS Cyg was, in 1938, classified as a Bn star—a B star with very broad absorption lines—at maximum luminosity, and broad emission lines at minimum luminosity = Be.

We now proceed to consider the variety of cataclysmic-variable stars and their defining characteristics. The first such characteristic is the *sign* of the change from the "habitual" stage of the star—i.e., where it spends most of its time. There are a very few stars where the abrupt change is a luminosity decrease: e.g., 3-6 magnitudes for the R Cor Bor stars, of late type, showing strong carbon bands, whose accompanying feature at minimum luminosity is the appearance of ionized lines up through He II. Most cataclysmic stars, on which we focus, show luminosity increases. The prototype of such stars were the novae, classified into various kinds according to amplitude of luminosity increase, and recurrence time. As in the pulsating stars, the longer the recurrence time, the greater the amplitude; but unlike them, the bolometric magnitude, not just visual magnitude, appears to show this correlation. "Appears," because farUV, IR, etc. nonvisual observations are quite new—the last 15 years—relative to the frequency of occurrence of ordinary novae. Fig. 3-4 shows a current light-curve of Nova Cyg 1978, in the visual, farUV, and IR; but the great predominance of accumulated data are still only visual. Various kinds of novae, following the Gaposchkins, with estimates of the energy liberated during one outburst taken from Robinson (1976), are listed in Table 3-2.

In any classification like this, one raises the question of the symbiotic stars, which we treat in Section C as a prototype peculiarity. Some astronomers, focusing on binary mass-transfer origins for the cataclysmic stars, include the symbiotic stars with the slow (recurrent) novae (cf Allen, 1980). In 1938, as mentioned, the Gaposchkins emphatically disavowed Z And as an ordinary nova, but avowed it as being binary, with a distinct third component, a nebula. In their 1978 summary, the Z And class included T Cor Bor, now identified by most as a recurrent nova. I emphasize the problem here, as well as in Section C, as a strong piece of evidence on the general problem of multi-atmospheric regions vs. binarity. In that respect, discussing the novae variation in luminosity without including that spectral sequence of changes brought into strong focus by Nova Pers is myopic; so Table 3-2's abstract of the combined summaries by McLaughlin and the Gaposchkins complements both Fig. 3-4 and Fig. 3-5, on luminosity, which is put into perspective below.

Then in terms of orientation on thermal vs. nonthermal aspects of the cataclysmic-type variability, a primary question is the meaning of the "energy" column in the above Table 3-2. The kinetic energy contained in the ejected shell is reliable to the accuracy of the estimate of mass in the shell, because one can measure spectral line-displacement to obtain velocity, *if* one assumes a one-time ejection of the shell. Otherwise, one measures a mass-loss rate, and a model of the whole "atmospheric" region is essential, to associate a local density to a local velocity as a function of time. Essentially, mass estimates result from converting total H α emission into mass of emitting gas (cf Potasch, 1959a, b, c, d). One can also estimate the thermal energy content of the shell, from the assumed initial conditions prior to ejection. So there remains the energy radiated, its spectral distribution, and its source, as a function of time. The historical situation in the literature of nova luminosity, and its meaning, is confused. A fundamental

Table 3-1
Sequence of Spectra During Nova Outburst

SPECTRAL-PHASE LEVEL	CHARACTER	EXCITATION-LEVEL	VELOCITY
Preoutburst	Few observed: B-A continuum; indistinguishable lines.	B-A star	No lines
Premaximum spectrum	Mainly B-A; some F; absorption spectrum. During rise to maximum, lines become stronger and spectral type cools; type at maximum ranges A0 to late F; few K. α Cyg, sg, type spectrum at maximum. Only H α remains in emission at max.	Na I through He I	Ranges -200 to -2000 km/s absorption-line displacements
Principal spectrum	Considered to be the typical nova spectrum of broad emission-lines with absorption edges on blue wings. Appears just after maximum. Sometimes multiple lines, showing same accelerations. Color temperature increases after maximum, sometimes doubling, to reach B-type, again.	Na I through He I. Initially, H I, Ca II, Na I, Fe II strongest. About 3 mag. below max, [O I], [N II], and He I appear; eventually He II, N III, [N III], [O III] appear at end of this phase.	Larger than premax. They accelerate in time, from 1.1 to 2 in ratio initial: final.
Diffuse-enhanced spectrum	Overlapping principal spectrum, at about twice velocity, so distinct. Broad emission lines with absorption edges on blue wings. The lines sometimes are resolved into several components, which disappear and re-appear, whose displacements can vary rapidly. Novae brightness fluctuations are accompanied by line fluctuations. Mg II disappears first in this spectrum.	Na I through singly-ionized metals.	Twice velocity of principal spectrum.
Orion spectrum	Single absorption lines of He I, N II, O II, sometimes H I begin to appear when diffuse enhanced spectrum is at maximum strength, at similar or larger velocity. Chief character is a broadband at $\lambda 4640$, assigned to N II + O II, then N III, then N V, successively in time. This marks the transition stage: spectrum changes from stellar to nebular.	He I and ionized metals, many forbidden lines; N II to N V.	Similar to diffused-enhanced stage, but can be quite larger.
Nebular stage	In fully-developed nebular stage, nova and PN spectra are very similar. As nova fades, successive stages produce higher excitation, and more forbidden lines. (Fe X) red line present in some novae. (Fe XIV) green line present in several recurrent novae and a few novae.	Two distinct characters: (i) Radiative-excited spectrum of very-hot star; (ii) Solar-coronal lines requiring 10^6 K and very low density.	Ambiguous
Postnova spectrum	Novae show hot star continua; some without lines; some with narrow H I and He II, C III. Recurrent novae show coronal lines persisting until essentially the next outburst stage; some look like Be stars at minimum; some show M-type spectra; many resemble symbiotic stars at minimum.		-200 to -2000 km/s.
FarUV addenda	Read the text, Chapter 3. Apparently a continuous outflow of o (1000 km/s) persists.	FarUV superionized lines; the forbidden coronal lines in visual supplement these.	o (10^3 km/s) continuous outflow and episodic ejections.

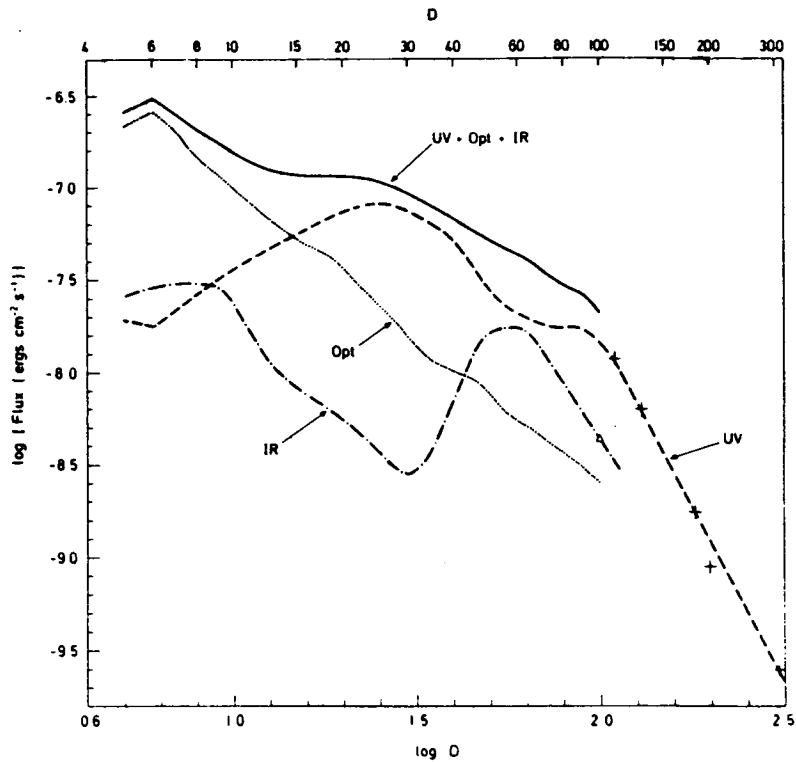


Fig. 3-4. The variation of the farUV, optical and IR fluxes for Nova Cygni 1978, and total observed flux as a function of time (from Stickland et al., 1980).

Table 3-2
Characteristics of Varieties of Novae

Class	Amplitude (visual mag)	Recurrence	Energy (ergs)
Classical novae	9-17	10^6 y; never ?	10^{44} - 10^{45} ?
Recurrent novae	7-9	10-100y	10^{43} - 10^{44}
Dwarf-novae types:			
SS Cyg (Z Cam)	2-5	10-50d	10^{38} - 10^{39}
U Gem	2-6	15-500d	10^{38} - 10^{39}

y = year; d = day

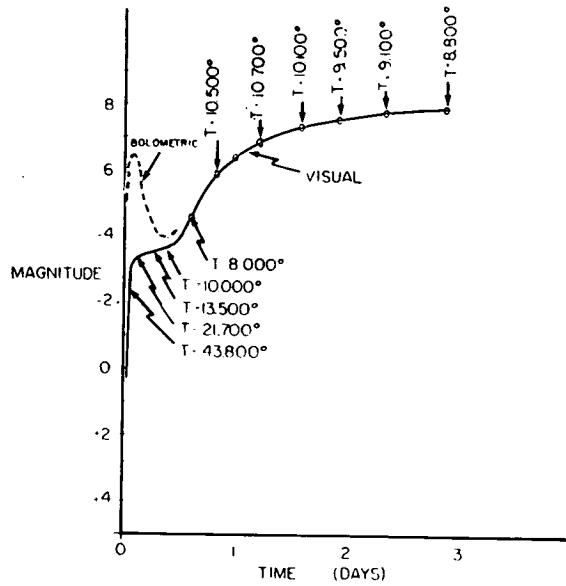


Fig. 3-5. "Light Curve" of the expanding shell. The energy emitted by the shell as visible radiation is plotted as visual magnitude, while the total energy emitted is plotted as the bolometric magnitude. The surface temperature is shown at each stage (from Pottasch, 1959).

observational paper, always quoted, is Arp (1956), summarizing a study of 30 novae in M31, thus with no correction necessary for relative distance. The data are wholly visual, so their bolometric value must be inferred. His energy measures are always cited as establishing various relations, especially the conclusion that slowly-declining novae radiate more total energy than rapidly declining novae. The only energies given by Arp are those in his table I, which represent the area under the visual light-curve, expressed in luminosity.

Gallegher and Starrfield (1976, 1978) use Arp's empirical relations, plus early farUV, and IR, data on Nova FH Ser; plus their theoretical time-behavior of the energy produced by binary mass-transfer (constant nonthermal energy output for 100 years or longer) to argue against the bolometric energy dropping off as rapidly as the observed visual. They suggest the data imply constant total radiative energy output, hence energy input by their mechanism, over at least 100 days following the outburst. Here, we note only that the observed luminosity is supposed to measure a major, even predominant, part of the energy produced by this mass-transfer. Under this theory, a mass-ejection from the system is not always a consequence of such mass-transfer within the system. For example, a 1974 version (Starrfield, Sparks, Truran) of the theory identifies the normal dwarf-nova as a system without such ejected mass. However, current farUV observations of dwarf novae show high-speed ejection to be normal, even sometimes at speeds as high as 4800 km/s (e.g., Cordova and Mason, 1982). The theoretical model also argues that the lower the initial luminosity of the white-dwarf component of the binary, the better the chance for a normal nova outburst to occur. However, the authors of the observational paper suggest the contrary, that mass-loss is preferentially observed in systems with relatively high luminosity.

To try to put these basic observational features of novae, and the suggestions on their origin, into focus, we proceed as we did for the pulsating variables. We abstract, by a simple model, the essential physics of the classically-succinct description of the nova phenomenon: "star swells up and burst," but interpreting "swells" and "bursts" less literally. To first approximation, in terms of a blackbody temperature and surface-area, the star "swells" by ejecting an opaque shell, whose surface temperature decreases with increasing surface area. The nova *apparently* "flares" because surface area times visual radiative emissivity increases rapidly. The area increases rapidly, the nova "erupts," from an imposed nonthermal kinetic energy. To second approximation, the system is not a blackbody, but linearly

nonEquilibrium: a central star continues to replenish the visual thermal energy radiated by the shell, by nonvisual thermal radiative energy input to the shell. The nonthermal mass-transfer expansion combines with a thermal radiative transfer within the shell, and radiative cooling at its top, to fix both surface temperature and opacity of the shell: the star “bursts” when the opacity of the shell-photosphere drops below 1. So long as the shell neither expands differentially, nor interacts with its environment, all energy coupling to the spectrum is radiative; so the model gives the spectral evolution of this time-dependent photosphere. It is the equivalent of the “instantaneous supergiant photosphere” representation of pulsation, but with much more rapid expansion; and the original star is dwarf rather than supergiant, hot rather than cool.

This linear nonEquilibrium picture is illustrated by a classic model devised by Pottasch (1958, 1959). The model-configuration is a hot, dwarf or subdwarf, central star, $T_{\text{eff}} \sim 200,000$ K and $R \sim 0.3$ solar, with an ejected shell containing 10^{29} gm of matter and expanding at a constant velocity of 800 km/s. The total radiative input from the central star remains constant. The model, shown in Fig. 3-5, reproduces the essential features of McLaughlin’s 1943 schematic light-curve of a nova, shown in Fig. 3-6, even the “pre-maximum halt,” and the post-nova configuration of a compact, hot, blue object that is so often quoted. By allowing the shell to collide with the ISM, and be decelerated to some 30 km/s, Pottasch can produce the PN-similar phase. And, by construction, the nonthermal kinetic energy of the shell is 3×10^{44} ergs; the bolometric energy radiated during the 3 days before the shell becomes optically thin is 1×10^{44} ergs; and the thermal energy of the gas, if it totally recombines and drops to the indicated 10,000 K, is some 3×10^{42} ergs. So the total energy produced in the first 3 days of the outburst is some 4×10^{44} ergs, of which three-fourths lies in the kinetic energy of the shell. During the “eruption” phase, one observes the energy radiated from the central star’s very small surface at 200,000 K— λ (max) at about 150Å—converted into radiation from the very large surface at some 10,000 K, λ (max) about 3000Å.

Under this simple, ad hoc, representation, the function of the ejected shell is simply to transform invisible (to present detectors) radiant energy into visible. I now caricature it to be a thin, fluorescing screen, ignoring radiation-transfer time-lags. To the accuracy of the modified blackbody approximation, T^4 of the shell decreases as r^{-2} . Introducing the nonzero mass-thickness of the shell, simply introduces a thermal capacity, allows the possibility of a thermal phase-lag, and permits a lower limit to the decrease in T by making the shell ultimately transparent. The changing luminosity—the nova light curve—has nothing to do with any nonthermal radiative energy supplement to the thermal radiation of the original star, nor requires any energy generated by mass-interchange within the binary. The nonthermal, or other, energy production is *only* that to eject the shell. If there is no ejected shell, there is no “fluorescing screen” conversion of energy, and one sees no “sudden rise” in radiation. “Sudden,” because one realizes that at these velocities, the photosphere doubles its effective radius in the first 250 sec, and raises λ (max) to

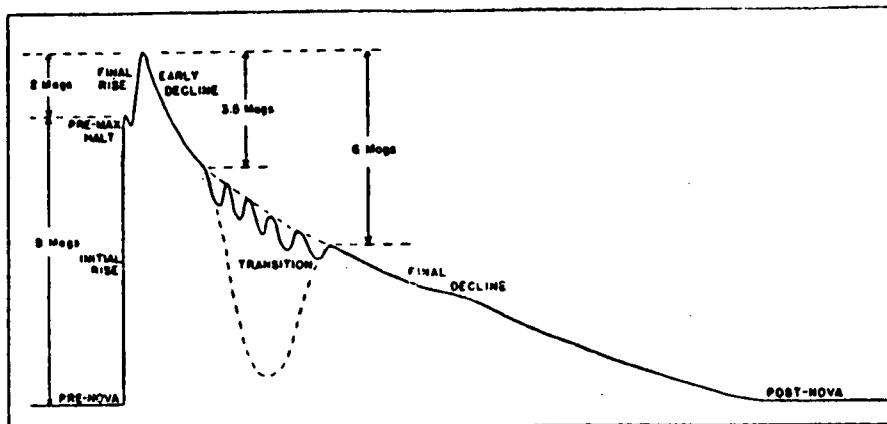


Fig. 3-6. Schematic light curve of a nova. The time is not uniform; it has been greatly magnified in the early stages (from McLaughlin, 1943).

200Å; in 4 hours, the area of the effective photosphere has increased by a factor 3000, and λ (max) to 1100Å, just inside the IUE observing range. Under Pottasch's particular choice of parameters, the shell becomes visually transparent after about 3 days: $T_{\text{eff}} \sim 8\text{--}9000$ K; $r/r_0 \sim 500\text{--}1000$; λ (max) $\sim 3200\text{--}3600$ Å, just short of the Balmer limit; total energy radiated to that date, $\sim 1 \times 10^{44}$ ergs. A more massive shell would permit greater expansion, and surface cooling, so produce relatively more energy in the visual, a larger peak intensity, and a greater duration, including the post-maximum drop. These are the above-remarked correlations from Arp's visual data. Note that the drop, after $\tau(\text{vis}) \sim 1$, is much slower than the rise, simply because one needs to double the r/r_0 of 500–1000 to decrease density by only a factor of 4, which takes 2-3 days. Also, of course, both farUV and IR opacities are larger than the visual, so one has the observed direction of the phase-lags in Fig. 3-4, for epochs of peak luminosity in these wavelength regions.

So, like the standard, single-star, model of pulsational-variability, Pottasch's single-star nova model represents cataclysmic variability as being, in origin, primarily a motion of the photosphere as a whole. The two models differ, kinematically, in the kinetic energy put into such photospheric motion. To first approximation, pulsational variability produces no mass-loss; the same photospheric material rises and falls. If differential motions, and velocity gradients, can be kept sufficiently-small, there is no nonradiative energy dissipation, hence, no change, over a cycle, of energy output from the star. One requires neither increase in nuclear energy production, nor additional energy source. To this first approximation, it is a closed-system thermodynamic model. However, even to first approximation, the nova-cataclysmic model produces a mass-loss; the whole of the moving photosphere is ejected from the star. No matter the size of differential velocity gradients, there is this additional (kinetic) energy output from the star, which must have some source. There is always the possibility of a gradual accumulation of energy, in some storage-reservoir, until the storage valve opens—so abrupt ejection does not necessarily imply abrupt production of the momentum/energy for ejection. But no matter the details, to first approximation the cataclysmic phenomenon stamps the star as an open thermodynamic system. When one asked complete thermodynamic consistency of the pulsation-model, we saw that it, too, produced a mass-loss, and additional energy loss; kinetic energy, to the mass-loss; nonradiative energy, to the rise in T_e and emission-line production. The difference between pulsational variability and cataclysmic becomes one of degree, rather than remaining a basic thermodynamic difference, as in the first approximation.

Even our superficial survey of variety of pulsational variability demonstrated a variety, across the HR diagram, in all the observable characteristics of a pulsating star: in the farUV as well as in the visual. But even more, it exhibited an even stronger departure from the imposed first-approximation character of closed thermodynamic system—there is a quasi-steady mass-loss, and nonradiative-energy dissipation, in addition to that accompanying the pulsation. Variable stars apparently share the *existence* of this last, quasi-steady, flow with other, nonvariable, neighbors in the HR plane. But, on the basis of existing data, we do not have a good idea on the relative sizes of these quasi-steady flows—and theory is presently incomplete.

So we ask insight into precisely the above questions, for the range of cataclysmic stars: What varieties of such objects are there? Is their ejection only episodic? But we note that “similarity” extends beyond the simple list of varieties of novae in Table 3-1. There are also such objects as the central stars of planetary-nebulae. As already noted, there is continued confusion in the literature, in low-dispersion classification, whether a star is a planetary-nebula or an old nova. The “nebular spectrum” is the outstanding feature of both. They are distinguished, in the visual spectrum, by the difference in velocity. Both are associated with a hot, dwarf or subdwarf, central star. In Pottasch's nova model, the small size, and hot character, of the central star are crucial—the combination is the only alternative not requiring a major increase in the star's radiative output during the outburst. The planetary-nebular central star characteristics are similarly inferred from “fluorescent-sensing” of “atmospheric” regions far from the exciting source. And, for the PN as for the novae, these “sensing atmospheric regions” reflect ejection of a shell. The historic classical picture of a PN differs, in considering ejection at some 30–50 km/s, the velocities of the nebula itself observed in the visual spectrum; and one has never observed the “birth” of a PN as one does for the nova shell, for which visual-spectral velocities are $o(10^3 \text{ km/s})$. But one notes recent PN investigations in the farUV (Benvenuti and Perinotto, 1980; Feibelman, 1981, 1982), which show the region between star and nebula to be filled with material moving at $o(10^3 \text{ km/s})$. Clearly, the PN nebula marks the locus of material which has been decelerated, by a factor of 10, and cooled. We remark, below, that current farUV spectra of old novae show velocities of $o(1000 \text{ km/s})$.

One also notes objects identified as “possibly proto-PN” where these same large, $\sim 10^3$ km/s, velocities are observed, e.g., V1016Cyg, HM Sge, HBV 475 (Feibelman, 1982). The interesting thing is that these objects were all originally observed as faint *reddish* stars, and the “eruption” was but several visual magnitudes. In the succeeding decade of observations, they have shown increasing ionization-excitation levels; they show IR and radio bursts; their spectra resemble symbiotic stars as well as PN. Such data put into focus the similarity and contrast between ordinary, presumed-one-time-event, novae and the recurrent ones. Both of these show “cool” stages, late in development: strong IR and radio excesses, TiO bands, *sometimes* dust silicate signatures. The “quiet” stage of recurrent novae and symbiotic stars is “statistically” a late-type star, by contrast to the hot subdwarf usually identified with postnovae. If one models all these as binaries, with a hot and a cold component, one asks why the direction of “favoritism” in the quiet phase: possibly the ordinary novae have dwarf red stars, the other, giant. The same problem arises in the multi-region atmosphere, as we see in Part III: the chromospheric-coronal regions being enhanced for the novae, as for the WR stars; the cool, decelerated outer regions being enhanced for the quiet-phase recurrent-novae, symbiotic—and similar stars, such as the Be. We reconsider this all in various succeeding sections of this chapter. Here we simply stress the great similarity, in many apparently different types of phenomena and stars, when one considers phenomena involving mass-ejection.

Clearly, one can—and must—modify Pottasch’s simple, first-approximation model, to represent all these additional features, just as one must enlarge the Willson-Hill model of pulsation. It is clear that the first direction of modification, for the classical nova, is to admit at least several ejected shells: of the several sets of spectra associated with the premaximal, and immediate postmaximal, spectra of the novae. If one admits widely different levels of mass-ejection, observations to date suggest that it is likely these several shells simply correspond to strong, transient, increases in ejected mass against a general background of a steady mass-flux—over a wide range of time-intervals and background levels. It is here that the distinction between “cataclysmic” variability, and those other aspects of variability found throughout the HR diagram enters. In caricature, and drawing upon Pottasch’s simple model for illustration, *we might define “cataclysmic” variability as being primarily—but not necessarily exclusively—being associated with an unpredictably-abrupt change in mass-flux from a star.* This is the interpretive counterpart of the definition based on visual luminosity variation. By simply saying *change*, we imply—as modern observations in the farUV imply—that mass-loss is a general quasi-steady property of stars, which can increase or decrease. As we saw in Chapter 2, a thermal diffusive mass-loss, as expected from the standard thermal model, is inadequate by orders of magnitude to match the observed mass-losses; so, generally, we admit a nonthermal mass-flux from stars. The distinctive aspect of *cataclysmic* is abrupt, generally unpredictable, and significantly-different from whatever is that mass-flux level that maintains that type of star in *whatever* atmospheric pattern we generally observed. So, for example, we do not distinguish between *novae (of all types) which increase their visual luminosity by an increase in their mass-flux,* and *R Cor Bor stars,* which we interpret as *exhibiting an unspecified direction of change in mass-flux accompanying the decrease in visual luminosity.*

It is equally clear that the second direction of modification of Pottasch’s first-approximation model is to admit additional radiative energy-fluxes—whether associated with the initial ejection of the photosphere, or subsequent events such as nonradiative heating and radiative cooling, or even the presence of a binary-companion. We have already discussed the effect of a moving photosphere on chromospheric emission. Pottasch’s model emphasizes the role of changing radiative opacity. That one does not model the primary cause of cataclysmic-variability via mass-ejection to lie in binary mass-transfer, does not imply that one must neglect the possible presence of a companion, even a close one. After all, as we will see in Section D, a major method of probing extended-atmospheric structure lies in eclipse observations of close binaries: the Sun-Moon-Earth, the WR + O in V444Cyg, the M + B components in 31 Cyg, etc.

But the basic physics involved in extending Pottasch’s model beyond the classical novae for which it was devised lies in retaining its character of being basically a mass-ejection effect. The gas flow is characterized by reaching escape velocities low in the atmosphere. (The binary-transfer model has the mass-flow of the mass-flux come from the accretion disk.) At the classical nova ejection phase, the photosphere already moves at escape velocity. At best, the planetary-nebular members of the cataclysmic class represent a late phase of such episodic mass-ejection. So, we

turn to consider the observational/empirical situation for other members of the class. As for the novae, the big development in recent years is the addition of the farUV data, sometimes supplemented by farIR and radio data. But the striking characteristic of most discussions of farUV observations is their taking for granted the validity of the binary mass-exchange model. So, too often, the data are presented in such terms, not in more simple ones, asking what range of models are compatible with the data, not whether the data agree with just this particular binary hypothesis. Payne-Gaposchkin (1977) posed the question as double-edged: Are all novae close binaries? How does one interpret a close binary which is not a nova? So, in the following, we abstract the variety of farUV information on cataclysmic variables from this aspect of keeping jointly in mind the caricature models of both Pottasch and binary mass-exchange—but above all, the question of which is basic: abrupt mass-ejection, or abrupt increase in stellar radiative flux—or possibly a mixture.

Then, as for the pulsating variables, we see best this problem of episodic vs. quasi-steady mass-flow—and accompanying phenomena—by looking at farUV spectra, of the variety of types of novae. We survey the planetary-nebulae under the emission-line peculiarity in Section B.3.c; but we have already mentioned the most essential aspect—the presence of a continuous outflow, between star and nebula, of ~ 1000 km/s. This much exceeds the classical ejection velocity of ~ 50 km/s, adopted simply because this is what is observed, now, at the nebula itself. There is also no evidence that such flow is episodic. So, one requires a strong deceleration; we will see the Be, and similar, stars demand the same. We also survey the symbiotic stars later, in Section C.

The significant addition to the nova picture of Table 3-1 comes from farUV spectra of old novae. Typical results are those on HR Del (1967), V 603 Aql (1918), RR Pic (1925) from Duerbeck, et al. (1980a, 1980b), Hutchings (1979), Dulcina-Hacyan et al. (1980). All authors report P Cyg type line profiles in the superionized N V, C IV, Si IV lines, with velocities $\sim 10^3$ km/s from the absorption-component shifts. Values up to some 3000 km/s are given for HR Del; Hutchings reports variations in C IV absorption by a factor of 2. Thus, at representative phases from 60 through 10 years after the episodic nova outburst, a strong, quasi-steady nova mass-flow continues. Hutchings gives a value of $10^{-8} M_{\odot}/y$ for HR Del; I think the uncertainty is a good factor of 100; but the point is that the quasi-steady flow is significant.

In the same references, Duerbeck et al. report that the nova-like variable TT Ari shows strong, violet-displaced, absorption lines. I reproduce one of their low-resolution, SW, spectra, for interest here, and eventual comparison to the Be situation: see Fig. 3-7. Velocities are $\sim 10^3$ km/s. This variable is described as resembling a dwarf nova during outburst—but even more, a Be star. One should compare the descriptions of the visual spectrum of this star—vis a vis its alleged binarity—with those of the Be star 88 Her (Doazan et al. 1982a, b); especially focusing on the differing periodicity of different kinds of features. Note that the period from velocity variations has been good to three significant figures for 60 years; note that none of the authors believe that binarity has been demonstrated.

Finally, there is an increasing variety of studies of the farUV behavior of dwarf and recurrent novae vis a vis the velocities, but nothing so definitive as for the novae has emerged (possibly it will have, by the time this book is published). There is, however, growing evidence for a background quasi-steady flow in addition to the episodic. This quasi-steady velocity can vary, over time-intervals long compared with the abrupt, nova-like, ones. We will also see such variation in the Be stars. Here, I simply cite several, illustrative, studies. Fig. 3-8a, b reproduce diagrams from La Dous showing, respectively, what she characterizes as two classes of spectra of dwarf novae at minimum. Note that her one minimum class resembles other kinds of novae at minimum or maximum: relatively flat continuum, superionized emission lines. The other minimum class spectrum more resembles TT Ari; also, it resembles the blue component, seen at *minimum* luminosity, of the so-called “binary-cepheids”—as S Mus in Fig. 3-3B; and also the Be spectra of Section B.3.b. But also, it resembles Fig. 3-9a, a dwarf nova at *maximum* luminosity. It also resembles (Cassatella et al. 1982) the appearance of the recurrent nova T Cr B at *maximum* luminosity during a curious, 2-year, phase showing a variability in the farUV, but none in the visual-spectral V-band (a 1000Å-wide continuum measure, centered on λ 4000Å). Note that T Cr B is a double-line spectroscopic binary, the nova plus an M3 giant. Recall that the cepheid binary cited above is the (F8 to G0, sometimes K0) cepheid plus the supposed B-type companion. That is, there is a “switch” in the relative spectral type of that binary component which is varying. Then, we note the reference already cited, in discussing dwarf-nova binary modeling: Cordova and Mason (1982), showing the

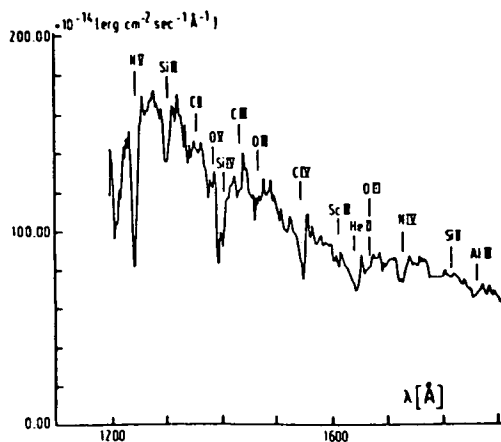


Fig. 3-7. The farUV spectrum of the nova-like variable TT Ari (from Duerbeck et al., 1980).

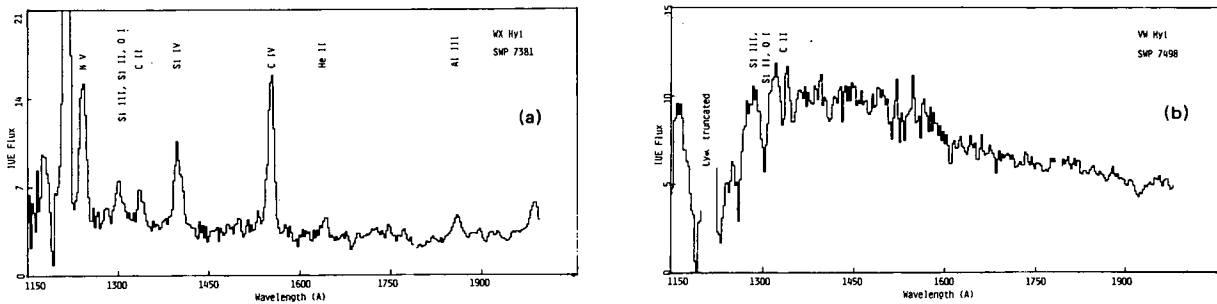


Figure 3-8. FarUV spectra of dwarf novae. (a) and (b): Two types of spectra during minimum (from la Dous, 1983).

dwarf nova TW Vir with a prominent P Cyg profile for C IV, and displaced; but essentially absorption NV, and the edge velocity of the absorption component extending to some 4800 km/s. The observation was made at an epoch of brighter-than-minimum luminosity; there were no detailed light curves at that epoch, to know the precise phase. Klare, et al. study six dwarf novae, of various subtypes, all during some aspect of outburst. The results are similar to that cited on TW Vir; except that asymptotic velocities and mass-loss rates were derived from comparing observed to theoretical line-profiles. Velocities range 2500–3000 km/s; mass-losses range 10^{-10} – 10^{-12} .

But finally, we have an excellent perspective on this whole problem of dwarf novae and phenomena: the data; the broad choice of physical models; the relation to continuous vs. episodic mass-loss; and the multi-“period” phenomena already mentioned in the pulsational variables, which will reoccur in following sections of this chapter, in Whelan’s (1980) summary of a group-program on these stars. Hassall et al. (1982) report its current progress. One distinguishes three “phases, maybe aspects” of dwarf-novae behavior; quiescence—an emission line spectrum, as one of La Dous’ minimum alternatives, above; an outburst, lasting several days, at intervals of ≈ 10 days; super outbursts, lasting ≈ 10 days, at intervals of ≈ 100 days; the amplitudes of the latter differ by about 1 V-magnitude. Individuality is strong—in some stars outbursts and superoutbursts can have the same relation, but each multiplied by a factor 10 in size of interval between eruption. Complimentary to the preceding discussion, I reproduce these authors’ sequence of spectra over a “cycle” for one star (Fig. 3-9). The farUV line behavior follows that already given as characterizing SS Cyg in the visual: emission lines overlying broad absorption lines during quiescence are replaced by strong absorption lines during eruption. As in Fig. 3-9, P Cyg lines often appear during the rise, and at the peak, of the outburst. Velocities and mass-loss inferred from them increase from some 3000 km/s, $0.8 \times 10^{-11} M_{\odot}/y$ during the rise, to some 5000 km/s and 2×10^{-11} at peak. The authors stress the order-of-magnitude uncertainty

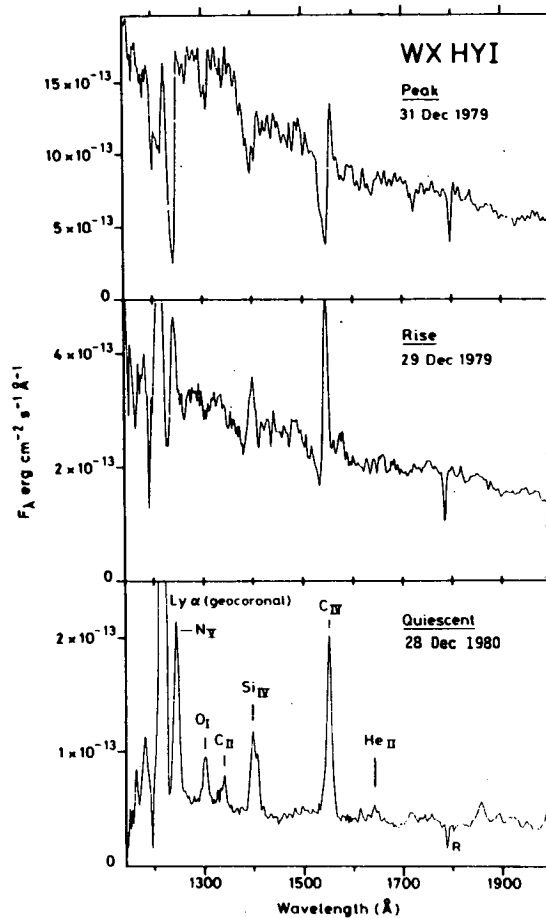


Fig. 3-9. Spectra of WX Hyd (from Hassall et al., 1982). The development of the line spectrum is shown as the superoutburst progresses. The characteristic strong emission lines of quiescence are replaced by absorption or P Cygni features (at C IV, Si IV). The flux scales are different for each spectrum; "R" marks a resonance near 1970Å.

of the latter, from ionization-uncertainty. The velocities are line blue-edge values, thus larger than P Cyg absorption-component displacement. However, the direction of change during the "episode" is clear: enhanced velocity, enhanced mass-flux, during enhanced luminosity. Finally, there is about a one-day time-lag of farUV luminosity maximum behind optical—in the same direction as for the classical novae, already quoted.

The authors give a detailed discussion of the inadequacy of the binary model to represent the data; it is unnecessary to repeat here. We note only that all aspects are well represented, grosso modo, by a Pottasch-type model, of a single-star, multi-structured, evolving atmosphere. We note the presence of background mass-flow, the short periods of an episodic enhancement, and the longer periods of a larger, episodic, enhancement; each as found for the pulsating variables; each, as we will find for Be and similar stars.

We note another difference between our focus on a Pottasch-type model and the binary mass-exchange one. The former is kinematic—we have not discussed why or how the photosphere is ejected; we have tried only to establish, empirically-theoretically, what kind of atmospheric structure accompanies such a photosphere. And, in the following sections, we ask what other kinds of stars exhibit the same kind of structure, and with what kinds of

photospheres—both continuous and episodic mass-flux—are the structures associated. The binary model focuses on the cause of the observed mass-ejection, without too much attention on the kinematics of how such mass-flow from an accreting disk produces the observed features. We note one typical difference between prediction and observation. Gallegher and Starrfield remark that the nuclear outburst theory predicts some 100 years of quasi-constant, enhanced, energy output, with continuous time-evolution toward a more energetic—bluer—spectrum; whereas, the observations appear to show only some 100 days of quasi-constant enhanced energetic output. They argue that if the nova phenomenon were primarily one of mass-ejection, the shell should cool, as it expands—which they assert it does not. Unfortunately, they apparently overlook the observed progressive shift toward later spectral classes until, and even beyond, visual maximum. But the Pottasch-type model faithfully reproduces all these observed features: the initial cooling, shift toward later spectral type, of the expanding, optically-thick shell; the progressive blue-shift of the spectrum as the shell becomes optically-transparent, and the retardation of farUV maximum behind visual; the increasing ionization level of the nebular spectrum as the shell becomes increasingly transparent. The retardation of the IR maximum to follow the farUV; radio data; Ti O bands—these must all be added to the first-approximation picture. I emphasize: there are many incomplete aspects of this simple Pottasch model; thermodynamic and observational, especially the continuous plus episodic flow. But its main point, a focus on subatmospheric mass-ejection as representing the main time-evolution of the system, seems useful as a starting point.

iii. Spectrum-Variability. This type of variability was, at the 1938 epoch, in contrast to cataclysmic variability, thought to have its *primary* origin in temperature changes, which must then affect the spectrum, rather than in changes in surface-area. Indeed, as originally defined, spectrum-variability need not, although it might, be accompanied by variation in luminosity. Thus, it lies outside the above classification scheme, which is based on luminosity studies, and it requires more sophisticated observation. But still, the level of such sophistication is not high: simply the presence, and relative strength, of absorption or emission lines, not their profiles nor positions. Although the Gaposchkins devoted relatively little space to this category of variability, they emphasized the rich possibilities of its future exploitation, *that it alone warranted treatment as extensive as they had given to all other categories of variables combined, in their book*. Further, they emphasized that the largest, and best known at that epoch, category of spectrum variables was the Be stars (Section B.3.b following; also Underhill and Doazan, 1982).

These Be stars are main-sequence but hot and bright, hence easy to observe by comparison with other main-sequence classes of emission-line, spectrum-variable, stars like the T Tauri (see Section B.3.c following; also Cram and Kuhl, 1984). Variability is primarily in the appearance of the line-spectrum: hydrogen Balmer lines pass from emission to absorption (Be to B-normal); from having relatively-unreversed emission profiles (Be) to such profiles with deep central absorption-components (Be-shell), including even normal absorption lines with deep central absorption components (B-shell), although the Be-shell and B-shell difference is not usually emphasized except in modern work (cf Doazan, Be stars, in Underhill and Doazan, 1982). Of equal interest to these hydrogen lines is the behavior of the Fe II lines, normally produced in stars of much lower T_{eff} , and of the superionized species like O VI, N V, C IV in the farUV, and of their X-ray spectrum. *ALL* these aspects of the line-spectrum are variable; thus far, in no discernable period; only in some cases do vague patterns begin to appear under detailed study of individual stars, *not* simply from statistics of many stars observed, each, at only a few phases.

Furthermore, one notes that at the epoch of the Gaposchkin book, the P Cyg type stars (B supergiants in which emission-line profiles in the visual-spectral region show violet-displaced absorption wings) were included among the Be stars. And we note that P Cyg itself, that star which shows the most extreme individuality of almost any star thus far studied, was historically described as nova Cyg (1600). Roughly, 20 percent of the main-sequence B stars are Be, so the “peculiar” stars are hardly a minor population. We note that the Gaposchkins found some one-third of the 413 emission-line B and A stars, in the largest catalog existing at their epoch (Merrill and Burwell, 1933), to show luminosity, as well as spectrum, variability. A very significant datum, when taken together with the observations showing that a Be star can pass from B, to Be, to B-shell and return, in all directions, is that, statistically, Be stars are generally one magnitude brighter than B stars, *in the visual*. Doazan (Underhill and Doazan 1982) discusses the relation of visual luminosity variations to that in the farUV, remarking that stars can stay in one or the other of

the Be and B-normal phases for periods as long as 35 years. Thus, we see very well the implications of this long-term, *but not unidirectional*, change in *total* luminosity of the star on internal-structure, not just envelope-structure, of the star. I stress this, relative to the *apparently envelope-storage* luminosity variations in the pulsating variables. We return to this point, in summarizing this Chapter 3, and in Part III.

Although we do not discuss the high-resolution, farUV spectral observations until Section B.3.b, we note that such studies (Doazan in Underhill and Doazan, 1982 and parts of this volume) show very clearly the presence, and variability, of large mass-fluxes from these stars. Thus, these plus the H α emission line behavior, show that at least this type of spectrum variable exhibits strong variations in surface-area of at least those “surfaces” where arise the line-spectrum. The total luminosity variations mentioned above suggest the same thing, more generally. So, temperature variations alone do not suffice to describe such “spectrum-variability.”

The Be stars are hardly the only spectrum variables. These others are discussed in more detail throughout the several volumes in the series. The Ap and Am stars are particularly interesting, re the above-mentioned alternatives of “rotating, spotted, stars.” The same is true for the symbiotic stars, re “binarity.” And, indeed, *all* the emission-line stars show such spectrum-variability. The dMe “flare” stars are excellent examples which link emission-line variability and “solar-like” behavior characteristics.

So, looking broadly at the three examples of kinds of stellar variability, it was the diversification and extension of visual luminosity observations to include spectra—of even rough quality—which introduced sufficiently-precise restrictions on empirical modeling to understand where, in the star, and by what means, such variability arises. The supplementing of luminosity measures by simple spectral line-shift measures is the obvious first example, to separate stellar-positional changes (which specify binary motion) from stellar-surface changes (which specify surface-velocity). Such suffice to separate binarity from intrinsic stellar-structural phenomena. Then the more detailed spectral measures of line characteristics (absorption vs. emission, profiles, etc.) gave more details of what *kind* of structural changes, atmospheric or interior, exist. And, the correlations among these, *for individual stars, not just statistical for groups of stars, where phase-relations are lost*, make further precise these details which real-world models must satisfy, that exclude purely thermal modeling.

To continue in the same logic, we note that one did not, at that 1938 epoch, ask too deeply into what caused the temperature changes thought to underlie spectrum-variability. (And, of course, we note the other types of spectrum-variability associated with magnetic fields, as in the Ap stars, and with rotation of spotted-stars, as in the Am.) But there are only two possible sources for such anomalous temperatures: either by modified radiation fields, or by “mechanical” effects of compression or dissipation associated with nonthermal velocity fields. One has no idea how to induce the former without the latter, unless one collapses magnetic fields, which is again an “aero/hydro-magnetic phenomenon.” Discarding sufficiently-large-amplitude velocity fields to be observable in line-shifts, hence, lying in the province of mass-fluxes, one is reduced to mechanical energy-fluxes which do not transport mass, *locally*, or *grossly* from the star. Phenomenologically, one comes to the “picture” introduced to produce the solar chromosphere-corona: nonradiative heating.

So, once again, we see the tendency of diverse phenomena of “peculiarity” to close on themselves. None appears *really* distinct from an origin linked to the two additions to (closed, thermal) modeling: mass-flux, non-radiative energy-flux, the characteristics of (open, nonthermal) structures.

2. 1978 Modification of 1938 Classification Scheme

In the pre-1938 scheme, the one class excluded from interest in the (closed, thermal) adequacy question was that of binaries. For these, variability was only geometrical, not physical. But whereas in 1938, the cataclysmic variables were placed by the Gaposchkins in a class parallel to the intrinsic—they restricted intrinsic to pulsational, whereas in my summary I included cataclysmic—in 1978, they concluded that *all* cataclysmic variables occur as components of binary systems. Thus a binarity impact on variability is admitted to arise *not just* from geometrical effects, but possibly also from physical. Particularly in our era when modeling is increasingly empirical, more aided by observed correlations between different phenomena than by speculation, *it is necessary to separate phenomena*

arising in noninteractive association from those arising in causal linkage. Thus, if it is true that all cataclysmic variables are members of binaries, one asks whether binarity is the *cause* of such variability, or simply an added feature. This is particularly essential for our review of *thermal* vs. *nonthermal* origin of atmospheric structure, and delineation of *kind* of nonthermal origin.

A “cataclysmic” variability that arises from a tidally-induced mass-ejection from one or both stars of the binary is one thing, not necessarily linked to a nonthermal structure of an *individual* star. But an impact of a mass-flux from one star on the other, with such mass-flux arising primarily because of a nonthermal structure of its parent star, even though possibly accelerated by the gravitational field of the second star, is quite another thing. It is this last possibility where current interpretations of the phenomena of “cataclysmic” variability are weak. Whether such investigations are correct or not is not our present problem; we note only that they depend, primarily, upon a nonthermal structure for the star and/or atmosphere, to produce cataclysm. So, “cataclysmic” \equiv (open, nonthermal), in 1978 as in 1938, only from different aspects.

Further interest in such “binarity” interpretation of variability lies in discussions of “symbiotic” peculiarity, to which we return below, in Section C. Again, we shall see that they focus on the two alternatives for interpreting the significance of “peculiarity” in spectral and luminosity features: (1) superposition of effects from *two* stars, not usually resolvable and so existing only by inference/speculation, each star being modeled “normally;” (2) superposition of radiation coming from two or more *different atmospheric regions of the same star*, such regions having their origin in nonthermal effects. Alternatives (1) and (2) may combine.

This, then, is the “evolution” between 1938 and 1978 in categorizing and interpreting variability: putting into stronger focus the choice between “binarity” of stars and “multiplicity” of atmospheric region, when diagnosing the spectrum of a *superficially* single star. Reaching ahead, we will see that the evolution in recent years—already forecast by solar studies for several decades—is toward putting into focus the choice between multiple atmospheric layers arranged in radial “layers” vs. those where there is significant nonradial structure. And again, in such choice and such diagnostics, we must carefully distinguish “global” from “dermatological” effects, when asking the main thermodynamic characteristics of atmospheric structure.

3. The Gaposchkins’ Contrast of Stellar and Atmospheric Variability

I can do no better than to quote this, sans comment. The above discussion, in which I have borrowed heavily from their writings and private discussions, suffices for elaboration:

The present chapter (spectrum variables) actually covers a subject as extensive as, and largely distinct from, the rest of the book. Earlier chapters consider variable *stars*; here, we deal with variable *atmospheres*. All *true variable stars* have *variable atmospheres*, but a *variable atmosphere is probably the property of all stars*, whether obviously variable in brightness or not (as witness the solar envelope). In the present chapter, we consider not only the atmosphere proper (to be defined, perhaps, in gravitational subservience to the star) but also the more extended stellar envelopes, which may (the novae) or may not (the Pleiades) have originally been part of the star they surround.

Thus, in concluding their chapter on the peculiarity characteristic of *variability*, the Gaposchkins launch a bridge to the peculiarity characteristic of *atmospheric-extent*, having already done so explicitly for *emission* peculiarity, and implicitly for *symbiotic* peculiarity.

In 1920, Payne-Gaposchkin published her book, *The Stars of High Luminosity*, in which she summarized the essential “hopes” of (closed, thermal) modeling by applying the Saha, and Fowler and Milne approach to Equilibrium ionization and excitation to discuss the high-luminosity stars within the 2-dimensional HR diagram taxonomy. Thereafter, she spent her life contrasting the ideals of such stellar normalcy to the facts of stellar peculiarity. The Gaposchkins’ above, 1938, remark on the solar envelope, at that epoch just before its actual thermodynamic nature became clear, served to put universal atmospheric variability into focus: all stars, including the Sun, show it,

it is just a matter of degree and detail. Her comment on seeing the first solar farUV, emission-line, superionized spectrum served equally to put into succinct focus the pervasive prevalence of a variety of peculiarities: “My God, the Sun’s a symbiotic star—GO in the visual, WC 6 in the farUV.” The universal symbiocity of atmospheric regions and phenomena as contrasted to stellar type; nonthermal energy-fluxes in hot and cool stars alike; the ubiquitous pitfalls of abundance-evolutionary questions—all in the spectrum of the Sun and “stars like it.” So, we move on to the emission-line stars; and exhibit *a*, the WR phenomenon, including classical WR stars; exhibit *b*, the Be stars; exhibit *c*, the planetary nebulae; exhibit *d*; the T Tauri stars.

B. EMISSION-LINE PECULIARITY AND STARS

1. General Existence of Such Peculiarity and Stars

Throughout the HR diagram, there are stars in which *some* spectral lines from *some* abundant elements appear wholly or partly in emission in the visual spectrum. These same lines are predicted to be in absorption by (closed, thermal) modeling, and observed to be in absorption in the majority of stars of the same MK spectral class as the emission-line ones. These majority are the “normal” stars, so designated because they are the majority and because they accord with classical modeling predictions; the minority are the “emission-peculiar” stars. When such emission-peculiar stars are main-sequence (MS), i.e., in luminosity classes V, IV, and III, their peculiar status is usually designated by suffix “e” following the MK spectral class. Among the O stars, the designation is by an array of (f)-brackets, depending upon which combination of H, He, N emission lines is observed. For the other stars, *e* implies *at least* Balmer H α emission, with possibly other emission-lines also. Emission-line stars are universally variable (but the converse is not true); so that the star does not necessarily show H α emission at a particular observed epoch; it suffices to have shown it at *some* epoch.

Examples of such *e* stars are the Be, Ae, and dMe. The emission-line MS stars of the FGK classes are mainly the T Tauri stars. These latter are generally considered to be “pre-main-sequence;” both because they are enveloped in nebulosity and because they are observed to lie above the MS. The Herbig Ae, Be stars are thought to be pre-main-sequence stars, evolving toward it from above. By contrast, classical Be stars often lie above the MS, are sometimes assigned luminosity class IV; and many authors call them “evolved” stars which are leaving the MS. The first two emission-line stars discovered were the Be stars γ Cas and β Lyr; the Be stars are the most extensively observed of all emission-line stars. The characteristics of γ Cas are discussed in detail in the B-Be volume, and should be read, especially in comparison with the other Be stars discussed there, to put the present abstracted summary, and our use of these stars in Part III, into focus. We compare the Be and T Tauri stars to illustrate the comparative importance of mass-flux and nonradiative energy-flux in interpreting such emission-line formation, hence the importance of such (open, nonthermal) modeling. Such a comparison of these “hot” and “cool” emission-line stars again puts into focus the similarity, rather than difference, re “peculiarity,” hence modeling correction, across the HR diagram.

There are a variety of other emission-line stars beside those designated by *e* (or *f*). These generally fall into classes of stars that are peculiar from some sense other than emission-line, but for which emission lines are a strong, additional, characteristic. Examples are members of the cataclysmic-variables class already mentioned (planetary-nebulae, novae, symbiotic, R Cor Bor, etc.); many of the pulsating stars at particular phases; the T Tauri stars have already been mentioned; the FU Ori stars, which combine the T Tauri and “cataclysmic” characteristics, showing emission lines in both pre-and post-“eruptive” phases. These stars are all admitted to be “peculiar” or a priori excluded from conventional (closed, thermal) modeling. But, two broad classes of “unlabeled” emission-line stars, the OBA sg and the WR, present an interesting “dilemma” re definition of “normality” from “majority-of stars” and “classical modeling” aspects.

The B sg illustrate the point. Such luminosity class I stars that show emission lines are grossly distinguished from Be stars by the very large luminosity difference, and by their emission lines being confined to H α . Then they, in turn, are divided into two subclasses, Ia and Ib, again by luminosity differences: Ia is about 1 magnitude brighter than Ib. But observationally, no type Ia star has been found which does not at some time show H α in emission;

whereas, while some Ib stars have been found to show such, the majority do not. Thus, the Ib class is like the MS B-Be amalgam, *without* the “e” distinction. But under the “majority-of-stars” definition, the “normal” B Ia sg would be one with emission H α ; while such “normality” would conflict with (closed, thermal) modeling normality, and we would abandon all such B Ia as being susceptible to such modeling, as we did the MS Be. Doazan, in the B-Be volume, points out the historical basis of this dilemma; too limited spectral coverage in classical taxonomy. MK classification is based on the blue, hence excluding H α , so all sg “appear” normal from *both* definitions, simply because of the limited taxonomic basis. This point is expanded, and illustrated, by the contrast between Epoch I, normal MK taxonomy, and Epoch II, taxonomy in the farUV and X-ray, in the several volumes of the series. There are other characteristic differences in these stars. We have already mentioned variability for the B Ia and at least some of the B Ib. The same behavior characterizes the O and A sg. As discussed in the variability-type of peculiarity among the later-type sg, many of them also show this emission-line-type peculiarity. Thus, the sg should, generally, simply be added to the above list of types of stars which, although not labeled with “e,” are emission-peculiar.

For use in Part III, we should emphasize here another distinction between Be and B sg emission characteristics. The *maximum emission-line strengths*, relative to the adjacent continuum, are much stronger in the MS than in the sg stars—with the exception of the WR class, following. However, over short time-intervals, and low spectral resolution, emission-line variation is much more apparent in the sg. The sg show greater short-term variation in *line-profiles*; while the Be stars show greater, but longer-term, variation in *total line-emission*. Also, over long time intervals, the Be stars show the greater variation in line-profile; we discuss this later.

Then, in the same logic, the WR-type stars also are “normal” stars, in their perpetual and universal exhibition of emission lines, instead of absorption. We return to these later, for more detailed specification of their “peculiarity.” Here, we emphasize only this “normality” of emission lines, *and* that the WR-type “peculiarity” occurs in both sg and those “quasi-MS” stars forming the central stars of some PN. Indeed, Conti and associates have identified WR-N stars across a range of M_V from -2 to -10 . The central stars of PN identified as WR are (thus far) only type WC; and the range in M_V has not yet been well specified. But the point is clear—among some classes of stars, emission-line stars are the *normal* stars.

In an overall statistical abstract, we note Merrill’s comment that 95 percent of emission-line stars appear to lie in the OBA and M classes; only very few lie in the FGK classes. We have already noted that some 20 percent of B MS stars are Be, and increasing with each new survey. When one considers the selection effects coming from the ~ 4 magnitude difference between Be and T Tauri stars, such statistics as Merrill’s should be taken cautiously. We note that just in the last few years are the same kinds of detailed surveys being made of types of profiles, and variability, for the T Tauri stars as have existed for decades for the Be stars. Again, consult the B-Be and FGK volumes.

Similarly, we should comment on the use of emission lines for classification purposes, among the stars which exhibit them, to supplement the MK absorption-line approach. Although in the bright Be, and WR stars, these emission lines have been studied for well over a century, there is much “mythology” in the literature, especially among theoreticians, but also among taxonomists. One finds statements asserting that: “There is a definite relation between the net emission strength of H α and the stellar luminosity.” Such statements are simply not correct; the strong variations found in the Be stars, where the star passes from an emission-line to an absorption-line star, are the most direct evidence. Possibly such statements refer to the supergiants; and even there, the already discussed situation among the Ia and Ib B sg shows the fallacy of taking emission-line intensity and stellar luminosity as showing any kind of isomorphism.

The same kind of error—ignoring the very basic point that emission-line stars are variable; the only uncertainties are time and amplitude scales—lies in attempts to classify emission-line stars by types of profiles of emission lines (cf the summaries by Jaschek et al., 1981 for the Be stars; and by Ulrich and Knapp 1978 and by Schneeberger, 1979 for the T Tauri stars). The same star, observed at different epochs, very often shows a transition from one classification category to another. Refer to the changes in profiles for typical Be stars by Doazan (1982), and in Kuhl (1984) for the T Tauri stars; indeed, even among some of the profiles shown at different epochs in the material of those proposing such classification. My objections are hardly just formal. *IF* we could identify characteristics of a given star, or class of stars, which led the star to always produce a given emission-line profile, we would have made

a strong step forward in the problem of modeling the production of such profiles; we would have found at least *some* time-independent factors, which determined the departures from thermal models. We have not, at least thus far. But, one of the strong aspects of peculiarity—variability—is linked to another aspect, the production of emission-lines. Apparently, all stars exhibiting emission lines are significantly variable, although the converse is not true. This tells us something about the thermodynamics of that stellar structure producing emission lines—it is not thermally “quiet,” with change only over evolutionary times.

Finally, in this quick overview, it is useful to put into perspective the meaning of emission lines: what storage modes, what distribution of storage modes, and what fluxes does it take to produce emission lines? There are exceptional circumstances in which particular lines from particular atomic configurations can be produced in emission in nonLTE standard-star models. But these are not those strong emission lines from abundant elements which characterize emission-line stars. And the assertion, which still persists in the literature, that the correct kind of scattering processes in radiative transfer can produce emission lines is, like some of the above statements, a myth, resulting from erroneous boundary conditions applied to a quasi-LTE treatment of a nonLTE situation (Gebbie and Thomas, 1968; Harrington, 1969). In essence, one has but two alternatives to produce such emission lines as we discuss in emission-line peculiarity: an extended atmosphere, which demands a nonthermal mass-flux; or a nonradiatively-heated atmosphere, which demands a nonradiative nonthermal energy-flux. And, equally, one has but two alternatives in diagnosing variability in such emission lines: to infer the existence of a variable mass-flux, or that of a variable nonradiative energy-flux, or of both. So when we observe variable emission lines from ions: (i) some of which are normally expected, in that MK taxonomic class; (ii) some of which are superionized, for standard photospheric conditions of that class; (iii) some of which are subionized, for those same conditions—the inadequacy of standard models, and in which directions to seek change, do not require profound thought.

2. General Characteristics of Observed Emission-Lines in Emission-Line Peculiar Stars

a. Range of Ions Producing Emission Lines. I stress that to be included in the category of emission peculiar, it suffices that a star show at least emission- $H\alpha$, at least once. $H\alpha$ is the widest occurring across the HR diagram. Many current emission-region surveys are based on it. Its classical handicap is its falling outside the visual spectrum, where most classical exploration/taxonomy was done. So emission- $H\beta$ replaced it, historically-operationally, but not physically-phenomenologically. We must realize this lack of data on emission- $H\alpha$ is our, not the star's, inadequacy. So I equally stress that a star is not excluded from this category, nor from the specific varieties of it such as WR, Be, PN, T Tauri “emission-line” type *phenomena, not just stars*, if it shows equally-anomalous emission lines other than $H\alpha$, or the hydrogen Balmer lines, or hydrogen lines generally. To demand that a stellar model permit some particular line to appear in emission rather than in absorption, even episodically, is to demand some minimal range of thermodynamic conditions in the atmosphere, which is broader than those permitted by allowing only absorption lines to be produced. Equally, to exclude emission in any other lines, than the one defining minimal membership in the class, is to impose a strong—and usually unjustified—limitation on that minimal range. For example, in Chapter 2, we noted the generally photoionization-dominated character of hydrogen $H\alpha$ and the Balmer lines, except in abnormally-dense regions such as flares. At the end of Section 1 preceding, we noted that the presence of emission lines generally requires either nonradiative heating, or extended atmospheres. If a class of stars is restricted to showing *only* $H\alpha$, or Balmer, emission, one implicitly restricts that class of stars to having only extended atmospheres, and prohibits their having chromospheres. A priori, of course, everything is possible. But as we will see in this section, the historic, and contemporary variety of phenomena observed in stars showing, at least episodically, $H\alpha$, and Balmer, emission argues that such restricted class would be as physically unreal as the classical standard model.

So it is that one regrets the mis-labeling of the Be category in de Jager's stimulating survey of *The Brightest Stars* (1980), where the class is restricted to stars producing only Balmer emission lines. As above, the point is hardly just semantic-taxonomic. It produces much confusion in his discussion of that variability of the Be stars—and their three phases of Be, Be-shell, B-normal—upon which we lay such stress here, and the influence of that variability upon extended-atmospheric and local-environmental structure. It further confuses the empirical relations between Be and

stars similar to them. Because the Be are such phenomenological crossroads, their liaisons must be recognized. Finally, it introduces much factual inaccuracy in the discussion of that earliest observed Be star, γ Cas, which is presently enveloped in enough observational misunderstanding re its asserted binary character (cf Doazan 1982, and Doazan et al., 1983).

There are other examples of unjustified limitation imposed on those broad ranges of thermodynamic conditions demanded by the presence of some emission lines. An inverted example is the restriction of stars having "chromospheres" to those showing emission cores in Ca II and Mg II—because this is what is observed in the Sun, where a chromosphere exists. Emission or absorption in the superionized lines of O VI and N V, but without Ca II or Mg II core emission, are considered grounds for excluding such stars from those having chromospheres. One errs, thermodynamically, in defining chromosphere *only* in terms of the nonradiative heating to produce a particular emission line, independent of other thermodynamic considerations, whose presence is as much demanded by N V in hot stars as by Mg II in cool stars (cf. Chapter 4). One errs observationally, in confusing observational inability to detect—from insensitive instrument, faint star, etc.—with actual absence of an ion. The ludicrous extreme, is the establishment, from emission lines observed in hot OB sg, of categories of warm winds, $T_e < 10^5$ K, because one sees no ions hotter than O VI, N V, C IV in Copernicus and IUE, *whose spectral range ensures that resonance lines from hotter ions are unobservable*. As soon as X-rays were observable, the physical travesty was clear; but the modeling inertial error persists even in an "expert" survey of research priorities for the coming decade (Field, 1982). Let us hope our monograph series is as widely read.

So, in the following discussion of emission-peculiar stars, and what thermodynamic enlargement of standard-model conditions the particular emission lines demand, I try to not overrestrict possible atmospheric models by imposing what is not observed, or ignoring what is. Probably the biggest handicap of atmospheric modeling, today, is also the most stimulating; whatever nonthermal feature is not observed today, is, by experience, highly likely to be observed tomorrow. Interpretative-dilemma: bad detector yesterday, or variable star?

Then in a very gross way, the exceptional spectral line is that which does *not* appear in emission, somewhere, at some time, across the HR diagram. As noted, the hydrogen Balmer lines, especially H α , are those most frequently observed, in a wide variety of stars. One sometimes observes hydrogen Paschen lines in emission, generally when the Balmer lines are in strong emission. Lines of He I and II are observed. We have already noted the prevalence of emission cores of Ca II and Mg II lines in stars cooler than mid-F; they show variable emission wings in the hotter stars—a fact often overlooked in discussing the prevalence of "chromospheres." Various lines of the abundant elements—Fe, Si, C, N, O, Ne—appear, from various stages of ionization, and in both permitted and forbidden transitions. Especially in cataclysmic and symbiotic stars, in the visual, one sometimes observes forbidden lines from highly-ionized atoms; e.g., the (solar) coronal lines, like [Fe VII, X]. In the farUV, in all sg, and cooler MS stars, one observes superionized emission lines. The same lines are observed in absorption in hot MS stars. Their presence is equally anomalous to standard atmospheres, whether they are in emission or absorption, as Menzel emphasized for H α .

Above, I stressed the two major alternatives on atmospheric configurations to produce such variety of emission lines: nonthermally heated, or/and extended-atmosphere. Usually, especially today, discussions of such lines focus on such modeling alternatives, not on trying to survey common and contrasting properties of particular lines across the HR plane. I mentioned the diagnostic importance of the Balmer lines in this choice; we survey more details, in comparing the Be and T Tauri. Zirin (1976) surveys the appearance of He I λ 10830 across the HR plane; mainly in absorption, but also in emission; and its implication on ubiquitous chromospheric-coronal existence. He stresses its variability. One should keep λ 10830 in mind for perspective on the current debates between cool (10^4 K), warm (10^5 K), coronal (10^6 K), ultrathermal velocity (10^7 K) winds. One has debated for years over chromospheric-collisional vs. coronal-radiative origin for λ 10830; one has remarked its presence ever since helium was identified in the Sun, and realized that no standard-model structure can produce it. Given its presence, in emission or in absorption, one can hardly dispute nonradiative fluxes in those stars. In the same way, whether one produces O VI collisionally, or radiatively, its environment must have $T_e > 10^5$ K; and its environment *is* the wind. To decelerate this $\sim 10^3$ km/s wind to reach those exterior regions where emission H α is formed, and which move at $\sim 10^2$ km/s

velocities, produces, at the interface, T_e near 10^7 K; X-ray emission supports these super- 10^5 K T_e levels. But any discussion of emission lines which restricts attention to the chromospheric-coronal atmospheric regions is myopic. The importance of these regions, and that of the farUV observations which detail their structure, is dual. First, it demonstrates that such nonradiatively heated regions universally exist. Second, it shows that such hot, ultraspeed regions can exist interior to those regions, moving more slowly and being much colder, that are needed to produce the classical visual emission spectrum of the Oe, Be, Ae, PN stars—and stars similar to them.

At the end of Chapter 2, I abstracted the various elaborations of the standard model to show that, grossly, a quasi-isothermal surface layer—containing T_e -variations by factors between 1 and 2—was not a bad approximation for the photosphere. In essence, our preceding discussion of cataclysmic variability shows that equally well, their photospheric layers can usually be represented by the same degree of quasi-isothermal, but moving, photosphere. But the simple existence of emission lines, the observed variety of ions producing them in a given atmosphere, and their relation to corresponding equally-anomalous absorption lines demonstrate that the range of T_e over the regions producing them is by factors between 10 and 10^3 . In the same way, the range of differential nonthermal velocities in classical and moving photospheres is small; that in the regions of emission-line production is by factors between 10 and 100. In a phrase, these emission lines, and associated absorption lines, demand a greater range in atmospheric conditions within one star than the standard-atmospheric model permits across the whole range of stars in the HR plane. It is useful to keep this in mind, when one discusses the thermodynamic significance of stellar atmospheres on stellar structure and evolution, and the ISM—and the general structure of concentrations of matter and energy. We proceed to illustrate all this.

b. Kinds of Emission-Line Profiles. Such lines can be wholly in emission, with or without reversals, which can be central or displaced, shallow or fall below the continuum, symmetric or not. Such lines occur all across the HR diagram: from being nearly the unique type in WR stars; strong and variable in Be, Oe, Ae, PN, novae, symbiotic, and T Tauri stars; being seen transiently in both dMe and sg stars; and variable in OBA sg (cf. Figs. 3-10, 3-11, 3-12). Also, emission can occur as quasi-central emission cores in strong absorption lines—sometimes themselves having absorption cores: e.g., Balmer lines in Be, and the Ca II H and K lines in cool stars (Figs 3-13a, b). Emission can also appear in the wings of absorption lines, of which good examples are the Ca II lines in some Be stars (cf Fig. 3-14). Lest one think that emission lines always imply “hotter” conditions (as in the appearance of He II lines in R Cor Bor), note that “subionized” Fe II lines can appear in emission in Be phases, and emission-bordered absorption cores in Be-shell phases.;

The *spectroscopically-empirical* “shell-spectrum” illustrates how precisely particular kinds of emission profile can establish boundary conditions on empirical modeling. Such a spectrum is characterized, in the prototype Be stars, by the broad emission line changing into a line with a deep, narrow, absorption core, with or without emission wings, in Be-shell phases (Fig. 3-15). (A corresponding B-shell spectrum corresponds to the broad absorption profile characterizing the B-normal phase being replaced by an absorption line having a narrow and deep central absorption core, cf Fig. 3-16.) An added feature characterizing the shell phase is that remarked above: the presence of “subionized” singly ionized metals, with the “shell-line” being a narrow deep absorption, which may (Be-shell) or may not (Be-shell and B-shell) have emission wings. The term “shell” was originally introduced by Struve, as part of a modeling scheme for Be-stars, and referred to the geometry of absorbing material. Today that significance has vanished; leaving the term to refer *only to the appearance of a particular kind of spectrum in the visual*: narrow, deep absorption core for hydrogen, plus Fe II presence. Confusion can arise, when one discusses ejection of a mass-shell, such as in a nova. There is no problem, so long as no *a priori relation is imposed between shell-type-spectrum, and shell-mass-ejection.*

Finally, we must mention one velocity-oriented emission-line profile: the so-called “P Cygni” (Fig. 3-17a) and “Inverse P Cygni” (Fig. 3-17b) profile. The former consists of an emission line with an absorption component on its extreme blue wing; the latter, with the inverted configuration. These were first observed in the visual spectrum of the highly-individual star P Cyg, for many lines of different ions. They were then observed in the WR stars, then eventually in many other stars, including the hydrogen Balmer lines in Be and T Tauri types. Today, some T Tauri

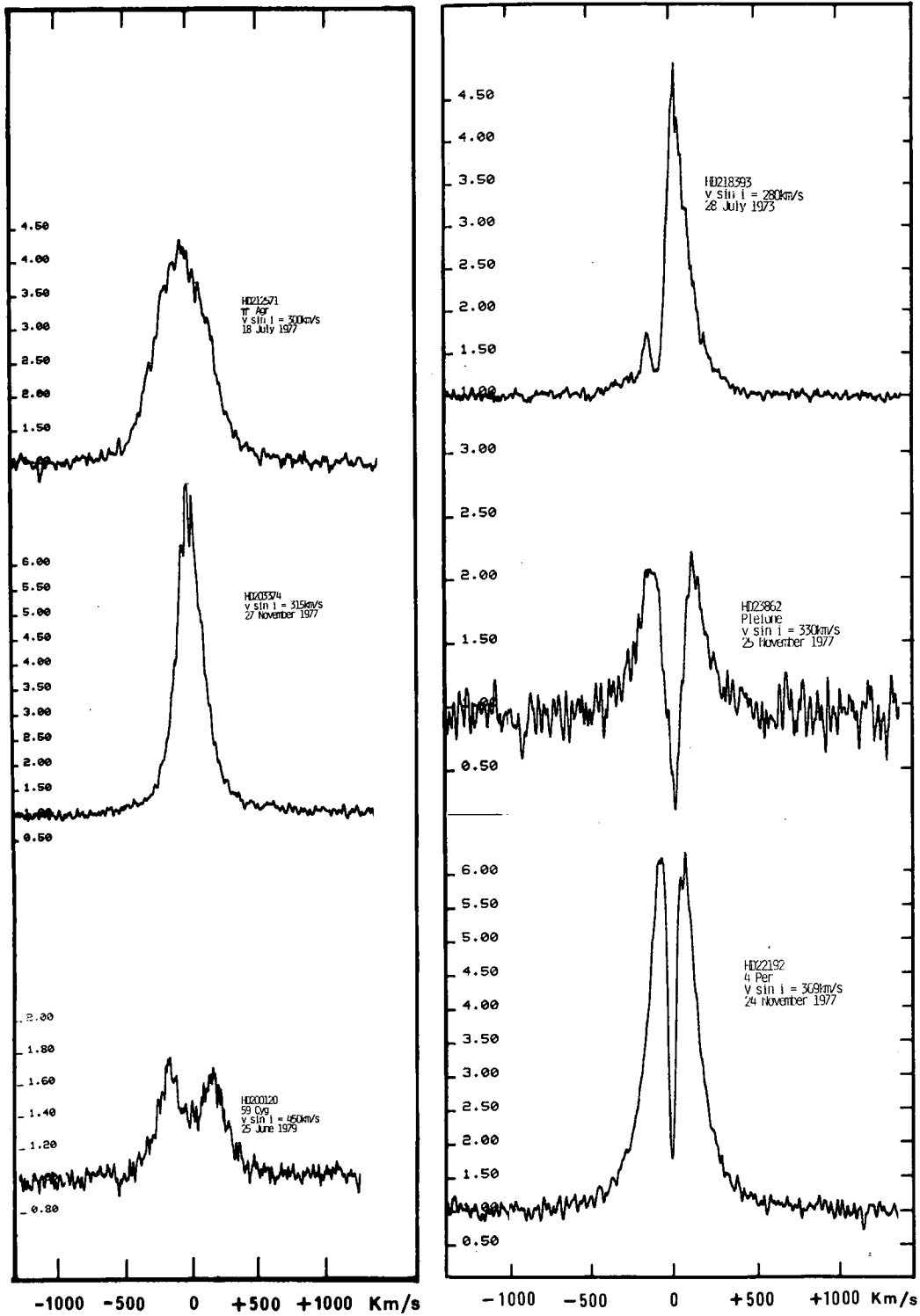


Fig. 3-10. A sample of H α emission-line profiles in Be spectra (left) and shell spectra (right). The characteristic feature of shell lines is the narrowness of the self-reversal (from Doazan, 1982). A given star may show different characteristics at different epochs (see Fig. 3-22).

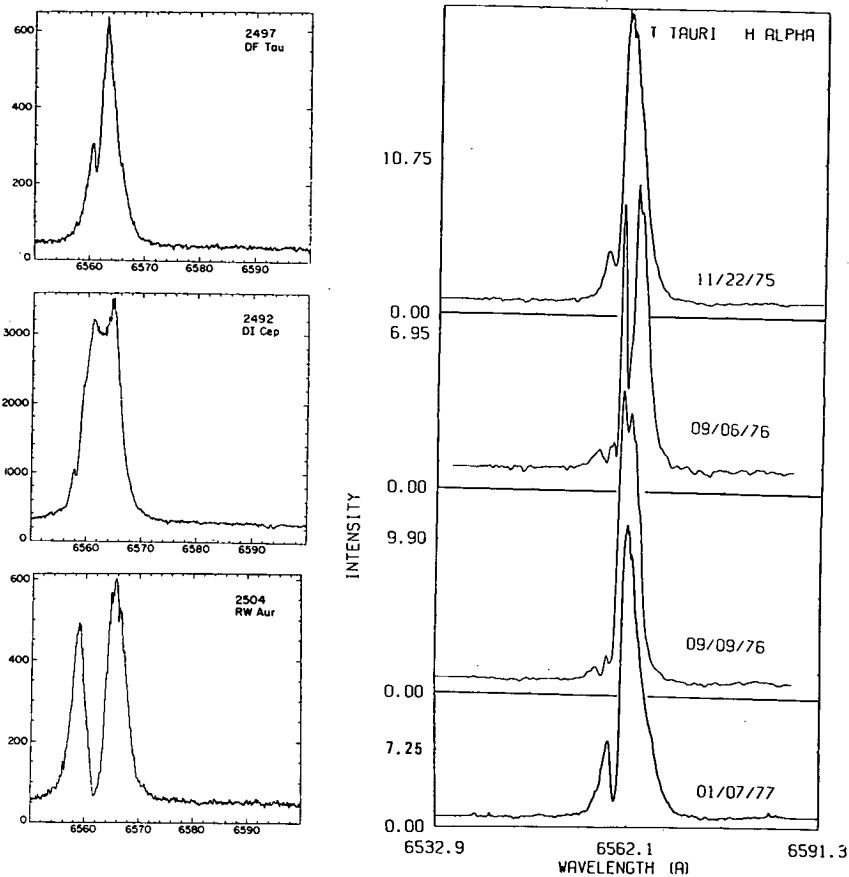


Fig. 3-11. A sample of H α emission-line profiles of T Tauri stars (left), (from Hartmann, 1982). The variation of the H α line of T Tau (from Schneeberger et al., 1981) (right).

stars have been observed to show direct P Cyg profiles in lower Balmer lines, and inverse P Cyg profiles in higher lines (Bastian and Krautter, 1980). This duplicity makes difficult the early, pictorial interpretations of such profiles as arising in extended atmospheres around a “normal” star, within which temperature continued its photospheric, RE, outward decrease. The expanding atmosphere was postulated to be opaque in the lines, extended but transparent in the continuum. Thus, the emission component arose from the greater geometrical extent of the star in the line over the continuum, *not because of a hotter* external atmospheric region but *in spite of a colder* one. The absorption core corresponded to that part of this colder region which was projected against the hotter continuum disk. An expanding atmosphere gave the normal P Cyg profiles; a contracting, the inverse P Cyg, under that epoch’s “theory.” So the atmosphere must be both expanding and contracting to reproduce the today’s observed simultaneous presence of both direct and inverse P Cyg profiles, under this simplistic “pseudo-thermal” modeling.

In the spirit of trying to provide unified empirical atmospheric modeling among these P Cyg, WR, and some other hot stars, Beals (1951) tried to establish a sequence of “modified P Cygni” emission profiles, extending the “classical” one with absorption core in the far wings, by the core moving progressively inward to a final, limiting, no-absorption-core type: (Fig. 3-18). There exist in the literature attempts at applying, and enlarging, this Beals sequence to classify Be and T Tauri stars by comparing/ordering their Balmer emission profiles from this sequence. Such attempts are a priori negated by the great variability observed in such profiles; a given star’s H α profile, for example, often traversing nearly the entire Beals sequence in sufficient time, and repeating. Again, cf B-Be and FGK volumes of this series.

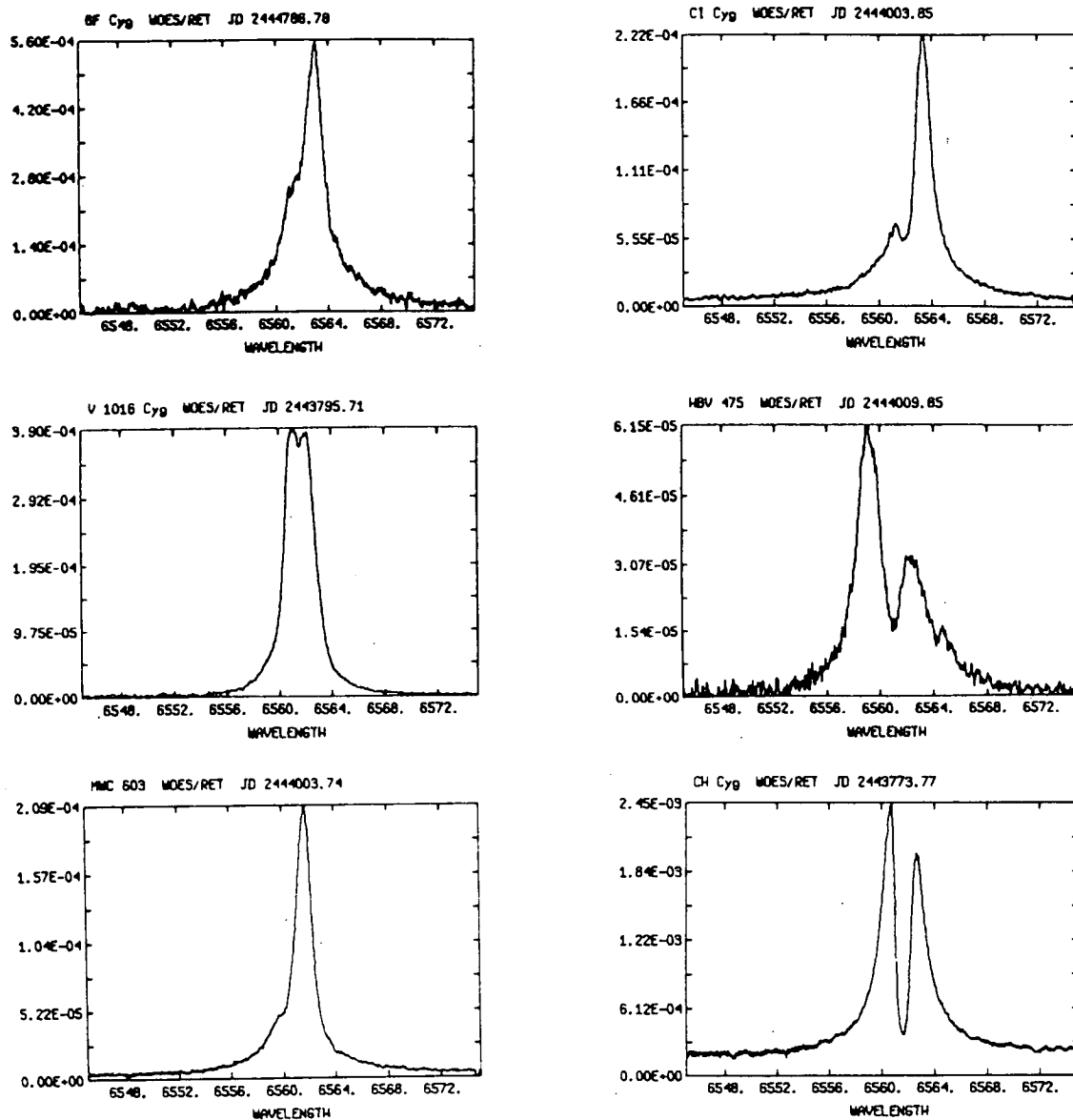


Fig. 3-12. A sample of H α profiles in symbiotic stars (from Oliverson and Anderson, 1983).

We should add that such emission lines are often displaced, and greatly broadened, relative to thermal broadening at photospheric T_e -values. The displacement, and line-breadth treated as a broadening velocity, can be super-thermic relative to classical-modeling T_e -values, is often highly variable, and can differ from ion to ion within the same star. The profile can also change with the size of displacement, although no real correlations between form and displacement have yet been established. All these effects are most marked in the farUV, there for superionized absorption lines as well as for emission, although for certain stars it can be equally striking in the visual. The *largest* "inferred velocities," for both emission and absorption lines, and line-breadths, are usually found in the farUV; notable exceptions in the visual are the novae, the WR stars, and H α in many stars where it is its width, rather than displacement (which is generally small, $\lesssim 100$ km/s), which is striking.

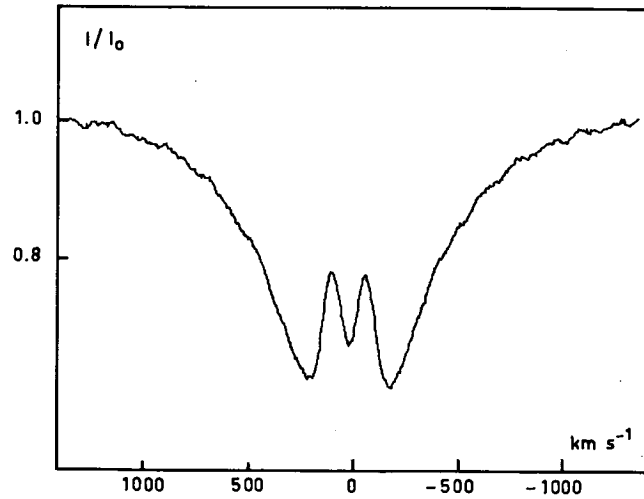
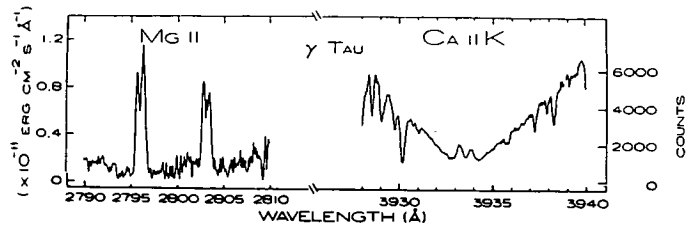


Fig. 3-13. At the top: the Mg II h and k lines and the Ca II K line in the K0 giant γ Tau (from Balinas et al., 1981). At the bottom, the H β profile of a Be star, a Col (B7V $_e$) (from Bijaoui and Doazan, 1979).

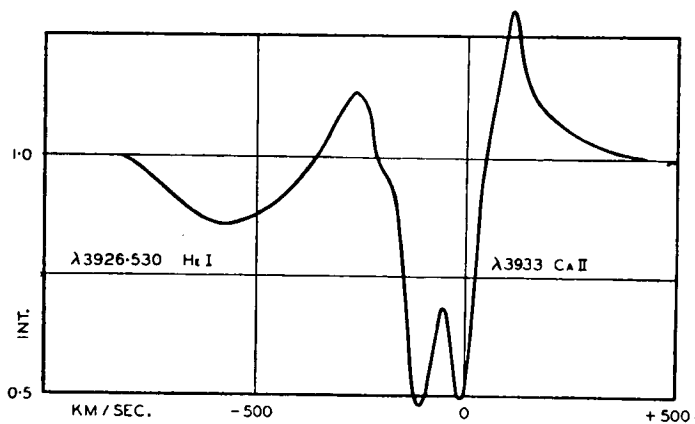


FIGURE 23.

Fig. 3-14. The Ca II K line in the P Cygni-type star, MWC 374. Note the emission wings which borders the narrow and deep absorptions (from Beals, 1951).

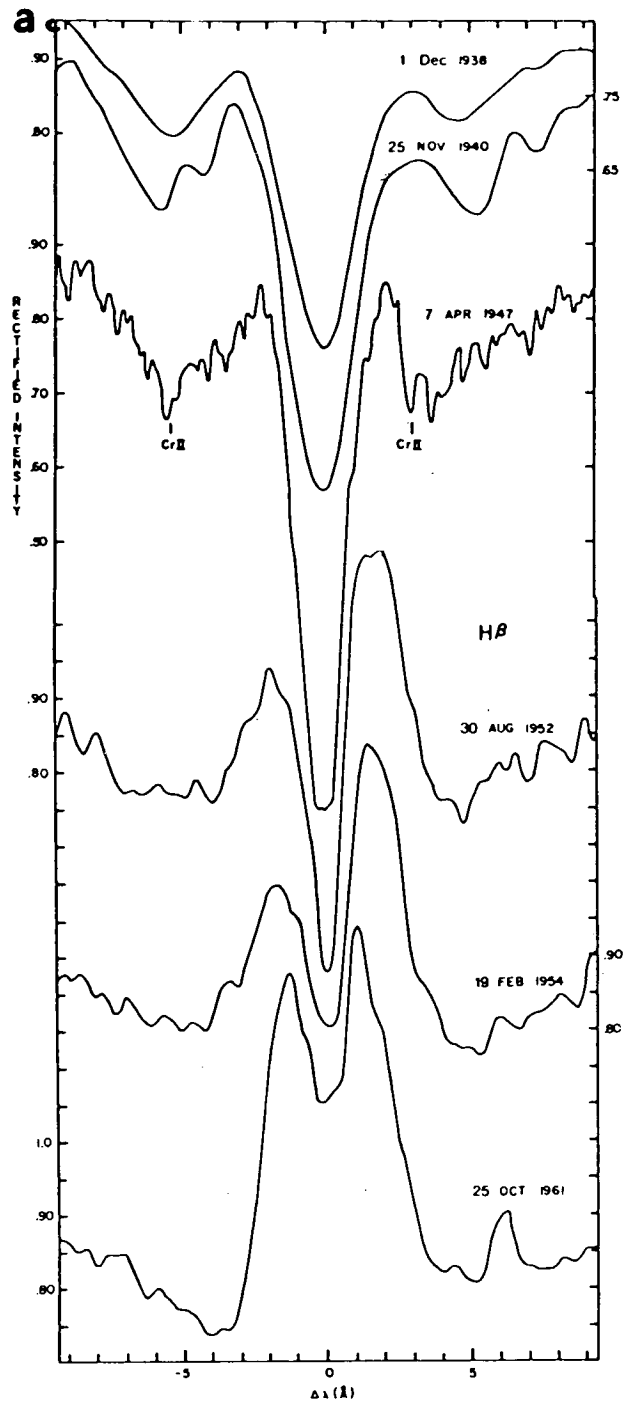


Fig. 3-15. $H\alpha$ -profiles of Pleione from 1938 to 1973 (from Gulliver, 1977). The figure shows the transition from the shell phase to the Be phase. Note the progressiveness of the transition.

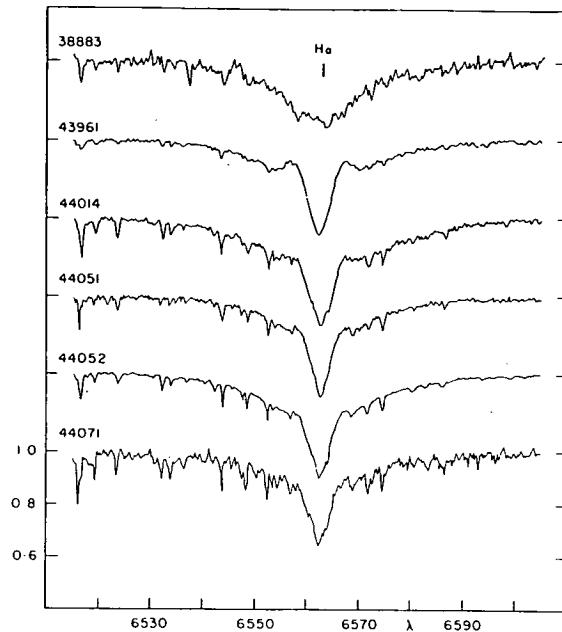


Fig. 3-16. Profiles of the H α line in the spectrum of θ Coronae Borealis, at the beginning of a weak shell phase (from Poeckert and Duric, 1980).

c. **Interpretation/Implication of the Presence of Emission-Lines on Atmospheric Modeling.** As continuously stressed, the presence of the kind of emission-lines characterizing emission-peculiarity implies either or both of a nonradiative heating, and a greater atmospheric extent in the lines than in the adjacent continuum. In terms of our perpetual reference-caricature, there is implied a rise in source-function, and/or an increase in surface area, for that region of line-formation mimicked by the equivalent blackbody source. I use source-function rather than T_e to characterize the radiating surface, because as we saw in Chapter 2 and Vol. 2, it is the integrated radiation field in the line, rather than the value of T_e at the effective atmospheric place of origin of the observed I_ν , which fixes the local value of the source-function. And, this local value of the energy stored in the line is fixed by the distribution of source-sink terms over an extended region around that point. Thus, while the existence of an emission line may imply a nonradiative heating, and rise in T_e , somewhere in the atmosphere, it may not imply this at the place of immediate origin of the observed I_ν . H α , with its photoionization-dominated character, is the outstanding example. But this characterization holds for all other members of that photoionization-dominated class of lines also. As we saw in Chapter 2, the effect of the presence of such lines on a RE T_e -distribution, which is determined by radiation transfer in the continuum alone, can be quite different from that of a line whose source-sink terms are collisionally-dominated. The situation is the same in photosphere or exophotosphere. These facts are critical, when we ask the diagnostic implications on atmospheric extent of an observed strong Balmer emission, and the implications on atmospheric heating that such Balmer emission mainly originates in regions external to the nonradiatively-heated chromosphere-corona. These fundamentally nonLTE facts again become of critical concern when we ask why it is that not only are the H α envelopes located exterior to the corona, but that their T_e lies *below* any strictly-radiatively-controlled values, in regions full of aerodynamic motions. As we saw in Chapter 2, such a nonLTE focus on equivalent blackbody source-function, rather than T_e , to describe emissive properties of, and diagnostic inferences about, atmospheric regions becomes increasingly important as one progresses outward from the low photosphere. Especially for emission lines, it is important to keep such outward evolution in perspective. So, I abstract/preview it.

In discussing classical, geometrically-thin but optically-thick, photospheres, we focused primarily on the thermal, or T_e , character of the equivalent blackbody. Classically, the stellar mass and luminosity fix the surface-area

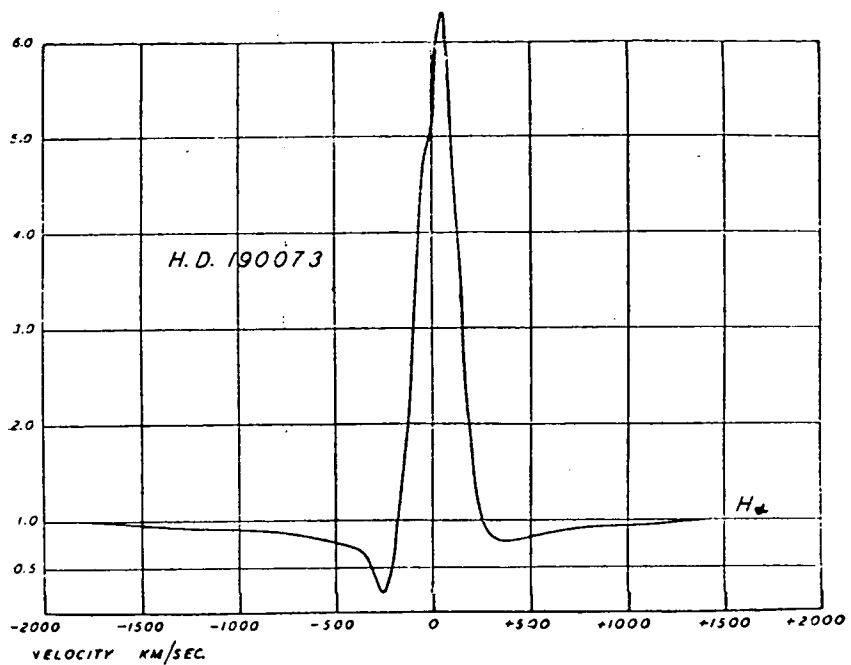


Fig. 3-17a. The P Cygni-type profile of the $H\alpha$ line in the P Cygni star HD 190073 (from Beals, 1939).

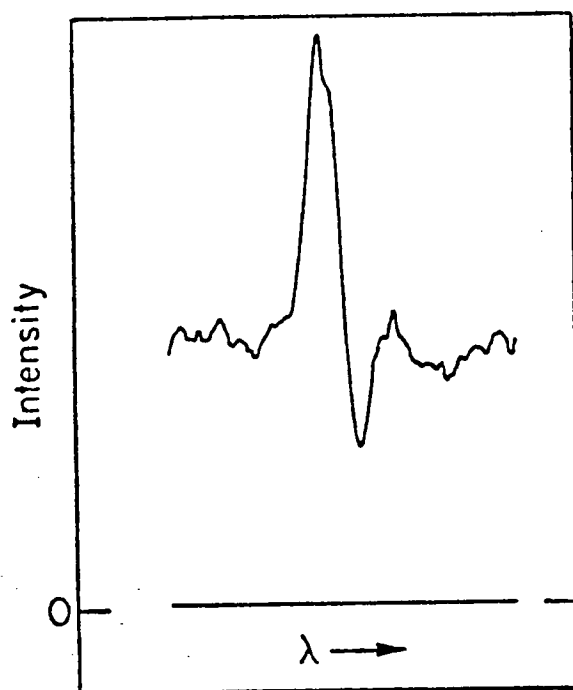


Fig. 3-17b. The $H\alpha$ line of ScrA showing an inverse P Cygni profile (from S. Edwards 1979).

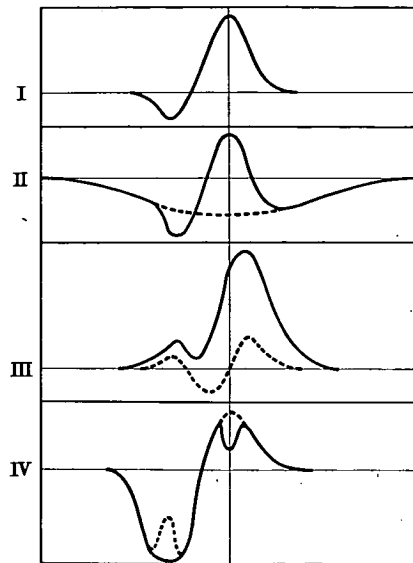


Fig. 3-18. P Cygni-type line profiles
(from Beals, 1951).

of such thermal models. RE, and collisionally-dominated source-sink terms for each radiative continuum, ensure that the emergent radiative flux determines, and is stamped with, the thermal character of the photosphere. NonLTE affects the details, but not the basic relation between flux and T_e (photosphere). In such models, emission lines do not appear. For pulsational, low-radial-amplitude photospheres, the same gross thermal relations hold between radius, radiative-flux, and photospheric temperature. Emission lines reflect only nonlinear pulsation-wave energy dissipation. The cataclysmic photosphere is, during the early stages of the shell-mass-ejection phase, just that finite opacity, effectively RE, ejected mass-shell. Its effective area increases with the expansion; its radiative-flux, and temperature, vary inversely with this area. But this ejected shell ceases to be the "effective photosphere" as soon as it becomes transparent in any spectral region. So at least two effects occur. First, the shell's opacity no longer satisfies LOS, so strong nonLTE effects can occur in its state and spectrum. Second, but with increasingly smaller contribution, it shares the photosphere role with the underlying "newly-emerging photosphere" of the central star. And, as we saw in Section A, such shared role can lead to diagnostic confusion. The "rejected" photosphere, the ejected-shell, evolves through all the aspects of the atmospheric transition-zone as it moves outward. It traverses that particular sequence (Chapter 5) of distinctive atmospheric regions (Chapter 4) which corresponds to the time-history details of the mass-ejection by that particular cataclysmic star. I use the term "mass-ejection" rather than the term "mass-loss" or "mass-flow" to emphasize that, empirically, this mass-loss is indeed an ejection imposed from below, rather than one pulled out from above—by hot-coronal expansion, or radiative-acceleration in nonLOS regions, or etc. As already stressed, a major problem is to distinguish between episodic and continuous such mass-ejections. But the essential point I emphasize here, is the panoramic, striking, guidance given by the cataclysmic stars—or phenomena. In the time-evolution of one episodic outburst of the cataclysmic star, one previews the quasi-time-independent spatial-sequence of atmospheric structure—albeit for a particular pattern of structure—in other stars. In the steady flow between episodic outbursts, one sees the quiet photosphere, overlain by this spatial sequence of regions. The closest "similar," time-dependent, configuration to the cataclysmic stars is that of the Be stars, as they traverse the B-normal, Be, Be-shell phases: but the temporal progression is so slow, and so individual in the relation of episodic and quasi-steady, but time-dependent, mass-ejection as to not yet exhibit the clarity of the cataclysmic events.

Thus, we see that in this evolving-cataclysmic example, the appearance and evolution of emission lines reflect a melange of: radiative heating from a source much hotter and smaller than was the “original shell-mass-ejection” surface during its observed phase of rise to maximum visual luminosity; nonradiative energy dissipation; a mass-flow enlargement of the radiating-surface-area. The problem is to diagnose the relative roles and contributions of these effects in determining the thermodynamic states of the several atmospheric regions and the particular sequence of regions existing for that star, at that epoch.

In each situation of emission line peculiarity, we confront the same simple diagnostic alternatives for interpreting why the lines are in emission relative to the adjacent continuum: either differences in thermodynamic state (in T_e or source-function), or differences in area of radiating surface, of the equivalent “nonEquilibrium blackbody.” And we confront the same necessity to delineate the relative roles of radiative-energy, nonradiative-energy, and mass-fluxes in producing those differences in thermodynamic state and radiating-surface area.

The need for differential T_e effects—i.e., departure from the quasi-isothermal outer atmosphere of the standard model—has long been evident in the visual spectrum of cool stars from the observed Ca II emission cores; in the visual spectrum of hot WR-type stars from observed O VI emission lines; in symbiotic, PN, and novae from the observed forbidden coronal lines; and across the HR diagram in the presence of He I λ 10830, emission or absorption. In the last decade, the ubiquitously-observed presence of superionized lines (Section E), emission and absorption, in the farUV made evident the pervasive T_e effects across the HR diagram, in all stellar types. The need for seeking at least some contribution to the emission lines from enlarged-surface effects is essentially twofold. First, the observed sizes of the emission lines—both intensity and breadth—are very difficult, if not impossible, to produce by only a rise in T_e . The situation is particularly striking in the case of H α , and the arguments are particularly clear, because the source-function for H α is photoionization-dominated, hence, independent of the local T_e , over a wide range of atmospheric regions. We return to the problem in detail, in discussing T Tauri and Be stars in Sections 3.b and 3.c. Here, we only remark that if only chromospheric effects were to dominate, observations of H α and the BaC in the same star must show *detailed correlation in size. It is not enough that emission H α correlates with a reversed BaC jump; the emission-rise across the BaC must match, in size, the H α emission intensity.* This is generally not observed, even though there is a correlation between *presence* of H α emission and *presence* of reversed BaC jump. Second, the general observation of nonthermal mass-fluxes, and superthermic velocities carrying them, means that density distributions in the outer atmosphere are not exponential, but must decrease at the much-slower $(r^2 V)^{-1}$ rate. Present evidence suggests that stars showing visual emission lines have also higher mass-fluxes, at least at some epochs, than stars not showing them. Any relations between actual H α emission at a given phase, and farUV-inferred mass-flux, are not yet well established; indeed there is strong evidence for strong phase differences. So, while the problem is open, the more extended density distribution coming from a mass-flux, and its change with epoch, does seem required. This is the operational definition of an extended atmosphere—equivalently, an increased radiating surface.

The competition between radiation field, nonradiative heating, and mass-flux—as *independently-variable quantities*—becomes increasingly clear: historically, from visual data; currently, from farUV, farIR, and radio.

In the historical approach to peculiar stars, in the various ad hoc models introduced to represent them, one customarily took the radiation field as uncoupled to the thermal state of those exophotospheric regions introduced to produce the peculiarity. We saw that the general radiation field of even pulsating stars and novae is taken as photospheric. Either exophotospheric regions were assumed to be optically-thin, so that the radiation field was wholly determined by the classical photosphere; or the coupling terms, the source-sink terms discussed in Chapter 2, were ignored and the atmospheric interaction with the radiation field was “pure scattering.” Classically, the emission lines in the normal, hot stars were interpreted as arising via Schuster’s scattering mechanism; we have already emphasized the illegitimacy of such interpretation. Such a photospheric-radiative control of the exophotospheric regions of peculiar stars has been widely applied, even up through the modern era of farUV observations, which show superionized species moving at highly superthermic velocities. Such radiative control was imposed equally for the superionized species in the hot, “normal” OB stars—sg, d, sd alike—and the subionized species for the Be stars. In the hot OB stars, one used much imagination to speculate that even O VI was produced under RE and a photospheric radiation field which was opaque in the farUV although transparent in the visual (Castor, 1979). The speculation could

not be supported, and was dropped, but is still quoted. The cool H α envelope of the Be stars was equally speculated to be maintained, under RE, by the photospheric radiation field; the problem of how T_e in this dense envelope, differentially expanding at 1–200 km/s, could be maintained at 10,000 K by a 30,000 K photosphere—as in γ Cas, ζ Oph, 59 Cyg—was set aside. The 10^4 K planetary-nebular H α envelope, surrounding central stars of photospheric $T_e = 3\text{--}10 \times 10^4$ K, was maintained, as already remarked, by impurity cooling, in a low-density nebula, by C–N–O. Ionization was speculated to decrease monotonically outward from the photosphere of the central star; and much supporting evidence was contributed. Such a model is the basis of the classical Stromgren spheres for the extent of H II regions, under RE. Any transfer problems only appeared in the LyC; the source-sink terms were always photo-ionization-dominated, but only in the LyC; the BaC was ignored, as being optically-thin.

Today, we must include the chromospheric-coronal contribution to this general photospheric radiation field of the star. The problem centers around how much nonradiative energy is dissipated, at what atmospheric densities, at what “phases” of the star. Since reliable theory of the size and character of the nonradiative energy-flux is lacking, one must proceed empirically. The cataclysmic example of the phase change in energetic character of the actual photospheric, not chromospheric-coronal, radiation field—from $< 10^4$ K to $> 10^5$ K—exhibits the problems in assuming, a priori, that one knows the reference radiation field against which to infer nonradiative heating. All emission-peculiar stars are hardly as extreme as the cataclysmic. But we note that statistically, Be stars—i.e., B stars exhibiting some degree of emission-line phase—are 1 visual magnitude brighter than ordinary B-stars, of the same MK spectral class (Doazan, in Underhill and Doazan, 1982). In contrast, the statistical visual-excess of the emission-line similar T Tauri stars is less, between 0.1–0.5 visual magnitudes (Kuhi, 1982). And, of course, one can consider that the configuration is not a luminosity excess, but a T_e -deficit in the region of origin of the classification-lines: for both Be and T Tauri. We will comment, in the T Tauri section, on the difficulty of assigning a spectral class—hence, a photospheric radiation field—to some stars, placed in the T Tauri class because of their emission-line spectrum. Our first type of emission-peculiar star/phenomenon considered, the WR, places the problem in even stronger perspective.

And so, at a time when the thermal-coupling between radiation field and chromosphere-corona was being developed for the Sun “and cool stars like the Sun”—presumably including T Tauri—only standard photospheric radiation fields were retained for the hot stars. The suggestions of Joy (1945) and Herbig (1962, 1969) that the Balmer emission in T Tauri stars might originate in a low-lying chromosphere were enthusiastically explored (Herbig, 1962, 1969; Calvet, Kuhi, and Vogel, 1981; Dumont et al., 1973; Cram, 1979; Heidmann and Thomas, 1980)—noting that excited H I was a superexcited, H II a superionized, species for these T Tauri stars. But Balmer emission in the Be, and similar, stars was attributed solely to an extended atmosphere and standard photospheric radiation field—because such atoms are subexcited, subionized in such stars as the Be, and similar. But today, the farUV observations show that the Be as well as the T Tauri, the stars hotter than the 1972-theoretical cutoff in nonradiative energy-flux at spectral class about F4, as well as those colder, have chromospheres-coronae. Thus, all these stars should have contributions to their radiation field from such nonradiatively heated regions. For the Sun, our 1961 empirical-theoretical models—cf Section D—gave a factor 10^6 increase in the LyC over photospheric models, from T_e , not area, effects. So, neither the presence of Ca II emission, nor the absence of H α emission, were any longer anomalous—just peculiar, in the sense of departing, in visual-spectral observations, from either standard thermal models, or LTE diagnosis/modeling of “slightly-perturbed” thermal models. The presence of radiative, and nonradiative, independent fluxes and their effect on structure and diagnostics were self-consistent. But, whereas in the cataclysmic example the increased-area effect of a mass-flux is exceptionally strong, for the Sun it is exceptionally weak.

Thus, we have used as examples two extremes—cataclysmic stars and Sun—to put into focus: (thermal vs. areal) and (radiative-flux, nonradiative-flux, mass-flux) alternative interpretations and causes for emission-line peculiarity. And, we exhibited the diagnostic melange in separating all these. So, we now pass to more-intermediate examples, to which we have already made reference in the above. We have emphasized the photosphere vs. chromosphere-corona contrast in thermal gradients as the first step away from standard thermal modeling and resulting from nonradiative energy-fluxes. Superionized emission lines put this contrast into focus. But, equally, we stress the chromosphere-corona vs. regions exterior to it as the crucial step toward areal differences, and resulting from mass-fluxes.

3. Varieties of Emission-Line Stars; Their Characteristics; and Their Implications on Atmospheric Regions and Regional Patterns

I summarize the characteristics of selected varieties of those stars which are emission-line peculiar in the visual spectrum. I choose these particular varieties, because each illustrates a configuration where the particular characteristics of the particular emission lines, in that star, when viewed against the background of other characteristics of that star, appear to define the characteristics of an exophotospheric atmospheric region, or pattern of such regions. Presumably, such departures from (closed, thermal) models can be linked to what, observationally, distinguishes (closed, thermal) from (open, nonthermal); namely, the several nonthermal fluxes. So I try to make such links explicit, that they may be used in the empirical-theoretical modeling in Part III of the monograph.

Section 3.a focuses on the WR-*phenomenon*, where both visual and farUV emission lines demand both large T_e and large area, hence, nonradiative-energy and mass-fluxes, to produce them. These also produce such large radiative opacities, and such low variability, as to essentially obscure any photosphere produced by radiative fluxes alone, and to permit a free-expansion, free-cooling "upper-corona" to extend very far from the star. Section 3.b focuses on the Be stars and their strongly-variable *phases* where the *visual-spectral emission-lines* demand subionization, low density gradient, and low superthermal velocities, while the *farUV-spectral absorption lines* demand superionization and ultra-superthermal velocities. Their variability pattern, and comparison of phase-behavior of Balmer and farUV measures of mass-flow, demand highly-extended, low-velocity cool envelopes, beginning a few radii from the star, overlying a hot, high-velocity, chromosphere-corona. The Bep phases, when they exist, exhibit low-excitation, low-velocity forbidden lines of those "impurities" which cool the planetary-nebulae. Part of Section 3.c focuses on those cataclysmic stars, the planetary-nebulae, to which the Be, and Be-similar, stars form an actual and conceptual bridge. Their visual-spectral emission lines demand subionization and low-velocity, dilute-atmospheric, extended-atmospheric regions; their farUV-spectral emission and absorption lines demand superionization and ultra-superthermal velocities throughout the interior of the nebula. Their variability is less than the Be, more than the WR; their "local-environment" begins far more distantly than for the Be and the Bep, but is more pronounced and nearer than for the WR. The remainder of Section 3.c "interrupts" the crossroads sequential-pattern of the Be and Be-similar hot stars, to exhibit a Be-similar atmospheric pattern in the T Tauri stars. Taken alone, its visual-spectral emission lines would imply superexcitation. Combined with its farUV-spectral emission lines, the visual plus farUV spectra demand that the visual-spectral emission lines, produced in a cool, extended H α envelope, be subionized, relative to an underlying chromosphere-corona.

This Section B.3 of the discussion of emission-line peculiarity makes a natural bridge to the discussion of symbiotic-star variability, Section C. The "original" symbiotic stars are, indeed, a cool-star extension of the hot star, Be-similar, sequences of stars discussed by early workers in the field. At our epoch, either a literal or conceptual adoption of the basic physics of "symbiotic spectra" broadens enormously the class of stars to which the term should be applied. It also makes clearer the physical significance of such "symbiotic" spectra, in terms of phenomenological patterns linked to patterns of atmospheric regions. When sequences of stellar types are identified, as they have been, it appears that along such sequences, the sizes and variability of nonthermal fluxes and effects progress, resulting in different atmospheric regions, and their characteristics progressing in relative observational importance. In the recognition of such sequences among the emission-peculiar stars, from visual spectral data, I am indebted to, and mainly follow, the pioneering work of the Gaposchkins, Beals, Struve, Swings, McLaughlin, Merrill, Joy and others. To the material upon which their original sequential, and structural, pictures were based, I simply adjoin more modern data, especially from the farUV, and some considerations on thermodynamic consistency. I am particularly indebted to Vera Doazan for an introduction to, and collaboration on, the crossroads nature of the Be stars, as earlier emphasized by the Gaposchkins, Struve, and McLaughlin; and as extended by those modern, farUV, Be-star studies summarized by Doazan in the B and Be volume in the series (Underhill and Doazan, 1982). I am similarly indebted to Len Kuhl for an introduction to the schizophrenic character of Balmer emission in the T Tauri stars—partially from a deep hot chromosphere, partially from an extended cool H α envelope, parallel to that of the Be stars.

I am particularly indebted to Doazan and Kuhl jointly, for the chance to join them in that combined visual and farUV Be star study which has placed in such clear perspective the variable mass-flux aspects which link Be and T Tauri stars to the PN in delineating “local-environmental” effects.

a. WR-Type, Emission-Line Stars, as Limiting Prototype and Precursor

Among all emission-line stars, those showing the WR-type spectrum merit the title of *the* emission-peculiar stars, especially in our sense of peculiarity as guiding the way toward the general pattern of atmospheric structure for real-world, not speculative-theoretical, stars. The general appreciation of this character has evolved enormously over the years, even since 1972 when the speculative-theoreticians dismissed these stars as too peculiar to warrant attention in the controversy over the existence of hot-star chromospheres and coronae (Kippenhahn-Thomas dispute; Jordan and Avrett, 1973). Today, they are often cited as the stars which contribute most to our understanding of stellar evolution under mass-loss (cf Conti, 1980). But actually, those stars showing WR-type spectra are unique among the hot stars in the sense of their farUV spectra showing no surprises, except in minor detail, over the super-ionized, steady-flow at ultrathermic expansion velocities, historically observed in their visual spectra. Also, visual-spectral analysis of eclipsing binaries containing a WR star as one component had long shown strong departure from an exponential density gradient in a vastly extended atmosphere, the gradient being more nearly represented by the $(Vr^2)^{-1}$ distribution in a mass-ejecting atmosphere; and the so-determined, visual estimates of the mass-loss, 10^{-5} – $10^{-6} M_{\odot} / y$, have simply been confirmed by farUV and radio studies. Such yearly mass-loss lies near that produced in one nova outburst (cf Thomas, 1947, 1949; and Section D, here).

Observed *visual* energy distribution, and variety of ionization levels, make this WR-type spectrum, and stars showing it, also unique among *all* stars, hot or cold, with the exception of the Sun. They show no surprises between visual and farUV spectral regions: in demonstrating the production, within the atmosphere of a single star, of those spectral mixtures introducing the concept of a symbiotic spectrum. Indeed in the visual spectrum they show a more extreme mixture of high- and low-temperature phenomena than do the “usual” symbiotic stars themselves, which we survey in Section C. In these stars, and the Sun, it is the variety of atmospheric regions, and of physical conditions characterizing them, rather than variety of “standard-model star” components of a multiple system, which produce symbiotic spectra: *observationally*, not speculatively. We note Payne-Gaposchkin’s comment on seeing the first solar, rocket, farUV spectrum: “It’s a WR star, spectral type WC-6.” We should recognize this same symbiotic character in the spectra of other kinds of single stars, especially Be-similar, but there the range of symbioticity is not so extreme, in the visual spectrum alone, as for the WR. We need adjoin the farUV to the visual, to attain such extreme symbiotic range. So the WR, emission-peculiar, type stars exhibit a range of peculiar phenomena quite beyond only emission lines, in both visual and other spectra.

Third, we note that the WR-type stars do not universally exhibit, or exhibit only sparsely, that variety of peculiarity which in the Be, and Be-similar, stars is so striking. This is the presence of subionized, decelerated-flow, atmospheric regions, which appear to result from an interaction between a variable mass-flow and an induced local-environmental-medium. This is, observationally, a link to the planetary-nebulae. Speculatively, the stellar evolutionists consider it a mark of late-type evolutionary phase. Our focus lies on the requirement of a knowledge of the time-history of the mass-loss. We return to the point. Here, we only stress that just as the Sun and WR stars are linked in clarifying the problem of stellar symbiosis, so are the Sun, WR, planetary-nebulae, novae, Be—possibly the T Tauri—linked in clarifying the problem of subionized, highly-variable, local-environmental media: sequentially, in closeness to star.

Finally, in this abstract of WR-type peculiarity, and probably the most essential in asking what the observed spectrum of a stellar atmosphere tells us, unambiguously, about the general character of the underlying star, we note that the variety of stars showing a WR-type spectrum is very large. Among “field-stars” showing some variety of WR spectrum, Conti (1982) and collaborators have shown that absolute visual luminosities range from -2 to -10 . Masses, inferred from binary studies, range from a few to 50 solar masses. If one adds “strange and massive” objects, such as the exciting object of the 30 Doradus complex (Cassinelli, 1981), or similar central objects in giant H II regions of our own and other galaxies (Walborn, 1981; Conti and Massey, 1981), which show WR-type spectra, the ranges of

luminosities and masses increase by factors of 10. We also note the number of central stars of planetary nebulae showing both WR, type WC, and strong O VI-dominated spectra. If we adopt current evolutionary scenarios for the pre-planetary-nebular phase, their central stars are subdwarfs, masses near the solar. Those WR nuclei among them have spectral type WC. And finally, we cannot overlook the WC6 character of the solar transition-region between chromosphere and corona. *So we apparently have no direct relation between kind of spectrum and mass of the object producing the WR-type spectrum, or its evolutionary phase:* contrary to what is implicit in all standard-model analyses, or taxonomic usages, of stellar spectra.

I long ago suggested (1949) that the WR spectrum of whatever object we regard does not refer to any particular variety of RE and HE photosphere, standard-model or otherwise, but to a chromosphere-corona, produced by the observed, highly-superthermic, velocity field. For these objects, the opacity of chromosphere-coronal regions is so high, that one never sees a photosphere, at least of the "thermal" variety. In this case, where the *observed* mass-fluxes are so large, the mass-flow creates its own "lower-atmosphere;" all the considerations on "normal" stellar spectra, and their diagnostics, fall by the roadside. I suggested, indeed (1968), that one should not discuss *WR stars*, but *WR phenomena*. The chief characteristic of the WR phenomenon would be just this dominant mass-flux, at highly superthermic velocity, which heats as well as distends the atmosphere. Each star has also a radiative energy-flux; just what size radiative flux—per unit area and total—is not clear, from observations. We discuss the modeling of such an atmosphere, as part of a sequential link to other varieties of peculiar stars and atmospheric patterns, in Part III of the monograph—with of course continued reference and contrast to other aspects of peculiarity in the remainder of this Chapter 3.

Evolution in understanding just how a stellar atmosphere arises, just what parameters suffice to specify its state, and the relation of these to stellar-evolution is a slow process. As illustration, I compare my summary of the 1968 JILA colloquium on the WR stars (Thomas, 1968b) with summary comments by Renzini at the 1982 Mexican symposium on WR stars (de Loore and Willis, 1982):

THOMAS (1968): Primary among these questions is whether the WR class consists of a distinct group of objects with a unique initial configuration and evolutionary history, or whether the class consists of objects having an atmospheric configuration which produces the WR spectrum, but which can be reached from a variety of initial conditions along a variety of paths. It seems clear that the atmospheric model required to produce the WR spectrum differs drastically from "normal" stellar models, and that a distinguishing characteristic is a supply of mechanical energy produced by some instability of the structure of the star. But until we can decide whether the "pure" WR spectrum requires only a very large mechanical energy supply, or whether it requires a very special kind of mechanical energy supply, it appears that no conclusive choice between "WR object" and "WR atmospheric phenomenon" can be made.

RENZINI (1982): The fact that similar spectra are exhibited by stars of so different mass, internal structure, and evolutionary phase, can be interpreted as a strong indication that the WR effect is indeed an *atmospheric* phenomenon, always arising once however some particular combination of the atmospheric parameters [temperature, gravity, and composition] are produced.

Stellar evolutionists, spurred by WR-objects, are apparently ready to accept that different evolutionary paths for different objects can produce *apparently* identical atmospheric configurations. As yet, however, they are apparently unaware that classical atmospheric modeling (based on temperature, gravity, composition alone) is insufficient to produce the spectra of those peculiar stars with whom they now collaborate.

Given this abstract, we summarize the details of the underlying observational characteristics of the WR, emission-line, *phenomena*, on which the abstract rests. I base this summary on the evolution from Beals' classical work (1930), described mainly in: the Proceedings of the 1938, CNRS, Paris colloquium already cited; the 1968 JILA Colloquium (Gebbie and Thomas); the 1971 Buenos Aires Symposium (Bappu and Sahade); and the 1982 Mexico

Colloquium (de Loore and Willis). Kuhl's resolution of the problem of increase, or decrease, outward, of T_e in the region covered by visual spectra is summarized in the Proceedings of the 1968 and 1971 symposia. Sahade's 1980 lectures on WR stars at the College de France collects much material, and develops his ideas on a 2-coronal model of these stars in an attempt to reconcile visual and farUV correlations between excitation/ionization and emission-line widths. Willis presented preliminary material on a further discussion of this problem (Stalio, 1983) at the 1982 Trieste Workshop on stellar velocity fields: where Garmany summarized work by herself, Conti, and associates on the range of luminosities and mass-fluxes in the O, Of, and WR stars. Finally, I am indebted to Conti for preliminary material from his WR and O star volume in the present series (Conti and Underhill, 1985). One should also consult the associated work on evolution of WR stars, and their proposed linkages to the Of stars, by Conti, de Loore, Maeder, Chiari, and others, which is summarized in the 1982 symposium reference, as well as in the Proceedings of the 1980 Trieste Symposium on mass-loss and its evolutionary effects (Stalio, 1981). However, these evolutionary aspects are not a focus in this monograph. We ask what is the WR phenomenon, and puzzle at its small variability.

Then from all these detailed references, which contain up-to-date summaries of observations in the visual, farUV, X-ray, radio, and farIR, it is possible to succinctly summarize the observational basis for the above abstracted picture of WR-peculiar stars, without becoming preoccupied with the detailed exposition and substantiation which Conti will present in the WR and O star volume proper. I am indebted to him for much discussion; so far as I can see, we agree in the "kinematic" picture and model of the WR *phenomenon*, as primarily reflecting such a large mass-flux as to dominate the structure of the atmospheric regions where originate the observed spectrum from visual, farUV, and radio. We differ, possibly, in our understanding of the source and origin of the mass-flux and in level of radiative energy-flux; and I set aside those regions of preoccupation with internal structure and evolutionary questions on which Conti focuses so heavily. Then one can summarize the essential features of the WR phenomenon as follows.

CHARACTERISTIC FEATURES OF THE WR-SPECTRUM

Let me first re-emphasize that the WR stars are unique in showing no real surprises in their farUV spectra. One already knew from the visual spectrum that the atmosphere embraces conditions producing a wide range of ionization, extending upward to species like O VI and N V. The WR visual spectra show subordinate lines of such ions, in contrast to the resonance lines observed in the farUV for WR, and most other kinds of stars. So the WR visual spectra simply tell us that such superionized regions, now recognized as universal among all stellar types, contain much more material in those stars showing WR-type spectra. Nonradiative heating begins deeper, in mass and opacity. In the same way, the prevalence of superthermic—indeed reaching superescape—velocities in such visual-spectral ions simply tell us that these ultravelocity atmospheric regions also contain much more material than do these regions in most other stars. Acceleration, impulsive or gradual, begins deeper, in mass and opacity. Ordinary novae—possibly other varieties of cataclysmic stars—eject their photospheres; so at least their *episodic* mass-fluxes are very large. A strong acceleration—apparently impulsive—begins deep, in mass and opacity. Apparently WR stars eject their chromospheres; so their *continuous* mass-fluxes are very large. A strong acceleration begins deeper for them than for other stars, except novae. We already remarked that the *continuous* mass-flux of a WR star, integrated over one or a few years, gives the same value as the one-episode ejection of a nova. One must be careful on such estimates of mass-flux; especially where, as for the novae, it is based on integrated H α observations. We return to the point, in discussing Be stars. But the point is nonetheless valid. Set aside the question of *why* and *how* a nova ejects its photosphere (and regions above), and a WR-object ejects its chromosphere (and regions above). That they do—i.e., that the outflow velocities are so high at such large densities—is a *kinematic, not dynamic, representation of the large mass-fluxes of these objects*. And it shows—observationally—that the time-integrated mass-loss, and kinetic energy contained in it, are not so different for WR and novae. We continually return to this point. Here, we stress it simply in terms of putting into perspective visual and farUV results, and contributions to the picture of the WR phenomenon. We stress that the farUV addition to the nova—and other cataclysmic stars, including the PN—lies in showing the continuous as well as episodic nature of mass-loss, possibly of other nonthermal fluxes. In the WR case, the farUV data offer more details, not strikingly new results. *But* they offer these details as more firmly establishing the sequential location of WR among other peculiar stars.

So in the following listing of WR characteristics, I first give the visual-spectral picture; then adjoin what the farUV has added. One more point must be emphasized. Contemporaneously with spatial observations have come increased, ground-based, farIR and radio data. These are presently not too extensive, but they have added important information. I include these, to the extent they are available. So the following is an update of my 1968 abstract, where I proposed *WR-phenomenon, rather than WR-star*, as more consistent with observations; I hold to that viewpoint.

[1] The outstanding spectral character is that the WR is an emission-line spectrum, with the following qualifications:

[1.a] P Cygni absorption components are observed on the blue edges of some emission lines: not always the same lines, in different stars.

[1.b] Some few WR objects exhibit intrinsic absorption lines; even one has observed hydrogen Balmer lines proper (Niemela, 1973). Usually, but not always, when such absorption lines are observed in WR objects, they are attributed to binarity, and to arise in the second companion. Recently, however, the existence of hydrogen absorption lines in some definitely-single WR stars (Massey et al., 1981) has been shown.

[2] The emission lines are very broad, 10–50Å; the breadths vary with the line, and with the star. Interpreted as nonthermal velocity broadening, velocities of $\approx 10^3$ km/s are required. This is the same size as that expansion velocity required by the P Cyg absorption-component shifts. Discussions of velocity correlations with other things are *usually* based on such line-widths, not P Cyg absorption shifts.

[3] The emission lines represent a wide range of ionization, and excitation within a given ion. Ionization levels range from H I to O VI, in the visual; but Barlow, Blades, and Hummer (1980) claim to have identified O VII and O VIII in at least one WR star. In the farUV, a wide range of ionization is observed, up through the C IV, N V, O VI isoelectronic Li sequence. Only novae and some symbiotic stars show, in the visual, such an ionization range. But again we have Payne-Gaposchkin's remark: the visual WR ionization range is characteristic of the solar chromosphere-corona transition region, as observed in the farUV, which also characterizes the WR farUV, and the farUV of most other stars (cf Section E).

We also note that forbidden Fe X, XIV, and Ca XIV lines are observed, faintly, in the visual solar spectrum, essentially because of the large solar atmospheric volume at those T_e where such lines can be produced. In both Sun and stars, resonance lines of such ions are excluded from observation in the farUV by the present spectral cutoff near λ 1200 for the IUE. We have remarked that the forbidden coronal lines have been, on occasion, observed in novae and symbiotic stars. To my knowledge, no such observations have been reported for WR stars.

[4] I have called the emission lines in [3] superionized. For nonWR stars, where some continuum is observed, and photospheric properties inferred, superionization is relative to photospheric T_e . The history of attempts to attach a color-temperature, or effective-temperature, to WR stars does not inspire great confidence in such photospheric T —indeed, even in the existence of such photospheres which, as remarked above, it is not obvious that we see. The earliest attempts (cf 1938 CNRS Colloquium) at estimating T_c ranged from some 15,000 K to 10^5 K. Kuhl's 1968 summary found T_c highly variable with λ : in the visual spectrum, it ranged from 10^5 K at λ 3500 Å to 10^4 K at λ 9500Å. Underhill (1982) adds farUV data to her earlier visual studies to set a range 1.8 – 4.0×10^4 K for T_{eff} , with concentration between 2.5 – 3.0×10^4 K, for nine WR stars. A careful study by Fitzpatrick, et al. (1982) of a WC7 star, continuum observations in the spectral range λ 1200– λ 12,500Å, finds a $T_{\text{eff}} \sim 43,000$ K. This result is *highly* dependent on the extinction correction; indeed, it is essentially fixed by it. Comparison of their discussion with a similar one for a Bep star by the same authors (Sitko and Savage, 1980) exhibits the generality of the problem, and uncertainty of conclusion. Studies by Willis and Wilson (1978) and Nussbaumer et al. (1982) add more data to these farUV and visual studies, and the extinction-correction problem. All these results are for “field-WR stars,” not for the WR-type central stars of PN. If one argues that these latter stars have the very high T_{eff} associated generally with such observed central stars, the situation is interesting, especially as regards the following.

Here, in discussing WR stars, and especially the problem of their mass-flux, our principal interest lies in asking just how much energy does lie, intrinsically, in the radiative flux—for itself, for “photospheric” structure, and relative to the energy in the mass-flux. For the ordinary nova discussed by Pottasch, we found a factor of 3 greater

energy in the mass-flux than in the radiative energy-flux at outburst. Willis (1982a, 1982b) gives factors ranging between 0.04 and 0.60 across the range from WN to WC stars. *Statistically*, and one should be cautious, the WC stars show the larger values. We return continuously to this problem, in discussing our (empirical) sequence of emission-line stars, in comparing them to the cataclysmic, and to other varieties of peculiar stars. The value of this parameter (energy in mass-flux/stellar luminosity) is obviously highly significant in any discussions of origin and size of mass-flux.

[5] Beals' early work on the visual spectrum established an anticorrelation between line-width and ionization-level: the higher the ionization, the smaller the line-widths. By a variety of observational arguments, Kuhl (1968, 1971) established that ionization, and T_e , decrease outward, while expansion velocity increases outward, in the atmospheric regions where these lines arise. I tried, unsuccessfully (1949) to construct models with an outward-increasing T_e associated with a deceleration of the expansion velocity.

In the farUV, the observed inverse correlation between line-width and ionization-level found in the visual spectrum is reversed. Line-width increases with both ionization, and excitation-level of the lower level of the transition. Sahade has used this trend to infer an outward increase in T_e , in regions exterior to those covered by the visual data, to a second T_e -maximum. He and Zorec (1981) attribute this T_e -rise to the mass-flow from the WR star impinging on a second stellar component, producing a shock. So, for these authors, this phenomenon is theoretically limited to binaries; observationally, it does not seem to be the case. We note, of course, that a second-shock-produced, T_e maximum is to be expected in all those single-star atmospheres showing a decelerated mass-flow, as in the PN, Be, etc. stars. The whole question is the geometrical and opacity extent of such a region, that is permitted by radiative cooling. We return to the point in Part III, and here in Chapter 3.

By contrast, Willis (1982a, 1982b) recasts these correlations of line-width with excitation-ionization into one with excitation of the lower level, across visual and farUV regions alike. All show a decrease in line-width with increasing excitation. For several stars, he shows that using a velocity from P Cyg absorption component displacements, instead of emission-line-width, gives a similar trend. To interpret this result, he adopts a monotonic outward increase in expansion velocity, but a "frozen-in" excitation-ionization state of the material, for flow densities below a certain value. Thus, relative to our present focus on monotonic or nonmonotonic expansion velocity, and its link to variability vs. nonvariability of mass flow, this model expects a similarity between solar and WR outflow, on which, indeed, Willis and Zirker have remarked (Stalio, 1983).

[6] A major fraction, possibly as many as 50 percent, of WR objects are associated with nebulosity: H II regions, and planetary-nebulae. By contrast to the Be stars, the radii of the H II-region nebulosity are large: small nebulae, associated with individual stars and called *ring-nebulae*, have some 10 psc diameters: larger H II nebulae are associated with OB clusters. Planetary-nebulae whose central stars are WR-objects *apparently* have no distinct size-differences with other PN but such data are very sketchy. Sahade stresses the difficulty of distinguishing between PN and ring-nebulae, suggesting that one criterion be radio thermal emission, and $\lesssim 100$ km/s nebular expansion velocity. FarIR and radio data are not extensive, but suggest IR and radio excesses, variously attributed to low-temperature plasma and dust emission, from regions at 5–100 photospheric radii (Cohen and Vogel, 1978). One should note the recent speckle-interferometric study by Dyck, et al. (1982) of a WC9 star, which shows an IR halo at about 3×10^{16} cm—about 10^4 photospheric radii. They interpret the halo as produced by scattering from circumstellar grains. So we have distinctly conflicting evidence as to whether the WR mass-flow is decelerated, then cooled, far (\gtrsim psc) or near (\lesssim PN nebular dimensions, $\sim 10^4$ – 10^6 photospheric radii, < 0.1 – 1 psc). The question is a basic one, as we stress in Part III. Willis (1982a, 1982b) summarizes the literature on the production of ring-nebulae, especially in its relation to energy or momentum balance. I stress that our present focus lies on whether or not such "nebulae" are produced—empirically, not theoretically—close to the star: *very* close, as for the Be stars; or far, as for the PN; or *very* far, as for the WR—as a "variable mass-flux created" local environment. Or does such interaction only occur with the local ISM, very far away?

Finally, one notes that those WR stars associated with the far-out, H II region nebulae are usually WN type, contracting to the WC found in PN.

[7] Evidence for a marked variability in the WR phenomenon, especially its outstanding characteristic of large mass-flux, is small. While very strong variations in line-profiles have been observed, these occur, mainly, only in binaries. Among definitely-single stars, small, irregular changes have been noticed. Indeed, prominent He II lines have been observed to disappear at some epochs. But variability is in no way as pronounced as in the Be stars, nor is it as marked as among other hot sg. The possible exceptions are the WC central stars of some PN, in giving "close" nebula, but not directly measured—only inferred—variability, as for other PN. We return, to stress this point, in those stars that exhibit strong, but also variable, mass-loss, when discussing local environment changes, in the Be stars. The idea of a variability in mass-flux being linked to the production of a "near" nebula, rather than all nebulae being linked to a constant mass-flux interacting with the local ISM, arose in considering the origin of the planetary-nebulae (Kwok, 1980, 1982; Purton et al., 1978). The association of such variable mass-flux with the properties of the H α envelope in Be stars (cf summary in Doazan, 1982) extended the idea. So, these points [6] and [7] are strongly linked.

[8] The ensemble of the preceding observed characteristics show the WR emission spectrum as something which is characteristic of a particular star for a long time interval (4000 years, for γ Vel), varies little (during 100 years spectroscopic observation), and gives little evidence of a decelerated flow near the star (during 15 years spatial observation). These characteristics serve to put into perspective what is the most striking feature of the inferred mass-loss for the classical, or field, WR stars: it is practically constant across the whole range of such stars, at a mean value of about $3 \times 10^{-5} M_{\odot}/y$. There is a small range, compared with that found in the OB stars, from about 10^{-5} for an Of sg like ζ Pup, to some 3×10^{-5} for a late-type WN star (WNL), to some 3×10^{-4} for early-type WN (WNE) and WC stars. But there is much scatter about this subclass dependence. These data are from Willis (1982a, 1982b). He stresses that there is also a growing strength of emission lines along the (sg and/or g, not MS) sequence: O V—Of—WNL—WNE—WC; hence, he infers a development of denser winds along this sequence. Finally, he also finds a steady increase in "terminal" velocity of the mass-flow toward earlier type, individually within the WN and WC sequences. I reproduce his velocity data in Figs. 3-19a, b; the mass-loss data for OB and WR stars of Conti and Germany in Fig. 3-20; and the details of the WR mass-loss data compiled by Willis in Fig. 3-21. To reconcile all these data, Willis infers that the velocity acceleration must be progressively less-steep along the above-mentioned O V—WC sequence.

One wants to put into careful perspective any conclusions on steepness of velocity laws, especially as they relate to size of mass-fluxes. We note that practically all discussions of hot-star velocity fields, including those of the WR stars, are made relative to the radiative-acceleration theories of mass-loss. We comment on these, especially relative to observations, in Section F. Here, we note only that such theories effectively reduce to motion under quasi-constant acceleration, and give a velocity-dependence on radius which is effectively $(1 - (r_p/r)^a)^\beta$, where r_p is photospheric radius and a and β are parameters. But as we continually stress, the important quantity in fixing *size of mass-flux* is the geometrical location of the thermal-point—that point where flow-velocity comes within a factor 2–3 of the 1-dimensional flow velocity. Below this point, density decreases exponentially outward; above it, as $(r^2 V)^{-1}$. So, kinematically, the lower the thermal point, the larger the mass-flux, *exponentially in height of thermal point*. Thus, the velocity law in the region where one observes the WR emission lines has little to do with the size of the mass-flux. What is important, is knowing what fixes the size of the velocity in the region below that observed. We emphasized this in discussing cataclysmic stars, again here, and in the following. It forms the basis for our empirical-theoretical modeling in Part III. Empirically, we note that the thermal point for the Sun occurs at particle concentrations near 10^5 – 10^6 ; for the WR stars, $\geq 10^{14}$ (cf Section D). Kinematically, this is the difference in their mass-fluxes.

[9] I have deferred to the last characteristic spectral feature, that one usually stressed first, after emission lines: the division of WR visual spectra into carbon, WC, and nitrogen, WN, varieties. In the visual WC spectrum, lines of carbon and oxygen predominate, with few lines from nitrogen. In the visual WN spectrum, lines from N dominate, with few from C and O. However, the C IV farUV doublet at $\lambda 1550$ is observed in essentially all WR spectra, WN as well as WC. Often, the $\lambda 5801$ and 5812 C IV lines are also seen in WN spectra. But generally the strongest C III lines are not seen in WN spectra; when they are, the object is called "mixed," WC+WN. One says that rarely are N lines

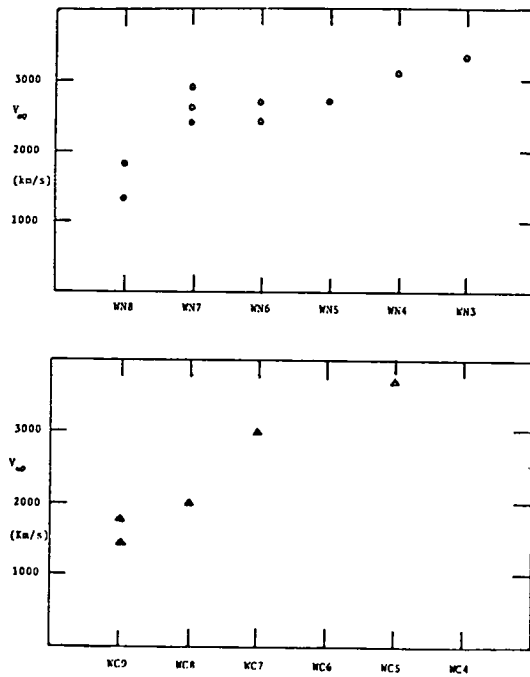


Fig. 3-19. Stellar wind terminal velocities measured from high-resolution IUE P-Cygni profiles of UV resonance lines, plotted as a function of WN and WC subclass. A good correlation of V_{∞} with WC subclass is apparent (from Willis, 1982).

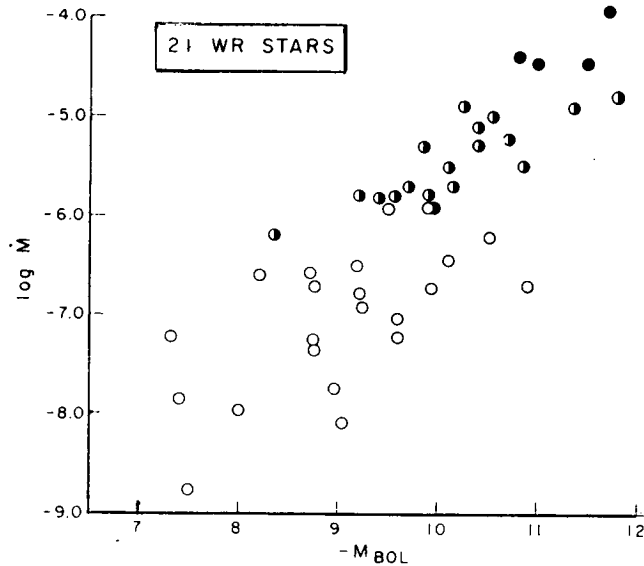


Fig. 3-20. Mass-loss rate as a function of luminosity: \circ —rates determined from UV data; \bullet —rates determined from optical and/or continuum data; \bullet —rates determined from radio data (VLA) alone. Different methods sample different mass-loss rates. There is some overlap in determinations for those stars indicated by half-filled symbols (from Conti and Garmany, 1981).

theories, introducing multiple scattering, still do not suffice. Hot-coronal type mass-losses are even more inadequate. The WR stars simply join the cataclysmic to put into strong focus the significance of the mass-loss as *the* parameter giving to stars their character of being open thermodynamic systems. Simply recognizing such character alone does not, of course, tell us anything about the structure of the star, or its evolutionary state, nor does it specify the precise nonthermal mechanism, or configuration, producing the mass-ejection. And, of course, the cataclysmic plus WR categories of stars apparently demonstrate that it is inadmissible to assume that the luminosity measures the energy produced by the star, by whatever mechanisms. So, I make no further comment on the WR stars, but pass on to other peculiar stars—but with the same questions, on the basic thermodynamic character, and how to represent it, of stars, their atmospheres, and their environments—ambient, or stellar-manufactured.

b. The Be Emission-Line Stars: Crossroads of a Variety of Stellar Peculiarities; Intermediate Between WR-Phenomena and Cataclysmic-Ejection in Mass-Flux Characteristics; Sequentially-Linked to Symbiotic, T Tauri, and Planetary-Nebulae in Local-Environmental Creation Via Variable Mass-Flux

Among the emission-peculiar stars, those showing the greatest number of other types of peculiarity are the Be stars. Again, I use peculiarity not only in its visual-spectral definition, but also in our broader sense of guiding the identification of the variety of exophotospheric regions, and atmospheric patterns, which exist in real stars. In the Be and Be-shell visual spectra alone, one observes strong: *variability*; *emission-lines*; *extended-atmosphere effects*; *symbiotic* effects, but in the sense of *subionization* being prominent rather than *superionization*; *superthermal velocity* fields. When one adjoins the farUV, X-ray, farIR and radio spectral regions, the great wealth of peculiarity relative to thermal atmospheric structure—and its links to the nonthermal fluxes of energy and mass—multiplies. Their subionized emission lines in the visual link these Be stars to a broad range of emission-peculiar hot stars, with cool extended-atmospheric regions, expanding at superthermal, but small, velocity, and variable in time-scales ranging from abrupt and short to very long. But the superionized, ultra-superthermic absorption lines in the farUV show that the cool regions producing the emission lines are underlain by hot, rapidly expanding chromospheric-coronal regions. These expand so rapidly that the atmospheric material must be strongly decelerated, to form those overlying cool, slowly-moving atmospheric regions which evolve, in a way similar to the planetary-nebulae, into a local environment produced by the star itself, not by the collapse of its aboriginal environment. And, the incompatibility of mass-fluxes inferred from the farUV, rapidly moving, superionized lines with those inferred from steady-state models of the H α envelope, demonstrate the need to know the time-history within “cycles of mass-flux enhancement” for these Be, and Be-similar, stars. This is an abstracted panorama of our present empirical-theoretical understanding of the Be star contribution to exhibiting the variety of stellar atmospheric and local environmental structure. We proceed to summarize its basis.

In Section 2.a above, we defined a Be star as one in luminosity classes III-V which has shown, at least once, H α in emission. We noted that historically, most sky surveys were made in the visual; so most Be stars were detected from H β , rather than H α , in emission. We also noted that when the Balmer lines are strongly in emission, there is often observed emission in Paschen lines. Finally, hydrogen emission lines are often accompanied by singly-ionized metallic, usually Fe II, emission-lines. We noted that a Be-shell spectrum is simply one with narrow and deep absorption cores in the hydrogen and metallic lines, with or without emission wings. A B-normal star is simply that: an absorption-line B star; such absorption lines are broad, not at all shell-like. Some 20 percent of the stars in the B-class satisfy the Be/shell criteria, this designation being for a star which is *either* Be, *or* Be-shell. Some 80 percent of the B-type stars have, during the various epochs of their observation, shown only a B-normal spectrum; other stars have shown at least two kinds; some, have shown all three of Be/shell and B-normal, sometimes more than once. Wholly empirically, then, it seems not justified to consider these three spectral types as being different objects, but justified to regard B-normal, Be, Be-shell as simply phases, between which at least some stars can pass, even though we do not know how or why. We adopt this convention: putting all B-type stars, luminosity classes III-V, in one of the three phases, *at a given epoch*. The degree to which the phase-characteristics are shown, can range from very small to very large. Fig. 3-22 shows the succession of phases shown by 59 Cyg, at the indicated dates; Fig. 3-15, Pleione. The appearance is a strong function of resolution. Fig. 3-23 shows E W Lac under high and low resolution at the same date. Given these definitions, it is hard to see where any confusion arises on the *spectral definition* of B-star phases;

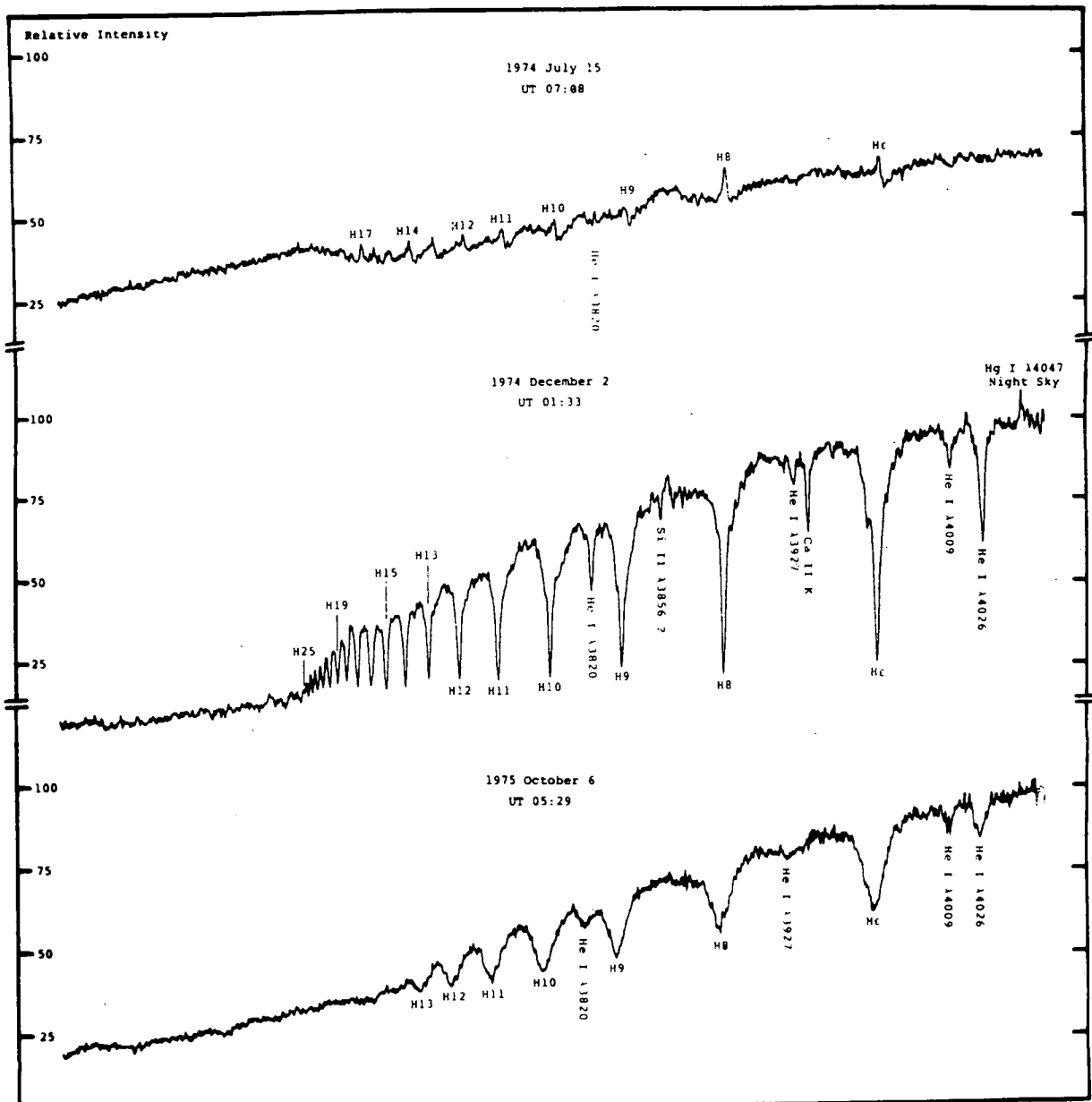


Fig. 3-22. At the top, is shown the spectrum of 59 Cyg in July 1974 during the strong second Be phase. The Balmer line emission is seen until H17. He I, $\lambda 4471$, and Mg II, $\lambda 4481$, are both in emission; the Balmer discontinuity is in emission.

Below is shown the spectrum of 59 Cyg in December 1974 when the shell spectrum is completely developed. Shell absorption in the Balmer lines is observed until H25 and singly ionized metals are strong in absorption. All the photospheric lines are enhanced and strongly affected by the shell component, as is seen in the He I lines, for example. Note the large Balmer discontinuity in absorption.

At the bottom, the spectrum of 59 Cyg in October 1975 looks like that of a normal B star in the photographic region although H α is still fairly strong in emission (from Barker, 1979).

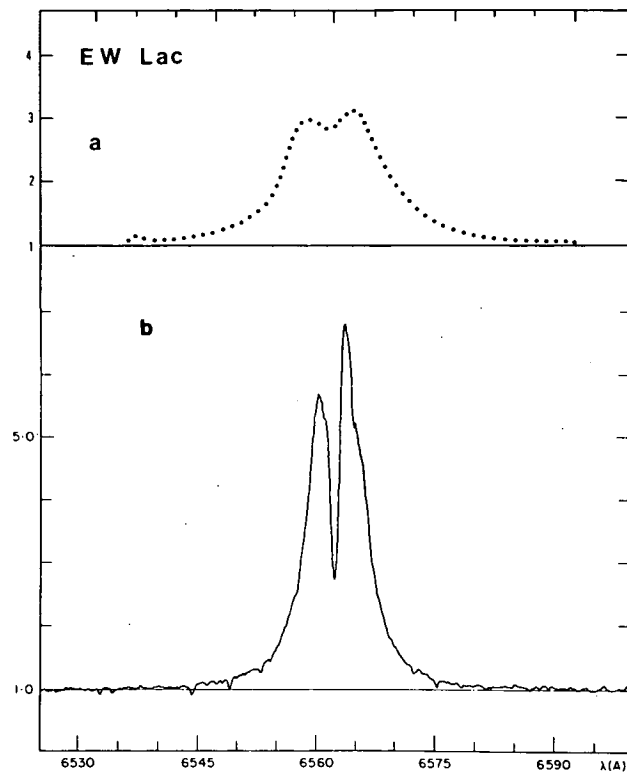


Fig. 3-23. H α profile of EW Lac whose spectrum shows pronounced shell characteristics: (a) at low resolution (Slettebak and Reynolds, 1978); (b) at high resolution (Poekert, 1980). Note that the shell characteristic, i.e., the narrow and deep self-reversal, is completely wiped out at low resolution and is similar to a self-reversal of a Be spectrum.

clearly, there can be much confusion in explaining how the spectra, and phases, are produced. Struve (1931a) was the first to suggest an extended atmosphere as the origin of the emission lines, following models of WR stars and novae by Menzel (1929) and Beals (1930). Struve's last model (1942) of Be, and Be-similar, atmospheres rested on analogy to the extended solar atmosphere. In the following, we summarize all this, following the pattern of these analogies and similarities in atmospheric structure, and their relation to nonthermal fluxes, as we did for the cataclysmic and WR stars in the preceding.

Along with the WR stars and the Sun, the Be are the oldest known, and the longest studied, of the peculiar stars; each of these type were identified in the 1860's, because for us, they are *bright* peculiar stars. This same characteristic has, over the years, given us details on their atmospheric structure, and stimulated that non-standard atmospheric modeling whose need was not so observationally-demanded in other stars. The Sun gave us the first evidence, and numerical details (cf Section D), of low-density atmospheric regions of very great extent: their sizes are measured in photospheric radii, rather than in standard-photospheric density scale heights. Both quasi-static and dynamic such regions exist. Today, most solar studies focus on the effect of hydromagnetic "activity" on such extended atmospheric structure, and its extension to solar-similar stars (cf Jordan, 1981). As we just saw, the WR stars gave us the first evidence that such extended atmospheres are linked to a continuous, significantly-large mass-flux from the stars; and that such mass-flow can change completely our picture of atmospheric structure in even high-density regions. Today, most WR studies focus on the stellar-evolutionary effects of such mass-loss (Chiosi and Stalio,

1981; Conti and de Loore, 1979). The Be stars gave us the first evidence of extended, cool, high-density atmospheric regions for hot main-sequence stars; and that such atmospheric regions must apparently disappear and reappear, as a given star changes its spectral appearance to B-normal (absorption-line star) to Be (emission-line star) to Be-shell (shell-line star), in any and all directions, in a variety of time scales. These stars also inspired the first suggestions that a main-sequence mass-loss was produced by a subatmospheric nonthermal structure (Limber, 1964, 1967, 1969), rather than by a radiation-pressure (Gerasimovic, 1934). Over the years, the classical ad hoc models of the Be outer atmosphere as a uniformly-cool, equatorial disk, controlled by the photospheric radiation field and a superthermic, but slow and non-dissipative, mass-ejection have very considerably evolved. Today, most Be studies focus on diagnosing ever-improving data to learn just what actual atmospheric model—and its time-dependence—it is, that an adequate theory must predict—or at least represent. We are certain only that it must be more spheroidal than disk-like, must include a very hot chromosphere-corona above the photosphere, where velocities can reach 2000 km/s; must retain an overlying, cool, relatively-slow moving H α envelope; and must incorporate a cooler region to produce permitted Fe II, and forbidden nebular, lines, possibly dust, far enough out from the star. But most important of all, we have learned the great importance of gross time-dependent changes in post-coronal structure. A century of visual observations has shown us what such changes are; a decade of farUV data has shown their phase-lagged link to the mass-flux and its variability. We find the same need to consider the interaction between a continuous, and an episodic, mass-ejection that arose in discussing the cataclysmic-peculiar stars. We find the interesting contrast between cataclysmic, Be, and WR stars already remarked. The most direct way of putting into focus the details of this material on the Be stars is by being more explicit on just this WR, cataclysmic, Be comparison. We proceed to do so, as the first aspect of the following.

In addition, both historically-accumulated visual data, and newer farUV data, emphasize the strong variability of atmospheric patterns for the Be stars: within a given star, and between two stars of the same visual luminosity and gravity. Contrasting with, and complimenting, such individuality is the strong sequential link found between the Be and “Be-similar” stars. This last aspect should not be surprising; it was the basis of the model of the exospheres of hot, Be-similar, stars proposed by Struve (1942), cf (ii) following, based on analogy with the solar chromosphere-corona, at an epoch when these solar regions were still modeled as cool, but progressively-dynamic, as one went outward in the solar atmosphere. So, just before the “hot solar-corona” epoch arrived, and considerably before the spatial epoch, Be-star modeling had progressed from Struve-Epoch-I, equatorial disks; to Struve-Epoch-II, spheroidal solar-Be-similar. The problem seems to be that among most Be modelers, one focused on Struve-equatorial, ignoring Struve-solar. Among the solar-modelers, high-density, cool, H α emission regions did not seem particularly useful for solar studies, even though such solar-stellar links are always useful for better understanding stellar atmospheres generally. Unfortunately, solar coronal densities, at the thermal point, have already decreased to 10^6 , while Be emission-envelope densities are 10^{13} – 10^{10} . As we will stress in Part III—cf the preview of Part III bis—it is the Be-similar PN—the Be stars being “little planetary-nebulae,” according to McLaughlin—where the comparison is most appropriate: solar-coronal densities are reached only at an r/R (photosphere) of 10^4 – 10^6 – 10^8 , for the PN. The solar-system environment is a vacuum, compared with that of the PN. Which is, of course, all the more reason to study the two simultaneously, if one has a really catholic interest in atmospheres + environments—simply to ask, *WHY* the difference? To which a tentative answer *appears* to be: size, and variability of a mass-flux.

So I structure this empirical-theoretical summary of the Be stars around these two comparisons: WR-cataclysmic-Be; and Be + Be-similar stars. Clearly, I draw heavily on the Be volume in this series (Underhill and Doazan, 1982) which represents the most current global survey of available observational material on Be stars, and a critical discussion of current modeling. One should also read carefully the Be sections of three other volumes which have appeared this year, as well as the extensive journal and IUE symposia literature. IAU Commissions 29 and 36 sponsored a symposium on Be stars in April 1980 (Groth and Jaschek, 1981) which gives a good idea of the diversity of thinking, and the data supporting it, on the Be problem. de Jager (1981) and Kitching (1982) devote considerable space to putting these stars into perspective. Unfortunately, I find these last two books not as current as one would like, on contemporary observations, modeling, and such physical concepts as electron-scattering being *not* useful in emission-line production. For this reason, I follow the comparison of Be to the other mentioned peculiar stars with a quick commentary on the current status of such things as equatorial disks, binarity, etc.

i. Be vs. WR-Type Phenomena, Against the Cataclysmic Star Background

α. The Visual Spectrum. The immediately-striking, visual-spectral, similarity between the two categories, WR and Be, is the presence of strong emission lines. The immediately-striking visual-spectral contrast between the two is the superionization character of the WR emission lines—up through O VI; and the subionization character of the Be emission lines—hydrogen and Fe II lines. To produce the WR-type lines, we require chromospheric-coronal T_e . In normal star taxonomy, the hydrogen absorption lines reach their maximum strength in the A stars, decreasing in strength from A0 throughout the B class. Emission H α reaches strengths more than 10 times the continuum, in early Be stars like the first one observed, γ Cas, or that for which the widest range of spectral and temporal data currently exist, 59 Cyg. Moreover, Fe II, characteristic of the normal A0 sg α Cyg, is not found in normal B stars, but is strongly characteristic, in absorption, of the Be-shell phases; occasionally, it is observed in emission, at such phases. Especially for such hot stars as ζ Oph, γ Cas, 59 Cyg, we have to cool the exophotosphere, relative to the photosphere, very considerably, to produce such emission lines—not heat it, as for the T Tauri stars. Small wonder that Struve left his 1931, WR + nova-analogous model to propose the 1942 pre-Edlén, cool solar chromosphere-corona-analogous model. Moreover, this shift in thinking was aided by the further contrast in the visual spectrum: the ultrasuperthermic velocities associated with the superionized lines in the WR-spectrum are, typically, ~ 1000 km/s; while the Be emission lines show no line-displacements, or displacements of their absorption components, exceeding about 100 km/s. Finally, a major visual-spectral contrast between the two types of stars lies in their variability: it is minor in the WR stars, major in the Be stars. Indeed, the character of the Be spectrum can change very abruptly. McLaughlin's 1948 description of 59 Cyg is still typical—"characterized by long periods of quiescence and short periods of activity." Data are not yet sufficiently precise to attach typical time-scales to the several variable features of Be spectra—if indeed there are typical values for such; what exists, is summarized in Doazan (1982). What is important, is the "long quiescent period, unpredictable and abrupt change" characteristic. We recall that this was also our characterization of the cataclysmic variable stars; where the visual-spectral abrupt variability is overwhelmingly in the luminosity, with following, longer-term, changes in spectrum. For the Be stars, the striking variability is in spectrum; although, but developing over a very long time-scale, such a spectral change is, at least statistically, a precursor of a luminosity change.

So, in the visual spectrum, the strong similarity between WR-type and Be-type stars lies in the presence of strong emission lines, and the necessity for an extended-atmosphere to produce them. Possibly the need for an extended atmosphere to produce the superionized WR lines is not as obvious as for the subionized Be lines—but we observe, directly, the extended atmosphere for the WR (cf Section D), to confirm this conclusion. The strong contrast between WR and Be stars lies in just those emission features producing the similarity: (i) their variability—small for WR, striking for Be; (ii) the nonEquilibrium thermo-dynamic nature of the atmospheric regions where the emission lines arise—ultra-high nonthermal expansion velocity $> 10^3$ km/s for WR; superthermic but much smaller velocity $\sim 10^2$ km/s for Be; (iii) high, superionized energy level for emission lines of WR; low, subionized energy level for Be. Indeed, ionization level for Be atmospheric regions is incompatible with the inferred velocity gradients unless they are simple, monotonic, expansion.

A final similarity and difference lies in the range of objects embraced by WR-type phenomena, and Be-type phenomena. We stressed the enormous range in mass, size, luminosity of WR-objects; and the common time-invariance of the WR-type spectrum. We have alluded to, and will stress increasingly in following pages, the variety of objects showing the H α envelope, variability, low-velocity Be character. They also share the characteristics of individuality, and small-to-large amplitude range. Here, we briefly elaborate on the Be-phase aspect, already remarked to put these into perspective.

Originally-historically, during many years of statistical collections of observations, the B-normal, Be, Be-shell types of spectra were thought to represent quite different types of stars. Struve's 1931 model of the emission lines, as coming from an extended atmosphere, associated the existence of the atmospheric extent with a rotational instability of the Be and Be-shell stars. Each was assumed to be rotating at the critical velocity for mass-ejection: gravity is just balanced by rotation. The actual velocity observed is a projection effect: $V \sin i$. Within this model, Be

differs from Be-shell simply in the inclination, i , of the rotation axis. But observations at several epochs for many stars, and detailed observations over long baselines for a few stars like γ Cas and 59 Cyg, show that some stars can, and do, exhibit each of these types of spectra, at different temporal epochs, moving back and forth between these phases, not linked to any evolutionary change; Fig. 3-24 exhibits such behavior for γ Cas (Doazan et al., 1983). Thus, rather than characterizing different *objects*, these differing phases of one star characterize a variability in whatever produces the emission lines and the shell features. For the Be stars, the emission lines are produced by that density distribution giving an extended atmosphere; for the shell features, one infers an even stronger cooling than that required to obtain sufficient neutral hydrogen to produce the strong Balmer emission lines. So, if emission lines come and go, so must come and go those sufficiently small density gradients that produce extended atmospheres. Therefore, there must be episodic variations of those mass-fluxes which, dynamically, produce such small density gradients relative to the thermal. But because in some stars, at some epochs, Be phases often last many decades, there must also be long intervals of quasi-continuous mass-flow. So the phase-behavior of these Be stars forms an empirical and conceptual bridge to the effects of such combinations of normally-steady, but occasionally-large and rapidly-changing, episodic nonthermal fluxes, whose prototypes are the cataclysmic stars of various kinds. Indeed, in this respect, the Be stars, when *studied only in the visual*, provided a melange of equally-only-visual behavior of the WR and cataclysmic stars. WR provided continuous mass-flow; cataclysmic stars, especially ordinary novae, apparently provide only episodic mass-flow; the Be, and Be-similar, stars provided examples of both continuous, and episodic, mass-flow—*under the assumption that emission lines measure atmospheric extent of a freely-expanding mass-flow*. Again, we stress: $\text{o}(10^3 \text{ km/s})$ for WR; the same for novae; $\text{o}(10^2 \text{ km/s})$ for Be and PN and other “similar” stars—including P Cyg. Such comparisons are stimulating and tantalizing—the last, because of the complete unpredictability—other than from long years of observing “intuition”—of episodic outbursts.

Not all B stars have been observed to show a range of phases; indeed some 80 percent of B stars have shown only B-normal spectra. Even those stars that have been observed in several phases often rest in a given phase many years, even several decades. There exist no precursors as to when a phase change will occur, nor to which other phase the transition will go, nor any periods associated with any pattern of change—nor, indeed, any pattern characteristic of many stars. Doazan discusses an apparently-similar pattern for γ Cas and 59 Cyg over the last 80 years of observations; but there is as yet no evidence that this pattern holds for any other stars, or even for these two outside the present epochs of observation. Indeed, the characteristics of *individuality*, and *gradualness* (a continuous range of emission amplitudes among stars, from very small to very large) best describe any “statistics” of Be stars. “Trends” are more accurately descriptive than are “correlations” or “relations” among the several observed quantities for a given sample of stars. So in the sense of departure from the WR quasi-steady character of its emission lines, hence in that atmospheric structure, hence mass-flux, producing them, the Be and cataclysmic stars share, in the visual, more

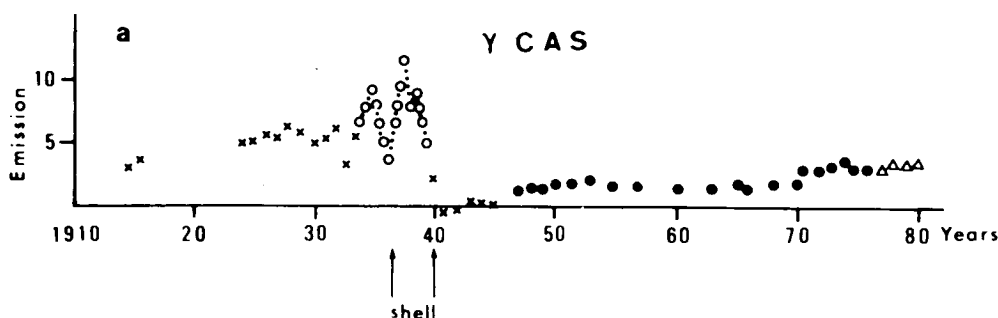


Fig. 3-24. A schematic representation of the variation of Balmer-line emission in γ Cas (from Doazan et al., 1980b). The intensity scale is arbitrary.

common characteristics. I stress, however, that the abrupt variation in mass-flux from the cataclysmic stars is inferred from a large increase in visual luminosity, accompanied by large absorption-line displacements. But this is highly individual. Some novae have increased by a factor 10^4 in luminosity in less than 2 days; some take 2 months to rise by a factor 40; RT Serp remained at maximum luminosity for 15 years and after 30 years had decreased in intensity only as far as had Nov Aql after a week; the latter reached “normalcy” after 11 years. In the Be stars the “abrupt” rise in mass-flux is inferred, *in the visual*, from the appearance, disappearance, and change in line-profile of the emission lines, accompanied by only small, if any, spectral line-displacements. The “abrupt” changes in phase of Be stars should be taken in the same sense. Some stars have shown the emission lines to disappear in weeks; 59 Cyg went through several shell phases in a few years, was in its last B-normal phase for about a year, and has taken over 5 years without fully recovering to a bright Be phase yet. Fig. 3-24 above for γ Cas places the problem in perspective. The V/R ratio has suggested, for several years, that γ Cas is ready for an “episode.” One waits.

β . The FarUV Spectrum. In the farUV spectrum, that primary aspect of similarity between WR and Be spectra in the visual-emission lines—is now a contrast. WR farUV lines retain their emission character, some with P Cyg-type violet-displaced absorption components. But, there are no emission lines in farUV Be spectra. Presumably, this implies the farUV lines are produced closer to the star than is emission H α . But what was a primary contrast in the visual spectrum is a similarity in the farUV; the presence of superionized, ultra-superthermic velocity, spectral lines. Both WR and Be spectra show them: the WR, in emission; the Be, in absorption. Thus, the farUV spectrum shows that the Be atmosphere must have a rapidly-expanding chromosphere-corona; an atmospheric region of high ionization and gas-dynamic energy; precisely the basic character of the WR-phenomenon. But whereas this chromosphere-coronal region is of enormous extent in the WR stars—beginning so deep that we do not observe an (RE, HE) photosphere, extending so far we see cool exophotospheric regions only at distances of parsecs—it is much more limited in the Be stars. One sees a normal B-star photosphere, “veiled” to varying degree among different stars and at different epochs by the chromosphere-corona. But one observes the same superionized spectral level in *all* phases of some Be stars. In each of the B-normal, Be, and Be-shell, phases of *some* stars one observes the Si IV, C IV, N V, O VI sequence, which covers as much of the farUV spectrum as is observable with the IUE. With Copernicus, one observed O VI in a B-normal (τ Sco) and in the Be, Be-shell 59 Cyg. Moreover, those X-ray observations to date—detection in τ Sco, γ Cas, ζ Oph; 59 Cyg was inaccessible—imply an equal T_e (max) level of 10^6 – 10^7 K in this range of stars showing this range of phases. If anything, the B-normal phases show somewhat higher X-ray emission than the Be and Be-shell phases. X-ray emission from the prototype B-normal star, τ Sco, is six times larger than from the Be-Oe star, ζ Oph, for example. While these data are *highly* incomplete—*no* basis for statistics—they reinforce the physical picture, and its cause, that distinguish B-normal and Be-phases in the visual: the presence of an extended, cool, H α emitting envelope which begins quite near the star (a few radii), in the Be phase and terminates the high- T_e chromosphere-corona without ending the high-density aspect. Evidence for such an extended, cool, envelope following the corona is lacking, in the B-normal phase; evidence against its presence is provided by the lowered X-ray opacity inferred from the higher X-ray values.

Those detailed studies of variability in the farUV, for a few stars, over the 5 years of IUE operation, complemented with some earlier data from Copernicus, are summarized by Doazan (1982), and supplement the atmospheric structure of the above picture. The superionization level, for a given star, does not change significantly with time, and remains at the same level among “similar” stars: e.g., ζ Oph, γ Cas, τ Sco, 59 Cyg. Not enough studies have been made to compare these bright, early Be (and Oe) stars and later Be stars, especially to distinguish simple brightness effects and variability effects. One does see, universally, C IV, in high-resolution observations; N V is at the end of the IUE usable range; O VI was detectable only by Copernicus. So apparently the nonradiative heating, to produce chromosphere-corona, remains always, for these stars, at significantly-high level. Occasionally, C IV intensities drop strongly (59 Cyg, Dec. 1981; θ Cr B, Sept. 1982); the significance is to be studied.

But the size of the velocities accompanying the mass-flux changes drastically; and there is evidence for change in the atmospheric-density level at the location where a particular outflow velocity is reached. At the steady, high level of H α emission in the well-developed Be phase, velocities of the several observed line-components do not change

very much; variability is in intensity of the line, especially of the high-velocity components. One does see additional line-components come and go, in times of a few weeks. However, in the phases between Be-minimum, almost B-normal, and well-developed Be, one observes the largest, and most variable, mass-fluxes and velocities in the case studied in most detail, 59 Cyg. One observes, in the farUV, two strong line-components during this increasing-Be phase. One component, near 100 km/s, changes little. The second, high-velocity, component, has been observed to vary, in line-displacement, from 300 to 1000 km/s, within a few weeks, without pattern. Very occasionally, one has observed additional, intermediate, displaced components. Fig. 3-25 exhibits a sequence of C IV observations, as illustration. So apparently, and in agreement with inference from the visual $H\alpha$ spectrum and the random farUV data, the significant difference between Be-phases, and between different stars, lies in the mass-flux parameter, and its effect in producing the extended-atmospheric density structure. This is the essential basis of the Be emission-peculiarity: an "areal" rather than a "temperature" effect.

But a combination of simultaneous observations in the farUV and visual $H\alpha$ shows that this areal effect is not simply that of an atmosphere distended by simple mass-outflow. By statistics on a variety of stars at random phases, and systematic observations of particular stars, especially 59 Cyg, over a variety of phases, Doazan and Thomas (1982) established a lack of correlation between $H\alpha$ emission—or atmospheric extent—and farUV mass-flux. Apparently, one has maximum mass-outflow during period of minimal, but increasing, $H\alpha$ emission. A graphic example is 59 Cyg; where, after 5 years from Be-minimum, and outflow of some 1000 km/s, the $H\alpha$ intensity is still 5 times less than at the bright Be phase preceding Be-minimum. Under simple outflow, the mass-flux would have filled a region, some 20,000 photospheric radii in extent. Historical and current estimates require the $H\alpha$ emission to come from a volume less than some 15–25 radii in extent; a few days flow should fill it. Also, as already emphasized, the velocities in the $H\alpha$ envelope do not exceed some 100 km/s; so the flow must have been strongly decelerated between "top" of corona and "bottom" of $H\alpha$ envelope. Instead of a simple mass-flow expansion, the Be stars require the creation of a "storage-cavity," or balloon, from some region within a few radii of the star, extending an indeterminate distance outward. The question is what produces it; what produces the deceleration?

Once again, we close with a cataclysmic example: not the nova, with its *apparently* simple outflow, but the planetary-nebulae, which exhibit an $H\alpha$ envelope, but beginning only some 10^5 , and greater, radii from the central star. We summarize more details in the following section. Here, we stress only the similarity following McLaughlin: the Be stars are little planetary-nebulae; the $H\alpha$ envelopes of the Be star begin a factor 10^3 in radius closer to the star than they do for the PN. Without the simultaneous visual and farUV data, we would not have established this picture. We defer further comment until we summarize how such combined farUV and visual data have changed the picture of planetary-nebulae. The only additional comment to make on the WR-Be-comparison, is to re-emphasize that any $H\alpha$ envelope—any H II shell—does not occur, for the WR, until *much* greater radii: 10 psc, or 10^{18} cm instead of the 10^{13} cm for the Be stars.

ii. Be-Similar Stars: Visual and FarUV Spectrum

Struve presented an extensive summary, and general atmospheric pattern, for such hot, peculiar stars, in 1942, based on analogy to, and extension of, the observed, extended, outer-atmosphere of the Sun. Primary to this pattern was his pre-Edlen picture of the solar chromosphere-corona as a cold, dynamically-extended region. The chromosphere was supposed extended by random nonthermal motions; so its density distribution was quasi-exponential, pseudo-thermal, with a scale-height fixed by random nonthermal motions rather than thermal. The corona was dynamically extended by superthermic, nonrandom motions. The variety of "shell-stars," as he called these hot peculiar stars embraced by this pattern, depended upon the opacities of chromosphere and corona, and the sizes of the velocities. Especially in view of the evolution in Be-modeling from visual to farUV data, one should note his choice of γ Cas as the prototype of a static shell, based only on these visual-spectral regions, at that epoch.

In our search for continuity of exophotospheric modeling across the HR plane, the essential characteristic of what we earlier called "Struve's-Epoch-II" model was its ignoring Be-rotation in favor of a focus on emission lines plus variability as the guide. Re rotational instability, Be-stars were considered unique. Re variability of strong, low-energy, emission lines, Be stars are simply a "crossroads" member of intersecting sequences of a variety of other

59 CYGNI
C IV 1548.1551 Å

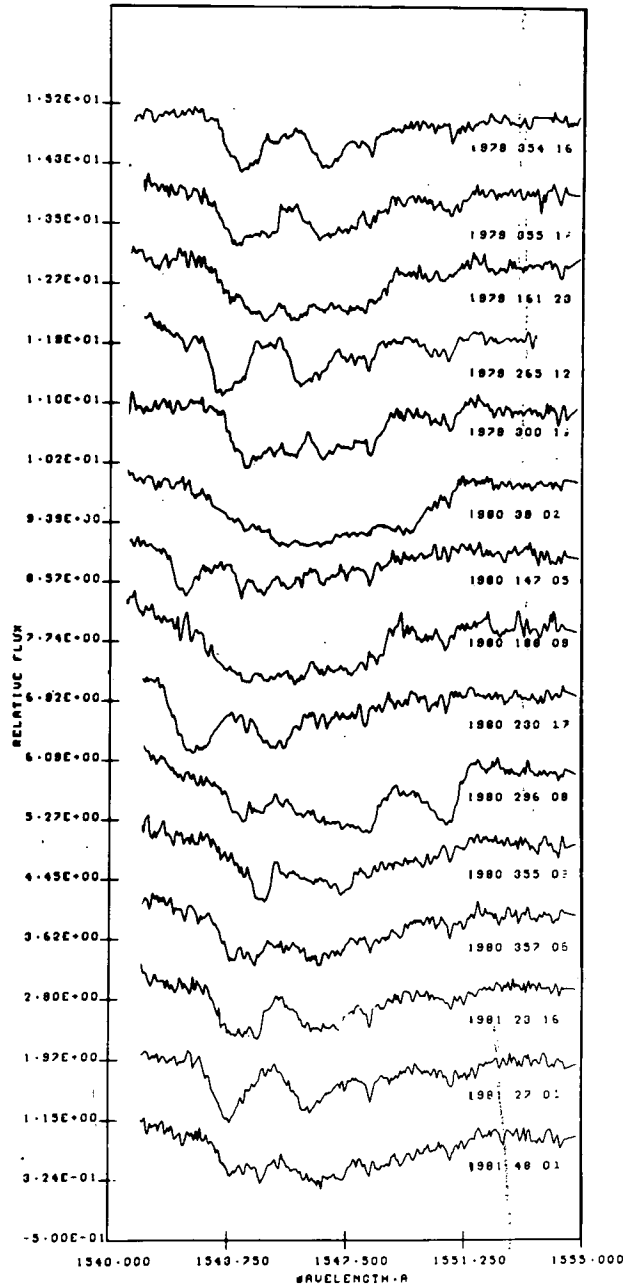


Fig. 3-25. Variations in the C IV resonance lines of 59 Cyg during the period 1978 to 1980 observed with IUE. Most of the spectra show two components, the high velocity of which varies from about -600 to -1000 km/s. Note the changes in the profile (from Doazan et al., 1983).

kinds of peculiar stars. The great range in Balmer emission-line intensities and profiles across the Be and Be-shell phases, and additionally among the Bep stars, and those stars called symbiotic—such as Z And, already emphasized in discussing cataclysmic-peculiar stars—had led Beals (1939) to see a continuous progression of such line-profiles from the supergiant, α Cyg, through the Be stars to the P Cyg-type supergiants, and the symbiotic. On one end lay the purely-absorption, static, sharp, deep profiles of α Cyg, which the Be-shell spectra resemble. So one expects extended, low-density, cool atmospheric regions. On the other end of the progressive sequence, lay the distinctive, kinematic, P Cyg profiles, whose extrapolated variety embraces WR, Be, Bep. So we also expect hot, dynamic, regions. Noting that P Cyg and Z And had once been considered as novae, Beals included novae in the sequence. Noting that the symbiotic stars wander—both historically-taxonomically, and time-dependently in their spectral changes—throughout this sequence, they are obvious members. Struve adopted the sequence, with the remark prefacing this Chapter 3, which can be paraphrased: “such tenuous outer atmospheres probably characterize the majority of stars, at some evolutionary phase; our confidence in stellar modeling will rest on its ability to produce such atmospheres.” To this sequence of Be-similar stars—based on variable emission lines, characterized by the individuality of those stars defining the sequence—I would add the planetary-nebulae, as particularly similar to the Be stars, as emphasized by McLaughlin’s (1931) characterization of Be stars as little planetary-nebulae. So, here—trying to put them into that empirical-theoretical perspective which constantly recurs in our abstracts of Be, cataclysmic, and symbiotic “phases”—we define and summarize: *Be-similar star*: one showing hot-star visual continua, some Balmer emission lines, and cooler star (α Cyg type) metallic absorption, sometimes emission, lines. Recall this definition when we come to Section C, on symbiotic stars.

Struve’s model has been rediscussed by Doazan and Thomas (1982), in its necessary evolution under the recognition of the “hot” chromosphere-corona. The essential aspect, for us here, is the recognition of the chromospheric density distribution as being fixed by HE under an outward rising T_e that is produced by a nonradiative energy-flux, which does not transport mass. We discuss this picture, as explored and verified observationally/empirically in the Sun, in detail, in Section D: *Extended-Atmospheric Peculiarity*. In that discussion, we emphasize this HE but non-thermal chromosphere as the lowest exophotospheric region. In the present section, we focus attention on the observational evidence delineating the post H α -envelope regions, in transition to the planetary-nebular discussion.

We noted that the WR emission lines are superionized in character, as are those in the farUV spectra of the Be, and B-normal, stars; all indicating $T_e \lesssim 1-2 \times 10^5$ K. The X-ray data suggest T_e (max) $\sim 10^6-10^7$ K. So the farUV lines can be formed on either side of the T_e -maximum, above or below the X-ray origin. The several velocity components, near 1–200 km/s, and near 1000 km/s, in the Be stars suggest such distribution on either side of the T_e (max) (Doazan and Thomas, 1982). The H α envelope has T_e in the $1-2 \times 10^4$ K range (cf the models discussed below); and velocities have been strongly decelerated. There is one variety—or extremity, in terms of extended atmosphere—of Be stars which exhibits emission lines of even lower excitation, and density: the Bep stars, which show—in addition to all the above—lines of [C I], [O II], [S II], [Fe II], and [Ni II]. Such lines require particle concentrations of some 10^8 , and T_e nearer 5×10^3 K, than the $10^{10}-10^{11}$ and $1-2 \times 10^4$ K of the H α envelope. These stars are further notable for their strong farIR excesses; even, for some of them, observed radio excesses. While the usual Be stars show farIR excesses, radio excesses have not yet been detected.

The literature debates whether such farIR excesses, and radio excesses, arise in emission from dust grains, or from f–b and f–f emissions. If the latter, they can be produced in all the regions considered above: the hot regions, the cool H α envelope, and whatever succeeds it. It is simply strongly indicative of differential atmospheric extension, that such large IR excesses, and such radio excesses, are not produced in *all* Be stars; just in the Bep, defined by the presence of the forbidden lines, requiring low-atmospheric densities. We have the indication that such stars have atmospheres of even greater extent than the usual Be. Whether this comes from an initially-greater mass-flux, leading to outflow gas concentrations being larger, at the same radius (cf Part III on modeling); or whether it results from a more efficient “balloon-storage” in these particular stars, remains to be “seen,” and empirically-theoretically explored.

We note that such strong farIR excesses, and radio excesses, are also characteristic of the planetary nebulae and the symbiotic stars. But we also note that there are exceptional stars, even among the few Bep stars, whose

emission lines are the higher energy forbidden lines of [O III] and [N III] characteristic of planetary-nebulae. For these exceptional Bep stars, the farIR and radio excesses are even larger. Such stars fill in, even more strongly, the gap between Be and PN stars. And they raise even more strongly the question: Do these excesses reflect a larger mass-flow, or a more efficient balloon-storage mechanism in the post-coronal regions—or do they represent the presence of dust grains, and if so, how are they produced? Manufacture them in the atmosphere, or do they come from primeval environment? Note that this balloon-storage mechanism, which must exist in the Be stars to satisfy all the above variety of data, produces a “local environment” from the star itself, from its mechanism of mass-flux production, *whatever* it is. The character of the farIR spectral distribution gives further information. If dust is the origin, one expects some indication of its presence, from such evidence as the silicate signatures near 10 and 20 μ . One has *not* observed such signatures in ordinary Be or Bep stars; one *has* observed them in Herbig Oe and Be stars. The distinguishing characteristic of these latter, over ordinary Oe and Be stars, is their location in strong nebulosity. We have not explained the mechanism of Be balloon storage. One alternative is some interaction with an existing, more dense than normal, ISM. Another alternative is a self-interaction between mass-fluxes produced at different epochs (to which we return, in the planetary-nebulae). Implicitly, we have favored the latter, in our stating that the data “require” a time-history of the mass-flux from a star, to construct a complete exophotospheric atmospheric model, empirically-theoretically. These data, just discussed, exhibit the alternatives.

Finally, in terms of the sequence of types of emission-line, and Be-similar, stars, we should note that the forbidden solar coronal lines from Fe X and Fe XIV have been observed in symbiotic stars and novae—but not in the Be, Bep, nor planetary-nebulae. And we note that some WR stars exhibit farUV and radio excesses. As we shall see in Part III, the deceleration plus cooling process for the Be stars requires, somewhere below the H α envelope, production of a second corona, with a “momentary” T_e probably higher than the original one. Clearly, the relative geometry of all these regions—the radial distribution of velocity, density, T_e —as a function of size and time-history of the mass-flux, remains to be carefully investigated. We can only be certain that this whole exophotospheric structure—and especially exocoronal structure for these Be-similar stars—is nonthermally-rich in variety.

iii. Rotation and Binarity: Visual and FarUV Spectra

For perspective, we should conclude this abstract of Be, and Be-similar observations and empirical-theoretical guidance on atmospheric structure by commenting on rotationally—and binary—inspired syntheses of data. Doazan (1982) critically details such efforts. One should supplement this by reading Poeckert’s (1981) status-summary of the Struve-Epoch-I, critical-rotation-source, models, because it is Poeckert and Marlborough who have explored this model the most exhaustively. Likewise, one should read the Harmanecz and Doazan discussion of 88 Her (1983), because Harmanecz and colleagues have been foremost among those urging a binarity-interpretation of Be phenomena. I only abstract the three summaries.

α *Rotational-Instability*, to produce extended equatorial disks, inspired by Struve’s interpretation of the observed broad absorption lines in Be stars as rotation, is put into perspective by Collins (1970): “There is not a single piece of observational evidence that Be-stars rotate at the critical velocity.” A further compilation of observed velocities (Slettebak, 1976) in comparison with theoretical-critical velocities (Collins, 1974) substantiates the conclusion (Slettebak, 1979). Yet it is the assumption that *all* Be stars rotate at this critical velocity, that underlies the model. At Struve’s epoch, such a rotation inferred from broad absorption lines was the only unusual character of Be stars that it seemed possible to link to that atmospheric extension required to produce the strong Balmer emission lines. One usually ignores the fact that for every Be star with such a derived rotation, one can find a B-normal star with the same absorption-line width. One argues that statistically, there are more broad-lined Be than B stars; so that it is the inclination between rotation axis and line-of-sight that confuses the inference of the actual critical velocity from the observed one. So, assuming the actual Be rotational velocity to be the critical one, for that star, one should expect an observational correlation between absorption-line widths, expressed as $V \sin i$, and size of Be effects. Certainly, no star should change its basic character, such as always producing a shell-spectrum (viewed equatorially); or never a shell-spectrum (viewed pole-on); or some melange for stars of intermediate inclination. But, in the visual

spectrum: some stars are observed to have exhibited the full range of phases; and some emission-line breadths much exceed the absorption-breadths, for some stars, at some epochs. Such variability was early recognized (1931) by Struve and Swings as a vulnerable point of the model.

FarUV observations have now provided the definitive death-blows. Copernicus observations of Fe III shell lines show no correlation with $V \sin i$ (Peters, 1976; Snow et al., 1979). Some "pole-on" stars show strong shell lines; others, do not (Snow, 1976; Peters, 1979). If, indeed, critical rotation is the source of the extended atmosphere, it should occur only in the equatorial plane; so there should be a strong correlation between observed line-displacements and inclination. Four Be stars—59 Cyg, γ Cas, 66 Oph, ω Ori—show $V \sin i$ values of 450, 300, 275, 190 km/s, thus cover the equator-on, pole-on range. Yet for each of these stars, the observed (expansion) farUV line-displacements of C IV and N V reach at least 750 km/s, which exceeds the photospheric escape velocity. We have already commented on its variability, and multi-line-component structure, for 59 Cyg and γ Cas, ranging from -200 to -2000 km/s. The two other stars also show such multi-component line-structure (Peters, 1982). So, there are much greater variations in mass-flow velocity for a given star than between equator-on and pole-on stars. Early reports, from Copernicus data, of a correlation between mass-loss and $V \sin i$ (Marlborough and Snow, 1976) using only asymmetries of Si IV farUV absorption lines as a measure of flow-velocity, apparently rest on insufficient data. More extensive data, and using also C IV lines, show no correlation between $V \sin i$ and mass-loss inferred from these observations by this approach (Snow, 1981; Doazan et al., 1981). I make one caution here, already made above, and return to it in Section F: the inference of an actual mass-flux from line-profiles. Some of the just-mentioned mass-loss values came from line-asymmetries. Our observations of 59 Cyg (Doazan et al., 1980, et seq.) showed, for some years, quite symmetric Si IV lines but highly-displaced (1000 km/s) C IV and N V lines. (Now, asymmetry, and other components, appear, for Si IV.) Inferences of mass-loss from total H α emission, and from IR and radio excesses, depend only on density distributions, not on mass-flow, for the emitting atoms. A mass-flow is introduced, by whatever one assumes to fix the density distribution. In discussing "balloon-storage" above, we show the weakness of assuming a simple expansion to relate density-distribution and mass-flow. Clearly, all such mass-loss inferences are highly model-dependent, and not just in the sense of ionization computations, for given density distribution.

Finally, the classical equatorial-disk model was, as mentioned, subionized, not superionized and chromospheric-coronal. When the pervasive presence of chromospheres-coronae was first discovered, the equatorial-disk advocates "permitted" chromosphere-coronal regions at the poles. Arguments were made that a "turbulence" would be introduced in the equatorial-disk, produce upward-propagating acoustic waves as in the classical solar model, hence heat the upper, more diffuse, regions. The higher densities in the equatorial disk would cool any nonradiative heating too rapidly to permit chromospheres-coronae (Marlborough et al., 1978). Again, farUV observations show no dependence of superionization on orientation. Equator-on, pole-on, intermediate stars alike show the same superionization phenomena. X-ray data are insufficient, at the moment, to provide evidence either way.

(β) *Binarity*. As in all discussions of the origin of some stellar peculiarity, speculatively attributed to binarity, one wants to carefully distinguish between *the phenomenon as occurring in a star which is a binary*, and *as occurring because of binarity so that it would not occur if the star were not a member of a binary*. So, for Be stars, one asks if the *Be-phenomenon* occurs *only* in binary stars—hence, has its origin in binarity—or if there are only some aspects which are present, or enhanced, by binarity. There are sufficient Be stars for which there is absolutely zero evidence of binarity, that one can say the Be phenomena discussed above do not have their origin in binarity. At the moment, the principal focus on binarity in Be stars lies in those stars—like 88 Her—showing a "perfect" binary-type radial velocity variation, for many years, but with zero other evidence of binarity (Doazan, 1982; Doazan and Harmonecz, 1983). It also lies on those stars like γ Cas, for which X-ray observations suggest to some astronomers the presence of a degenerate companion, but for which other evidence is lacking (Doazan, 1982). For γ Cas, the problem is complicated by the similarity in its phase-behavior to other stars, like 59 Cyg. X-ray interpretations are complicated by the strong X-ray emission from Unsold's prototype B-normal star, τ Sco, relative to that from ζ Oph, an Oe-Be star whose MK class is effectively identical to that of τ Sco. In short, there are undoubtedly B-stars in binaries which have shown B-normal phase, some which have shown Be phase, and some have shown Be-shell phase. But, at the

moment, there is zero evidence that binarity has any major effect on what causes these phases, and on the mass-flux, nonradiative energy-flux, and other factors which may contribute to those causes. There may be such effects; as yet we have no evidence on them; speculation does not seem as useful as continuing the empirical-theoretical investigations summarized.

c. Two Other Varieties of Be-Similar, Emission-Line Stars, Which Further Illustrate the Be-Crossroads Character.

In Section *b.ii*, we defined Be-similar stars as those following the Struve-Beals sequence of hot-photospheric, emission-line, variable, peculiar stars: each enveloped by an extended-atmospheric, cool, shell within which all of the broad Balmer emission lines, α Cyg-type sharp singly-ionized metallic lines, and sometimes P Cyg-type profiles were produced. The conceptual model was solar-like: quasi-static chromosphere, dynamic corona, in atmospheric-regional sequence. If one ignored the historically-early, but later than its nova, classification of P Cyg as a Be star, then the representative Be star in this sequence was γ Cas, used to illustrate the quasi-static chromospheric regions, overlain by the P Cyg-exemplified dynamic corona. Ironically, although current farUV data show γ Cas to be much more dynamic than P Cyg—expansion velocities up to 1500 km/s contrasting to the 2–400 km/s values for P Cyg—these data show the relative locations of analog regions are correct. The hot, ultravelocity, chromosphere-corona of γ Cas—exhibited only in absorption lines—is overlain by a slower-moving, apparently not as highly excited, P Cyg outer-atmosphere. We note that, like the WR stars, P Cyg shows the same expansion velocity in visual and farUV spectral regions. However, in its farUV spectrum, P Cyg shows no superionized P Cyg profiles. Even in the farUV spectra, the α Cyg analog persists for the cool, sharp—especially absorption—line-cores.

So this sequence of photospherically-hot, Be-similar stars shows a common atmospheric structural pattern among its members: (1) monotonic outward increase in expansion velocity to superescape values, until some abrupt deceleration occurs, thereafter a slow expansion, still at (local) superescape values; (2) monotonic outward increase in T_e , until—associated with the deceleration but presumably with spatial phase-lag—a strong cooling below standard-atmospheric values, for the local T_e , occurs; (3) there exist some evidences for higher-excitation/ionization “symbiotic” phenomena, in these stars. Among the members of the sequence, there is a very large range in the details of this structural pattern; indeed, some aspects of it may not even occur in the “near” environment of the star; e.g., deceleration + cooling for the WR stars, *if* it occurs at all. So the WR stars exhibit a bridge to normal-star lack of exocoronal, local-environmental, structure. They exhibit it, because of their very large mass-flux. We noted other “bridges” at the extremities of the sequence. Apparently the line-spectrum, at least, of the WR stars begins with the chromosphere-coronal region; the description of the continuum, and its (photospheric ?) origin, rests open. One links to the cataclysmic stars by adjoining, for these WR objects, a photosphere which is already “superescape,” for at least some of the varieties; again, the possibility of transition-types remains to be explored.

So, in asking how this atmospheric pattern arises, from nonthermal fluxes, these Be and Be-similar stars give the broad bridge—they are the intermediate range between cataclysmic and WR types. In the visual spectrum, mass-ejection for the cataclysmic stars is episodic; in the farUV, one finds a continuous mass-flow, apparently undetectable in the visual. In both visual and farUV spectra, the WR stars exhibit a continuous, but very high level, mass-outflow. The Be stars, especially in a few well-studied examples, like 59 Cyg and γ Cas, exhibit a melange of both episodic and continuous mass-ejection, in both visual and farUV spectra—*when we understand how to diagnose the data, in terms of thermodynamic consistency of spatial evolution of atmospheric regions*. Unfortunately, we do not have as much evidence on the effect, and variability, of nonradiative energy-fluxes which do not transport mass. In the visual spectrum, superionization is strongly detected in the WR; marginally, in cataclysmic; not at all in the Be. In the farUV, it is presently difficult to distinguish between lack of nonradiative heating to produce superionization, and simply low-level atmospheric density—as produced by a drop in the mass-flux level—in the regions where such heating occurs. Such data as those presently becoming available on later-type stars, such as that on θ Cor Bor, in its Sept. 82 drop in C IV intensity, provide examples, which our observing programs should try to exploit. (Obviously, the programs try; it is the observing time available that is the problem; specifically, the allocating committees.)

There is a second kind of bridge, again involving Be-similarity; linked to the first. We added the PN stars to the Struve-Beals sequence. They satisfy the criteria except for variability; and here, the ordinary, “field,” WR stars are

also marginal. PN and WR phenomena are also linked through the central stars of some PN. We have already noted the historic link of PN to cataclysmic stars, in terms of a *presumed* episodic mass-ejection, and the current link in terms of farUV evidence for continuous mass-flow, undetected in the visual. So, they join the Be stars proper in this intermediate aspect, and in that of their intermediate position of H α envelope being formed exterior to the Be, but interior to any WR-associated nebulosity. But finally, there is another, symbiotic, aspect: the nearby presence of cool H α and of hot ions in regions far away from the central star. This symbiotic aspect provides a transition to the symbiotic stars proper, in Section C following. And it is this last transition which links these stars, via the Be-stars proper, to another kind of emission-line, variable, but photospherically-cool, stars, the T Tauri. As stressed in discussing cataclysmic stars, the "quiet-phase" of ordinary novae seems to be a hot OB sd; but that of recurrent novae seems to be a late-type, cool star. And we note that quiet-phase T Tauri stars show late spectral type, KO, for most of them. So while the Struve-Beals Be-similar sequence of stars focuses on the "deceleration" aspect—which we will see leads to questions of manufactured local environment—the other Be-similar sequence now abstracted focuses on symbiotic effects—in PN, T Tauri, and symbiotic stars themselves. But overall, these two sequences intersect, in many of their properties—and with other types of peculiar stars, especially the cataclysmic.

i. The Planetary-Nebular Emission-Line Stars: Extreme of the Be-Similar, and Infant of the Cataclysmic. This title-categorization of the PN abstracts the preceding attempt to place into perspective the several varieties of Be-similar sequences of stars, and the intermediate place of such stars in exhibiting the consequences of a combined episodic and continuous mass-flux. Then, in this perspective, the evolution of observational and theoretical studies of the PN places into strong contrast the empirical-theoretical vs. speculative-theoretical approaches to atmospheric structural patterns. The impact of current farUV data from IUE is as disruptive of PN speculative models based only on visual observations as it is of Be and novae historical modeling; yet, similarly, it also unifies the thermodynamic structure and basis for such models.

(α) *Visual Observations, and Inferences on the PN.* There are five visual-observational characteristics of the nebulae of the PN, and one characteristic of their central stars. The latter is quickly summarized: evidence points to most of the central stars being very hot, and subdwarf in size. Because of the faintness of the objects, actual resolution of the spectrum of the central star is difficult; Lutz (1978) summarizes what has been found, and I reproduce it as Table 3-3. Before such studies, inferences on the central stars were indirect, coming from calculations of what radiative fluxes were needed, in what spectral regions, to produce the ionization-excitation features summarized below. Universally, one found central-star "equivalent blackbody" temperatures of $\approx 10^5$ K. Essentially, these depend on the energy in the hydrogen and helium continuum required to produce the observed hydrogen and helium nebular spectra. There are a variety of atmospheric models for these central stars: blackbody, LTE standard atmospheres, nonLTE atmospheres of various kinds. The situation is periodically summarized in the various PN symposia (Osterbrock and O'Dell, 1968; Terzian, 1978; the Proceedings of the 1982 London symposium are not yet in print); books by Aller (1956), Gurzadian (1966), Osterbrock (1969), and two in preparation (by Aller and by Pottasch); and references contained therein, which I do not reproduce here. In effect, a definitive atmospheric model of the central star clearly awaits the inclusion of chromospheric-coronal and mass-flow effects. Until then, the actual character of the central star is, like that for most of the cataclysmic and symbiotic stars, open for discussion. *Apparently*, the star must be very hot, to radiatively excite the following nebular phenomena. But, because we will see—in Section β following—evidence for a strong shock-deceleration, the ionization/excitation near the nebula must be reexamined. The same holds for the ultra-velocity superionization between star and nebulae. Then, here, the second significant item is the evidence for *some* A-K type stars, in Lutz' tabulation. One must first verify its accuracy. Then if true, one uses it, in examining the nova, recurrent-nova difference in type of central stars, in terms of the sequential analogies we pursue.

Then we turn to the five characteristics of the nebular visual spectrum.

Table 3-3
Classifications of Central Stars of Planetary Nebulae

Classification	No. of stars
Continuous	21
Wolf-Rayet	7
Ofp or Of	10
O-type	9
O VI	10
WR+O or WR+Of	6
O-subdwarf	6
Peculiar	8
Emission unclassified	7

The spectra can be categorized roughly as follows:

- (1) Continuous. No spectra features are present except the continuum of a very hot star.
- (2) Wolf Rayet. These stars have broad emission lines of H, He, C, N, and O. There are six WC central stars and one possible WN.
- (3) Ofp. Emission lines of H I, He II, N III, and C III are present in the spectra. O-type absorption features are also present.
- (4) Of. There is only one Of central star known. The spectrum is the same as an Ofp star except that C III is not present.
- (5) O-type. The absorption lines of an O star are the only features present.
- (6) O VI. These stars have prominent emission lines of O VI, $\lambda 3811,34$; otherwise their spectra look like those of Ofp or Wolf-Rayet central stars.
- (7) Of+WR; O+WR. These spectra have combinations of WR, O-type, and Of-type emission and absorption features.
- (8) O-subdwarf. These spectra have broad absorption lines which are indicative of a hot, high-gravity star.
- (9) Peculiar. The absorption features indicate a spectral type somewhere between A and K.
- (10) Emission unclassified. These spectra are believed to show emission lines from the central star but they do not fit into any of the above categories.

The numbers in the Table are not necessarily representative of the true distribution of central stars among the various classifications. There are strong selection effects in that numerous faint central stars have not been observed spectroscopically, and in some planetary nebulae the central star is so faint that it is lost in the bright nebulosity.

From Lutz, 1982

The first striking characteristic, of which we shall make much use in Part III, is the high concentrations of material—inferred from all the following characteristics: particle concentrations 10^3 – 10^5 cm^{-3} at the nebular distances of 0.01–1 psc; mean values are 10^4 cm^{-1} and 0.1 psc, respectively. Under simple expansion at constant velocity, one requires a concentration of some 10^{18} cm^{-3} at a photospheric radius of 0.1 solar (the mentioned subdwarf), or some 10^{12} cm^{-3} at giant-type photosphere (cf below). These values are quite high; it was the basis for the historic idea that PN were phenomena of the ISM, not of any particular stellar atmosphere.

Second, the PN are emission-peculiar stars, as defined by their strong Balmer emission spectrum. But they are extreme, as are the WR stars, in showing mainly emission lines in their spectrum. For the WR stars, it is not clear whether the emission lines represent a T_e as well as areal effect; for the PN, it appears that the permitted lines, in the visual spectrum, represent wholly an extended-atmosphere effect. But, by contrast to the Be and T Tauri stars, the $H\alpha$ envelope exists at the distances, and with the concentrations, mentioned above. So it poses, but more acutely, the balloon-storage vs. simple expansion problem, discussed for the Be stars.

Third, the PN resemble, but do not equal, the WR and P Cyg stars, and the symbiotic, in the range of their spectral excitation. Aller (1956, table III.1) gives 5 pages of lines observed. For us, it suffices to note that permitted transitions range from the H I, neutral and once-ionized atoms characterizing cool stars—but *not* Ca II and Fe II; through He I and He II; up to C IV and O V, of hot stars. Forbidden lines range from neutral and once-ionized metals and C–N–O up through Ca VII and Fe VII.

Fourth, expansion velocities of the nebula are slow, 15–50 km/s, a mean near 20 km/s. Wilson (1950) showed that many lines are double, indicating small (5–10 km/s) differential velocities; the smaller the velocity, the higher the ionization.

Fifth, the morphology of the PN remains under constant discussion:

(a) whether there is a void, or a continuous distribution, of material between central star and nebula—i.e., does a 1-episode ejection suffice, or is a continuous outflow required?

(b) whether one requires significant nonradial “clumpiness” of material, particularly to produce sufficient emission from the low-ionization material to match the observed, from models based on producing the high-ionization material—i.e., do “symbiotic” spectra require something other than radial sequences of regions to produce them? Capiotti (1978) summarizes this work; further details are not important here, for us.

Then given these visual-spectral characteristics, we abstract what conclusions were reached from them—on atmospheric structure and its spectral excitation, and on the origin and significance of that structure.

Chapter 2 already summarized the utility of the PN in the development of a self-consistent nonLTE diagnostics. The Balmer spectrum is excited by the radiation field of the central star: but the density distribution of the atoms producing it is controlled by something other than that radiation field. Hence, the principal hydrogen-spectrum diagnostic difference between PN, Be, T Tauri etc. lies in the opacity effects, controlled by that density distribution. However, the second aspect emphasized in Chapter 2—impurity cooling—is brought into sharp focus by the PN just because of the distant-location, and low-density, character of the nebula. There are two aspects. First, that T_e in the nebula is held to some 10^4 K by the impurity cooling of the low-lying metastable levels of low-ionized species, like O II, O III, N II, N III. We require low densities, otherwise collisional deexcitation would kill the radiative cooling. Then second, we observe high-ionization forbidden lines, [Fe VIII], [Ca VII], etc.—which require $T_e > 10^4$ K but also low density, for the same reason. This situation is common to other Be-similar stars than the PN, and is important for guiding modeling. Even from the visual spectrum, the atmospheric structural scheme of: a hot central star, ionization decreasing outward as the farUV spectrum is absorbed; a low-velocity mass-outflow at sometime in the past, and a quasi-static doughnut structure, perturbed by “clumps” of gas; was hardly complete. But note that it was as structurally complete as the scenario for the ordinary nova. Each, from the visual data, was modeled as the result of a 1-episode ejection; they differ only in mass ejected; 10^{-4} solar masses for the nova; 0.2 solar masses for the PN, are the “popular” values.

The physical picture resulting from standard diagnostics of these visual-spectral observations is conventionally translated into a PN model having no linkage to the variable, extended-atmospheric, emission-envelope + α Cyg-shell, atmospheric structure of the Be-similar stars in the Struve-Beals sequence. Also, any resemblance to the McLaughlin

characterization of Be stars as little-PN is wholly fortuitous. The PN were thought to represent a 1-episodic, low-velocity, ejection of a significant fraction of the mass of a (grossly) solar-mass star; the residual star has the more-or-less standard photosphere of a very hot subdwarf; the ejected mass lies in a distant nebula, continuing the same, slow, outward expansion. The PN is nova-like in its 1-episodic character; nova-unlike in its velocity. The latter more nearly resembles the slow, continuous, mass-loss found by Deutsch (1956, 1961) for red giants. Hence, for the speculative-theoreticians working on evolutionary problems, the PN linkage is to the evolutionary climax of the red-giant phase for stars in the 1–5 solar-mass range. The PN episodic ejection is associated with a presumed instability arising in the change from He-core burning to double-shell burning. Exactly what the slow, some 20 km/s, nebular expansion represents is blurred. Whipple's original proposal (1933) to use it to compute PN life-times assumed an original nebular ejection at this value. Later evolutionary pictures (summaries by Osterbrock, Field in Terzian, 1978; Renzini, 1981) attributed this 20 km/s to the red-giant mass-flow, following Deutsch's observations, and its perturbation by the episode of the large mass-ejection at the onset of the nuclear-burning instability. The detailed characteristics of this picture, where the mass in the nebula is attributed primarily to this 1-episodic ejection, are vague. Renzini argues that the 0.2 solar masses in the nebula can not have been produced by the steady mass-flow of about $10^{-6} M_{\odot}/y$ associated with red giants, over the $o(10^3)$ years which the 20 km/s flow, and observed PN dimensions, give for the PN lifetime since "birth," following Whipple. He notes that these values would require a continuous flow exceeding some $10^{-5} M_{\odot}/y$ —which we note would place them in the WR category. So, he argues for a nova-like, at least very short-lived, 1-episode ejection. Various of the evolutionists argue that the slow red-giant mass-loss peels off successive atmospheric layers, leaving less "cold atmospheric material" overlying the "hot underlying envelope;" eventually just enough "cold" atmosphere is left that it can be ejected by radiation-pressure from the envelope, as the 0.2 solar-mass shell nebula. The picture is reminiscent of Menzel's (1935) picture of symbiotic stars as a hot "core" surmounted, but only at the equator, by an extended cool envelope. Oblique rotation gives the symbiotic "phases." All these models are vague as to how such a differential thermal state can be maintained. O'Dell (1963) correlated nebular-location against temperature of central star; finding the smallest nebulae associated with coolest, and largest, central star; thus suggesting the central star contracts as the nebula expands. Since this requires the central star to shrink by a factor 100 in radius—1.0 solar to 0.01 solar, T_r increasing from 4×10^4 to 10^5 K—in some 30,000 years, such models pose interesting problems in stellar, as well as atmospheric, structure. Osterbrock (1964) extends this size-age correlation to note that the central stars of the smallest PN show the broadest emission lines; interpreted as velocity broadening, he infers 400–1000 km/s.

(β) *This conventional picture of the PN changed strongly with high-resolution farUV observations via the IUE* (Benvenuti and Perinoto, 1980, 1981, 1982; Feibelman, 1981, 1982; Surdej and Heck, 1982). One observes a continuous outflow, in C IV and N V as well as in lower-ionization lines, from $o(100$ km/s) to 1–2000 km/s in the N V lines. *Very* roughly, the velocities are the larger, the higher the ionization; but there are strong exceptions. Clearly, the investigations are preliminary. But the essential aspect is that the region between central star and nebula is filled with high-velocity, highly-ionized continuous outflow. Whether the material is called superionized depends on how one models the central star. For $T \lesssim 0.5 \times 10^5$ K, the mass flow is superionized; for $1-2 \times 10^5$ K, it is not. HD 138403, studied by Surdej and Heck, has low excitations; so the material is superionized. Benvenuti and Perinoto give estimates of some $10^{-8} M_{\odot}/y$, but stress that the values are highly uncertain. The similarity to the nova situation is clear. One knows the nova has an episodic outburst, which could well be composed of several closely-spaced shell-ejections; one now observes, many years after the outburst, a continuous, low-level, mass-ejection. Apparently, novae do not create long-lasting nebular concentrations around them. One surmises that PN result from at least one, large, episodic outburst. By a combination of observational diagnostics and evolutionary arguments (Renzini, 1981; Peimbert, 1981), one infers that the PN "accumulated" mass-outburst produced something about 10^3 larger than did the ordinary nova outburst. Observationally, a long-lasting nebula results/exists.

The currently-most-interesting replacement for the above conventional PN picture views the PN nebula as the resultant of the high-speed episodic outburst and the preceding red-giant outflow (Purton, Fitzgerald, and Kwok, 1978; Kwok, 1981, 1982). Kwok, at least, considers the matter accumulated in the nebula as almost wholly the mass-flow from the preceding red-giant phase; there is a problem with total nebular mass. The picture is not necessarily wholly a large outburst, as for Renzini; but a mass-flow that is continually accelerated as the "veiling" of the

underlying hot stellar core decreases, following the ejection of the cold atmosphere. So, continuously, the mass-flux from the star at one epoch overtakes that from earlier epochs, resulting in the nebula, at some distance fixed by the history of the flow—of the red-giant, post-red-giant mass-flow. Observationally, one should see the nebula itself, plus an exterior region corresponding to flow in the red-giant phase, plus the interior region corresponding to present-epoch flow. And, indeed, Kwok discusses observations which can be interpreted as supporting the existence of each of these three regions.

So observationally, and in terms of this kinematic model of Kwok and associates, one returns to the Be-similarity. Pictorially, the difference lies in the rarity of the PN episodic ejection: whatever their highly individual time scales of episodic outburst, these occur more frequently for the Be stars. The similarity lies in the production of a “storage” envelope, rather than a simple expanding envelope, to represent the details of this kind of emission-peculiarity. Osterbrock (1964) stressed that whatever the mechanism, the PN nebula must represent a local enhancement of the density. Today, such a conclusion is not at all evident, given these results on a continuous outflow; and the picture of an interaction between the mass-fluxes of different epochs determining the form of the observed nebula. One returns to interpret McLaughlin’s characterization of the Be as “little” planetary nebulae, not so much in terms of size of mass-ejection, but in its history of variability. The nova outburst appears to be one superimposed on a relatively small, preceding, mass-flow; the PN, an outburst superimposed on a larger preceding mass-flow—if the sequence is correct, the Be continuous outflow, before the enhanced episode, must either be still higher or sufficiently more frequent in episodic enhancement.

In terms of the dynamic-cause aspect, we note that “popular” cataclysmic origin rests on a binary mass-transfer to provide a nuclear origin; the pre-IUE PN origin lay in single-star, He-flash nuclear enhancement—the literature continues to ascribe the exceptional Be mass-loss to rotational instability. Given this checkered-array of explanations, the continued re-enforcement of the Be-similar kinematic sequence is amusing.

ii. The T Tauri Emission-Line Stars: The Cool-Branch at the Be-Similar Crossroads. Our continuing attempts to exploit similarities between the Be and other emission-peculiar stars to delineate common patterns of nonthermal atmospheric structure and their causes, finds strong similarity and strong contrast between them and the T Tauri stars. We try to exploit these, also, toward the same objectives.

Re similarity, the H α emission profiles of Be and T Tauri stars are remarkably alike, in appearance, and in behavior. Figs. 3-10 through 3-11 show illustrative examples. For each kind of star, the peak intensity in the observed profiles can reach 10, sometimes 20–30 times the continuum adjacent to the line; but the range among stars is enormous, in intensity and in profile shape. Cohen and Kuhl (1980) have surveyed some 500 T Tauri stars, photo-electrically, and find ranges in H α equivalent width from a few to 200Å. By far the most Be observations are photographic; because of saturation, very large equivalent widths are difficult to measure, but the range still goes up through 100Å, from again very small values, especially when the line goes into absorption. In both kinds of stars, H β and later lines can be in absorption when H α is in emission. Accompanying Balmer emission, both kinds of stars show emission in single ionized metals, and sometimes in He I and II. While in T Tauri stars, neutral metals are also seen in both emission and absorption, such lines—as NaD and Fe I—are only seen in absorption in Be stars, and that during shell phases, when they are very sharp. The absorption lines in both Be and T Tauri stars are characterized as abnormally-broad, relative to nonemission-line stars of the same MK classes. Because of this broad, often diffuse, character, one customarily reads in the literature the phrase “probably due to rotation.” For T Tauri stars, $V \sin i$ values from such line-widths are usually quoted as ranging 25–100 km/s (Herbig, 1962, but see below); while for the Be stars (and indeed the normal-B stars) values range up to some 400 km/s. While one often hears that normal FGK stars show $V \sin i \sim 15$ km/s, there are some few, nonemission-line, stars with values exceeding 100 km/s. Emission-line breadths are large for both kinds of stars: extremes of 500–1000 km/s are sometimes reported for H α in Be stars; 2–400 km/s are the corresponding T Tauri values. P Cyg absorption on the blue edge of the emission lines is observed in some stars of both Be and P Cyg type; there is sometimes emission at the blue edge of such absorption components for both types of stars. Inverse P Cyg components are also observed in both T Tauri and Be; Kuhl estimates some 5 percent of the former show such. Very occasionally, in the same spectrum, some Balmer lines showing direct, some showing inverse, P Cyg lines are observed.

Spectral-variability is as distinguishing a feature as emission-peculiarity for both kinds of stars. The outstanding gross feature of the Be stars, the existence of the 3-phase variability, has thus far not been found for the T Tauri stars. But we note that a fundamental difference between Be and T Tauri stars, in terms of accumulation of basic empirical data, lies in the difference in luminosity associated with spectral type (cf below): 8–10 visual magnitudes, some 10^3 – 10^4 in visual luminosity. When one has the impression that T Tauri studies are retracing the path made clear many years ago in the Be stars, the reason is evident: it takes time to accumulate sufficient data to make clear all the characteristics of individuality and variability. One criticizes attempts to classify Be stars by classifying their Balmer emission-line profiles (Jaschek et al., 1981), because the H α profiles of some stars have been observed to traverse, over succeeding observational epochs, the whole range of profiles used to define the classification scheme that differentiates between stars. Preliminary indications are that the same situation holds for the T Tauri stars (compare the profiles, at different epochs, of the studies by Knapp and Ulrich, 1981, and Schneeberger et al., 1979). Nonetheless, only these kinds of extensive data-collecting projects (those just cited; those of Kuhi and collaborators; etc.) can give us the information needed to evaluate the conclusions motivating, or resulting from, them. The new multi-photon detectors should permit the photographic-based Be-type historic programs to be greatly accelerated. So, results thus far do not give indications of that major phase variability of the Be stars which so strongly affect conclusions on their post-coronal atmospheric structure. But these T Tauri data do exist in sufficient quantity to show just how profoundly variability must be included in modeling. Kuhi (1982) illustrates NaD profiles changing from emission to absorption in a half hour. Schneeberger et al., exhibit H α profile changes in 3 days that show variation of 40 percent in equivalent width. I reproduced this latter, as Fig. 3-11, to caution that it is not just a rectangular profile changing its size by 40 percent; but that the basic change lies in the characteristics of the self-reversed quasi-central “component.” Schneeberger et al., assert that 70 percent of their profiles give evidence of (variable) expansion velocities, in the range 30–250 km/s, on the basis of just such profiles. One takes this information against the background of a study by Herbig (1977), showing that a bisector of the emission-line profiles for a number of stars shows no shift—up to a 10 km/s blue-shift uncertainty—from velocities determined from both photospheric absorption line velocities, and those of the nebulae in which the stars are immersed.

Finally, in this gross abstract of similarity, we note that *the Be and T Tauri stars alike are considered main-sequence stars, but each lies above the main-sequence.* Statistically, stars in the Be phase lie about 1 visual magnitude above it. Popularly, they are for this reason often called “post-main-sequence,” with the implication of being slightly-evolved stars. But, as summarized, more and more evidence finds an increased luminosity—at least visual—accompanying the growth of the bright Be phase. Thus far, we have no evidence for evolutionary link to such phase variability. Equally statistically (Kuhi, 1982), one finds that T Tauri stars lie about 0.1 visual magnitudes above the MS; among stars showing this excess, the effect is even greater, about 0.5 mag. Because they are so often associated with nebulosity, they are popularly often called “pre-main-sequence.”

We return to this star-nebulosity association below, because our main focus, in discussing Be and Be-similar stars, lies on this star-environment aspect, especially in its effect on exocoronal atmospheric structure. But here, we note the existence of the Herbig Ae/Be stars (1960), often called early-type analogs to the T Tauri stars because their primary characteristic is being Ae/Be type immersed in nebulosity. Garrison and Anderson (1977) observed high-resolution H α profiles of 14 such stars, over a 7-month period. The variety of line-profiles seen in ordinary Be stars, and in the T Tauri profiles mentioned above, is seen also in these stars. For those showing P Cyg absorption components, all but one show blue-edge emission. The authors compare their double-peaked profiles to Marlborough’s Be profiles, computed for expansion and rotation; these Ae/Be profiles are considerably wider, and show a rough increase in width with earlier spectral type. These Herbig stars are often called pre-main-sequence because of this nebulosity association; but observationally, this association is the only distinguishing feature between them and the ordinary Be stars. We should note also the “peculiar” T Tauri-like star, V1331 Cyg (Chavarria-K. 1981). Its characterizing feature is to lie intermediate to “ordinary” T Tauri stars and the Herbig Ae/Be; its spectral type is called F0-A8. A number of the emission lines are called P Cyg, with absorption component displacements of some 200 km/s. He derives a mass-loss lying between 10^{-6} – $10^{-7} M_{\odot}/y$, as compared with Garrison’s (1978) value of 10^{-5} – 10^{-8} for the Ae/Be stars. The point I make here, in citing these intermediate stars, is that these discussions

of pre- and post-main-sequence stars are wholly speculative. There is no *observational* reason to call the Herbig Ae/Be *pre-*, and ordinary Ae/Be *post-*main-sequence; that they are associated with nebulosity is only speculation-provoking. To date, such evolutionary calculations as Larson's (1972, et seq.) have no link with observed phenomena. The very great prevalence of mass-outflow rather than inflow, and the similarity between exophotospheric spectra of all varieties of Be/Ae, T Tauri, and these "intermediate" objects only suggest that we concentrate, for the moment, on understanding atmospheric structure—what and why it is. So here, the nebulosity link to the mass-loss is mainly diagnostic, asking—observationally—can we decide which is primeval ISM, and which is stellar ejecta.

Then given all these aspects of spectral similarity between Be and T Tauri stars, and in full awareness of the strong difference in basic MK spectral type—i.e., in radiative flux, hence standard-model photosphere—we ask whether it is possible that they have the same exophotospheric atmospheric structural pattern? Or, at least, does any difference in pattern fall within the range of patterns exhibited by the hot-photosphere, or the cool/cold-photosphere, stars among themselves? We have seen that one gross dividing line among hot peculiar stars is the post-coronal pattern: a monotonic ultra-speed, hot post-corona; or a decelerated, cold post-corona. Such a pattern as the latter is associated with other "cool/cold" phenomena—low-energy forbidden lines, large farIR and radio excesses, dust-signatures in the farIR. Such phenomena are seen in cataclysmic stars with hot and cool "quiet"-phase photospheres alike. So we ask the situation, again comparatively, between hot-Be-like and cool/cold T Tauri-like stars. And here, we find a greater emergence of differences, especially re nebulosity. Because such nebulosity is of particular interest in any focus on local-environment—primeval or manufactured—we are particularly interested in it, in this hot/cool comparison, and especially in questions of any collisional interaction between it and any stellar mass-flux—again with the primeval or manufactured varieties. But to compare post-coronal behavior, we must first put chromosphere-coronal behavior in focus, after photospheric.

To place the difference in photospheric spectral class into focus, note that Kuhi's current statistics (1982) give 70–80 percent of T Tauri stars as showing K-type spectra, when there are not such a large number of emission lines that the photospheric, absorption, spectrum is "veiled" by it. There are a few F, a few G, a few more early M photospheric spectral types; and some 10 percent so heavily emission-line that an absorption spectrum cannot be classified. To cope with this veiling-by-emission, Kuhi has extended the MK classification to λ 7000. Thus, the problem earlier mentioned of H α exclusion in routine Be patrol studies is eliminated for his T Tauri studies. Apparently, this emission-veiling makes the spectrum appear earlier, especially by filling in absorption lines, which accounts for the historically-earlier placing of the T Tauri mainly in F–G classes. We also note that an extensive study of some 64 stars by Vogel and Kuhi find that only a few percent of them give $V \sin i \gtrsim 25$ km/s; two or three exceed 100 km/s; none approach anywhere near the 2–400 km/s critical rotation velocity. So, one can hardly look for the origin of extended atmospheres in rotational instability, for these T Tauri stars. Kuhi suggests that the historic characterization of the T Tauri absorption lines as "broad and shallow, probably due to high rotation" more probably arises from a filling-in of the central regions of strong lines by the emission-veiling effect. We also note the possibility of nonthermal line-broadening from velocity gradients in any outward flow velocity. Smith and Karp (1978) consider this possibility for τ Sco, in the B-star analogous situation, but reject it as requiring too large ($10^{-5} M_{\odot}/y$) mass-loss. However, the cited work on the unusual T Tauri star, V1331, returns to this possibility in discussing the line-broadening by P Cyg-type absorption on the blue edge. Smith (1981) also summarizes the possibility of oscillations, nonradial and radial, introducing such line-broadening. For us here, the essential aspect is simply the anomalous line-broadening, apparently not due to rotation, whether it comes from a nonthermal chromospheric-emission filling in of absorption lines, or actual nonthermal motions.

The importance of *chromospheres-coronae* for T Tauri stars was put into focus long before the spatial era's demonstration of their universal prevalence in all stars. It was placed there by Joy's (1945) observation that the T Tauri spectrum resembles that of the solar chromosphere—one usually forgets to add "as seen at eclipse." The suggestion was further developed by Herbig (1962, 1969), and enthusiastically explored by a number of us (Kuhi, 1964; Dumont et al., 1973; Cram, 1979; Heidmann and Thomas, 1980; Calvet, Kuhi, and Vogel, 1981). It has many advantages: particularly, it is easier to obtain rapid line variations if their formation occurs in a small volume. The passing of the NaD line from emission to absorption in a half-hour (Kuhi, 1982) is a good example. I return to the

H α problem below, and in Part III, but after spending some years, collaborating with Nicole Heidmann and discussing with Cram, trying to produce the observed H α profiles in a deep-lying chromosphere, I conclude that a chromosphere alone cannot produce the whole profile (Heidmann and Thomas, 1981). A major objection is that, because H α is photo-ionization-dominated, its emission peak should be directly proportional to a BaC *in emission*. No such increase in the BaC is observed to come anywhere near the large observed peak intensities of H α , even though our earlier work found a correlation between H α and BaC (Dumont et al., 1973). But now, I briefly abstract the farUV and X-ray results, to put modern support of Joy's suggestion into focus.

First, one should realize what Joy's suggestion means, in comparing T Tauri and solar chromosphere. H α is in emission, hence resembles T Tauri stars, in the *solar-chromospheric eclipse spectrum because that solar atmospheric region is very transparent to the Paschen continuum*, so there is no continuum adjacent to H α . For H α to be in emission on the solar disk, where there is a 6000 K PaC, would require: *either* a strong nonradiative heating in solar atmospheric regions having significant BaC opacity, to raise the BaC emission relative to the PaC sufficiently to produce a large source-term in the H α source-function (cf Chapter 2); *or* a several orders of magnitude increase in n_e , and some increase in T_e , in those eclipse regions. The last alternative is excluded, except in flares. The first alternative requires the nonradiative heating to occur much deeper in the T Tauri, than in the solar, atmosphere. Hence, Joy's suggestion requires a deeper-lying chromosphere, in the T Tauri stars relative to the Sun; i.e., a larger non-radiative energy-flux. In the same way, seeing the singly-ionized (superionized, for this spectral type) metals on the disk, rather than in the eclipse-limb spectrum, means a larger T_e in regions of greater density. Because the density distribution is exponential, in these atmospheric regions, the actual height-decrease for the origin of the chromosphere is not necessarily large; but the chromospheric density values are.

Second, for optimum production of H α , one would like an atmospheric region with $T_e \sim 1-2 \times 10^4$ K. For Sun and T Tauri stars, this means a T_e -rise from photosphere to chromosphere. For Be-stars, as already emphasized, it means a T_e -drop: anti-chromosphere. The ionized-metal emission lines require the same kind of differential T_e change. The presence of the *neutral* metal lines, and especially that they are seen only in absorption in the Be stars, at shell-phases, further compounds the apparent difference between Be and T Tauri stars. The presence of low-excitation forbidden lines of O, C, S—observed in all the T Tauri stars, but only Bep stars—restores harmony: it requires low-density, $n_e \lesssim 10^8$, cool regions: clearly these lie outside any chromosphere-corona, especially a low-lying one. This was the situation from visual, ground-based observations prior to spatial ones: implications of outward increase in T_e , then decrease. We ask how such spatial observations—farUV and X-ray—complement the picture.

There our picture of chromospheric-coronal regions is currently a strongly-evolving one, as data accumulate. Gahm summarized the 1978 situation (IAU commission 27 report) as farUV lines generally detected up through C IV. His 1981 summary (Goddard First IUE meeting) noted that N V was increasingly-detected in many stars. Si IV, C IV, N V lines show fluxes some 10^3-10^5 times solar values, with correspondingly large values for the emission-measures ($\int n_e^2 dh$). Even given T Tauri radii 3–10 times solar values, such farUV values completely support the idea of lower-lying, hence, denser, chromospheric-coronal regions in T Tauri stars, relative to normal FGK stars, like the Sun. By contrast to the involved discussions of hot star observations, where various astronomers debate radiative vs. collisional production of such lines, hence extent of RE vs. nonradiatively-heated regions, it seems universally accepted that these Si IV, C IV, N V lines require sizable regions of $T_e \sim 10^5$ K, in T Tauri, and stars like them. Typical, more specific and detailed discussions of farUV observations of T Tauri stars are given by Cram et al. (1980), Jordan et al. (1982), Bertout (1982). These references stress that the total energy radiated from such superionized regions is very large; it corresponds to some 2×10^9 erg cm $^{-2}$ s $^{-1}$, which is some 10^{-1} of the photospheric radiative-flux. Again, these values are some 10^4 larger than for the Sun—and they correspond to the non-radiative flux necessary to heat the regions where these lines are emitting. There is an important corollary to this comment on size of nonradiative heating required. Both Cram et al. and Jordan et al. conclude that their data—on quite different stars—require quite small T_e -gradients. Cram et al. note that this resolves, for the T Tauri stars, a point which has been controversial for the Sun. There, it has often been asserted that the solar chromosphere-corona transition-zone is heated by downward conduction from the corona, rather than by local heating from some mechanical dissipation. The mentioned T_e -gradients require, for the T Tauri stars, the local-dissipative, not the heat-conductive, nonradiative energy-source. Both the Cram et al. and Jordan et al. references find n_e ranging $10^{11}-10^9$ in these

regions of the atmosphere. Jordan et al. distinguish between lines requiring the lower densities—intersystem (forbidden) lines of C II and C III—and those requiring the higher; hence they suggest two distinct emitting regions; one of $n_e \sim 10^{11}$, the other of $n_e \sim 10^9$. We return to this point. Finally, we note that none of today's data—visual or farUV—give evidence of the 1–2000 km/s variable velocities found in the chromospheres-coronae of some Be stars, or of the 3–800 km/s variable velocities found in the solar outer- and far-corona, cf Fig. 3-33 in Section F. We have already remarked on the Schneeberger et al. interpretation of the absorption components of their H α profiles as suggesting expansion velocities as high as 250 km/s. Chavarría-K gives blue-edge velocities of 300–550 km/s for the P Cyg absorption depressions in V1331 Cyg. One notes, as already emphasized, that no direct spectroscopic measures of $V \gtrsim 50$ km/s over the solar surface as a whole exist. One can only wait for more data, not speculate. We return to the point in Section F.

The same characterization as a currently-evolving problem can be made of our picture of T Tauri coronae from existing X-ray data: cf Feigelson and DeCampli (1981) and Walter and Kuhi (1981). In abstract, X-ray emission in the 0.1–4.5 keV band range 10^{29} – 10^{31} erg/s, by comparison with the values 10^{32} (the Oe/Be star ζ Oph) to 10^{33} (B-normal star τ Sco). The range of Be values in the Bradt et al. catalog is 10^{33} – 10^{37} ; but most of these Be stars are poorly observed. For our present interests, the significant point is the anti-correlation between H α emission and X-ray emission for the T Tauri stars found by Walter and Kuhi. If the total H α emission is mainly chromospheric, this Walter-Kuhi correlation implies greater X-ray emission with lesser chromosphere, which is difficult to understand. If the H α emission is mainly extended-atmospheric, and post-coronal, the Walter-Kuhi correlation implies that the larger the cool H α emitting envelope, the more the absorption of X-rays from an underlying chromosphere. This is quite reasonable. We note that this is consistent with the *very sparse* Be-data: more X-ray emission from the B-normal star—i.e., less X-ray absorption. And again, both these sets of data—T Tauri and Be—are consistent with the picture of independent nonradiative-fluxes (which heat chromosphere-corona) and mass-fluxes (which provide the extended H α envelope).

So, *the importance of the post-coronal atmospheric regions, and their linkage to the local stellar environment*, come naturally into focus when we try to explore further the regions where the C II, C III low-excitation forbidden lines, and X-ray absorption, occur. The former aspect, forbidden lines, recalls for us an historical-alternative to “emission-peculiar” for characterizing T Tauri stars; i.e., “nebular variables,” based on their association with nebulae. The latter aspect gives us, for both Be and T Tauri stars, a focus on the properties of a cool, H α -emitting, envelope. For the Be stars, such an envelope was apparently linked to the production of a “local-environment” by self-interaction between variable mass-fluxes at different epochs. A primary problem is to distinguish between interaction with the actual local ISM, and with the mass-flux of earlier epochs. So we have the two alternative ways of approaching these post-coronal regions. One is a focus on the distant environment of these stars, with Aller (1964), who abstracts the T Tauri characteristics under those of “variable nebulae and the associated stars.” We ask if a “nebular-environment” can collapse and produce atmospheric peculiarities; we have already commented on the puzzling nature of so few inverse P Cyg profiles if this alternative is literally true. The other approach follows the Be picture: a focus on a local “manufactured” respect. We have too little data to distinguish ordinary, and Herbig, Be behavior in this environment. I highly abstract the T Tauri stars from the first focus, and fill in details from the second, to try to put these atmospheric, environmental, nebular questions into perspective.

Then Aller's (1956) focus lies on various kinds of nebulae, and the stars associated with them, for purposes of comparison with the planetary-nebulae, in which the associated star is centrally-enveloped. Nebulae showing emission lines are far most often associated with the hot O–B stars, which have no fixed location relative to the nebula, but are simply presumed to excite it radiatively. All O stars in the galactic plane are associated with emission nebulae—the so-called H II regions of ionized hydrogen—the only requirement being that such regions lie within the “Stromgren-sphere” about the star, earlier discussed. Such stars lying $\gtrsim 300$ psc from the galactic plane show very few such H II associations; hence the classical implication that these nebulae are ISM, not produced by any mass-flux from the star. Hubble found that if the exciting star were colder than about B1, the nebular spectrum would usually be that of the star. Aller introduces those variable, bright-line nebulae associated with the T Tauri class of the cool G–K dwarfs as the exception to the Hubble rule, noting that extended nebulae associated with T Tauri itself has been known since Hind's 1852 observations; thus we have known their existence as long as we have that of the Be stars. Herbig (1952) found that the brightest, and most distant from the star, nebula is a reflection nebula, apparently

excited by T Tauri, similar to those excited by B stars. But there exists a smaller, condensed, nebula—having its own forbidden-line spectrum of [O I], [O II], [S II] but not [O III], plus H α —surrounding T Tauri itself. Since then, the T Tauri class of stars has much evolved; and its characteristics, elaborated, as summarized above. We simply emphasize that the strong [O I] and [S II] in the stellar spectrum must actually refer to the low density, enveloping, nebulosity—only not as distant as in the (resolved) PN situation. In the early historical days, one had the same problem of confusion between different classes of objects; Z And, the prototype symbiotic star of the following section, wanders in and out of the literature of all these classes.

In passing from Aller's focus on the distant environment to ours on the local, and a further elaboration of T Tauri characteristics by comparing them to those of the Be, it is better to continue from the environment inward, rather than from the photosphere outward as we have done in discussing the preceding kinds of emission-peculiar stars. Because, we have seen that two things measure the production and character of a local environment by an interaction involving the stellar mass-flux. One is the properties of the medium with which the mass-flux produced at that epoch collides: it can be the ambient, local, ISM; it can be the mass-flux of a preceding epoch. This effect is measured by where the exocoronal density distribution become less steep than r^{-2} . (This is by contrast to the pre-corona, where chromosphere-corona transition is measured by where density-gradient takes an r^{-2} character as contrasted to an exponential.) The density distributions of WR and solar atmospheres already mentioned (and to be made more explicit in Section D), and that of the PN, are illustrative. The second effect comes from the energy involved in the interaction, the mass-flow velocity; the nova is the prime example, again relative to the Be, and similar, stars. So we compare data on atmospheric extent of the T Tauri to the Be, and Be-similar, stars.

Then we noted that while the "ordinary" Be stars show small IR excesses, they show neither radio excesses; nor the low-energy forbidden nebular lines like those from [O I], [O II], [S II] quoted above for T Tauri + its enveloping nebula; nor the higher-energy forbidden lines like those from [O III] and [N III] shown by the PN; nor the coronal-level [Fe VII]—[Fe X] etc. seen in symbiotic stars (Section C following) and novae. By contrast, the Bep stars show much larger IR excesses, the low-excitation forbidden lines, and sometimes radio excesses. Neither Be nor Bep stars show dust "signatures" in the farUV. Now, in comparison (Cohen, 1980; Bertout, 1982), the T Tauri stars behave like a more extended-atmosphere Bep star—but not an excited one, like the symbiotic and novae stars. In addition, however, some T Tauri stars show the silicate-dust signatures near 9.7μ , and also ice signatures near 3.1μ . In the radio region some T Tauri stars, including T Tauri itself, show just marginal radio excesses. Thus, the picture we have of T Tauri atmospheric extent is a structure much more extended than a Be star, possibly comparable to a Bep star, and less extended than either a symbiotic or PN star. There is the complication of the nebula enveloping the star, as possibly providing the dust, radio, and a part of the IR excess. For insight, we turn to the Herbig Be and Ae stars, which appear to give the same visual spectrum as ordinary Be and Ae stars, but are, like the T Tauri stars, enveloped in nebulosity. Their added feature to the ordinary Be stars is a stronger IR excess, radio detection, and sometimes silicate-dust signatures. They do not exhibit the high-energy forbidden lines, nor the coronal-type forbidden lines. Thus, it is tempting—but certainly not proven—to associate, as an extension of Aller's comment on the [O I], [S II], [O II] observed in T Tauri, these low-energy forbidden lines, the large IR excess, the radio excesses, and the dust-signatures in the IR with the enveloping nebula, not with the star proper. It would appear, by comparing ordinary and Herbig Be stars, that such nebulosity is "fortuitous"—unless one prefers parental—local ISM, rather than manufactured ISM: but this is, to the extent of present data, conjectural. What is significant, is that neither Be nor T Tauri—ordinary or nebular-enveloped—show signs of high-excitation forbidden lines. Thus, we do not find evidence for that kind of collisional interaction, which is produced by a strong mass-flow, at these distances where particle-concentration has dropped to the $\lesssim 10^8 \text{ cm}^{-3}$ values required to avoid collisional de-excitation of the metastable levels giving these forbidden lines. As mentioned above, and as will be stressed in Section C following, both symbiotic stars and novae do give evidence for such high-excitation collisions at low densities, hence far from the central star. So we conclude that Be, Bep, Herbig Be/Ae, and T Tauri stars do not have collisions between wind and "local-environment" as far from the star as do the cataclysmic and symbiotic stars.

Thus, if we take the characteristics of the H α envelope of both T Tauri and Be stars—and their strong resemblance, which we have already discussed—as indeed cool and low-velocity ($V \lesssim 100 \text{ km/s}$), we conclude that any high-velocity ($V \gtrsim 2\text{--}300 \text{ km/s}$) flow must have been decelerated *reasonably-close* to the star. We know such flow exists

for the Be stars, observationally. We *assume* that it must exist, at the 2–300 km/s level, for the T Tauri stars, to produce an extended atmosphere by a $V \geq q$, the local thermal velocity, at high-enough densities to maintain such an extended atmosphere. We consider all these details in Part III: here, we only focus on the basic observational material. And, in this T Tauri, Be star comparison, the basic material is three-fold: (i) the existence of a high-density extended atmosphere, as evidenced by the range of material from H α to X-ray emission; (ii) the existence of a chromosphere-corona just above the photosphere; (iii) any collisional deceleration of mass-flow, and production of a “local-environment,” occurs relatively near the star, not at PN-type distances.

Finally, in discussing such cool regions overlying chromosphere-corona, we have taken for granted that the deceleration and cooling must result from a collisional interaction between mass-flux and “local environment.” Bertout (1982) has proposed the same kind of structural model, but with different origin. The post-coronal cooling is supposed to result simply because of the greater particle concentration in the T Tauri, relative to normal FGK, corona; so radiative cooling is much larger. This also reduces the energy content of the gas, and it decelerates. An empirical decision between the two alternatives will depend upon whether evidence for collisional interaction can be found, such as the two T_e maxima earlier discussed. From a theoretical standpoint, as we discuss later, there is strong evidence that the original Parker-type acceleration of the gas from its (adiabatic) energy storage is insufficient to match the observed final velocities in the Sun, a typical, non-T Tauri, FGK star. So, a radiative cooling is insufficient to produce the required deceleration. Bertout also stresses the utility of radio—and of course farIR—measures in deciding between the several possible density distributions (Bertout and Thum, 1980). A spectral dependence of $\nu^{0.6}$ corresponds to the r^{-2} distribution; other values, to other distributions (cf Panagia and Felli, 1975). For only a few stars have T Tauri radio-spectral measures been made (Bertout and Thum, 1980; Cohen, 1981). The real problem is that we would like to investigate such density-dependence in the region of mass-flux interaction, which—for Be and T Tauri—is too far interior to the radio diameter, *if* the above discussion and conclusions are correct. On the other hand, the region of such interaction does, for symbiotic stars and novae, appear to fall within the range where these radio studies can be critical, in complementing results from high-excitation/ionization forbidden lines.

C. SYMBIOTIC STARS AND SYMBIOTIC PECULIARITY

In this section, we focus explicitly on that type of peculiar star called SYMBIOTIC, by Merrill (1933), because they show what he called “combination spectra.” Such spectra combine features observed in stars classified cool (or late) under the MK system, which have low-photospheric temperature, with emission features requiring high-excitation conditions. Note the hot/cold definitions are not parallel. *Cold* is defined in terms of a normal-star observational characteristic: e.g., TiO absorption. *Hot* is defined in terms of a *peculiar* star observational characteristic, which is anomalous in even hot normal stars: emission lines. The superficial temptation is simply to conclude that one observes two stars which lie so close as to be unresolved; indeed, Sahade’s summary in the Greenstein volume (1960) combines, under “composite systems,” a summary of close binaries and symbiotic stars. If one always had two spectra, reflecting the orbital motion, there would be no problem. But, we do not have two spectra; and we have already referred to the notation “single-lined binary (?),” and its ambiguity; Are there really two stars, or do the spectroscopic peculiarities arise, somehow, in only one star? Actually, this category is a storehouse of ambiguity, just because of that variety, and intensity, of spectra implied by using the term “symbiotic” to characterize *visual* spectra. We have already noted that the prototype star of the class, Z And, has variously been labeled: nova, Be, nebular-variable, PN, etc.

As we have continuously stressed, an historical ambiguity between binarity and single-star was prejudiced toward binarity as long as one believed that real-world stars can be described by the standard atmospheric model consisting of a quasi-isothermal photosphere, and nothing else. Under such conditions, it was hard to imagine the same star producing—simultaneously or even sequentially—the TiO absorption bands characterizing an M-type star, but also He II in emission—even though R Cor Bor, showing no evidence of binarity, produces such He II emission and various C molecules, episodically. As Harwit (1981) emphasizes, it is hard to consider such arrays of symbiotic, speculative star-contradictory, data on individual stars to be the proper nourishment for training speculative-theoretical astrophysicists: too many details, too few generalities. In a crude way, one can regard a study of symbiotic

stars to be the height of a study of stellar individuality. First, there is that decision on class of stellar peculiarity into which any particular “symbiotic” star might best be placed. Then there is a decision how to subclassify it—in terms of what physical parameters—when it is found to be extraordinary even among the peculiar star class to which it has been assigned. In that sense, today, the WR stars are perfect symbiotic stars: essentially all types of stars show, in some member-star of that type in the farUV resonance lines, some trace of the Si IV–C IV–N V–O VI superionization indicators; only the WR are so crude as to show these ions, via subordinate lines, in the visual spectrum.

But in the preceding pages of this chapter, we have seen that *it is the presence of some degree of symbiocity, in all stars—single or multiple—which is “normal,” not its absence.* The situation changed from the historic speculative one because we find, empirically, that the stellar atmosphere is generally multi-, not mono-, regional. We find, empirically, that what characterizes all stars is not just a photospheric radiative-flux and gravity: but also a nonradiative energy-flux; a mass-flux; maybe, in some of them, other fluxes such as magnetic, etc. The observational level to which the several regions appear, and the sequences in which they appear, can vary strongly, among “like” stars, and in the same star at different epochs. Apparently, such individuality and variability reflect the different sizes of these several fluxes, and the perturbation of gravity by the velocity associated with the mass-flux. Empirically-theoretically, we find the star is a thermodynamic (open, nonthermal) system rather than a (closed, thermal) one. And we ask the variety of stars, under the framework of this nonlinearly nonEquilibrium open-system thermodynamics, to guide us to the correct variety of equations needed to model such structure. So, in a sense, the visual-spectral defined, hence blatant, symbiotic stars should give us the extremes of what we must model: in variety of atmospheric regions, of sequences of regions, of kinds of fluxes, and of kinds of terms to include in our equations. Under the caution that certainly some of these symbiotic “phenomena” must reflect multiple-star symbiocity, not just single-star, we briefly survey them, for additional perspective on the range of symbiotic phenomena that modeling must encompass. As in the preceding sections, I continually stress the properties of regions, and sequences of regions, required to produce these peculiarities—here, symbiotic.

1. Gross Considerations on Sequences of Atmospheric Regions vs. Binarity to Put Symbiotic Stars into Perspective

We have discussed the evolution of such sequences of atmospheric regions in passing from observed-cataclysmic stars as exemplified by varieties of novae, to WR, to Be, to Be-similar, to inferred-cataclysmic stars as exemplified by PN, through T Tauri and some stars intermediate to them and Herbig Be/Ae. The basic observational phenomena which are similar in this progression are a photosphere partially characterized by a radiative flux; a chromosphere-corona partially characterized by a nonradiative energy-dissipation; and a variety of atmospheric regions whose density distributions are determined dynamically rather than thermally-statically. Among the basic observational phenomena which characterize the particular atmospheric regional sequence, and which evolve among the types of peculiar stars discussed, are: kinetic energy and total matter in the mass-ejection, and (possibly coupled) energy level of the spectroscopic state, in each atmospheric region; the location, if it exists, of an exophotospheric, possibly mixed pre- and post-coronal, low-energy H α emission region; the location, if it exists, of a region producing an α Cyg-type spectrum of narrow, low-energy absorption lines (sometimes replaced by emission lines); the location, if it exists, of a post-coronal region producing low-energy forbidden lines; the same, for high-energy forbidden lines; and the same, for various farIR and radio excesses; the same, for dust and ice species. For all these, one tries to establish relations to the size of the mass-flow, its velocity distribution, and any association between such flow and nonradiative-heating effects.

By contrast to the single-region atmosphere of the standard-model, the total spectrum across a wide range of λ of each such sequence of atmospheric regions is a combination of what is produced by the enumerated sequence of regions. Precisely what is the range of ionization/excitation level depends upon the particular star, and sequence of regions. But in the broad sense of the term, at any one epoch, one expects to see some aspects of a “symbiotic spectrum” in the above sense of Merrill.

We have stressed variability as a characteristic of most of the above types of stars and sequences of atmospheric regions. The variability lies in both luminosity and spectrum. The extreme of such variability lies in that between the

quiet and active phases of the cataclysmic variables. And there, the symbiotic character of such spectral variability is most marked. We recall that the nova traverses phases where its visual spectrum varies from early B-type absorption, through nebular, through coronal, to showing the TiO bands of an M-type star. Recalling McLaughlin's characterization of the Be star, 59 Cyg, as exhibiting "long periods of quiescence and short periods of activity;" and also recalling that such activity consisted of reasonably-abrupt increases in luminosity, followed by the production of sharp-cored Fe II absorption lines, we recognize again a high-excitation/low-excitation combination: bright B main-sequence, then faint A supergiant. And we note the T Tauri, where a fading of an emission spectrum in the blue leaves an M-type absorption spectrum in the red. In this sequence of "symbiosis," the range and size of the effects progressively diminish. When we adjoin the farUV spectrum, we find—as for the Sun—another dimension of symbiocity—an enormous increase in the high-ionization/excitation aspect. And, indeed, we find a variable X-ray component. Merrill's recognition of a *symbiotic phenomenon* is a ubiquitous character of most, not just confined to a few, stars. One must just observe across a sufficiently broad spectral region. In our new understanding of the multi-regional aspect of stars, this means simply that one must observe many regions, not just the photosphere, to recognize such generality. In some stars, notably Merrill's symbiotic, it suffices to observe the photosphere, in the visual spectrum, to recognize that the symbiotic character is the predominant one.

Then, to put the binarity alternative into focus, it suffices to quote Payne-Gapsochkin's characterization of the physical features associated with binarity, in their nova application: (a) the orbital period is not correlated with the range of the outburst; (b) the orbital period is unrelated to the outburst-cycle; (c) there is no correlation between orbital period and velocity of mass-ejection; (d) brightness varies on many time-scales, which are unrelated to the orbital period. (Again, one could be describing Be-star binaries; cf the 88 Her discussion by Doazan and Harmonec, already mentioned.) She further summarizes the properties of eight stars in systems which were called cataclysmic, but in which the red-companion is not low-luminosity, but a late-type giant. T Cor Bor is a well-defined nova; R Aqu is enveloped in an expanding nebula that is interpreted as an explosion of (200 yr) ago; four stars show repeated cataclysmic outbursts; four are listed as of "Z And" type. Again, we note that Z And itself started its astronomical career by being identified as a nova; later, it was removed from the class because of insufficiently large luminosity range, and is generally accepted as the prototype symbiotic star. We proceed to consider it.

2. Photospheric and Pseudo-Photospheric Symbiotic Characteristics

We have stressed that in WR stars one sees little, if any, trace of a "standard-like," HE and RE, photosphere. In other stars, such as the T Tauri, we stressed that the photospheric MK class was *usually* recognizable, even though veiled by the exophotosphere, which gives slight hotter-star character to a red-star photosphere. In other stars, the veiling effect is the inverse; intrinsically-hot photospheres are reddened, as in such stars as the central ones of the PN. Even in the B stars, as they change phase, the photospheric MK class remains *largely* recognizable, in spite of reddening effects. In the novae, the situation is different; the large ejection introduces a nontrivial change in standard MK class, and energy distribution. An initial, usually B, premaximum spectrum shifts to class A, even F and later at maximum and immediate postmaximum. When the opacity of the "ejected photosphere" decreases sufficiently, we obtain the gradually-emerging effects of the "underlying," very hot photosphere: the star reverses the change, and becomes bluer. Presumably, this latter persists, throughout the posteruptive phase. For "ordinary" novae, this last phase is of undefined duration. For "recurrent" novae, the quiet-stage photosphere is presently considered to be late-type, hence, cool. But we really have, at this moment, no real basis for rejecting the possibility that ordinary novae eventually erupt again. Then, we ask just where—at what kind of star—does the underlying photosphere change its quiet character from "blue" to "red?" Clearly, this question demands much data collection, unless some new physical picture can be produced from what data we have.

The essential aspect of all this, for us here, is to recognize that the photospheric character of the star is not something always defined *only* by the continuum, and certainly not by the visual continuum alone: it sometimes requires strong extrapolation to remove the effects of this exoatmospheric "veiling." One can express this another way, in terms of "causes." To a first approximation, the photosphere reflects the effect of the radiative energy-flux

and gravity; the exophotosphere reflects the effects of nonradiative energy, and mass-fluxes—and “other” nonthermal phenomena. So, the presence of nonradiative fluxes introduces certain atmospheric effects, whose existence perturbs empirical inference of the size of the radiative-flux, hence, of the character of the photosphere, in certain stars and at certain epochs. Not all “corrections” to reduce observed, to “standard-atmospheric,” values come from the effects of the ISM; nor can they be determined “empirically” by studying stars satisfying standard-atmospheric models at differing distances from us. On the contrary, study of these peculiar stars are the best indicators of which of the deviations from standard-star predictions are ISM, and which are exophotospheric, because the effects are usually the strongest in these stars.

Then, when one studies the classical, visual, symbiotic stars, their primary characteristic is a spectrum, and spectral distribution of energy, showing both “blue” and “red,” hot and cold, features. In general, the blue spectral regions show the hot, and the red regions the cold, features. The contrast is strongest between different epochs, but some hot-cold features are shown at the same epoch. Historically, these stars showed quasi-regular (visual) luminosity variation, over the several phases; and usually one discussed these in terms of the combination of a classical B star with a classical M star, to get blue and red colors. In the earliest days of low-resolution observations, the simplest interpretation of variability was eclipsing-binarity: a low-luminosity M star, and a low-luminosity B star at sufficiently-small separation that eclipses could occur. As spectral resolution increased, one observed that the “B-star” must instead be a Be-star, then a “Be-shell” star, and eventually a “peculiar” Bep star. That is, the occasional presence of emission lines distinguishes Be from B; the presence of forbidden lines distinguishes Bep from ordinary Be; but in addition, the forbidden lines are high-excitation rather than just low, so we have a “peculiar” Bep. Indeed, during some phases, at luminosity minimum, one observes, in some stars [Fe VII], [Fe X], [Ca VII] lines. Similar lines have been observed in post-eruptive phases of novae, and in some planetary-nebulae.

Today, under observations at even better resolution, spectral and temporal, one recognizes a quasi-regular sequence of phases in these quasi-periodic symbiotic stars, by contrast to the situation in the Be stars and novae. At minimum light, what one might identify as the quiet phase, one sees a cool-star photospheric continuum, in the red, and a cool-star absorption spectrum of, e.g., TiO bands. The prototype symbiotic star, Z And, has spectral character M at this phase. Other symbiotic stars range from G through M. Thus, they fall in the same MK range as the T Tauri, but more numerous M than K. At maximum light, one has the Bep phase, with Be-shell spectrum, B-type continuum in the blue spectral region and forbidden “nebular” lines. As the star decreases in brightness, the Be-shell spectrum weakens, and the “nebular” character of forbidden, *high*-excitation lines appears. This last phase bears resemblance to planetary-nebulae, and very, very postmaximum phases of novae. Then, the cycle repeats. In a sense, one had better regard the system as “triple,” not binary: an M star, a Be-shell or Bep star, and a planetary nebula.

We have already remarked on the variety of “WR-spectra” occurring in stars other than “WR-stars.” We can similarly remark on the variety of “symbiotic spectra = hot + cool star characteristics” in various types of stars. In the prototype symbiotic star, the quiet-level phase shows the *photospheric* spectrum of a *cool* star; whereas, some of these other, “symbiotic-similar” spectra show, as just mentioned, *hot or cool* quiet-phase photospheric spectrum. We have remarked on the evidence that the prototype Z And showed, at one epoch, a nova-like abruptness in outburst; although generally, symbiotic stars show gradually varying, and more-or-less regular, changes in phase. We note Viotti’s characterization (1980) of Z And: “periods of intense activity followed by quiescent phases.” The comment is virtually the same as that quoted several times by McLaughlin on the Be star 59 Cyg. What is unspecified is the time-scales; which, apparently, are much more regular for symbiotic than for Be. Another aspect of importance is that, in marked contrast to normal M-stars, one has on a few occasions measured velocities of ≈ 200 km/s in the visual spectra of symbiotic stars. Later, in summarizing mass-flux measures across the HR plane, we will note that there *is as yet no direct evidence* for $V \gtrsim 100$ km/s in normal M stars. However, very recent farUV observations of the M sg TV Gem, at low dispersion, suggest that the star, at some epoch, shows a combined B-star + M-star continuum + strongly-displaced C IV lines, some 8A, or 1500 km/s, and not-displaced Si IV lines (Michalitsianos et al., 1980). Most symbiotic stars show their farUV superionized lines in emission; the C IV and Si IV lines, just described, are in absorption, in TV Gem. The authors reject the possibility that these lines at $\lambda 1540$ can actually be C IV, because of the large velocities, relative to what is commonly seen in other symbiotic stars. We note that precisely this

behavior of C IV and Si IV absorption lines is what we found in 59 Cyg (Doazan et al., 1980). One clearly has the alternatives of TV Gem being an unusual variety of symbiotic star, or an actual binary. One eagerly awaits high-dispersion SWR farUV observations; thus far, the authors have high-dispersion observations only in the LWR.

This last comparison places in focus another characteristic of classical symbiotic *stars* vs. symbiotic *spectra*. Classically, symbiotic *stars* have been considered to be composite of an M *giant* plus a B *main-sequence*, star or spectrum. We note that Be stars are, statistically, about 1 visual magnitude brighter than B stars. Often, for that reason, they are given luminosity class IV (eg γ Cas B0 *IVe*), but not always (e.g., 59 Cyg B2 *Ve*); but in any event they are not III(g) or I-II(sg). Also, novae are MS stars, as are *most* other cataclysmic-class stars, *except* prototype-symbiotic. So, in this sense, *prototype*-symbiotic stars represent, *classically*, a “larger” star in their quiet phase, “basic-photospheric” structure, than do other “symbiotic-like” stars (except the WR, with their ionization range from H I to O VI, so that they are “symbiotic-like,” in spite of lack of classical photospheric continuum). Thus, this prototype-symbiotic star brings into focus two problems, as contrasted to most “symbiotic-like” stars: that of the T_{eff} , and that of the *size* (radiating-area, radius, or luminosity class, as you prefer) for the basic, classical, stellar *photosphere* of the underlying star. The remaining phenomena, which give the symbiotic appearance, come from the extended outer-atmosphere produced by the mass-flux, the heated outer-atmospheric regions produced by the nonradiative flux, and the ultimate cooled and decelerated far-outer-atmosphere. (That is, this would be the picture *if* one rejects binarity, or triplicity as explanation of the composite, variable spectrum.) Clearly, much remains, observationally, to be done to clarify these two aspects of *size* (of photosphere, of the various regions of outer-atmosphere) and T_{e} (of photosphere, of the various regions of the outer atmosphere). A clear delineation of the difference between these prototype-symbiotic, and symbiotic-like stars, together with a clarification of which phases are “quiet” (i.e., characterized by minimal mass-flux perturbation of the atmospheric structure), are essential.

3. Exophotospheric Symbiotic Variability

We quoted Viotti's characterization of the phases of symbiotic stars: “periods of intense activity followed by quiescent phases” to parallel McLaughlin's summary of Be-star phases, as exemplified by the large collection of observations of 59 Cyg and γ Cas. Similarly, detailed studies of the prototype star, Z And, make clear the details of this characterization; around this prototype other, less detailed, data exhibit the “individuality” of symbiotic stars and phenomena.

We noted that Z And was first classified as a nova, and this classification characterizes the active phases of such stars: these active phases exhibit recurrent, nova-like eruptions of varying amplitude (Mattei, 1978; Altamore et al., 1981). An abstract of the line-spectra of Z And across the phases summarizes the situation which must be modeled.

a. Variability of the Line-Spectrum. During minimum light, which occurs in the quiet phases, one observes *almost* as large a range of ionization as in the WR stars. In the blue, one sees emission lines ranging from O I to [Fe VII]; the highest-ionized permitted lines come from N V and O V. In the farUV one observes N V and C IV in emission. Line-displacements do not exceed a few hundred km/s. In the red, one sees absorption bands of TiO.

During active phases, at luminosity maximum, the higher-ionized lines weaken. Hydrogen Balmer and Fe II emission lines are prominent; and sometimes show P Cyg absorption components, with velocities near 200 km/s. Boyarchuk (1968) comments that the increased luminosity appears to come from increased emission in the blue; the red continuum stays essentially constant. The blue-increase “veils” the blue part of the spectrum. Boyarchuk and Altamore et al. suggest this implies the Z And “system” is surrounded by an expanding opaque envelope.

b. Individuality of the Line-Spectra—and “Objects.” In addition to the above features of more-or-less permitted lines, Z And symbiotic stars generally exhibit a planetary-nebular type spectrum as the brightness declines at the end of the active phase. Sahade (1976) suggests that there appear to be two main types of symbiotic stars: those showing no evidence of IR emission from dust, and those which do—and the latter exhibit a high-excitation, largely forbidden

spectrum. This spectrum includes [C III], [N V], [Fe VI], [Fe VII]. There are indications that the latter class includes “cold components” whose energy distribution is more yellow than red. Among some few symbiotic stars, as among some planetary-nebulae and novae, one observes the [Fe X] red (solar) coronal line. Sahade discusses (1976) possible identification of such stars with X-ray sources.

The planetary-nebular characteristics are so strong, among some stars, that they were indeed first classified as planetaries, only later as symbiotic stars. And even now, one debates the adequacy of such classification. Those symbiotic stars showing a strong farIR excess, often also show radio excess. V1016 Cyg shows strong farIR and radio excesses. After a 1965 outburst, the ionization-level of its nebular spectrum rose steadily to [Fe VII], possibly [Ca VII]—but including [Fe II], and some evidence for the TiO absorption band. Inferred velocities are low, lower than for the more usual symbiotic, and closer to the PN. Consequently, Mammano and Ciatti (1975) propose that it is an “incipient” planetary-nebula, rather than typical symbiotic.

In the same way, Blair et al. (1981) note the resemblance of HM Sag to V1016 Cyg. HM Sag rose 5 magnitudes in 5 months. However, precise data suggest its “cool-component” is more likely a K subgiant, rather than M giant. So, the authors suggest it is a “symbiotic cousin” of the RS CVn—the “binary” counterparts of the T Tauri stars. Suggested line-identifications range from the Balmer lines, [Fe II], through He I and He II, to [Fe VI] and [Fe VII]—[Ca X] is listed with a ?.

Thus, we see that the sequence of stars which centers on the diagnostic ambiguity between multiple-stars or multiple-atmospheres, and multiple-atmospheric-regions, is hardly provincial in membership. Starting with the Be and Bep stars, we went in two directions. One, the Be-similar, hot, stars. In the other, discussing the T Tauri stars, we stressed that its Balmer emission lines might be considered as superionized, if there were no regions between where they are formed and an FGK star standard photosphere. However, given the ubiquity of chromospheres-coronae, the T Tauri simply fall into the Be-similar sequence of cool, decelerated “local-environmental-producing”—and “interacting” stars—and the Balmer emission lines are a subionized species. Neither Be nor T Tauri stars can be excluded from that variety of objects showing symbiotic phenomena; indeed, it is hard, at our epoch, to find stars which can be excluded. And now, in these last pages, we close on the T Tauri stars from another direction, the proposed cousin of the RS CVn stars—HM Sag.

There is a link left unclosed—or at least, unremarked: the high and low ionization categories in the symbiotic stars, and the Bep peculiar in the Be stars, and the problem of the rare, but occasionally present, forbidden, highly-ionized lines from [N V], [Fe VI, VII] up through [Fe X], maybe [Fe XIV]. The “ubiquitous” chromospheric-coronal presence leaves unsurprising such lines produced in low-lying chromosphere-corona. But one notes that one observes these lines in the Sun because the solar corona is very extensive—it cools gradually all the way to the Earth; coronal lines are produced over a region of several radii. The solar wind does not take over as the density-control until some 3 radii (cf section following, on extended-atmospheres). To see such forbidden coronal lines, requires a large emitting volume. If the Be mass-flow is stopped within a radius or so, as required to produce Balmer emission lines of the observed intensity; the density is too high and volume too low to expect such [Fe X], etc. lines to appear strongly. But we note that this deceleration of the mass-flow should produce a second corona, at whatever location the mass-outflow interacts with that from earlier epochs. If, indeed, there is a sequence of such cool envelopes, beginning at varying distances, depending upon this interaction and its details, some stars should provide the proper combination of density and atmospheric extent to produce such [Fe X], etc. We defer this problem to Part III. Here, we simply note it, as one more bit of evidence for use in such empirical-theoretical modeling.

We have already remarked that Sahade has proposed the existence of such a second corona (1980) to reconcile the farUV and visual WR spectral correlations between line-widths and ionization level. His later modification of it to depend on binarity, and Willis’ argument that such a second maximum of T_e is not necessary, does not remove its possibility.

Finally, we should note, in the above connection, the suggestion by Altamore et al. (1981) that the highly-ionized lines arise in the chromosphere-coronal transition region of the M-type component of the symbiotic-binary. The essential aspect of such a suggestion is that the lines arise in the atmosphere of one star, with no relation to the binary character of the symbiotic system, as contrasted to their arising in the postulated accretion disk. The essential

aspect of the suggestion—or, better, recognition—lies in its acceptance, as an essential part of symbiotic modeling, that *actual*, rather than standard-speculative, stellar atmospheres be adopted to indicate what a multiple-star model must provide. Given that understanding of single-star atmospheres which our preceding discussion of stellar peculiarities puts into focus, one must re-think the multiple-star problem. We need neither accreting disks nor mass-flow impacting on them to provide enough energy for chromospheres-coronae and X-rays. Nor do we need, a priori, “cold-companions” to match Balmer, or farIR, or radio emissions. What we do need, is self-consistency of all those atmospheric regions the observations tell us exist in single stars. So, by continuing this study of sequences of stars, which map sequences of regions as one goes farther and farther from the photosphere, we hope to establish the variety of atmospheric patterns and possibly sequences of them.

As examples of the historical evolution, as data improve, we note that the first ad hoc model of a symbiotic star was Plaskett’s (1928) picture of a cool star surrounded by a nebula. The difficulty of heating the nebula, imposed by the classical RE, was attacked in Aller’s (1954) proposal of applying the solar chromospheric heating by shock-waves. Gauzit (1955, 1958) replaced “nebula” by “extended-corona,” and shocks by solar-like prominences, similar to my own (1948, 1949) heating of solar and WR atmospheres by spicules-jets-prominences. On the other extreme was a return to the planetary-nebular configuration of a hot central star enveloped by an extended, cool outer-atmosphere, which was quasi-homogeneous for Sobolev (1960), and existed only at the equator, for Menzel (1946), so resembling a similar model for Be stars (cf Marlborough’s models, 1969 et seq., and review, 1976). For more details on these, see the reviews by Sahade (1960, 1976) and the cataclysmic volume in this series.

If one adds to this historical perspective on single-star symbiotic modeling the current preoccupation with multiple-star modeling, one finds essentially the same kind of models adopted for no matter what kind of peculiarity. Because, simply, as we have seen, the various kinds of peculiarity are strongly related. So: hot star, cold star, disk, and mass-flow. While usually the mass-flow is from cold to hot star, the reverse is occasionally the case. But one notes that for single stars, hot-star mass-loss is usually larger than is cold-star. We return to the point, in summarizing the superthermic velocity field peculiarity.

We now turn to three other kinds of peculiarity, quite different from the preceding three. *For those three, distinct features were immediately, strikingly, contradictory to observed features of normal stars. For the three remaining, differences are striking relative to the expectations from normal modeling.* Thus, in a sense, they are a bridge between peculiarity and anomaly, as we have defined these two terms. They are more striking than anomaly, because their sizes, under the simplest observations, are so clearly in contradiction with the classical, normal model that only trivial computations are needed to show this. For anomaly, the required calculations are more refined. Furthermore, in the preceding discussions, we have already considered some evidence for the remaining three peculiarities: extended-atmospheres, superionization, and differential atmospheric motions. However, those considerations involved distinguishing between several mechanisms for producing each of those three peculiarities, not its simple existence. Thus, they represent those refinements beyond simple, low-resolution visual observations with which we continually supplement such observations in this chapter.

D. EXTENDED-ATMOSPHERE STARS

1. General Summary

An “extended atmosphere” implies a density-gradient that is strikingly less than an exponential one at the classical boundary-temperature, T_0 . Classical modeling, as in Chapter 2, gives a density gradient that is exponential, with a scale-height, H , fixed by gravity and T_0 as

$$H = kT_0/\mu g \quad (3.1)$$

in the notation of Chapter 2. The classical radiation intensity, I_ν , in a direction tangential to the stellar limb has essentially a constant source-function, $S_{\nu 0}$, in these boundary regions, so that we have

$$I_\nu (\text{tangential}) = S_{\nu 0} \left[1 - \exp(-\tau_{\text{tg}}) \right], \quad (3.2)$$

where τ_{tg} is the tangential optical depth, given by

$$\tau_{\text{tg}}(p) = \alpha_{\text{ab}} \int_{-\infty}^{\infty} n_{\text{ab}}(r) ds. \quad (3.3)$$

The relation between the tangential line-of-sight distance, s , the radial distance, r , and the radial distance to the line-of-sight, p , is given by

$$r^2 = p^2 + s^2, \quad (3.4)$$

and the distribution $n_{\text{ab}}(r)$ of absorbing atoms is, in a plane-parallel atmosphere,

$$n_{\text{ab}} = n_0 \exp[-(r-R)/H], \quad (3.5)$$

where R is some photospheric radius, above which conditions are isothermal in T_e , and excitation-ionization do not change with height. The change of I_ν with τ_{tg} , within $1 \lesssim \tau_{\text{tg}} \lesssim 10$, gives the limb of the stellar disk. Thus, we see that τ_{tg} changes exponentially with height, $(r-R)$; and the intensity at the limb drops exponentially with τ_{tg} until τ is very small, then exponentially with $(r-R)$. So, the limb should be *very* sharp. And, regardless whether the actual value of $n_0 \alpha_{\text{ab}}$ changes greatly from one spectral region to another, the double-exponential behavior in the vicinity of $\tau_{\text{tg}} \sim 1$ means that the sharp limb of the star does not vary a *great* deal, certainly not a large fraction of a radius, with λ . Then in a phrase, *extended-atmospheric stars* are those where the density scale-height near the visual-continuum limb, or the apparent radius of the star at some λ , or log density in outer-atmospheric regions differ by factors of 3–10 and more from the classical-atmospheric predictions of eqs. (3-1)–(3-5). For a spherically-homogeneous atmosphere, the *cause* of an extended atmosphere is: *either* a departure from RE in the sense of heating to a larger T_e with correspondingly larger scale-height; *or* a departure from HE, hence, from exponential density decrease; *or* some combination of the two. The *empirical* problem is to distinguish between these alternatives; *then*, one asks *why* RE and/or HE fail.

Stars which have historically been labeled “extended-atmosphere peculiar,” because of striking observations in the visual spectrum that demand such categorization for them, essentially fall into two groups, according to the observational methods of detection: (a) eclipses, (b) other. Actually a third group should be included, the most extreme of all, the planetary nebulae, which classically was considered a phenomenon of the ISM, not of the star itself, being apparently physically separated from the star. We have already summarized how it has become recognized as giving the most directly obvious evidence of the existence of far outer-atmospheric regions, in a continuous distribution of matter from the photosphere outward.

a. Eclipse Material: A faint atmospheric extension out to several radii has been observed for the Sun at solar eclipses since 1860, de la Rue and Secchi, and by Lyot coronagraphs since the 1930’s. Quantitative measures of mass densities in the low outer-atmosphere have existed since the work by Menzel and collaborators in the early 1930’s. While few in number, there are striking examples of stellar binaries in which the “large” component, of which there are both hot-star and cold-star examples, shows an extended atmosphere by virtue of a gradual—rather than an abrupt as would correspond to applying eqs. (3-1)–(3-5) to an I_ν from the eclipsed secondary component—eclipse of the secondary. Systematic observations of such stars (ξ Aur, 31 Cyg, etc.) date from the 1930’s. We consider such eclipse material in the following Section 2.

b. Non-Eclipse Material: Since the first observations by Secchi in 1866, an increasingly numerous variety of early-type, hot stars have been noted to show striking features, such as emission lines and other radiative-flux excesses in a variety of spectral regions, for whose ensemble of characteristics no other interpretation than an extended atmosphere has yet been proposed. There was a great concentration of efforts to delineate, observationally in the visual, these features in the late 1920's and throughout the 1930's. Such efforts climaxed in Struve's 1942 empirical summary-model. We have combined these efforts, subsequent visual data, and farUV data in our summary in the preceding section B.3.b of this chapter. See, in more detail, the B-Be volume (Underhill and Doazan, 1982) and the WR volume (Conti and Underhill, 1985.) More recently, since Joy's (1945) and Herbig's (1962) pioneering work on T Tauri stars there have been other, cooler, stars, in which the same ensemble of characteristics is exhibited. For these stars, the separation between the effects of a low-lying chromosphere and simply an extended atmosphere in producing many of the enhanced radiative-fluxes is not so immediately obvious; but the separation process places these two effects into strong focus (cf the section by Kuhl in FGK monograph; Heidmann and Thomas, 1980; and Section B.3.c above).

I stress these dates, the common awareness of solar and stellar extended-atmosphere peculiarity by the early observers, and this summary article, by Struve, to emphasize that by about 1940 the phenomenological existence of this "extended-atmosphere peculiarity" among many stars, hot-warm-cold, was well established, *empirically*; and ad hoc attempts were well underway to at least model it, if not to understand its origin; but all such attempts lay within the (closed, thermal) thermodynamic framework. The physically inconsistent aspect lay in the recognition of the existence of superthermic velocity fields in these extended, outer-atmospheric regions *without* asking the effect of such superthermic velocities on the RE condition. With the postwar rush of the 1950's, 1960's, and 1970's to apply the large-scale computing machines developed in the war and postwar years to replace the simplified numerical approximations earlier adopted, astronomers tended to lose sight of the actual, observational, stellar atmospheric situation summarized by Struve, and to focus on "arithmetically-rigorous" classical atmospheric modeling, because the physics and equations under these approximations were so simple. So, aside from more-decimal-place emphasis on what we already knew to be the characteristics of such classical models, such telephone-book modeling has been largely an aberration in the evolution of extended-atmospheric, or outer-atmospheric, or "shell"-atmospheric (Struve's term) modeling. The significant *empirical* advances, relative to extended- or outer-atmospheres, since those upon which Struve based his summary have been:

- Edlen's identification of the solar coronal lines (which had been also observed in novae, symbiotic, and other stars) as superionized species of the most common elements, in 1941-42, just after Struve's article appeared. This caused the really striking "discontinuity" in thinking, which marks the 1942 epoch as significant.
- Redman's (1945) measures of differential line-profile widths in the *low* outer-atmosphere of the Sun, the chromosphere, at eclipse, to suggest nonRE values of T_e in these regions.
- The HAO 1952 eclipse observations, which firmly established such a low-atmospheric rise in T_e above RE values, and gave its details.
- The solar IR and radio observations of the 1950's which further elaborated this solar outer-atmospheric structure.
- The spatial farUV and X-ray, and the IR and radio, data of the 1960's and 1970's, which have firmly established the four basic empirical properties of extended atmospheres, solar and stellar alike: (1) superionization in the low outer-atmosphere; (2) extent of the outer atmosphere to several-to-thousands of photospheric radii, depending upon the individual star, not its classical spectral class; (3) an acceleration in the low outer-atmosphere to highly superthermic velocities; and then, for some stars, a deceleration in the far outer-atmosphere, *well inside* distances which interaction with the "normal" ISM would require for such deceleration; (4) a cooling, for some stars, to subphotospheric T_e , to produce subionization. Various stars are *observed* to show these four properties to greater or lesser degree, with such observations variable in time, again to greater or lesser degree among different stars.

Before summarizing eclipse evidence, type *a*, for these categories of extended-atmosphere peculiar stars, it is useful to simply quote an introductory abstract of Struve's summary article, which places his preliminary outer-atmospheric model into the perspective of the subsequent empirical developments just abstracted. We referred extensively to this paper in discussing Be stars; the following shows just how suggestively encompassing were these ideas already in Struve (1942):

"There has been in recent years, a growing realization that some of the peculiar phenomena generally ascribed to a tenuous outer atmosphere in some early-type stars are not confined to a few freaks in the stellar population but are probably characteristic, in a small degree, of the majority of stars in certain stages of their evolution. Beals has called attention on several occasions to the fact that there exist certain definite similarities between such widely different groups of stars as those of classes Be, W, P Cygni, and α Cygni. The tendency to show bright lines of the P Cygni type is pronounced in class A supergiants, and probably even a few members of class F show them. It is common among the W stars and occasionally is seen in stars normally designated as Be. Swings and I have called attention to the fact that several O stars with emission lines also show indications of P Cygni type structure. My own studies of dilution effects have led to the recognition of a considerable number of stars which are surrounded by outer shells or extended atmospheres, where the pressure is low and the dilution factor of the order of 0.1–0.01. Some of these shells expand, as in 17 Leporis. Others are stationary, as in ξ Tauri, ϕ Persei, γ Cassiopeiae, Pleione, etc.

The different types of shells are not yet clearly related to one another. But we do know the following facts: (a) Shells of the Be type may become transformed into shells producing strong absorption lines (γ Cassiopeiae, Pleione). (b) Normal B stars without emission lines may become at times Be stars, and vice versa. (c) Expanding shells of the P Cygni-type stars may become transformed into peculiar Be stars without P Cygni-type structure in their lines (Z Andromedae), and vice versa. (d) A-type supergiants with P Cygni type lines may at times lose the P Cygni lines (β Orionis) or show marked variations in their intensity and structure (α Cygni). (e) All phenomena of outer shells are more or less violently variable (17 Leporis, P Cygni, *V/R* variation in Be stars, etc.).

The question arises whether any star of early type may be regarded as being free of these peculiarities, or at least of a certain predisposition to develop them from time to time. This question is of great importance, because upon its answer will depend the degree of confidence which we are prepared to bestow upon discussions of "normal" reversing layers, built up according to the standard procedure, where mechanical equilibrium is assumed by setting equal gravitational acceleration and gas pressure plus ordinary continuous radiation pressure."

After elaborating on this abstract by summarizing the observational material upon which it was based, Struve sketched an ad hoc outer-atmospheric model, consisting of: (i) a "normal" reversing-layer (he focused on the line-spectrum; here we would combine photosphere and reversing-layer, and put many more lines than did Struve in the outer-atmosphere); (ii) a "chromosphere," or a layer producing static but strong hydrogen absorption lines out to large quantum number, and other absorption lines, similar to the spectrum of α Cyg (an A-type sg, so showing Balmer lines, which are sometimes in emission, much stronger than those in the normal, higher- T_e , B stars); (iii) a "corona," or a layer containing the outward-expanding material that produces P Cyg-type profiles. The essential thing to note is that when Struve wrote this article, the solar chromosphere-corona had *no* association with a rising T_e , nor with a mechanical energy dissipation, but only with the characteristics of an extended and differentially-expanding *cooler* (than photospheric T_e) outer-atmosphere. Indeed, he stressed that the degree of ionization represented by the observed emission lines was almost always lower than that of the reversing-layer: it was normal to observe Fe II and H in emission while He I was observed in absorption.

Today, using the observations subsequent to his summary that are abstracted above, and anticipating many sections of this monograph, we would indeed retain his low outer-atmospheric structure, nomenclature, and solar

analogy—but replacing the pre-1942 by the post-1942 understanding of the solar chromosphere-corona as *primarily* characterized by nonradiative heating. We would admit expansion velocities in the corona up to the corresponding thermal velocity, then adjoin an “accelerated-postcoronal” region of further increase in velocity where further non-radiative heating may or may not occur. And finally, we would displace the hydrogen, and other subionized species, origin from chromosphere to a “decelerated-postcorona,” the far outer-atmosphere, whose empirical characteristics are even today, as we have seen, only badly understood. The contrast between the hot stars of Struve’s survey, and the later, similar cool stars like T Tauri, lies in the necessity to admit a chromospheric component for ions like H, which are not subionized species in the *photospheres* of these cool stars.

But these latter-day modifications of the Struve model are only evolution, based on more extensive data and thermodynamical framework, *not a profound change in his basic picture that most stars, not just freaks, require an extended-, or outer-, or shell-atmosphere, not satisfying normal or classical modeling.* And we can certainly echo his emphasis on variability, especially the “phase-variability” of Be stars which he anticipated so clearly. The “new” elements which have been added, empirically, are those characteristics of *individuality* and *gradualness*, stressed by Doazan in the Be, Kuhl in the T Tauri, all the authors in the cataclysmic; the need to know time history of mass-loss, shown empirically by Doazan, to model postcoronal structure.

When he came to the question of *why* such outer-atmospheric regions exist, and in some stars more strongly than in others, Struve had earlier fallen into the trap of “rotational instability-induced ejection.” The basic contradiction of this idea with the data, especially on variability, is thoroughly discussed by Doazan, and need not be repeated here. While the data summarized in this monograph point, indeed, to an origin of the two additional fluxes of nonradiative energy and mass in a nonstatic structure of the star, the dynamic configuration must apparently be more general than simply rotational.

So we consider first the low outer-atmosphere of the Sun, as the most complete, observationally, among the stars. This discussion puts into empirical focus both the summary just presented and the contrast between effects of nonradiative energy, and mass-fluxes. We will see that the former alone produces a *low-density* extended-atmosphere; the latter can produce a *high-density* one. Sun, and Be and/or T Tauri, stars illustrate the two extremes. Clearly, because high-density regions are easier to observe than low, this contrast has an important bearing on ease of observation of these extended-atmospheric stars and regions, and on attempts to classify stars according to the degree in which they show evidence for such atmospheric regions. Again, I orient the discussion around contrasting effects of increased radiating area of the star, associated with a mass-flux, and increased temperature of the radiating area, associated with a nonradiative energy-flux.

Finally, for the rest of the monograph, we will be discussing extended atmospheres—exophotospheres, especially postchromospheric regions—in contrasting HE-exponential density gradients to those arising dynamically, $\sim (Ur^2)^{-1}$, with U in the transthermic, superthermic, ultrathermic, and ultraescape ranges, and possibly time-dependent. So, it is always useful to have some reference equations, which suffice to give at least roughly approximate quantitative relations. So I use eqs. (2.27), and (2.27) + (2.29), including sufficient time-dependence, radiative-acceleration, and viscosity terms to avoid those demands for discontinuities coming from incomplete equations, not physical necessity. Also, here we need only the mass and macroscopic energy equations. In the spherically-symmetrical case, these become, in Chapter 2 notation: (We label them (3.A) etc. because we will use them extensively, here and in Part III.)

$$\partial\rho/\partial t + (4\pi r^2)^{-1} \partial(4\pi Ur^2\rho)/\partial r = 0 \quad (3.A)$$

$$\rho\partial U/\partial t + \rho U\partial U/\partial r + \partial(p+p')/\partial r = -\rho GM/r^2 + (\rho/c)\int F_\nu K_\nu d\nu \quad (3.B)$$

where $U, \rho, M, p, F_\nu, K_\nu$ are radial-velocity, density, stellar-mass, gas-pressure, monochromatic flux, mass absorption coefficient, respectively. Also we use: $p' = \text{viscosity term} = -\theta \partial U/\partial r$, where θ varies slowly with T_e . $q^2 = kT_e/\mu$,

where μ is mean particle mass of *all* the gas. v_{th}^2 = thermal velocity of the mean absorbing atom providing the radiative acceleration = $2kT_e/\mu_{\text{abs}}$. Note that q and v_{th} do not refer to the same "mean" particles. Then Castor-Abbott-Kline (1975) represent the radiative-acceleration term as:

$$c^{-1} \int F_\nu K_\nu d\nu = \left(\sigma_e L / 4\pi cr^2 \right) [1 + M(s)] = \left(\Gamma GM / r^2 \right) \left\{ 1 + K \left[(4\pi / \sigma_e v_{\text{th}} dM/dt) r^2 U \partial U / \partial r \right]^\alpha \right\} . \quad (3.6)$$

The first term represents electron-scattering; the second, $M(s)$, the line-effect, which they assert can be represented by:

$$\Gamma = \sigma_e L / 4\pi GMc \quad ; \quad M(s) = K s^{-\alpha} \quad ; \quad s = \sigma_e \rho v_{\text{th}} (\partial U / \partial r)^{-1} . \quad (3.7)$$

To avoid confusion with the usual use of t for time, I have used s where CAK use t in their expression for the opacity. Also, in eq. (3-6) one should replace $4\pi r^2 U / (dM/dt)$ by ρ^{-1} , CAK having considered only the time-independent situation and so made this substitution, in order to express all velocity terms symmetrically in the form $(r^2 U dU/dr)$ when $U \gg q$. I introduce the time-dependent terms here simply for illustration below, but also carry the CAK expression as it stands. Then the usual combining of these equations gives the two equivalent equations; one expressed in terms of U ; the other, in ρ .

$$[r^2 U \partial U / \partial r] [q^2 / U^2 - 1] + \left(\sigma_e L / 4\pi c \right) K \left[(4\pi / \sigma_e v_{\text{th}} dM/dt) (r^2 U \partial U / \partial r) \right]^\alpha - r^2 \partial (\theta \partial U / \partial r) / \partial r + \quad (3.C)$$

$$+ r^2 U \left[(q^2 / U^2) \partial \ln \rho / \partial t - \partial \ln U / \partial t \right] = \left(GM [1 - \Gamma] / r^2 - 2q^2 / r + \partial q^2 / \partial r \right) r^2$$

$$U^2 [q^2 / U^2 - 1] \partial \ln \rho / \partial r + \left(\sigma_e L K / 4\pi c \right) \left[(4\pi / \sigma_e v_{\text{th}} dM/dt) (r^2 U \partial U / \partial r) \right]^\alpha + \quad (3.D)$$

$$+ U [\partial \ln U / \partial t - \partial \ln \rho / \partial t] = - \left[(GM / r^2) [1 - \Gamma] - 2U^2 / r + \partial q^2 / \partial r \right] .$$

I do not discuss in this Chapter 3 the legitimacy of the CAK representation of the radiative-acceleration term, except to say that they consider only pure scattering to compute the radiative transfer in the lines. So, by definition, there is no coupling between the thermal state of the atmosphere and the velocity field, except in estimating the Doppler width of the line, through v_{th} . Our interest in the following is simply asking how well do the various approximate solutions to these equations, for hot and cold stars, under ad hoc boundary conditions, represent the observations. We defer any other considerations of the theory to Part III, except in commenting on the various rationalizations of why these theories do not, indeed, represent the observations. This applies, alike, to the radiative-acceleration theory, and to the hot-corona theory.

2. Extended-Atmospheres Inferred from Eclipse Observations

a. The Sun

During the period 1860–1900, one photographed, progressively, the extent of the faint outer atmosphere of the Sun as seen when the Moon covered the central, bright, disk. One first photographed the "white-light" corona, coming from a combination of electron and dust scattering of photospheric emission, and indicating an "extended-atmosphere" with at least these two constituents. Second, one photographed the "red-light" of the lower part of this outer atmosphere, the chromosphere, coming mainly from H α , so showing the abnormal extent of the line-spectrum emitting regions. Later, one photographed the remaining elements in the "flash-spectrum," so called because it

appeared abruptly, in emission, when the Moon covered the solar limb. That the lines appeared in emission, showed that the opacity in the continuum adjacent to the lines decreased much more rapidly than that in the lines. Resolution, spectral and in height, increased steadily after that epoch. The first really modern data, with sufficient height resolution that one could actually attempt an analysis of the changing thermodynamic structure with height in the very-low outer-atmosphere, was that obtained by Menzel at the 1932 eclipse. Successive, evolving analyses of these data by Menzel and Cillie (1935, 1937) and Thomas (1950 a, b) at once developed the necessary *thermal non-Equilibrium* diagnostics necessary for their treatment, and obtained preliminary results on the chromospheric structure. On this basis, a more sophisticated set of observations, and diagnostics, was planned and conducted for the 1952 solar eclipse (Evans, Robert, Thomas), whose observational results (Athay, Billings, Evans, Roberts, 1954) have been discussed at length (Thomas and Athay, 1961). These, and subsequent observations, are summarized in the Solar Volume of the series by Athay, so they need not be discussed in any detail here. I do, however, simply abstract their highlights, re the solar-stellar comparison of the relative effects of mass-flux, which nullifies HE and increases effective emitting area, and nonradiative heating, which nullifies RE and increases effective emitting temperature. The Sun provides us with a wealth of observational detail, unmatched by any other star, on the evolution from classical photosphere to nonclassical chromosphere-corona in the classical-boundary regions of the atmosphere. It is unfortunate that its mass-flux is too small to provide equal observational detail on the evolution of the change from HE to dynamic density distribution, especially detail on the outward evolution of mass-flow velocity. Hopefully, one is in the process of delineating, from this possibility of solar detail, at least one kind of nonradial atmospheric effect, under these solar conditions of small mass-flux, significant nonradiative heating, and the presence of magnetic fields. I do not discuss this third aspect here; it is covered, to present knowledge, in the Solar Volume (Jordan, 1981); my present emphasis lies on the broad radial distribution of atmospheric regions, which *apparently* the nonradial effects perturb only slightly.

i. The Low Solar Chromosphere

We use the high spatial resolution given by solar proximity to show the details of the transition from quasi-classical photosphere to nonclassical outer-atmosphere under solar-type—i.e., low mass-flux—conditions. In terms of producing a high-density, very extended, outer-atmosphere, this *solar* transition has relatively-small effect; we obtain a low-density, reasonably-extended one. In terms of introducing a large rise in T_e , this *solar* transition is indeed large. In the demonstration, we want to make clear the actual *solar* situation, but also how it would change were the solar mass-flux much larger than it is, for use in discussing mass-flux theories. For this solar illustration, I abstract the data and its discussion from Thomas and Athay (1961), updating its focus.

In brief, the solar eclipse data show an increasingly larger radiative-flux, at heights above the photospheric radius, R_p , than what the classical model predicts; and the size of the increase varies with λ . We ask an interpretation in terms of *either*: effective size and “temperature” of an optically-thick extension of the classical atmosphere; *or* conditions in an optically-thin “nebular” outer-atmosphere; *or* something intermediate; *all* these alternatives *may* be present, each in a different wavelength region.

Then we recall from Chapter 2 that:

$$I_\nu(\mu, 0) = \int_0^\infty S_\nu(\tau_\nu) e^{-\tau_\nu/\mu} d\tau_\nu/\mu \quad (2.10)$$

$$F_\nu(0) = 2\pi \int_0^1 \mu I_\nu(\mu, 0) d\mu \quad (2.11)$$

$$L = \pi R_p^2 \int B_\nu(T_{\text{eff}}) d\nu \quad (3.8)$$

That is, T_{eff} is the temperature the star would have if it radiated like a uniform blackbody surface with photospheric radius R_p . Now, as seen in Chapter 2, the opacity-emissivity in the Sun is essentially H^- throughout the classical photosphere, and the approximation $S_\nu = B_\nu(T_e)$ is very good for $\tau > 10^{-2}$ or so. Thus, with $S_\nu = B_\nu(T_e)$, the continuum emission across the solar disk is well represented by eqs. (2.10)–(2.11). The monotonic decreases of the I_ν from center to limb across the disk correspond to decrease in “effective” optical depth with μ , which corresponds to decreasing “effective” T_e from disk-center to limb, where it reaches T_0 . This *thermal* “limb-darkening” is, at the very limb, replaced by the abrupt drop in I_ν given by eq. (3.2), which is *wholly* an opacity effect given by the predicted exponential decrease in density, not in T_e . We note that the ratio of column-density of absorbing atoms above a given height in the radial direction, to column-density of absorbing atoms along a tangential line of sight at that same given height, which is the ratio of radial to tangential optical depths, is, for a distribution (3.5),

$$\tau(\text{radial})/\tau(\text{tangential}) = (H/2\pi R_p)^{1/2} \sim 5 \times 10^{-3} \quad (3.9)$$

for the Sun. So, the region of the limb-drop, $\tau(\text{tang}) \lesssim 1$, is the region $\tau(\text{rad}) \lesssim 0.005$, truly an isothermal one, in classical modeling. In such models, the only change in opacity conditions across this isothermal boundary region is an increase in H^- ionization, from the lower density, hence, an increase in importance of free-bound and free-free emission and absorption from atomic hydrogen, as we saw in Chapter 2. This *can* result in a minor rise in T_e , at very low τ , as we saw. Again as discussed in Chapter 2, this simple isothermal model of the extreme outer photosphere is, in the neoclassical model, slightly perturbed by the combined effects of line-blanketing and a nonLTE rise in source-function, both of which effects have still not been well modeled; but in no event can T_0 rise above T_{eff} (Sun) ~ 5800 K; nor can H rise higher than the value corresponding to that T_{eff} , about 175 km.

So given all this, we could expect three, alternative, kinds of “radiative emission gradients” at the solar limb, from eq. (3.2), *if* the classical or neoclassical atmospheric models are correct.

Either (C-1) the H^- concentration follows the density concentration and, after an initial slow decrease of I_ν (tangential), eq. (3.2), from large τ_{tg} until $\tau_{\text{tg}} \sim 1$, I_ν decreases as τ_{tg} , with n_{H^-} given by eq. (3.5). That is, the emission scale-height should be 125–175 km, for $4200 \text{ K} < T_{\text{eo}} < 5800 \text{ K}$.

Or (C-2) recognizing that the concentration of H^- is given, in LTE, by the Boltzmann-Saha relation between H^- , neutral hydrogen, and electron concentrations

$$n_{H^-} = n_H n_e f(T_e), \quad (3.10)$$

and that n_e is given by the singly-ionized metals whose degree of ionization is fixed in this (solar) region, $n_e n_H \sim (\text{density})^2$, and τ_{H^-} has a scale-height of $H/2 \sim 75\text{--}90$ km. Thus, the emission scale-height should also be 75–90 km.

Or (C-3) the continuum emission and opacity in these limb-regions comes from Balmer free-bound instead of H^- . Recognizing that each of these varies as $n_e n_p$, we should again expect τ_{tg} , hence emission, scale-heights to be $H/2 \sim 75\text{--}90$ km.

Alternatively, *if*, for *whatever*, nonclassical, reasons, the solar *limb*-diameter, and “temperatures” in the limb-regions increase (because of increase, or less rapid than classical decrease, of density and T_e), we again would have two alternatives for emission gradients.

Either (P-1) these additional limb-extension regions are opaque, and we obtain

$$L_\nu = \pi R_p^2 B_\nu(T_{\text{eff}}) + 2\pi R_p B_{\nu}(T_{\text{limb},\nu}) dR_{p\nu}. \quad (3.11)$$

Then, the continuum emission at the limb regions above the *classical* photospheric radius, R_p , should continue to “change” outward for $r \leq R_p + dR_{p\nu}$. Whether there is an increase or decrease depends, of course, on the sign and size of the change in the $T_{\text{limb},\nu}$ entering B_ν as compared with the increase in $dR_{p\nu}$. T and R have subscripts ν to allow for such dependence.

Or (P-2) there is not sufficient opacity rise at the limb to make the “nebular addition” optically thick, at the observed ν , and we simply obtain hydrogen, or H^- , ff, fb continuous emission, and line emission from all elements, corresponding to whatever are the distributions of density and T_e in this region. Again, emission scale-heights are completely unknown and they must be inverted, to infer, empirically, the “corrections” to these classical models.

The actual eclipse observations give the total emission, at each wavelength interval, from a 1-cm-wide column above the Moon's limb, which is located at $h(t)$ above the solar limb; i.e.,

$$E_{\lambda} = \int_h^{\infty} I_{\lambda} (\text{tangential}) dh, \quad h = r - R_p. \quad (3.12)$$

Then we abstract what the data tell us about the thermodynamic structure of the low solar chromosphere by giving: $E_{\lambda 4700}(h)$, the emission at a typical wavelength in the Paschen continuum *region*, which is free from spectral lines; $E_{\lambda 3640}(h)$, the Balmer continuous emission, obtained by subtracting an empirical λ -extrapolation of the continuum in the Paschen region from the observed emission at $\lambda 3640$; and $E_{n_2}(h)$, the total emission in the several Balmer lines. Height $h = 0$ is chosen at the inflection point of $E_{\lambda 4700}(h)$, thus corresponds to $\tau_{\text{tg}}(\lambda 4700) \sim 1$ for exponential opacity distribution as in eq. (3.5). Then, the data are:

$-120 < h < 6300$ km:

$$E_{\lambda 4700}(h) = 385 \exp(-7 \times 10^{-8}h) + 67.5 \exp(-2.2 \times 10^{-8}h) + 10 \exp(-6 \times 10^{-9}h) \quad (3.13)$$

$$+ 12.1 \exp(-4 \times 10^{-9}h) + 8.5 \exp(-7 \times 10^{-10}h) + 17.4 \exp(-5 \times 10^{-11}h)$$

$500 < h < 2400$ km:

$$E_{\lambda 3640}(h) = 780 \exp(-2.2 \times 10^{-8}h) \quad (3.14)$$

$$E_{n_2}(h) = E_{n_2:0} \exp(-\beta_n \times 10^{-8}h), \quad \beta_n \leq 2.2 \times 10^{-8} = \beta(H_{28} - H_{31}). \quad (3.15)$$

Remarks on Additional Data:

1. For $100 < h < 500$ km, $E_{\lambda 3640}$ and all E_{n_2} show a decreasing slope toward smaller h , such that one infers—from *very* few data points and a double numerical height-differentiation of E_{λ} —that the emission per unit volume, $S_{\nu_0} d\tau_{\lambda}$, at the Balmer limit increases outward in the height-range $0 \lesssim h \lesssim 500$ km, reaching a maximum at about 500 km, and thereafter decreasing with increasing h .

2. The slope of $\ln E_{n_2}$, $-\beta_{n_2}$, flattens, differentially with n , toward smaller h ; the smaller n show the smaller slopes.

Gross Interpretation of These Data:

The first exponential term in eq. (3.13) shows an emission height-gradient corresponding to an H of about 150 km; and, comparing its size to those of the remaining terms, one sees that it clearly controls the emission gradient in the first few scale-heights. This is particularly true, if one notes that I_{ν} (tangential) = dE_{ν}/dh , so that the weight of this first term in eq. (3.13) is even greater in I_{ν} than in E_{λ} . So the *initial* emission, hence opacity, decrease at the limb lies in accord with classical alternative (C-1): apparently, n (H^-) follows the HE, RE density distribution. But nowhere is the emission-gradient as steep as the $H \sim 60-90$ km required by alternatives (C-2) or (C-3). So we can only conclude that n_e does not decrease as fast as it would if metals were its only source, with these keeping constant ionization and following n_H .

But gradually out to $h \sim 500$ km, and definitely after that, the emission gradients are much flatter than correspond to $H \sim 150$ km. For $h \sim 500$ km, $H \sim 500$ km is a good representation for emission in the Balmer continuum, which varies as $n_e n_p T_e^{-3/2}$; and below this height, $n_e n_p T_e^{-3/2}$ actually rises. This, and the preceding, agree in demanding an outward rise in T_e , accompanied by increased ionization of hydrogen, beginning at least in this 0–500 km height-range.

Finally, a comparison of the height-dependence of the relative emission in the Balmer continuum, and the several terms representing the emission in the Paschen spectral region, implies a gradual height-evolution of the source of the emission in the Paschen region from H^- , through hydrogen free-bound, to electron-scattering as one traverses this height range from 0 to 2400 km. Above this last height, and well out into the corona (continuum measures out to some 50,000 km were made in these observations) electron-scattering continues to dominate in the continuous emission and opacity. All this implies a continued outward increase of T_e , throughout the range covered by the data, with hydrogen becoming predominantly ionized at some $1000 < h < 1500$ km where, from eq. (3.14) and comparing second and higher terms in eq. (3.13), these latter terms begin to dominate, indicating the predominance of electron-scattering. And, overall, the *sizes* of these emission height-gradients accord with an HE quasi-exponential density distribution, with scale-height evolving with T_e , not with an $(r^2 V)$ -dominated density gradient corresponding to a mass-flux. (Cf, also, Table 3-5.)

This semiquantitative abstract of the transition region from photosphere into outer-atmosphere was made quantitative in detail and used to predict emission *outside* the two continua whose observations provide the empirical basis for this atmospheric model. These details of the construction of the first nonLTE empirical model of the lower *solar* chromosphere, which is the transition region to the *solar* outer-atmosphere from the classical photosphere, are given in Thomas and Athay (1961), and subsequent applications to later eclipse, and other data are summarized in Athay (1976). The details of the development, and empirical verification, of this nonLTE diagnostic approach are given in that reference and in Thomas (1965). Here, for use in the rest of the monograph, it is useful to sketch the essential structure of this empirical approach.

Because the atmosphere is optically-thin in the Balmer and Paschen and H^- continua for $h \gtrsim 500$ km one can invert the data in eqs. (3.13)–(3.15) to obtain the emission per unit volume, ϵ_λ , which relates to E_λ by:

$$E_\lambda = \int_h^\infty \int_{-\infty}^{+\infty} \epsilon_\lambda ds dh. \quad (3.16)$$

Then we have:

$$\begin{aligned} \epsilon_{\lambda 4700} = & n_e \text{-scattering} + n_{H^-} \text{-scattering} + H^- \text{-emission (ff + fb)} \\ & + \text{H-Paschen fb emission} \end{aligned} \quad (3.17)$$

$$\epsilon_{\lambda 3640} \text{(BaC)} = \text{H-Balmer fb emission} \quad (3.18)$$

where we give these several terms, together with the corresponding expressions for absorption, and each for the hydrogen Balmer lines.

Absorption:

$$\text{electron-scattering: } n_e \alpha = 6.65 \times 10^{-25} n_e \quad (3.19)$$

$$\text{neutral-H scattering: } n_H \alpha_\lambda = 1.51 \times 10^{-29} (4700/\lambda)^4 n_H \quad (3.20)$$

$$\text{H}^-: \text{bf}: n_{\text{H}}^{-1} \alpha_{\text{H}^- \text{bf}}: \alpha_{\text{H}^- \text{bf}} \text{ tabulated (Chandrasekhar, 1958)} = 3.14 \times 10^{-17} \text{ at } \lambda 4700 \quad (3.21)$$

$$\text{ff}: n_{\text{H}} n_{\text{e}} \alpha_{\text{H}^- \text{ff}}: \alpha_{\text{H}^- \text{ff}} \text{ tabulated (Chandrasekhar and Breen, 1946)} = 3.1 \times 10^{-27} \text{ at } \lambda 4700 \quad (3.22)$$

$$\text{H}: \text{ff}: 1.42 \times 10^{-38} n_{\text{e}} n_{\text{p}} (10^{-4} T_{\text{e}})^{-1/2} (\lambda/4700)^3 [1 - \exp(-h\nu/kT_{\text{e}})] g_{\text{ff}} \quad (3.23)$$

$$\text{bf}: 2.81 \times 10^{29} k^{-5} \nu^{-3} n_{\text{k}} [1 - \exp(-h\nu/kT_{\text{e}})] g_{\text{bf}} \quad (3.24)$$

Emission: (in all directions)

$$\text{scattering: } 4\pi J_{\nu} (n\alpha)_{\text{abs}},$$

$$\text{H}^-: \text{bf}: 4\pi n_{\text{H}}^{-1} \alpha_{\text{H}^- \text{bf}}^* B_{\nu}(T_{\text{e}}) \quad (3.25)$$

$$\text{ff}: 4\pi n_{\text{H}} n_{\text{e}} \alpha_{\text{H}^- \text{ff}}^* B_{\nu}(T_{\text{e}}) \quad (3.26)$$

*denotes LTE values at that $T_{\text{e}}, n_{\text{H}}, n_{\text{e}}$ actually present.

$$\text{H}: \text{bf}: 2.15 \times 10^{-32} n_{\text{p}} n_{\text{e}} (10^{-4} T_{\text{e}})^{-3/2} \exp(X_{\text{k}} - X_{\nu}) g_{\text{bf}} k^{-3} \quad (3.27)$$

$$\text{ff}: 6.72 \times 10^{-40} n_{\text{p}} n_{\text{e}} (10^{-4} T_{\text{e}})^{-1/2} \exp(-X_{\nu}) g_{\text{ff}} \quad (3.28)$$

$$X_{\nu} = h\nu/kT_{\text{e}} \quad ; \quad X_{\text{k}} = h\nu/kT_{\text{e}}$$

the g are the Gaunt-factors tabulated by Menzel and Pekeris (1935).

Substituting these expressions for the emissivities, eqs. (3.25)–(3.28), into eqs. (3.17) and (3.18), we see that we have two observational equations in the three unknowns: $n_{\text{e}}, T_{\text{e}}$, and either n_1 or b_1 . The situation is resolved by expressing b_1 in terms of the local $n_{\text{e}}, T_{\text{e}}$, and the intensities of the various radiation fields to which this atmospheric region is not opaque. For those to which the region is locally-opaque, one would need to solve a radiative transfer equation. To a quite-good accuracy, one can use a 3-level hydrogen atom to express b_1 and b_2 in terms of $n_{\text{e}}, T_{\text{e}}$, the *observed* radiative-intensity in the BaC (which comes from the photosphere, for the solar situation), a transfer solution in the LyC, and a rough transfer solution in H α . For details, cf Chapter 2, Section III.B.3 and chapters 4 and 6 of Thomas and Athay (1961). X, Y are $h\nu/k(T_{\text{e}}, T_{\text{c}})$.

Regions opaque in LyC:

$$b_1 = b_2 = W_2^{-1} Y_2 e^{Y_2} X_2^{-1} e^{-X_2} [1 + \Delta_{\alpha}] \quad (3.29)$$

$$\Delta_{\alpha} = b_3 K_{32} e^{X_3} [\text{NRB}]_{\text{H}\alpha} F_{\text{c}2}^{-1} \quad (3.30)$$

The notation is that of Chapter 2; rate-coefficients are defined in the appendix to that chapter. The transfer solution in H α need only be rough because: $0 < \Delta_{\alpha} < 0.65$; a 50 percent uncertainty in b_1 . As in all the boundary regions discussed in Chapter 2, $W_2 \cong 0.5$.

Transition region in LyC:

$$b_1 = X_1^{-1} e^{-X_1} Y_1 e^{-Y_1} \quad (3.31)$$

and as discussed in Chapter 2, Section III.B.3.b, we have a 1-point transfer solution in the LyC to give

$$Y_1^{-1} e^{-Y_1} = \frac{\psi}{\Lambda} \left\{ 1 - \frac{\exp(-\sqrt{3\Lambda} \tau_1)}{1 + \sqrt{\Lambda}} \right\} \quad (3.32)$$

ψ , Λ are specified in terms of local quantities.

One is thus able to do a step-by-step determination of the values of n_e , T_e , b_1 , b_2 from the *observational* eqs. (3.17) and (3.18), the *theoretical* representations eqs. (3.25)–(3.32), and the assumed condition of HE. One obtains the results of Table 3-4, taken from tables (6-9) and (6-10) of Thomas and Athay; Table 3-5 gives the relative contributions of the various terms in eq. (3.18), taken from their table 6-7. Finally, Table 3-6 gives the ratio of the *empirical* value of gravity—computed under the assumption of HE and using the density distribution from a preliminary version of Table 3-4—to its actual value (for various assumptions on the solar He: H abundance, this still being unknown). We see from these empirical results that there is no reason to question HE, and thus there is no evidence of a mass-flux effect, in these regions $h \lesssim 3500 \text{ km} \sim 0.004 R_p$. For such evidence, one needs to go to observations of the far corona (cf Section *ii* following) to find a strong flattening near about $2\text{--}3 R_p$, the height-decrease being less than a quasi-exponential decrease at coronal scale-heights of $0.6\text{--}1.2 \times 10^{10}$, which correspond to $T_e \sim 1\text{--}2 \times 10^6 \text{ K}$. The slowest-varying term in eq. (3.13), which covers data only up to 50,000 km, corresponds to a scale-height $\sim 2 \times 10^{10}$.

So, we find four essential characteristics of this first, empirical, thermal nonLTE model (1961) of the transition region between photosphere and outer-atmosphere of a very-low mass-flux star, the Sun; which model was constructed wholly from visual, although eclipse, data.

First, the classical photospheric model becomes inadequate quite low, at quite high densities: $\tau_{\text{rad}} \sim 10^{-3}\text{--}10^{-4}$, $n \sim 10^{15}$. Then, over the next 2000 km, or $\Delta R_p \sim 0.003$, the density drops only by about 10^6 , as contrasted to the about 10^7 expected from the classical model, isothermal at $T_{\text{eo}} = 4200 \text{ K}$. But, *above* that $R = 1.003 R_p$, the actual solar density decreases with a scale-height $0.6\text{--}1.2 \times 10^{10} \text{ cm}$ as contrasted to the classical scale-height $1.2 \times 10^7 \text{ cm}$. Thus, in another 2000 km, the classical atmospheric density is 10^7 lower than the actual solar.

Second, this behavior of the density corresponds *wholly* to an abrupt rise in T_e , a departure from RE but not from HE, over this same height interval, from about 4000 K to about $1\text{--}2 \times 10^6 \text{ K}$. So of the 10^6 actual density drop, about a factor 10^4 comes from the quasi-exponential decrease across the 1500 km “gradual” rise in T_e from about 4000 K to about 20,000 K; and about a factor 100 from the “quasi-abrupt” rise from 20,000 K to the $1.2 \times 10^6 \text{ K}$ coronal values, to preserve static, thermal pressure, HE.

Third, these densities are high enough in this photosphere-chromosphere transition-region that even in the visual, disk, spectrum, the centers of all the strong, and some of the intermediate, spectral lines are affected by the presence of this *solar-type* outer atmosphere. For some lines, this nonclassical effect is obvious, even under medium-spectral resolution and medium-theory diagnostics. Examples are the emission-cores of the Ca II lines and the presence of the $\lambda 10830$ lines from He I. For other spectral lines, even strong ones, more refined observations and diagnostic theory are needed to show the presence of an outer atmosphere. Examples are the profiles of the hydrogen Balmer lines, which—especially the central intensities—were used for solar *and* stellar diagnostics of $T_e(\tau)$ under the assumption of LTE. It was not until our eclipse data showed that T_e inferred from such LTE analyses, and T_e inferred from our eclipse observations, had different *signs* for dT_e/dh ; until our eclipse data showed the optical thickness of the chromosphere to exceed ≈ 100 in H α ; and until our nonLTE theory showed how bad was such an LTE approximation for precisely these Balmer lines; that a chromospheric origin for the central cores of these Balmer

Table 3-4
Model of the Lower Solar Chromosphere (Thomas and Athay, 1961)

Model Corresponding to an Upper Bound on T_e ($h < 500$ km)

h , km	$10^{-4} T_e$	$10^{-14} n_1$	$10^{-11} n_e$	$10^{-5} n_{H-}$	tang $\tau_{\lambda 4700}$	rad $\tau_{\lambda 5000}$
0	0.505	37.8	6.36	38.8	0.24	1×10^{-3}
100	0.525	16.0	5.04	11.5	0.078	4×10^{-4}
200	0.546	6.99	4.65	4.10	0.029	2×10^{-4}
300	0.568	3.15	4.58	1.62	0.012	6×10^{-5}
400	0.591	1.46	4.63	0.670	0.0051	3×10^{-5}
500	0.615	0.695	4.72	0.290	0.0023	1×10^{-5}

Model of the Chromosphere for $750 \text{ km} < h \lesssim 1320 \text{ km}$
Hydrostatic Equilibrium

h , km	$Z = 10^{-4} T_e$	$10^8 \frac{d \ln Z}{dh}$	$10^{-11} n_e$	$10^{-11} n_1$	$10^{-5} n_2$	τ_{LVC}	$\tau_{L\gamma\alpha}$	$\tau_{H\alpha}$
750	0.665	0.284	4.04	121.0	9.98	1×10^3	1×10^7	34.5
850	0.684	0.291	3.69	62.8	8.38	—	—	28.5
950	0.704	0.303	3.38	31.9	7.02	—	—	23.4
1000	0.715	0.314	3.24	22.7	6.44	2×10^2	2×10^6	21.7
1050	0.727	0.329	3.10	16.0	5.92	140.0	—	20.5
1100	0.740	0.356	2.97	11.0	5.42	96.0	—	18.7
1150	0.754	0.390	2.86	7.79	4.98	58.0	—	17.7
1200	0.770	0.464	2.75	5.05	4.61	35.0	3×10^5	17.0
1225	0.779	0.519	2.70	4.08	4.44	28.0	—	—
1250	0.7901	0.633	2.65	3.19	4.28	19.8	2×10^5	—
1260	0.7954	0.714	2.64	2.87	4.22	16.0	—	—
1270	0.8016	0.836	2.62	2.55	4.16	13.5	—	—
1280	0.8090	1.008	2.61	2.26	4.11	11.2	1×10^5	—
1290	0.8183	1.285	2.60	1.98	4.06	9.0	—	—
1300	0.8310	1.820	2.60	1.71	—	6.6	7×10^4	—
1310	0.8504	2.840	2.62	1.42	—	4.7	—	—
1320	0.897	8.110	2.69	1.1	—	2.5	—	—

Table 3-5
Relative Importance of Various Terms Entering Observed Eclipse Emission in the Paschen Continuum at $\lambda 4700\text{\AA}$

h	n_e	n_{H-} (Rayleigh)	H-fb	H-ff	Paschen	f-f
500	10	3	72	5	10	0.3
750	30	2	37	3	27	1
1000	50	0.5	8	1	38	2
1500	65	0.5	4	0.5	28	2
2000	85	—	—	—	15	—
2400	85	—	—	—	15	—

Table 3-6
Rough Values of Effective Gravity to Give Hydrostatic Equilibrium Under the Empirical Density Distribution in the Lower Solar Chromosphere; Parameter Is Helium Abundance. Tabular Entry = Ratio of Effective to Actual Solar Gravity

Height Interval (km)	0.05	He:H 0.10	0.20 (by number)
500-750	1.18	1.06	0.90
750-1000	1.40	1.26	1.06

lines was recognized. We should note that the eclipse behavior of the Balmer lines permitted a check on the Balmer opacity predicted by the empirical, continuum-derived, model of Table 3-4; the agreement is very good.

Fourth, although in the visual spectrum, only the lines, not the continuum, are influenced by the outer-atmosphere of this “solar-type” Sun, *both* lines *and* continuum are affected in the farUV, IR, radio, and X-ray. These are discussed in the solar volume (Jordan, 1981). Here, we note only two things, relative to Table 3-4. First, use of the farUV line-spectrum to derive a chromospheric model (e.g., Vernazza et al., 1976, 1981) results in models differing in details of the height-scale, but not in the gross features and conclusions, of Table 3-4. Use of the IR spectrum to obtain a better model in the region $h < 500$ km is summarized by Athay in the two references cited, who also summarizes radio contributions to modeling, especially as relates to inhomogeneities. But second, I want to emphasize here that this first empirical model of the photosphere to outer-atmosphere transition region permitted, for the first time, a good *empirical* estimate of the effect of this T_e -rise in the outer-atmosphere on the *Lyman continuous emission* from a star. To know that T_e rises is not enough; one must know what is the T_e -rise in the region of the origin of the LyC—i.e., where $\tau_{\text{LyC}} \sim 1$. For this, the results of Table 3-4 could be applied to compute the source-function at the head of the LyC

$$S_{\text{LyC}-\nu_1} = (2h\nu_1^3/c^2) (b_1 \exp X_1 - 1)^{-1} \quad (3.33)$$

at the location $\tau_{\nu_1} \sim 1$. We obtained $1-2.3 \times 10^{10}$ for $b_1 \exp X_1$ at this optical depth, which corresponds, empirically, to $T_e \sim 8-8500$ K. The then-current data (Morton and Widing, 1961) give $T_{\text{rad}} \sim 6900 \text{ K} \pm 200 \text{ K}$, which corresponds to $b_1 \exp X_1 \sim 8 \times 10^9 \pm$ by a factor 2. Note that an LTE estimate of this LyC flux, for a boundary $T_{\text{eo}} \sim 4200 \text{ K}$, is a factor 10^6 less than this value. This comparison of the predicted and observed LyC flux has two important consequences.

(*LyC-1*). The first is that we can trust this relatively-simple nonLTE diagnostic approach to give an estimate of at least the gross structure of the outer-atmosphere. Of course, for stars generally we do not have that height-behavior of the excess radiative emission given in the solar case. But we do have the ν -dependence over a wide spectral range of observations, and this is equivalent to an emitting-depth, or emitting-area, probe. The modeling by Vernazza et al. (1976, 1981) exemplifies this approach, again for the solar case, so that it can be compared with the eclipse modeling. As mentioned, these two approaches do not differ in their results on the gross structure just summarized: a relatively-rapid onset of the lowest parts of the solar outer-atmosphere, due only to a T_e -rise; densities greater than some 10^7 times what classical modeling predicts: LyC fluxes greater than 10^6 times what classical modeling predicts, but LyC disk-size little changed from the photospheric. (Compare the models in Fig. 2-4.)

(*LyC-2*). The second relates to the classical notion of the so-called “Stromgren-sphere,” the region around a star which its LyC radiation field *was* thought to maintain in an H II, or hydrogen-ionized, state. The radii of such spheres have been tabulated for all stars: for the Sun, classically, it lies within the photosphere. For the Sun, observationally, it includes at least the Earth’s orbit. Not only is the solar LyC stronger than classical, because of the non-radiative increase in T_e in the region of its origin in the chromosphere-corona, but this increased T_e itself provides an ionization to produce an H II region—collisional rather than radiative, which is of course the source of the excess LyC. *This* H II region extends throughout the coronal, and postcoronal cooling down to some 10^4 K, regions. Moreover, in addition to the nonradiative-flux that provides such heating—and the data in Table 3-4 show the non-radiative energy dissipation is greatest in the low chromosphere (cf Athay’s discussion in the solar volume)—there is the energy in the solar wind which, being superthermic, will eventually dissipate by a shock-wave (cf Part III) and again, locally, produce hydrogen ionization by collisions, so an H II region. Thus, the “classical” Stromgren sphere evaporates, being replaced by a combination of: chromospheric-coronal collisional ionization; enhanced radiative ionization by the LyC produced in the *outer atmosphere, not the photosphere*, which LyC excess is a factor 10^6 for the Sun; and an ultimate ionization-shock when the wind is decelerated by the ISM. The extent of the “enhanced,” nonclassical, Stromgren sphere associated with the existence of the *outer atmosphere* is unknown, from the spectral class alone. One needs to know nonradiative- and mass-fluxes to compute it, for each star. This solar section simply shows how much classical estimates of such effects can change, for a rather mediocre star.

We note the effect of this excess LyC radiation on the interpretation of peculiar stars discussed earlier, especially the symbiotic, where often a “hot companion” is *postulated* to explain “superionization” of the “nebulae” associated with these stars. But we note that such interpretations generally ignore, even today, with the 1961 solar example at hand, the effects of the “chromosphere-coronal” regions of the (cool) primary star, and of winds large enough to shock-ionize circumstellar regions. Some astronomers argue (cf following sections in this chapter) that many of the kinds of cool stars forming the “primary” of symbiotic stars have low- T_e coronae and low-velocity winds. I respond only that the Sun has a 2×10^6 K corona, and on occasion, an 800 km/s wind, even though the mass-flux level is low; *while in no other cool star, not even the Sun, have systematic, nontransient, outflow velocities $\gtrsim 100$ km/s been measured, spectroscopically.* The solar wind velocities have been measured by a collector at the Earth’s orbit, and *extrapolated* backward to the Sun. Thus, for the cool stars, as discussed later, much remains to be done in observational diagnostics (cf Section F, Fig. 3-33).

ii. The Solar Corona: Gross Radial Structure

I gave detail on the structure of the photosphere-chromosphere, and the beginning of the chromosphere-corona, transition-regions because the empirical relation between its density and T_e -structures identify the cause of the beginning of the outer-atmosphere in the solar situation: i.e., simply a nonradiative heating. The details of the (n_e , T_e) distribution throughout the remainder of the chromosphere-corona transition region depend upon disk, not eclipse, analysis of the line spectrum, not the continuum. So, it is doubly complicated by: the necessity to construct a height-scale from an optical-depth scale, which involves the question of a “turbulence” inferred from line-widths; and the necessity to consider nonLTE radiative transfer in the lines. These problems are discussed by Athay, by Cram, and by Zirker in the Solar Volume (Jordan, 1981). Only high-enough in the corona can one get simple and direct measures of n_e from the continuum. Because hydrogen is effectively ionized, $n_e(r)$ gives density (ρ). In the chromosphere-corona transition region, eclipse data—requiring the double height-differentiation for analysis—are not capable of resolving the behavior in that few thousand kilometer region.

Once into the corona, one believes the gross, radial variation of T_e is quite small, lying in the range $1-2 \times 10^6$ K. The Solar volume considers the situation in detail; we comment quickly on nonradial variations below. But, on the contrary, the radial variation of density is very large, and characterizes the “extended-atmosphere” properties of the Sun for $r > 1.004 R_p$. We ask what this density variation tells us about the relative importance of nonradiative heating and mass-flux, in fixing these *solar* extended atmospheric properties.

The 1952 eclipse data give n_e out to about 50,000 km, $r \simeq 1.072 R_p$, subject to the uncertainty mentioned above. Then the compilations by van de Hulst (1961) and Newkirk (1967) of $n_e(r)$, extending to $6R_p$ and $30R_p$ respectively, suffice for our discussion. These data are compared in Table 3-7 where we also give $\beta_e = -d \ln n_e / dr$ and $\beta_e r_1 r_2 / R_p^2$, obtained by simple differencing of the data between successive heights r_i, r_{i+1} . We note that under isothermal conditions, HE in a plane-parallel atmosphere is represented by eq. (3.5), whereas HE in a spherical atmosphere is represented by

$$n = n_p \exp \left\{ - (Mg_p / kT_e) (r - R_p) / (r/R_p) \right\} \quad (3.34)$$

We can cast eq. (3.34) into the *form* of eq. (3.5)

$$n = n_p \exp \left\{ - (r - R_p) / H_e \right\} \quad (3.35)$$

by defining

$$H_e = H_p (r/R_p) \quad ; \quad H_p = kT_e / Mg_p \quad (3.36)$$

Table 3-7
 n_e -Distribution

van de Hulst (1953)				Newkirk (1967)	
r/R_p	$\log n_e$	$\beta_e \times 10^{10}$	$\beta_e (r_1 r_2 / R_p^2) \times 10^{10}$	$\log n_e$	$\beta_e (r_1 r_2 / R_p^2) \times 10^{10}$
1.0036	10.71				
1.057	8.36				
1.072	8.18				
1.02				8.60	
1.03	8.50				
		1.43	1.57		
1.06	8.37				
		1.12	1.30		
1.1	8.20			8.15	
		1.16	1.53		1.35
1.2	7.85			7.84	
					1.38
1.3		0.81	1.36	7.57	
					1.27
1.4	7.36			7.36	
		0.60	1.33		1.33
1.6	7.00			7.00	
		0.50	1.42		
1.8	6.70				1.46
		0.41	1.50		
2.0	6.45			6.45	
		0.35	1.76		1.65
2.5	5.92			5.95	
		0.28	2.07		1.74
3.0	5.50			5.60	
		0.19	2.00		
3.5	5.21				2.06
		0.17	2.39		
4.0	4.95			5.08	
		0.099	1.95		
5.0	4.65				2.36
		0.063	1.85		
6.0	4.46			4.49	
					3.00
8.0				4.11	
					1.59
10.0				3.99	
					5.8
15.0				3.40	
					5.8
20.0				3.11	
					8.9
30.0				2.66	
50.0				(2.00)	
100.0				(1.30)	
215				0.40	

Thus, in a strictly-isothermal spherical atmosphere, $\log n$ should vary as r^{-1} . van de Hulst considered that his data were sufficiently well represented by such a relation, with $T_e \simeq 1.5 \times 10^6$ K. For our present purposes, we can see the situation a bit more explicitly by considering the data differentially, so computing at each r :

$$2.3 \left\{ \frac{\log n_{e1} - \log n_{e2}}{r_1 - r_2} \right\} = -\beta_e = -(Mg_p/kT_e) (R_p^2/r_1 r_2), \quad (3.37)$$

and tabulating $(r_1 r_2 / R_p^2) \beta_e$. This last should be H_p^{-1} , whose value should be between $1.65 - 0.81 \times 10^{-10}$ for T_e between $1 - 2 \times 10^6$ K. (Note that we use the van de Hulst distribution labeled "solar max, equator and pole." Since these distributions are the same as the other equatorial ones in the $\Delta \log n_e$ structure, which is what we use in our discussion, there is no difference in models for our present purposes.)

Either from Table 3-7 itself, or from plotting $(r_1 r_2 / R_p^2) \beta_e$ against r/R_p , Fig. 3-26, we see that both sets of data would be reasonably well satisfied by a mean value of $H_p^{-1} \sim 1.4 \times 10^{-8}$, for $r/R_p \lesssim 2$. Such an H_p corresponds to $T_e \sim 1.2 \times 10^6$ K, a reasonable value from what has been said above. For $r/R_p \gtrsim 2$, H_p^{-1} rapidly increases, with the two sets of data showing increasing scatter, and diverging. So, either (α) one tries to interpret this trend in terms of a gradient in T_e , or (β) one accepts a quasi-isothermal "mean" corona and looks for something else for $r/R_p \gtrsim 2$.

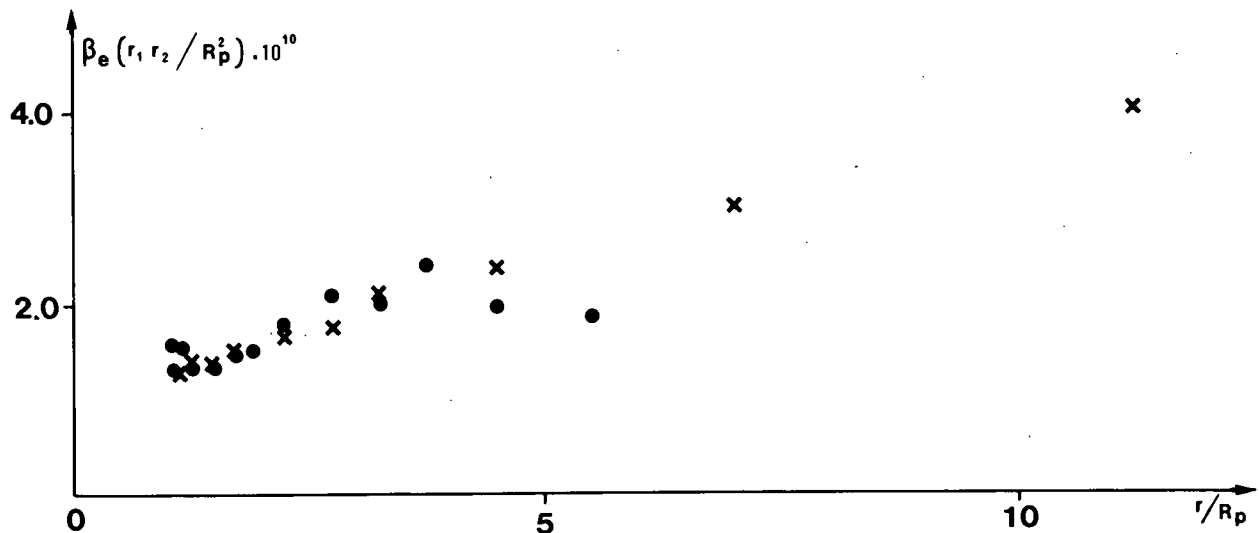


Fig. 3-26. Solar density gradient.

α . If one takes the data in Fig. 3-26 *completely* literally, overlooks the very large observational scatter, and considers them to reflect wholly a variation in T_e —although a slow one—one would find an initial increase in T_e , from about 1×10^6 K at $r/R_p \sim 1.03$, to maximum $T_e \sim 1.3 \times 10^6$ K at $r/R_p \sim 1.4$, followed by a monotonic decrease through the values: 1×10^6 K at $r/R_p \sim 2$; 0.8×10^6 at about 3; 0.75×10^6 at about 5; 0.5×10^6 at about 7; 0.45×10^6 at about 10; to less than 25,000 K at the Earth. Such a T_e -distribution for the “average” Sun is not obviously absurd compared with inferences from other data, although the absolute sizes of the T_e are small. Mariska and Withbroe (1978) ask what can be said on the T_e -distribution for $r/R_p \lesssim 1.4$ from farUV line intensities. The data are not internally consistent; e.g., the Mg X/O VI ratio suggests a mean $T_e \sim 1.2 \times 10^6$ K while Si XII/Mg X suggests 2×10^6 K. They try various models $T_e(r)$ to match these farUV lines; conclude that no model with $dT_e/dr \leq 0$ in the range $1.1 < r/R_p < 1.4$ is compatible with the data; and suggest a model with $T_e(r/R_p = 1.4)$ lying between $2.5 - 3.0 \times 10^6$ K, decreasing for smaller r/R_p to reach about 1.2×10^6 K at $r/R_p \simeq 1.1$, and 1.0×10^6 at about 1.02. A similar treatment by Saiko (1970) finds similar results, with slightly lower T_e : 1.5×10^6 K at about 1.05, and 2.4×10^6 K at 1.4. Nakada et al. (1976) find 2.5×10^6 K at 1.2, decreasing monotonically outward, to reach 1.5×10^6 at $r/R_p \simeq 3$. So the above estimates of T_e , and dT_e/dr , from density gradients, inferred from electron-scattering data, agree with the estimates of T_e from line-intensity observations of various ions, in placing a T_e (max) for the average corona at about $r/R_p \simeq 1.4$; but the density gradients are too large, implying too small T_e , by about a factor 2, relative to the line data. Before commenting on the effects of a possible radially-inhomogeneous structure, we should consider that kind of an alternative (β) which, for the sun, underlies it: a wind, or mass-flux.

β . Making reference to the thermodynamics of such a mass-flux as developed in Part III of this volume, we can ask into the self-consistency of the data under such an effect. We see that a mass-flux does not perturb an HE atmospheric structure, isothermal or not, until the flow-velocity, V , exceeds about one-third the (one-dimensional) thermal velocity, $q = (kT_e/M)^{1/2}$. From the Solar Volume, we have that the mean solar mass-loss is 3×10^{-14} solar masses per year. Then we have for the particle-concentration \simeq electron-concentration at that radius where V first comes to within a few percent of q :

$$n_q = (\dot{M}/4\pi m_H q r^2) = 2.9 \times 10^6 (10^{-6} T_e)^{-1/2} (r/R_p)^{-2}. \quad (3.38)$$

From the n_e -values of Table 3-7, we see that a self-consistent solution between n_q and r/R_p would be: for $T_e = 1 \times 10^6$ K, $n_q \simeq 3 \times 10^5$ at $r/R_p \simeq 3$; for $T_e = 1.5 \times 10^6$ K, $n_q \simeq 2 \times 10^5$, at $\simeq 3.25$; for $T_e = 2 \times 10^6$ K, $n_q \simeq 1.5 \times 10^5$ at $r/R_p \simeq 3.5$. Since the mass-flux effect begins when $V \simeq 1/3 q$, and between there and $V \simeq q$ we expect a drop in density by 3 even for constant r , we see that the Table 3-7 data are also compatible with this mass-flux representation, with $V \simeq q/3$ at $r/R_p \simeq 2$, where departure from an isothermal exponential density distribution apparently starts, and $V \simeq q$ at $r/R_p \simeq 3 - 3.5$.

Again setting aside (until just below) the question of nonradial inhomogeneous structure, we try to push this self-consistency aspect further. The “mean” solar wind has $V \simeq 500$ km/s at the Earth’s orbit, reaching half this value at $r/R_p \simeq 5$ (Zirker, Solar Volume). Using these mean wind values, and if we take $V \simeq q = 130$ km/s ($T_e = 1 \times 10^6$ K) and $\log n_e \simeq 5.50$ at $r/R_p \simeq 3$ —the values just found—and use the mass-flux density distribution of constant ($r^2 V n_e$), then we would expect $\log n_e \simeq 4.75$ at $r/R_p \simeq 5$, and $\log n_e \simeq 1.2$ at the Earth’s orbit ($r/R_p = 215$). If we use the values found for $T_e = 2 \times 10^6$: $V \simeq 180$ km/s and $\log n_e \simeq 5.20$ at $r/R_p \simeq 3.5$, we again would expect $\log n_e \simeq 4.75$ at $r/R_p \simeq 5$, and $\log n_e \simeq 1.2$ at the Earth. If, instead, we take the maximum value of $V = 800$ km/s at the Earth’s orbit during sunspot minimum (Zirker, Solar Volume), and repeat the above with only that change of $V = 400$ km/s at $r/R_p \sim 5$ and 800 km/s at the Earth, we would expect $\log n_e \simeq 4.55$ and $\log n_e \simeq 1.0$ at these two positions, respectively. Thus, the predicted $\log n_e$ at $r/R_p \simeq 5$ bracket the observed value, while the values for both V (max) exceed the observed value by about a factor of 4 at the Earth.

Such a level of self-consistency for the mass-flux modeling of the density distribution above $r/R_p \simeq 3$ is not bad, but the factor of 4 over-estimate of the density at the Earth is not trivial. That is, the (radially-homogeneous) mass-flux model gives too low a density gradient, relative to the observed, in the same sense as the deviation of the quasi-exponential, thermal, model of alternative (α).

Let us put these results from the upper-part of the chromosphere-corona transition region and the corona into the same focus as those from the chromosphere and lower-part of the transition-region in Section *i*, always aiming at the stellar application of distinguishing between effects of nonradiative-energy, and mass-fluxes. In Section *i*, we saw that the classical photospheric model becomes, for solar-level nonradiative-flux, inadequate at densities $n \approx 10^{15}$, compared with the $n \approx 10^{16} - 10^{17}$ at τ_{vis} (radial) ≈ 1 . Over the next 2000 km, $\Delta R_p/R_p \approx 0.003$, n decreases by about a factor of 10^6 —including the effect of the jump to coronal T_e —as contrasted to the 10^7 from the classical, RE, model. Extrapolating from this low-chromospheric model, through the chromosphere-corona transition region, into the low corona under the assumption that only the effect of the nonradiative flux is important, we expected an actual, further, density drop of $e - e^2$ in the next 2000 km or so, up to $r/R_p \approx 1.007$, by contrast to the factor $\geq 10^7$ predicted by the classical model. In this Section *ii*, we see that this is indeed the case, and that a quasi-exponential thermal structure represents well the data out to between $r/R_p \approx 2 - 3$, where $n \approx 10^6 - 10^5$, for the *mean* solar atmosphere. Above this height, one is uncertain whether a quasi-exponential, with decreasing T_e , or the $(r^2 V)^{-1}$ behavior of a mass-flux, are *empirically* better. But for us, the essential thing here, is that over a drop of $\geq 10^{10}$ in density from the height of first evidence of the effect of a nonradiative energy-flux, an HE, but nonRE, atmospheric model for the *mean* Sun suffices, for this star with an $F_M \approx 3 \times 10^{-14}$.

Correspondingly, T_e —again for the mean solar atmosphere—lies between $1-3 \times 10^6$ K in this region, apparently passing through a maximum of $2-3 \times 10^6$ K near $r/R_p \approx 1.5$. The nontrivial discrepancy between “kinetic” T_e and “ionization/excitation” T_e remains to be resolved; reference is made to the Solar Volume in the series. We note that the differences in T_e inferred from density-gradients, line-profiles, and ionization-excitation studies from line-intensities are long known, in the Sun, and in stars generally.

Finally, we comment on the nonradial-inhomogeneous structure of the outer solar atmosphere. One realizes that such a structure exists throughout the solar atmosphere, from the granulation observed everywhere, and the sunspots observed more locally, in the lowest photosphere, out to the spectacular plumes and streamers observed at eclipses. In the same sense, one observes strong variation in the terrestrial atmosphere, ranging from cloudwhisps to hurricanes. Nonetheless, one contests that equally in the solar and terrestrial atmospheres there is a mean structure that varies with height, and which consists of systematic density and temperature variations with height that, with the exception of highly-transient events like solar active-regions, and terrestrial hurricanes and cyclones, can be considered to be a “mean,” radially-distributed, atmosphere. And here, when we discuss the difference between a classical, RE and HE, photosphere enveloping the star considered as a (closed, thermal) system, and the atmosphere enveloping a star considered as a (open, nonthermal) system, which is composed of a quasi-RE + HE photosphere, surmounted by an outer-atmosphere whose properties are fixed by nonradiative-energy- and mass-fluxes, possibly plus other fluxes—then we contest that present evidence shows the difference between these two atmospheric representations to be given in very predominant first-order approximation, by differences in radial distributions of density, T_e , and outward systematic velocity. That there are also nonradial-inhomogeneous effects, one could hardly deny. The question is their first-order importance in resolving this choice between (closed, thermal) and (open, nonthermal) modeling, and how to do it. These are primarily empirical questions, given our current state of knowledge of how to produce the nonradiative energy-, and mass-fluxes.

In the solar outer atmosphere (referring to Zirker’s summary in the Solar Volume), one distinguishes, in a rough way, three kinds of regions: quiet-Sun; coronal-holes; active-regions. In the chromosphere the quiet-Sun and coronal-hole regions are essentially indistinguishable. Table 3-8 taken from Vaiana and Rosner (1978), summarizes the situation in the corona well below the $r/R_p \approx 2$ level. For our present purposes, the essential result of this table is to show the small nonradial variation between these regions, relative to the gross, radial variations we have discussed above. The quiet-Sun and coronal-hole regions differ trivially, in n_e : both their T_e lie within the $1 - 2 \times 10^6$ K range of uncertainty; and their “scale-heights,” or density gradients—especially taking into account how they are determined in these regions, lie within the range of uncertainty of such data. The “active-regions” have significantly higher T_e and n_e ; but they are hardly the regions we try to discuss in our attempts to delineate the mean, radial, sequence of atmospheric regions. We note only that if the relative importance of the active regions—i.e., their relative contribution to emission and scattering—decreases with increasing height, then the “mean” effect would be in the direction observed: too great value of β_e , the inverse scale-height, hence too small inferred “effective” kinetic T_e .

Table 3-8
Typical Isothermal Coronal Model Parameters (Vaiana and Rosner, 1978)

	OSO-4				Skylab ATM (S-054) ^c				
	1953 ^a (van de Hulst)	X-ray AR	EUV ^a AR	EUV ^a QS	CH ^b	LSS ^d	BP	AR	Small (C) flare
Temperature T_6 (10^6 K)	1.5	3	2.5	1.8	1.3 ^b	2.1	1.8	2.5	10
Characteristic vertical size L (cm)	—	10^{10}	H ^c	H ^c	H ^c	H ^c	3×10^8	7×10^9	7×10^8
Electron density N_e (cm^{-3})	10^8	10^9	1×10^9	1×10^8	1.3×10^8	2.0×10^8	4×10^9	5×10^9	5×10^{10}
Pressure $\equiv 2N_e kT$ P (dyne cm^{-2})	0.04	1	0.7	0.07	0.05	0.11	2.0	3.5	140
Energy density $\equiv 3N_e kT$ U_T (erg cm^{-3})	0.06	1	1.0	0.11	0.07	0.16	3.0	5.2	210
Scale height $\equiv 5 \times 10^3 T$ H (cm)	8×10^9	1×10^{10}	1×10^{10}	9×10^9	6×10^9	1×10^{10}	9×10^9	1×10^{10}	5×10^{10}
Total fraction of surface area	1	—	—	—	0.1	0.9	< 0.01	10^{-3} – 10^{-2}	—
Equipartition magnetic field $\equiv (16\pi N_e kT)$ B_{eq} (Gauss)	1	5	4	2	1.0	2	7.1	9	—

Abbreviations are as follows:

AR, active region; QS, quiet Sun; CH, coronal hole; LSS, large-scale structure; BP, bright points.

^aValues at $h \sim 10^{10}$ cm (\sim height at which temperature gradient vanishes in model).

^bThe S-054 data permit a range of allowed temperatures. $T_6 = 1.3$ is assumed in the calculations (Maxson & Vaiana, 1977).

^cThe pressure scale height is used as the characteristic size.

^dLarge-scale structures (LSS) are identified with the quiet Sun (QS).

^eX-ray spectrographic telescope.

iii. Stellar Extrapolation from Solar Configuration

At this point in our summary of extended-atmosphere peculiarity, we have two choices: either we can proceed directly to other stars showing such evidence of extended atmospheres, or we can first try to place such possible evidence in perspective via the results of the above solar summary. Again, we emphasize that apparently the only alternatives for producing such an extended atmosphere are some combination of a nonradiative energy-flux which increases T_e , hence scale-height under HE, and a mass-flux which negates HE. I proceed first via solar guidance, because of the much greater, and more detailed, solar data.

Then we have shown, empirically, that the Sun is an extended-atmosphere peculiar star because of an increased T_e over the RE, classical model predictions from a radiative-flux alone. This thermally-induced atmospheric extension suffices to represent at least the first factor of 10^8 drop in density from its value where a significant departure from the RE distribution of T_e occurs; the origin of such departure is the dissipation of some nonradiative energy-flux. Any effect of mass-flux on such atmospheric extension does not, empirically, appear until $r/R_p \gtrsim 2-3$, $n \lesssim 10^5$. Thereafter, again empirically, there appear mass-flux effects, associated with a velocity which accelerates from low values in the corona to some 5–800 km/s at some $200R_p$, apparently being continuously accelerated in the interval. The nonradiative heating continues from its first visible effects near $n \sim 10^{15}$ until at least $r/R_p \sim 1.5$, where $n \sim 10^7$, thus through a range of n of at least 10^8 . All these inferences on effects of nonradiative energy-, and mass-fluxes are empirical, there being as yet no adequate theory of origin or amplitude of either nonradiative-energy-, or mass-fluxes.

If, then, we want to extrapolate from solar *empirical* knowledge to stellar—to aid in diagnosis, crude prediction, or simply visualization—we can only proceed via thermodynamic considerations: assuming *first*, that those stars considered are also (open, nonthermal) thermodynamic systems, rather than classical (closed, thermal); and *second* that this radially-symmetrical modeling gives a reasonable approximation to a gross atmospheric structure. Then one uses the stellar observations *first* to establish, or contradict, these two assumptions and *second*, as for the Sun, to ask what details can be inferred, under this framework. Any additional theory introduced on origin or amplitude of these two fluxes, nonradiative energy and mass, coming from the (open, nonthermal) character is, today, essentially speculation.

Then, from thermodynamic considerations alone, we restrict attention to radiative-flux, nonradiative energy-flux, mass-flux, and gravity. From radiative-flux and gravity, under HE and RE, as in Chapter 2 we obtain a photospheric boundary T_e , T_0 , and a density distribution in these quasi-isothermal boundary regions. From a nonradiative-flux alone, unless we know its form and details of propagation and dissipation, we have no simple way to ask the perturbation on the RE distribution of T_e . We know only that *if* a mass-flux occurs, then when $V \sim q$, an energy dissipation will occur, because the flow velocity is differential, producing shocks, etc. in such a transsonic flow regime (cf Vol. 2). So RE becomes invalid *at least* where HE becomes invalid, probably lower in the atmosphere. So, we focus attention on the point R_q , as the *maximum* height where the outer-atmosphere begins. Then we highly abstract our development of Part III to put, here, the preceding into quick focus.

With a given value of F_M , and the R_p corresponding to the photospheric radius of that star, we can compute from eq. (3.38) with the stellar, rather than solar, R_p and q , a value for n_q . The range of uncertainty corresponds to uncertainty whether nonradiative-heating just begins at this point R_q , in which case we use $q(T_0)$, or whether it has already begun, in which case we use $q(x \times 10^6 \text{ K})$, where $x \sim 1-3$. This value of x corresponds to thermal stability conditions for the corona, cf Thomas and Athay (1961) and Athay (Solar Volume). This computed value of n_q , compared with n from whatever photospheric model one thinks applicable, gives the number of density scale-heights between that representative photospheric point and R_q ; thus, by iteration, one obtains a better value of R_q . The tables in Chapter 4 give several representative “beginning points of the outer atmosphere,” for several stellar types, using F_M values associated with such stars, *empirically*, in the literature (cf the discussion of F_M later in this chapter). The striking result of the tables is simply the large increase in n_q as F_M increases; essentially, n_q is proportional to F_M . Because *above* R_q the density decreases outward as $(Vr^2)^{-1}$, instead of exponentially at the thermal density scale-height, this n_q essentially fixes the density of the outer atmosphere. Thus, for a Be star like 59 Cyg or γ Cas, the atmospheric density in the regions of producing the superionized spectral lines, and the superthermic velocities, is some $10^{13} - 10^{11}$; and even if H α and the Fe II lines are produced at $50R_p$, and even farther out, n has only

decreased by a factor of $10^2 - 10^3$, to $10^{11} - 10^8$, as contrasted to the solar situation where the mass-flux outer-atmosphere begins near $n_q \sim 10^5$. This is what we mean by *just large nonradiative-fluxes alone produce only low-density extended-atmospheres, whereas large mass-flux effects produce high-density extended-atmospheres*. With this orientation, based *wholly* on thermodynamic properties, independent of origin or details of nonradiative-energy-, and mass-fluxes, we proceed to consider the extended-atmospheric phenomena of other stars as inferred from eclipses.

b. Eclipse Probing of a Hot-Star Extended Atmosphere

In the preceding Section a, we saw the results of eclipse-probing of the atmosphere of a main-sequence cool star, the Sun. If the Sun were at normal stellar distances, and observed only in the visual spectrum, it would be seen, and considered, to be “normal.” But because of the favorable location of the Earth, Moon, and Sun, there occur eclipses of the bright central solar disk, as seen at the Earth, by the Moon. So, we can see the radial distribution of *emission* above the photosphere. Such observations transform the Sun into an extended-atmosphere peculiar star. Anomalous intensities of well-known spectral lines and continua make quantitative the density-measure of the extent; the identification of normally-unknown lines, and their intensities, help us distinguish between thermal and nonthermal immediate causes of this anomalous atmospheric extent. Subsequent observations in the X-ray, farUV, farIR, and radio spectral regions confirmed, detailed, and enlarged this “historical” pattern of regions of the extended solar atmosphere.

Unless we visited one of its planets, such method of measuring outer-atmospheric peculiarity will not work for any other star. We can only use a similar, eclipse, approach by substituting for the Sun some star whose atmospheric extent is much larger than the size of its binary companion, which replaces the Moon. “Much-larger” refers to the photospheric disk of the companion; an extended-atmosphere, with very small emissivity, of the companion will not perturb the situation. Then the increasing transmittivity of the extended atmosphere of the “peculiar” star as the companion emerges from eclipse, and conversely as it enters, gives a radial distribution of the *absorbing* (or scattering) material above the photosphere. If the companion is also the brighter, its eclipse will also be the deeper: so one will contrast a deep, broad eclipse at one minimum with a shallow, narrow eclipse at another. One should read the Kopal and (Martha) Shapley (1946), and Kopal (1946) discussions of the extended-atmospheric implications of this kind of observed alternating minima in exceptional stellar eclipses, in a search for, and probe of, extended-atmospheric peculiar stars. Clearly, neither the height resolution nor the accuracy of density values will approach those in the solar situation; and we have seen the problem there at the greater radii.

Then from the standpoint of the utility of “confirming” information on peculiarity, the binary V444 Cyg is a particularly useful one. One component is a WR, classified as WN5; the other, an O6 main-sequence whose brightness is some 1.75 magnitudes greater than the WR. In Section II.B.3 of this chapter, we summarized the properties of WR stars, which we called the generally-peculiar stars, even when observed only in the visual, at normal stellar distances. Then we note that the WR component of V444 Cyg is also “location-peculiar,” like the Sun, in giving the chance of eclipse-probing of its atmosphere. I base the following on the discussion by Kopal and Shapley (1946) of the Gordon and Kron observations (1943). A subsequent discussion of other properties of this system by Munch (1950) should be read.

The WR atmospheric dimunition of the O-star light is by electron-scattering; so like the solar case, the results give directly $n_e(r)$; the observed ionization state guarantees that, like the solar corona, $n_e(r)$ is density (r). There is a nontrivial ambiguity coming from uncertainty in the orbital inclination; Kopal and Shapley give solutions for $i = 70^\circ, 80^\circ, 90^\circ$ ($i =$ inclination of pole of the orbital plane to observer’s line of sight). Discussions by S. Gaposchkin, Russell, and Kopal are cited for the 1.75-magnitude difference between the stars, and for a preference of the 80° value for i . In Table 3-9 we reproduce their values for $n_e(r)$. As for the Sun, we difference these values to form $\beta_e = d \ln n_e / dr$ and $\beta_e (r_1 r_2 / R_p^2)$. We also tabulate $n_e r^2$; the value of V necessary to give a constant mass-flux; and the T_e required to match the β_e by a thermal quasi-exponential density distribution. We arbitrarily choose $V(R_p) = 2000$ km/s. Note that this value gives an \dot{M} ranging from 0.3×10^{-5} at $i = 90^\circ$ to 7×10^{-5} at $i = 70^\circ$, with 1×10^{-5} at $i = 80^\circ$; all these lie within the range found from modern farUV data on WR stars. Note also that

Table 3-9
Atmospheric Structure of WR Component of V444 Cyg

a. $i = 80^\circ$							
r/R_p	r/R_{orb}	$10^{-12}n_e$	$10^{12}\beta_e$	$10^{10}\beta_e (r_1 r_2 / R_p^2)$	$10^{-6}T_e$	$n_e r^2 / R_{orb}^2$	V (km/s)
1.	0.12	1.786				2.57	2000
	0.14	1.541	2.82	0.0340	23.8	3.03	1700
	0.16	1.330	2.98	0.0444	18.2	3.30	1550
1.5	0.18	1.147	2.98	0.0596	13.5	3.72	1400
	0.20	0.985	3.03	0.0756	10.7	3.94	1300
	0.22	0.844	3.14	0.0960	8.4	4.08	1250
2.	0.24	0.720	3.18	0.117	6.9	4.15	1250
2.5	0.30	0.432	3.42	0.171	4.7	4.15	1250
3.	0.36	0.258	3.45	0.259	3.1	3.89	1300
	0.42	0.157	3.32	0.358	2.3	3.34	1550
4.	0.48	0.090	3.72	0.522	1.5	2.77	1850
	0.54	0.044	4.80	0.865	0.93	2.08	2500
5.	0.60	0.017	6.35	1.46	0.55	1.28	4000
	0.66	0.004	9.7	2.7	0.30	0.61	8500
						0.17	30,000

b. $i = 70^\circ$							
r/R_p	r/R_{orb}	$10^{-12}n_e$	$10^{12}\beta_e$	$10^{11}\beta_e (r_1 r_2 / R_p^2)$	$10^{-6}T_e$	$n_e r^2 / R_{orb}^2$	V (km/s)
1.	0.3000	1.856	5.42	0.631	1.11	1.67	2000
	0.3500	0.944	4.87	0.756	0.93	1.16	2900
	0.4000	0.514	4.32	0.865	0.815	0.822	4000
1.5	0.4500	0.300	4.28	1.07	0.659	0.608	5500
	0.5000	0.176	4.14	1.26	0.560	0.440	7600
	0.550	0.105	4.21	1.55	0.455	0.318	10,500
2.	0.6000	0.062	5.06	2.20	0.320	0.223	15,000
	0.6500	0.033	8.82	4.45	0.158	0.139	24,000
	0.7000	0.011				0.054	62,000

c. $i = 90^\circ$							
r/R_p	r/R_{orb}	$10^{-12}n_e$	$10^{12}\beta_e$	$10^{11}\beta_e (r_1 r_2 / R_p^2)$	$10^{-6}T_e$	$n_e r^2 / R_{orb}^2$	V (km/s)
1.	0.075	1.415	2.66	0.355	31.3	0.797	2000
	0.100	1.197	2.64	0.588	18.9	1.197	1300
	0.125	1.015	2.63	0.880	12.6	1.59	1000
2.	0.150	0.862	2.70	1.62	6.9	1.94	800
3.	0.225	0.521	2.87	3.45	3.2	2.64	600
4.	0.300	0.305	2.92	5.85	1.9	2.74	600
5.	0.375	0.177	2.95	8.85	1.25	2.49	650
6.	0.450	0.102	3.50	14.7	0.75	2.06	800
7.	0.525	0.053	4.45	24.9	0.44	1.46	1100
8.	0.600	0.023	5.65	40.6	0.27	0.83	1900
9.	0.675	0.008				0.365	4500

the “kinetic- T_e ” given in our tables differ from those in the Kopal-Shapley results, because they used a plane-parallel atmosphere density distribution rather than that for the spherical case required in this situation. Then, note the large range in photospheric R_p —defined as the smallest “non-opaque” disk in the data analysis by Kopal and Shapley: values given are $2.7 R_{p\odot}$ ($i = 90^\circ$), $4.3 R_{p\odot}$ ($i = 80^\circ$), $10.7 R_{p\odot}$ ($i = 70^\circ$). And finally, note the corresponding range in g_p : 3.8×10^4 ($i = 90^\circ$), 1.3×10^4 ($i = 80^\circ$), 2.4×10^3 ($i = 70^\circ$); compared with 2.7×10^4 for a main-sequence Sun and the common value near 10^4 for main-sequence, g, sg O and hotter stars, among which should probably be included the WR. One sees why the choice of $i \sim 80^\circ$ appears to represent a compromise.

Then taking account of all this uncertainty on the parameters of the WR star and orbit, and the accuracy of analysis of the data to obtain $n_e(r)$, we ask what conclusions we can draw on the extended-atmosphere of the WR component of V444 Cyg, following the approach in the preceding Section a to the Sun.

(1) Each of the several alternatives agrees in giving β_e , and the resulting H_p , *much* lower than solar values: $0.03\text{--}0.05 \times 10^{-10}$ as contrasted with the solar values near 1×10^{-10} . These would correspond to an “effective-kinetic- T_e ” near 20×10^6 for the $i = 80^\circ$ and 90° cases, 1×10^6 for $i = 70^\circ$, compared with 1×10^6 K for the Sun. Alternatively, the density distribution would be reasonably-well matched by a mass-flow of $1\text{--}2000$ km/s for $i = 80\text{--}90^\circ$ in the lowest regions, as contrasted to the Sun where the thermal case is the only alternative in the lowest corona. For this WR case, while we cannot really exclude them, the 20×10^6 K for “mean” coronal T_e , in these lowest regions seem quite high. This leaves the mass-flux alternative throughout the atmosphere, from the smallest measurable r . While we will return to the point in Part III, we only note here that *if* we tried to find the *origin* of the mass-flux in a hot corona—as in the Parker theory for the solar wind—we would be obliged to accept a “mean” corona, not just active regions, with such a $T_e \sim 2 \times 10^7$ K.

(2) Values of $\dot{M} \sim 10^{-4}\text{--}10^{-5}$, and velocities $1500\text{--}3500$ km/s, are frequently quoted in the literature from IUE observations (cf Section B.3.a preceding). If we apply the methodology around eq. (3.38) to the WR situation with $\dot{M} = 3 \times 10^{-5}$, we find

$$n_q = 3 \times 10^{15} (10^{-6} T_e)^{-1/2} (r/R_{p\odot})^{-2} \quad (3.39)$$

for the density at the *thermal point*, i.e., where V first exceeds the 1-dimensional *thermal* velocity, which is 130 km/s for 10^6 K. So, we see that the predicted $n_q \sim 10^{14}\text{--}10^{13}$ indicates that, indeed, the transition to a mass-flux dominated, as contrasted to thermal-dominated, flow occurs well below the beginning of the Kopal-Shapley “opaque” disk. That is, it suggests that the whole WR atmosphere is mass-flux controlled, in strong contrast to the Sun. This also means, of course, that a nonradiative heating extends throughout the whole measurable atmosphere. Since the lowest-ionization species observed in WR stars—like N II and C II—are hardly compatible with such a region, this would imply their formation in a postcoronal, cooled, region: just as are, apparently, the “shell” lines in Be stars, but as for the Sun, with no evidence of decelerations. The interesting aspect of this conclusion is that it comes only from the value of \dot{M} , and a crude estimate of r ; decreasing T_e only demands the heating start lower, at larger n_q . *The eclipse observations simply substantiate these large values of \dot{M} inferred from IUE.* Even if we dropped the 2000 km/s used in Table 3-9 to as low as 100 km/s, it would only drop \dot{M} to $10^{-5}\text{--}10^{-6}$, and n_q to $10^{13}\text{--}10^{12}$, which remain larger than the beginning values in the solar case, thus continue to require the low-atmosphere onset of nonradiative-heating, at least that heating required by the velocity-gradients of a mass-flux.

(3) The above conclusions on where subionized species are formed should be considered in the light of what we have already discussed: an initial outward *decrease* of ionization, from the lowest levels observed (e.g., Beals, 1930; Aller, 1943; Kuhl, 1968). One must reconcile the two sets of data: from the visual, an outward velocity *increasing* with *decreasing* ionization: from the farUV, an outward velocity *increasing* with *increasing* ionization. Sahade (1980) has proposed a model with two coronal-like T_e maxima; Willis (1981, 1982) discusses a frozen-in ionization. We spend no further time on it here, deferring it to Part III. Here, we only mention it to illustrate how, even for the

generally-peculiar WR stars, their extended-atmosphere peculiarity sharpens the focus on the problems of outer-atmospheric modeling. And, again, they illustrate how, by continually contrasting them to the Sun, we obtain a global viewpoint on the effects of these two nonclassical fluxes: nonradiative-energy and mass.

I must strongly admit that all these data, when analyzed as for the solar corona, and taking into account the IUE material, completely invert the picture I advocated during 1947–1968. The broad picture of insisting on a chromosphere-coronal presence, needing to be analyzed by a nonstatic, nonLTE diagnostic approach; and that joint diagnostics of the WR stars plus Sun will aid our understanding of the general stellar atmosphere; these, remain correct. But the *results* of the original diagnostics are wrong. I argued that a mass-loss $\sim 10^{-5}$ demanded by the eclipse results and an expansion velocity ~ 1000 km/s could not, a priori, be correct: so rather than systematic mass-flux velocities, there must be a system of in- and out-moving prominences, supporting a globally-static extended-atmosphere. And, consequently, T_e must increase outward, as would the ionization state. It is a good example of erroneous, a priori prejudice (against such large mass-loss) applied to what the data say, literally; so, inverting their conclusion.

c. Eclipse Probing of a Cold-Star Extended Atmosphere

The WR binary V444 Cyg exemplified eclipse-probing of the extended atmosphere of a hot star, or of the transition-region or coronal atmospheric region of *any* kind of a star where the continuous opacity comes from electron-scattering so that there is no ambiguity in converting distribution of such opacity into density-distribution. In each of these circumstances, the main ambiguity centers on accuracy of data vs. the differential density-gradient required to discriminate between thermal and mass-flux density distributions. In regions of coronal-level T_e , where the mass-flow is still accelerating outward, the differential density gradient between these two alternatives is not always large compared with accuracy of the data. A second ambiguity centers on the possible presence, and size, of nonradially-inhomogeneous distributions of absorbing material.

We have seen, in the analysis of eclipse observations of the *chromosphere* of the cool star, the Sun, where opacity is not by electron-scattering alone, how nonLTE distributions of populations of ionization and excitation levels must be included in converting opacity distribution to density distribution. Moreover, a self-consistent diagnostics, *which determines T_e , n_e , etc. from the data rather than imposing it from a priori models*, must be adopted. Also, we have seen how the radiative excitation/ionization must be modified, when its source is a radiation field produced in the nonradiatively-heated regions of this extended solar atmosphere.

Then the existence of eclipsing binaries where the primary extended-atmosphere star is cold, and in which occur the above complications in converting opacity-distribution to density-distribution, has been long known. The first-observed, ζ Aur, has been studied for some 50 years; 31 and 32 Cyg, VV Ceph, ϵ Aur are almost as well known; others, more faint, have been less well observed (cf reviews by Wilson, 1960; Wright, 1970; and details for ζ Aur by Wilson and Abt, 1954 and by Groth, 1957). What has not been so well recognized and included in analyses is the presence of *all* the above complications in converting eclipse observations of opacity-variation with outer-atmospheric position into density-variation. Ignorance of some of them has led to apparent contradictions in the analyses, which I summarize below. The situation is presently very much in diagnostic flux. Here, I only abstract what presently exists in the literature on analysis of the *visual* spectrum, adding a few comments on the very preliminary results from the farUV which are beginning to appear. I restrict attention to ζ Aur, as the most widely studied. But I do note that, while the “probing,” secondary star in the eclipse is always a hot MS star, usually B, compared with the cold sg primary component, usually K, VV Ceph is composed of an M sg and a Be secondary. Thus, the possibility of interesting differences with the remaining binaries exists, for this one, and indeed they are mentioned in the literature.

Then by contrast with the WR, and solar, eclipse studies, those of ζ Aur rest on analyses of the change in equivalent widths of several strong, and several reasonably-strong, lines as the B star goes progressively behind the K star extended atmosphere, before and after total eclipse. One analyzes a change in *absorption*-line intensities of the combined B + K spectrum as contrasted to the change in *emission*-line intensities in the solar case. That is, one has an extra-atmospheric $I_{\nu 0}$ incident on the K-star atmosphere from behind, due to the B star; for the solar case, $I_{\nu 0} = 0$. Although the fact is usually not emphasized, essentially all analyses of ζ Aur, and similar stars, assume that they

can simply subtract the eclipse-line from the noneclipse-line, obtaining what is called the “chromospheric component” of the line, and then analyze this “residual” as giving the atmospheric absorption. Thus, in the out-of-eclipse spectrum, the Ca II H and K lines are attributed to the K star; the Balmer lines, to the B star. The “enhanced,” or “chromospheric” absorption is attributed to the K-star atmosphere. As in discussions of the so-called “flare equation” in solar studies, such a subtraction approach is quite illegitimate (Zirker and Thomas, 1961); one badly underestimates the opacity. A simple example is a photoionization-dominated line formed in an isothermal atmosphere. Provided that the atmospheric layer remains transparent to the photoionizing radiation, but not to the line itself, increasing the extent of the atmosphere alone, keeping constant the ratio of line and continuous opacity, does not change the profile. So, until those analyzing such data have shown, by solution of a nonLTE transfer equation, including the atmospheres of both stars, under such boundary-conditions, that their approach is self-consistent, one does not find surprising the several contradictions summarized below.

First, consider the overall characteristics of the system. I do not summarize that part of the work having to do with the eclipse determination of photospheric radii and masses except to quote: Wilson’s tabulation of minimum radii and masses give K-star, $14 M_{\odot}$ and $190 R_{\odot}$, B-star, $8 M_{\odot}$ and $7 R_{\odot}$; and Wright’s, $8 M_{\odot}$ and $200 R_{\odot}$ for the K-star, $6 M_{\odot}$ and $4 R_{\odot}$ for the B star. Similar ranges of a factor 2, between authors, exist for the other stars, for M and R . Thus, the ranges of uncertainty in gravity are also about a factor 2. The luminosity difference *in the visual* is about 2 mag, the B-star being the brighter, as inferred from the depths of the two eclipses. The MK classification would suggest M_v of -2.3 for the K4 II star, and -0.8 for the B7 V star, following Wilson; Wright gives types K4 Ib and B6 V, corresponding to -3.7 and -1.5 for M_v , respectively, with again $\Delta m_v \sim 2$ from eclipse data.

The star also gives an interesting illustration of why symbiotic and binary stars are hard to distinguish. In the normal, out-of-eclipse, spectrum, one sees type K 0 at the red end, with the K spectrum disappearing more and more toward the blue where, finally, only the Balmer and He I lines of a B-star spectrum appear. During primary light minimum, interpreted as primary eclipse, the B-type spectrum vanishes. Also during out-of-eclipse phases, one observes Ca II H and K showing the central emission components associated with the presence of a chromosphere across the whole cool part of the HR diagram. In normal B stars, one observes no Ca II emission cores; only emission wings in some Be stars. Thus, one associates this emission Ca II profile with the K star. And, one notes that for a month or so on each side of primary minimum, the Ca II widens progressively toward totality, with no emission core until it reappears *just* at totality.

Then the basic data consist of profiles, and equivalent widths, of Balmer, Ca I, II and metals. Applying standard curve-of-growth analyses, the various authors, summarized in the above references, translate these data into the usual column densities of absorbing atoms, “excitation-temperatures,” and “turbulence.” All authors adopt the plane-parallel, HE, quasi-isothermal representation of eq. (3.5). We reproduce Abt and Wilson’s Table 9 (1954) as Table 3-10 to illustrate the several β_e ; Groth’s tabulation (1957) shows the same relative β_e . Using $10 M_{\odot}$ and $200 R_{\odot}$ for the K-star, we obtain $g \sim 10$. Hence H_p^{-1} , for the K star, should be about $3 \times 10^{-11} \text{ cm}^{-1}$, compared with the *observed maximum* 1×10^{-11} at $r \sim 1.1 R_p$ and about 1×10^{-12} at $r \sim 1.5 R_p$. “Should be” corresponds to using the upper limit on T_0 for the RE solution, LTE or nonLTE, of $T_{\text{eff}} \sim 3500 \text{ K}$ for this K sg, and applying an HE thermal model. So, if we interpret the data in terms of an HE, but not RE, thermal model, we require a $T_{\text{kin}} \gtrsim 10,000 \text{ K}$ at $1.1 R_p$ and $T_{\text{kin}} \gtrsim 100,000 \text{ K}$ at $1.5 R_p$. Alternatively, if we try to interpret the data in terms of a mass-flux extended atmosphere, we see that these β_e are too large to be matched by an $(r^2 V)^{-1}$ density gradient, *unless* there is a *very* rapid acceleration through these atmospheric regions; a factor between 30 and 10^{17} in a distance $0.5 R_p$, depending upon which β_e one tries to match.

We ask what information any other “contradictions”—or *anomalies*—add, to help in interpreting the differential values of these β_e . I summarize the results of the various authors.

(1) “Excitation-temperatures” exceed the classical boundary-temperature and increase with height. These range from 4–5000 K for the metals, to about 6800 K for the Balmer ground-state of hydrogen. All authors judge that the differential β_e between Ca I and Ca II at low heights, and between these and the essentially-similar β_e for neutral and ionized metals, is a strong problem and guide to atmospheric structure.

(2) Inversion of the column densities inferred from the equivalent-width analysis, via the observed values of the β_e determined from these column-density height-variations, leads to internal contradictions, which have been variously

Table 3-10
Spectroscopic Logarithmic Apparent Gradients, $\Delta \ln N/\Delta h$, AT
 $h = 10 \times 10^6$ km and $h = 40 \times 10^6$ km for Zeta Aurigal

Element	$\Delta \ln N/\Delta h$ (cm ⁻¹)			
	$h = 10 \times 10^6$ km		$h = 40 \times 10^6$ km	
	A*	B [†]	A*	B [†]
H [‡]	~ 0	~ 0	1.2×10^{-12}	0.5×10^{-12}
Ca I	12.7×10^{-12}	9.9×10^{-12}	—	—
Ca II	6.0×10^{-12}	3.9×10^{-12}	1.3×10^{-12}	0.6×10^{-12}
Fe I	4.4×10^{-12}	3.7×10^{-12}	—	—
Mn II	3.7×10^{-12}	2.8×10^{-12}	1.0×10^{-12}	0.6×10^{-12}
Fe II	4.2×10^{-12}	2.8×10^{-12}	1.2×10^{-12}	1.0×10^{-12}

* Ingress and egress, 1939–1940; egress, 1947–1948.

From Wilson and Abt, 1954.

† Ingress, 1947–1948.

‡ Population of first excited level.

interpreted. Combining data on Ca I and Ca II lines gives an estimate of Ca-ionization, as well as total Ca-concentration. Use of an assumed Ca: H abundance gives, from that of Ca, the hydrogen concentration. Comparison of that with the ground-state Balmer concentration gives the 6800 K excitation temperature cited above, and shows hydrogen to be mainly neutral, as is to be expected if the sole ionizing source in the K-atmosphere is the (diluted) radiation field from the B star. Use of an assumed Fe: H abundance gives a total population for Fe which, combined with an Fe I population inferred from the Fe I lines, gives an Fe I ionization. The ionization degree for Ca and Fe differ by an order of magnitude, Ca being the lower, in the lower atmosphere; in the upper atmosphere, they essentially agree. All authors consider this strange, since the ionization potentials of 7.9 and 6.1 eV for Fe I and Ca I, respectively, are so close; they attribute the difficulty to Ca. Use of these estimates of the concentrations of Fe I and Fe II, combined with the Stromgren substitute (1937) for the Saha equation under conditions of a dilute radiation field, and an estimate of radiation temperature and dilution factor to enter that equation, gives the electron concentration. This value is essentially that for the total concentration of hydrogen, obtained from calcium, as above; so it demands that hydrogen be essentially all ionized. This contradicts both the earlier conclusion that hydrogen must be mainly neutral, and the general consensus that the electrons must arise from ionization of the metals. In interpreting these results, the authors diverge. Wilson and Abt suggest this requires the K-star chromospheric material to lie in concentrations of small size and high density. Relative motions of these “balls or bubbles” account for the “turbulence” summarized below. On the contrary, Groth resolves the internal contradictions by simply stating that the ionization/excitation processes are simply characteristic of the thermodynamic state of the K-star atmosphere, and have nothing to do with the B star.

(3) “Superthermic turbulence” exists in the K-star chromosphere, *if* the chromosphere has its pre-1941 sense of a simply extended, not heated, atmospheric region. From curve-of-growth analysis, values of “microturbulence” range 7–22 km/s. The significance of this range is complicated by systematic differences in equivalent-widths deduced from different observatories’ data. The authors suggest, from profiles of Ca II H and K lines, particularly the latter as being free from effects of Balmer ϵ , the presence of individual line-components corresponding to the presence of moving clouds; cf particularly the line-profiles reproduced by Wright (1970). Such profiles increase in width from

$< 1A$ at large distances from the limb, to about $3A$ at smaller distances, about 6 weeks and 2 weeks, respectively, from totality. “Satellite” lines of Ca II K have been observed at some 2 diameters from the limb for 31 and 32 Cyg as well as for ζ Aur.

The above data are visual, and well known for some 30 years. Recently, farUV data provide strong supplements; e.g., those by Chapman (1981) and Hack and Faraggiana (1980) for ζ Aur. They find lines of N V, C IV, Si IV, and Mg II, among others. The Mg II lines show marked P Cyg profiles (one can, in Wright’s diagram for Ca II cited above, find weak P Cyg profiles, at some phases); but they do not show the strong variation in equivalent widths across the eclipse noted for Ca II. They do, however, show variable components. The C IV profiles show strong changes, and displacements of the point of maximum absorption; but velocities associated with such show $\Delta V \lesssim 100$ km/s. In a preliminary way, Chapman interprets the presence, and behavior, of the superionized lines as coming from their formation in a shock produced on the other side (from the K star) of the Be star, by the wind from the K star moving around the B star, which produces a wake in it. This wind material is then supposed to accrete onto the B star, after being slowed by this wake-shock configuration. He estimates an accretion rate of $4 \times 10^{-10} M_{\odot}/y$. Hack and Faraggiana suggest that these superionized lines originate in a K-star corona, possibly formed in the discrete clouds pictured by Wilson and Abt, but hot rather than cold.

Comment on these anomalies and their interpretations:

First, if one compares the analysis of the *visual* eclipse data with that summarized earlier for the solar case, and particularly if one goes back and reads in detail the discussion of both continuous, hydrogen-Balmer, and metallic solar eclipse data (Thomas and Athay, chaps. 6 and 9; Zirker, 1956, 1958), it is clear that both data and its analysis for these ζ Aur stars have been extremely rudimentary. Discussions of variation in excitation-temperature; differential β_e for different elements, and degrees of ionization; inhomogeneous vs. homogeneous atmospheres; “turbulence;”—all these “effects,” found in the early solar-eclipse data, and its interpretation, have been greatly systematized, and contradictions/anomalies removed, by the modern solar-eclipse treatments summarized. The essential aspect in the solar diagnosis of eclipse data was to determine T_e , n_e , n (hydrogen) as a function of height *empirically*, under an unrestricted nonLTE approach. Concepts of excitation-temperature, and such things as the Stromgren modification of the Saha equation, *were not imposed*: they were decided by the data, plus admitting whatever atomic interactions were compatible with T_e , densities, and imposed photospheric radiation fields. Any radiation fields to which the atmosphere was opaque, were computed from nonLTE transfer methods. Under such approach, the excitation/ionization anomalies, and problems associated with differential β_e , were mainly resolved, in terms of a mechanically-heated outer atmosphere. One would guess that modern data and diagnostics, without imposing preconceptions, would have the same result for the ζ Aur stars.

Second, we saw that the problems remaining, for the Sun, after the above-type analysis, are precisely: (α) Where do wind effects take over from nonRE heating effects, in fixing radial density distribution? and (β) Where do any nonradial inhomogeneities significantly perturb the “mean” radial density distribution?

α . We see that thermal vs. nonthermal effects on density distributions *can* differ significantly between solar and ζ Aur cases. *If* Chapman’s estimate of $10^{-9} - 10^{-10} M_{\odot}/y$ is anywhere near correct, then we have at most a factor 10 increase in n_q —the location of the thermal point—*but*, for this sg K star, the photospheric density is a factor 10^3 smaller than for the Sun. So, the thermal point lies about a factor $10^3 - 10^4$ closer to the photosphere, in *relative* density value. The “extended-atmosphere” for this K-sg begins, relatively, closer to the photosphere than it does for the MS Sun. *But*, it begins at almost the same *absolute* density, only about a factor of 10 larger. We will see that this illustrates an important point: the beginning of an extended-atmosphere effect, *for the same size mass-flux*, at a greater *absolute* density for a MS than for a sg star. This will be important in understanding why the *extent* of the extended atmosphere, in terms of H α emission, is greater for a Be MS, than for a Be sg, star.

We should take cautiously Chapman’s attribution of the C IV and N V to the “accretion” region. We know that such ions are seen in normal B stars; and that mass-fluxes for such stars (e.g., τ Sco) can easily be the same size as that for the K star, in Chapman’s model. Further, many single, cool and cold, stars show, themselves, such superionization. This, plus their observation that late-B MS stars do not often show C IV, is undoubtedly the basis for

Hack and Faraggiana's attribution of the superionized lines to the K-star corona; although we must note that Chapman's C IV profiles are absorption, thus, more nearly resembling those from B MS than the P Cyg type in sg, hot and cold. We have already remarked on this, in the symbiotic star section.

Finally, we should note the farUV observations, and modeling, of 32 Cyg by Stencel et al. (1979). The interesting thing is that while they do not observe either N V or C IV, only Si IV and that weakly; they deduce from their data a mass-flux of $4 \times 10^{-7} M_{\odot} / y$. They cite Saito's derivation of $\sim 10^{-8} - 6 \times 10^{-7}$ for ζ Aur to show similarity between the two stars. And, they conclude that the B star actually moves within the upper-chromosphere, lower circumstellar envelope, of the K star. They also measure differential gas motions up to 400 km/s. It is difficult to reconcile all aspects of this picture; one would think that such a "dynamical" model, and such velocities, would produce ionization larger than the highest they measure, Si IV; via shock-waves, even if any chromospheric, transition-region, or coronal temperatures are not sufficiently high.

β . The uncertainty re nonradial inhomogeneities is clearly strong. From diagnostics of both visual and farUV data, we see that various authors argue for moving "clumps" of gas. Stencel et al., made the same cautions as I have, above, re the reliability of such inferences from LTE, curve-of-growth diagnostics. Saito (1970) suggests that the combined effects of mass-loss, nonsteady chromospheric velocities, and chromospheric-produced radiation would introduce shocks and asymmetries, without requiring multiple condensations. Clearly, not much *really* reliable can be said. The existence of separate, displaced, components of various lines certainly requires velocity gradients; whether these also require discrete elements, remains to be seen.

In short, while the diagnostics and data of the visual spectrum are crude, one has the same feeling re the completeness of the farUV data. We will return to "individuality" of mass-flux, and superionization, later; it is an outstanding question. Here, we emphasize only that whatever else one can say, these ζ Aur-type stars certainly have extended atmospheres, at least *some* nontrivial nonradiative-heating effects, and certainly very-significant mass-fluxes. But, the modeling, even empirical, quite apart from any theory, remains completely open.

E-F. SUPERIONIZATION AND SUPERTHERMIC VELOCITY: PECULIARITY AND ANOMALY

I have stressed the WR phenomenon as the prototype of hot-star stellar atmospheric peculiarity, even when observed in the visual spectrum under low resolution; and the Sun as the prototype of a cool normal star, which is also peculiar and anomalous when observed under high spectral and spatial resolution, especially in the farUV and X-ray spectral regions. The WR spectra, in the visual and farUV, show superionization in permitted lines up through O VI; one observes thermal X-rays in the 0.2–3.5 keV range. The Sun shows such superionization in the visual spectrum, at eclipse and with a coronagraph, up to [Fe XIV], [Ca XIV]; in the farUV, superionized permitted lines up to O VI; in the EUV, up to Mg X, Fe XVI; in the XUV, up to Fe XVIII; in the X-ray spectrum, a wide range corresponding to $T_e \sim 10^6 - 10^7$ K. The solar farUV spectrum resembles a WC6 spectrum, in its symbiotic variety. In the visual spectrum of classical WR stars, and some central stars of PN showing a WR spectrum even under low resolution, one observes velocities, from P Cyg absorption component shifts, and infers velocities, from line widths, up to 2–3000 km/s. In the visual spectrum, over limited areas of the solar surface, one observes velocities up to ~ 50 km/s; at the solar limb, one observes shell-ejections of $\sim (100-1000)$ km/s; in the radio spectrum, one infers ejected material moving at $\sim (10^3)$ km/s; collectors near the Earth measure solar-wind velocities in the 300–800 km/s range.

In the preceding sections on stellar peculiarity, we found superionization and superthermic-velocities in some atmospheric regions of each star in each category of peculiar stars. We found their presence, and specific characteristics, strongly linked to the sequential structure of exophotospheric, sometimes even photospheric, atmospheric regions; and to the sometimes production of local stellar environments by that mass-flux from the star associated with some superthermic velocity fields.

In the following Sections E and F, we survey these two phenomena across the HR diagram. We find that each of them is observed to be present in some atmospheric regions, of at least some stars of each spectral and luminosity class, normal or peculiar, independently of how the class is defined, all across the HR diagram. Statistically, across all

classes, most stars have been observed to show these phenomena. So, by our earlier definitions, *all* such stars are peculiar and anomalous, relative to standard thermal models. The presence of these two phenomena in an atmosphere destroys the fundamental basis for any thermal modeling. Superionization invalidates radiative equilibrium; superthermic-velocities invalidate hydrostatic equilibrium, in at least some atmospheric regions. But the standard thermal atmosphere has only one region, the photosphere; the several opacity subregions all retain the thermal character of the photosphere. So in any event, the presence of any atmospheric regions showing superionization and/or superthermic-velocities invalidates the standard model as a description of the atmosphere of that star, of which examples exist in all spectral classes.

We have seen that these two phenomena occur in peculiar stars in a wide range of degree, and are there associated with other peculiarities/anomalies, which occur with varying amplitudes among similar stars and can be variable in time. Since these two phenomena are observed in most normal stars, of all classes, we ask the significance of their lack of detection in some stars: too feeble amplitude, or actual absence? And are the stars in which they are not yet detected a random sample, or do they share some common characteristics? We try to put such nondetection into perspective, noting the increasing numbers of stars showing some characteristics of peculiarity, as observational refinement increases.

We have already conjectured that peculiar stars are simply normal stars with large-amplitude nonthermal properties of various kinds. We have also noted, in surveying these peculiar stars, the interrelation between different aspects of peculiarity. For example, superthermic velocities transporting a mass-flux provide a nonthermal extended atmosphere; variability in such velocities can cause an apparent local environment to begin in the atmosphere, very close to the star. We can use these relations exhibited by the peculiar stars as indirect indicators of superionization and superthermic-velocity. Finally—and it is the reason we continually stress the Sun and WR as a joint exhibit—we note that such large ($\sim 10^3$ km/s) surface-averaged superthermic velocities would not be directly detected in the Sun, spectroscopically; and their variability between 800 km/s and 300 km/s extremes would not be suspected, were the Earth not so close to the Sun that particle collectors could be utilized. How many stars share this solar characteristic?

A major interest in surveying these two phenomena lies in asking what relation, if any, observations show to exist between them. Are they independent, or does the existence of one imply the existence of the other, and which one is primary? In Vol. 2, we discuss the laboratory evidence and matching theory which shows that a gas flow accelerating from the small subthermic values of the photosphere, to the strong superthermic values of the outer atmosphere, generally dissipates mechanical energy; certainly it does, when decelerated from $o(10^3$ km/s) to $o(10^2$ km/s), as in some stars. The exception is the so-called perfect expansion, perfect wind-tunnel flow, etc., where a smooth transition from subthermic to superthermic velocity can occur at the equivalent of a “nozzle-throat” without an energy dissipation such as by shock-waves. In Part III, we discuss the evidence—accumulated in this Chapter 3—that shows the flow velocity to reach thermal velocity, in most stars, much below this equivalent nozzle-throat, which is where flow velocity equals escape-velocity. So, we expect the existence of such superthermic velocities to generally imply a nonradiative heating, hence, a superionization. But, on the contrary, from laboratory evidence and matching theory, we can have a nonradiative transport, and dissipation of energy, without the presence of a superthermic velocity field. For example, there can be wave-motions. In short, we have no problem finding a real-world situation where we can have a nonradiative energy-flux without a mass-flux; the question is whether this situation can exist in a stellar atmosphere. In this survey of observational material, we keep these laboratory constraints in focus, and ask how stellar atmospheres behave. Do some stars have nonradiative energy-fluxes without mass-fluxes? Do others have mass-fluxes without nonradiative heating?

At this point, we should put into sharp focus the popularly accepted difference between hot-stars and cold-stars in this aspect of interrelation between superionization and superthermic-velocities. For the Sun, and cool stars like it, most astronomers consider the production of a chromosphere-corona—the home of the superionized lines—by a nonradiative energy-flux to be the primary phenomenon. A superthermic mass-flux is then produced by thermal expansion of the hot corona (Parker, 1958, 1981). The compensating mass-flow from subcoronal regions is “pulled-out” by the coronal mass-loss. According to the associated speculative-theory, one needs specify only the radiative

and nonradiative energy-fluxes; the transfer and dissipation of these specify density and temperature structure of chromosphere-corona; in turn, these characterize the mass-flow by giving its size and velocity distribution. By contrast, in the hot stars, the mass-flow has historically been considered to be primary. Either a strong radiation field drives it (Gerasamovic, 1934), or it results, somehow, from a subatmospheric instability, e.g., rotational (Struve, 1930; Limber, 1964). In recent years, the radiative origin has been reactivated: initially by Lucy and Solomon (1970); expanded, by Castor, Abbott, and Kline (1975); and elaborated by Abbott (1980, 1982). But in any event, it is the mass-flow which is primary. Any nonradiative dissipation is neglected; no terms are admitted which could provide it, in the equations describing the flow. However, the existence of such dissipation is *implicitly* admitted, because the high-velocity characteristics of the mass-flow are mainly diagnosed from such lines as O VI, N V, C IV, Si IV. Nevertheless *the effect of its existence is imposed to be negligible, on the characteristics of the velocity field.* So neither of the two currently fashionable alternatives for the superthermic velocities—hot-corona and radiative-acceleration—take as primary a mass-flux imposed by the structure of star. The primary character of the star as an open thermodynamic system is considered to be a derived one, not characteristic of a nonthermal structure of the star, or of some subatmospheric region. The hot-coronal theory is content with radiative and nonradiative energy-fluxes, and gravity, to be specified by the subatmosphere. The radiative-acceleration theories are content with only radiative flux, and gravity, being specified; but in their present forms, these theories do not predict the existence of chromospheres-coronae. A discussion of the thermodynamic inadequacies of these two kinds of theories is deferred to Part III. Here, we only put into focus what their speculative-theoretical basis requires. So, if our data summary concludes that, indeed, the superthermic-velocity, and mass-flux, aspects are independent fundamental parameters, not derivable from energy-fluxes, these two theories can be discarded along with the standard model. This does not mean that *parts* of them are not useful. There is undoubtedly a radiative acceleration, *once a flow has been initiated.* There are some photospheres that the standard-model RE and HE can represent. But there are other factors, and terms in the descriptive equations, which these speculatively-limited approximations ignore. It is in the observations, and their thermodynamic implications, that we find these omitted terms—and atmospheric regions. The examples of the peculiar stars guide the way. The reader may wish to refer to Chapter 4, from time to time, where the results from this Chapter 3 are translated into the variety of atmospheric regions they demand.

We proceed to summarize the breadth of occurrence of these two phenomena, separately, but seeking all examples of their interrelations. We simply do not impose, a priori, that total nonradiative energy-flux and mass-flux cannot be specified independently. On the contrary, we consider that stars have observationally shown they are open systems, for which, generally, energy and mass-fluxes must be independent in size and origin, although they can interact, to produce common phenomena.

E. SUPERIONIZATION PECULIARITY AND ANOMALY

1. Perspective

Throughout this chapter, and on the basis of what ionization level an RE photosphere under the observed T_{eff} and g can produce, we have taken an observed superionization as diagnostically equivalent to the presence of a non-radiative heating which, somewhere in the exophotosphere, raises T_e significantly above T_{eff} . We have also seen, from some peculiar stars, that such rise need not occur in all exophotospheric regions. But any other evidence of the existence of atmospheric regions where $T_e > T_{\text{eff}}$ is equivalent to the presence of superionization, in this survey of the kind of thermodynamic inadequacies of the standard RE and HE thermal atmosphere. We ask how large is $T_e - T_{\text{eff}}$; where; and why. Then here we come to an ambiguity, in interpreting the significance of an observed superionization in any particular atmospheric region. As we have already stressed, and as the observations of the peculiar stars have demonstrated, the existence of an exophotosphere implies that the atmospheric radiation field departs from what would be predicted if only a photosphere were present. Thus, while an observed ionization that is “super” relative to that produced by the photospheric T_{eff} implies nonradiative heating somewhere, such heating need not be in the region observed in that superionization. If not, the superionization is controlled by the local radiation field

shortward of the ionization wavelength. Generally, the radiation field at such λ is unobservable, with present instruments. So as in the historical planetary-nebular modeling, one depends on conjectures as to the spatial location, and the emissive character of those regions which are heated; and one obtains as wide a range of radiative-ionization as one is willing to speculatively-admit for spatial distribution and emissivity. For the PN, the spatial location is unambiguous: the geometrical center. But the spatial distribution is a major problem: for an inferred total luminosity, $T_{\text{eff}} \sim (\text{assumed radius})^{-1/2}$, giving T_e a range $3 \times 10^4 - 2 \times 10^5$ K. The range in quality of ionizing radiation is thus enormous. A more correct emissivity requires not only nonLTE models, but asks the perturbation of both a low-lying stellar chromosphere-corona, and a T_e -rise in the outer regions associated with decelerating the mass flow. We also saw the problem in the eclipsing systems like 31 Cyg. The classical radiative excitation of the K-star envelope by a standard B-star is too low; one needs to give the K star a chromosphere, to reproduce the observed ionization state and excitation temperatures. But then one encountered the problem of the wind, and asked what produces C IV, and where.

The Sun is a simpler illustration. One identified the corona as superionized, historically first, before the chromosphere, by its *very* high superionization: [Fe X], [Fe XIV], [Ca XIV]. The first models (Wooley and Allen, 1950) had a cool, photospheric- T_0 atmosphere out to some 4000 km, then an abrupt rise, in $\sim 10^2$ km, to a 10^6 K corona. Any heating in that first 4000 km, e.g., to produce He I, was radiative back-heating from the corona. The chromosphere was cold; its anomalously-low density gradient, known since the 1860's, continued to be represented by McCrea's 1929 model of a "supersonic turbulence," Mach number about 2.5. All gas-dynamics laboratory experience demands that such motion dissipate energy. But most astronomers postulated an entirely new kind of phenomenon, *astrophysical-turbulence*: which is speculatively-prohibited to dissipate energy even though it is super-thermic, contrary to laboratory experience. Then the atmosphere satisfies RE. We have already summarized the resolution of the problem, into a totally different model. Nonradiative heating in the actual low chromosphere raises T_e to 6000 K at some 500 km height, and to 10,000 K at some 1500 km, height. HE, under these empirical T_e , gives a density distribution self-consistent with the observations. The 10^6 K coronal T_e is reached already at some 2000 km; and persists for some 3–5 radii. We have already discussed its departure from HE, at about 2–3 radii. Today, no one questions that a nonradiative energy dissipation heats the low chromosphere, and produces its excitation and ionization, with the possible exception of He I excitation. One also requires a nonradiative heating of the corona; the precise mechanism is disputed (cf the discussion in Jordan, 1981). One also debates whether the abrupt rise in T_e , from some 10^4 K to 10^6 K—in the so-called *chromosphere-corona transition region*—is accompanied by local nonradiative heating of this transition-zone, or by a thermal conduction downward from the corona induced by the steep T_e -gradient. In discussing the T Tauri stars, and their inferred nonradiative heating at lower atmospheric depths than in the Sun, we have already noted the conclusion by Cram et al. (1979) that this transition-zone is, for such stars, heated by local nonradiative energy dissipation, not thermal conduction downward.

So it results that a discussion of the variety of superionization phenomena, and of their several diagnostic equivalents, begins with an immediate focus on that need for a variety of exophotospheric regions, and that need for understanding any coupling between superionization and superthermic velocities, which became paramount in surveying peculiar stars. The first aspect of the need is to distinguish between exophotospheric regions whose T_e is locally-dissipatively-controlled, and those whose T_e is externally-radiatively-controlled. The second aspect of the need is to be self-consistent between those T_e interpreted as kinetic-temperatures, the local nonthermal velocity fields in the regions and their local energy dissipation, and the dependence of density distributions within these regions upon these two kinds of velocity fields. But in this process of self-consistent distinction between atmospheric regions re size, location, and cause of $T_e - T_{\text{eff}} > 0$, we cannot forget the priority: first, what is the evidence that there is a greater T_e -rise than that coming from nonLTE; second, what is the size of $T_e - T_{\text{eff}}$, in what general parts of the atmosphere; third, how does the size relate to density and velocity values; and only last do we ask how, then why. That was our emphasis in surveying peculiar stars; it must be the same here. Only then can we try to combine these facts with other information, in Part III, to specify the thermodynamic properties of distinctive atmospheric regions, their sequential occurrence, and their algorithmic modeling. During, and after, the algorithmic modeling we ask what physics imposes its pattern. There, we emphasize physical consistency: internal, and with laboratory experience. We do not begin with an assumed atmospheric configuration, then impose it on the diagnostics.

So our survey of superionization differs from those usual in the literature, which survey superionization in terms of its possible origin under the physical conditions presumed to exist in speculatively-defined atmospheric regions. For example, Cassinelli and MacGregor survey "Stellar Chromospheres, Coronae, and Winds" (1983). But only for cool stars are all three categories of phenomena admitted; hot stars are restricted, a priori, to possessing only coronae and winds. They then attribute the observed C IV, N V, O VI superionization to coronal X-rays. This hot-star speculative-restriction of lower-atmospheric structure to an abrupt photosphere-corona transition, omitting a chromosphere, is precisely the equally-speculative Woolley-Allen (1950) solar model. This last was proposed without making an empirical-theoretical study of the photosphere-chromosphere-corona density distribution, to relate it to kinetic-temperature and mass-flow. It was discredited by the 1952 eclipse data + analysis. In the same way, for the hot stars, Cassinelli and MacGregor forgo a two-aspect study of chromospheric structure, as abstracted above, replacing it with the one-aspect focus on ionization. Ionization state, density distribution, and mass-flow are, by their a priori assumption, decoupled. One has not much confidence in such a survey, as other than speculation. This impression is reinforced by their carelessly-wrong abstracts of some aspects, and of empirical-diagnostics of observations. For example, they assert that: (i) solar mass-flow velocities are 1/5–1/10 the 2000 km/s of OB stars. (ii) Mass-flow in Be stars is barely discernable. (iii) O VI superionization is restricted to stars hotter than B 0.5, and N V and C IV, to stars hotter than B 2.5 and B 6; and T_e (postcorona) $\sim 0.8 T_{\text{eff}}$. (iv) The first conclusive evidence of hot star mass-loss came in 1967 (thus ignoring the significance of WR, P Cyg, novae etc. in mass-flux modeling). (v) The hydrogen Balmer lines are efficient radiative coolants, and their ground state is collisionally populated. (vi) Ca II H and K are absent in stars of spectral type earlier than F0. *ALL* these assertions are wrong, as we see from the preceding material in this chapter, and from the discussion of nonLTE radiation fields in Chapter 2.

Other surveys of superionization, and its implied nonradiative heating, via a priori definitions of atmospheric regions, lead to the same confusion on hot-star chromospheres, the atmospheric-location of the superionized C IV, N V, O VI sequence of ions, and the details of the density gradient in the precorona—even in the corona and postcorona. Linsky (1977, 1980, 1981a) defines chromosphere, transition-region, and corona to match his interpretation of the solar situation; wholly in terms of the energy balance; not involving momentum balance and density distributions; incapable of being extended to meet the preoccupation of Cassinelli and MacGregor with RE regions in hot stars. For Linsky, the basic character of all three regions of the solar exophotosphere is their domination by non-radiative heating; T_e -gradients are small in chromosphere and corona, but large in transition-region, relative to the pressure scale-height. The corona is defined to distinguish itself from the chromosphere by its nonradiative heating being largely magnetic, and this being balanced by a combination of X-ray and EUV radiative cooling, and thermally-driven wind energy-loss. Like Cassinelli and MacGregor, he then finds that his definition leaves him with little hard evidence for chromospheres among stars hotter than type F0. Unfortunately, again like them, he falls into the same trap of misleadingly-inadequate summary of crucial observational facts, in asserting the lack of observed Ca II emission earlier than F0, main-sequence and giants; and only otherwise-unconfirmed Mg II observations in O8, B1, and B7 stars by Kondo et al. (1976, 1977) from Copernicus. Our Fig. 3-14 shows Ca II emission to have been observed by Beals since 1951 in P Cyg; Mg II is often observed in Be Stars (Doazan, 1982); Blanco et al. (1980, 1981, 1982) report Mg II emission, and the presence of C IV in stars as early as A5. Our own observations show C IV out to B8 stars; and in Herbig Ae stars, as find Djie and The (1982). Again following Cassinelli and MacGregor, Linsky suggests that the C IV–O VI observed in hot stars does not establish the existence of subcoronal, exophotospheric regions, but rather, reflects coronal X-ray ionization in a cool postcorona, so differing from cool stars. These concepts persist, noting the Böhm-Vitense and Dettman (1980) suggestion that chromospheres exist only on the red side of the Cepheid instability strip, whose cause they find in the lack of theoretical expectation of convection in such hot stars. But now we reach that fundamental point disputed at the 1972 Goddard colloquium on stellar chromospheres, which touches the physics of nonradiative heating, not the semantics of terminology. Böhm-Vitense and Dettman assert that there is no nonradiative heating earlier than their dividing line—at least none by convection—and they offer no alternative. However, the observed superionization in hot stars, whether coronal X-ray-produced or by local nonradiative heating, contradicts the assertion. We return to the question below. It is simply a matter of where, not whether, such heating occurs, in the exophotosphere. It is a question to be resolved, whether

such superionization as C IV–N V occurs on both sides of a coronal maximum T_e —sub- and post-corona, for a 10^6 – 10^7 K corona. It is also a question to be resolved, whether there are indeed some stars, for which nowhere in the atmosphere does it become hot enough to produce C IV–O VI locally by collisions, or distantly by locally-produced X-rays. But it is, especially at our epoch, not useful to focus on nomenclature, ignore observations and issue categorical dogma that, e.g., can confuse an otherwise excellent and informative paper like that by Eichendorf et al. (1982) into echoing the statement, quoting the Linsky, Böhm-Vitense, etc. work: “giants and supergiants later than G5–K0 do not have transition regions, and supergiants earlier than F5–F8 do not have chromospheres.” The above-cited observations show the presence of Ca II and Mg II in supergiants earlier than F5; a number of so-called “hybrid” giants and supergiants, spectral type cooler than K0, show at least C IV (e.g., Reimers, 1980; Hartmann et al. 1981). We return below to this question of the existence of a dividing line, which excludes a group of cool giants and supergiants from showing any phenomena hotter than 10^4 K envelopes, and which is linked to their producing larger mass-losses than stars showing hotter exospheres. We note that the basic question is: Do there *exist* independent fluxes of nonradiative energy and mass, of *some* size, in all stars across the HR diagram? The question is not whether their size, origin, and specific consequences are the same. Refer to the discussion in Chapter 4.

2. Character and Locale of Superionization

From our summary of the variety of nonthermal phenomena observed in a variety of peculiar stars, including superionization, we have a good idea of the variety of this last, and of the superionization-equivalent phenomena. Also, we have a good idea of the characteristics of the conditions which produce these phenomena. Roughly, such conditions are associated with: T_e -rises in the immediate postphotosphere, resulting from dissipation of nonradiative energy-fluxes of one kind or another; T_e -rises associated with some variety of accelerated flow which is not “perfect” expansion; T_e -rises associated with some deceleration of the flow; and nonphotospheric radiative-fluxes, produced in one or more of these regions, which are superenergetic relative to T_{eff} . Also, we have an enormous range of density in the observed locales; so we can have density-dependent ionization as well as temperature-dependent, if conditions depart from simple collisional-ionization balancing recombination; i.e., things depend upon the particular nonLTE processes involved. So, these studies of peculiar stars give us a good reference basis. If our conjecture is correct, that peculiarity simply reflects greater amplitudes in some of the nonthermal fluxes, our survey can consist simply of examining those phenomena found for the peculiar stars, asking are they present generally. We need proper precaution to ensure that we don’t overlook something, because the conjecture may not be correct. We also note that we found a considerable variety of subionization phenomena. Because we associated this with significantly-large, and variable, mass-flux, we do not expect it to be as prevalent among normal, as among peculiar, stars. But, we must be careful that observation of *only* such subionization—from instrumental limitation such as seeing only H α and Fe II in Be stars when only the visual spectrum was available—is not taken as a general character of some star or class of stars, prior to observing them more broadly. So, we proceed according to this scheme: asking general prevalence, across the HR diagram, of those superionization, and superionization-related, phenomena found earlier, and for any exceptions not earlier encountered.

Then we note three varieties of superionization-equivalent phenomena, in order of associated nonradiative energy supply: superexcitation of quasi-normal photospheric-level ions; superionization itself; X-ray emission. We note that all three of UV, farIR, and radio continua excesses can be considered superionization-equivalent under the proper circumstances. We have already commented on the strikingly-obvious nature of these in such things as BaC in emission (largely from the Chalonge group studies); the solar LyC observations; and various farIR and radio excesses. But here, we concentrate on the first three items as those most generally considered.

Then I would first put into primary focus just one, categorical, observational, conclusion: *there appears to be some variety, to some degree, of nonradiative energy dissipation, resulting in a $T_e > T_{\text{eff}}$ somewhere in the exosphere, in every star in the HR plane*, which has been studied with sufficient spectral resolution. One can be even stronger, admitting that the statistics are not as complete: *it appears that every star has a T_e , somewhere in the exosphere, which is at least a factor 2 larger than T_{eff}* . Often the factor becomes as large as 100–1000. I stress

this point, attaching no significance to the particular factor 2 as a lower-limit other than it is very much larger than any uncertainty—physical or mathematical—which arises in modeling the standard thermal, RE and HE, atmosphere, just as we have emphasized in Chapter 2. A second reason for stressing the result is to show just how necessary it is to regard the star as a nonlinearly nonEquilibrium thermodynamic system. For, one often hears quoted the characteristic of such a linearly-nonEquilibrium, where entropy can be defined, system, which results from applying the Second Law of Equilibrium Thermodynamics: A system cannot, by itself, transport energy from a colder to a hotter region. And here, we see that *all* stars violate this principle in their exophotosphere—i.e., they would if they were Equilibrium, or only linearly nonEquilibrium systems. They are not such systems; so they do not violate such Equilibrium principles/Laws; and it is meaningless to introduce any discussions in terms of entropy, which is undefined, in these circumstances. A third reason for stressing the result was the repeatedly mentioned general belief, up through the 1972 Goddard symposium on Stellar Chromospheres (Jordan and Avrett, 1973), persisting among most astronomers until the Lamers-Rogerson observations of O VI in τ Sco (1975), persisting among some modelers even today (Abbott, 1980), that there is a dividing line, at about spectral class F2–F4, for the existence of nonradiatively heated regions. Earlier-hotter stars live under RE; later-cooler, solar-like, stars have hot chromospheres-coronae, etc. We have seen that peculiar stars have disputed this belief for a half-century: observationally, once O VI was identified in WR stars, PN, etc.; thermodynamically, once superthermic velocities were discovered (Section F). The conceptual problem has been to establish that peculiar stars were peculiar only in possessing large amplitudes in those fluxes which produce observable nonradiative heating effects only in the farUV, under low-resolution spectra and diagnostics, for many stars.

In proceeding to the details underlying the preceding generalization, we note that the existence of such non-radiatively heated regions is generally discussed in terms of “spectral indicators.” We began these Sections E + F by listing these for the WR stars and the Sun. Too often, the solar ones are simply adopted, to define the various atmospheric regions, as above. One forgets that there had to be an initial calibration to establish that such “indicators” do indeed have anything to do with nonradiative heating and $T_e > T_{\text{eff}}$. Such forgetfulness often leads to dogma which loses the initial objective. We abstract these three varieties of superionization indicators, from this respect.

a. Superexcitation. The historically-oldest indicator, occurring widely across the HR plane, is the presence of He I $\lambda 10830$, whether in emission or absorption, in stars cooler than B-type where He I is normally and photospherically observed. I have already cited the summary article by Zirin (1976). Now, however, debating between collisional and radiative excitation/ionization generally, we note that Goldberg’s (1939) suggestion of photoionization of He I, at $\lambda \lesssim 500\text{\AA}$, by an EUV excess is the most generally accepted. This was proposed in the pre-Edlen period of accumulating evidence for hot exophotospheres. Goldberg demanded regions producing an EUV radiative excess. And still today, in geometrically-chromospheric regions, photoionization from the corona, for He I, rather than a 20 eV collisional excitation to the ground state, seems favored. Indeed, such radiative processes seem to govern the He I spectrum in the solar chromosphere (cf Athay’s summaries; 1961, 1976). But if we accept this interpretation, then the prevalence of $\lambda 10830$ measures the prevalence of coronae rather than of chromospheres—i.e., 10^5 – 10^7 K regions rather than 10^4 K regions. We note that it is not important, energetically, in this decision, whether $\lambda 10830$ is in emission or absorption. The suggestion is reinforced by Zirin’s finding little correlation between it and the Ca II K line, the latter being thought chromospheric collisionally-excited (cf below). Then Zirin’s statistics show 80 percent of all G and K stars, some F stars, a few M giants and at least one M2lab, an M3.5II, and an M IIIa showing $\lambda 10830$ in absorption. The essential thing, in such statistics, is that half the stars are estimated to show variability, although a major fraction were observed only once. Thus, that such a large fraction show $\lambda 10830$, and variable, suggests not only that all such stars *can* produce nonradiative heating, but that its size can vary. $\lambda 10830$ is found in emission, in about one-fourth of the stars, including some late M and S stars, where also hydrogen Paschen- γ is observed in emission. Again, re the P- γ emission, we face the problem of extended atmosphere vs. heating. There is evidence that H α emission in the above M2lab star, α Ori, is chromospheric rather than “postcoronal;” interferometric studies are in progress (Goldberg et al., 1982). So given this $\lambda 10830$ evidence, and given that these stars also show Ca II H and K

(cf below), one concludes that there is strong evidence for widespread coronal-level T_e as well as chromospheric: 10^5 – 10^7 K as well as 10^4 K; evidence for T_e/T_{eff} in the 10^3 range as well as 2. So the results are impressive on the prevalence of a nonradiative heating, to “coronal” levels. Because it is variable, and in analogy to the Sun, Zirin attributes such heating to magnetic effects. Here, we should only emphasize again, that the solar coronal holes (thought magnetically-unconfined) and nonholes (thought magnetically-confined) do not differ much in T_e , some 10 percent; both show $T_e \sim 1$ – 2×10^6 K, in the corona. Only at $r/R \sim 200$, do the solar wind T_e drop to some 10^5 K. $\lambda 10830$ is also observed in emission in WR and P Cyg stars; but this hardly requires coronal radiative ionization/excitation in such stars. So, it cannot be taken as evidence of nonradiative heating; rather, of atmospheric extent. But normally-present He I is hardly a good “chromospheric indicator” for hot stars.

The most popularly used “chromospheric”—i.e., $T_{\text{eff}} \lesssim T_e \lesssim 3 \times 10^4$ K—indicators, for cool stars are the emission cores of Ca II, H and K, lines at $\lambda 3900$ and Mg II, h and k, lines at $\lambda 2800$. Let us put them carefully in perspective, for use here and in Section b, because their significance is too often used carelessly. In Ca II H and K, these self-reversed emission cores, cf Fig. 3-13, are observationally long-known, in the Sun and in other cool stars. *But the primary focus on them concerned only the widths of these cores* (Wilson and Bappu, 1957; Wilson, 1957; Goldberg, 1957; Hoyle and Wilson, 1958; de Jager, 1958; Kraft, 1958). Attention to the self-reversed feature was variously discussed in LTE-terms of cold clouds overlying regions of a few hundred degree-rise above the photospheric boundary T_e (McMath et al., 1956); or in nonLTE terms of noncoherent scattering in the core vs. coherent scattering in the wings (Miyamoto, 1947–1958), with the amplitude of the K2 emission peak fixed by T_e at the photosphere-chromosphere boundary. Jefferies and Thomas (1958) called attention to the importance of nonLTE diffusion effects, or thermalization effects for these collision-dominated lines, in a static, thermal atmosphere which is both optically-thick and has a strong outward increase in T_e . In such an atmosphere, the source-function in the core of the line—and particularly at the K2 peak—will be $\ll B_\nu(T_e)$. The observed self-reversed center of the observed emission core of the absorption line corresponds to the diffusion-decrease of S_ν to the limb. That such a region exists in the solar atmosphere—high Ca II opacity in a region of rapidly-rising T_e —was shown (calibrated) by our 1952 eclipse observations and diagnostics. We calculated (Jefferies and Thomas, 1959) the first Ca II line-profiles showing precisely the mixture of those effects abstracted in Chapter 2, cf Fig. 3-27. There are the two competing effects which should be kept well in focus.

(1) Moving inward from the boundary, J_ν always tries, but fails, to reach LOS at the local $B_\nu(T_e)$ —this is the self-reversed central core. In an *isothermal* upper photosphere, as remarked in Chapter 2, at the core-center, $\tau = 0$, $S_\nu(0) = \epsilon^{1/2} B_\nu(T_e)$; and when LOS is reached, $S_\nu(\text{K2-peak}) = B_\nu(T_e)$.

(2) But T_e falls steeply from chromosphere toward photosphere; so S_ν always lags below B_ν ; and the K2-peak $< B_\nu(\text{local-}T_e)$; so the observed small peak intensity *does not* imply small T_e -rise. The details depend on the n_e -gradient, to fix ϵ , and the T_e -gradient, to fix the source-term, $\epsilon B_\nu(T_e)$, distribution. Distributions are in line-opacity, not linear distance. Fig. 3-27 imposes a chromospheric $B_\nu(T_e)$ rising exponentially outward, and a constant n_e . We see that as the amplitude of the chromospheric rise decreases, so does the K2 peak. In principle, under our original treatment of a ν -independent line source-function, at the K1-minimum, the influence of the chromospheric rise in T_e has disappeared; the remainder of the profile reflects the inward rise of T_e in the photosphere. We have reached the saturated, LOS-LTE region, as abstracted for both line and continuum in Chapter 2. But in practice, the situation is confused by the degree of coherence in scattering; and a wide literature has developed on the Ca II problem after our initial treatment (cf Thomas, 1957, 1965; Jefferies, 1968; Avrett and Linsky, 1970; Cannon, 1983).

In addition to these two competing effects, there is the third one of what determines the ν -dependence of the absorption coefficient, which converts the τ -dependence of the source-function into ν -dependence of the line profile. All our original discussion was in terms of a thermal Doppler-broadening dominating the emission core; it gives too small a line-width. We return to the problem in Section F. Here, however, we are simply concerned with the diagnostic meaning, calibration, and use of this observed, central, self-reversed, with large range in amplitude, emission core of these Ca II and Mg II lines; whose source-function is nonLTE and collision-dominated, so reflects the T_e -rise outward. Its calibration in the Sun has been taken to apply to all other stars showing the phenomenon.

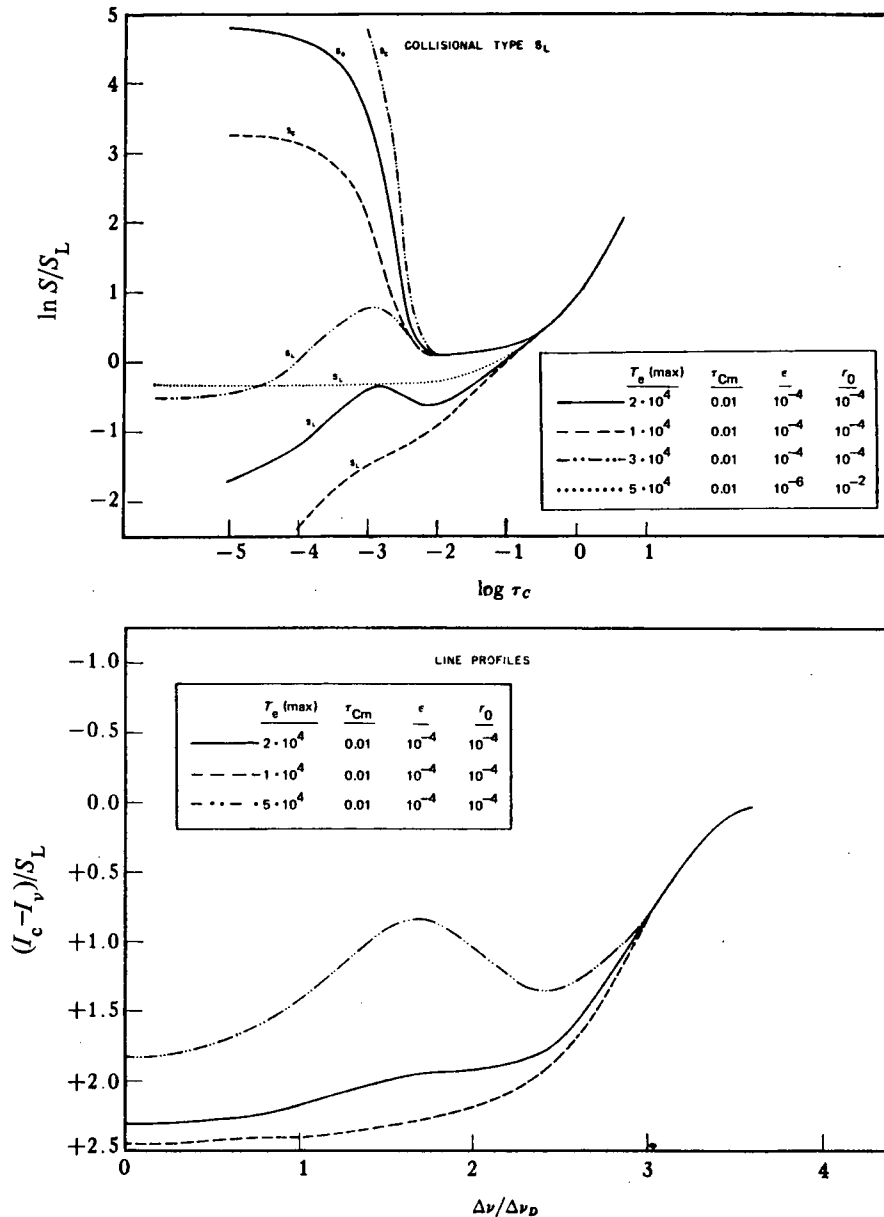


Fig. 3-27. At the top, $S_L(\tau_c)$ relative to $S_c(\tau_c)$ for a collisional-type source-function. At the bottom, line profiles corresponding to $S_L(\tau_c)$.

Then the significance of such calibrated results, for atmospheric diagnostics, lies in the following chain of thermodynamics applied to upper-, and exo-, photospheric conditions: (1) This environment requires that the line source-function be nonLTE, dominated by the scattering-term, so that S_v only approaches its atmospheric-coupling value, the source-term/sink-term, at large optical depth, which means in the line-wings. These line-wings are not our primary diagnostic concern. (2) The atomic configuration of Ca II and Mg II requires that these lines be collision-dominated, with very small ϵ in this environment; so that S_v is coupled to the T_e -structure of that atmospheric region where the line arises by the source-term/sink-term $\rightarrow B_v(T_e)$ only asymptotically, in depth. For lesser τ , $S_v < B_v(T_e)$, by an amount depending on the radiative transfer under the particular atmospheric and line-broadening configuration. (3) The observed K3-K2-K1 contours are those produced in an atmosphere of significantly-varying T_e ,

whose size—given a computed ϵ and observed intensity—is significantly larger than T_{eff} . (4) The solar calibration, in an atmosphere of known $T_e(\tau)$ —which was determined independently of the Ca II, Mg II observations—shows a rapidly-increasing T_e at just those values where the ionization of Ca II and Mg II, hence, H and K line opacity, change rapidly. (5) Because of the similarity of ionization energies of Ca II (11.82 eV) and Mg II (14.96 eV) to hydrogen (13.54 eV), the behavior of these ions is similar to, and brackets, that of hydrogen, *once hydrogen leaves the region of optically-thick LyC, in which its ionization is photoionization-controlled by the BaC*. For the Sun, this passage from optically thick to thin in the LyC, the τ -interval where we need a transfer solution in the LyC for diagnostics, occurs just where T_e begins its rapid rise, 10^4 K to 10^6 K, with a brief pause at the Ly α plateau near $2-3 \times 10^4$ K. So we know that the Ca II and Mg II, H and K, lines are magnificent indicators of the existence of a T_e -behavior of the kind which we associate with the solar photosphere-chromosphere, and chromosphere-corona picture, because that is the detailed calibration which we have.

We can take this calibrated diagnostics over to any other star, which is solar-similar in the sense of this rapid rise in T_e , and the values from which it starts and where it ends, occurring just where these Ca II and Mg II line-centers are formed. We can add a theory of size and origin of nonradiative energy-fluxes as a function of spectral type to try to predict this $T_e(\tau)$, because we can't generally measure it. We can add thermodynamic attempts to predict atmospheric response to general nonradiative heating, such as the T_e -plateau (Athay and Thomas, 1956 et seq.), and argue that the solar T_e -structure is typical for a wide range of stars, independent of size and character of nonradiative fluxes. But we recognize that observationally—in various stars, and over the solar surface—the emission-core size and appearance changes. We also recognize, observationally, that the T Tauri, solar-similar, cool-type star where we know there is a very much larger— 10^3 —nonradiative energy input, shows a marked difference in Ca II line-widths (discussed in Section F), and that it has a very much larger mass-flux than the Sun. And, we recognize that it is the size of the mass-flux which fixes the density distribution, after reaching the thermal point (cf Part III). So, we should be cautious in following the usual, oversimplified dogma; no observed Ca II \rightarrow no chromosphere \rightarrow no nonradiative energy-flux. Note, in Fig. 3-27, the size K2 peaks for a $T_e(\text{max})$, *in the Ca II region*, of only some $2 \times T_{\text{eff}}$. Particularly, one should be cautious in echoing the too-often read conclusion: no Ca II is observed, but X-rays are; therefore there is only a corona, not a chromosphere. Such incorrect diagnostics rival the speculative concept of non-dissipative superthermic turbulence, in their thermodynamic novelty. But it is useful to comment on the extension of the Ca II “indicator” to stars colder and hotter than the Sun.

If we go to stars significantly cooler than the Sun, in the sense of most Ca being Ca I; but if we admit a non-radiative heating which carries T_e up to values capable of producing that quality radiation to back-ionize He I and produce $\lambda 10830$, then we first produce, then traverse, such a Ca II, Mg II region as for the Sun. And, because the energy balance finds the same kind of radiative loss as in the solar picture—somewhere on the upward rise of T_e —we expect to traverse a thermodynamic situation *roughly* like that above. So, again, Ca II and Mg II will be good “indicators” of this T_e -structured, heated, atmospheric region; which is *one* of the characteristics of a chromosphere for these kinds of stars (cf Chapter 4). It is just preceded by a more extensive cool region than for the Sun; so presumably requires more nonradiative heating than the Sun, to reach a given T_e . So a lesser $T_e(\text{max})$, for the same nonradiative energy, is not surprising.

But if we go to stars significantly-hotter than the Sun, where Ca II is less predominant, and especially where a nonradiative heating to raise T_e in the upper photosphere will destroy what small Ca II may exist in the photosphere, its use as an indicator fades. *Not because there is no chromosphere, not because there is no nonradiative heating to produce a chromosphere*—but because we fry the diagnostic chicken, so it produces no more modeling eggs. We note that the convective instability producing the original Biermann-Schwarzschild acoustic energy, and the κ -instability producing the cepheid pulsation, are all associated with being able to descend from the photosphere, increase T_e and reach stronger hydrogen ionization. So, in such stars, we can also ascend from the photosphere, nonradiatively raise T_e , and reach stronger hydrogen ionization. In a hotter star, we can neither descend, nor ascend to produce hydrogen ionization—it is already ionized. The same for the Ca II and Mg II, as above. If we want them for diagnostic purposes, we must do the reverse of the preceding; we have to subionize the atmosphere: produce a cool envelope; as for the Be, and similar, stars. In normal B stars, we find no Ca II emission or absorption; but in

some Be stars, we find absorption cores, *but emission wings*, in Ca II. At shell phases, in the visible spectrum, one observes not only Ca II and Mg II lines, and of course the narrow Fe II lines, but also, in some cases, Na I. Whereas Mg II λ 4481 disappears for luminosity class V B stars at spectral class 5; it persists to class 2 for class IV, and is even stronger in class III (Lesh, 1968). In the farUV, the Mg II h and k λ 2800 lines sometimes show emission wings, and absorption cores. Some show blue-shifted absorption components, variable, in the -50 to -200 km/s range. Very clearly, Ca II and Mg II in these hot B and Be stars arise in the cool envelope. Diagnostically, they indicate the presence of a cool postcorona. The emission wings indicate extended-atmospheric effects, not at all any T_e -rise in a chromosphere. One cannot do diagnostics of only one ion, or one type of line. We have already emphasized how the T Tauri stars have a cool spectrum produced in two regions: a low-lying chromosphere, a postcoronal envelope. In which of these, do we diagnose an observed Ca II, Mg II, H and K lines?

But we need go to neither Be stars, nor T Tauri stars, to find exophotospheric, exocoronal Mg II lines. Hartmann et al. (1981) note two displaced components in each of the Mg II h and k lines: at -13 km/s and at -84 km/s; for the "hybrid" K4 II star α Tra. Note both components are on the blue side of the emission peak, which is not resolved. This differs from the central K3 components discussed by Deutsch and Reimers (cf below) for Ca II. They interpret the -13 km/s component as referring to expansion in regions before the chromosphere-corona, transition-region, rise to $T \gtrsim 1 \times 10^4$ K. At large distances from the star (but smaller, in r/R , than the Sun-Earth distance), they consider that the gas has cooled sufficiently that Mg II is again the dominant ionization stage; and the -84 km/s velocity reflects the postcoronal asymptotic velocity, which they also find in a Ly α blue-shifted component. They observe Si IV, C IV and N V, but they find no measurable lineshifts, only estimated line-widths. From these, in C IV, they infer 150–200 km/s. Si III and C III give them < 100 km/s widths; Si II, S I, O I progressively less. They model the star with a 80,000 K corona, 95 km/s velocity reached at 2.5–3 radii. A 15,000 K region, with flow-velocity some 15 km/s, is reached at 1.2 radii. The maximum velocity is 105 km/s at 4–5 radii, below the observed 150–200 km/s attributed to C IV. Also, the T_e -values in their model are too low to produce the observed N V. All the model discrepancies simply reflect the present inadequacy of the Hartmann and MacGregor (1980) attempt to use Alven waves to produce both heating and drive the mass-loss. But these attempts do model the double origin of the observed Mg II resonance lines. Their greatest uncertainty lies in how hot is the intermediate region. Hartmann et al. (1981) find the same kind of Mg II, double-velocity component, behavior in α , β Aqr, two G Ib stars, also labeled hybrid, and offer the same interpretation. They call these stars hybrid because they show both the "chromospheric," low-excitation spectrum, and the "transition-region" farUV lines. By contrast, the last reference also exhibits λ Vel, K5Ib, which shows just the "chromospheric" type spectrum—no N V or Si IV; vanishingly-weak, if present, C IV. Mg II λ 2800 shows just one, lower-velocity, component. We return to "hybrid."

Our essential point here is wholly observational-diagnostic, complimentary to the preceding, on Ca II, Mg II "indicators." Not only does evidence of chromospheric, and coronal regions exist—but also postcoronal; and one can diagnose observations in terms of superexcitation before and after the corona, self-consistently with the velocity field. (We overlap with Section F, but a certain amount of such is necessary.) Ca II and Mg II are indeed good indicators of the heated regions with $T_e \lesssim 3 \times 10^4$ K. Their use becomes marginal in stars where major nonradiative heating is not required to raise the atmospheric T_e into regions where Ca II is inappreciable; and it becomes ambiguous when Ca I predominates in the photosphere (cf Section b). Note that the rapid upward rise in T_e for the solar chromosphere-corona transition begins at about 8500–9000 K; this is T_{eff} for a mid-A class star. We have already noted the persistence of Mg II emission cores up to some A5 stars, presumably associated with the precorona; and emission winds in Be stars, presumably associated with the postcorona.

As a final comment on the superexcitation aspects, we have already compared the changed character of T Tauri type stars, under a larger mass-flux than the Sun: an extended atmosphere, and strong Balmer emission, much larger than could be produced by chromospheric heating to give the observed BaC, and so the Balmer-line source-functions. But we have also noted the observational evidence for a lower height at which nonradiative heating begins in the T Tauri atmosphere. This configuration gives additional "indicators;" that is, some lines which are photospheric, and always in absorption, in the Sun, like the NaD lines, go into emission, with rapid variability, in T Tauri stars. We already quoted Cram's estimate of a factor 10^3 larger nonradiative energy dissipation in a typical T Tauri

star, to bring the ratio of nonradiative to radiative flux to some 10^{-1} , rather than the solar 10^{-4} . So when we survey the broad variety of stars, and ask: Must we include a variety, for given spectral class, of nonradiative flux, in modeling? The answer is yes—admit a large variety in size, and probably type, of this flux. Then before commenting on “hybrid” stars, mentioned above, we consider superionization which, with the above comment on multicomponent mass-flow line-displacements, and this one on variability and individuality, places the problem into better perspective.

b. Superionization Itself. We have so constantly exhibited the evidence for this, that discussion here is almost anticlimatic. Such lines as Si IV, C IV, N V, O VI (with Copernicus), are *almost* ubiquitously observed across the HR plane. But three points must be placed into perspective. First, the question of whether the T_e -regions these ions span, if collisionally-ionized— $3-4 \times 10^4$ to $2-3 \times 10^5$ —refers always to a postphotospheric, precoronal region, or also to a postcoronal. Second, there is the question of cool “hybrid” stars, those in whose spectra these ions are seen, also lines characteristic of $T_e \lesssim 2 \times 10^4$ K, and possibly X-rays—but which fall in regions of the HR plane where various astronomers suggest there should be only atmospheres with $T_e \lesssim 2 \times 10^4$ and heavy mass-loss, no regions of $T_e \sim 10^5-10^6$. These last form a transition to Section F. And third, there is the question of what means the “trend” of these, observed in absorption in normal hot main sequence stars, to gradually become weaker with decreasing T_{eff} , then to reappear in emission in cooler stars. And, on the contrary, among peculiar Be stars, one sometimes observes as strong C IV absorption in B8 stars as in B0 but the strength of the C IV line can also be highly variable, in B2e as in B6e-types (cf Fig. 3-28): 59 Cyg (B2e), and Θ Cor Bor (B6e), each at two differing phases. The literature on these superionized components is rich, and becomes richer daily. I cannot adequately summarize it, especially in its aspects of individuality and variability. For the hot stars, Doazan and Underhill (1982) give a superb synthesis of material, as of today; the same will come in future volumes for other spectral classes. Here, I can only try to highlight the essential thermodynamic points. In addition, we return to Ca II, Mg II, as superionization in late stars.

Then re the first point, drawing upon this extensive B-Be material for hot stars, one should note the same situation, re Si IV, C IV, N V as found above for the Mg II lines in cool stars; two components: one low-velocity, less than coronal thermal velocities; one high-velocity, exceeding escape velocities. The situation varies between stars. For example, at our epoch, the low-velocity component is the stronger, in γ Cas; and the behavior is common to all three ions. Intensities vary strongly in the high-velocity component; velocity change is minor. In 59 Cyg, until recently, the Si IV, essentially undisplaced component, was enormously the strongest; there were only slight traces of a high-velocity component. The strongest C IV, N V components were the high-velocity; and the velocities varied, randomly, by a factor of two, within weeks. The low-velocity component was faint, and essentially unchanging in location. Occasionally, several high-velocity components appeared. The shocking surprise (27/01/83) is the appearance of a *red-shifted* absorption component in Si IV of γ Cas; not detectable in C IV or N V. Other stars behave similarly. At the moment, Θ Cor Bor shows a strong variability in strength of its C IV line; on two occasions, over 9 months, it became almost invisible—then recovered. 59 Cyg behaved the same, and recovered. *None* of these changes are reflected in luminosity variations of the star. At least for these stars, where we have so much material, the Cassinelli suggestion of no significant precoronal material and all observed superionized lines being produced in a postcorona by X-ray Auger ionization must be firmly rejected. These hot stars seem much more parallel to the cool stars in their chromospheric-coronal behavior, than they do to the speculative no chromosphere models. (Again, I emphasize the incomplete definition of a chromosphere from *just* this nonradiative-heating aspect; cf Chapter 4.) Because of the similarity of those Oe stars we know, to the Be, and the same, for the Herbig Be and Ae, I see no reason whatsoever to accept Cassinelli’s speculation.

From a similar interest in the existence of pre- and post-coronal regions of similar ionization, we turn to consider the cool “hybrid” stars, and those associated cool stars whose classification led to the “hybrid” idea. I continually assert that chromospheres-coronae are ubiquitous across the HR diagram. The cool stars just mentioned have been offered as exceptions; they are presumed to have only slightly-heated atmospheres, $T_e \lesssim 2 \times 10^4$ K, producing only the spectrum of the lower solar chromosphere, nothing hotter, and to have strong mass-fluxes, nothing more. Hybrid stars are those of the same MK classification which behave “normally”—they have atmospheres where, in addition to a lower solar chromospheric spectrum, one also observes the solar transition region spectra of Si IV,

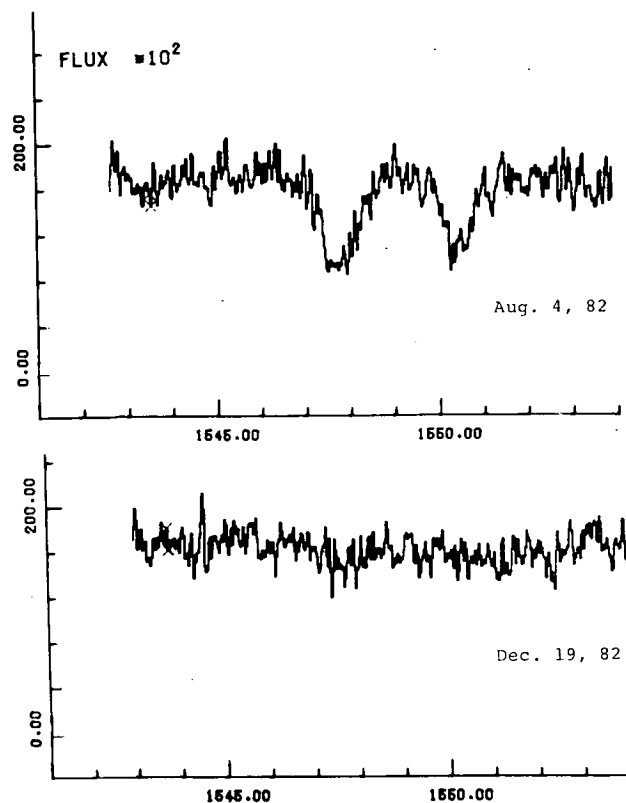


Fig. 3-28. Abrupt change in the C IV resonance lines of the Be star θ CrB (from Doazan et al., 1983)

C IV, N V, possibly, in some cases, X-rays. Also, as already discussed, they show displaced spectral lines indicating mass-flow, sometimes two components, arising in different regions. They would not be noteworthy, the term hybrid would not have been invented, were it not for the possible existence of restricted “only chromosphere, large mass-flux” stars. Consider the evidence.

Such a restricted-star class, and hybrid exception, arises from a chain of observational studies begun by Deutsch (1956, 1960, 1961) of displaced absorption components of low excitation lines in M giants and supergiants, continuing earlier observations showing occasional line-doubling in ground-state lines. The displaced component shows velocities are ≈ 10 km/s, are not found in giants earlier than M0, but are, in earlier supergiants. The Ca II H and K lines always show the strongest lines, which Deutsch labeled “circumstellar, CS”; these lines are sharp, and superposed on the emission cores earlier discussed. That is, apparently the K3 cores are displaced, for these stars. Wilson (1960) found the accompanying K2 peaks displaced, statistically, about 40 percent of these K3 values. Both Wilson and Deutsch concluded this demonstrates mass-flow at the chromospheric level. Among giants, luminosity class III, Deutsch found that the K3 absorption increases in equivalent width by a factor 10–100 between M0 and M6. The velocities reach some 30 km/s at M0, and 5 km/s at M6. From these data, Deutsch estimated mass-losses of $10^{-12} M_{\odot}/y$ for an M1, 10^{-8} for an M5, giant, dropping off abruptly for stars earlier than M0, where the CS lines were not observed. Deutsch cautioned, however, that Ca II ionization in these CS regions, by a K giant UV continuum, would explain the absence there. But, these lines continue to be observed in hotter sg.

Reimers (1975, 1977) extended the observations to cover M and K giants, G–M supergiants. One should carefully separate results on M giants, from the others. Then for the giants, he substantiated Deutsch’s results on velocity

of K3 core, its relation to the K2 velocity, and the increase in absorption to later M subclasses. He increased Deutsch's value for an M1 mass-loss to 10^{-9} , reducing the abrupt dropoff. He added that one given star can show strong variability, during which an increased equivalent width accompanies a larger displacement. The K3 blue edge stays fixed; the variability comes from motion of the red edge. He further emphasized Deutsch's suggestion that increased ionization, toward the K giants from the M, introduces the cutoff, and that the data demand a velocity increasing outward in the atmosphere. He therefore proposed a model where the Ca II line comes from two quite different atmospheric regions: before and after whatever is the T_e -maximum produced by the nonradiative heating, and its associated superionization, whether collisionally or radiatively produced. According to this model, the earlier M giants have a greater superionized region surrounding them, and a higher terminal velocity of the mass-flow; hence, Deutsch's relations follow. For M0 giants, he finds $10 R$ as the outer radius of the no-Ca II region, and $V \sim 25$ km/s. We return to the model, below.

Reimer's second broad result, by adding the K giant and G–M sg data, was the identification of higher-velocity components, sometimes outside the Ca II emission core. Broadly, he obtains an increase of velocity toward hotter stars, in the direction of the M giant subclass trend; he suggests that the relation $V \sim V_{\text{esc}}^2 = 2gR$ (photospheric values) grossly represents the asymptotic velocity. His calibration from his data is compatible with a solar value of 500 km/s. For the hotter M giants, he notes the tendency of the Ca II K3 velocities to exceed those from other lines, which just exceed the K2 values; but in cooler giants and in M sg, the K3 velocities are less than from other lines. Deutsch (1960) and Weyman (1962) consider this implies deceleration at large distance. Finally, he finds that all class II K giants, and a few class III K and M giants, show a second, high-velocity component outside the emission core—which he calls K4. Velocities are -75 to -95 km/s. Thus these K4 results are the same as the later ones by Hartmann et al., for Mg II—but cf below.

Then in summary, Deutsch and Reimers together noted the existence of a locus in the (M_{bol} , spectral-type) plane—passing through $(-4, G5)$, $(-1.8, K2)$, $(0, K5)$. Roughly, stars cooler and more luminous than the locus show low-velocity, $\lesssim 100$ km/s displaced components of Ca II; stars hotter, less-luminous, with higher gravity do not show such CS displaced components of Ca II; but the maximum observed atmospheric velocity increases as gR . He suggests that the mass-loss is roughly represented by $L/gR \sim L/V_{\text{max}}^2 \sim L/\text{escape-energy}$. Thus, always the same fraction of the stellar energy production goes into mass-loss; and the kinetic energy remaining in the mass-loss, after escape, is also a constant fraction of the escape energy, and of the luminosity. Reimers (1980) summarizes these results as only reflecting trends in the evolution of the characteristics of chromosphere-corona, T_e (max), wind-velocities, possibly mass-loss rates. He emphasizes that observations, particularly of such “hybrid” stars, indicate only a gradually-evolving character, with individuality and variability about such trends.

By contrast, using low-resolution farUV data, Linsky and Haisch (1979) adopted the Deutsch-Reimers locus, elaborating it to demand a *sharp* division into two types of cool stars: solar-type, with high ionization and low mass-flux; and nonsolar, having no superionization exceeding $T_e \sim 2 \times 10^4$ K, but larger mass-fluxes. Hartmann et al. (1980), Dupree et al. (1979), Brown et al. (1979) support such a division, but insist, with Reimers, on its gradualness, again because of the hybrid star existence. Linsky pictures the sharp division as a choice for the star in the use of the nonradiative energy supplied its atmosphere: it can either create a hot atmosphere, with small mass-loss, or a warm atmosphere, with large mass-loss. Above the locus, the stars have made one choice; below it, another. To support his conjecture, he introduces a false, quite misleading, analogy to solar coronal-hole, and non-hole regions, calling the former “cool, with large mass-loss,” and the latter “hot and no mass-loss.” We have already noted that hole and nonhole each have $T_e \sim 1.5\text{--}2.5 \times 10^6$ K, and only some 10 percent difference in density, in the corona (Vaiana and Rosner, 1978).

It is useful to try to put these results into better diagnostic perspective, especially the use of the Ca II lines. There, we do indeed find a difference between M-giants and the Sun—also the K, G giants. The solar calcium is Ca II, and the circumstances of forming the H and K lines have been outlined. The roughest calculation, LTE or nonLTE, shows photospheric calcium is Ca I ($n_e \sim 10^{11}\text{--}10^{12}$) for the M giants, until M0–K9, when Ca II takes over, as for the Sun. So the major part of the M-giant Ca II profile is chromospheric, except K3, which is formed in an observationally-established, distant cool envelope. That is, the Ca II locale for these stars consists of two shells: one

chromospheric, one postcoronal, separated by a hot void in Ca II, which produces EUV radiation capable of photoionizing Ca II. So whatever the ionization mechanism in the postcoronal shell, its T_e will not exceed that in the chromospheric Ca II shell; while n_e drops enormously. In short, ϵ and $\epsilon B_\nu(T_e)$ —sink and source terms in the H and K transfer equations—will have a discontinuous drop in the line-center, as contrasted to the strong rise in $\epsilon B_\nu(T_e)$ in the solar case. So, the cool-envelope K3 minimum intensity drops strongly. (But the situation is not pure scattering, as Reimers suggests, any more than it is in the normal atmosphere; it is simply a question of the size of ϵ , as outlined.) Moreover, as one goes to the hotter stars, the outer radius of the hot Ca II void, the inner radius of the cool Ca II shell, increases; while the total number of Ca II atoms in the cool shell decreases. The effect is accentuated if we simply recall that most of the nonradiative energy is, in the solar case, used to heat the low chromosphere, not the subsequent hotter regions: by a factor 10^2 – 10^3 . So, since $T_{\text{eff}} \sim 3000$ K for the M giants, we recognize that the same nonradiative energy input to an M giant and the Sun leaves much less energy available to energize the postchromospheric atmosphere and wind for the M star. So if the cool Ca II envelope for these cool stars is produced simply by cooling, independently of any relation to deceleration, its decreased importance toward hotter stars, and its apparent absence in the Sun, are hardly surprising. Nor is a decrease in mass-flux inferred from the total number of Ca II atoms in it—from the K3 equivalent width—surprising, or credible—as warned by Deutsch and Reimers. It is difficult to find any serious observational or thermodynamic support for the Linsky-Haisch suggestion of alternative possibilities to partition a given energy between heating and producing a strong wind, under their hole, non-hole, presumably magnetic field, analogy. It seems preferable to study the gradual height-evolution of heating as the initial photosphere varies, as above, and with Reimers' emphasis upon gradual trends, rather than strict and abrupt changes between stellar types, according with that suggested by other data in hot and cool stars alike.

There is an apparently ambiguous point in the above modeling of pre- and postcoronal cool regions which is actually clarifying. In the M giant, Ca II data, the displacement of the emission peaks and the K3 minimum were taken to measure the chromospheric and cool-envelope velocities, respectively. In the K4 region of the K stars, the implication is that the K3 velocities refer only to the chromospheric shell, no longer the cool-envelope shell, so that the velocity of the latter is the K4 one. In the Mg II, hybrid-star, discussions, the position of the emission peak is ignored, and both chromospheric and exocoronal, terminal, velocities are inferred from components lying to the blue of the (unresolved) emission peaks. So in passing from the cool M giants, and their two Ca II shells, to hotter stars, via the hybrid stars and their two Mg II shells, we supplement the Ca II by Mg II shells in the diagnostics: always a precoronal “chromosphere-shell,” and a postcoronal “cool-envelope-shell.” And continuing the Ca II, Mg II progression toward hotter ions, and *if* we have the proper thermal structure of the exophotosphere, we can have precoronal “transition-region-shell” and postcoronal “cooling postcoronal” shells for O VI, N V, C IV, Si IV etc. ions. Whether such shells have sufficient total concentration of such ions to be visible, depends on the (T_e , density) structure of the shell and exophotosphere. So, we progress from M giants, through the remaining cool stars, into the hot-star domain and the Be stars in particular, simply because we have so much data on them. So we must recognize that the term “hybrid” for the stars so labeled is completely misleading; the stars are quite “normally peculiar,” re standard models, in their exophotospheric structure. The Hartmann et al. models may or may not be correct in seeking the nonradiative energy (and possibly mass-flow accelerative) source in Alfvén waves. They must, however, be modified to incorporate the production of the N V, possibly higher superionization stages, possibly X-rays. Then the major observational-theoretical problem is the velocities of these C IV, N V ions: Are they indeed as high as the inferred 150–200 km/s? Or even higher? Clearly, at the moment, any theory is in such a state that we had best hope for observational clarification of the problem.

This last question, then, leads to that of the relation between these postcoronal, “cooler-than-corona shells” and the cool H α envelopes in the T Tauri, Be, and Be-similar stars. For at least the latter, a deceleration of the mass-flow before the cool envelope is observationally established. It is inferentially-reasonable, for T Tauri, if (cf Part III) one believes the flow-velocity = 1-dimensional thermal velocity after the low-lying thermal point, up until an escape point. We recall that prior to space observations, we had only evidence for $V \lesssim 200$ km/s for the Be stars; now, we observe pre-cool-envelope values up to 2000 km/s. So the question is the maximum velocity reached in the T_e (max) regions for these cool stars. We know, for the Sun, that at some phases, V reaches 800 km/s. The Reimer's suggestion

of $V \sim V_{\text{esc}}^2$ clearly rests on too small a range of data, and does not admit variability in a given star, or individuality in stars of the same, classical (T_{eff}, g); both are characteristics stressed by Reimers in discussing “trends.” We will find the same, in abstracting the various velocity laws proposed for the hot stars and radiative-acceleration, in Section F. The resolution of these questions are crucial, in deciding whether the postcoronal “cool” regions of various types can sometimes represent only static cooling, or whether—*empirically*—they must always be associated with a deceleration, of whatever origin. We continue the discussion, from the mass-loss viewpoint, after abstracting the X-ray aspect of superionization.

c. **X-Ray Emission.** Like the discussion of Si IV–C IV–N V superionization across the HR plane, a discussion of X-ray prevalence is anticlimactic. The bulk of the material comes from the Einstein satellite, created by Gaicconi, his chief collaborator Vaiana, and many enthusiastic co-workers. The Erci (1979) lectures by Vaiana and Rosner give details of the results; but they are essentially surveyed by Vaiana et al. (1981), with diagnostic interpretations suggested by Pallavicini et al. (1981) from the standpoint of a strong focus upon solar-analogous, coronal, magnetic phenomena. The last should be leavened with individual investigations on dispersion among classes of similar stars, like that on the T Tauri already cited by Kuhi and Walter (1981). The major accomplishment of all this work has been the demonstration that hot coronae are found in stars of nearly all varieties in the HR diagram, the possible exception being very cool supergiants and some giants. The major inadequacy thus far was the limited life of Einstein, relative to IUE, hence the lack of sufficiently complete data on individuality and variability. The former exists; dispersion of 2–3 powers of 10 within a given class of stars is found; and again, trends rather than rules seem preferable. So I only briefly abstract the results, just calling attention to the diagnostic disagreements, where they exist. I stress the essential harmony among IUE and Einstein results, in indicating the “normality” of very hot exospheric regions in all stars, but the details necessary for modeling are quite complementary, not duplicative, from these two sources.

In abstracting this X-ray material, one wants to carefully distinguish between the observations, any trends they show across the HR diagram, any quasi-correlations with any other parameters such as rotation, and any theoretical modeling. The easiest way to abstract the first and second is simply to reproduce the summarizing diagrams of Vaiana et al. (1981), which gives Fig. 3-30 for total X-ray luminosity in the 0.2–4.0 keV band; and Fig. 3-29 for flux (erg cm/s) in that band, in main-sequence stars. Fig. 3-30 shows that there is a trend of total X-ray luminosity to decrease with cooler spectral class: about as rapidly as total luminosity between O5 and M5 for MS stars, a factor 10^4 – 10^5 change, in the X-ray median values. However, there is a scatter of individual values about this mean, which ranges from 10 – 10^4 , the scatter increasing toward later types. The relative decrease among giant and sg stars seems slightly larger in the X-ray, with equally large scatter, but there is no detection among giants and sg later than M0. Fig. 3-29 shows no significant change in X-ray flux from early to late stars; only *possibly*, a slight decrease, but the scatter is enormous, again 10^3 , increasing toward the red. We recall that values of the nonradiative energy-flux needed for the Sun range from 10^6 – 10^7 erg cm⁻²/s to heat the low chromosphere, and some 10^4 for the corona; while the T Tauri stars demand about 10^3 larger values. The X-ray fluxes, for G–M, MS, stars range over some 10^4 – 10^7 . The so-called theoretical values of the acoustic energy-fluxes cited in these diagrams are meaningless. But the observed scatter in observational results shows the futility of expecting that any theory which specifies only (spectrum, luminosity, or gravity) input data can be useful in modeling actual stars. Data on variability are woefully incomplete; but those on the cited individuality are striking, in substantiating the evidence from other sources already summarized. What is uniquely important about the X-ray observations, of course, is their numerical size.

Inferences on correlation with other parameters come from the Pallavicini et al. (1981) material, which is that of Vaiana et al., supplemented by collaborative programs, published and unpublished, summarized in the article. Then Pallavicini et al. focus on two correlations between stellar parameters and X-ray luminosities: rotation for late-type stars; and total luminosity for early-type stars, where no correlation with $V \sin i$ is found. It is too much to reproduce here the whole array of scatter-diagrams by which the authors have searched for correlations; the reader should examine them carefully, and other individual studies such as that by Kuhi and Walter on X-ray, rotation

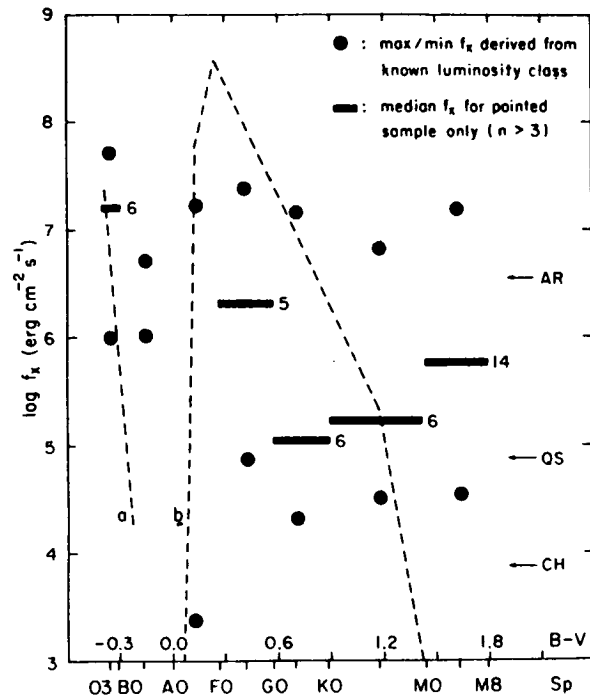


Fig. 3-29. Variation of derived X-ray surface flux f_x vs. spectral type for main-sequence stars (from Vaiana, et al., 1981). Circles indicate the maximum and minimum observed f_x for main-sequence stars optically well-classified, bars indicate the median f_x for the pointed sample of main-sequence stars only. For comparison, the authors give the variation in total available acoustic surface flux f_x as a function of spectral type predicted by: (a) Hearn (1972, 1973) and (b) Renzini et al. (1977). As a guidepost the authors have also indicated in the right-hand margin the typical values of soft X-ray surface flux for various solar features (AR = active region, QS = quiet Sun, CH = coronal hole) taken from Vaiana and Rosner (1978).

correlations for the T Tauri stars, where such correlation with rotation was not found. I reproduce only their two summary diagrams: L_{bol} vs. L_X for types O3–A5; and L_X vs. $V \sin i$ for types F7–M5: Figs. 3-31 and 3-32.

The trend with luminosity, and the varying correlation with $V \sin i$, confirm what we have already summarized for the peculiar stars. Re the luminosity trend, we should be very clear. The luminosity is a measure of the energy produced by the star; that it represents the *total* energy, is a conjecture. Calculations of interior structure and evolution, based on thermal models, are presumed to support the conjecture; but as we have seen from the peculiar stars, there are many observations that put the conjecture into question. So if we take radiative luminosity as one aspect of the energy production, it would be surprising if, as it increases, other aspects do not also increase: for example, the nonradiative energy-flux not transporting mass, and that flux which does. We continually stress this point. Here, we note that Fig. 3-31 simply says that L_X goes in the same direction as L_{bol} . There is no mechanism proposed by which L_{bol} produces L_X . There is only the implication that nonradiative energy-flux increases with radiative flux.

The correlation of L_X with rotation, and any interpretation of it, should be treated cautiously, as the authors do. They carefully distinguish, in any expectation that rotation might be associated with an increased energy supply,

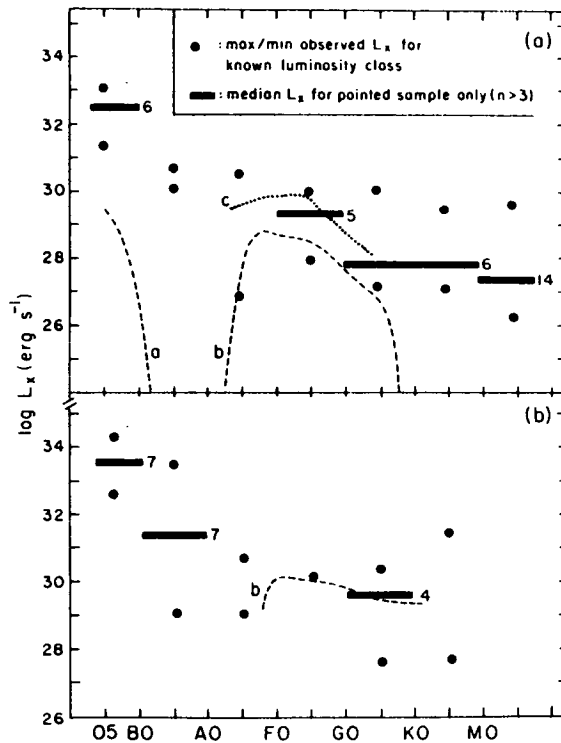


Fig. 3-30. Variation in X-ray luminosity L_X vs. spectral type for optically well-classified stars: (a) main-sequence (b) giants and supergiants (from Vaiana et al., (1981). Circles indicate the maximum and minimum value of L_X found in this sample and, horizontal bars, the median value of L_X for the subset of pointed-survey stars. For comparison, several theoretical predictions of X-ray emission levels are plotted, all based upon acoustic coronal heating: (a) and (b) from Mewe (1979); (c) from Landini and Monignori-Fossi (1973). Note the gross discrepancies between such theories and observation.

between convecting (late) and non-convecting (early) stars, in the sense we have already stressed. If one regards the production of a magnetic field as a way of converting rotational energy into energy supplied the atmosphere, then independent rotation and convection can indeed provide such a magnetic field, and dynamo action: this is the cool-star situation, as they stress. They also note, however, that there is insufficient energy in rotation of the Sun—always the primary example of dynamo action—to allow rotation to be the sole source of the energy; it should suffice for a maximum of only some 10^8 years. So one requires that some aspect of the mechanism also convert solar radiative energy into mechanical—as in the original thermal-turbulent instability of Biermann and Schwarzschild. The problem remains to be explored. Here, while their data look convincing, one asks why the correlation does not hold for the T Tauri stars which, in the mean, rotate somewhat more strongly than the FGK average. We have already noted the diagnostic complication stressed by Kuhl and Walter: the inverse correlation of L_X with $H\alpha$; thus the suggestion that large mass-flux masks X-ray emission. This aspect is particularly important in trying to understand the lack of X-ray

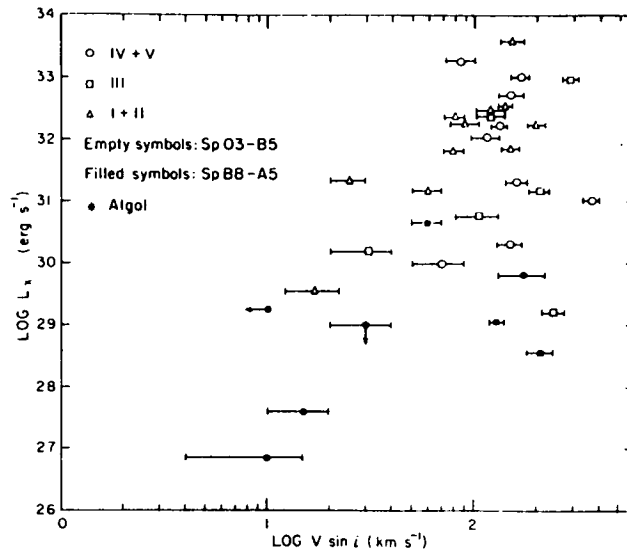


Fig. 3-31. Scatter diagram of X-ray luminosities vs. projected rotational velocities $V \sin i$ for stars of spectral types O3-B5 (empty symbols) and of spectral types B8-A5 (filled symbols). Different symbols indicate different luminosity classes. The horizontal bars indicate the probable errors on the adopted values of $V \sin i$. There is no obvious correlation between X-ray luminosities and rotational velocities for both groups of stars O3-B5 and B8-A5. The peculiar system Algol may not belong to the same subset of stars, since X-ray emission is likely to originate from the K0 IV component, rather than from the B8 V primary (from Pallavicini et al., 1981).

detection in M giants and sg. We have discussed above the evidence of differential behavior of Ca II and Mg II cool shells in such stars, relative to the K and G classes. If it is simply a matter of that low-level ionization, the X-ray opacity is not affected. If, however, the earlier K and G stars behave like the Sun, with greatly extended 10^6 - 10^7 K coronal regions, while MS sg always fall below 10^5 - 10^4 because of not enough energy remaining after heating the 3500 K photosphere to the 10^4 - 10^5 K level, then differential opacity becomes significant. Here, the evidence of the T Tauri stars, and the Be/Oe (e.g., ζ Oph) vs. B (e.g., τ Sco) becomes very significant, because of the extended cool H α envelope present in T Tauri and Be, but not B, stars.

Finally, again, one should keep in careful perspective just what effects one might expect from the rotation, especially in comparing what effects correlate with X-ray emission. Rotational velocities for the cool stars do not exceed some 50 km/s; they reach some 350-400 km/s for the hot Be stars. The authors state that the *effect of rotation has been well established as being present in the Be stars*, probably due to diminution of the effective gravity. *This is simply not true*, as we have abstracted earlier and is detailed in the B-Be volume (Underhill and Doazan, 1982); the persistence of such statements in the literature simply reflects early, marginal, and incomplete observations and faulty theory. There is no question that much energy is stored in rotation; the question is how to un-store it. We have already speculated sufficiently, on whether an independent mass-flux can provide the second independent velocity, with rotation, to build magnetic fields; it remains to be shown.

In summary, the X-ray evidence is invaluable for demonstrating the pervasive nature of coronae across the HR diagram. The existing gaps, such as the M g and sg, remain to be explored. The evidence for individuality is inescapable; we need more data to demonstrate variability to the same level of empirical assurance. Correlations with rotation are stimulating; those with luminosity require much thought on whether they imply origin or parallelism; we continually return to the question.

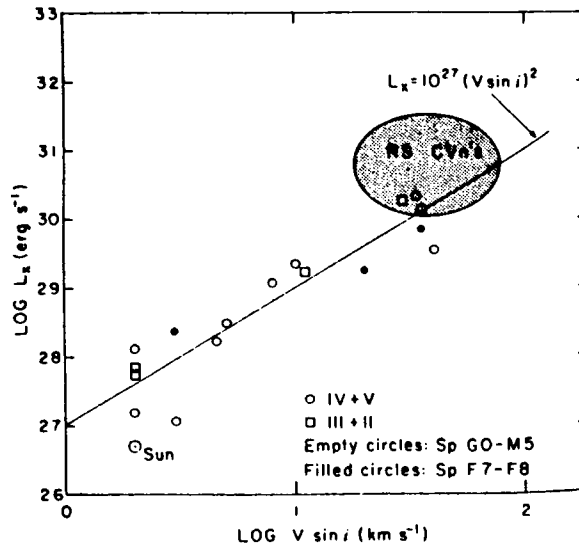


Fig. 3-32. Scatter diagram of X-ray luminosities vs. projected rotational velocities for stars of spectral type G0-M5 (empty symbols) and F7-F8 (filled symbols). Different symbols indicate different luminosity classes. The position of RS CVn stars (both short- and long-period systems) is indicated (from Walter et al., 1980); the plotted X-ray value for the Sun is an average over the solar cycle. Note that the entire sample of stars from F7-M5 shows a correlation of the X-ray luminosity with the rotation rate: the straight line corresponds to the relationship $L_x = 10^{27} (V \sin i)^2$ with $V \sin i$ expressed in km/s (from Pallavicini et al., 1981).

F. SUPERHERMIC-VELOCITY PECULIARITY AND ANOMALY

The use which has been made, in modern theoretical work to date, of the ensemble of data on the superionization and superthermic-velocity peculiarities and anomalies provides an outstanding example of the inertial sclerosis of wholly speculative theory. Prior to spatial observations, few such theoreticians admitted the implications of observing these phenomena in even just a few stars, just in the visual; because such data demand a fundamental change in thermodynamic character of stellar-atmospheric, even stellar-environmental, modeling. WR and P Cyg stars, where both these phenomena are strong, were considered as too exceptionally-peculiar, and relegated to the status of novae (Paris colloquium, 1938). Novae also show the phenomena, but their later interpretation as an effect of binarity broadened the tranquilizing label of "exceptionally peculiar." Solar observations of such phenomena were set aside as appearing only in unimportant atmospheric regions, undetectable in other cool stars, not present in nonconvective stars hotter than class F. Such divorce of the normal Sun and its low-amplitude, nonthermal effects from the historically-contemporary, Be and WR, peculiar stars with their large-amplitude, nonthermal effects characterizes dogma. Each new observational fact, and extension of the stellar domain and phenomenological range, have been reluctantly accepted because of lack of speculative theory to represent them and predict tomorrow's new results. The simple characterization of the atmosphere as enveloping an (open, nonthermal) system, from which generally independent fluxes of matter and energy emerge, with values fixed by a subatmospheric nonthermal structure, would demand revision in that subatmospheric structure before being able to specify the values of the several fluxes entering the

atmosphere. And this, few theoreticians computing structural-evolution find it pleasant to admit. This inertia persists, in spite of increasing evidence that a “peculiarity” distinguishing two stars in their visual spectra, very often vanishes in the farUV. Peculiarity reflects amplitude, not thermodynamic character. So, in abstracting where we stand on the presence, and implication, of superthermic velocities in stellar atmospheres, we must be particularly careful to stress what the whole variety of observations demand of future models, not restrict attention only to those observations, and those stars, which current speculations can partially represent. The situation is even more striking for these superthermic velocities than for superionization, because their observed characteristics demand an even wider range of conditions than do those of the superionization. As an example, superionization alone could, usually, be satisfied by just one of the often-double ionization-shells discussed in Section E: for example, speculative rejection of hot-star chromospheres in favor of only postcoronal X-ray ionized regions to produce C IV–N V–O VI: or rejection of postcoronal cool envelopes in both hot and cool stars in favor of only precoronal chromospheres to produce emission H α . The simultaneous observations of the velocities of the studied ions resolves the problem—*empirically*—as we have already seen. This empirical distribution of superionization regions, and their associated velocities, then suggests—at least empirically—the characteristics of those thermodynamic fluxes which must at the least be associated with such models. Whether the association is causer, caused, or parallel from common source remains to be shown.

Then I emphasize four points at the beginning of the abstracted survey. (1) We must demand that the thermodynamic structure of the star as a whole, and of the range of atmospheres and environments enveloping such stars, be capable of producing and representing the whole variety of observed superthermic-velocity phenomena across the HR diagram. Then our abstracted summary of some peculiar stars has already exhibited a formidable array of such requirements. Mainly, we ask what should be added to, not subtracted from, these data. As an example, any theory or model which does not include variability and individuality, self-consistent with their observed characteristics, cannot be taken seriously. Such a speculative model would again simply be a set of equations looking for an application, not a theory or model of actual stellar atmospheres. (2) In this abstract, I focus on velocities, not on mass-fluxes carried by the velocities when they are radial. The choice is deliberate: a line-displacement shows directly that there exists a velocity at least as large as the displacement of the absorption minimum or maximum of the line. The velocity can be much larger; out to the line’s edge; but its value depends on the line broadening mechanism admitted to consideration. So here, in quoting values, I give both: the first is soundest. Measurement of total emission or absorption in the line is open to a model-dependent ambiguity. The array of data show that no model, at present, is sufficiently reliable to trust estimates of the total mass, moving at given velocity, in the geometrical region producing that line-component, to better than several orders of magnitude. The uncertainty arises in distribution over the whole atmosphere of ions of that given velocity; what is their ionization state; and the approximations made in the transfer problem for the radiation in the line. So, at best, we ask what even an uncertainty of several orders of magnitude in mass-flux, for the observed velocity and ionization level, lets us conclude. Again, I emphasize that we must take into consideration variability and individuality. (3) We have already emphasized that it is a theory to be proven, when one asserts that an observed superionization implies the existence of a nonthermal mass-flux. But it is simply the thermodynamics of superthermic gas-flow, encompassing many theoretical modeling alternatives, that lets us say an observed superthermic velocity *gradient* almost invariably demands that there must be an accompanying, nonzero, nonradiative energy dissipation. (4) Given the above uncertainty on mass-flux, observations still suffice to put into strong question the assumption that effectively all of the energy generated in the stellar interior lies in the observed radiation field for all stars except supernovae and some novae, and to give quantitative demonstration of the conclusion. Finally, in the survey, I emphasize the systematic-flow velocities over the quasi-random ones, often called “turbulent;” the latter are too-often only speculation.

1. Systematic-Flow Velocities

I re-emphasize. In this abstract, I try to summarize what the actual measured velocities are, across the HR diagram; from which of (i)–(iv) following they come; and with what other features they show trends or correlations. Then in order of confidence, one has: (i) Whole line-displacement measures, which can of course be associated with the line becoming asymmetric. (ii) Displacement of some feature within the line, such as the absorption minimum in a classical P Cyg profile, where one also observes the undisplaced emission peak. Of the same variety, but less reliable since it involves a transfer problem, are the several types of “other” P Cyg-type profiles introduced by Beals (cf Fig. 3-34), and modified by others. (iii) A line-asymmetry, for which there is some good reason to attribute the asymmetry to a mass-flow. (iv) Simply the breadth of a line, for which no other interpretation than macroscopic velocity-broadening has come to mind.

I also re-emphasize. *Absence* of any or all of (i)–(iii) does *not* prove the star has no velocity field: it simply means *there is no observable velocity field in the atmospheric region where the line is produced, of kind and size to affect that line*. Negative surveys, finding no such evidence, and proclaiming the dogma “there are no outflow velocities, no mass-fluxes” in such stars, have severely held up progress. I quote what has become almost biblical dogma: the survey, using asymmetries in the Si IV line, largely in Copernicus data, showing no observed mass-flow for M_{bol} fainter than -6 ($L/L_{\odot} \lesssim 2 \times 10^4$) (Snow and Morton, 1976; Lamers and Snow, 1978). This was qualified to except Be stars with rotational velocities, $V \sin i > 200$ km/s (these same references). This limit was lowered to $M_{\text{bol}} \sim -5.3$, possibly -4.2 for B stars, and -3.2 for Be stars. In 1980, Lamers reasserted that the limit of observable mass-loss occurs at $M_{\text{bol}} \sim -6$ over the entire range from $7500 \text{ K} < T_{\text{eff}} < 40,000 \text{ K}$. He has continually stressed the exceptional nature of Be stars, where (he speculates) rotation makes mass-loss very significantly easier; and the mass-loss is confined to the equatorial plane. We abstracted the Be results in Section B; and they have been discussed in detail in Doazan (1982). There is, as yet, no observable dependence of Be mass-loss on $V \sin i$. Furthermore, there are B stars showing the same rotational velocity as Be stars, without showing similar mass-flow velocities. Finally, in the same star (59 Cyg), at the same epoch, when the C IV and N V lines showed velocities, between -300 and -800 km/s, the Si IV lines were undisplaced, with no measurable asymmetry. The diagnostic problem is the same here as emphasized in discussing superionization. The atmosphere is not homogeneous; there are enormous variations along r ; velocities can apparently range from thermal or less, in the lowest regions, to highly superthermal and superescape; lines observed in one region will not necessarily show the same velocity, atoms will not show the same ionization, as those in other regions. To say that undisplaced, symmetric Si IV implies the same for C IV, N V, O VI is as unfounded a statement as to assert that the observation of only C IV–N V–O VI shows that coronae cannot exist because such ions would be destroyed in such regions in that star. In the same way, for cool stars, one has the classic solar example. No solar spectroscopic measures have yet shown nonlocalized mass-flow greater than some 50 km/s; but collectors near the Earth give velocities 300–800 km/s, depending upon the epoch. Again, in many cool stars, because of the long exposure time needed, far more long- λ observations of Mg II exist than short- λ measures of C IV. So, one can study the kinematic properties of the Ca II and Mg II ionization shells; not of the C IV one, from such data. WR, P Cyg, novae warned of what was coming, given proper detectors. So do the Sun, symbiotic, Be, T Tauri, etc.

I try to abstract the material in terms of how long we have known what, to emphasize just this rapidly-unfolding panorama which faces any modeling plus theorizing. The thermodynamic structure must be elastic enough to accommodate tomorrow’s new data. I can remember being shocked at a 1976 Space-Telescope proposal to design an instrument, to be flown in 1986, to reconfirm the 1975 Copernicus Lamers-Rogerson identification of O VI in τ Sco, by one of the astronomers who had worked on the O VI, WR class of PN central stars.

Then, the historically-oldest direct observations of superthermic velocities in stellar atmospheres were the “exceptionally-peculiar” novae, WR, and P Cyg stars. Velocities are *measured directly* from line-shifts and the absorption-component displacements in P Cyg profiles. Velocities are also *inferred from* the breadths of undisplaced emission lines. Also as discussed in earlier sections, the class of novae became increasingly diffuse: subdivided into classes of novae, based on recurrence-frequency and amplitude; and into other categories such as symbiotic. Moreover, mass-flow is now recognized as being continuous as well as episodic. (I set aside super-novae from the discussion; possibly I make the same error of “too peculiar” that I have attributed to others, above.)

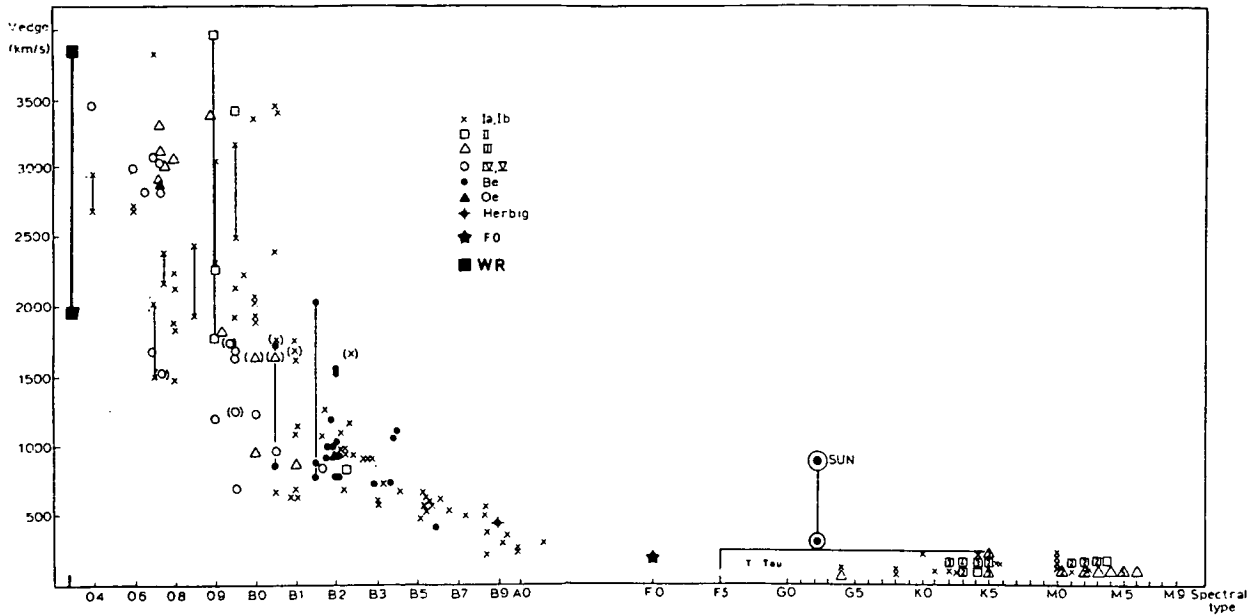


Fig. 3-33. Edge-velocity vs. spectral type across the HR-diagram. Data from: Reimers (1973a, b, c, 1977), Snow and Morton (1976), Abbott (1978), Cassinelli and Abbott (1980), Hutchings and Von Rudloff (1980), Chavarria, K. (1981), Underhill and Doazan (1982), Willis (1982), Jordan (1982), Kuhl (1983). Straight lines join values obtained for the same star at different epochs or/and by different authors. WR stars are represented by one straight line showing the range of measured velocities. T Tauri stars are represented by a horizontal line at the maximum observed value in the visible.

Fig. 3-34. Non-typical line profiles in P Cygni spectra (from Beals, 1951).

But in any event, these historically-superthermic nova-type stars produce velocities ranging from some 3000 km/s to 100 km/s in the rise phase, and some 2–3000 km/s to some 500 km/s in the later phases, of the episodic ejection. The continuous-flow velocities are $\text{o}(1000 \text{ km/s})$. Thus, while statistically there seems to be a continuous acceleration of the episodic-ejection material, data on the early phases are sufficiently sketchy that no definite characteristics can be assigned to that acceleration. The velocity characteristics of these hot, sd, stars are thus coherent, while showing much individuality, and of course variability. In any event, there is nothing to suggest that the size of the ejected material at one episode—some $10^{-4} M_{\odot}$ —is fixed by any identified properties of the radiation field. Yet there are sufficient sequential properties to let us recognize novae-cataclysmic as not glibly set aside as “binarity.”

If we take the quiet-phase character of the nova central star to be an OB hot dwarf, then the two similar classes—OB sd proper, and central stars of PN—show the same velocity character. The Kiel group (Hamann et al., 1982) find velocities of 1000–1500 km/s for two of four OB sd: line-displacement plus model fitting: thus dropping to $\dot{M}_{\text{bol}} \sim -4$ the region of mass-loss. Their model calculations find at least $\dot{M} \sim 10^{-8}$ – $10^{-11} \dot{M}_{\odot} / \text{y}$ and $F_M \sim 10^{-5}$ – $10^{-8} \text{ gm/cm}^2 \text{ s}$. Darius et al. find blue-edge velocities of 2500 km/s in OB sd (1979). The PN already discussed (e.g., Harrington, 1982) show blue-edge velocities of 1500–2000 km/s and $\dot{M} \sim 10^{-9}$ – 10^{-10} .

Both WR and P Cyg show reverse-correlations between flow-velocity (higher) and ionization-degree (lower), which appear the inverse of any parallel sequence of chromosphere-corona and increasing-outward velocity, unless, as mentioned, the lowest level one sees is a chromosphere and the gas accelerates as it cools. Nonetheless, this is the association; and WR show velocities from $\text{o}(100)$ to 2–3000 km/s; while P Cyg shows velocities from -100 to -450 km/s, exhibiting several components. $\dot{M} \sim 10^{-5}$ is assigned WR and P Cyg alike. Lamers suggests P Cyg, and the similar B1 Ia ζ^1 Sco, are examples of early type sg which have large winds and low ionization, because both show Fe II, Al II, Mg II. Here, however, by contrast to the situation in the M-type sg discussed in Section E, the C IV marks them as being superionized to at least the 10^5 K level; so it is hard to see the basis for his suggestion. He states the situation resembles the presence of Fe II in “early-type shell stars,” which, as we have seen, is a complete misrepresentation of the situation, unless he implies that P Cyg has also an outer atmospheric deceleration. But this contradicts the inverse correlation between ionization and velocity; and, indeed, Fe II shows, according to Underhill (1982) some 300 km/s velocity. So, we recognize P Cyg as “anomalous,” among the bright stars, because of its low velocity and unobserved N V; with the anomaly here, as in the M sg, to be diagnosed, to interpret it in terms of fluxes and atmospheric structure peculiar to those stars. Then from these two types of hot, massive stars, WR and P Cyg—observationally different in maximum observed velocity, inferentially very similar in size of mass-loss—we have three paths: toward hotter g and sg; toward cooler g and sg; toward cooler MS, the latter intermediate to the hot sd already covered.

Because the brightest stars are the easiest observed—hence present data are the most extensive—most of the hot-star reviews focus on the hot sg (Conti, 1978, 1981, 1982; Lamers, 1980, 1981; Barlow, 1982; Abbott, 1978, 1982a, 1982b). Conti’s reviews are the most objective on observational accuracy and scatter; unfortunately his results are invariably expressed in terms of \dot{M} , not some velocity parameter. He emphasizes that in using the farUV data—the only ones for which velocities can be directly estimated (I exclude H α , for reasons already discussed)—one usually fits simulated P Cyg-type profiles computed according to some oversimplified modeling scheme (e.g., Castor and Lamers, 1979); i.e., assuming the same $U(r)$, $\rho(r)$, often ionization (r) distributions in the atmosphere for *all* stars. One thus assumes the only change is in size of mass-flux as a scale-factor, nothing else. (We discuss in Part III that this is hardly physically self-consistent.) We also note that in such procedure, a velocity-law is a priori imposed, based on the various versions of the radiative-acceleration theories, which contain no mechanical energy dissipation. Since the observed lines used for diagnostics are usually those which could not be produced without such mechanical heating, the representation of the energy in the equations entering the theory is hardly self-consistent, unless one assumes that the microscopic energy of the gas can be neglected relative to the macroscopic. So, to abstract Conti’s results, one has available only his compilation of \dot{M} , not V . Fig. 3-20 reproduces his and Garmany’s (1981) results, down to M_{bol} brighter than -7 . He emphasizes that this shows a trend of \dot{M} to increase with L , not a correlation,

because of the scatter in \dot{M} by a factor 10–100 at given L . So, this is contrary to the basic assumption of the radiative-acceleration origin for mass-loss, as we have continually stressed in this Chapter 3 in emphasizing such individuality and variability. He further emphasizes the important result, for ultimate hot-star modeling, of the small scatter in \dot{M} among the WR stars in spite of their wide difference in spectroscopic details, as compared with the much greater range in \dot{M} , but smaller spectral differences, among the normal O–Of stars. But also recall, from Section B.3.a, the equally-small scatter in U (max) \sim 2000–3500 km/s. Then Lamers' focus lies equally on \dot{M} and F_M ; but on trying to impose their representation as functions only of the standard-atmosphere, and standard (closed, thermal) star parameters $L, M, R, T_{\text{eff}}, g$. Thus variability and individuality are, a priori, excluded. He tries to force the observations into such a framework by rediscussing all the data under the assumption that all stars have the same $U(r/R)$, etc., atmospheric model, and the same conditions at a large distance from the star. When the discrepancies are too strong, as in any aspect of variability, he ignores them. When there is too much individuality and variability, as for the Be stars, he asserts that the discrepancies “must” arise from rotation effects; but does not say how; and ignores the observational attempts to find such a relation, which have failed. Needless to say, he does not try to look at any “peculiar” stars. For these reasons, given that the goal of these observational studies is to seek $U(r)$ and its variation among stars, not a priori impose its uniformity, it is hard to have confidence in either his diagnostic approach or results.

For actual data summaries on U , of any variety, one turns to the above reviews by Barlow, on the hot OB sg and WR stars; by Abbott, on these hot sg plus those MS OB stars covered by Copernicus; and to other sources from which such data for such reviews come. I have used Snow and Morton (1976); Abbott (1978); Cassinelli and Abbott (1981); Abbott et al. (1981); Hutchings and von Rudloff (1980); Underhill (1982); and the data on Be stars (Doazan, 1982) already summarized. It is actually more illustrative to combine all these data with those summarized, in earlier sections of this chapter, on the cooler stars. There, the data came mainly from Reimers (1975, 1977, 1980) plus particular stars mentioned in this Chapter 3 text. Fig. 3-33 gives the combined display. I plot U against classical spectral class, in the same way—and for precisely the same reason, no better alternative—as the X-ray data are usually displayed. One should note that among the above, those collections of data which give both velocity at minimum absorption and blue-edge velocity are those by Snow and Morton, Hutchings and von Rudloff, and Doazan on the several Be stars at various phases, probably because they focus on observations sans preconceived imposition of velocity “laws” and their dependence on stellar parameters. In the same way, Hutchings and von Rudloff very clearly summarize their wholly empirical search for any U (max)—dependence on spectral class, M_{bol} , escape-velocity, etc.; they find trends, not laws. In the same spirit, I stress: Fig. 3-33 exhibits trends, about which there is a *very* large dispersion, to which one must attach physical reality, not regard it as observational error. This obvious conclusion for that dispersion resulting from variability and individuality in the case of the Be stars is generally accepted; consequently, the Be stars are generally excluded from modeling discussions which try to relate U (max) to other parameters. One should simply recognize that the Be stars are not unique, in such physical-source scatter. We ask some insight into what are the largest velocities produced, in stellar atmospheres of various kinds; is there evidence of systematic change in U through the atmosphere; and is U generally time-dependent, over what time-scale, or just occasionally so, in particular stellar types?

Then I make two kinds of comments: one kind, in broad perspective, with four aspects; the other kind, consisting of a number of comments on details, looking at hot and cool stars separately, and ensemble.

Broad Comments

B-1. There is evidence for $U \sim \text{o}(10^3 \text{ km/s})$ among various kinds of stars, for all stars of spectral type earlier than, and including, the Sun. But, if we did not have collector-measures of the solar U (max), coming from our peculiar-proximity to the Sun, we would not be able to claim evidence for $U \gtrsim 400 \text{ km/s}$ later than about B9 for sg and about B5 for MS. We can, however, claim evidence for $U \gtrsim 1\text{--}200 \text{ km/s}$ up through spectral class M, in all luminosity classes. So we cannot, in any way, exclude that $U \sim \text{o}(10^3 \text{ km/s})$ will be found in spectral classes later than the Sun, with increased observational sensitivity.

B-2. There is clearly a trend for this maximum U to increase toward earlier spectral classes, but not necessarily toward brighter luminosity classes. U as large as 3000–3500 km/s is found in WR, O sg, OB sd, and novae alike; U of at least 2000–2500 km/s is observed in some phases of at least one B 1.5 eV star; 1500–2000 km/s, in many B 3 eV and earlier. Other than flare-surges, no mass-flow velocities have been reported in excess of the 1000 km/s in stars at the cool end of the HR plane later than the B-stars. The Sun shows the largest *measured* values, ranging about a mean of 450 km/s, from 300 to the maximum solar value yet reported, 800 km/s. Because there is a tendency for the higher U to be found in stars with larger F_M —i.e., more matter/cm² flowing with such U —and because, except for (4) following, U increases outward; it is possible that this trend toward higher U in earlier stars may be an artifact of observational selection among stars of large mass-flow, hence, larger outer-atmospheric densities. But, in any event, any model or theory of U must be able to reproduce at least these $U(\max)$ in at least those stars where they have presently been observed, *and their variability*. Note that this range of stars covers a large variety of $V \sin i$; that the magnetic field is largely unknown; that the stars are mainly single; that they cover a large range of T_{eff} , or *photospheric* radiative-flux; and they cover a large range of g and L .

B-3. Within the observations from a given star, there are a number of examples where $U(\max)$ changes, between different epochs, by a factor up to 5. But we can only say with certainty that we observe, for a given star at a given epoch, several velocities at which more absorbing atoms are concentrated than at other velocities; and that total, and relative, numbers of such absorbing atoms also vary between observing epochs. So, as for (1) above, we cannot say with certainty that a once-observed $U(\max)$ does not exist, somewhere in the atmosphere, for that star, at all epochs. All we can say, is that—expressed as a function of number of absorbing atoms along the line-of-sight—the $U(r)$ pattern has changed, between observing epochs. The same remark holds, when comparing $U(r)$ for “similar” stars—i.e., of the same MK and luminosity class: there is very strong individuality.

B-4. The remarks (1)–(3) relate to $U(\max)$ and other velocity components observed at its same epoch *in the superionized lines*. But as we have continuously emphasized in earlier sections of this chapter, there is much evidence, among some kinds of stars, for an eventual strong deceleration of the flow in the atmosphere, not in any way linked to gravitation, but observationally-apparently linked to variable mass-flux. Doazan (1983) has emphasized that as a result of this deceleration there may be, indeed, a further gravitational effect, possibly even an infall if the strong deceleration is strong enough. Again, the suggestion is observationally-linked to red-shifted absorption lines. But the initial deceleration’s existence, in some stars, and apparent association with strongly-variable mass-flux, should be emphasized here in discussing asymptotic velocity and velocity patterns. Too often $U(\max)$ is taken as obviously being the U (asymptotic) at very large distances from the star, for all stars. IF the observations gave no evidence of anything but monotonically-increasing-outward velocities, such an assumption might possibly be justified—at least as a first approximation. Clearly it is not justified, however, given the existing observations.

These broad comments abstract the broad observational picture which any satisfactory theory, or simply empirical and ad hoc modeling, must be able to represent. If, to construct a simple theory or model, one ignores (1)–(4), then the material abstracted by Fig. 3-33 will remain anomalous, under that theory or model.

Specific Comments

As just emphasized, especially in (4) but also in considering the behavior of $U(\max)$ across the HR diagram, too often diagnostics of observations to give these velocities, and the associated mass-fluxes, are based on the model which is to be tested. Then, when one asserts that the data support the theory, one is uncertain how much this support has been, a priori, built into the result. We already stressed this point in the Chapter 2 discussion of diagnostics of lines and continua for T_e . So the following specific comments are aimed at just this preconditioning of diagnostic results. I stress again: this monograph proposes no theory for the origin, or size, of velocity fields, mass-fluxes, or nonradiative energy-fluxes. It simply focuses on asking their observational characteristics, and whether they can be considered mutually independent of each other, and of (T_{eff} , g), even though there may be trends under which one or several of the quantities may vary in parallel, with large time-variability and individuality. Then, in Part III, we ask how to obtain some characteristics of atmospheric structure from the assumption that these three fluxes, and gravity, are independent quantities.

Then we recognize that most of the diagnostics of hot stars have been made under the assumption that the radiative-acceleration theory for origin and size of mass-flow velocity, and of mass-flux, is at least grossly correct. And, likewise, most diagnostics of cool stars have been made under the assumption that the hot-coronal-origin theory is, equally-grossly, correct. So, it is useful to have explicitly in front of us those algebraic expressions, from the theories, used in the diagnostics to justify a dependence upon the various standard-star parameters, and clear insight into their origin.

Radiative-acceleration: CAK (1975), Abbott (1978) present the essence of those algebraic predictions commonly used in those diagnostics related to the theory. CAK discussed an RE atmosphere with T decreasing outward as r^{-n} ; Abbott focuses on isothermal atmospheres. As we saw from Chapter 2, under RE an isothermal atmosphere is reasonable; the strong departure from reality comes in the neglect of departures from RE, which is universally ignored in the velocity pattern from these radiative-acceleration models. "Adjustments," when introduced, lie in the production of C IV, N V, O VI as contaminants, by Auger ionization with coronal X-rays, in an otherwise RE atmosphere. The effect of a corona, presumed to be geometrically very-small, on the velocity field is ignored. Then the solutions discussed are characterized by: (1) time-independence; (2) effectively-constant T_e ; (3) $U \gg q$; (4) $2q^2/r \ll GM(1 - \Gamma)/r^2$. Thus, their solutions are limited to that atmospheric region where U is strongly superthermic, but the neutral-particle escape velocity, $V_{esc}^2 = 2GM/r \gg 2q^2$; i.e., thermal velocity is not escape velocity. Under these conditions, eq. (3.C) is:

$$(r^2 U dU/dr)^\alpha \left\{ (\sigma_e LK/4\pi c) [4\pi/\sigma_e v_{th} dM/dt]^\alpha - (r^2 U dU/dr)^{1-\alpha} \right\} = GM(1 - \Gamma). \quad (3.40)$$

The pair of relations:

$$r^2 U dU/dr = \text{constant} = \alpha(1 - \alpha)^{-1} GM(1 - \Gamma) \quad (3.41)$$

$$dM/dt = \alpha(1 - \alpha) \left\{ (1 - \alpha) K \Gamma / (1 - \Gamma) \right\}^{1/\alpha} (1 - \Gamma) 4\pi GM/\sigma_e v_{th} \quad (3.42)$$

satisfies eq. (3.40)—which is valid only under the stated conditions, and in the stated atmospheric regions. One requires $\alpha < 1$. Eq. (3.41) leads to the velocity law used in their, and other, data analyses

$$U^2 - U_s^2 = \alpha(1 - \alpha)^{-1} 2GM [1 - \Gamma] (R_s^{-1} - r^{-1}) \quad (3.43)$$

and to the asymptotic-velocity, which they state is not changed by whatever happens in the regions outside that considered:

$$U_\infty^2 - U_s^2 = \alpha(1 - \alpha)^{-1} (2GM/R_s) (1 - \Gamma) = \alpha(1 - \alpha)^{-1} V_{esc}^2 (1 - \Gamma). \quad (3.44)$$

They identify R_s as the radius where $U = q$ is first reached, so $U_s^2 = q^2$; which they state is essentially the photospheric radius, because the acceleration to thermal velocity is very rapid.

Note that this distribution $U(r)$, and the corresponding U_∞ , are supposedly produced by a radiative-acceleration: yet the solutions do not depend upon the radiation-field, only on the surface gravity. (Γ , in the term $(1-\Gamma)$, is negligible; $\Gamma \lesssim 0.2$ in the cases they consider.) This is, physically, a curious result, whose origin is obscured by the authors' insistence upon characterizing theirs as a theory which fixes \dot{M} as an eigen-value problem—but without saying why. It indeed produces a value of \dot{M} as an eigen-value solution, but without making clear what limiting—indeed invalidating—assumptions they introduce to obtain such a result. Eq. (3.C) is a single equation which, in all generality, applied to an open thermodynamic system, should predict the $U(r)$ behavior of a specified \dot{M} ; or, alternatively of a specified F_M . CAK et seq., try to produce two quantities from this single equation by *imposing* two conditions which severely condition the derived results. First they *impose* that the contracted form (3.40), which requires (1)–(4) above, of eq. (3.C) is valid. Second, they *impose* that the solution conform to one or the other of two equivalent conditions—(a) that the solution give $r^2 d(U^2)/dr = \text{constant}$, or (b) that it produce an \dot{M} proportional to some power of L (or Γ) under the condition that $(1-\Gamma)$ is a negligible correction. It then requires only algebraic manipulation to produce eqs. (3.41) and (3.42) from eq. (3.40) under (a) or (b). By imposing an r^{-2} variation of $d(U^2)/dr$, one imposes a dependence upon *either* gravity *or* L , the only physical quantities entering which vary as r^{-2} ; and $\Gamma \ll 1$ ensures that gravity dominates. The eigen-value nature of \dot{M} results: it is the only way one equation produces two quantities. However, the long chain of assumptions—beginning with the representation of many lines by a single value of α —leads, as we see below, to discord with what is observed. Basically, I emphasize: the problem arises from trying to predict \dot{M} from radiative-acceleration, instead of using such acceleration to predict the $U(r)$ of an \dot{M} imposed at the base of the atmosphere as a lower boundary-value.

Note also that condition (3) above constrains their solution to a region with an outer radius:

$$r \ll GM/2q^2 = 4.0 \times 10^{13} (M/M_\odot) (10^{-4} T_e)^{-1} \text{ cm.} \quad (3.45)$$

For a sg with $T_e \sim 35,000$ K, $M/M_\odot \sim 10$ – 25 , and $R \sim 50R_\odot \sim 0.3 \times 10^{13}$, one has r (outer)/ $R \sim 30$ – 80 , which is effectively no limitation. If, however, the star has a low-lying chromosphere-corona, r (outer)/ $R \sim 1$ – 3 ; and the size of the accelerating region covered by the above approximation is severely limited. But in this situation, the size of dM/dt drops; the radiation-field must include the contribution from the chromosphere-corona, etc. In the same way, the Castor-Lamers computation of the expected kind of P Cyg profiles under the above approach of purely scattering solutions of the transfer equation, monotonic variation of opacity, T_e , etc. with r adopts a velocity-law resembling the above

$$U(r) = U_\infty \left[0.01 + 0.99 (1 - R_s/r)^\beta \right]. \quad (3.46)$$

Such computations do not produce lines wholly in absorption, but only those of the classical P Cyg type, with a ratio of emission to absorption increasing with the size of β . The Castor-Lamers profiles cover $\beta = 0.5$ (the above case), 1, 2, 4.

Thus, the predicted features of the radiative-acceleration theory for the *origin and size* of mass-flow velocity and mass-loss are: (i) A U (max) given by eq. (3.44), thus varying only with V_{esc} , with the proportionality-factor having a universal value fixed by the absorbing lines, not L . Both Abbott and Barlow abstract Abbott's consideration of 1000 spectral lines of the 27 most cosmically-abundant elements in stars A through O, 1×10^4 K $< T_{\text{eff}} < 5 \times 10^4$ K, to conclude $\alpha = 0.5$ – 0.6 throughout this range: thus, $U_\infty/V_{\text{esc}} \sim 1$ – 1.2 . (ii) The rise to $U \geq q$ is so rapid that the theory does not consider its details; (iii) The passage from $U = q$ to $U \sim U_\infty$ occurs within a radius given by eq. (3.43), and according to the formula eq. (3.44). None of these considerations (i)–(iii) depend on the radiation field; only on V_{esc} ; any variability or individuality must then result from such in V_{esc} , i.e., gravity. (iv) Only the size of the

mass-loss depends on L , via eq. (3.42). Because this equation is valid only if eq. (3.41) describing dU/dr is valid, under the assumed eq. (3.40), failure of any of (i)–(iii) implies failure of this (iv). Then, in addition to a variability and individuality in mass-loss possibly arising from such behavior in V_{esc} , it can also arise from that in L . One thing should be noted: in this radiative-acceleration, it is the farUV, not the visual, which is important. So, if thermal models, RE and HE, are discarded for the exophotosphere, L –and its variability–need not be that L used in this RE theory. In the same way, the actual numerical predictions of dM/dt will decrease as $T_e^{-1/2}$, if a chromosphere-corona replaces RE: *if* the theory remains applicable.

Hot-coronal mass-loss: The standard Parker theory (1958) contracts eq. (3.C) to the form:

$$(r^2 U dU/dr) (q^2/U^2 - 1) = (GM/r^2 - 2q^2/r + dq^2/dr) r^2. \quad (3.47)$$

In addition to this contraction of the equations, the approximation consists of imposing that, because of the contracted form of the equations, the vanishing of the LHS of the equation at $U = q$ requires, in an isothermal atmosphere, $q^2 = W^2/2$ at the same atmospheric point. $W^2 = GM/r$; so W is the scape velocity of an ionized particle. These two conditions then lead to the predictions of the velocity and mass-flux at the *critical-point*, where $U^2 = q^2 = W^2/2 = GM/2r_c$:

$$U_c^2 = q^2 = kT_e/\mu = 1.66 \times 10^{12} (10^{-4} T_e) \quad (3.48)$$

$$r_c = GM/2q^2 = 4.0 \times 10^{13} (M/M_\odot) (10^{-4} T_e)^{-1} \quad (3.49)$$

$$dM/dt = 4\pi r_c^2 U_c \rho_c = 6.8 \times 10^{-16} n_c (M/M_\odot)^2 (10^{-4} T_e)^{-1.5} \quad (3.50)$$

Thus, the predicted features of the hot-coronal-theory are the velocity U_c at the critical point, as a function of *only* the coronal T_e ; the radius, r_c , at the critical point as a function of *both* T_e (corona) and stellar mass; and the mass-loss as a function of the *three* quantities— T_e (corona), stellar-mass, and the particle (hydrogen) concentration at the critical point. That is, this is a theory *if* it can also predict T_e (corona) and n (corona). The *presumption* is that a sufficiently-detailed knowledge of the nonradiative flux, coupled with radiative flux and gravity, will suffice to predict n_c and T_e (corona). No one has yet identified the actual F_{NR} , of the Sun, or of any other star, sufficiently well to use it to compute a chromosphere-corona model to test these assumptions which define the hot-coronal model. Indeed, even simply assuming a nonradiative flux having arbitrarily-imposed characteristics and computing a rough atmospheric model, no one has yet predicted a mass-flux significantly larger than the solar one (cf Hearn and Vardevas, 1981; Hammer, 1982); nor has anyone yet predicted a mass-flow velocity as large as the observed solar ones. To extend the above U_c to whatever is the maximum U , one must make some additional assumption on $q(r)$, in order to integrate eq. (3.47) outward from r_c . Effectively, this means making some assumption on the energy balance of the gas, and the heating and cooling processes which produce the balance. If one assumes adiabatic behavior of the gas flow after this coronal maximum T_e , one adjoins the adiabatic form of the energy equation (2-28) to obtain, with the $\gamma = 5/3$ of a monatomic gas:

$$U^2 (\text{max}) = U_\infty^2 = U_c^2 + \left[2\gamma kT_e/\mu \right] (\gamma - 1) - 2GM/r_c = 2U_c^2 = 2q_c^2. \quad (3.51)$$

For a solar corona of 2×10^6 K, one obtains $U_c \sim 200$ km/s, $U(\text{max}) \sim 300$ km/s. If one adds energy, in whatever way, one can of course increase $U(\text{max})$; if one loses energy, one diminishes $U(\text{max})$. Thus, whether one considers this hot-coronal-theory to be an empirical-theory or a speculative-theory depends on what quantities one starts with. If one starts with T_e (corona) and n_H (corona) at a particular radius, it is an empirical theory: one has started with a specified mass-flux. If one starts with $T_{\text{eff}}, g, F_{\text{nR}}$, plus the condition that thermal velocity is reached for the first time at the critical point, where $q^2 = GM/2r_c$, it is a speculative theory—which remains to be tested. Prediction of $U(\text{max})$ from U_c under the adiabatic assumption gives too small a $U(\text{max})$ by a factor of 1.5–2.5, depending on the epoch observed.

It is essential to put the difference between the radiative-acceleration and hot-corona theories into sharp focus in discussing the observed velocities. Basic to the difference, of course, is that the former depends only on F_R and g to predict velocity and size of mass-flux; while the latter needs also F_{nR} . But, relative to maximum velocities, one notes that the radiative-acceleration theory has no dependence of maximum flow velocity on radiation field or any other energy input; whereas, the hot-coronal mechanism depends entirely on F_{nR} to fix the coronal thermal velocity and on something unknown to further raise it. Then, in actually discussing the solution, the radiative-acceleration approach takes a very rapid rise in U to q as obvious; and focuses on the region between $q = U$ and $q^2 = GM/2r$ as that accelerating region that is critical to fixing the value of $U(\text{max})$. Because the atmosphere is only radiatively heated, $q = q$ (RE value of T_e); so this outer bound on the region considered lies far from the star. Adding a corona changes the solution, and region of acceleration *very fundamentally*. By contrast, the hot-coronal theory imposes a (relatively) very slow rise in U to q —because $U = q$ only occurs at $q^2 = GM/2r$, the outer boundary of the region of interest to the radiative-acceleration theory. So, relative to the radiative-acceleration model, the point $U = q$ in the hot-coronal model occurs very far from the photosphere, while $q^2 = GM/2r$ occurs very near the photosphere—this common point $U^2 = q^2 = GM/2r_c$ occurring at just a few radii. This point is critical in discussing the immediate physical cause of a very extended atmosphere—i.e., an atmosphere where the density decreases sufficiently-slowly that one observes atmospheric structure many radii from the photosphere. For the radiative-acceleration model, the low-lying $U = q$ point means the exponential decrease of density stops low in the atmosphere, where the density is high; thereafter the $(Ur^2)^{-1}$ law keeps it high. For the hot-coronal model, pushing the $U = q$ point far away, by forcing it to agree with the critical point, gives low densities, at the critical point, hence, beyond it also. Our empirical-theoretical approach of Part III preserves the low-lying $U = q$, if the mass-flux is sufficiently large; otherwise, not; hence, the basic difference between the Sun and a T Tauri star. Against this background, we make the specific comments on the relation between theories and the observations summarized in Fig. 3-33.

(S-1) The first thing to note is the discrepancy between the largest observed $U(\text{max})$, emphasized in comment (B-1) above, and predictions from either theory. These $U(\text{max})$ of ~ 3500 km/s were long-observed in the “peculiar” WR and novae; were first brought into general focus by Morton’s (1967) rocket observations of hot sg; formed the basis for the Lucy-Solomon (1970) assertion that the hot-coronal theory was inadequate and for their, CAK, Abbott et al. attempts to construct a radiative-acceleration theory: but today these $U(\text{max})$ still lie far outside any values predicted by either theory. But, to them, we must add the solar 450–800 km/s as being equally outside the hot-coronal theory constructed to represent it. It is amusing to note that a solar 800 km/s, when compared to its V_{esc} of 617 km/s, is in better agreement with the radiative-acceleration theory than are the hot stars. But it is also clear that our observational measures of $U(\text{max})$ in the cool-star range are woefully inadequate underestimates, unless one really believes the Sun is a *physically*-unique star, not just proximity-unique. The direction of the necessary theoretical modification is clear: one needs to add energy to the flow, for both hot and cool stars. Myself, I have always found it curious that a theory of radiative-acceleration could be proposed that predicts a flow-velocity which has no dependence on the radiation field. And again, one emphasizes the conclusions of Section E; that chromosphere-coronae are ubiquitous; so that a theory using only a photospheric radiation field is hardly realistic. So, as for the hot-coronal theory, one must incorporate a hot-coronal (+ chromospheric) radiation field in the radiative-acceleration theory, as well as a radiation field in the hot-coronal theory, and introduce a dependence of $U(\text{max})$ on the radiation field, and probably other, energy sources.

One should stress here that even those astronomers who admit problems in modeling $U(\text{max})$ are apparently content with the modeling of dM/dt . For example, for the hot stars, the above-cited authors note the agreement between the predicted L^2 (for an $\alpha = 0.5$, Abbott's latest results) and the "presently-observed" exponent of 1.8–2. But here, one should strongly stress: possibly the L^2 dependence is *empirically* valid, even though its diagnostic inference depends on observational diagnostics applying the questionable $U(r)$ from the theory. But, if the theoretical basis for using eq. (3.41) for $U(r)$ is incorrect, so also is it incorrect to use the theoretical expression (3.42) for dM/dt . These two theoretical expressions are either mutually required, or mutually excluded; there is no middle ground. One can always repeal the validity of the parent eq. (3.40) and try to find another parent equation producing the expression (3.42). There is nothing sacred in any of these equations; they are all approximations, to some degree. One must simply admit that as it stands, the radiative-acceleration theory doesn't work, in representing $U(\text{max})$ and $U(r)$. Nor, of course, does the hot-coronal theory, as it stands. But for it, a minimum change is obvious: don't contract (3.C) to produce (3.47). Without this contraction, the so-called Parker condition, or perfect wind-tunnel condition, of $U = q$ for the first time at $q^2 = W^2/2$ is neither necessary nor justified. We see in Part III that this contraction also contracts the number of distinct atmospheric regions, in contradiction to observations. We consider these points further, there. Here, we only emphasize the failure of both theories to represent the observed $U(\text{max})$, and the clearly inadequate data on $U(\text{max})$ for the cool stars.

(S-2) Because the literature is so full of references to the so-called observational confirmation of the $U(r, \text{max})$ predictions of the radiative-acceleration theory, it is useful to put the actual situation into sharp focus. The original broad discussion of Copernicus data on 47 OB stars by Snow and Morton (1976) found a lack of correlation between U (blue-edge) and V_{esc} . The original CAK theory, and various summaries of it, produced various α in the range 0.7–0.9, or U_s/V_{esc} lying between 1.5–3. Abbott (1978) added 18 stars to the Snow-Morton measures; but discarded half of these 65 stars because their blue-edges were not abrupt, hence, not suitable to test the theory. His least-squares solution of a linearized approximation— $U = U_s(\text{thermal}) + a V_{\text{esc}}$ —to eq. (3.43), like eq. (3.46), gave $U_s = 540$ km/s and $a = 2.4$. Abbott ignored U_s , and stated that uncertainty in the data meant a could be taken as 3; this has been the basis for his widely-quoted "empirical law" $a = 3$, $\alpha = 0.9$ (Cassinelli, 1979). Clearly, $a = 2$ is preferable from these data; nor should U_s be ignored. Cassinelli also noted that this result was in apparent accord with the Barlow and Cohen (1977) empirically-determined $dM/dt \sim L^{1.1}$ which, from eq. (3.47) corresponds also to $\alpha = 0.9$. Abbott's late-1981, early-1982, already-quoted results give $\alpha = 0.5\text{--}0.6$, $a = 1\text{--}1.2$. Barlow emphasizes that this means the theory is inadequate for stars hotter than about B8, because the Hutchings and von Rudloff data show $a \sim 3$ only earlier than about B1, dropping monotonically thereafter. Abbott's and Cassinelli's (1980) observations show the same. Abbott's most recent, mid-1982 (1982b) approach takes, empirically, $U_s = 0$, and: $a = 2.5$ at $T_{\text{eff}} = 5 \times 10^4$ K; $a = 3.5$ at 2.5×10^4 K; and 1.0 at 1×10^4 K. In (1982b), Abbott feels confident enough in this procedure to assert that he can predict $U(\text{max})$ for OB stars, when one lacks direct measures, with an uncertainty of some 20 percent. The literature is now too full of well-documented variability and individuality, in addition to the above-summarized departure from the predictions of this radiative-acceleration theory, for such statements to be taken seriously: cf Fig. 3-33. Unfortunately, such statements continue to be quoted, particularly by speculative-theoreticians wanting simple relations to be used in various applications which are, therefore, of dubious value.

(S-3) Barlow (1982) also focuses on other problems connected with the $U(r)$ distribution. He particularly emphasizes the problems with the too-small observed ratio of emission to absorption parts of the line, in those theoretical computations based on this radiative-acceleration theory. The reference-frame, for such statements, is the Castor and Lamers catalog of the expected P Cyg profiles (1979) coming from such a model. Relative to eq. (3.46), the analysis of Copernicus data on N V profiles in 82 stars by Abbott et al. (1982) would require $\beta \lesssim 0.05$ for some MS, and $\beta \sim 0.1\text{--}0.2$ for sg, thus suggesting very steep $U(r)$. To this material, of course, one should add that no B MS stars show P Cyg profiles in the farUV, only pure absorption profiles; so the worry is aggravated. Barlow notes various proposed remedies, including superthermic turbulence (Hamann, 1981). He also cites the discussion by Lamers et al. (1981) of multiple absorption components in some superionized lines of some stars; which Lamers et al. label "discrete shell absorption components" and assert have velocities of some $0.75 U(\text{max})$. (We referred to these in Section E; we return to them in Part III.) One alternative suggested by them is separate, and

colliding, mass-shells. Barlow compares these components with the “superthermic, colliding, blobs” of Lucy and White (1980) and Lucy (1982). Clearly, such differential superthermic motions heat the atmosphere strongly. In the same way, Cassinelli’s suggestion of a low-lying, thin, corona is variously suggested as an alternative source to produce the superionized lines. The interesting thing in all these phenomena is their neglect, in formulating the basic flow pattern of the radiative-acceleration theory, of any atmospheric pattern coming from nonradiative heating. Those source-sink terms associated with nonradiative heating are also neglected in the radiative-transfer calculations underlying the above catalog of predicted line-profiles. As mathematical exercises, possibly such models are interesting; but it is hard to take seriously their suggested ways to remove observational discord until these ways include what we know about real-star atmospheric structure. Again, I stress: the basic problem is a decision on the independence of mass-flux, or its predictability, from other atmospheric parameters. Such decision characterizes the basic problem of the hot-corona theory. The problem of the radiative-acceleration theory is even more basic: to decide to include *both* nonradiative flux and mass-flux as parameters additional to the radiative flux and gravity that it presently uses. The hot-corona approach, which Lucy-Solomon and their successors reject, had already taken the step of including the nonradiative flux as a parameter to be specified independently of radiative flux and gravity. Some of its proponents had narrowed this freedom, by imposing that only a particular kind of nonradiative flux was admissible—that speculated to be applicable to the Sun—but that restriction was, observationally, shown invalid. And, at the moment, those applying the hot-corona model do not demand that all stars have the same kind of nonradiative energy-flux; so there are three independent parameters to be specified.

(S-4) Effectively, (S-1)–(S-3) focus on U (max), and the quantities upon which the several theories permit it to depend. But a major point is the phenomena of individuality and variability. Under the radiative-acceleration theory, there is no way these two phenomena can be incorporated, without changing the basic structure of the theory. For U (max) to vary, one demands a change in V (esc)—that is, in either g or photospheric radius, or both. The models considered do not include such change. Presumably, the models could incorporate a variable, or individual, dM/dt by allowing L to vary. Again, under these models, there is no freedom to permit such change in L . And, again, the simplest way to include such variability seems simply to incorporate those features excluded, a priori, from the model: a nonradiative energy-flux, and a nonthermal subatmospheric structure which imposes the size, but not velocity nor energy, of the mass flux. The last comment can also be made for the hot-coronal theory. But, at the moment, its proponents are trying to see whether adding magnetic effects can resolve their problems: either by inhibiting flow, as in solar-coronal magnetically-closed, non-hole regions; or in adding energy, as by Alfvén waves (cf the Solar volume, Jordan, 1981). It is difficult to see how these effects, alone, can resolve such individuality and variability across the HR plane.

So a summary of our present empirical knowledge of superthermic, systematic mass-flow finds it universally present, across the HR plane, in some parts of each exophotosphere. Generally, U (max) is *very* superthermic; our uncertainty in U (max)/ q (max) lies in both U (max) and T_e (max). Also, for some stars like the Sun and most WR stars, expansion continues at this U (max) to very large distances; in others, like the Be and T Tauri types, U (cool, H α envelope) is considerably less than U (max), close to the star. For the Be stars, the velocity ratio is as small as 1/10; for the T Tauri, we are uncertain about both U (max) and U (envelope). The major question remains the uncertainty in the precise value of U (max), in various stellar types, and what this signifies in terms of the energy loss from the star by such mass-flux, as compared to radiative loss. We recognize the considerable variability and individuality among stars. Then, to answer the question, there are two major uncertainties.

[1.] What is the actual U (max), as compared with the various values measured by presently-accessible means? The solar case, compared to its cool-type neighbors—both quasi-normal and the peculiar like T Tauri—presents the outstanding example/proof of our present observational limitation. Note that a major aspect of the problem is just where the acceleration occurs, in terms both of having sufficient material there to detect the velocity, and of the location of the decelerating regions for some stars. For the Sun, Zirker (1981) abstracts the situation as at least half U (max) reached before 5 radii. With a highly-variable mass-flux, and its presumed effect on deceleration, one is simply ignorant. We know only that the Be star 59 Cyg reached U (max) \sim 2000 km/s, for brief periods, during

epochs of strong mass-flux variability. In my eyes, the uncertainty on U (max) begins in the mid-B-Be stars and extends to the whole cool part of the HR plane, excepting only the Sun; and for it, we need diagnostics of the type that only SOT + EUV will produce.

[2.] What are the nonradiative energies associated with the mass fluxes moving at these U (max)? Table 3-11 simply takes the U (max) of Fig. 3-33, and the range of mass fluxes found in the literature for the various types of objects, to compute $0.5 (dM/dt) U^2$ (max). Note the range of stellar types for which this nonradiative energy-flux associated with the mass-flux is hardly insignificant relative to the radiative flux. But, to me, its variability for a given star, and individuality among stars of the same "normal-standard type" are as significant as its actual size, in terms of modeling: both for the thermodynamic basis of the modeling, and the actual models. Also note the difference if we take the solar 800 km/s for U (max) of all the cool stars, instead of their presently-assigned values. Let me emphasize: these energy values are those which, somewhere, at some epoch, are carried by the mass-flux. They are not necessarily those carried away from the star by the mass-flux. For the Sun, and WR, and other stars, they are. They are not, for the Be, and other, stars; for these stars, some of this energy is dissipated in the atmosphere, by the decelerations which produce the "local environment" including the H α envelope. Let me equally emphasize: this maximum energy carried by the mass-flux at some atmospheric point is not necessarily given it at the base of the atmosphere, as is apparently the case for the novae. Depending on the star—and possibly the phase of the star—this energy is supplied by both that nonradiative flux which does not transport mass and the radiative flux. These two conclusions emphasized are empirical-theoretical, not speculative-theoretical. They must be incorporated into any modeling, then into any explanatory theory.

2. Quasi-Random Flow Velocities

There were epochs when any discussions of velocity fields in stellar atmospheres focused wholly on that type of convection thought responsible for solar granulation and associated phenomena; on thermal diffusion to provide that chemical separation thought necessary to explain the Am star spectra; and on quasi-random motions called "astronomical turbulence," which were invoked to explain both anomalous line-widths and total absorption. The two former were distinctly subthermic. The latter was mainly subthermic in most stars; but there were many cases where the inferred velocities were superthermic. The classic historical examples covered a wide range of stars. Roseland (1929) suggested stellar atmospheres should be turbulent, if they rotate, because a Reynolds' number based on stellar diameter and rotation velocity far exceeds the 10^3 value set by historic laboratory studies for the onset of turbulence. McCrea (1929) introduced the idea of turbulent elements, maintained in a near-Gaussian distribution as are thermal gas atoms, to provide the support mechanism for the solar chromosphere. Struve and Elvey (1934) introduced an astronomical turbulence to describe the line-broadening mechanism, and its effect on total absorption, in 10 F-type supergiants. Many of the inferred velocities were superthermic. Chandrasekhar (1934) objected to McCrea's Gaussian distribution as requiring collisions, which would stop the turbulence by dissipating its energy; and proposed instead a checkerboard chromosphere composed of gently rising and falling columns. The idea of turbulent elements was more popular, and universally adopted; Chandrasekhar's objection of collisional energy dissipation was simply ignored, for a decade; all models were RE, and HE under this "kinetic pseudo-temperature" of combined thermal and turbulent motions. Under the impact of Edlen's hot corona, the energy-dissipation problem was re-opened. Unsold (1930) had identified solar granulation with convection, which could be laminar or turbulent. Biermann (1946) and Schwarzschild (1948) proposed that the turbulent pressure fluctuations of such convection produce acoustic waves which, as they propagate upward, steepen into weak shock-waves and heat the corona. Under the combined stimuli of Redman's (1942) demonstration of the atomic-mass dependence of chromospheric line-widths, and Roberts' (1945) investigations of Secchi's spicules, Thomas (1948a) extended Chandrasekhar's objections by proposing that *all astronomical turbulence, in whatever star, was a blend of a T_e ($>$ RE value) and systematic mass-motions*. Observation or inference of any superthermic motion, whether called systematic or turbulent, must be taken to imply a T_e larger than the RE value in that atmospheric region. One was forbidden, thermodynamically, to postulate a superthermic turbulence without admitting also a nonRE value of T_e .

Table 3-11
Mass-Loss Kinetic Energy Relative to Radiative Energy

Stellar Type	L/L_{\odot}	$U(\text{max})$ km/s	\dot{M}'	KE/L_{\odot}	KE/L
WR-field	$1-6 \times 10^5$	1000-3500	3×10^{-5}	$10^3-3 \times 10^4$	0.003-0.3
O sg	$1-20 \times 10^5$	1000-3500	$10^{-8}-10^{-5}$	$1-1 \times 10^4$	$10^{-6}-0.2$
B0-B1 sg	$1-8 \times 10^5$	1000-3500	$10^{-7}-10^{-5}$	$10-10^4$	$10^{-5}-0.1$
B2, etc. sg	$2-10 \times 10^4$	1000-2000	$10^{-7}-10^{-6}$	10-300	$10^{-4}-0.1$
A0 sg	$1-6 \times 10^4$	250	$10^{-9}-10^{-7}$	$10^{-2}-0.5$	$10^{-7}-10^{-5}$
M sg	3×10^4	10-100	$10^{-7}-10^{-6}$	$10^{-3}-1$	$10^{-7}-10^{-5}$
O9-B0 IV-V	$1-7 \times 10^4$	1000	$10^{-9}-10^{-8}$	0.1-1	$10^{-6}-10^{-5}$
O9e-B0e IV-V	1×10^5	1000-2000	$10^{-9}-10^{-7}$	0.1-30	$10^{-6}-10^{-3}$
BXe	10^3-10^4	500-2000	$10^{-10}-10^{-7}$	$10^{-3}-30$	$10^{-7}-10^{-2}$
Sun	1	300-800	3×10^{-14}	$<10^{-6}$	$<10^{-6}$
novae (episod)		See text, Chap. 3, Sect. II.A.1.b.ii.			3
PN, OBsd, etc.		See text, Chap. 3, various.			

Since the epochs of these above sets of suggested alternatives to the problem of modeling line-widths, and total absorption or emission in lines, which exceed the values permitted in thermal atmosphere under an RE- T_e , and of modeling extended atmospheres, the astronomical literature has simply continued to present, side-by-side, treatments of "superthermic turbulent" and nonRE-dynamic, atmospheres. The treatments are both diagnostic of observations, and modeling of atmospheres or atmospheric regions. Almost invariably, those models which impose the existence of superthermic random motions without energy dissipation, also continue LTE-R, or pseudo-LTE-R, modeling, because it is difficult to develop a nonLTE source-function in the presence of random superthermic velocities without asking the coupling between them. We recall from Chapter 2 that the diffusion-scale, or thermalization-scale, is strongly dependent on the opacity, and this is related to the broadening function for the absorption coefficient. Indeed, a major motivation in the development of the modern nonLTE approach was to understand how to treat an atmosphere where T_e and T (radiation field) differ much more than RE permits (Thomas, 1948b).

I do not propose to try to summarize here all the background-observational, diagnostic, empirical-theoretical, speculative-theoretical-which exists on such quasi-random velocity fields in stellar atmospheres, their relation to more systematic velocity fields, and the relation of each to radiative-transfer problems. A number of us collaborated, in two symposia, to bring this material together: the IAU-IUTAM Cosmical Gas Dynamics Symposia, numbers 4 and 5, on Aerodynamical Phenomena in Stellar Atmospheres, at Varenna (1960) and Nice (1965) (Proceedings ed. Thomas, 1961, 1967). The situation relative to the impact of such quasi-random, nonthermal velocity fields on the structure of stellar atmospheres has not changed that much, in the intervening years. What has changed, is the situation summarized in Section E and preceding parts of this Section F: the characteristics of those atmospheric regions

not in RE, and of those where the systematic velocity field fixes the density distribution. But the reader should judge for himself, by reading the several articles in these two cited volumes, relative to the Proceedings of the 1979 Colloquium on Stellar Turbulence (ed. Gray and Linsky, 1980). Particularly, he should compare the 1979 summary by Traving, of the current approach to stellar atmospheric turbulence, to the several summaries in the 1961 and 1967 proceedings. And, a useful homogeneous comparison of evolution in thinking comes from comparing the 1979 summary by Bohm-Vitense, who is responsible for much of the modern development of the mixing-length approach to stellar atmospheric turbulence, to her 1960 and 1965 summaries. Again, I would simply caution against taking uncritically her picture of stellar chromospheres as only occurring, by definition, in stars which can produce them in the solar narrow range of T_e , instead of a chromosphere as representing the combined effect of a thermal, but non-RE, scale-height and the necessary range of T_e —varying with stellar type—to produce that situation. This distinction is critical, in distinguishing between a “turbulence” and a nonRE T_e to produce the density gradient of the immediate exophotosphere (cf Part III).

Part II

Some Thermodynamic and Gas-Dynamic Background for Use in Discussing Stellar Atmospheric Structure

Page intentionally left blank

Page intentionally left blank

SOME THERMODYNAMIC AND GAS-DYNAMIC BACKGROUND FOR USE IN DISCUSSING STELLAR ATMOSPHERIC STRUCTURE

Overall, the Foreword and Chapter 1 present the objectives of this monograph, and to some extent those of the series of which it is a part. The remainder of Part I compares the speculative-theoretical atmospheric models of a star assumed to be a (closed, thermal) thermodynamic system, in Chapter 2, to the real-world appearance of actual stellar atmospheres, in Chapter 3. The comparison negates the (closed, thermal) speculative character. Part III assembles, empirically-theoretically, the detailed characteristics of the distinctive atmospheric regions comprising the actual atmosphere, the several types of distinctive radial sequences into which these regions are distributed, and the local environments which form a prominent part of some types of such sequences. Throughout these diagnostics and syntheses we draw upon a broader range of thermodynamics than those Equilibrium and linearly nonEquilibrium varieties customarily considered in astrophysics. This is particularly necessary when we attempt to demonstrate that the stellar mass-flux, whose existence demands an open thermodynamic system, must be treated as a quantity specified by the star's subatmospheric structure; such mass-flux is *not* predictable from those parameters which suffice to characterize a closed thermodynamic system. It is also important when we recognize that the star evolves from the disorganized ISM to the organized stellar concentration. Such evolution violates Equilibrium and linearly nonEquilibrium thermodynamics. We also draw more explicitly upon laboratory gas-dynamic studies than is customary in astrophysical attempts to represent those velocity fields inferred to exist in stellar atmospheres. This is especially marked in our attempts to synthesize the astronomical observations into coherent velocity patterns of different types depending upon the variability characteristics of the several nonthermal fluxes of matter and energy from the star.

So Part II was projected to contain a summary of these nonEquilibrium thermodynamic and laboratory gas-dynamic aspects which are underemphasized in the usual astronomical literature. In the thermodynamic aspects, such background makes more readily comprehensible our assertion/assumption in Chapter 4 that each aspect of the nonlinear transition in thermodynamic state of star to that of the ISM is represented by a distinctive atmospheric region and vice-versa. It was projected that the summary of some aspects of laboratory gas-dynamics would focus upon the nonlinear aspects associated with the gas-flow becoming superthermic and upon the phenomena attending the deceleration of such a superthermic flow. Thus we would focus upon the atmospheric density gradient being fixed by the gas-flow rather than the converse.

This Part II is now transferred to a second, supportive, volume to this one on atmospheric structure. The focus of this second volume will be just that mentioned on these two aspects—nonEquilibrium thermodynamics and astrophysical applications of laboratory gas-dynamics. As mentioned in Chapter 1, I am not sure whether this second volume will mainly contribute to, or mainly draw from, the observational/empirical results of this first volume.

Page intentionally left blank

Page intentionally left blank

Part III
**Overview of the Empirical Structure
of the Stellar Atmosphere
and Local Environment**

Page intentionally left blank

Page intentionally left blank

INTRODUCTION TO PART III

OVERVIEW OF THE EMPIRICAL STRUCTURE OF THE STELLAR ATMOSPHERE AND LOCAL ENVIRONMENT

A. EMPIRICAL-THEORETICAL PERSPECTIVE FROM PARTS I AND II

The star is a self-gravitating, exothermic, evolving, quasi-equilibrium concentration of matter and energy in the nonEquilibrium interstellar medium. Because it is self-gravitating, the star's structure cannot be homogeneous. Because it is exothermic, its structure cannot be modeled as either isothermal or locally-adiabatic. Because of the observed sizes of the radiative fluxes from the stars, we infer the principal source of the exothermic character to lie in nuclear reactions rather than in simple gravitational contraction. Because visually, most stars, at most epochs, do not exhibit large radiative, nor gross structural, variability; and because such nuclear energy production is highly sensitive to the local temperature and density; in a first-approximation one models stellar internal structure as hydrostatic, under quasi-thermal velocity fields. That is, energy transport is either by radiation or quasi-static mass-motion. That is, any nonthermal differential velocities such as stationary turbulence, and laminar or turbulent convection, are required to be sufficiently subthermal to neither perturb hydrostatic equilibrium nor dissipate significant nonradiative energy. Also, in such models, the rate of nuclear energy production is allowed only the very slow changes accompanying stellar evolution. It is not allowed any significant variation in short time intervals, such as would accompany transient, not evolutionary, thermodynamic changes in those regions where the nuclear reactions occur.

This first-approximation structure gives the star a (closed, thermal) thermodynamic character. Such quasi-Equilibrium stellar structure divides the star into three gross parts. Central are those regions where densities and temperatures are large enough to produce nuclear reactions, and whose detailed structure is fixed by these reactions and the imposed quasi-thermal conditions. Surrounding this central region is the stellar envelope, which simply transmits the energy generated in the center; and across which the quasi-Equilibrium thermodynamic parameters of pressure, density, and temperature decrease from their very high values in the energy-generating regions to their relatively-low, subsurface values. The upper boundary of the envelope is defined by the condition that no radiation directly escape from it to the ISM. Then the third part of this quasi-Equilibrium model is simply that surface region from which radiation directly escapes to the ISM. The function of the surface region is simply to radiate away from the star all the energy the star produces, but in quite different spectral regions from those in which it was produced, and from those in which it is transported from the envelope into the atmosphere. Because gravity significantly inhibits particle, but not photon, escape, this model explicitly neglects energy carried away by a mass-flux, as well as the mass-loss itself. So "fluorescing-screen" is an appropriate description-caricature of the role of the surface region, as it was in our use of the term to characterize the role of the ejected photospheric shell in Pottasch's nova model, because this first-approximation to the surface region focuses only on the imposed thermal states of its lower and upper boundaries, not on the self-consistent physics of its internal structure. Its lower-boundary interface with the upper envelope is imposed to be a hot LTE region, with *hot* defined by the radiation *density* there; and its upper boundary is permitted to be a cooler, nonLTE-R region, with *cooler* defined by the radiation *flux* there. The structural/diagnostic relations between radiation flux, radiation-density, matter-temperature, and matter-density in this surface

region are provided by modeling it as a particular kind of gaseous atmosphere, in a hypothetical kind of thermodynamic state, whose properties are fixed wholly by the gravity and radiative flux from the star. Stellar atmosphere and environment are uncoupled except by the radiative flux. So long as all the above is physically self-consistent, and presents no strong contradictions with observations, such an atmosphere consisting of such a single region, the standard photosphere, suffices to translate observations into reasonable inferences on the structure and evolution of the stellar interior, and atmospheric chemical composition.

So long as one could continue to describe the atmosphere as this kind of a fluorescing-screen, which responds as a whole to changes in thermodynamic conditions at the envelope/atmosphere interface, one could extend its use beyond wholly-thermal HE models in translating observations into nonthermal interface conditions and change in conditions. As discussed in Chapter 3, one could diagnose *some* observations of pulsating variable stars, where the pulsations reflect thermal instabilities in the envelope. One might even diagnose observations of the early phases of cataclysmic stars, if these consisted simply of ejection of an atmospheric layer without differential motions of compression, and unchanged thermodynamic state of the envelope. That is, one could describe leisurely mass-motions of the atmosphere as a whole which do not lead to mass-loss; or violent motions leading to mass-ejection, or intermediate phenomena; so long as mass-motions and radiative fluxes were only quasi-adiabatically, not dissipatively, coupled. In essence, one would preserve the single-region, standard-photospheric, character of the atmosphere by restricting the size of differential motions.

However, Chapter 2 showed that the structure of the surface regions of the star cannot be described by any variety of LTE without risking significant error in relating size and spectral distribution of the radiative flux to T_e and to atmospheric structure. Also, Chapter 3 showed that nonRE effects sometimes accompany nonHE effects during some phases of the above atmospheric motions. Then admission of a possible nonthermal nonLTE structure of these regions becomes imperative. Guidance comes from the Chapter 3 exposition of the contrast, similarity, and variety of atmospheric conditions observed among the different kinds of stars. When one observes some atmospheric regions, in some stars, to be much cooler than the boundary temperatures predicted by quasi-thermal nonLTE modeling, one questions the validity of exophotospheric T_e fixed by photospheric RE. When one observes atmospheric regions whose T_e are much hotter than T_{eff} —even hotter than T_e at the top of the envelope—the neglect of all fluxes except radiative becomes inadmissible. When one observes atmospheric regions moving at speeds higher than thermal ones corresponding to the T_e in any part of the stellar atmosphere, the restriction of models to thermal cannot be retained, nor can the relation of such velocity fields to atmospheric structure be ignored. When one observes significant continuous mass-loss from stars, these cannot be modeled as closed systems. When one observes an apparent self-interaction of variable mass-flux in some stars, producing a local-environment at widely-varying distances from the photosphere, one realizes the atmosphere must be modeled as a symbiotic transition-zone to the ISM, not simply a boundary for the star. When one observes coronal phenomena inversely correlated with extent of this local-environment, one realizes it may veil some atmospheric regions. When one observes continuous variability in some of these atmospheric regions in some stars, and occasional variations in them in most stars, in times short compared with evolutionary, one questions the utility of quasi-Equilibrium, thermal, modeling. When one observes time-dependent, disparate observational prominence of these different atmospheric regions among stars exhibiting the same radiative flux and gravity, one begins to question the whole thermodynamic basis of the modeling—of subatmospheric conditions as well as atmospheric.

We recognize that we must allow the star to have, a priori, an unrestricted thermodynamic character; we must ask, not tell, each star, what is its thermodynamic character, and what is its detailed thermodynamic structure—atmospheric and subatmospheric.

The basic question is whether the various items in the above list—of thermodynamic inconsistencies, and anomalous atmospheric regions—are particular or general? The thermodynamic inconsistencies are quite general, as regards the need for at least a thermal nonLTE; one searches the possible variety of nonthermal nonLTE. One asks whether various kinds of nonthermal conditions and regions, not all of which are found in all stars at all epochs, are intrinsically different in different parts of the HR diagram? A primary example is the existence of atmospheric regions

showing superthermic and superescape flow-velocity. Among the cool, solar-like, stars these winds are theorized to originate in a hot corona, which is in turn assumed to be heated by a nonradiative energy dissipation linked to rotation and magnetic fields. Among the cataclysmic—and possibly symbiotic—stars, binary mass-exchange and resulting subatmospheric explosions are theorized to eject the wind. If indeed all mass-loss arises in such particular circumstances, then, presumably, somewhere on the HR diagram there do not intersect such a particular set of circumstances which invalidate the proscription of the first-approximation, standard model of no such mass-loss. If, however, such mass-loss is indeed ubiquitous over the HR plane, then one must change the basic thermodynamic character of stellar modeling to (open, nonthermal) from (closed, thermal), and ask how to incorporate a nonthermal mass-flux into the thermodynamic scheme. Under the (closed, thermal) thermodynamic characterization, a star *must* return a radiative energy flux to the ISM; and production and propagation of the flux must be modeled in generality. Under the (open, nonthermal) character, a star *must* return radiative and nonradiative energy fluxes, and a mass-flux, to the ISM; and propagation of each of these fluxes must be modeled, in equal generality.

We can only decide between the particular-circumstance, or general-thermodynamic, character of these thermodynamic inconsistencies and anomalous atmospheric regions by modeling them everywhere across the HR diagram, among peculiar and normal stars alike. One realizes that at this moment, there exists little general theory for describing the expected characteristics of general, nonlinear, nonthermal, open nonEquilibrium thermodynamic systems. So, one appreciates the potential guiding role of the observational characteristics of the distinctive regions comprising the transition-zone between one kind of (open, nonthermal) system, the star, and its environment, the ISM. So in this Part III, we try to synthesize: the thermodynamic inadequacies of existing astronomical models; the observational characteristics of the various kinds of atmospheric regions that occur in various stars at various epochs; the several radial sequences of such regions as they appear in various stars at various epochs; and inferences on what physical quantities appear to determine these observational characteristics and sequences. This, I call an empirical-theoretical model: generally, for all stars, in the sense that it represents the variety of atmospheric patterns permitted in a star that is an open thermodynamic system; specifically, for some star, at some epoch, if one is given values of all those parameters necessary to specify such an open thermodynamic system. How this atmospheric pattern relates to the sub-atmospheric structure of the envelope, and to the structure of the central, energy-producing regions, is another problem, lying outside this monograph. And, I stress that this empirical-theoretical atmospheric structural pattern, general or specific, and the algorithms to produce it, are presently highly preliminary and highly incomplete. I hope they will be rapidly improved and extended—but without substituting mathematical rigor at the expense of omitting some of that basic physics which the observations show to be absolutely necessary. Again I stress: we search equations to represent the observations; not observations to satisfy some set of equations that were produced, speculatively, without looking at the data. We saw the example, in Chapter 3, of equations contracted from their general form in order to produce a theory, not satisfy observations, of mass-flux.

The approach of this Part III is the following. Chapter 2 put into focus the thermodynamic approximations, and their consequences, which underlie the structure predicted by the standard atmospheric models—LTE, LTE-R, or thermal nonLTE. It also summarized the presently-incomplete status of the models' predictions on T_e in their upper regions. But it emphasized that this incompleteness is important mainly in trying to compute how much non-radiative energy must be dissipated to cause a significant rise in T_e . For this Part III, this incompleteness is reflected in estimates, using such standard models, of maximal beginning heights for the chromosphere, from a given mass-flux.

Chapter 1 summarized the immediate stimulus for looking at the possibility of nonthermal, exospheric atmospheric regions: namely, the long-observed presence of various kinds of nonthermal, differential, velocity fields in stellar atmospheres; some of which appear to be superthermic; all of which appear to be linked to atmospheres extended beyond thermal-model predictions. All available gas-dynamic experiments and theory would demand a mechanical energy dissipation from any differential superthermic velocities which are not of the linear, perfect-nozzle, thermal-expansion, type. So the program focuses on taking the nonthermal velocity fields, especially the superthermic ones, as observationally-given, and asking their thermodynamic consequences on atmospheric structure. The problems in such an approach were, historically, two: (i) Almost all the existing data came from low-resolution observations in the visual spectrum. (ii) Almost all observational diagnostics of these data rested on the assumption

that the methodology, and results, of such diagnostics were not perturbed by the presence of such nonthermal velocities, and by any phenomena associated with their presence, such as nonradiative heating and nonthermal atmospheric extension.

(i) Chapter 3 outlined how a focus on peculiar stars could use even low-resolution visual data to exhibit the presence, in the atmospheres of such stars, of nonthermal phenomena—especially velocity fields, atmospheric extension, variability in a given star, and individuality in amplitude of such phenomena among “similar” stars. Higher-resolution data, and observations outside the visual region, elaborated and detailed these phenomena. Chapter 3 also outlined how nonvisual spectral observations exhibit the common existence of some nonthermally-produced atmospheric regions in normal and peculiar stars alike, across the HR diagram.

(ii) Part II, which is Volume 2, puts into focus the effects of allowing nonlinear, rather than imposing linear, distribution functions and boundary conditions. Such effects occur in both diagnostic methodology and results, and in those thermodynamic conditions in stellar atmospheres required by such diagnostics. Part II also puts into focus the thermodynamic effects of adding nonthermal terms to the thermal equations of, and conditions imposed on, standard modeling; and of not restricting the amplitudes of the nonthermal terms. Part II is now Volume 2, hence not available simultaneously with this Volume 1. However, it contains only well-known aerodynamics, and some less-familiar thermodynamics, simply discussed from the observational-astrophysical viewpoint of stellar atmospheres and thermodynamically-open systems.

So given these data on what kind of thermodynamic conditions exist in the atmospheres of both peculiar and normal stars, coming from observations in both visual and nonvisual spectral regions, we can proceed to ask what kinds of distinctive, nonthermal, regions exist in stellar atmospheres. That is, we ask whether we can represent this range of observations of the variety of physical conditions existing in the variety of stars in terms of a limited variety of distinctive atmospheric regions. This variety of distinctive atmospheric regions is to exist everywhere across the HR diagram—not just among limited classes of stars. These regions all have nonthermal properties, and are both photospheric and exophotospheric. Observationally, some regions are more prominent than others, in different kinds of stars, and in different stars of the same kind, and in some phases of a given star relative to other phases. We do not speculate, theoretically, that such distinctive regions exist: we are led to their existence, and the definition of their characteristics, observationally. Ultimately, as stressed above, we seek to construct sets of equations which will predict the existence of such regions, with these distinctive characteristics, as functions of the fluxes imposed from the subatmosphere. The difference in importance—thermodynamic and observational—of different regions sometimes produces sequences of stars based on that relative importance. Chapter 4 considers the regions: Chapter 5 details the several atmospheric structural patterns which, empirically, seem to exist in the gross pattern of radial distribution. The variability of such patterns, and of the observational prominence of the several atmospheric regions, is also heavily stressed, as giving insight into subatmospheric structure.

Finally, in Chapter 6, I present perspective on those empirical atmospheric structural patterns displayed in Chapter 5. The patterns are specified by the outward radial evolution of the parameters characterizing their thermodynamic states. The patterns are interpreted in terms of size and time-dependence of energy and mass-fluxes, of the gravity that conditions their relative importance and so the thermodynamic character of the system, and the properties of the self-interaction, and interactions with the local ISM. Hopefully, the final conclusions will not only give a better picture of the stellar-solar atmosphere-environment ensemble, but also begin a case study of one kind of open thermodynamic system, which arises from exothermic concentration in its parent medium, and ends in a configuration more highly-organized than was its beginning.

Thus the discussions in Chapters 4-6 rest fundamentally on the variety of atmospheric conditions found in the variety of stars observationally-summarized in Chapter 3. Any attempted synthesis of such data into a pattern of coherent thermodynamic properties of distinctive atmospheric regions must rest, equally-fundamentally, on observational details from individual stars and stellar types: the variety of such details, the sometimes apparent contradictions of such details. To avoid regional, and pattern, characteristics being obscured for the reader by such detail, I try to bring the overall picture painted by Chapter 3 into perspective, before starting the step-by-step developments of Chapters 4-6 based on these details from Chapter 3.

B. EMPIRICAL-SPECULATIVE PREVIEW OF DISTINCTIVE ATMOSPHERIC REGIONS, THE STAR'S LOCAL ENVIRONMENT, AND ATMOSPHERIC PATTERNS

The step-by-step, empirical-theoretical modeling launched in Chapters 4-6 may eventually lead us to a satisfactory model of star + environment, when we have enough data to reach unambiguous conclusions. At the moment, as will be seen in reading Chapters 4-6, there are too many gaps in the observational material for all the results to be unambiguous. So, many of the details necessary for solid conclusions are incomplete. Nonetheless, I think the broad outlines of the thermodynamic picture are clear enough that the eventual model can be previewed, at least broadly. Here, I try to present such a preview.

Given the predictions of the standard model, and their contrast to real-star observations in Part I; and the much-broader thermodynamic alternatives than those permitted in (closed, thermal) systems, as outlined in Part II; the gross thermodynamic problem of stellar modeling is clear. From among the three thermodynamic alternatives discussed in Part II—isolated, closed, or open thermodynamic character for the star—the presence of radiative fluxes excludes that stars are isolated systems; and the increasingly-general presence of mass-fluxes from any star carefully measured implies that few, if any, stars are closed systems. The only remaining choice is whether: (a) the actual mass-fluxes are so small that the star can be satisfactorily-modeled as a (closed, thermal) system, in which the mass-fluxes are only a small perturbation; or whether (b) the mass-fluxes are sufficiently-large, and have sufficient effect upon atmospheric structure, that the star must be modeled from the beginning as an (open, nonthermal) system. Then we can order, in six points, the observational evidence from Chapter 3—against the background of the standard, speculative-theoretical, thermal atmospheric model—in terms of increasing testimony from the stars, that alternative (b) is the only one compatible with the whole array of observations. If so the mass-flux is imposed, not predicted.

(1) Ubiquitously, in all stars in the HR plane for which sufficiently discriminating observations exist, we observe, to some degree, superionized and superexcited spectroscopic phenomena, relative to standard-atmosphere predictions. In some stars, of nearly all types across the HR plane, observed X-rays demand that the rise in T_e implied by these phenomena reaches $\text{o}(10^6 \text{ K})$. Such thermal energies, relative to stellar gravity, imply mass-loss from the star—a nonstatic outer atmosphere. But by themselves, these phenomena demand only a nonradiative energy flux and its dissipation; not that the mass-loss provides a major perturbation of the (closed, thermal) atmospheric structure. A chromosphere-corona is a major perturbation of that *standard* variety of a (closed, thermal) atmosphere, where only radiative energy fluxes are permitted. But a mass-loss from such a corona, if produced only by thermal evaporation (Chapter 2), or by linear atmospheric expansion under perfect-nozzle flow, does not provide a major perturbation on the density structure in the easily-observable regions. Such small-perturbation modeling is only quasi-adequate in the asymptotic limit of very small, and time-independent, mass-flux. As we saw from Chapter 3, Fig. 3-33, stars which can be approximately described by this limiting case have such low-densities in those atmospheric regions where very-large flow velocities occur, that these large velocities are undetectable by the usual spectroscopic methods. The Sun is a good example of what these large $U(\text{max})$ actually are, and of the collector-techniques necessary to observe them. These solar data demonstrate the inadequacy of the small-perturbation model even for the low-mass-loss solar case, where generally we cannot observe $U(\text{max})$.

(2) Again referring to Fig. 3-33, we find a wide variety of stars exhibiting, even by normal spectroscopic techniques, highly superthermal and superescape velocities—reaching $\text{o}(10^3 \text{ km/s})$ in even main-sequence stars, usually not exceeding some 10^4 km/s . The values can be highly variable within a given star; and highly individualistic among stars of the same (closed, thermal) classification. We have as yet no satisfactory way of predicting, or estimating, the nonradiative energy flux whose dissipation produces (1) above; it need not be that energy carried by a mass-flux. But we note that a mass-flux does carry nonradiative energy; and if its flow velocity is superthermal, or even reasonably-close to thermal, it can both dissipate nonradiative energy, and perturb the local density distribution away from an HE exponential law. In Table 3-12, we saw that taking the observed mass-flow velocities, and combining them with the range of estimates of the mass-loss, we find the kinetic energy in the mass-flow to be a significant fraction of the radiative flux of the star, in some cases. We note, of course, that this kinetic energy in the mass-flow can vary strongly

over the atmosphere; cf especially, (4) below. But the production of mass-fluxes with such energy content anywhere in the star removes them from the category of being small perturbations on (closed, thermal) models prohibiting mass-loss.

(3) From Chapter 3 we also saw the great variety of stars having a very extended atmosphere, and the variety of phenomena produced by such extent. The most extreme among such stars—the PN—reach 10^6 – 10^8 radii before particle concentrations have dropped to the 10^5 – 10^3 level required to produce the nebular spectrum. We also note that concentrations of 10^5 – 10^6 are those exhibited in the Sun at only some 3 radii, where the gas-flow becomes thermal. Such large particle concentrations far from the star occur in those stars having large mass-fluxes—the WR stars provide the outstanding example, but, as we summarized in Chapter 3, they are hardly exceptional. Large concentrations can also occur because of interactions between mass-flows having different velocities, produced at different epochs, which piles up material in a snowplow effect. Thus we distinguish two kinds of atmospheric patterns: extended atmospheres associated simply with a large mass-flux; and extended atmospheres associated with a variable mass-flux. The former represents a continuous gradation of atmospheric extent. For stars with common photospheric properties, we will see in Chapter 4 that the size of the mass-flux fixes the density concentration where the density gradient changes from exponential to an $(r^2 U)^{-1}$ law, thus it is the density scale-factor for the whole atmosphere. The WR stars and the Sun represent opposite extremes in the category of stars showing essentially-negligible variability in mass-flux; so that atmospheric extent is measured by only size of mass-flux. Out to $\alpha(>10^2)$ radii from these stars, the mass-flow velocity either accelerates or remains essentially constant. Thus estimates from (2) above of the amount of energy carried by the mass-flux also represent estimates of the amount by which the radiative luminosity underestimates the energy output from the star. This total energy, radiative output plus energy carried by the mass-flow, thus represents the total rate of energy return to the ISM from the star. In this sense, during one outburst, the novae resemble the WR stars; for apparently, at that episode, the nova only interacts with the ISM very far from the star, like the WR. We would, however, be most unrealistic if we insisted on such similarity; because even from classical, visual observations the novae and WR represent the opposite extremes of episodic vs. continuous mass-flow. And today, with the discovery of the continuous outflow from novae, they do not at all fall into this WR + solar class of stars having extended atmospheres; but, instead, into the class of extended atmospheres associated with variable mass-flux. And here, the major problem is just that of episodic vs. continuous mass-flow. Again, as above, we emphasize that certainly the WR size of extended atmospheres, but also the solar size—each corresponding to a star with constant mass-flux—cannot be modeled as only a small perturbation on a (closed, thermal) system, from whose energy flux, radiative and nonradiative, plus gravity, one can predict size of the mass-flux.

(4) From the preceding, we see that the thermodynamic property which distinguishes the second pattern of extended atmospheres is that of episodic combined with continuous mass-flux. Such variability for a given star, and individuality among stars of similar types, of the mass-flux and velocities associated with it, are strongly-observational features. But so are the basic features which distinguished this class of stars even before the detailed farUV studies of the velocity patterns. The universal existence of chromospheres-coronae represents a major perturbation on standard-atmosphere models; for extended atmospheres of the type discussed in (3), such high T_e , and superionization and excitation, can extend 10^2 – 10^7 radii from the star, in solar and WR types alike. But in this second category, (4), of extended atmospheres, there occurs, observationally, a decelerated and cooled envelope, at distances ranging from 3–10 radii for Be and T Tauri stars at some phases, to 10^6 – 10^8 radii for the PN. The interruption of a continuous mass-flow by episodic ejections, and variability of the velocities associated with each, occurs much more frequently for the Be than for the PN. In Chapter 3, we summarized the historical evolution of our picture of the PN envelope from this standpoint—the Be stars as “little” PN in terms of envelope size. We also summarized the historically-remarked similarity between nebular phases of novae and the PN—and the historic presumption that the episodic mass-ejection from each was a one-time affair—and today’s attitude change in each, coming from the farUV observations of a continuous outflow from each, at $\alpha(10^3 \text{ km/s})$. For each, we have no evidence of collisional interactions of the mass-flow at distances smaller than PN dimensions. We also summarized the sequential-continuity from the novae through the variety of cataclysmic stars—recurrent and dwarf novae—leading to the symbiotic stars, which

re-link to the Be and Bep. All are similar, in the sense of the presence of “quiet” phases between episodic eruptions; the quiet phases mimicking a late type cool star, molecular spectra, evidence of dust, very extended cool envelope; the eruptive phases producing a hot-star spectrum, resembling the Be, even Bep. In the following, we define these cool, very-extended but variable in distance from the central star, envelopes as the “local-environment” of the star. The star manufactures it, as it returns mass to its parental environment; but the variability in such return produces an environment closer to the star than in the case of constant outflow. Also, since there is a strong deceleration close to the star, the energy contained in the mass-flux is not transformed directly to the parental environment as in the item (3) kinds of extended atmosphere; unless one indeed chooses to regard the local environment as already part of the parental. But in any event, one would make the same underestimate of the star’s energy production, as in (3), if one identified it with the photospheric radiation field, as observed in the visual, and extrapolated to other wavelengths via a standard-atmosphere-model. We have already discussed the error we would make if we used only the visual radiation energy—or indeed only the total radiation energy—as measuring the star’s energy output during a nova outburst. Even though probably to a lesser degree, we have the same problem in assessing the total stellar energy output, and its partition among radiative and mass-flow energies, in this wide variety of stars showing this kind of extended atmospheric pattern. Again, the Be stars provide a provocative example: the Be phase is, statistically, one visual magnitude brighter than the B-normal phase—and it is significantly redder, a later, cooler, continuum. The Be-shell phase mimics an even later spectral class. The early, pre-maximal stages of the nova give a rise in visual brightness, but a cooling of the star—corresponding to the “veiling” effect of the ejected nova-shell, or mass-flux. In the post-maximal phases, when the mass-shell becomes transparent, this veiling diminishes, allowing the underlying hot-star spectrum to appear—and photoionize the expanding material—just as in the case of the post-episodic ejection of the PN. Clearly, in these *not*-ubiquitous phenomena of the “local environment” we have an even stronger perturbation of the (closed, thermal) model than in the chromosphere-corona perturbation. But the configuration is not at all what some speculative-theoreticians try to model as the post-corona: an RE-controlled, ultra-velocity expansion to the parental environment. Neither of the two broad classes of extended atmospheres fall into such speculative-theoretical replacement of the standard atmosphere.

(5) We summarized the fact-of-its-existence of the local environment. In discussing the range of stellar types exhibiting it, we alluded to its possible veiling effect—in the sense of both continuous and line spectral veiling and transformation, at whatever is the local T_e , and nonLTE, where $\tau_\lambda = 1$ occurs. But there are other diagnostic consequences of the existence of this local environment, to which we have referred in Chapter 3. Prominent among these was the discussion of the observed X-rays. Statistically, we noted the inverse correlation between X-ray intensity and strength of local environment, as measured by $H\alpha$ emission from the cool envelope, from the T Tauri stars. We also summarized the supporting evidence from a very few B vs. Be stars: the B stars, without local environment, producing stronger X-rays. But the results summarized by Fig. 3-33 suggest an even more provocative veiling: an obscuration of both corona, and the coronal-level velocities $U(\max) > q(\text{corona})$. For extended atmospheres of the first, nonvariable mass-flux, type, we suggested that those stars having such a small mass-flux as the Sun would have correspondingly-small particle concentrations in the regions of large U . So, as for the Sun, we would not detect it, spectroscopically. But for stars having extended atmospheres of the second, variable mass-flux, type, the local-environment may mask, as just suggested, both corona and coronal-level U . We note that the suggestion is hardly only conjecture. In Chapter 3, we summarized the Deutsch-Reimers evidence for Ca II ionization shells, the inner boundary being fixed by chromosphere-coronal ionization. The shells, and associated shell expansion velocities, are highly-variable in these MO–M5 giants. We also noted the Ca II K4, higher, velocities detected by Reimers for K-type stars. And finally, we emphasized the even-higher velocities found in the Mg II ionization shells, presumably occurring at higher T_e —closer to any “corona” than the Ca II shells. We have, in the marginally-observable veiling phenomena in the late-type stars, challenges to both improved observational delineation of what is actually there, and any modeling, even empirical-theoretical.

(6) Last, in this ordering of the evidence for considering the effects of an independent mass-flux to be overwhelmingly major, we have a kind of kaleidoscope finale: the phenomena of stellar symbiosis, of which the symbiotic stars simply represent an extreme concentration. Taking such phenomena in their historically-literal definition—a

combination of high-temperature and low-temperature spectral features; and the essentially homogeneous character of the standard photosphere; one requires either multiple exospheric regions or binarity to produce such features. Again, we distinguish the several kinds of extended atmospheres. The WR-solar type, constant mass-flux, can produce that variety of symbiosis typified by the Sun: cool photosphere, hot farUV chromosphere-corona. But symbiosis is, classically, visual: a cool M-type, a hot B-type, at varying phases. And this is precisely the variety of phenomena we have discussed as composing the pattern of distinctive atmospheric regions for the variable-mass-flux kind of extended atmosphere. So, we can readily represent the phenomenological range of symbiotic phenomena—the symbiotic stars themselves, and the symbiotic phenomena in stars not primarily classified as symbiotic in type—if the size and time-dependence of the mass-flux are admitted as being independent parameters, determined by a sub-atmospheric nonthermal structure. As emphasized in Chapter 3, this does not at all mean that some symbiotic stars cannot be binaries. It simply means that the binary character is not necessary to produce the observed symbiotic phenomena. It means that if we admit the mass-flux as a parameter, independent in the same sense that radiative and nonradiative energy fluxes are independent, then the atmospheric regional structure that results will produce, observationally, those phenomena labeled “symbiotic.” If the particular star observed is a binary, then each component will contribute to an observed “symbiosis” to its capacity according to the type of extended atmosphere it has. If, of course, one star is solar-WR type, and the other Be, one will observe essentially the symbiotic variation coming from the Be type. If both have a variable mass-flux, then since the relative observational contribution from the several regions depends upon the phase of episodic mass-ejection, the two stars can produce a combined pattern that is much richer than from one star alone.

Thus, I preview the eventual development of the several distinctive regions of the atmosphere, the several patterns they may form, and the physical parameters upon which regions and patterns depend. We recognize three, gross, radially-distributed atmospheric “sectors,” the characteristics of each depending upon the amplitudes and time-variability of the several fluxes of matter and energy. Lowest is the photosphere—whose character need not be that of the standard thermal model, so that several varieties appear. Next comes the chromosphere-corona, the “nonradiatively-heated” sector, which appears to exist, to some degree, in all stars. Then comes the post-coronal, dynamically-extended, sector, whose character is basically linked to that of the mass-flux. We recognize two gross varieties of the post-corona: one associated with a mass-flux that is effectively-constant over very long epochs; the other, with a mass-flux comprising a continuous flow and episodic ejections. The latter variety produces what we call a local environment, sometimes beginning very close to the star, often quite variable in location. Thus this third sector blends into the parental ISM. Each sector may comprise more than one distinctive region. If the subatmospheric structure is wholly thermal, we obtain only a radiative flux from the star; this energy flux measures the total energy output from the star; the atmosphere consists only of a photosphere. It is the nonthermal structure of the subatmosphere which produces the other fluxes, and their effects in producing the multi-regional atmospheric structure. In this monograph, we do not ask what is the subatmospheric nonthermal structure; neither its variety; nor its cause. We ask only its observed consequences. Part I surveyed these observational consequences.

Thus our basic problem is to obtain a kinematic delineation of the distinctive regions and patterns. Second, we ask what kinds of terms, in what equations, can provide this kinematic description. Third, we must ultimately ask the relation between these terms and subatmospheric nonthermal structure. We offer little progress on the third problem; marginal progress on the second; and sufficient progress on the first to delineate a first-approximation to regions and patterns. However, we at least recognize the existence of these three problems, and put them into perspective in terms of the star as a thermodynamically open and nonthermal system. This is in contrast to the great bulk of current speculative-theory, which does not put these problems into such focus, universally, everywhere across the HR diagram.

4

CHARACTERISTICS OF DISTINCTIVE REGIONS COMPRISING STELLAR ATMOSPHERES

I. INTRODUCTION

To be precise in characterizing the distinctive regions comprising the stellar atmosphere, we return to Chapter 1. There, we defined the atmosphere as the transition-zone between stellar and interstellar states of matter and energy. If the atmosphere has distinctive regions, the transition between stellar and interstellar states must have distinctive aspects; and each such aspect must be associated with some region. Specifying “state” means specifying: (i) storage-modes of matter and energy; and (ii) propagation modes for their fluxes, which exist because neither star, nor atmospheric regions, nor storage-modes are adiabatically isolated. So “transition” means the spatial evolution of storage and flux-propagation modes across the atmosphere; and each aspect of the transition evolves across a distinctive atmospheric region with which it is associated. Such spatial evolution lies in both the kinds of modes and in the degree of nonEquilibrium characterizing the particular state-parameters required to specify storage and propagation. Then we must carefully distinguish two kinds of spatial evolution: that in numerical value of a particular state-parameter across a distinctive region; and that in a particular mode of storage or propagation. We presume that such spatial-evolutionary aspects are observationally-exhibited in the distinguishing characteristics of the several distinctive atmospheric regions comprising the atmosphere. To establish consistency between transition-aspect, and characteristics of distinctive region, we iterate. We iterate between nonEquilibrium-thermodynamic understanding of transition-aspect, and empirical-theoretical delineation of characteristics of distinctive atmospheric region in their thermodynamic formulation. In this Chapter 4, we make precise the results of such iteration to identify regional characteristics with thermodynamic transition aspects.

For example, the classical, speculative, standard, thermal atmosphere consists of one distinctive region, the photosphere, across which the LTE state-parameters of temperature and density change. But in parallel, the form of the photon storage function, J_ν , evolves from locally-Planckian at the base of the photosphere to distinctly non-Planckian at the top; and the photon transport quantity, I_ν , evolves from near-isotropy at the base to essentially equaling the flux at the top. The neoclassical, speculative, standard, thermal atmosphere consists of two distinctive regions: classical and neoclassical photospheres; LTE-R lower-, and nonLTE upper-, photosphere. The thermodynamic characteristic of the latter is the evolution of thermal storage in energy states of matter: from LTE-R to thermal nonLTE across it. But when one goes to the nonspeculative, real-world photosphere, one adds another storage quantity, nonthermal energy modes, and another transition aspect, the evolution of some of these from pure storage to dissipative across the photosphere. A priori, we do not know what these nonthermal modes are; they are to be determined. But a star having a photosphere without them, and their spatial-evolutionary character, will have no exophotospheric, chromospheric-coronal, regions.

The photospheres discussed in Chapter 2 are speculatively-theoretically-predicted distinctive atmospheric regions. By contrast, our focus in this chapter, and this Part III, lies on those distinctive atmospheric regions whose existence, and properties, have generally been identified empirically-theoretically; but which, generally, have no classical-theoretical basis for existing. The distinction arises because general astronomical focus has, historically, been

on regions compatible with the (closed, thermal) modeling of a single star, and on the kinds of physics necessary and sufficient for modeling, and diagnosing observations, of such regions. When there have been significant observational discrepancies with such theoretical atmospheres, the tendency has been to try to vary any theoretical predictions wholly speculatively, within the hypothetical (closed, thermal) framework, and see what “perturbed” atmospheric scheme could be produced. Or, alternatively, some astronomers look for resolution in multiple stars—each of the (closed, thermal) variety—so that each star has a “standard” atmosphere. Here, by contrast, we seek resolution in anomalous and peculiar, empirically-inferred, single-star, atmospheric regions whose existence demands an (open, nonthermal) star. I re-emphasize: the approach of this chapter *assumes* that the peculiarities and anomalies summarized in Chapter 3 can be resolved by this empirical-theoretical introduction of a multi-regioned atmosphere, even though there is no accompanying theoretical justification for the several regions produced by the approach. A strong justification for such a multi-regioned atmosphere can be exhibited if one demands that all stars be (open, nonthermal) systems, and produce independent fluxes of radiative and nonradiative energy, and of mass. In that situation, a sufficiently-varied array of aspects of transition between star and ISM can be found to produce an expectation of multiple distinctive atmospheric regions. The theory for such a configuration has not been developed to the point where characteristics of such regions can be actually predicted—indeed, we do not know precisely which characteristics of a star, added to its mass and composition, must be specified in order to predict values for such fluxes. Consequently, the validity of the assumption that a star *must* be characterized as an (open, nonthermal) system—consequently that the atmosphere *must* be multi-regioned—remains to be shown. As already stressed, the observational decision between the two alternatives of (closed, thermal) and (open, nonthermal) lies mainly in how we interpret the observed mass-fluxes: as something basic to the star, of wide range in possible amplitude; or as something of limited amplitude, capable of being produced by a small perturbation on a (closed, thermal) system. In this Chapter 4, and Part III, the only real test is which alternative gives the most thermodynamic consistency.

Then the overview of this Part III raised a major question. Can we interpret as general-thermodynamic, or must we consider as particular to the coincidence of several circumstances, the several characteristics of peculiarity and anomaly in demanding the existence of some particular distinctive atmospheric region? If the former—if the existence of the particular distinctive region requires some general thermodynamic characteristic of the star that is not included in models based on the (closed, thermal) character of the star—then the region should be intrinsically present in all types of stars across the HR diagram. It may differ in its observational prominence, and in values of the parameters characterizing it, but it must exist. If the second alternative is correct—if the distinctive region arises just from the coincidence of several particular circumstances, not all of them common to all stars—then we expect to find the region present only in some types of stars. In deciding between these two alternatives, for some distinctive region, one must be careful to distinguish between differing thermodynamic types of region, and differing ranges in values of the state-parameters characterizing some type of region as it occurs in stars of differing MK spectral class.

The thesis that a chromospheric-region must characterize the atmospheres of all stars provides a good example. As demonstrated in Chapter 3, the observed solar chromosphere has two basic thermodynamic characteristics: (i) a departure of the actual T_e -distribution from that in the underlying RE photosphere, resulting from a nonradiative energy flux and its local dissipation; (ii) a continuation of the photospheric characteristic of thermal HE to fix the density distribution, but a thermal HE under the actual nonRE distribution of T_e . These basic thermodynamic characteristics are reproducible everywhere across the HR diagram simply by demanding a nonradiative energy flux dissipation, and no differential nonthermal velocities larger than about 1/3 the local thermal velocity. A number of astronomers have insisted that a chromosphere exists only when it falls into the solar range of T_e , and thus exhibits a solar-type chromospheric spectrum. They would exclude from being called a chromosphere, a region in a hot star which satisfies (i)–(ii) above, but whose range in T_e lies outside the solar chromospheric one. Such definition/exclusion distorts the thermodynamic principles on which the definition of distinctive region exists. It replaces a thermodynamic precision by a semantic confusion between change in state-parameter values and spatial-evolution in thermodynamic effects. We can imagine modifying our definition of chromosphere by modifying (i) or (ii) in thermodynamic implication on the role of gravity and T_e in fixing density distribution, but for all gravity and T_e . For example, as we shall see, we can have a variety of photospheres where pulsation modifies gravity without affecting

RE. Then we could carry the same modification of density distribution over into the chromosphere, retaining RE or nonRE as the photosphere-chromosphere distinction, with a chromospheric nonRE T_e entering the gravity + pulsation relation there. But this is a quite different state than one corresponding simply to a change in the value of T_e , under the same RE or nonRE conditions, simply because one considers pulsation phenomena in another MK spectral class.

By the continued comparison of similar and contrasting features in such objects as the Sun and WR—the latter in its multiple varieties ranging from field stars to central stars of PN, so that these are phenomena rather than a particular kind of star; by highlighting the common character of some peculiarity across the HR diagram such as cool H α emission envelopes in Be, T Tauri, and PN stars; by emphasizing sequences of stars across which some peculiarity evolves, such as location of H α envelope in Be, symbiotic, T Tauri, PN stars, and the strength of episodic ejection in the cataclysmic stars, blending into the symbiotic, then Bep etc.; and above all by trying to bring into focus the basic thermodynamic character of each of the proposed distinctive atmospheric regions, I hope to avoid the enforced particularity of this “semantic-chromosphere” example.

One should never forget that a non-trivial variety in some unpredicted, but generally-observed, kind of phenomenon is the essence of attributing it to some omitted general thermodynamic property. For example, thermodynamically characterizing a star as necessarily having an energy flux, because we observe it, does not at all mean that the energy fluxes from all stars must have the same origin. It simply means that, *thermodynamically, a star cannot contract from the ISM, and evolve, as an isolated system; it must expel energy*. Indeed, requiring that the energy source must be nuclear reactions does not imply that all stars, or the same star at different phases, have the same nuclear reaction as energy source. Nor does it require that any or all of the reactions be capable of operating “quietly and thermally.” Nor should it require that the energy flux be wholly radiative; nor that any nonradiative flux be produced in only one way, nor transported nor dissipated in only one way.

By the same logic, thermodynamically characterizing a star as necessarily having a mass-flux, because we observe it, does not at all mean that the mass fluxes from all stars must have the same origin. It simply means that, *thermodynamically, a star cannot contract from the ISM, and evolve, as a closed thermodynamic system, simply expelling radiative energy. It must also expel mass*, which carries with it a certain amount of energy. But there is no proscription that all mass-fluxes—from all stars, or from the same star at different epochs—are produced in the same way, or have the same size, or that all must be variable, or not variable. Our theoretical understanding of mass-flux origins is, at the moment, essentially zero; it is the increasing variety of observations which will give us that insight and, eventually, understanding. In diagnosing the data, I impose the (open, nonthermal) character because closed is a special case of open, and thermal is a special case of nonthermal. Just as thermal nonLTE, or statistical equilibrium, is a special case of unproscribed nonLTE.

So, in establishing the compendium of such distinctive atmospheric regions—all across the HR diagram—in this chapter, I try to put into perspective this variety among regions of a given distinctive kind. Thermodynamically, one identifies the role and function of some one kind of such region. From the observational data of Chapter 3, one then tries to identify the observational appearance of this particular kind of region in each of the wide variety of stars, even in different phases of a given star. This gives us the observational variety within one kind of region; indeed, *this observed variety may even help us to learn, iteratively, what are its essential thermodynamic characteristics*. As emphasized in the preceding chromospheric illustration, such approach requires reducing to its absolute essentials the basic thermodynamic characterization of each distinctive region, if we are to avoid the confusion of a multitude of only semantically-different regions. We do not want to confuse variety among examples of one kind of distinctive region with different kinds of distinctive regions. The chromospheric example cautioned against becoming sidetracked by trying to force the solar range in nonRE T_e as uniquely defining a chromosphere. We stressed that, instead, one should focus on preserving just two thermodynamic essentials, independently of the particular values of state-parameters: (i) T_e -evolution from photosphere to chromosphere as reflecting evolution from RE to nonRE as some, required-to-exist, nonthermal energy storage modes become dissipative; (ii) maintaining the particular thermodynamics of the photospheric density-gradient, in the particular variety of photosphere-corona studied, into the chromosphere,

while introducing the nonRE, rather than RE, T_e . The variety of nonradiative energy dissipation gives, and is measured by, one aspect of chromospheric variety. But it also gives information on the variety of photospheric nonthermal storage modes, hence on the variety of photospheres that do exist. In the same way, the variety in kinds of linked photospheric-chromospheric density gradients gives further information on the variety of nonthermal mass and energy storage modes, hence on the variety of photosphere-chromosphere combinations that actually do exist. We will see, in Section II following, the structural importance of demanding both the two characteristics, (i) and (ii), and not just (i).

In a similar way, the observational variety in each of the other kinds of distinctive atmospheric regions gives us information on both that kind of region itself, and on the variety of photospheres—and other underlying, and sometimes overlying, distinctive atmospheric regions—required to be compatible with these observations. The chromospheric example refers to a kind of distinctive atmospheric region which exists everywhere, but with such existence not prominent in the visual spectrum, only in the farUV and X-ray. Relative to the photosphere, it is a high-energy phenomenon. It is useful to put all these aspects into focus for another kind of distinctive region, whose universal existence is presently ambiguous, but which is most prominent in the visual: the cool, low-velocity, H α emission envelope. Historically, it was not obvious that all H α emission envelopes could be considered as simply different varieties of one distinctive kind of region; the adjectives “cool” and “low-velocity” were never used. It was not obvious that, relative to the photosphere, they were appropriate: for the Be stars, the H α regions are cold and near the star; for the T Tauri, hot and near the star; for the PN, cold and far from the star; for the symbiotic, mixed, depending on the assumed photosphere. Such variety in H α regions is detailed by: temperature and mass-flow velocity relative to the photosphere; the distance where the H α emission begins; that, where it ends; and its variability. Whether these differences were variety about one, or several, kinds of distinctive regions was not clear from visual data alone. Unambiguity comes from adjoining farUV and X-ray observations. These establish a chromosphere-corona as existing immediately contiguous to the photosphere; and mass-flow velocities to continually accelerate outward through the chromosphere to superthermal and superescape values somewhere in the hot, superionized atmospheric regions. So the H α envelope, when it exists, is universally cooler than its immediately-underlying neighboring regions; and the mass-flow has been decelerated to values lower than in these underlying regions, but larger than photospheric. Note the problem posed by Fig. 3-33, in our certainty as to just what are the actually-existing maximum flow velocities, especially in the cooler stars. But we see the observational, and thermodynamic, importance of this H α emission envelope; and of joint visual and farUR observations of it. Relative to immediately-underlying regions, the envelope is a low-energy phenomenon. Relative to the photosphere, its energy level is ambiguous, varying from the hot to cool stars; without the farUV data, one might try to model its lower boundary as contiguous to the photosphere, a profound error in thermodynamic state.

We stressed the ambiguity of its universal existence: not only from one star to another, but at different phases of some given stars. Again, this behavior is made coherent by simultaneous farUV and visual data, which show, respectively, the behavior of the underlying chromospheric-coronal regions, and of the envelope itself. Apparently, there is a stronger variability in superionized velocities, the closer the region lies to the star: this is a trend, not a correlation, at the moment. As stressed in Chapter 3, these data show the importance of combined episodic and continuous mass-ejection patterns: in the study of a given star, in the study of sequences of stars, showing these phenomena to varying degrees of observational prominence. So the key to the existence of such a distinctive atmospheric region, the H α envelope, lies in the existence of photospheric storage modes, which produce mass-fluxes, and which have a highly time-dependent character. So in a general way, we include the H α envelope among the class of universally-existing distinctive atmospheric regions by considering stars, or phases of stars, in which it is absent as simply having such slow variability as to not produce, or produce only very far from the stars, these cool, decelerated regions.

So we see the problem in deciding how to construct our compendium of distinctive atmospheric regions, beginning with a photosphere. Possibly the historic, Chapter 2, definition of a photosphere can be “effectively” satisfied in the lowest atmospheric regions of some stars: a nondissipative region of matter and energy storage, with all storage modes completely coupled to the local thermal state, and the energy level of this thermal state fixed by the

local radiation field because of its predominance in microscopic interactions. But to model this photosphere, we must generally go far beyond Chapter 2 modeling, where we considered only thermal storage modes. We must establish, for each star, just what is the set of nonthermal storage modes, for both mass and energy; establish their time-dependence; and try to model their coupling to the radiation field. This last is essential; both for the coupling itself, and because the radiation field remains the major diagnostic tool. In the Sun, one currently progresses by studying the several oscillatory modes, including hydromagnetic, by direct photospheric observations (cf the several summaries in Jordan, 1981). Solar chromospheric-coronal, and wind, studies offer the kind of possibilities on which we focus here: trying to infer from exophotospheric regions information on the photosphere and subphotosphere. But so far, for the Sun, progress is ambiguous and not great: amplitudes are too small. The wide variety of stars offer richer possibilities, in their variety of atmospheric regions.

We note, as seen in the examples and the modeling approach above, that the types of the variety in distinctive atmospheric region are often linked, between the distinctive regions in a given star at given epoch. So, cataloging them in isolation would be incomplete. Almost, we should wholly organize the summary in terms of regions in a particular atmosphere at a given phase: the aim of Chapter 5. But there, we focus on relative amplitudes between different sequences, and here, on variety of different regions. So, here, we look at variety of regions by discussing them in order of gross classification of photosphere. But the classification is not in terms of values of the thermal parameters—as the MK system—but in varieties of nonthermal storage, independently of their, or thermal, amplitudes. We consider quasi-thermal, spherically-pulsating, and ejected-shell photospheres as forming three, gross, illustrative categories. We define each more precisely in the following; where we ask what variety of the several distinctive atmospheric regions are associated with them.

II. DISTINCTIVE ATMOSPHERIC REGIONS FOR QUASI-THERMAL PHOTOSPHERES

We do not consider stars having rigorously-thermal photospheres; i.e., those in which all nonthermal velocities are rigorously zero, and the amplitudes of all nonthermal storage modes are zero. These are the province of Chapter 2, where they have been adequately abstracted. As we saw, even such wholly-thermal modeling is not yet complete, in its treatment of the nonLTE coupling between lines and continua to specify T_e (upper-photosphere). But, there appear to be no real-world stars of this rigorously-thermal variety, which would have no exophotospheric regions. So, we do not consider them further in this Part III.

Then we consider those photospheres which we call quasi-thermal. We have already characterized the *classical* quasi-thermal photospheres as those where nonthermal storage, and velocities, are not set everywhere equal to zero; but on which, in the upper sub-regions, this condition is imposed. So, there, RE and HE are valid; and no exophotospheric regions arise. Energy fluxes are only radiative; upper-regions are wholly radiatively controlled; the radiative flux measures the energy production by the star. Any uncertainty in T_e -distribution in the lower photosphere comes from uncertainty in energy partition between thermal and nonthermal modes. Because there appear to be stars where this description seems reasonably adequate, except in the upper photospheric regions where nonthermal amplitudes and velocities do not fall to zero—as diagnosed by the presence of chromospheres-corona—we retain it, except in the upper boundary regions. And, these upper boundary regions are defined not by densities dropping to ISM values, nor nonLTE effects entering, but by RE failing. HE may also, in some stars, begin to fail in the same atmospheric region where RE begins to fail. But we have also examples of stars where thermal HE remains valid in regions where RE fails—notably the Sun. So, either possibility must be admitted, in proscribing the way this quasi-thermal photosphere can depart from its classical version. The departure begins to be significant in the upper-photosphere, as in the onset of thermal nonLTE effects described in Chapter 2, and for the same thermodynamic reason: amplification of nonlinear effects toward the boundary-transition regions of low density and opacity. So, based on observational guidance, but with direct thermodynamic specification, we *define*:

A. A QUASI-THERMAL PHOTOSPHERE is a distinctive atmospheric region, where:

(1) *OBSERVATIONALLY*, its lowest geometrical region is the deepest region seen in the visual continuum;

(2) *THERMODYNAMICALLY*, its radiation field measures its energy storage:

(2.a) Any energy storage and propagation in nonthermal modes is quasi-adiabatic rather than dissipative. *Quasi-adiabatic*, because radiative interchange is pervasive, but velocities and velocity-gradients are so small that no aerodynamic dissipation occurs.

(2.b) The coupling between thermal and nonthermal modes is sufficiently-strong that one can specify the storage in nonthermal modes from the distribution of thermal parameters, supplemented by lower-boundary values of radiative and convective energy fluxes, plus those of various nonthermal parameters such as mass-flux, rotational-velocity, subphotospheric magnetic field. The essential restriction on the size of these lower-boundary values is that they not exclude the existence of photospheric regions where differential nonthermal velocities do not exceed some 1/3 the thermal velocity. We see the origin of this last condition in eq. (3.D): $U/q \gtrsim 1/3$ introduces a departure of some 10% or more from the logarithmic density gradient under thermal HE. The same holds, but less obvious in numerical size, for departure from RE induced by such differential velocities. So, we cannot permit, for these quasi-thermal varieties of photosphere, lower-boundary values which already invalidate photospheric conditions at the lower base of the photosphere.

(2.c) The level of the photospheric thermal energy is measured by that part of the radiation field which originates in the photosphere. Chapter 2 described a gross approximation to a multi-gray photospheric structure. At any level, the radiation field is divided into two parts: a wholly-storage, opaque, spectral region, satisfying LOS, with the energy storage, J_ν , fixed locally by S_ν ; a partially-propagating, not opaque, spectral region in which radiative transfer fixes T_e . Then T_e , these non-LOS radiation fields, and density fix S_ν in the nonLOS regions. In these photospheric regions, those opaque spectral regions in which I_ν (observed) originates in the exophotosphere have storage values of J_ν corresponding to these photospheric conditions. As discussed in Chapter 3, a diagnostic error would be to assume that the observed I_ν in these spectral regions, in which the photosphere is opaque, measure these photospheric conditions. It would be equally-erroneous to assume that the observed fluxes, integrated over all ν , could be used to define a T_{eff} in the Chapter 2, standard-atmosphere, sense. Possibly, they can, in particular circumstances; but this must be demonstrated, empirically-theoretically, not assumed. So, to model, and to diagnose photosphere, one uses only radiation from it.

(2.d) Any variability in photospheric conditions, or radiation field, can be incorporated in the above scheme, so long as all radiative relaxation rates are much faster than the time-scales of the variability. The situation is as abstracted from Whitney, in Chapter 3. The variability can, of course, lead to a termination of the photosphere at lower heights than would be the case without it.

(2.e) Effectively, this means that in some regions of the upper photosphere, RE and HE give the distribution of T_e and density. When these two conditions, and any of the above, are violated, the photosphere ends, and we enter the exophotosphere. So, we can use the grids of standard, HE and RE, models, corresponding to Chapter 2 conditions, to estimate, self-consistently, what distributions of T_e and density, and what emergent I_ν and F_ν , define a particular photosphere. One can also use the TCB approach to estimating T_e in terms of sequences of opacity sub-regions, which is well-adapted to this separation of photospheric and exophotospheric regions.

(3) *DIAGNOSTICALLY*, the photosphere ends, and the first exophotospheric distinctive region begins, when:

either (3.a) No distribution of thermal parameters, consistent with RE and HE, can be found which represents the whole observed spectrum. There are two sources of ambiguity. The first was stressed in Chapter 2: inadequate treatment of line-continuum coupling, with a proper distinction between different types of line source-function in its dependence on radiation field. The second is the limitation in observed spectral range. The farUV data have helped; even they cut off before the region of F_ν (max) for the hot stars. So one is too-often restricted to line-, rather than continuum-, diagnostics. Since the 1952 solar eclipse results (Thomas and Athay, 1961), one recognizes that for even such a banal star, the strong lines are exophotospheric in origin. Usually, only the wings are photospheric; and there the theory is the most uncertain.

or (3.b) Those nonthermal parameters, and their largely ad hoc introduction into thermal models, which can often produce a reasonable representation of observations, have sizes which contradict some of the thermal conditions

(2.a)–(2.e), above some photospheric height. Then, at these heights, we say the photosphere ends. So, generally, it is easier to use the sizes of such nonthermal parameters, deduced from crude diagnostics of upper photosphere and lower exophotosphere, to fix the end of the photosphere and beginning of the next distinctive region. Again, eclipse studies of anomalous density gradients, the presence of superionized lines, the observation of superthermal velocities provide the obvious examples. So, *we define*:

B. A CHROMOSPHERE is a distinctive atmospheric region, which

(1) *OBSERVATIONALLY*, lies just above the photosphere, which blends continuously into it, and which

(1.a) shows an outward increase in T_e , continuing that photospheric outward-increase associated with thermal nonLTE effects, but progressing very much above the photospheric nonLTE thermal limit of T_{eff} :

(1.b) shows a lower density height-gradient than in the upper photosphere, which can be represented by the same thermodynamic relations that describe the photospheric density gradient except that the chromospheric, non-RE, T_e replaces the photospheric, RE, T_e . If the neighboring photosphere is quasi-thermal, this chromospheric density gradient is thermal HE under the chromospheric T_e -distribution.

(2) *THERMODYNAMICALLY*, a nonthermal dissipation of energy causes the rise in T_e , and decrease in density gradient, relative to the photosphere.

(2.a) There are two kinds of fluxes associated with nonthermal storage modes: energy and mass. The mass-flux also transports energy; so “energy-flux,” sans qualification, hereafter means an energy-flux not carried by a mass-flux. Then, in the chromosphere, the mass-fluxes are restricted to being sufficiently-small that the associated velocities are distinctly sub-thermal. The upper-chromospheric boundary region begins where the mass-flow velocity, U , satisfies $1 > U/q \gtrsim 1/3$. Thus the mass-flow perturbs neither RE nor HE until the region of the upper-chromospheric boundary. So the r -dependence of U/q gives information on the r -location of the upper-boundary region.

(2.b) There are two kinds of energy storage and flux associated with nonthermal energy fluxes and their dissipation. One kind is where nonthermal storage modes, with negligible local dissipation, persist throughout the photosphere, possibly into the chromosphere, and only “untrap” their energy storage in chromospheric regions. Examples lie in the several types of oscillatory storage, described by Deubner (1981) and by Leibacher and Stein (1981a), and observed as the solar 5- and 3-minute oscillations. A second kind of energy storage-propagation is that originally proposed (Biermann, 1946; Schwarzschild, 1948) to heat the solar corona: a flux of acoustic waves, produced in the lowest photosphere, or subphotosphere, by convective pressure fluctuations. These are wholly-propagating, not storage, in the upper photosphere and chromosphere-corona. Interpreted as progressive waves, the energy flux required by the 5- and 3-minute oscillations is some 10^9 erg/cm² sec; as storage, the oscillations are compatible with fluxes, when their energy storage untraps in the chromosphere, lying in the 10^6 – 10^7 erg/cm² sec range usually discussed for solar chromospheric heating. Both these oscillatory modes have their origins in the subatmospheric hydrogen-ionization zone: the one, from convective instability; the other, from pulsational. To be compatible with the chromospheric definition, the wave is carried by a distinctly subthermal flow; the eventual shock-waves produced propagate, of course, superthermally.

(3) *DIAGNOSTICALLY*, the chromosphere begins, and the photosphere ends, where nonradiative energy fluxes dissipate sufficient energy to raise T_e significantly above the T_{eff} associated with the photosphere; the chromosphere ends, when U/q is sufficiently-large, $\gtrsim 1/3$, to significantly perturb that density gradient which would exist in the absence of a mass-flux. If there were no nonradiative energy flux not associated with the mass-flux, then there would be no nonradiative energy dissipation until U/q reached sufficient size to produce it. Thus, crudely, the chromosphere would begin where it ended; that is, it would be a region of very small extent, in strong contrast to its relatively-large extent in the Sun. There, photospheric density scale-heights are some 10^2 km; the chromosphere requires some 10^3 km to raise T_e from T_e (min) to some 10^4 K, or to double T_e . As we saw in Chapter 3, it requires 1–2 solar radii before U/q reaches unity. So the possible range in extent of the chromosphere, as we define it, is very large; its bottom is fixed by the nonradiative energy flux; its top, by the mass-flux. Specifically, it extends between

the beginning of significant heating by nonradiative energy fluxes not transporting mass, and the beginning of significant momentum input and nonradiative heating by mass-fluxes. The chromosphere marks the beginning of an extended atmosphere, and an important “transition” aspect across it is that from a thermal extension—resulting from a significant rise in T_e —to a nonthermal extension—resulting from the beginning of significant dynamic-support aspects. Conceptually, this change from nondynamic extension in the chromosphere to dynamic extension in the exochromosphere was the basis of Struve’s (1942) attempt to introduce unity in extended atmospheres between hot and cold stars; the lacking element was the realization that T_e could rise above its RE value, and provide the nondynamic atmospheric extension.

Note, as we have already stressed, that such a diagnostic definition of a chromosphere is not at all tied to a particular range in values of T_e . Nor is it tied to a radiative instability in T_e , or a plateau structure in T_e , which may accompany nonradiative heating. Rather, it corresponds to the linear amplification of mass-flow velocity with outward decrease in density; mass-flow does not perturb density, here.

So, to specify the chromosphere’s beginning, we need to know the details of the nonradiative energy storage, fluxes, and dissipation. The existence of a very large rise in T_e in the outer solar atmosphere was generally admitted after Edlen’s identification of the solar coronal lines (1942). The significant rise, at low heights, of the solar chromospheric T_e was generally admitted after the 1952 HAO eclipse observations (Thomas and Athay, 1961). The general existence of chromospheres-coronae has been gradually admitted over the last decade. But the identification of the source(s) of nonradiative energy dissipation, and their characteristics, even for the Sun, remains speculative (cf the solar discussion in Jordan, 1981). So, a priori, we have no solid foundation for predicting the beginning level of the chromosphere, in any star. One can equally-well assume a chromospheric T_e -structure as assume the characteristics of the nonradiative energy flux. One notes that it is not simply the value of the nonradiative energy flux which one lacks for such prediction; it is the height-distribution of its dissipation. In the enlarged chromosphere-corona-wind reference frame, this point has recently been demonstrated in detail by Hammer (1982, a, b, c) and Hearn (1982).

So the best one can do at the moment, to estimate beginning heights of chromospheres, is to place upper limits on these heights by estimating chromospheric terminal heights. In the sense discussed above, these give the beginning height of a chromosphere of very-small extent, which is heated only by a mass-flux. So, these are strong upper limits on where the chromosphere actually begins. We use the expression for the time-independent mass-flow of eq. (3.38), to obtain the atmospheric density where the flow first reaches thermal velocity. As we have already remarked, below the level $U/q \lesssim 1$, the mass-flow does not perturb the density distribution. So, eq. (3.38), and the time-independent version of eq. (3.A) from which it comes, state that—given some initial U_0 deep in the atmosphere—its outward amplification follows the density decrease. This decrease follows from the HE condition; and is given by any of the several photospheric models. The essential point is to use q (photosphere); although compared with the quasi-exponential outward decrease of density, uncertainty in q (T_e) has minor effect. The solar mass-loss is well-specified by collector measurements. Stellar values are certain to the extent one believes the various mass-flux diagnostics; we already discussed this point. Table 4-1 simply exhibits ρ/ρ ($\tau = 1$) and $\Delta r/R$ (photosphere), assuming a plane-parallel, exponential, density-distribution at T_{eff} , for a variety of stars and values of mass-loss. The essential thing to note is the very low value for this upper-limit on the beginning height of chromospheres, everywhere across the HR diagram. The low value comes simply from the small density scale height in photospheres generally; any small outflow in the low photosphere amplifies rapidly. I presented these general results in 1973 (Thomas, 1973), just after the Goddard stellar chromospheric colloquium (Jordan and Avrett, 1973), to show that the prohibition on the existence of chromospheres in early-type stars, because of theoretical inability to specify the origin of a nonradiative energy flux in them, was without basis. One simply has insufficient data to predict the true lower-boundaries of chromospheres. The observational existence of a mass-flux implies, as in Table 4-1, the existence of a chromosphere in that star, and provides an upper limit on height of chromospheric beginning. The measured solar mass-flux from particle collectors, values inferred from WR binaries, and crude estimates from other diagnostics let one confidently predict that low-lying chromospheres exist across the HR diagram. FarUV observations confirm the prediction. Predicted vs. observed solar values show the height *overestimate* under our approach.

Table 4-1
Upper Height Limit on Beginning of Chromosphere

Type Star	$10^{-3} T_{\text{eff}}$	$\log g$	\dot{M}'	$n_{\text{Hc}}/n_{\text{Ho}}$	r_c/R_p
*OB sg	20-30	4	10^{-5}	$10^{-2.2}$	1.001
*M sg	3	1	10^{-11}	10^{-8}	1.1
**B V	30	4	10^{-9}	$10^{-2.5}$	1.007
**B V	25	4	10^{-9}	$10^{-2.0}$	1.005
**B III	25	3	10^{-9}	$10^{-1.7}$	1.045
**Be V-IV	30	4	10^{-7}	$10^{-0.5}$	1.004
**Be V-IV	25	4	10^{-7}	~ 1	1.003
**Sun (pred)	6	4.4	3.10^{-14}	10^{-9}	1.004
**Sun (actual)	-----				1.0007

*values from Thomas (1973)

**values from Doazan and Thomas (1982); n_{Hc} at nonLTE $T_{\text{ox}} (T_{\text{e0 max}})$

The thermodynamic structural details of the upper-boundary region of the chromosphere, and of its overlying region, have been as controversial as was the existence of chromospheres. The essential thermodynamic question is whether there exists a reasonably-extended region where the flow-velocity is near-thermal, but distinctly sub-escape; or whether such a region has only trivial extent—to reach thermal velocity implying to reach escape velocity. We have discussed the observational evidence for such a region in Chapter 3; we call it the lower-corona; and we now give the empirical-theoretical “map” of its synthesis into the atmospheric structure.

C. A LOWER-CORONA is a distinctive atmospheric region, which

(1) *OBSERVATIONALLY*, lies just above the chromosphere, which blends into it in such a way that is, locally, possibly fluctuating in time and space; so that the lower-corona

(1.a) continues to show an outward increase in T_e , hence in $q(T_e)$, as inferred by the simultaneous presence of ionization stages ranging from photospheric through O VI in farUV spectra, to varying degree among different stars. Between spectral sub-classes there are trends; but there is no overall correlation with location in the HR diagram. For example, among the B and Be stars, O VI, N V, and C IV are observed in early sub-classes of B-type stars, but not in late. However, C IV and N V are again observed in some Herbig (late B, early A) stars, in some T Tauri stars, and solar-like late dwarfs and giants, as discussed in Chapter 3. In the Sun, degree of ionization increases steadily outward through what we define as the chromosphere, and does not change much through what we call the lower-corona.

(1.b) continues to show a decrease in density gradient with increasing height. The density gradient is represented neither by an HE expression with outward-increasing T_e , nor by an expression of the form of eq. (3.38) with constant U . The observational basis for this point (1.b) is *very* limited, having been summarized in Chapter 3, under extended atmospheres. So the strongest basis for this characteristic, aside from these limited observations, is thermodynamic and laboratory-aerodynamic.

(2) *THERMODYNAMICALLY*, the lower-corona is a region of trans-thermal flow in the aerodynamic sense: i.e., over a significant height-range, the flow lies very close to the thermal value. Since the latter increases outward, so does the flow-velocity. The beginning of the lower-corona is where the flow enters the range $U/q \sim 1/3-1$; the end of the lower-corona is where the flow increases significantly above $U/q \sim 1$, and thereafter increases monotonically through the upper-corona.

(2.a) This trans-thermal, or trans-sonic, flow-regime is discussed at length in Part II, which is Vol. 2. Here, we abstract the essentials. Figs. 4-1 through 4-6 show the character of the trans-sonic regime as illustrated by spark-silhouette photographs of spheres in flight, at velocities ranging from $U/q \sim 1/3$ through $U/q \sim 4$. Fig. 4-7 supplements these photographs of the flow-pattern by exhibiting the behavior of the so-called "drag-coefficient," K_D , defined by

$$dU/dt = - K_D [\rho d^2/m] U^2 \quad (4.1)$$

d is the diameter and m the mass of the sphere; the other symbols are as before. In the low subsonic region, the atmospheric deceleration—or "drag"—comes from viscous effects, which cause separation of the flow from the body contour, through increasing size of the boundary-layer shown in the photographs. The base-pressure becomes much lower than the nose-pressure, from this flow-separation; it is this base-pressure deficit which causes the deceleration. The flow in the turbulent wake, created by the separation, is locally time-dependent; that flow up to the separation point has only the feeble time-dependence corresponding to the sphere deceleration. In the flow-regime between $0.8 \lesssim M = \text{Mach-number} = U/a \lesssim 1.2$ ($a = \text{sound-velocity}$), one sees an instability of the flow as a major characteristic. Superposed on the main flow is a locally-time-dependent network of acoustic waves, which is stochastic rather than regular in its behavior. As M progressively increases, this network of acoustic waves—which, near the boundary formed by the sphere's surface, are the characteristics of the differential equation describing the flow—coalesces into the bow-shockwave and the tail-shockwave. And in this supersonic regime, the flow again becomes stable. Any small disturbance—for example, a local roughening on the sphere surface produces such—rapidly damps out. Again in this flow-regime, upstream of the turbulent wake, the flow is locally time-independent. The abrupt rise, then slow decrease, of the drag-coefficient, K_D , in that range $0.8 \lesssim M \lesssim 1.2$ corresponds to the increase in the relative amount of energy, furnished by the sphere deceleration, put into driving the acoustic waves. Asymptotically, one represents the air-resistance reasonably well by ignoring all except the bow-shock, and setting a vacuum at the sphere's rear.

Here, we study trans-sonic flow by observing a sphere. Clearly, one can consider it to be a half-nozzle, with a converging-diverging geometry. So, one can visualize the aerodynamics of nozzle-flow, as the upstream velocity of the gas stream is increased from low subsonic through trans-sonic to supersonic. One can also study nozzle-flow itself; cf Prandtl (1904), a solar application by Thomas (1950c), and the laboratory experiments plus interpretation in Vol. 2, as well as the great variety of aerodynamical literature not explicitly aimed at astrophysical application. All such studies demonstrate that, once the mass-flow has been initiated, the flow at velocities below $M \sim 0.3-0.8$, and above $M \sim 1.2-1.5$, is stable; and for such things as moving spheres/projectiles, and mass-flow in stellar atmospheres, it can be represented very well as time-independent over times longer than the thermal relaxation-time of the gas. However, in the trans-sonic, or trans-thermal, regime— $0.8 \lesssim M \lesssim 1.2$ —the flow is locally-variable, in space and time, as exhibited by Figs. 4-2, 4-3, 4-4. The instability is observable as a stochastic distribution of acoustic waves, whose energy is furnished by the instability of the systematic flow, and which are superposed on the main flow. So, we can apply this basic physical picture of gas-flow traversing the sub-thermic, trans-thermic, and super-thermic regimes to sketch the atmospheric flow-pattern. In case it is not clear, I emphasize that these free-flight sphere experiments can be replaced by a stationary sphere around which a moving gas flows. At very high velocities, free-flight experiments are simply easier to perform. For analytical reference, we use the general equations (3.A)–(3.D); their contracted variety under special circumstances (3.40)–(3.51); and the stability discussions by Cannon and Thomas (1977), preceded by Thomas (1973) and Cannon and Thomas (1975). Clearly, the behavior of the flow depends upon its gross acceleration, and upon any energy supply supplemental to that provided by the acceleration—i.e., directly to the internal energy of the gas.

Figs. 4-1–4-6. Photographs of a moving sphere at a sequence of increasing Mach number.

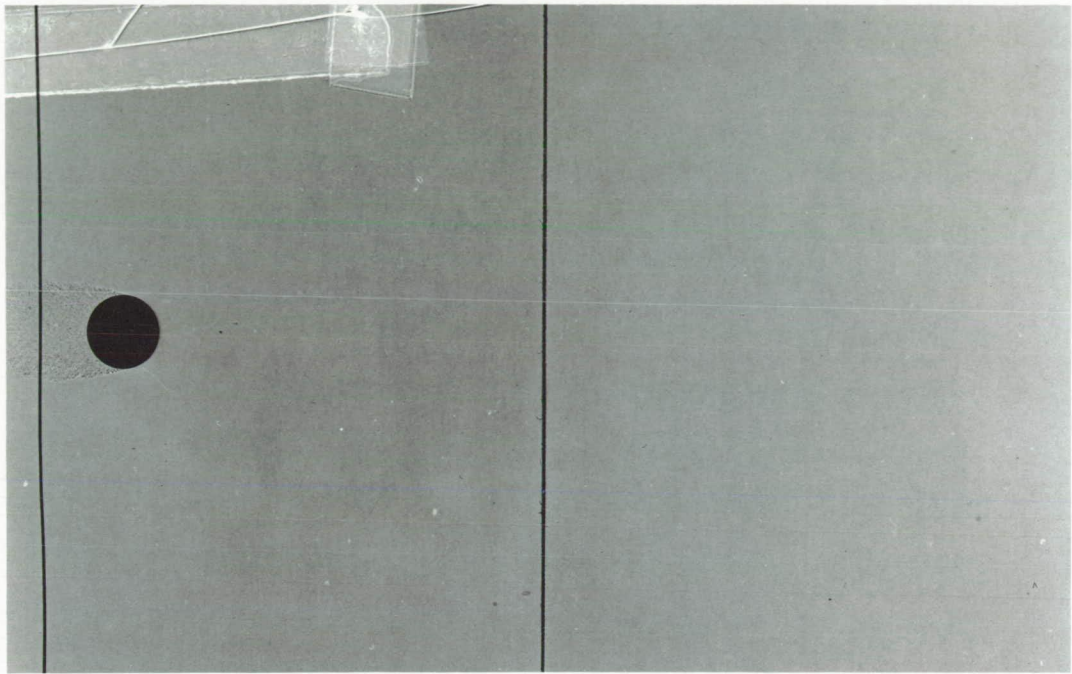


Fig. 4-1. $M = 0.60$.

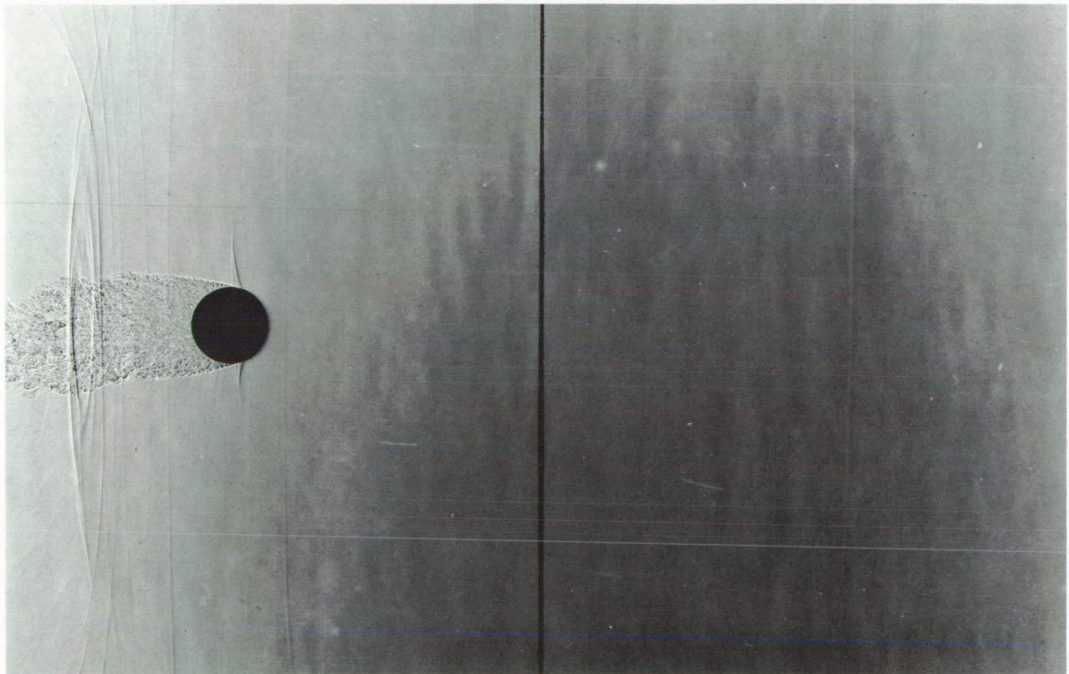


Fig. 4-2. $M = 0.94$.

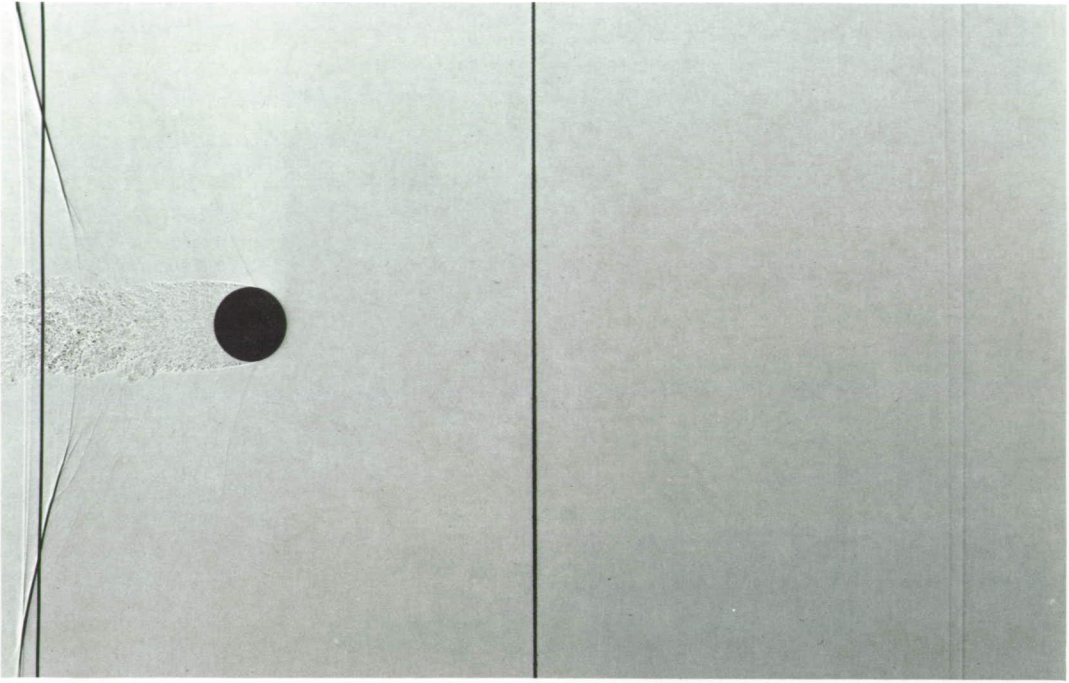


Fig. 4-3. $M = 0.98.$

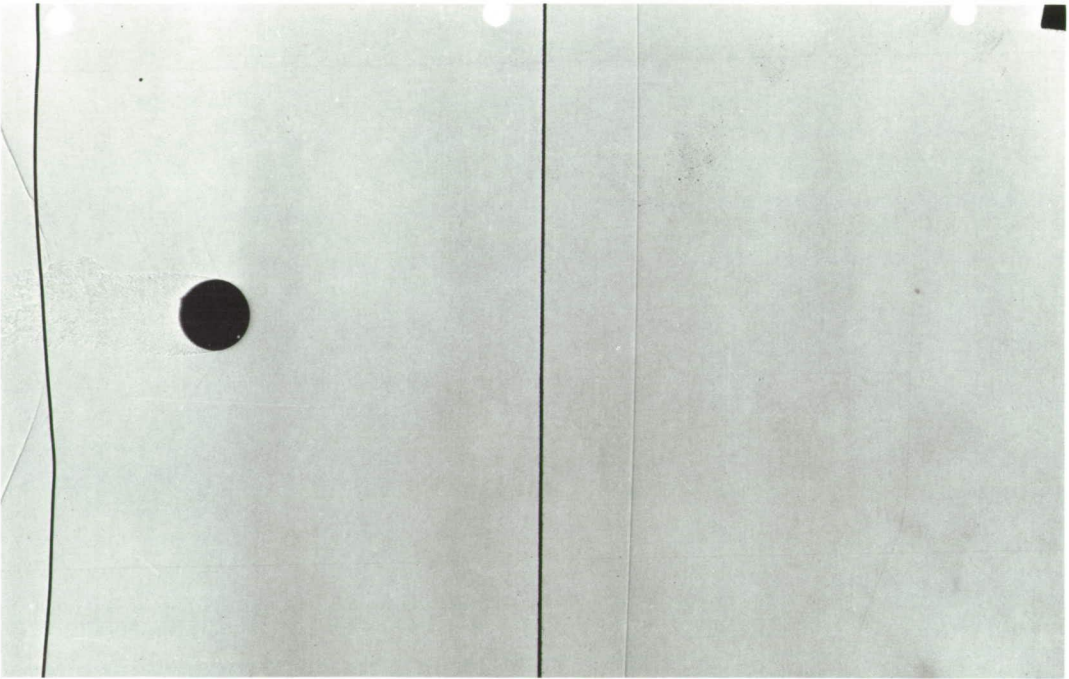


Fig. 4-4. $M = 1.06.$

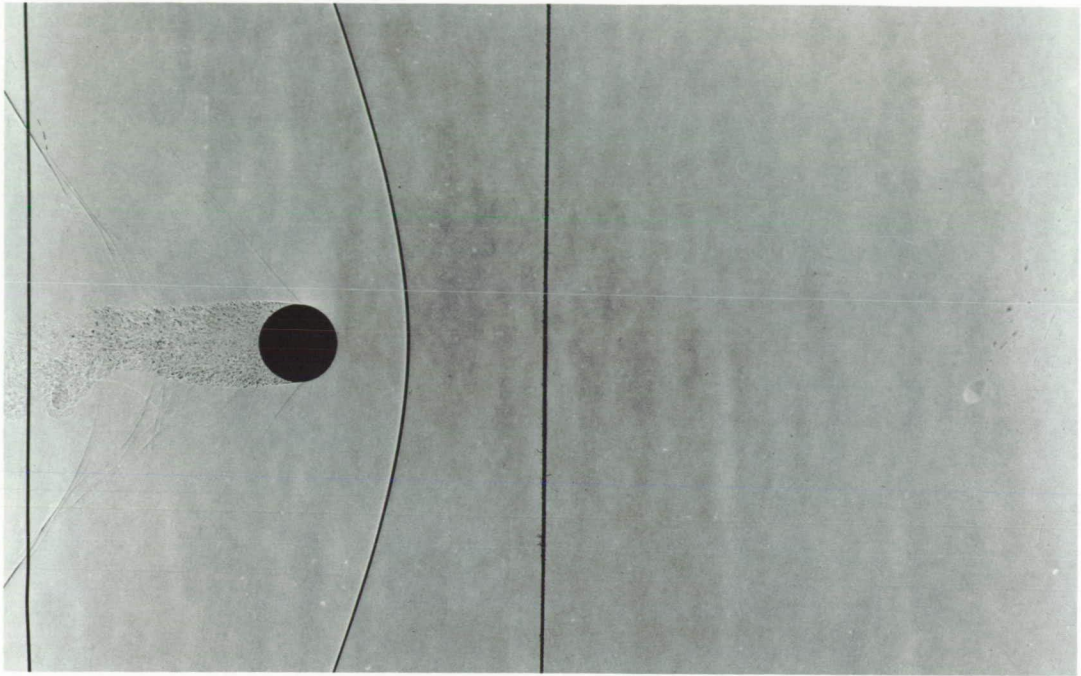


Fig. 4-5. $M = 1.12$.

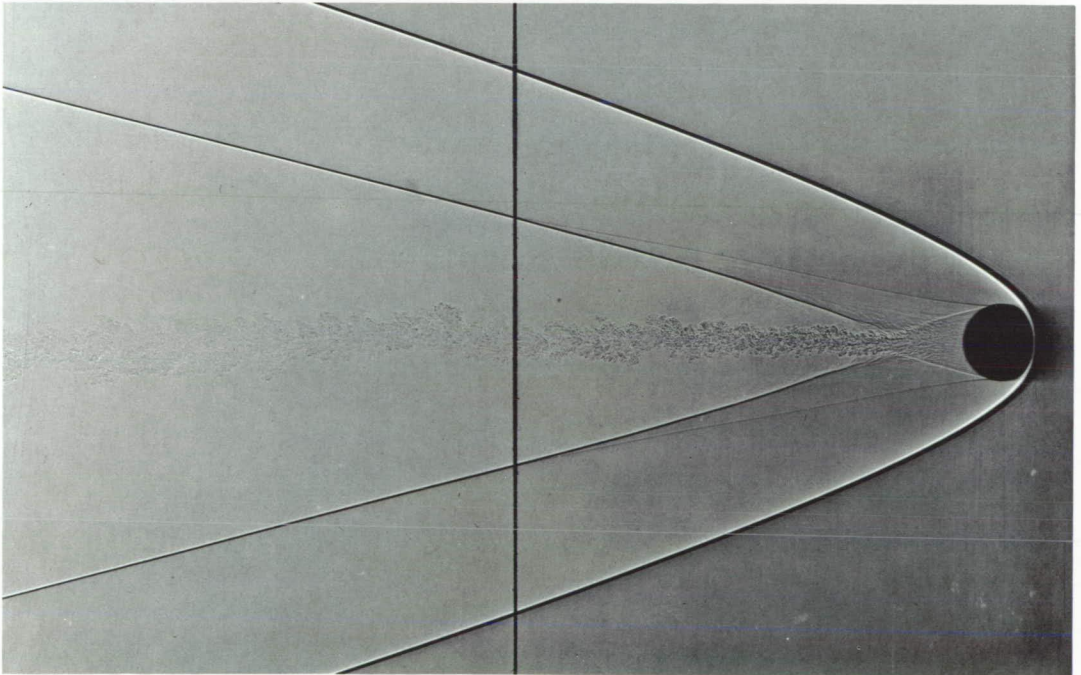
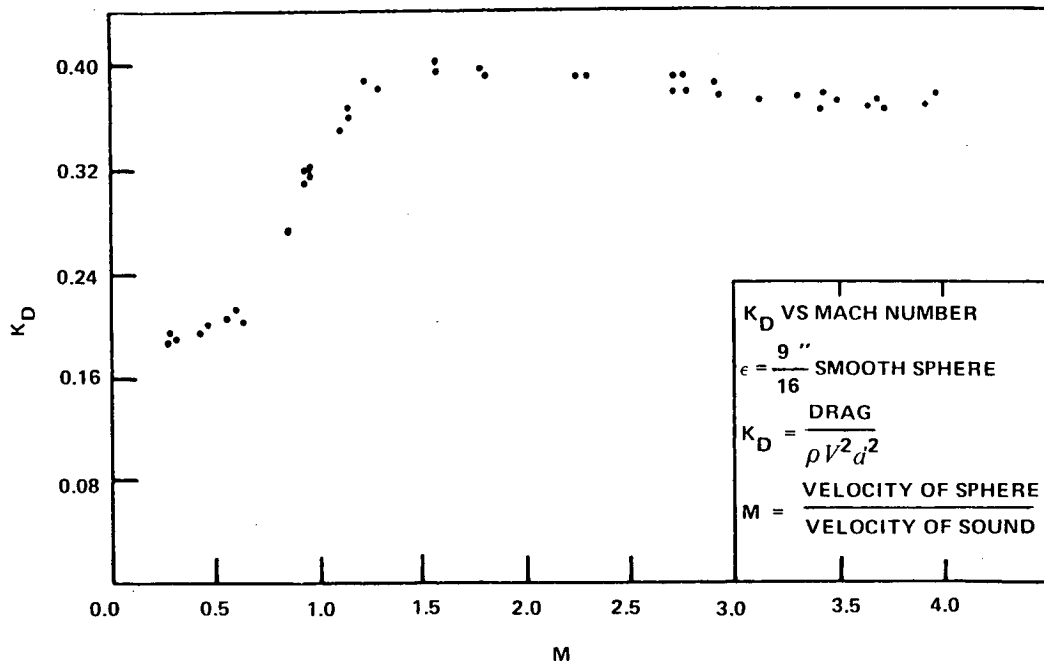


Fig. 4-6. $M = 4.01$.



"Subsonic"	$K_D = 0.192$	
$0 < M < 0.5$	(± 0.0029)	
"Transonic"	$K_D = 0.3173 + 0.2711 (M - 1.00)$	
$0.5 < M < 1.4$	(± 0.0018)	(± 0.0090)
"Supersonic"	$K_D = 0.3812 - 0.0140 (M - 2.75)$	
$1.4 < M < 4.0$	(± 0.0006)	(± 0.0008)

Figure 4-7. Air-Resistance vs Mach number.

i. Sub-Thermic Flow in Photosphere and Chromosphere

Whatever the mechanism which produces a mass-flow at velocity U_0 at the base of the photosphere, U accelerates outward because of the outward density decrease in the stellar atmosphere, following eq. (3.A), as discussed above. The flow-acceleration takes its energy from the thermal energy of the gas, which is maintained by the radiation field, under RE, in the photosphere, and additionally by the nonradiative energy fluxes in the chromosphere. Such atmospheres are always unstable against an outward mass-flow, as shown by Cannon and Thomas (1977), following Thomas (1973) and Cannon and Thomas (1975), abstracted as follows.

We define the flow in terms of optical depth, because of RE, defining

$$d\tau = -\alpha\rho dr; \quad \partial p_r / \partial r = -[\rho/c] \int F_\nu K_\nu dv \quad (4.2)$$

and look for perturbations on a steady-state flow given by U_0 and ρ_0 , in the form

$$U = U_0 + U_1; \quad \rho = \rho_0 + \rho_1. \quad (4.3)$$

Then, neglecting products of U_1 and ρ_1 ; from the t -dependent forms of eqs. (3.A), (3.B)

$$-\frac{1}{\alpha\rho} \frac{\partial\rho}{\partial t} + U \frac{\partial\rho}{\partial\tau} + \rho \frac{\partial U}{\partial\tau} = 0, \quad (4.4)$$

$$\frac{1}{\alpha\rho} \left[U \frac{\partial\rho}{\partial t} - \rho \frac{\partial U}{\partial t} \right] + \left[q^2 - U^2 + 2\alpha\rho\theta \frac{\partial U}{\partial\tau} \right] \frac{\partial\rho}{\partial\tau} = \left[g - \alpha \left(\frac{\partial_r p}{\partial\tau} + \rho q^2 \frac{\partial \ln T_e}{\partial\tau} \right) \right] \alpha^{-1} - \alpha\theta\rho^2 \frac{\partial^2 U}{\partial\tau^2}. \quad (4.5)$$

we subtract the steady-state forms of (4.4) and (4.5), written in terms of U_0 and ρ_0 , and using eq. (4.3), to obtain

$$\alpha\rho_0 U_0 \frac{\partial\rho_1}{\partial\tau} - \frac{\partial\rho_1}{\partial t} + \alpha\rho_0 \frac{\partial U_0}{\partial\tau} \rho_1 + \alpha\rho_0 \frac{\partial\rho_0}{\partial\tau} U_1 + \alpha\rho_0^2 \frac{\partial U_1}{\partial\tau} = 0; \quad (4.6)$$

$$\alpha\rho_0 Q_0 \frac{\partial\rho_1}{\partial\tau} + U_0 \frac{\partial\rho_1}{\partial t} + R\alpha\rho_0\rho_1 - 2U_0 \frac{\partial\rho_0}{\partial\tau} \alpha\rho_0 U_1 - \rho_0 \frac{\partial U_1}{\partial\tau} = 0, \quad (4.7)$$

where

$$Q = q^2 - U^2 + 2\alpha\theta \frac{dU}{d\tau}; \quad R = \frac{\partial q^2}{\partial\tau} + 2\alpha\theta \frac{\partial}{\partial\tau} \left[\rho_0 \frac{\partial U_0}{\partial\tau} \right] \quad (4.8)$$

We look for two kinds of perturbations; one about a static atmosphere, hence in the region of the lowest photosphere; the other about a well-developed mass-flow, hence the region of the upper chromosphere.

α . Lower Photosphere. The unperturbed, static, solution, $U_0 = 0$, corresponds to

$$T_{e0} = T_{e0}(\tau) \quad (4.9)$$

$$q_0^2 \frac{d\rho_0}{d\tau} = \left[g - \alpha \left(\rho_0 \frac{k}{M} \frac{dT_{e0}}{d\tau} + \frac{d_r p_0}{d\tau} \right) \right] \alpha^{-1}, \quad (4.10)$$

With $U_0 = 0$, then U in eqs. (4.4) and (4.5) is U_1 . Then the perturbation is about the time-independent configuration, so we have the simpler form of eqs. (4.6) and (4.7)

$$\frac{U d\rho_0}{d\tau} + \frac{\rho_0 dU}{d\tau} = 0, \quad (4.11)$$

$$q^2 \frac{d\rho_1}{d\tau} + \rho_1 q^2 \frac{d \ln T_e}{d\tau} = - \left(2\alpha\theta\rho_0 \frac{d\rho_0}{d\tau} \right) \frac{dU}{d\tau} - \alpha\theta\rho_0^2 \frac{d^2 U}{d\tau^2}. \quad (4.12)$$

We look for solutions of the form

$$U = U_1 \exp(i\Lambda\tau), \quad (4.13)$$

$$\rho_1 = \rho_{11} \exp(i\Lambda\tau), \quad (4.14)$$

and we obtain from eq. (4.11)

$$i\Lambda = - \frac{d \ln \rho_0}{d\tau}; \quad (4.15)$$

and from eq. (4.12)

$$\rho_{11} = - U_1 \left[\frac{\alpha \rho_0^2 \theta}{q^2} \frac{d \ln \rho_0}{d\tau} \right] / \left(1 - \frac{d \ln T}{d\tau} / \frac{d \ln \rho_0}{d\tau} \right) \quad (4.16)$$

Thus, from eq. (4.15), the atmosphere is unstable against a small radial velocity perturbation, U increases with decreasing τ , if density decreases outward. From eq. (4.10), this means as long as gravity exceeds the radiation-pressure plus temperature gradients. Too-large radiation pressure gradient makes the atmosphere stable; there is no driving acceleration in an atmosphere with no density gradient. Of course, we require a density gradient to make it possible for the atmosphere to merge, asymptotically, with the ISM. So, in those stars for which we have a quasi-static photosphere, radiation pressure must be smaller than gravity; but the atmosphere is unstable against a radial mass-flow.

From the preceding, one does not know the growth rate of any perturbation, so needs to return to the time-dependent form of the perturbations. One can also combine eqs. (4.11) and (4.12) in the form

$$\frac{dp}{d\tau} \left[q^2 - U^2 + 2\alpha\rho\theta \frac{dU}{d\tau} \right] = \left\{ g - \alpha \left[\frac{d_r p}{d\tau} + pq^2 \frac{d \ln T_e}{d\tau} \right] \right\} \alpha^{-1} - \alpha\theta\rho^2 \frac{d^2 U}{d\tau^2}, \quad (4.17)$$

to exhibit what we already remarked earlier from eq. (3.D); the perturbation on density-distribution of a velocity field is not significant until U^2 lies near q^2 . Until then, density perturbations depend on the viscosity, as in eq. (4.16), and are small outside regions of large $dU/d\tau$. The time-dependent perturbations to obtain the growth rate in this quasi-static situation in the low photosphere are described in the same way one describes those in the higher atmospheric regions where U has amplified to approach q : same approach, same equations. The only difference is that we study perturbations about $U_0 \sim 0$ in the low photosphere, and about $0 \ll U_0 \sim q$ in the upper chromosphere. So we replace the time-independent perturbations (4.13)–(4.14) with a time-dependent variety

$$U_1 = \bar{U}_1 \exp(i\lambda t - i\omega t); \quad \rho_1 = \bar{\rho}_1 \exp(i\lambda \tau - i\omega t); \quad (4.18)$$

which can describe disturbances like those in the sphere photographs. So we insert eqs. (4.18) into eqs. (4.6)–(4.7); introduce

$$w = \omega/\alpha\rho_0; \quad (4.19)$$

and eliminate U_1 and $\bar{\rho}_1$ between the resulting two equations. We obtain

$$[(Q_0\lambda - U_0 w)i + R] \left[\rho_0 \lambda i + \frac{d\rho_0}{d\tau} \right] + \left[(U_0\lambda + w)i + \frac{\partial U_0}{\partial \tau} \right] \left[-\rho_0 w i + 2U_0 \frac{\partial \rho_0}{\partial \tau} \right] = 0. \quad (4.20)$$

We consider both propagation and amplification of the disturbance by admitting real and imaginary parts of λ and w :

$$\lambda = \epsilon + i\eta; \quad w = \gamma + i\delta. \quad (4.21)$$

The real and imaginary parts of eq. (4.20) then give us two equations among the four quantities ϵ , η , γ , δ .

Consider the growth rate in the low photosphere, where the perturbation on the static atmosphere is about $U_0 = 0$. To accord with the result (4.15), we take $i\lambda$ as real—i.e., replace it by λ as real—but allow w to be complex, as in the second of eq. (4.21) corresponding to the use of eq. (4.19). Then in place of eq. (4.20) we obtain the simpler expression

$$[-\delta + i\gamma] [(-\delta + i\gamma)\rho_0 + V\lambda(P + \lambda/2)] - [P + \lambda][T + \lambda] = 0, \quad (4.22)$$

where

$$V = 2\alpha\rho_0^2\theta; \quad P = \frac{\partial \ln \rho_0}{\partial \tau}; \quad T = \frac{\partial \ln T_e}{\partial \tau}. \quad (4.23)$$

The imaginary part of eq. (4.22) gives

$$\delta = \lambda \frac{V}{2\rho_0} [P + \lambda/2] = \lambda [P + \lambda/2] \alpha\theta\rho_0 \quad (4.24)$$

Inserting this δ into the real part of eq. (4.22) gives

$$\lambda = \frac{-[P + T] \pm \left\{ (P + T)^2 - 4(P + \lambda/2)(T + \lambda/2) \right\}^{1/2}}{1 + s^2}, \quad (4.25)$$

$$s^2 = \frac{V^2 [P + \lambda/2]}{4q^2 \rho_0^2}. \quad (4.26)$$

Because we are in the region where all velocities are small compared with q , and thus also the viscosity terms are small, we see that

$$\lambda \sim -P \quad \text{or} \quad -T; \quad (4.27)$$

and before any mechanical heating sets in, $P \gg T$; so we obtain the result (4.15). Furthermore, the growth rate δ is, by eq. (4.24)

$$\delta \sim - \left(\frac{d \ln \rho_0}{d\tau} \right)^2 \frac{1}{2} \alpha\theta\rho_0, \quad (4.28)$$

or negative, proportional to the viscosity, as said at the outset.

β . Chromosphere

Then return to flow-perturbations in the region of the upper-chromosphere, where U_0 approaches q , and we use the complete expressions (4.21) for λ and w in the complete eq. (4.20). The imaginary part of eq. (4.20) gives the desired relation for generation-propagation of disturbances. We obtain

$$\epsilon U_0 = -\gamma(1 + \beta), \quad (4.29)$$

where

$$\beta = \frac{(Q_0/U_0)(\eta\rho_0 - \frac{1}{2} \partial\rho_0/\partial\tau) + \rho_0(U_0\eta - R/2U_0)}{-(Q_0/U_0)(\eta\rho_0 - \frac{1}{2} \partial\rho_0/\partial\tau) + U_0\partial\rho_0/\partial\tau + \rho_0(\delta + R/2U_0)} \quad (4.30)$$

Deep in the atmosphere, U_0 is small and Q_0/U_0 is large; hence we have there $\beta \approx -1$. From eq. (4.29), we see that no waves propagate; there is no acoustic radiation for any values of η and δ . This corresponds to what we see in the sphere photograph Fig. 4-1, for small velocity. Perturbations only arise because of the viscosity effects, which produce the boundary-layer, then separation, and the turbulent wake, as discussed above.

Higher in the atmosphere, where U approaches q , Q_0 becomes small. The quantity β increases positively into the upper atmosphere from its low-atmosphere value of -1 . An acoustic radiation loss, again as illustrated by the sphere photographs Figs. (4-2)–(4-5), corresponds to waves propagating away from their origin, amplifying as they move upward in the atmosphere and diminishing as they move downward. To accomplish this, we require both η and $\delta > 0$. Hence, the behavior of β . If it reaches zero, we see that the propagation velocity is just U_0 , which is expected in this region where $U_0 \sim q$, if the waves are indeed acoustic. So we see that as the flow enters the upper-chromosphere, lower-corona, the outward flow is indeed unstable. The instability is exhibited, observationally, in the production of these acoustic waves. Whatever is the energy source which accelerates the flow, it also provides energy for this wave-system which, observationally, is stochastic—or turbulent in the generalized sense of Moyal (1953).

ii. Trans-Thermic Flow in the Lower-Corona

Given the behavior of the flow as U approaches q , described and illustrated above, one might accept a contracted, time-independent, version of eq. (3.C) to describe the flow for $U \ll q$, and $U \gg q$, but not to describe the flow in the region $U \sim q$. One would expect to need the time-dependent terms in this equation. Possibly, also, one needs the radiative-acceleration terms. I say “possibly,” because one generally expects a significant radiative-acceleration to begin after some other acceleration has displaced the line from its rest position by about a Doppler-width, to get out of the central absorption core. That is, when the local flow-velocity begins to exceed q . So, as U approaches q , both the time-dependent and radiative-acceleration terms in eq. (3.C) become increasingly important. But cf. Section D.2.b following. Certainly, in this region, the contraction of the equations following the Parker hot-coronal approach is unjustified, without showing that it causes no serious problems. The same comment holds for the radiative-acceleration contractions, if one wants to study the transthermal part of the flow. The contraction described in Section F of Chapter 3, of course, ignores the description of the flow in the trans-thermal region. Such ignorance is dubious even if the atmosphere were “cool” as these theories assume; it is wholly unjustified in the actual case of the prevalence of chromospheres-coronae. If, then, one retains the full eq. (3.C), there is no reason to adopt the Parker boundary condition that U^2 only lies very close to q^2 when it also lies close to $GM/2r = W^2/2$, in the Chapter 3 notation. One must not impose this as a boundary condition; one must solve the flow pattern to see if it is satisfied, or if something else is more correct.

The difficulty in trying to solve such a stellar-atmospheric trans-thermal flow problem is that, generally, such problems have not yet been solved in even laboratory-aerodynamic situations, except in highly specialized circumstances. As we see, the stellar-atmospheric problem is highly-dependent on the nonradiative energy supply and dissipation, where we have already stressed our ignorance. Clearly, the flow takes its energy from the thermal energy of the atmosphere, up to the transition from quasi-thermal to strongly superthermic; which we place in the upper-corona. So rather than being able to call on laboratory knowledge of trans-thermal flow problems, in the presence of highly-dissipative energy sources, to guide our stellar atmospheric modeling, we have only the inverse situation. We must use empirical modeling to develop our understanding of such flow. But this requires we have some algorithmic approach to representing the data.

We see that our recognition of the physical cause of the instability, coupled with the form of eq. (3.C), provides just such an approach. The RHS of eq. (3.C) does not change significantly with U until $U^2 \sim W^2$. $\partial q^2 / \partial r > 0$ in this region; so it simply strengthens g , if it enters at all significantly. Then we see how the flow oscillates. If there were no terms other than the first, on the LHS of (3.C), the flow would accelerate until $U > q$; then decelerate, as the LHS changed sign while the RHS kept its sign, until $U < q$; then repeat. The behavior would persist until $U^2 \sim W^2$, and the RHS changed sign also. Indeed, we see from the sphere photographs that this is what actually happens, but locally. The sphere continues its monotonic deceleration, with the flow around it showing, locally, the fluctuations which produce the acoustic waves that we see. In the mass-flow in the atmosphere, the flow continues its monotonic acceleration outward because $U_0 \sim q$, in eq. (4.3), while it is U_1 which shows the fluctuations. U_1 is described by the t -dependent terms in eq. (3.C), while U_0 is described by the first two terms on the LHS—the aerodynamic and the radiative-acceleration terms. Clearly this is an oversimplification; the coupling between all terms is critical; but it lets us see a first-approximation picture that is much more realistic than those discussed under the hot-coronal and radiative-origin theories. Descriptively, we write eq. (3.C) as

$$r^2 U \frac{\partial U}{\partial r} \left\{ (q^2 / U^2 - 1) + \mathcal{K} L (\dot{M})^{-\alpha} (r^2 U \partial U / \partial r)^{\alpha-1} \right\} + f(r, t, U, \partial U / \partial r, \rho) = 2r (W_1^2 - q^2) \quad (4.31)$$

(In Chapter 3, we already remarked that \dot{M} in the above is already an approximation, to be corrected.) So we see that we have no problem of avoiding large $\partial U / \partial r$ when $U \sim q$, the motivation of the Parker condition; other terms remain to keep the LHS from vanishing. But we also see that, depending on the size of $\partial U / \partial r$, U_0 may not increase steadily outward under the relation $U_0 \sim q$; but rather $U_0 \sim q + kr$, with $kr > 0$, and depending on $L / (\partial U / \partial r)^{1-\alpha}$. The details of this, and of the cross-coupling with the fluctuating term $f(r, t, \text{etc.})$ remain to be established. Thus far, the arguments are by laboratory analogy, and from the observations, summarized in Chapter 3, of components of the super-ionized lines which fall into the velocity range to be expected if there is a pre- T_e (max) region where $U \sim q$.

So, summarizing Thermodynamic Characteristic (2.a): the lower-corona is characterized as a region where $U \sim q$; with q increasing outward as T_e rises; and where associated with the quasi-steady U_0 component of U there is a stochastic field of quasi-acoustic fluctuations. I use the term *acoustic* because of our reliance on laboratory observations; but one should realize that we actually mean compression-disturbances moving at about the 1-dimensional thermal velocity.

(2.b) This lower-corona ends where $U^2 \sim q^2 = W^2/2$: i.e., effectively, the flow reaches an escape velocity. Then, one enters the *UPPER-CORONA*. Conventionally, what we call *Upper-Corona* is called *Corona*; the *Lower-Corona* does not exist, in the usual theoretical modeling. An extended region of trans-thermic flow does not exist in these models. For the reasons summarized, its presence seems necessary.

(3) *DIAGNOSTICALLY*, the lower-corona begins, and the chromosphere ends, at the *thermal-point*; and the lower-corona ends, and the upper-corona begins at the *escape-point*. We define the thermal point as the end of the transition from quasi-thermal control of the density gradient in the low chromosphere to dynamic control at the upper boundary of the chromosphere. At the thermal point, U enters a region—the lower-corona—where U has effectively the value q , subject to the fluctuations of the velocity field just discussed. We define the escape point as the end of this “plateau” of $U \sim q$, across which the effective escape velocity, W , decreases and q increases, to reach equality between them and with U . At the escape point, the gas has sufficient flow-energy to escape from the star, *if* there are no subsequent decelerating forces or interactions, which inhibit a simple thermal-expansion type flow. At the escape point, the gas also has sufficient internal thermal energy to have a significant flow-energy far from the star, if there is any coupling between internal and translational energies, and all the internal energy is not lost by, e.g., radiation.

Because the chromospheric density gradient begins to be affected by the mass-flow when $U/q \gtrsim 1/3$; and because the instability associated with trans-thermal, or trans-sonic, flow is well-developed when $U/q \sim 1$; eq. (3.38) shows that the thermal point occurs at an atmospheric density about 1/3 the value where the chromosphere begins to lose its thermodynamic characteristic of quasi-static density decrease. That is, it occurs about one density scale-height above $U/q \sim 1/3$. So, we have a height-interval of about one density scale-height which marks the chromosphere, low-coronal thermodynamic transition. Table 4-1 set an upper height limit on chromospheric beginning, in

terms of density or particle concentration, by using eq. (3.38) and the photospheric value of q . We can now estimate lower-coronal beginning from the same equation, but using the chromospheric value of q , at the thermal point. Since, because of our ignorance of the nonradiative energy flux, we do not know, a priori, the chromospheric $T_e(r)$, we can only introduce T_e (thermal-point) as a parameter. Since it enters as $q \sim T_e^{1/2}$, an uncertainty in T_e , across its expected range of 10^4 – 10^6 K, only introduces an uncertainty of a factor 10 in n_H (thermal-point), much less than that coming from the admitted range in mass-flux. Finally, we saw in Table 4-1 that all values for the upper-limit on chromospheric beginning height placed $(r_{\text{chr}}/R_p - 1) \ll 1$. So these values were unaffected by our use of $r = R_p$ in eq. (3.38) to estimate chromospheric beginning height. For the chromospheric end, lower-coronal beginning, however, we need an iterative scheme; not all combinations of the parameters give $r_{\text{LC}} \sim R_p$. Roughly, the iteration simply consists of estimating the number of density scale-heights spanned by the chromosphere—since HE holds there—and adopting some scale-height to turn this number into Δr . We start from the density ratio $n_H(\text{chr})/n_H(\text{LC})$ from eq. (3.38) with $r = R_p$, then iterate. Clearly, we obtain lower and upper limits by using scale-heights computed with photospheric and upper-chromospheric values of T_e . Chapter 13, pp. 435–439, of *B-Stars With and Without Emission Lines* (Underhill and Doazan, 1982; Chapter 13, Doazan and Thomas), gives the details, and results, of such an iteration for characteristics of the thermal point for a range of Be stars. It is useless to simply duplicate those pages here, or to compute some other stellar type for variety. I simply adjoin here, as Table 4-2, table 13-4 from that volume, to illustrate the height range for the thermal point. Again, \dot{M} and $T_e(\text{chr})$ are parameters. Since these computations cover $\log g$ of 3 and 4, and \dot{M} of 10^{-9} – $10^{-6} M_\odot/y$, they are sufficiently illustrative for our present purposes.

First, we note that had we chosen the actual mass-flux instead of the total mass-loss rate—mass-flux integrated over the star— r would not enter the computation for n_H , and we would not have the iteration. However, mass-flow is generally discussed in terms of mass-loss, rather than mass-flux, for simplicity in stellar-evolutionary discussions; so we keep \dot{M} as the parameter measuring mass-flow. It is also a more useful parameter in discussing emission from post-coronal regions, such as the H α envelope. Emission $\sim n_H r^3 \sim \dot{M} r \sim F_M r^3$. So, with \dot{M} as parameter, uncertainty in geometry of an emitting shell enters as r , rather than as r^3 with F_M as parameter.

Then we have continually stressed the significance of the thermal point: there, the density distribution begins to follow an $(r^2 U)^{-1}$, rather than an exponential, outward decrease. So if the thermal point does not occur relatively low in the exophotosphere, particle concentration will have dropped too low before the range of exophotospheric regions begin, to let us see, and diagnose, the phenomena in such regions as high-velocity post-corona, low-velocity H α envelope, etc.—even if they exist. We saw the problem in detail, when discussing (Chapter 3) the distinction between thermal-point and escape-point for the Sun, and in measuring $U(\text{max})$ for the Sun and stars like it. We also continually emphasize that we see, and diagnose, the nebula in the PN type stars because particle concentrations persist as high as 10^4 – 10^6 at $r/R_p \sim 10^6$ – 10^8 ; the same range of values which the far-out thermal-point of the Sun places at a few solar radii. Our perpetual example of the Be stars is again striking: the variety of estimates of n_H in the H α envelope range over 10^9 – 10^{11} as a mean, spherical, concentration over a volume whose outer boundary ranges up to some $r/R_p \sim 25$. Given the presence of a chromosphere-corona, and the observed U ranging up to 2000 km/s, we need an inner “H α void” covering a few radii. So, Table 4-2 shows that we can hardly accept a thermal point lying above $r/R_p \sim 1.05$, for these stars, if we have the time-independent, spherical flow upon which these limits are based. The corresponding values of \dot{M} lie in the range 10^{-7} – $10^{-9} M_\odot/y$, values compatible with those summarized in Chapter 3. Also cf Section G.3.

So the essential significance of this low-lying character of the thermal-point for many stars is the same as the significance of the low-lying character of the chromospheric beginning point for all stars—their combined (diagnostic, structural, thermodynamic) implications. Diagnostically, we observe the chromosphere, and are aware of its significance in implying a non-negligible nonradiative energy-flux, because it begins low enough in the atmosphere that the particle concentration is still relatively large. Structurally, if the chromosphere didn’t begin low, we would neither see its effects nor think it and a nonradiative energy-flux were important in fulfilling the atmosphere’s role as the transition-zone between star and environment. In Chapter 3, we continually stressed the empirical-theoretical investigations which established just those facts; to do so, required the nonLTE diagnostic developments stressed in Chapter 2. Historically, although the solar outer atmosphere had been observed at eclipses since 1860, its effects on the radially-observed disk-spectrum had been a priori set aside as negligible; cf Van de Hulst, as late as 1953. It was not until the

Table 4-2
Lower Coronal Beginning Height

Log \dot{M}'	log g	T_{eff} (K)	T_{chrom} (K)	n_{H} Lower Limit	r/R_{p} Lower Limit	n_{H} Upper Limit	r/R_{p} Upper Limit
-9	4	30,000	5×10^4	3.5×10^9	1.005	2.16×10^9	1.01
			2×10^5			1.02×10^9	1.04
			8×10^5			3.95×10^8	1.19
			1.5×10^6			1.99×10^8	1.43
			3.0×10^6			2.68×10^7	3.27
	3	30,000	5×10^4	3.3×10^9	1.038	1.84×10^9	1.10
			2×10^5			4.77×10^8	1.53
			3×10^5			1.80×10^8	2.26
			1.5×10^6				
-7	4	30,000	5×10^4	3.6×10^{11}	1.003	2.19×10^{11}	1.006
			2×10^5			1.07×10^{11}	1.022
			8×10^5			4.87×10^{10}	1.07
			1.5×10^6			3.17×10^{10}	1.13
			3.0×10^6			1.72×10^{10}	1.30
			5.0×10^6			7.61×10^9	1.71
	3	30,000	5×10^4	3.5×10^{11}	1.015	2.08×10^{11}	1.03
			2×10^5			9.14×10^{10}	1.10
			8×10^5			2.24×10^{10}	1.58
			9×10^5			1.23×10^{10}	2.07
-6	4		5×10^4	3.5×10^{12}	1.001	2.20×10^{12}	1.003
			2×10^5			1.09×10^{12}	1.008
			8×10^5			5.36×10^{11}	1.020
			1.5×10^6			3.85×10^{11}	1.027
			3.0×10^6			2.72×10^{11}	1.029
			5.0×10^6			2.18×10^{11}	1.012
	3		5×10^4	3.5×10^{12}	1.004	2.20×10^{12}	1.002
			2×10^5				<1.0001
			1.5×10^6				
The Sun: $\dot{M}' = 3.0 \times 10^{-14}$; $n_0 = 3.8 \times 10^{15}$ ($6000/T_{\text{chrom}}$)							
T_{chrom}	1.0×10^4	2.5×10^4	5.0×10^4	2.0×10^5	4.0×10^5	4.5×10^5	
n_{H}	1.44×10^7	8.68×10^6	5.61×10^6	1.53×10^6	2.54×10^5	9.17×10^4	
r/R_{p}	1.018	1.043	1.088	1.47	3.06	4.93	

nonLTE diagnostics of the 1952 eclipse observations (Thomas and Athay, 1961) that astronomers became aware of just how low the chromosphere actually began; just how much material was involved in it; and just how much the source-functions for radiative diagnostics were affected by the combination of nonthermal heating and nonLTE distribution functions. Were the nonradiative energy flux, and its dissipation, less, the chromospheric beginning point, the mass contained in it, and the particle concentrations exhibiting its presence would all change in such a way as to make the importance of the chromosphere less, in the role of the atmosphere. I emphasize this point, now observationally and empirically-theoretically well-established, because it is precisely that same point which we must now put into perspective for all the other exophotospheric regions. What counts, is how much material is involved in them: in producing their observable effects, by their own particle concentration; and in veiling their effects, by the particle concentrations in overlying layers. And the sizes of those particle concentrations are fixed by just those sizes, and their time-dependences, of those non-thermal fluxes set aside, a priori, in speculative atmospheric modeling, but which we use here as the basis for our algorithmic, empirical-theoretical approach.

All these comments also hold, even more strongly, for the location of the thermal point—the beginning point of the lower-corona, where the density distribution ceases to decrease exponentially—and its relation to the mass-flux. If one permits thermal-points and escape-points to differ, the location of the first is fixed by the size of the mass-flux, not at all by the location of the escape point, which depends only on gravity and coronal- T_e . If, as in the Parker hot-coronal approach, one forces lower- and upper-corona to coincide—thermal-point to occur only at the escape-point—the size of the mass-flux is fixed by the location of these coinciding points and the HE, exponential, chromospheric density-distribution. One has extreme difficulty in producing the observed range of large mass-fluxes, and in producing solar-coronal-level particle concentrations at $r/R \sim 10^6$ – 10^8 in some stars. So, in constructing models of the full observed range in exophotospheric regions, one must be careful to avoid blurring any features, or contracting any descriptive equations, by a priori, speculative, imposition of conditions which do not accord with observations. So, *we permit, we do not force*, thermal-point and escape-point to differ; we restore just that essential freedom to maintain a large particle-concentration at large distances which the Parker hot-coronal approach suppresses. We ask, not tell, the stars what is their particle concentration at large distances, as a function of what mass-flux is compatible with their subatmospheric structure. We discussed the algebraic background for all this in Chapter 3, in considering that contraction of the underlying equations which is the Parker approach. We also noted, there, that the present radiative-acceleration theories suppress both chromosphere and all varieties of corona. So, we proceed to permit the lower- and upper-coronae, and thermal- and escape-points, to differ, and so define:

D. AN UPPER-CORONA is a distinctive atmospheric region, which

(1) *OBSERVATIONALLY*, lies just above the lower-corona, whose trans-thermic instability damps out as it blends into the upper-corona, and the mass-flow becomes a stable, monotonically-accelerated-outward, superthermic one. Thus the upper-corona:

(1.a) Continues to show a strong superionization, which, for some stars, culminates in the production of X-rays, to a highly individualistic degree among stars of the same MK class. As shown in Chapter 3, there is a trend in X-ray emission to decrease with decreasing visual luminosity; but the scatter is almost as large as the trend. There exist—comparing both hot and cool stars with and without H α emission—very preliminary indications of an increased X-ray emission with decreased H α luminosity. This suggests strong X-ray veiling in at least some stars, especially those with the more extended atmospheres associated with the cool, H α -emission envelopes. Because some stars of the same MK class show H α emission, while others do not; because the superionization levels of these two varieties of stars are the same; and because of this differential X-ray emission between the two varieties; a significant difference in post-coronal structure, but strong similarity in coronal structure, are suggested. Among the B, Be, Be-shell stars, these two varieties are further distinguished by the strong variability in these emission and shell features, and much smaller variability in other features by the B-normal stars. The small-scale variability is shown by the T Tauri stars; the emission-envelope, and shell, features have not yet been shown variable in them. But we note that some H α -emission is pre-coronal for the T Tauri stars, while it is wholly post-coronal for the Be, and Be-similar, stars.

(1.b) Continues to show a decrease in density gradient with increasing distance from the star. Under eq. (3.A), this implies a continued outward increase in U . For bright-enough stars that high-resolution, short-wavelength, farUV

observations can be made, the superionized lines show evidence of such outward acceleration, up to superescape values in the most highly-ionized ones. $U(\max)$ increases, statistically, with degree of ionization for the stars observed in most detail, which are the OB. We discussed in detail those stars which have individually been the most observed, the Be and some Oe, which generally show several components for each line, and are highly variable. One component is at 50–100 km/s, corresponding to chromospheric-coronal values of q . Other components range from some 300 km/s to some 2000 km/s, distinctly superescape. The particular ionization-velocity correlation of the WR stars, which mixes uncertainty in $T_e(r)$, hence ionization (r), with questions of frozen-in ionization and excitations states, was discussed in Chapter 3. That their maximum velocities, up to some 3500 km/s, are superescape is unquestionable. Solar values of $U(\max)$ are measured with collectors, at the Earth's distance, and are again superescape, ranging 300–800 km/s. So, observationally, we define the upper-corona as a region of continued outward acceleration of the mass-flow; beyond superthermic and superescape values even though we know neither kinematic nor dynamic details. Fig. 3-33 abstracts our uncertainty.

(1.c) Has an uncertainty in $T_e(\max)$, and in whether T_e continues a monotonic outward increase. Those stars in which X-rays are observed must have regions where $T_e \sim 10^6$ – 10^7 K. Those proponents of radiative-acceleration mass-flows, to avoid coronae, suggest such high- T_e regions are highly-localized “clumps” of material, produced by instabilities in the highly-superthermic flow. *As we saw above, such highly-superthermic flow is precisely where such instabilities do not arise*; they are immediately damped out by shocks, before they reach significant amplitude. Study any laboratory photograph of such flow, where some local inhomogeneity is introduced. Study the behavior of a solid object, in which a “tumbling” motion is induced: it is immediately damped, and the object moves steadily (cf Vol. 2 photographs). These authors suggest (Lucy and White, 1980; Lucy, 1982) that regions of differential opacity arise; the shielded regions have less radiative acceleration; differential flow, shocks, locally-high T_e arise. One has the same, laboratory-based objection to these wholly speculative proposals. Regions of differential density are *immediately* homogenized, by the stabilizing-shock occurrence, *unless* some strong barrier exists, such as a magnetic field. But the field must be strong enough to contain differential-flows of $o(10^3$ km/s). One must show how to produce them, under these conditions of such superescape flow—either experimentally in the laboratory, under stellar-simulated conditions, or by self-consistent theory, of which the essential thermodynamic aspects can again be laboratory-modeled. Lacking such real-world counter-evidence, we continue to associate those T_e demanded by X-ray observations *either* with the $T_e(\max)$ of the upper-coronae, *or* with the formation of the slow, cool, H α -emission envelopes discussed below. And again, in asking the prevalence of such T_e , we must, in each case of undetectable X-rays, ask into the possibility of veiling. It is the presence of such X-rays in *some* member-star of almost every class of stars which demands such consideration of veiling. The problem is the same as that attending Fig. 3-33 of $U(\max)$, vs. spectral type. It focuses on the existence of a local-environment; cf below.

So then, *wholly-arbitrarily*, we define, observationally, the end of the upper-corona to be that region where T_e begins to decrease outward. We introduce this definition, because it marks the region where a strong effect of a non-radiative energy dissipation ends. Note that we do not demand that T_e continue a monotonic outward decrease thereafter. We say only that the post-coronal beginning is characterized by the *first* change in the sign of dT_e/dr from positive to negative. We allow the possibility that the post-corona is itself ended by a region where T_e again rises, even briefly, as at the shock which must mark the deceleration of the mass-flow in those stars where U (H α -emission envelope) lies below its coronal values. So we have possible varieties of post-coronae.

(2) *THERMODYNAMICALLY*, the upper-corona is a region of superthermic—also superescape—flow, also characterized by nonradiative energy dissipation. The beginning of the upper-corona is where the flow enters the superthermal, superescape range; the end of the upper-corona is where that strong nonradiative energy dissipation which produces the chromosphere-corona becomes insignificant. At least over some part of the upper-corona, an outward acceleration continues; but we demand only that no deceleration mechanism dominates. By the nature of the transition from thermal to superthermal, superescape velocities, any mass-flow, not subsequently decelerated, will arrive arbitrarily-far from the star at nonzero velocity.

(2.a) The condition for the transition between lower- and upper-corona is fixed by the behavior of the RHS of eq. (3.C). It is not precisely the $q^2 = W^2/2 \equiv GM/2r$ relation that is valid in an isothermal region, nor the $U^2 = q^2$ relation for the LHS under the contracted form (3.47) of eq. (3.C); cf point (2.b) following. But effectively, at this lower-to upper-coronal transition, $U^2 \sim q^2 \sim W^2/2$; U passes from thermal to superthermal and superescape in a relatively short distance. The essential thing is to know the value of T_e in this transition-range; to know how high the nonradiative energy dissipation can heat the corona, in order to know how low must $W^2/2$ fall to reach q^2 , hence U^2 . So again, lacking detailed knowledge of the nonradiative energy flux, in any given star, and its dissipative properties, this T_e (escape-point) is not presently a theoretically-predictable quantity. If one wants simply to “guess” size and dissipation properties of a nonradiative energy flux, in order to “compute” T_e (escape-point), one might as well simply guess that T_e directly—because observationally, from farUV and X-ray spectra, we know the range of T_e . Observationally, we know that many stars reach a value of U that exceeds the photospheric escape velocity; we know that many more reach values of U that exceed the local escape velocity at exophotospheric escape points. So, it is not a question of *whether* such an escape point exists—it does; the question is where it lies, as a function of the several parameters characterizing the atmosphere of a given star. We return to its value at the end of Section (2.b).

(2.b) The question of the acceleration mechanism in the upper-corona is a critical one. Even for the Sun, it has not yet been resolved, nor has the question why the solar $U(\max)$ varies by a factor 2, while the mass-flux stays, statistically, constant (Zirker, 1983). That a radiative acceleration is important in the hot stars seems inescapable. That the proper radiation field producing such acceleration is not just the photospheric one, but is supplemented by that from the exophotosphere, seems equally clear. In such a situation, one must also admit the possibility of radiative acceleration in the cool stars. If, in the limit, the major radiative acceleration came from just those spectral regions in which chromosphere-corona were optically-thick and had continuum source-functions of comparable size across the HR plane, we would lose that distinction between hot and cold stars, in producing a radiative acceleration, which a focus only on the photosphere introduces. Because chromospheric-coronal radiative emission comes from dissipation of the nonradiative energy flux, and exochromospheric opacity comes from the mass-flow-induced density gradient, the radiative acceleration in this extreme case would be quasi-independent of the photospheric radiative flux. And, while it would not fix the size of the mass-flux, it would fix its maximum, even if not necessarily terminal, velocity. This extreme case is, a priori, no more correct than its omission.

The observed farUV and X-ray spectra already show that the range of ionization in the atmosphere of a given star is, observationally, much more homogeneous across the HR plane than would be inferred from the visual continuum alone. The faint cool star, the Sun, for which we have detailed observations because it is near, shows at least as high, and as varied, ionization as that shown by the bright, hot, WR objects—and equally as high $T_e(\max)$. Attempts to place the observed O VI, N V, C IV etc. ions of hot stars into regions of cool winds, by Auger ionization with coronal X-rays, are irrelevant—because it requires coronae in any event. So, roughly, we have the same variety of ions available for radiative acceleration, although not necessarily in the same concentration, across the HR diagram. For example, although the presence of C IV ions becomes decreasingly obvious as one goes down the sequence of Be stars from B0e to B9e, individual variations are strong—as reported in Chapter 3 for 59 Cyg (B2e) and θ Cr B (B7e). Moreover, C IV comes back into prominent visibility in the Herbig Be, Ae stars, and in the T Tauri stars, which range over classes F–M. Also, as stressed, X-ray observations in all spectral classes, except possibly the M sg, suggest the same level of $T_e(\max) \sim 10^6$ – 10^7 K, admitting veiling, cf below. So, in assessing the source, and degree, of radiative acceleration, what remain are largely questions of opacity, and nonLTE corrections to replace a simple-minded representation of that flux entering the radiative acceleration to be $B_\nu [1 - \exp(-\tau_\nu)]$. We note, of course, that the full effect of the photosphere + chromosphere-corona outward radiative acceleration will only be felt in the upper-corona. In the chromosphere, e.g., photospheric acceleration will be outward, coronal will be inward, and the difference gives the acceleration. In the cool H α -emission envelope, there will be a strong veiling of chromospheric-coronal continuum; its opacity will produce its own, local, radiation field. Thus, in eqs. (3.C) and (4.31), we expect a rapid outward increase in the radiative-acceleration term, but not just from the photospheric transfer problem. For this reason, we treated the behavior of the radiative-acceleration term as we did, in discussing the trans-thermic flow in the lower-corona.

So, in such considerations of the opacity of the chromospheric-coronal regions, we really return to Struve’s suggestion that the contribution to atmospheric structure of these two regions should be measured by the optical opacity

of each. His concern with such opacities focused on two aspects; ours, on three. His gross concern lay in the opacities being large enough to produce those atmospheric peculiarities observed in the visual. We stressed this point above, and in Chapter 3, re observable chromospheric features appearing in disk spectra. We emphasized the empirical demonstration, by solar eclipse diagnostics of the visual continuum at the limb, of the chromospheric contribution to disk observations of strong lines, and to the LyC and radio continua: i.e., the chromosphere is opaque in all these. Struve also focused on possible veiling effects on photospheric features by the exophotosphere. We stressed the observed existence of such effects in cool T Tauri, hot Be, and intermediate symbiotic stars; we also emphasized the apparent veiling of chromospheric-coronal features themselves, such as X-rays and possibly velocity fields, by the postcoronal, cool envelopes. But our third concern focuses on that chromospheric-coronal modification of the photospheric radiation field, because these regions are hot and variously opaque, in its accelerating effect on mass-flow: on Gerasimovic's, not Struve's, proposed origin of the dynamic corona. But here, we differ with Gerasimovic, and his successors such as Lucy and Solomon, and Castor-Abbott-Klein, in recognizing the radiation field as only an acceleration mechanism for the mass-flow, not as its source, which we attribute to the "open" boundary condition on a subatmospheric non-thermal configuration. Among other nonthermal modes, such configurations can include that stellar rotation, although not necessarily at the critical velocity, upon which Struve, and especially Limber, depended to produce the mass-flux. *What I try to put into focus here, is the convergence of the several—only superficially apparently-different—observational indications of modified exophotospheric structure, which demand that it itself produce appreciable opacity and radiation fields.* The apparent differences arise when each of the two basic directions of modification focuses upon *just one flux as primary*: either on a nonradiative flux which, as a corollary, produces a mass-flux; or on a mass-ejection which, as a corollary, produces a nonradiative heating. The converging unity arises when one recognizes that *both kinds of fluxes are independently necessary*, to produce that interaction which we observe. The mass-flux increases the exophotospheric opacity sufficiently that on the one hand, the heating of these regions by a nonradiative flux can be observed; and on the other hand, *the radiation field produced in the exophotosphere itself can be self-absorbed by, and accelerate, the exophotospheric mass-flow.* This is the interaction between the several fluxes which we emphasized above. Overall, each of these three aspects of chromospheric, coronal, and postcoronal opacities gives that empirical testimony which we need for empirical-theoretical characterization of radiative-acceleration.

Presently, strictly-theoretical predictions of exophotospheric opacities and emissions are unreliable; primarily because lack of knowledge of the characteristics of nonradiative energy-fluxes leaves $T_e(r)$ to be essentially conjectural. We have already stressed the exceptional cases where T_e and opacity can be directly diagnosed from observations, such as during eclipses. And we note that the approach of Table 4-2, to use the mass-flux to estimate particle concentrations at the base of the lower-coronal, $(r^2 q)^{-1}$, density distribution gives a rough measure of the total number of particles above the base of the corona, $N(L-C)$. Integrating eq. (3.38), with $U \sim q$, and taking a mean $q \sim q(10^5 \text{ K})$:

$$N(L-C) = \frac{\dot{M}}{4\pi\mu_H} \int_{r_{L-C}}^{\infty} \frac{dr}{qr^2} \sim 1.1 \times 10^{31} \dot{M}' \left\{ (10^{-5} T_e)^{1/2} r_{L-C}/R_{\odot} \right\}^{-1} \quad (4.32)$$

\dot{M}' is \dot{M} in units of solar-masses per year. With σ_e (electron-scattering) $\sim 10^{-24} \text{ cm}^2/\text{electron}$, we just reach $\tau(n_e) \sim 1$ for $r_{L-C}/R_{\odot} \sim 1$ and $\dot{M}' \sim 10^{-7}$; for $r_{L-C}/R_{\odot} \sim 10$, an OB photosphere, we reach $\tau(n_e) \sim 1$ for $\dot{M}' \sim 10^{-6}$; while the WR-type atmosphere, with $\dot{M}' \sim 10^{-4}-10^{-5}$, is, as continually remarked, opaque throughout the chromosphere-corona. For the radiative acceleration we are, of course, concerned with the line-opacity; but these figures show just how the mass-flux introduces a strong opacity. Note the opacity diagram, Fig. 4-8, in the (1983) treatment of that popular star, ζ Puppis, by Kudritzki, et al. In their nonLTE, but RE and HE model, even the "reasonably-photospheric" He II lines at $\lambda 4686$ and $\lambda 1640$ are formed at a factor 10 in n_e above the thermal point; they use an $\dot{M}' = 4 \times 10^{-6}$. As they emphasize, such lines are exophotospheric in origin. Thus, with the size \dot{M}' currently discussed in a variety of hot stars, the opacities induced by the mass-fluxes are sufficient to demand many lines are formed in regions where they will be absorbing in the exophotospheric radiation fields. The question, of course, is the size of these fields. We abstract the material collected in Chapter 3.

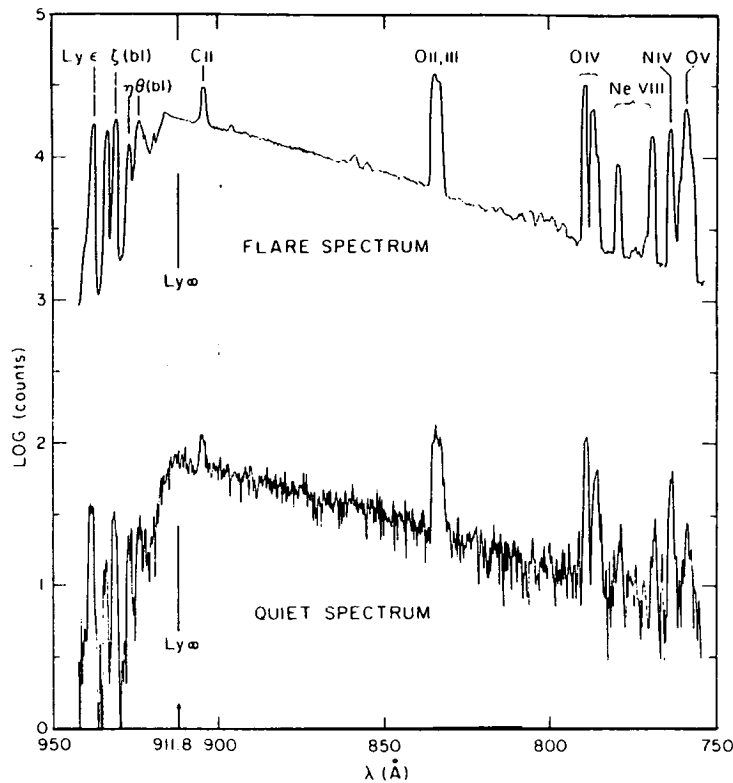


Figure 4-8. Solar chromospheric flare regions (from Machado, et al., 1980).

From an observational standpoint, we have data on a wide variety of stars, in the spectral region from the visual down to the Copernicus cut-off at about $\lambda 1100$. Such observations provide the basis for the often-remarked adequacy of standard, RE and HE, modeling to represent the continuum. Superionized lines appear throughout this spectral region; their formation is attributed to overlying layers; any radiative acceleration via them sees, usually, only a photospheric field. Although we have remarked a 1-magnitude, statistical, excess of the Be, over the B-normal, continuum, we have as yet established no correlation between radiation field variability and velocity variability in this spectral region. The strongest examples of phase-changes in radiative intensity in this region come in the cataclysmic, symbiotic, and pulsating variables. The cited behavior of the recurrent nova T Cr B during a two-year period (Cassatella et al., 1982) provides a striking example: strong changes in the $\lambda 1100$ – 3000\AA continuum; associated, but differential, change in the line-spectrum; no appreciable change in the visual continuum. But there were no striking velocity changes in these low-resolution spectra, nor in the two examples of high-resolution spectra during maximum luminosity. Usually, with the stated exceptions, cool stars have weak continua in the $\lambda\lambda 1100$ – 2000\AA region; and stars hotter than $T_{\text{eff}} \sim 25,000$ K have their photospheric maximum intensity below $\lambda 1100$. So, for both photospheres of hot stars, and chromospheres-coronae of all stars, the region $\lambda < 1100\text{\AA}$ is of the most interest, re radiative-acceleration, and its variability—with the above-cited exceptions.

In the spectral region above the X-ray and below the farUV, $100\text{\AA} \lesssim \lambda \lesssim 1100$ —that proposed to be studied in the NASA–FUSE and ESA–MAGELLAN PROGRAMS—the only detailed information is for the Sun, but there it is extensive, and provocative. In Chapter 3, we saw that we could infer from empirical-theoretical diagnostics of visual-continuum eclipse observations that the solar chromosphere is strongly-opaque in the LyC, with $\tau(\lambda 910\text{\AA}) \sim 10^5$ above the base of the chromosphere. In this LyC, the solar radiative emission comes from the level $\tau(\lambda 910) \sim 1$, where our visual continuum model gave $T_e \sim 8500$ – 9000 K, and $b_1 \sim 10^2$, producing $T_c \sim 6900$ K. This $\tau(\lambda 910) \sim 1$ comes in the region of rapid rise in T_e , associated with the rapidly-changing LyC opacity. Note that under RE modeling,

LTE or nonLTE, an outer-atmospheric, T_{eo} , of this size would correspond to a late B-type star. Then the LyC predicted by this model agreed with direct, disk-integrated, rocket observations of the LyC within a factor 2. Depending upon whether one wants to compare this chromospheric modification of the photospheric radiation field to the photospheric LTE-R modeled value of T_e (boundary) $\sim 4200\text{--}4800$ K, or to the nonLTE asymptotic value of about T_e (asyp) $\sim T_{\text{eff}} \sim 5800$ K, one has a LyC enhancement by a factor between 10^6 and 10^2 . That is, if stars behaved like the Sun, LTE-R models should have their LyC flux enhanced by 10^6 ; nonLTE but RE models, by 10^2 . And it should be these fluxes, not the photospheric RE ones, which one uses to estimate radiative acceleration of those winds which destroy, equally, HE modeling above the thermal point. For the Sun, actual radiative acceleration by lines in the LyC corresponds to a theoretical RE-photospheric radiative-acceleration by a late B star.

Current, high-resolution, disk observations in both quiet and flaring solar regions emphasize these remarks; cf Machado et al. (1980), reproduced here as Fig. 4-8. Note their similarity in spectral distribution of I_ν in this region of the LyC; the large change, a factor 10^2 between quiet and active regions, lies in the absolute size of I_ν . If, crudely, one represents the LyC source-function as $b_1^{-1} B_\nu(T_e)$ across the whole atmospheric region corresponding to the spectral range $750\text{\AA} < \lambda < 910\text{\AA}$, then the slope of I_λ corresponds to $T_e \sim 9200$ K in the quiet, and $10,000$ K in the flaring, regions; and the intensities, to a factor 50 decrease in b_1 from quiet to flare region. We note that the quiet-Sun chromosphere corresponds to $n_e \sim 10^{11}$, and the flaring to $n_e \sim 10^{13}$; that just this range of n_e marks the change from photoionization-dominated to collision-dominated H α and n_2 ; and that the change from opaque to transparent in the LyC marks the passage from $b_1 \sim b_2$ to strong departure from equality (cf Chapter 2). So, this change in b_1 is as expected, if we interpret, as becomes increasingly accepted, a flare region as one of large density at roughly the quiet-Sun T_e —at the height $\tau(\lambda 910) \sim 1$ —rather than as a region of extraordinary increase in T_e . That is, the nonradiatively-heated, chromospheric-coronal-equivalent regions occur at higher density, equivalently-lower in height, in what is called flare-areas. Then we recall, from Fig. 3-33, that in the quiet-Sun, $U(\text{max}) \sim 450$ km/s; while just before the minimum of solar activity—i.e., before that phase when the fraction of the solar surface covered by flare-areas is minimal— $U(\text{max}) \sim 800$ km/s. Brown et al. (in Jordan, 1981) summarize H α flare velocities as $U(\text{flare}) \lesssim 10^3$ km/s; while radio-burst data are diagnosed as giving $U(\text{max}) \sim 800\text{--}2000$ km/s. Note that with the exception of WR objects and novae, this range covers that observed in the brightest stars, and in the episodic-ejection phases of such things as Be, symbiotic, cataclysmic—and the Sun. We note, of course, the “veiling” comments on Fig. 3-33—both optically in terms of observations, and collisionally in terms of the cool envelope discussed later. And again, we insist on the WR spectrum as that produced in an atmosphere where the nonradiative heating begins low, so produces a radiative excess at higher densities—in most spectral regions, we see only the chromosphere-corona. We have already caricatured the novae as objects where the escape point lies below the observed layers, but where strong differential velocity effects have not yet arisen at the lowest observed heights.

Clearly, all flaring regions of the Sun do not cover the same surface area; nor do all stars behave like the Sun, especially those hot stars in whose atmosphere hydrogen is effectively ionized at layers below the chromosphere. But we note that this chromospheric-coronal enhancement of the radiation field is not confined to the spectral region of the hydrogen LyC, nor to the MK-taxonomic region of the Sun. Fig. 4-9 reproduces Skylab observations of quiet, active, and coronal-hole areas over the spectral region $300\text{\AA} < \lambda < 950\text{\AA}$ (Vernazza and Reeves, 1978). Fig. 4-10 reproduces rocket observations of the white-dwarf HZ 43, covering the same spectral region, from Malina et al. (1982). Clearly, both He I and He II continua are very significantly enhanced, over the predictions of standard photospheric models, LTE-R or nonLTE, based on RE values of T_e , and HE (at those T_e) values of opacity.

Further, speculative, discussion of radiative enhancement, and increased opacity, by chromospheric-coronal regions, across the HR plane, is not useful. One awaits either extensive observations in the $\lambda \lesssim 910\text{\AA}$ region—*but simultaneously with those in the farUV and visual*—or greater insight into the treatment of radiative acceleration by a chromospheric-coronal “shell.” That material on the variability of $U(\text{max})$, the form of the line-profiles reflecting the velocity distribution, and the “individuality” of such velocity characteristics, summarized in Chapter 3, provides strong boundary conditions on any theoretical representation of $U(r, t)$. We find the detailed information on phase-variability of Be, and Be-similar, stars provocatively-promising, especially if it can be supplemented by information on that $\lambda < 910\text{\AA}$ region. It is essential to separate those observational characteristics which arise from a change in mass-loss rate, and those which arise from a change in nonradiative heating, in order to separate those characteristics

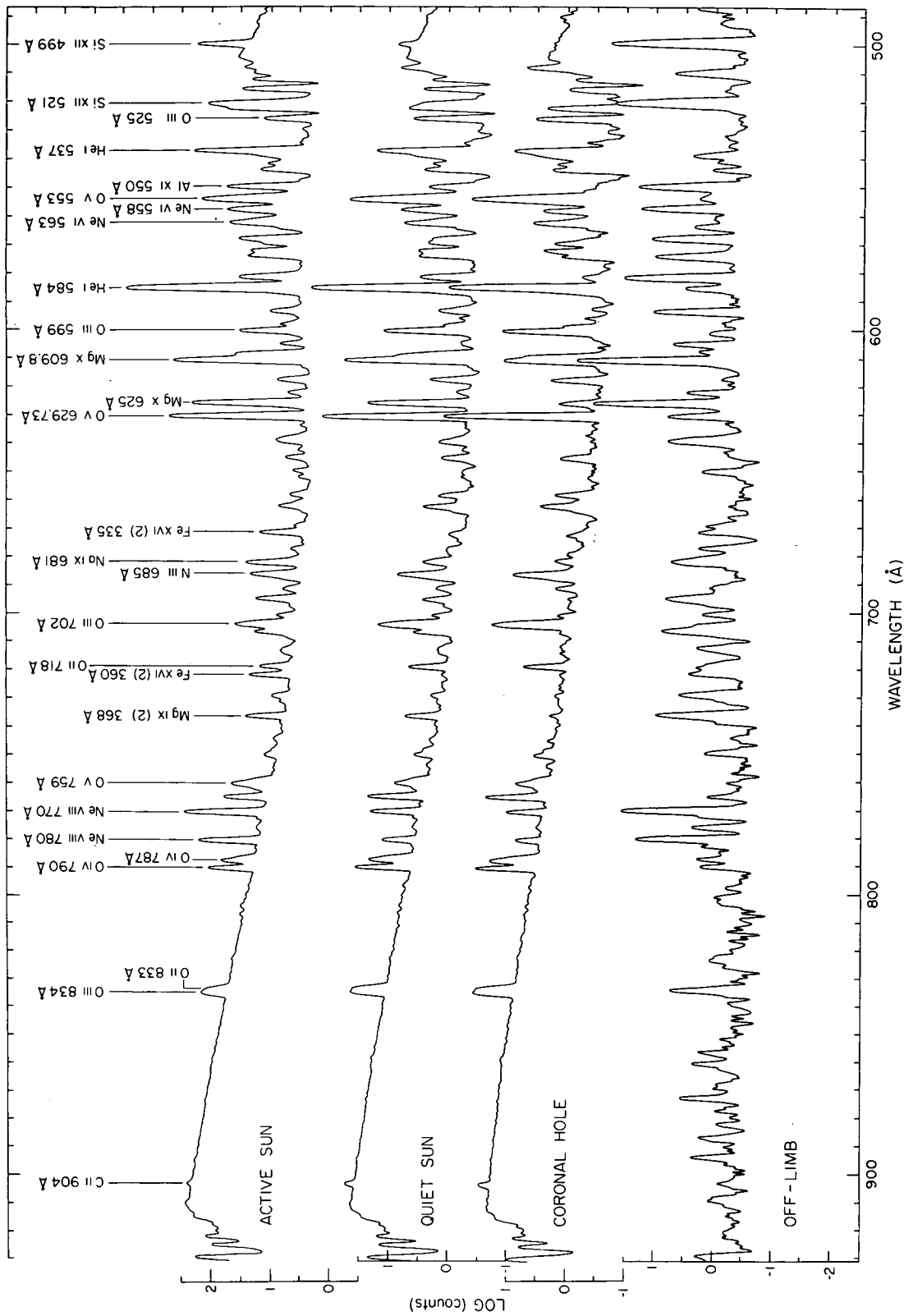


Fig. 4-9a. Average solar spectra between 950 to 450 Å of a quiet area, a coronal hole, an active region and a quiet area off limb (from Verrazza and Reeves, 1978).

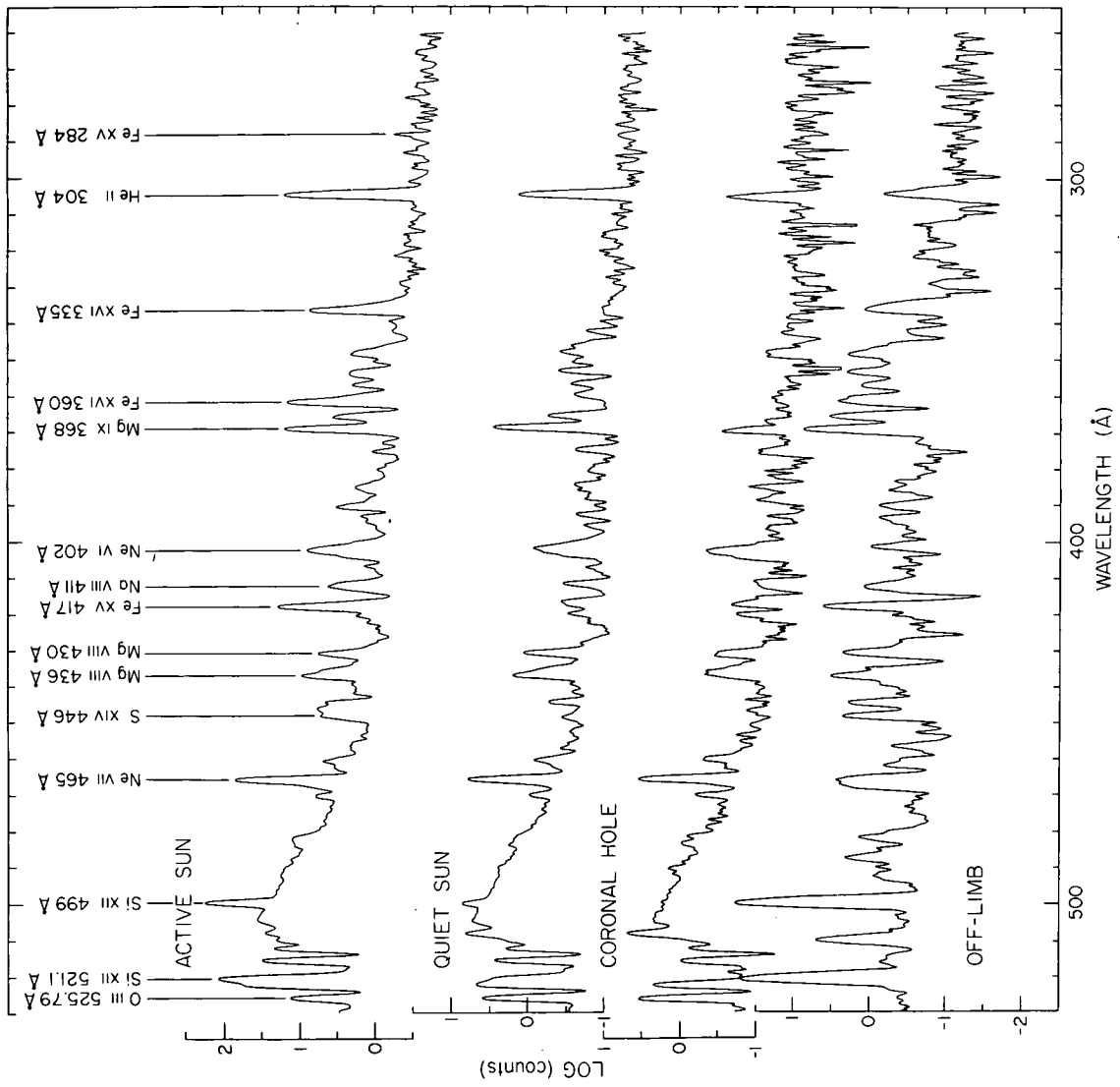


Fig. 4-9b. Average solar spectra between 550 to 280 Å of a quiet area, a coronal hole, an active region and a quiet area off limb (from Vernazza and Reeves, 1978).

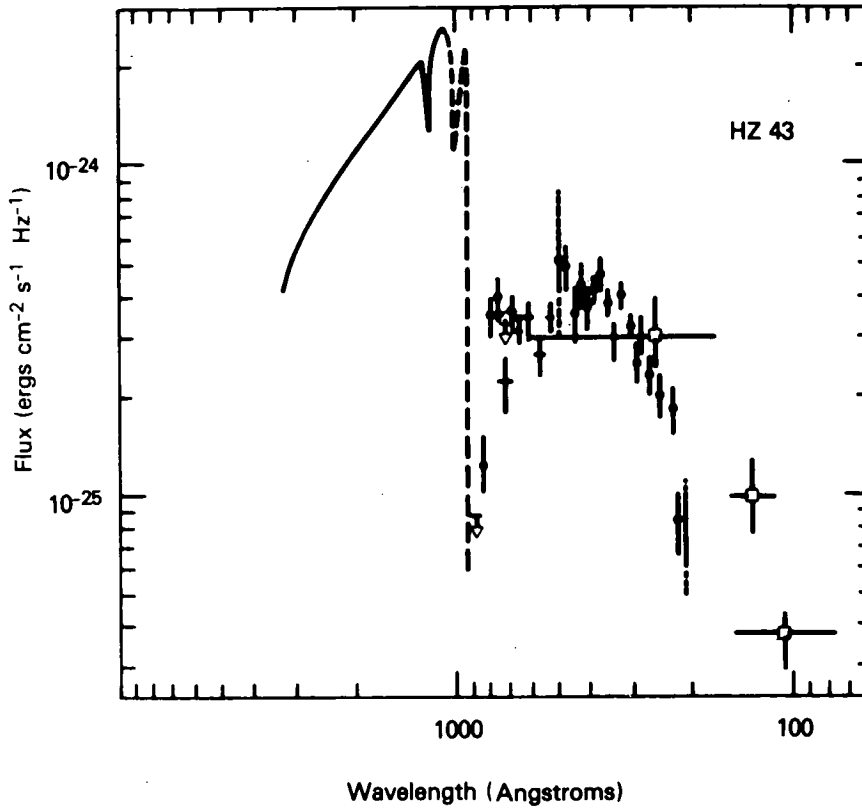


Figure 4-10. Extreme ultraviolet spectrum of the hot white dwarf star HZ 43 (distance 60 pc), obtained with a rocket-borne spectrograph (from Malina, et al., 1982).

arising from a greater mass-content of the exophotosphere from those arising from a greater energy content and dissipation. Thus far, the Be data are the most complete, in displaying variability and individuality of each aspect.

In Chapter 3, we have already shown the over-restrictive nature of that contraction of eq. (3.C) to the forms (3.40)–(3.46). In essence, an approach which produces a $U(\max)$ depending only on the escape velocity, not the radiation field, has lost its initial premise of a radiative acceleration. Its loss corresponds to turning eq. (3.C), which should describe the propagation of a specified mass-flux, into an eigen-value problem for determining the size of the mass-flux. That approach demands a thermal radiation field specify the size of a nonthermal mass-loss—a thermodynamic inconsistency. So we return to asking how a combined thermal (photospheric) and nonthermal (CC) radiation field accelerates a specified nonthermal mass-flux. From the above discussion, and Chapter 3's observational conditions, one has, schematically, an equation corresponding to (3.C), in any region where U exceeds q sufficiently that any trans-thermal instability of the lower-corona has damped out:

$$\begin{aligned}
 U \frac{dU}{dr} (1 - q^2/U^2) + kr. &= \sum_{i,\alpha,\nu} n_i C_{i\alpha\nu} (U dU/dr)^\alpha \left(b_{P\nu}^{-1} B_\nu(T_{\text{eff}}) \pm b_{CC}^{-1} B_\nu(T_e) \right) \frac{R^2}{r^2} \\
 &+ \frac{2q^2}{r} - \frac{GM}{r^2}
 \end{aligned} \tag{4.33}$$

R^2/r^2 is simply the factor relating areal flux to total flux. The sum is over the absorbing ion, the line at ν , and the CAK α -factor which, in their approach, gives the velocity dependence—i.e., the displacement—of the line-absorption. The b 's represent a mélange of the nonLTE, and any opacity, correction. The (\pm) represents the “location” of the point: interior to chromosphere-corona, the radiative-acceleration of the latter opposes the photospheric acceleration; exterior, the two accelerations reinforce. The “ kr .” simply represents those correction terms which, in the lower-coronal trans-thermal region, keep the LHS from vanishing. We have continued the representation of the flux by the expression earlier used, $b^{-1}B_\nu(T_e)$; and all the discussion of Chapters 2–3 can be taken over to assess its value, for each continuum. The $C_{i\alpha\nu}$ contains the line-transfer correction. Then the essential comments are the following:

α . If $U(\max)$ and $U(r)$ are to be fixed by the radiation field, then clearly it is the first terms on each of the LHS and RHS which are the important ones. The gravitational term—which also measures the escape velocity—is important in lower atmospheric regions, because it fixes that density gradient, for $U \ll q$, which provides the initial acceleration up to $U \sim q$. In the region $U \gg q$, on which the radiative-acceleration theories focus to estimate $U(r)$ and $U(\max)$, the gravitational term is a deceleration, not acceleration. That it appears as an acceleration in the CAK approach is an artifact, introduced by their erroneous contraction of the equations, and restricted solution.

β . Because the radiative terms are the larger, when the sign of the chromospheric-coronal contribution is positive, the major acceleration should occur above the region where the outward opacity of chromosphere-corona becomes negligible relative to the inward opacity—i.e., where the major chromospheric-coronal (CC) contribution to $J_\nu(r)$ comes from below, not above. For an r^{-2} density distribution beginning at r_{LC} , and a constant volume emissivity, equal contribution from above and below to the CC comes at $2r_{LC}$. So, noting that there is no need to introduce a dU/dr dependence in opacity until $U > q$, we would expect maximum radiative acceleration to occur above $r \gtrsim 2r_{LC}$. However, if nonradiative heating is peaked much lower in the atmosphere, so that a very thin coronal region is produced—as the radiative-acceleration advocates now suggest—maximum acceleration begins lower, terminating earlier the trans-thermal flow, and the lower-corona.

γ . In assessing the size of the radiative acceleration, hence the value of $U(\max)$, some approximation is necessary to avoid the overwhelming details of considering the variety of lines, their radiative transfer, and possible distributions of T_e . One could simply adopt the early Lucy and Solomon attempts to set limits (1970)—noting the correction to these by Thomas (1973) by neglecting dU/dr on the RHS—i.e., setting $\alpha = 0$ —by using some weighted value of T_e (CC) rather than their T_{eff} . One would obtain

$$U^2(r) - q^2(LC) \sim K \left\{ L(CC) \cdot W_{CC} + L(Ph) \cdot W_{Ph} \right\} (1 - r_{LC}/r) \quad (4.34)$$

where the W represent the weighting according to what lines of what ions absorb in what spectral region, of the photospheric, $L(Ph)$, and CC, $L(CC)$ luminosities. Alternatively, one could adopt the CAK approach to representing the dU/dr dependence by some mean α , without adopting those simplifications of the terms in the equations which we criticized. One would obtain

$$U^2(r) - q^2(LC) \sim K \left\{ L(CC) \cdot W_{CC} + L(Ph) \times W_{Ph} \right\}^{1/(1-\alpha)} \left\{ 1 - \left(\frac{r_{LC}}{r} \right)^{(1+\alpha)/(1-\alpha)} \right\} \quad (4.35)$$

That is, the larger the value of $\alpha < 1$, the stronger the dependence on radiation field, and the more rapid the acceleration. To obtain these expressions (4.34) and (4.35), we have simply neglected gravity and q^2/r . That is, we assume either that we are beyond the gravitational escape-point, or that already in the lower-corona, radiative-acceleration dominates.

δ . Gravity dominates below the upper-corona; the $2q^2/r$ term dominates sufficiently-far from the star. The essential physical point of Parker's approach lies in their equality near the star for sufficiently-large T_e . That common, escape, point is defined only by the value of T_e and gravity by:

$$r_{\text{esc}}/R_p = 2.1 \times 10^3 (10^{-4}T_e)^{-1} \times (10^{-4}g)(R_p/10R_\odot). \quad (4.36)$$

The particle-concentration there is fixed by adjoining a value of the mass-loss to those of T_e and g :

$$n_{H,esc} = 1.2 \times 10^{12} \dot{M}' (10^{-4} T_e)^{3/2} (10^{-4} g_p)^{-2} (R_p/10R_\odot)^{-4}. \quad (4.37)$$

Again, we simply give the results for a MS star like the B–Be, in Table 4-3. These would be the conditions at the top of the lower-corona, beginning of the upper-corona, if there were no radiative acceleration. We see that while the Sun reaches the escape point well-within the observationally-suggested region of some 3 radii, (Chapter 3), the Be stars require T_e significantly larger than the solar quiet-Sun value of some 2×10^6 K to produce, thermally, such small r_{esc}/R_p . Contrary to the belief at the epoch of the (1970) original Lucy and Solomon discussion, current X-ray data do not exclude such $5\text{--}10 \times 10^6$ values of T_e . But note that the observed strong variability in $U(\max)$, without corresponding strong variability in $F_p(\lambda > 1100\text{\AA})$, does not suggest a photospheric radiative acceleration can be responsible. The photospheric radiation of 59 Cyg (B2e), $T_{eff} \sim 25,000$ K, peaks just outside the $\lambda 1100\text{\AA}$ cut-off. Clearly, an empirical-theoretical discussion of 59 Cyg, γ Cas, ζ Oph, θ Cr B—those stars on which we have such extensive visual and farUV material—requires the data for $\lambda \lesssim \text{LyC}$. Given the long lead-time for satellite observations, the only near-future hope seems to be systematic rocket studies while IUE is still available for the coordinated studies. The alternative is attempts at theoretical prediction of the radiation field from a variety of arbitrarily-chosen chromosphere-corona models. Such arbitrary choice means arbitrary specification of upper and lower boundaries of the upper-corona—thus of its extent and transition to the postcorona—by the specification of $T_e(r)$ and of the mass-flux. The question becomes the consistency between the radiative-acceleration predicted by such models, and the well-observed variety of properties of the postcorona, as summarized in Chapter 3 and considered below.

(3) *DIAGNOSTICALLY*, the upper-corona begins at the escape-point, characterized by $U(r)$ rising above the local thermal and escape velocities; and it ends in the regions where nonradiative heating is not significant. If the beginning point lies in the $T_e \sim 10^6$ K range, its diagnostic problem is the lack of observing facilities for the spectral range where such coronal-type ions appear, to measure their $U(r)$. Generally, the range is, again, $\lambda < \text{LyC}$; MgX at $\lambda 610$ is the ‘coldest’ strong line. As continually emphasized, the characterization of stellar winds as ‘warm,’ because nothing hotter than O VI is observed, is incredibly naive diagnostics, given the IUE, Copernicus, and most rocket spectral limitations. The observations of forbidden coronal lines of the 10^6 K variety, in such a range of Be-similar stars, protest a ‘warm’ rather than ‘hot’ label. That we observe components of C IV and N V at both 50–200 km/s (thermal velocities, for T_e

Table 4-3
Characteristics at the Escape Point

T_e (chrom) K	5.0×10^4	2.0×10^5	8.0×10^5	1.5×10^6	5.0×10^6	1.0×10^7
Be stars						
$(10^{-4} g_p)^{-1} (r/R_p)$	410	104	26	13.9	4.2	2.0
$(10^{-4} g_p)^2 (F'_M)^{-1} n_H$	1×10^{13}	1×10^{14}	8×10^{14}	2×10^{15}	1×10^{16}	4×10^{16}
the Sun						
r/R_p	110	29	7.1	3.8	1.13	—
n_H	5.0×10^2	4.0×10^3	3.0×10^4	8.0×10^4	5.0×10^5	—

up to $1\text{--}2 \cdot 10^6$ K, and $> 3\text{--}400$ km/s, up to 2000 km/s, simultaneously, suggests that we are observing simultaneously the region of the lower-to-upper coronal transition, and the beginning stages of a cooling—but not yet cool or decelerated—postcorona. We observe such a range of farUV velocities simultaneously with velocities of 50–200 km/s in the cool H α regions, in the Be and Be-similar stars. However, in WR field-stars, we observe velocities up to 3500 km/s both visually and in the farUV—but most generally, we see no evidence of slow, cool regions. The Be-similar stars exhibit strong variability in $U(\text{max})$; the WR do not. The solar variability is in $U(\text{max})$, not total \dot{M} . Thus we have strong empirical evidence for an ambiguous variety of postcoronae, ambiguously linked to the upper-corona: decelerated and nondecelerated flow; rapid and slower cooling. So, we define:

The *POSTCORONAL DOMAIN* of the stellar atmosphere is an ambiguously-characterized set of distinctive atmospheric regions, of which set, even among stars exhibiting quasi-thermal photospheres, there appear to be at least two varieties. One variety, characterized by mass-flows in which the velocity continues to accelerate, or remains nearly constant, outward, relative to its upper-coronal values, includes stars with such widely-differing mass-fluxes as the Sun and *most* WR-type objects. Among such stars, there is some evidence for an ultimate deceleration, by collisions at some pscs, with extra-stellar media which do not appear to have originated in the star, at least not within times short compared with stellar-evolutionary ones. Such stars do not exhibit clear evidence for variable total mass-loss over times comparable with historical observations. In the mass-flow from such objects, T_e appears to decrease only very slowly in the postcorona, although there is evidence for some degree of frozen-in ionization and excitation. A second variety of mass-flow in the postcorona is characterized by a deceleration in flow-velocity, at a wide variety of distances from the star among stars belonging to this class. These include such widely different types as the Be and Be-similar, the T Tauri, the cataclysmic, the symbiotic; all showing strong H α -emission. So, with this deceleration, stars producing this second variety of postcoronal domain exhibit a rapid cooling from their coronal values of T_e , again quite close to the star relative to the locales of interaction with the ISM exhibited by stars of the first variety. These cooling and deceleration distances range from a few stellar radii for the hot Be and cool T Tauri to $10^6\text{--}10^8$ radii for the PN. The deceleration is in some cases as great as a factor 10 in $U(r)$: 2000 km/s to 1–200 km/s for some Be stars already quoted. The cooling is, quite generally, from the $10^6\text{--}10^7$ K coronal values to $0.5\text{--}2 \times 10^4$ K: from X-ray emission levels to those of hydrogen Balmer lines and ionized metals such as Fe II. Stars can pass from one of these two varieties to the other, in times shorter than historic spectral observations, thus very much shorter than evolutionary times. The universal characteristic of stars belonging to the second variety is a significant variability in mass-flux. Such variability can lie in both size of a slowly-varying continuous flow, and in size and recurrence of a short episodic mass-ejection. A star may, but need not, exhibit both continuous and episodic mass-loss. Thus it is difficult, presently, to assert that a star, assigned to the first variety at our epoch, will not join the second variety at some other epoch, for some undetermined duration. The taxonomic, and diagnostic, problems are the same as for a star classified as a classical nova—a star showing a one-time outburst: it may erupt again in the future, and so join the recurrent-nova class. The characteristic of classical novae to exhibit blue quiet-phase central stars; while recurrent novae exhibit red quiet-phase central stars; may simply be a “veiling” aspect of atmospheric structure. A redder appearance would correspond to a yet-present, as-yet-undispersed, mass-ejection from an earlier epoch. So episodic dispersion, as well as ejection, becomes a crucial characteristic. For all these reasons, I emphasize the term “ambiguously-characterized” for the postcoronal domain; and we try to clarify the situation by retaining these two varieties of stars. So, recognizing that such division may be ephemeral, we define:

E. A NONDECELERATED POSTCORONA is a distinctive atmospheric region, which

(1) *OBSERVATIONALLY*, lies just above the upper-corona; appears to exist only in those stars showing only minor variability of the mass-flux; and is the last region of the atmosphere-proper, for such stars. So the nondecelerated postcorona:

(1.a) Shows an only slowly-decreasing-outward T_e , which is maintained by an RE under the combined photospheric + chromospheric-coronal radiation field, at the density fixed by the mass-flow expansion.

(1.b) Exhibits mainly a recombination spectrum, under the radiative ionization/excitation from, and with the RE T_e corresponding to, the same radiation field as (1.a).

(1.c) Exhibits a velocity, $U(r)$, for the mass-expansion which either accelerates outward or reaches a quasi-asymptotic value. The density distribution is that for a time-independent flow at this $U(r)$.

(1.d) May, at large distances from the star, exhibit collisional-deceleration, and excitation/ionization, processes corresponding to interaction of the mass-flow with the ambient ISM—or IPM for the Sun.

(2) *THERMODYNAMICALLY*, the nondecelerated postcorona is a region where the mass-flow from the star is partially accelerated and heated by the total radiation field of the photosphere and exophotosphere. Other, as yet unverified, accelerating and heating mechanisms may exist, such as magnetohydrodynamic waves of various kinds. The essential aspect is that the nonradiative energy sources producing chromosphere-corona do not operate here; and the mass-flow has no self-interaction of the type resulting from a variable mass-flow, considered below. Any interaction with the stellar environment is with the ambient component, not that local component produced by the star, considered below.

(3) *DIAGNOSTICALLY*, the nondecelerated postcorona presents the classical problem of a differentially expanding flow illuminated by a dilute radiation field. Especially the PN and novae literature are rich in discussion.

This type of distinctive atmospheric region represents the whole of the exocorona, for those stars exhibiting it: those with nonvariable mass-flux. As such, it is the variety most often discussed in the current literature, where a variability in size of mass-flux has, with few exceptions, been ignored until very recently. Our strong exception to the usual discussions lies in our insistence that the chromospheric-coronal radiation be included. The only type of exophotospheric veiling from such kinds of stars is that by hot regions. So, we turn to the second variety of the post-coronal set of regions: those associated with stars showing variable mass-flux, of whatever size and time-scales. Clearly, the variety just discussed could be incorporated in the following, by considering it as the limiting case of vanishingly-small amplitude of the variable mass-flux component. So we define:

F. A DECELERATED POSTCORONA is a distinctive atmospheric region, which

(1) *OBSERVATIONALLY*, lies just above the upper-corona; appears to exist only for those stars showing significant variability in size of their mass-flux; and, for such stars, forms a transition-region between “hot, ultraspeed-expanding” chromosphere-corona, and a “cool, slowly-expanding” local-environment, the latter, itself, consisting of distinctive regions. So the decelerated postcorona:

(1.a) Shows, initially, a slowly-cooling T_e ; then an abrupt rise in T_e , across the shock occurring at the decelerating-collisional front, to some 10^7 K for an $o(10^3$ km/s) expansion; followed by a rapid cooling, to some 10^4 K; thereafter, again, a slow cooling. This T_e behavior is controlled by the mélange of chromosphere-coronal radiation field, the collisional interaction between the different mass-fluxes, and the progressive-outward radiative-input from the cool regions and their veiling of the coronal ones.

(1.b) Shows, initially, a decrease in excitation/ionization level corresponding to vanishing of the coronal non-radiative heating and its replacement by RE processes; then the sharp rise in collisional excitation/ionization at the shock, but with whatever the relaxation-lag is; then the subsequent cooling and again RE conditions.

(1.c) Shows, initially, those $U(r)$ corresponding to the radiative—and any other—acceleration of the upper-coronal flow-velocity; the subsequent deceleration at the shock; and the subsequent slow expansion. Note that if the post-shock flow velocity could fall below the local escape-velocity there could eventually be sufficient deceleration to produce an infall of material. This is Doazan’s interpretation of the inverse P Cygni profile in the Balmer lines, noting that one sees the greater infall velocity in the later Balmer lines, which come from the greater atmospheric depths. So, depending upon the location of the shock, one must admit a range of possibilities for the post-shock flow: either wholly expansion, or some infall.

(2) *THERMODYNAMICALLY*, the decelerated postcorona is a region: at whose base, the present-epoch mass-flow continues the upper-coronal outward acceleration, mainly radiative, but without nonradiative heating; in whose interior, this mass-flow is decelerated by collision with a slower-moving mass-flow from a preceding epoch; and which ends where T_e in the flow has decreased sufficiently to produce significant H α -emission, to $0.5\text{--}2 \times 10^4$ K. Such emission depends, thereafter, primarily upon particle concentration and radius of the H α -emission envelope, which is the overlying distinctive atmospheric region, in which the flow has stabilized to a quasi-steady, slow expansion.

(2.a) The value of $U(\text{max})$ reached before the decelerating collision depends upon the time-history of the mass-flow preceding the present epoch. The present-epoch distribution of nonradiative heating fixes both $U(\text{thermal, corona})$, the size of the radiative acceleration, and the extent of the upper-corona. The time-history of the mass-flux permits estimate of how far the present-epoch mass-flux “snowplows” into that of the preceding epoch before a quasi-steady configuration of the two mass-flows, separated by the interaction-shock, is established. The combined extent of upper-corona + decelerated postcorona gives the distance over which a free-flow expansion can be accelerated, radiatively-or-otherwise, before the abrupt deceleration: hence, $U(\text{max})$. Those investigations to date of this kind of decelerated flow have essentially been those of Kwok et al., cited in Chapter 3. Their focus lay on changes in mass-flux accompanying an evolutionary change in the late-stage M giant thought to produce a PN, and on the location of the PN as the locus of that shock-interaction. It is a “1-epoch” change in mass-flux, and the flow-velocity at each phase is unaccelerated-ejection. However, particularly the Be studies summarized in Chapter 3 show that a phase-dependent, accelerated mass-flow and $U(r)$ represent, for at least some stars, the single-star, nonevolutionary behavior. The summarized Be-similar, symbiotic, and cataclysmic stars’ behavior suggests the same. Our present knowledge does not permit unambiguous distinction between change in mass-flux size and in velocity—hence in acceleration and acceleration distance—in representing the variety of observations. Thus, to represent upper-corona and the lower part of the postcorona, we require the time-history of the distribution of nonradiative heating and of the mass-flux. At the minute, our knowledge of these is so rudimentary that theoretical prediction is simply unrestrained speculation. The best we can do, in thermodynamic characterization, is an empirical-theoretical abstract of certain features:

(2.a. α) $U(\text{decel})$ of the overlying H α shell cannot be less than $U(\text{max})$ of the slowest component of the preceding mass-flow; possibly, with a gravitational deceleration. So when, as observed, there are oftentimes large differences between $U(\text{max})$ and $U(\text{decel})$, it implies some of: (i) strong variation in size of radiative, or other, acceleration; (ii) strong difference in acceleration distance; (iii) an initially-large, photospheric nonthermal, episodic ejection velocity, as for novae and the model discussed by Kwok et al., (iii) does not come under the quasi-thermal photosphere category of regions. So, since most of the Be, Be-similar, etc. observations appear to imply quasi-thermal photospheres, we have (i) and/or (ii). We must admit an independent time-dependence in either or both of the nonradiative energy and mass-fluxes for stars exhibiting decelerated postcoronae and following regions.

(2.a. β) The postcorona cannot extend beyond the beginning of the H α envelope, by definition. So, Section G following gives an estimate of postcoronal end, from the strength of the H α -emission.

(2.a. γ) Because the slow expansion velocity of the H α shell is not zero, its distance from the star reflects the time-interval between significant changes in mass-flux, and/or radiative acceleration.

(2.a. δ) We can use the Kwok et al. (1978) modeling of the PN—which, for those stars, represents the collision-locale and the beginning of the H α envelope—as illustrative guidance to the case where the effect of any evolution of mass-flow outward (our exophotospheric regions through the upper-corona), and of any radiative-acceleration, have been suppressed. Thus the model has a photosphere, exophotospheric unaccelerated mass-flow, and collision-shock + H α envelope. The parameters are (mass-loss, flow-velocity) for each phase: \dot{M} , V for the earliest and \dot{m} , v for the last; \dot{M}_s , V_s refers to the nebula, whose internal structure is ignored, being modeled as a perfectly absorbing “black-box.” We cannot simply quote their tabulated results, because, unfortunately, they evaluated the momentum-change of the nebula as $M_s dV_s/dt$ rather than the correct $d(M_s V_s)/dt$. But this is only a detail in their objective of exhibiting the production of a slowly-moving nebula in an ultra-speed wind, very much closer to the star than any interaction with the ambient ISM would provide. More recently, Kwok (1982b) has rediscussed the problem, from another viewpoint, treating $d(M_s V_s)/dt$; the former discussion is more succinct. Their (corrected) equations are:

$$\text{mass:} \quad dM_s/dt = (v - V_s)\dot{m}/v + (V_s - V)\dot{M}/V \quad (4.38)$$

$$\text{momentum:} \quad d(M_s V_s)/dt = (v - V_s)^2 \dot{m}/v - (V_s - V)^2 \dot{M}/V \quad (4.39)$$

which produce the quasi-steady flow, $\dot{V}_s \sim 0$, at the nebula

$$V_s \sim V \left\{ \frac{[(\dot{M} - \dot{m})/4\dot{M}]/[1 - \dot{m}V/\dot{M}v]}{3 \pm (1 + 8\dot{m}\dot{M}[v - V]^2/vV[\dot{M} - \dot{m}]^2)^{1/2}} \right\} \quad (4.40)$$

in place of their eq. (4). They considered only the cases where $v \gg V$, and $\dot{M} > \dot{m}$; adopting only the “+” alternative in eq. (4.38), $\dot{m}V/\dot{M}v \ll 1$. One obtains, setting $\dot{m}/\dot{M} = x$:

$$V_s \sim V \left\{ [1 - x]/4 \right\} \left\{ 3 + (1 + 8xv/V[1 - x]^2)^{1/2} \right\} \quad (4.41)$$

Thus solutions range from $V_s = V$, when $x = 0$, to $V_s = (vV/2)^{1/2}$ for $x = 1$. They considered $V \sim 5\text{--}10$ km/s for the red-giant phase; $v \sim 500\text{--}1000$ km/s; and $x \sim 0.3\text{--}0.1$; so obtained $V_s \sim 20\text{--}60$ km/s, the actual PN range. Adding the cases where $\dot{m} > \dot{M}$ simply requires adding the “-” alternative in eq. (4.40). In the limiting case, e.g., of $v \gg V$, $\dot{m} \gg \dot{M}$, $\dot{m}/v \gg \dot{M}/V$, we obtain the two solutions: $V_s = v, v/2$; the latter, corresponding to the “-”, is the useful one. Thus the range of nebular characteristics is large, depending on the range assigned to the parameters.

The model illustrates its own limitation for detailed application: $V_s < V$; and V, v are implicitly $U(\text{max})$ in red-giant and post-red-giant phases, but the outward evolution of $U(r)$ is ignored. So we have again the problem posed by Fig. 3-33, but multiplied: how to avoid not only the solar $U(\text{max})$ level of 400–800 km/s, but the $q(T_e)$ level of 50–200 km/s. We would need to suppress the red-giant flow from reaching the escape point; or to reach it with so little energy, and add so little energy subsequently, that $U(r; \text{red-giant phase})$ decreases outward *before* the collisional-encounter with the succeeding-flow. Crudely, this argues for suppression of both mass-flux (to avoid close-in collision), and nonradiative heating (to avoid both thermal and radiative accelerations), for limited times between these phases of quite different mass-flow.

(2.b) The distribution of excitation/ionization across this postcorona is thermodynamically critical. It drops from coronal values to H α shell values, with a short-but-sharp rise at the deceleration shock. As detailed above, its modeling depends on the time-histories of mass-flux, and nonradiative heating of the chromosphere-corona. Above all, we need detailed observational studies of a variety of stars to develop insight.

(3) *DIAGNOSTICALLY*, the decelerated postcorona is, with the upper-corona, one of the most ambiguous regions to study. Its critical features— $U(r)$ at its beginning, peak-energy carried in the mass-flow, the abrupt rise and fall in ionization/excitation at the deceleration-shock—are best observed in the currently-unobservable spectral region $\lambda \lesssim \text{LyC}$. However, lower limits can be set on $U(\text{max})$ from farUV observations, and on $U(\text{decel})$ from H α and ionized-metal observations in the visual. Also, other diagnostics of the H α -emission envelope put other limits on conditions at the top of the postcorona. So, we proceed to consider

G. The H α -EMISSION ENVELOPE is a distinction atmospheric region, part of the postcoronal domain (PCD) of the stellar atmosphere, and a member of that variety of PCD regions which: has a phase-dependent character, even existence, associated with the existence of a strongly-variable, over both short and long time-intervals, mass-flux from the star; has as its lowest-lying member a decelerated postcorona, hence is stamped with its characteristics of a slower, cooler mass-flow than in the coronal regions; has a sufficiently-smooth transition to the ISM that we call its totality the *local stellar environment*, LSE. The H α -emission envelope is that region of the LSE which is observed, in the visual spectrum, the closest to the star—although this distance may vary greatly among stars exhibiting a LSE, and between phases of a given such star, and is apparently linked to the time-interval between major mass-flux enhancements. Major controversy continues, at our epoch, as to the location of this H α -emission envelope in the PCD, rather than between photosphere and chromosphere; and as to our quasi-spherical, rather than more conventional equatorial-disk, modeling of it as one among other such distinctive atmospheric regions along a radial sequence. We place the H α -emission envelope in the above perspective, because:

(1) *OBSERVATIONALLY*, historic visual, and current simultaneous visual + farUV and X-ray, observations are inconsistent with other alternatives, which violate the gross structural pattern we are, empirically-theoretically, assembling in this Part III of the book.

(1.a) A variety of stars, ranging from Be to T Tauri, exhibit H α peak intensities up to 10–30 times the local continuum, and emission equivalent widths up to 100Å. Even the crudest diagnostics, cf (3) below, require the H α -emission envelope, at such phases, to extend beyond the coronal escape point.

(1.b) Any mass-loss in the range quoted in the current literature for Be and T Tauri stars, which is required to produce an atmosphere of sufficient extent to produce the observed H α -emission, requires already—as discussed in the chromospheric-coronal sections preceding—a nonradiative atmospheric heating at $r/R_p \sim 1.1$. Such heating is useful to produce part, but far from most, of the H α -emission for cool T Tauri stars. To produce Be, and Be-similar, H α -emission requires cooling, not heating. So, such thermodynamic consequences of the observed mass-loss are incompatible with locating the H α envelope in the thermodynamic transition between photosphere and chromosphere, and with the small size of the H α envelope required by such location.

(1.c) Placing the cool H α envelope interior to the corona destroys that X-ray absorption by the envelope which is compatible with the observed anti-correlation between H α -emission and X-ray intensities, as abstracted in Chapter 3.

(1.d) Chapter 3 summarizes the lack of correlation between $V \sin i$ and any of those features diagnostically-useful in establishing the necessity for an equatorial H α -emission disk. Super- and sub-ionization; velocities of size $o(10^3 \text{ km/s})$ and $o(10^2 \text{ km/s})$; the variety of H α profiles—none of these correlate, in enhancement or suppression, with $V \sin i$; so none suggests the existence of a favored direction, relative to the stellar rotation axis. Crudely, sphericity remains.

(1.e) Chapter 3, and especially Doazan (1982), detail the examples of individual stars showing, at different phases, each of a B-abs, Be, and Be-shell spectrum. Equatorial-disk modeling is incompatible with such data.

(1.f) The size of the observed polarization (1–2 percent) is so small as to be reproducible with little departure from sphericity but proper location of ionized regions—i.e., interior to the H α envelope. Note that polarization falls, across the lines.

So observationally, for self-consistency among all the data, we must place the H α -emission envelope in the postcoronal domain rather than the pre-chromospheric; and its geometry must be grossly spheroidal.

(2) *THERMODYNAMICALLY*, there are three characteristics of the H α envelope which preserve its character across the HR diagram:

(2.a) From visual data alone, its particle concentration is greater than simple outward expansion under constant or accelerating mass-flow, under a mass-loss compatible with other data, would produce; and the size—and existence, which is tied to the existence of the H α envelope—of this excess particle-concentration varies under a range of time-scales. As summarized in Chapter 3, and the Introduction to this Part III, the evidence is most striking for the PN, and the most detailed for some Be stars during phase changes. Because of the steady secular rise of H α -emission from the B-abs to Be(max) phases, although broken by short-term fluctuations, we interpret the excess particle-concentration as a “filling” of the H α envelope by some mechanism related to the mass-flow, whose variation we studied in detail. Our earliest interpretation of individual Be-star history suggested a back-filling of the H α envelope via a shock propagating back toward the star from the mass-flow collision with the ISM, or possibly with some backward extension of it into the star produced in earlier phases (Doazan et al., 1980). But the Kwok et al., PN alternative discussed above—one mass-flow overtaking another and building a “snow-plow,” forward, concentration of material—seems a better, broader alternative to cover all stars having such an H α -emission envelope. It permits a superthermal, snow-plowing, collision between mass-fluxes anywhere above the thermal-point depending upon the mass-flux history. Thus it more easily represents those short-term fluctuations especially characteristic of the T Tauri, sometimes of the Be and Be-similar, but not of the PN. Depending upon the time-interval between strong changes in mass-flux, it also permits that strong observed variety in location of the H α envelope. So we have the first thermodynamic characteristic of the

H α envelope: a dependence of its properties on the time-history of the star's mass-loss, whose outflow fixes the distribution of particle-concentration above the thermal-point.

(2.b) Simultaneous visual + farUV observations add the second thermodynamic characteristic of the mass-flow in the H α envelope: it is slow relative to that in the underlying corona; it has been decelerated. This is consistent with, but not absolutely demanded by, (2.a) preceding. Nor does it usurp the thermodynamic transition-character of the decelerated postcorona: an initial outward acceleration of the mass-flow, even though its T_e may be simultaneously falling; then a deceleration to match conditions observed in the succeeding region, the H α envelope. This H α envelope reflects the characteristics of a flow which is already decelerated below its coronal and lower postcoronal values. The velocity-transition characteristic of the H α envelope is that of the further change in $U(r)$ —acceleration or deceleration? We have already remarked that the immediately post-shock flow depends upon whether U drops below V_{esc} in that region. Again, this depends upon the time-history of the mass-flow in locating the deceleration-shock. Immediately behind this shock, the flow is locally-sub-thermic. So if the other—including radiative—terms on the RHS of eq. (4.38) exceed the gravitational—i.e., if the flow has already passed the escape point—the flow will be decelerated, until it has cooled sufficiently to be superthermic, or until the radiative acceleration has been sufficiently veiled to let gravity predominate. If these happen, but thermal velocity drops below $(GM/2r)^{1/2}$, the flow may continue to decelerate. The 1–200 km/s velocities usually discussed in H α envelope modeling of Be stars (Marlborough, 1969; Poekert and Marlborough, 1978) are not superescape anywhere inside $r/R_p \sim 20$ –5 for MS, and 6–1.5 for sg, B stars. A superthermic, cool, flow anywhere inside these radii, for which radiative-acceleration does not exceed gravitational, will be gravitationally decelerated. It can even come to rest, and fall back toward the photosphere, as earlier discussed. However, if the flow cools sufficiently to become supersonic, and if the radiative-acceleration predominates, the outward acceleration can resume. So an important question is whether the H α envelope shields itself from the chromospheric-coronal radiative acceleration. The point is that we cannot, a priori, impose either acceleration or deceleration as a thermodynamic characteristic of the flow in the H α envelope. That character depends on the time-history of the mass-flux from the given star. A star which initially produces an H α envelope at only a few radii, or less, can maintain such a Be-like behavior if the episodic mass-flow change is sufficiently frequent; or it can evolve into a PN-like distant H α envelope, if the episodic variation is infrequent. Thus, all our earlier comments on ordinary-, vs. recurrent-, vs. dwarf-novae—relative to episodic vs. continuous mass-loss, and veiling—apply; we return to them in Section III. This ensemble of stars exhibits the “variety” in H α -emission envelope across the HR plane, while maintaining its thermodynamic character of being a slow-moving, PCD, distinctive atmospheric region, which takes on some of the character of being a local environment.

We noted that this slow-moving, decelerated characteristic is compatible with the excess particle-concentration characteristic (2.a) above. Given, observationally (Chapter 3), that the range in velocities of the H α envelope is 100–300 km/s—50 km/s for the PN; and in thermal velocities for 10^6 – 10^7 K coroneae, 100–350 km/s; we see that H α envelope particle-concentrations should be essentially the same as those in the lower-corona, but decreased by the factor $r^2(\text{lower-corona})/r^2(\text{H}\alpha \text{ envelope})$. Given, for Be stars that such H α envelopes begin only a few radii from the star, their particle concentrations differ from lower-coronal values only by about a factor 10. So for a Be, MS, star we have a quite flat density distribution between thermal point and H α envelope; with a “ripple” caused by the postcoronal flow reaching some 2000 km/s, then decelerating. However, this “density plateau” contributes little to the H α -emission; it is the hot “ring” in spheroidal structure; the same as the hot region between central star of PN and the nebula itself. The Be are indeed “little PN”: in size of central hot region, and therefore in radial location of H α envelope.

Thus, *kinematically*, we understand the large difference in presence, and observational prominence, of H α -emission envelopes among even stars of one visual spectroscopic class, the B. H α -emission, and strong variability, increase from being unobserved in B-abs MS and B1b, to observed as small but present in B1a, to large size in Be. Only in the latter is evidence for decelerated flow strong. But quoted values of mass-*flux*, for all these, are very similar. So, in terms of many interrelated features, H α -emission envelopes, and their variety, appear to come from individuality in frequency and size of mass-flux variability, not simply from large mass-loss, the quantity so prominently displayed by WR and OB sg alike. This variability provides that decelerated, slow, flow which builds up the particle-concentration in the postcoronal, local stellar environment; whose third thermodynamic characteristic, to which we now turn,

is so critical in introducing the symbiotic characteristic of “cool star properties,” complementing the “hot star properties” characteristic introduced by the chromospheric-coronal region. But to be observed, this characteristic needs sufficient particle-concentration.

(2.c) Simultaneous visual, farUV, and X-ray observations add the third thermodynamic characteristic of the H α -emission envelope: empirically, as summarized in Chapter 3, it is very cool relative to the underlying corona. Again empirically, this cooling can occur very close to the star, at a few radii, as for the hot Be and the cool T Tauri; or very far, as for the PN. But empirically, the PCD of all these stars cools very much more rapidly than does that of stars in the WR + Sun, nondecelerated postcoronal, class. Such enhanced cooling is consistent with, but does not necessarily demand, the increased particle-concentration of (2.a). But the result of (2.a) plus rapid cooling is the dense, cool H α envelope, and the even cooler succeeding regions of the LSE; all beginning at these varieties of distances from the star. The contrast between a Be star and a PN in the size of the “hot central ring,” thus the distance at which H α -emission is observed, is striking. For a sufficiently hot photosphere, this H α envelope may be the first place one could observe hydrogen in that star. The WR objects are such hot stars; they are often called hydrogen-deficient objects because none is observed; we note the few counter-examples cited in Chapter 3, of H α observed in distant cool, nebulae surrounding WR objects. One must be cautious, in abundance-diagnostics.

The cooling results from the absence of significant nonradiative heating in the PCD—except at the deceleration shock—thus the return of the local atmospheric configuration to one of RE. Aside from the lower density in this exophotosphere, the main difference between the photospheric RE treated in Chapter 2, and this H α envelope RE, lies in the radiation field incident on the latter being photospheric + chromospheric-coronal + emission from the deceleration shock. Additionally, the H α envelope density distribution is fixed by its mass-flow, not HE. Properly treated, of course, the Chapter 2 model photosphere would be replaced by the real-star one, on which the back-radiation from the exophotosphere must be included. Then in such self-consistent, real-star, models—and their observational diagnostics—it is not only the opacity of the ISM which inhibits our observational determination of those crucial radiation fields at $\lambda \lesssim \text{LyC}$, but also the opacity of the H α envelope and of the remaining regions of the LSE. We stressed the observational indications, in Chapter 3, that all “assumed” ISM effects may not be such, but LSE effects instead.

Then useful thermodynamic insight into the low- T_e characterization of the H α envelope, and the LSE generally, is provided by the results of conventional modeling of Be and PN H α envelopes, in spite of the very basic differences between their assumed, and our empirically-constructed, atmospheric structural patterns. Mainly, one needs to supplement conventional means by adding the hot “H α void,” and our simplified nonLTE algebraic approach. We recall that in Section F.2, we stressed that the boundary between decelerated postcorona and H α envelope occurs where T_e has dropped sufficiently to produce strong H α -emission; thereafter, the size of this emission is controlled by particle concentration and envelope size. If, as in the lower, very hot regions, H α -emission were wholly recombination in an optically-thin gas, its T_e -sensitivity would be low—as $T_e^{-1/2}$. But the major increase in n_3 , hence in H α -emission, corresponding to this drop in T_e is an opacity effect; which, after this T_e drop, is controlled by density and volume of the cool regions. This nonLTE behavior of a diffuse gas is familiar since the early PN discussions of Menzel et al., (MABG, 1935, et seq.); the classical Stromgren sphere; and our models contrasting collisional vs. photoionization effects under varying particle-concentrations and opacities (Thomas, 1948, 1949; Thomas and Athay, 1961, particularly pp. 102–5; Gebbie and Thomas, 1969). For given local values of (T_e, n_e) , the value of b_3 —hence of n_3 —increases monotonically through the sequence of opacity-configurations: from their being optically-thin in all lines and continua, through being optically-thick in only Lyman lines, then also opaque in the LyC, then also in H α , then BaC, et seq. We see this explicitly by adding cascade from levels $k \geq 4$, treated as LTE-R, to the populating mechanism for level 3, in the 3-level atom expression (2.269) for b_3 , to obtain, in the collision-free case:

$$b_3 = \left(F_{c3} + \sum_{k>3} \delta_{k3} \right) / \left(F_{c3} + \sum_{j<3} \delta_{3j} \right) \quad (4.42)$$

where F_{c3} and F_{3c} are given in Appendix 2-A; and δ_{ik} is given by eq. (2.270) in terms of T_e and $(\text{NRB})_{ik}$. For sufficiently-low T_e that $E_1(-X_k)$ can be represented by $ex(-X_k)/X_k$, eq. (4.42) gives:

$$n_3 \sim T_e^{-3/2} b_3 \exp(X_3) \sim \frac{C_1 T_e^{-1/2} + C_2 T_e^{-3/2} (\text{NRB})_{43} \exp(-X_{34})}{C_3 (\text{NRB})_{32} + C_4 (\text{NRB})_{31} + C_5 W_3 E_1(-Y_3)} \quad (4.43)$$

where the C_k are numerical constants and W_3 is the dilution factor for the Paschen continuum. The classical contrast of optically-thin to optically-thick cases comes from setting, respectively, the several (NRB) = 1 or 0. Thus, from the form of the terms in eq. (4.43), we see that this opacity-choice of terms can be much more significant than the T_e -effect. Where the value of T_e enters, is in the choice of a T_e -range where significant Lyman and Balmer opacity can occur—i.e., where significant n_1 and n_2 can occur; this is what limits the H α envelope to the range $T_e \sim 0.5\text{--}2 \times 10^4$ K, cf below.

The b_3 situation is illustrated by comparing classical PN and Be models. The classical, MABG, diffuse, distant-nebular PN example treats the (NRB) as 1 for all but the Lyman lines; and as either 1, optically-thin case, or 0, optically-thick case, for them; each case with $W_3 = 0$. Values of b_3 are 0.05–0.15, under $T_e = 1\text{--}2 \times 10^4$ K for the thin case; they double, for the thick case. Marlborough (1968) and Poekert and Marlborough (1978) treat the Be example similarly. In addition to the two cited cases, they consider a third, where (NRB) = 0 for Balmer and other lines also. Throughout, they consider only the photospheric radiation field, with the W_k fixed by estimates of H α envelope absorption of it. Their finally-adopted n_k —or b_k —results from a process of averaging over either cases 1 and 2, according to Ly α opacity, or over cases 2 and 3, according to H α opacity. But in any event, for $T_e = 1 \times 10^4$ K, they obtain b_3 ranging from ~ 2 at inner and outer borders of the envelope to ~ 40 at its interior; and for $T_e = 2 \times 10^4$ K, b_3 ranges ~ 40 to 300. We only note, from our discussions of transfer solutions in Chapter 2, Section III. β .3, that the limits on (NRB) are

$$0 < (\text{NRB})_{ki} \lesssim \eta_{ik}^{1/2} \quad (4.44)$$

which, for a radiation field determined by transfer within the nebula itself, reduces the range of solution by reducing the range of (NRB). Of course, the result (4.44) is the 2-level atom approximation.

Finally, we see the T_e -dependence of the opacity, hence the reason the H α envelope is, for strongest H α -emission, restricted to $T_e \sim 0.5\text{--}2 \times 10^4$ K in the expressions, resulting from eqs. (2.267) and (2.268), under varying opacity:

Opaque in LyC:

$$n_2 \sim 1.66 \times 10^{-15} n_e n W_2^{-1} T_r^{-1} T_e^{-1/2} \exp(Y_2) \quad (4.45)$$

$$n_1 \sim 0.25 n_2 \exp(X_{12}) \quad (4.46)$$

$$W_2 = (2r^2/R^2)^{-1} \quad (4.47)$$

Optically-thin LyC:

$$n_2 \sim n_2(\text{above}) (1 + \Delta_\alpha) \quad (4.48)$$

$$n_1 \sim 1.45 \times 10^4 T_e^{-2} (1 + X_{12})^{-1} n_e \exp(X_{12}) \quad (4.49)$$

$$\Delta_\alpha \sim b_3 \delta_{32}/F_{c2} \quad (4.50)$$

(3) *DIAGNOSTICALLY*, we see from the preceding that the H α -emission envelope continues the character of these LSE regions in being difficult to locate, in precise value of r/R_p . Lacking farUV + X-ray observations, and self-consistent thermodynamics, we see that visual data alone would place this H α envelope beginning at the thermal point; particle concentrations there and at its actual beginning differ only by an amount corresponding to their observational uncertainty. One would simply ignore—take as non-existing—the hot, very-high-velocity intermediate spherical shell. And, indeed, this is what has been done, historically. It continues even today, in the debate where to locate a

chromosphere-corona; everywhere, as a spherical shell; or only in limited locale, as a conical, polar, region arising from an equatorial, everywhere slowly-expanding, rotationally-ejected disk. It is only these simultaneous observations in visual and farUV which have produced the correct picture. And, as we have seen, it is a reasonably-complete picture for only a few stars, well-studied. We require equally-detailed study of examples covering the whole range of location of H α envelopes between close-in Be and T Tauri, and far-out PN. We conclude, here, by illustrating the ambiguity coming from visual, H α , data alone, on four Be stars, at very bright H α -emission phase.

We have H α -emission equivalent widths for γ Cas, B0 IVe–80Å; and three B2 IVe stars, ϕ Per, 66 Oph, ν Cyg–68, 36, 40Å, respectively. These spectral classes are observed; values of $\log g$, T_{eff} , and R are assumed, as characteristic of the classes: 4, 30,000 K, $10R_{\odot}$; and 4, 20–25,000 K, $5R_{\odot}$; respectively. Then if F_{λ} is the flux in the continuum adjacent to H α , we have for the observed energy output in H α , $\text{erg cm}^{-2} \text{ sec}^{-1} \text{ cm}^{-1}$. $W_{\lambda} = \text{H}\alpha$ equivalent width:

$$E_{\text{obs}} = 10^{-8} W_{\lambda} F_{\lambda} 4\pi R^2. \quad (4.51)$$

Treating the H α envelope as a diffuse gas, the total emission in H α should be:

$$E_{\text{cal}} = h\nu_{32} A_{32} N_3 = 1.3 \times 10^{-4} 4\pi R^3 n_{30} (r_0/R)^3 (1 - r_0/r_e) \quad (4.52)$$

if we assume n_e varies as r^{-2} , under constant U, and that the excitation of n_3 stays unchanged between radii r_0 and r_e of the envelope. Then combining the two equations, we obtain n_{e0} :

$$n_{30} = 0.55 \times 10^3 \left\{ \frac{W_{\lambda} \times 10^{-16} F_{\lambda}}{50A} \right\} \left\{ (R_p/R_{\odot})(r_0/R_p)^3 (1 - r_0/r_e) \right\}^{-p} \quad (4.53)$$

to accompany

the expressions for n_3 :

$$T_e = 1 \times 10^4 \text{ K:}$$

$$n_3 = 2.2 \times 10^{-20} b_3 n_e^2$$

$$T_e = 2 \times 10^4 \text{ K:}$$

$$n_3 = 3.2 \times 10^{-21} b_3 n_e^2$$

(4.54)

and the expression for n_H at the thermal point in Table 4-2. For a blackbody at $T_{\text{eff}} = 3, 2.5, 2 \times 10^4$ K, F_{λ} has, respectively, the values 2.8, 2.2, 1.5×10^{16} in the above units. The Kurucz (1978) photospheric models, without exo-photospheric perturbation, give, respectively, 0.71, 0.51, 0.35×10^{16} .

The expression (4.53), and our assumption of constancy of b_3 over the envelope, exhibit the uncertainty entering the diagnostics. Nonetheless we see that the values of $n_e \sim 10^{10}$ – 10^9 at the beginning of the H α envelope, thus, $n_H \sim 10^{11}$ – 10^{10} at the thermal point; an $r_0/R \sim 3$; and $\dot{M} \sim 10^{-7}$ – 10^{-8} are reasonably compatible with observations and range of theory. Without the deceleration to produce a low velocity at the H α envelope, n_e would have to decrease more between thermal point and envelope; so the inferred n_e at the envelope would require larger n_e , hence \dot{M} , at the thermal point. In the same way, a smaller emitting volume—an equatorial disk rather than spherical shell—would require larger n_{30} , hence n_{e0} , \dot{M} , and n_e (thermal point). We also note that an H α envelope beginning near $r_0/R \sim 3$ requires an escape point interior to this value. Admitting $T_e \gtrsim 5 \times 10^6$ K in the corona makes this no problem; there is also the possibility that radiative deceleration depresses the escape point, as discussed. Clearly, an r_0/R_p of 2 or 4 rather than 3 lies within the diagnostic range. However, a *very* thin chromosphere-corona, such that $r_0/R \lesssim 1.5$, requires an n_e range 10^{11} – 10^{10} at the envelope, hence 10^{12} – 10^{11} at the thermal point, and $\dot{M} \sim 10^{-6}$ – 10^{-7} . These \dot{M} , although falling in the range of the Marlborough-Poekert models, are high relative to values found in the literature from farUV diagnostics. 10^{-6} is the OB sg value; hence these would require Be MS mass-fluxes some 100 times those of the OB sg. As emphasized throughout Chapter 3, mass-loss diagnostics are presently primitive, until self-consistent models are developed; but all this suggests the values associated with $r_0/R_p \sim 3$, possibly 2.5–4, are preferable, in terms of current data, for these Be stars at strong H α -emission phase.

More important, we can ask the realism of assuming a thin envelope, using either T_{eff} or 1 – 2×10^4 K for T_r in eq. (4.45). The latter assumes that a transfer-solution in the envelope itself fixes T_r . Taking the base of the envelope to be located at $r/R_p \sim 3$; a (minimal) envelope thickness of one photospheric radius; and the range in n_{e0} found above, eqs. (4.45)–(4.47) give

$$T_e = T_r = T_{env} = 1 \times 10^4 \text{ K}$$

n_e	n_2	n_1	$\tau_{Ly\alpha}$	τ_{LyC}	$\tau_{H\alpha}$	τ_{BaC}
$10^{10}-10^9$	10^8-10^6	$10^{12}-10^{10}$	$10^{11}-10^9$	10^7-10^5	10^8-10^6	10^3-10^1

$$T_e = T_r = T_{env} = 2 \times 10^4 \text{ K}$$

$10^{10}-10^9$	10^7-10^5	10^9-10^7	10^7-10^5	10^3-10^1	10^6-10^4	10^2-1
----------------	-------------	-------------	-------------	-------------	-------------	----------

The n_3 from eqs. (4.54) and the above discussion give $\tau(\text{PaC}) \ll 1$ for an envelope even $100 R_p$ in extent.

Thus we see that the approximation of treating the $H\alpha$ envelope as a diffuse, optically-thin gas whose emission is given by eq. (4.52) is not, a priori, a satisfactory one—particularly for stars, like the Be at some phases, where a dense envelope occurs close to the star. The other extreme, treating it as optically-opaque, with emission given by $\pi r_{en}^2 B_\nu(T_{ex})$, gives only that r_{en} where $\tau(\text{tangential}, H\alpha) \sim 1$, and requires specifying T_{ex} . Then we have $W_\lambda \sim r_{en}^2 B_\lambda(T_{ex}, H\alpha)/R^2 B_\lambda(T_r, \text{PaC})$. From Chapters 2–3, we see that $T_{ex}(H\alpha)$ results from a transfer solution in the envelope for a photoionization-dominated line, with source-sink terms computed from $J_\nu(\text{PaC})$ and $J_\nu(\text{BaC})$. Because the envelope does not affect $J_\nu(\text{PaC})$, we know its value observationally, as we did for both in the solar chromosphere. We must do a transfer-solution for $J_\nu(\text{BaC})$ as we did for the LyC in the solar case. But because we know the solution gives $T_{ex}(H\alpha) < T_r(\text{PaC})$, the observed W_λ —given above—demand $r_{en}/R_p \gtrsim 10$. This is all we require, for our present objective of establishing atmospheric structural pattern. Thus, diagnostics based on the optically-thick, as well as optically-thin, envelope show that the $H\alpha$ envelope must lie well above and outside the chromosphere-corona. The evidence cited in Chapter 3 completes the picture by showing sphericity, rather than equatorial concentration, to be the observationally-acceptable geometry.

Finally, we emphasize that such optically-thick diagnostics provides only a density distribution, not any details on how it was produced—e.g., by a mass-flow. Only if one can show that a particular density distribution can be produced only by a particular mass-flow, and show why, can one say that such diagnostics gives a mass-flux. We showed that the *ensemble* of data—visual + farUV + X-ray—demand a decelerated flow; and invalidate the use of farUV mass-flow velocities to produce the $H\alpha$ envelope density distribution; the $H\alpha$ data alone are insufficient. Precisely the same caution must be applied to diagnostics by use of IR and radio data: each gives only information on density distribution. For stars with this LSE, strongly evidenced by the presence of an $H\alpha$ envelope, use of farUV velocities to diagnose $H\alpha$, IR, or radio data is, a priori, excluded. Only in the case of such stars as WR, Sun, etc.—showing no evidence of a decelerated postcorona—could such farUV velocities be used, as first approximation.

Thus, we recognize that $H\alpha$ envelope, and its LSE neighbors, must be admitted to produce a “veiling” effect of lower-lying regions; such observed effects are not necessarily produced by the ISM. So, we recognize the character of, and define:

H-I-J-? THE REMAINING REGIONS OF THE LSE, which are “blended,” possibly not distinctive, atmospheric regions; possibly they only reflect different levels of continued cooling from the $H\alpha$ envelope outward. Thus,

(1) OBSERVATIONALLY:

(1.a) We have a region producing both narrow and deep cores of the hydrogen lines, and narrow, deep, absorption lines of the singly-ionized metals, especially Fe II. Such data are more compatible with regions of $T_e = 0.5-1 \times 10^4$ K than with the $H\alpha$ envelope $1-2 \times 10^4$ K. The spectrum is highly transient, defining the shell-phase for the Be stars. Similar, sharp, absorption features of Ca II, Mg II, Na I are identified as produced in a “cool-shell” of T Tauri stars by Kuhl (1982), and associated with particle-concentrations $\sim 10^4$.

(1.b) Low-excitation forbidden lines are observed in both Be and T Tauri stars. Densities $\lesssim 10^5$ are generally associated with such lines, to avoid collisional de-excitations eliminating them.

(1.c) As discussed in Chapter 3, evidence for the presence of dust particles in atmospheric regions exterior to those producing (1.a) and (1.b) are found in a variety of stars. Such evidence is only conclusive where the actual dust “signatures” are found; and these occur in Be-similar, like symbiotic, rather than Be proper. But they also occur in T Tauri stars; occasionally, in some cataclysmic stars.

(1.d) A variety of strengths of IR and radio excesses are found both in stars exhibiting the LSE phenomenon, and in the other—WR and Sun—variety. Such can be produced in chromospheres-corona; they can be produced in cold atmospheres with dust; their diagnostics are ambiguous. In a sense it is similar to H α -emission production in T Tauri stars: it can be both chromospheric and H α envelope.

(1.e) One set of phenomena are more rarely-associated with these low-density regions of the LSE: the observed high-ionization, high-excitation forbidden lines. Apparently, in some stars, the deceleration-shock occurs at very-low density regions, as for the novae, and apparently also for some symbiotic stars. The PN are the obvious example. Whether the deceleration shock originally occurred close to the star, following a large episodic outburst, then slowly propagated outward; or whether the interaction occurred at present PN distances; the present-day result is the same. The interior of the PN is characterized by flows at $\text{o}(10^3 \text{ km/s})$ with $T_{\text{ion}} \lesssim 10^5 \text{ K}$; some forbidden lines correspond to 10^6 K or more; the nebula itself moves at $\lesssim 50 \text{ km/s}$, with $T_e \sim 0.5\text{--}2 \times 10^4 \text{ K}$. This configuration corresponds to the above-discussed H α envelope + LSE-remainder. Any nova interaction shock apparently corresponds to PN distances, or greater; but novae do not fall under our quasi-thermal photosphere category.

(2) *THERMODYNAMICALLY*, this LSE-remainder mimics the outer-atmosphere of a very cool star. Indeed, adjoining it to the H α envelope, the whole configuration of the decelerated postcoronal domain mimics the sub-atmospheric + atmospheric complex above the hot stellar interior—with the important condition that the whole complex is transparent in the visual—i.e., PaC—spectral regions, and that it is expanding at $\text{o}(10^2 \text{ km/s})$, at low density.

(2.a) The chromosphere-corona + deceleration shock mimics a very hot, $\text{o}(10^6\text{--}10^7 \text{ K})$, interior. The H α -emission envelope, plus the upper, cooling, part of the decelerated postcorona mimics the hydrogen ionization zone of a star whose $T_e \sim 5000 \text{ K}$ at $\tau(\text{BaC}) \sim 1$. But above this “photosphere”—which is transparent in the BaC—exists sufficiently-strong cooling mechanisms to drop T_e low-enough to produce, ultimately, dust. Because the whole configuration is very low particle-concentration, impurity cooling by the same “contaminants” as cool the PN can be effective.

(2.b) In discussing novae, in Chapter 3, we caricatured the atmosphere as a fluorescing screen, hot on its bottom-side, cold on its top-side; whose role was to covert the high-energy radiative flux from below, to a low-energy radiative flux from the star. The energy and mass-transport corresponding to the initial nova-shell motion was decoupled from the radiative cooling, until that exophotospheric level where the nova shell collides with the ISM, or a LSE resulting from earlier mass-loss. Here, we can make the same caricature; with the exception that radiative cooling in the PaC does not exist, because of the low exophotospheric opacity in this PaC.

(2.c) From our preceding logic, this LSE exists wholly because of a variability in mass-loss. If there is no such variability, we obtain a WR-type atmosphere, if \dot{M} is very large, or a solar-type, if \dot{M} is small. But if there is such variability in mass-loss, hence in postcoronal structure we must admit the possibility of variability in nonradiative energy-flux, hence in chromospheric-coronal structure. We have noted that a complete photospheric model must include back-radiation from chromosphere-corona, not rest on the Chapter 2 type models. Thus, we have the possibility of variation in the photospheric, PaC, observed spectrum, not directly associated with a mass-loss.

(3) *DIAGNOSTICALLY*: the presence of this LSE-remainder, plus H α envelope and decelerated postcorona, do indeed divide stellar exophotospheric structural patterns into two distinct varieties. We began the chapter with an attempt to simply identify the variety of distinctive atmospheric regions, independently of their sequential occurrence. We found them too inter-related, preceding and succeeding regions to that studied, for such objective separation. Initially, we recognized that the several types of photospheres required at least a division into atmospheric regions associated with

one type of photosphere. Eventually, in recognizing the importance of a variability in mass-flux for the regions associated with even one type, quasi-thermal, photosphere, we recognized the impossibility of setting aside sequential relations for even these. So, we proceed directly to abstract what we have learned, between Chapter 3 and this Chapter 4, of sequences of distinctive atmospheric regions, relative to atmospheric structural patterns.

OBSERVED DISTINCTIVE RADIAL SEQUENCES OF THE DISTINCTIVE ATMOSPHERIC REGIONS COMPRISING STELLAR ATMOSPHERES

I. A PERSPECTIVE FROM THOSE SEQUENCES WHOSE VARIETY INCLUDES QUASI-THERMAL PHOTOSPHERES

In Chapter 4, we identified, and summarized the characteristics of, each of those distinctive atmospheric regions on which we have enough observational material that empirical-theoretical studies can put them into clear focus. We identified each such distinctive region, whenever it is observed in a particular star, as always occurring as one member of a radially-distributed sequence of differing types of such regions, whose totality comprises the atmosphere. Thus far, we have sufficient data, and thermodynamic insight, to have been able to characterize well only those types of regions which occur in sequences that include quasi-thermal photospheres. Regions of these types may also occur in sequences which do not include quasi-thermal photospheres; and there may exist distinctive atmospheric regions which we have not yet sufficient data, and insight, to have identified. Each such region exhibits at least one aspect of that total nonEquilibrium-thermodynamic transition between stellar and interstellar-medium states of matter and energy, which it is the function of the stellar atmosphere to provide. Thus for a particular star, and for a particular environment, a particular sequence of distinctive regions appears to exhibit the particular total transition. Just as Chapter 4 focused on the question whether such distinctive atmospheric regions exist, their range in type, and in variety of a given type; so here in Chapter 5, we focus on the variety in which distinctive atmospheric sequences exist, to the extent that we presently identify their characteristics.

Because of the manner of its identification, each distinctive region was seen to have two kinds of characteristics: those nonEquilibrium-thermodynamic ones which specify its distinctive transition-aspect role; and those observational ones which exhibit its presence in a given star. Hopefully, we have reduced the thermodynamic characteristics of each type of distinctive region to their absolute essentials; so that all varieties of that type of region are unambiguously recognized by their common, distinctive, transition aspects. But we also stressed that a variety in the particular observational characteristics of a given type of region, between different stars or kinds of stars, is essential for being able to identify that distinctive transition aspect with a general thermodynamic property, not simply with a particular set of values of a particular set of thermodynamic parameters. For this reason, "sufficient observational material to identify the character of a given type of distinctive atmospheric region" means material across the whole HR diagram, not just observations of stars of one, or a few, limited varieties. Observationally, the specific appearance of a distinctive type of region may change between stars differing in values of only some, not necessarily all, thermodynamic parameters. Our standard example is superionization, which occurs in all stars observed under sufficiently-broad spectral coverage, and which is one observational characteristic of a chromosphere. It reflects the chromospheric thermodynamic characteristic of some nonradiative energy dissipation; which itself reflects the transition-aspect across the photosphere of passage from wholly-storage, to partially propagative and dissipative, modes of nonradiative energy concentration. The observed ions are identified as superionized relative to the ionization level of the underlying photosphere, which varies with T_{eff} , which is defined by the radiative energy flux. Thus, defining a

chromosphere across the HR diagram to have the particular ionization-level of the solar chromosphere would hardly satisfy any distinctive thermodynamic characteristics. The transition in thermodynamic character, between photosphere and chromosphere, is independent of the particular value of T_{eff} , and of the particular kinds of nonradiative-energy storage, propagation, and dissipation. The variety in these four quantities introduces the observational, but not thermodynamic-characteristic, varieties of chromosphere.

If there existed classes of stars, within each of which all its members had the same values of all characteristic parameters—mass, radius, gravity, composition, etc. and radiative and nonradiative energy-, mass-, and hydromagnetic-fluxes; and if all stars had precisely the same local ISM environment; then presumably all stars of each class would have the same sequence of the same kinds of distinctive atmospheric regions. These sequences of atmospheric regions—one for each class of stars—would replace the “standard atmospheric model,” consisting of the several photospheric subregions, of Chapter 2. Variety between one class and another would be similar to the kind of variety one finds between MK classes; the existence of exophotospheric, and local environmental, characteristics would simply give greater richness to the contrast between classes in this enlarged taxonomy. However, the variety in all the phenomena discussed in Chapter 3—especially in the summary-characteristics of variability, individuality, dependence upon time-history—makes it clear that such enlarged stellar classes either do not exist, or we do not presently see how to define them. At the moment, we must simply admit a greater variety in details of the sequences of atmospheric regions found in individual stars than we might expect if the above idealized classes existed. The primary question is whether we can identify, and define, *gross distinctive sequences* of distinctive regions; or are sequences simply polyglot?

So then, we appreciate the significance of our second standard example of a distinctive atmospheric region, identified in Chapters 3 and 4: the H α envelope, which is not found in all stars, and appears strongly only in those stars showing a significantly-variable mass-flux. The existence of such variability gives the invariant thermodynamic characteristics of a decelerated, and cooled, region relative to the underlying chromosphere-corona. The particular characteristics of the variability in the particular star produce the large variety in location and size of the H α envelope. A negligible variability depresses the observational prominence of this region—and of the whole of the associated LSE—by producing it, if at all, so far from the star, at such low density, as to make it inconspicuous. So the non-universal existence of this H α envelope distinctive atmospheric region lets us identify at least two gross distinctive sequences of distinctive atmospheric regions: those with, those without, an observationally-prominent H α envelope and a conspicuous LSE; thus presumably those with, and those without, a significantly-variable mass-flux.

The distinction between the two types of sequences is observationally striking. The simultaneous coexistence, in a particular star, of some combination of the three gross subsets of distinctive atmospheric regions—quasi-thermal photospheres with a variety of T_{eff} , much-hotter chromospheres-coronae, much-cooler LSE—produces the historic, visual, symbiotic character of some stars: a *mélange* of high-temperature and low-temperature spectral features. Our current ability to observe stars across spectral regions from the X-ray to the radio shows, unambiguously, the universality of this symbiotic character: universal in the thermodynamic-existence sense; highly individual in its observed variety. Such broad spectral range also introduces the modern enlargement of the symbiotic character: a concurrent *mélange* of high and low velocities. Then we note that the symbiotic character of a given star is the more pronounced, and exhibits the greater variety, the greater the range of distinctive atmospheric regions observationally-strong in the star; particularly, the greater the variety of their distribution among the above three gross subsets. Thus the WR + Sun sequence of atmospheric regions is the more limited—with the exception of those few WR objects exhibiting distant envelopes; its symbiotic aspects lie mainly in the contrast between photosphere, chromosphere-corona, and non-decelerated postcorona. Those varieties of the sequence of regions resting on a variable mass-flux are the richest, bringing into focus also the range of low-temperature phenomena. Moreover, since its low-temperature, relatively-slow-moving characteristics rest primarily on variability, its symbiotic aspects exhibit great range in ‘phases’ of the star. Thus it is no surprise that the name “symbiotic star,” based wholly on visual-spectral data, was given to objects which are not only very difficult to put into any particular class at any one phase—under any classification scheme based primarily on “temperature” effects—but whose uncertain classifications change strongly with phase. Their visual spectra alone show both TiO and (Fe X) and (Fe XIV) solar-coronal lines. Various, as emphasized, they have been classified Be, Bep, ordinary and recurrent nova. They are, indeed, proto-examples of the second, rich, type of

distinctive sequence of distinctive atmospheric regions. If you want to model the time-history of a symbiotic star—or any other in this second, gross, distinctive sequential category—then model the space-sequential distribution of distinctive regions, and devise a time-dependent “veiling and enhancement” scheme.

We cited the symbiotic stars as the proto-example of stars exhibiting the full richness of this second distinctive type of atmospheric sequence. But in developing its characteristics, and in presenting a crude conceptual model of the sequence of atmospheric regions, we relied most heavily on the B, Be, Be-shell stars because of the range of data, across these several phases, being greater than for other stars in the category. We modeled an observed subthermic mass-flow in the photosphere, amplifying to as large as 2000 km/s in the upper- and postcorona. For this reason, we stated that the sequence must include, as one of its varieties—the only one on which we have detailed observations—a quasi-thermal photosphere. Quasi-thermal, in the sense that the mass-flow does not perturb HE or RE, in the photosphere. The strongest complement to the picture came from the PN, and their interpretation of a variable mass-flux, which is low-frequency episodic. But we have no detailed observations, especially phase-dependent ones, of their photospheric conditions: only the low-resolution surveys of range in spectral type, and some tentative interpretations of some objects as proto-PN, abstracted in Chapter 3. So implicit in the identification of this second type of distinctive atmospheric sequence, and our crude conceptual model of it, lies the assumption that all phases of the mass-flux variability can be modeled with such a quasi-thermal photosphere. Thus far, the Be-data, and supplements from T Tauri etc., provide no detailed observations to the contrary; but this is hardly sufficient. We note that the symbiotic stars are nova-similar as well as Be-similar; and that the PN may have the same “abrupt-episodic” conceptual history as the novae, so possibly the same type photosphere. A quasi-thermal photosphere seems, on the basis of present data, a possible member of the second, mass-flux variable, sequence of atmospheric regions; but it has not at all been shown to be the only kind of photosphere which can fill that role. The proto-example of a star which exhibits the range of phenomena expected from a member of this class is a symbiotic star; but we have nothing like the range of observational material on them which we do for the Be-stars. So, conclusion on the outward evolution of their mass-flow, continuous or episodic, is, presently, essentially speculative.

We turn to less complete data, from which we have not yet the ability to unambiguously infer the character of regions comprising atmospheric sequences, even to the extent of Chapter 4. Nonetheless, these data, and their thermodynamic implications, supplement our picture of atmospheric sequences of regions.

II. AN EXTRAPOLATED PERSPECTIVE ON THOSE SEQUENCES WHICH INCLUDE EJECTED-SHELL AND SPHERICALLY-PULSATING PHOTOSPHERES

Initially, in Section I, I stressed that we have, as yet, sufficient observational data to unambiguously identify only those sequences which include quasi-thermal photospheres. Our unambiguous demonstration that there exists more than one distinctive sequence came from identifying with a variable mass-flux the production of that subsequence of regions called the LSE, prominent among which is the $H\alpha$ emission-envelope, which is not observed in all stars. As illustrated in Chapters 3 and 4, the amount and variety of evidence needed to establish the sequential properties of the regions comprising this second kind of sequence is very large; hence, the present rarity of this kind of investigation, which gives the sequential details. But the observational evidence characterizing the LSE is almost wholly exphotospheric. While the mass-flux variability is paramount, we do not find strong observational evidence for it in wholly photospheric—even chromospheric—behavior; with one possible, important, exception considered below. Thus, saying that our well-studied sequences produce only quasi-thermal photospheres means, simply, that among the well-studied stars, there are not yet included those for which well-defined nonthermal effects on photospheric structure stand out. To a first approximation, one models quasi-thermal photospheres under the condition $U(\text{photosphere}) \ll q$ at all phases. It leaves open the question of what sequences to expect when $U(\text{photosphere}) > q$, at some epochs, even though *differential* $U > q$ may or may not occur.

A. EJECTED-SHELL PHOTOSPHERES

First, we recognize that our initial division of stars into three photospheric categories separated from those with quasi-thermal photospheres, of which *some* have variable mass-flux, just those stars we would a priori associate with variable mass-flux: the (episodically) ejected-shell type. However, if we were to take literally the ordinary novae as one-time episodic ejection, we should consider their photospheres as “quasi-thermal” at all other epochs. Indeed, we simply have the above-invoked similarity to the PN, also usually described as one-episodic ejection, or one-episode enhanced mass-flux; the remaining time, they show quasi-thermal photospheres. Indeed, by combining them with the Be stars to exhibit the range in character of H α envelope, we have treated them thusly. We regard Be stars as “little PN” in strength of episodic ejection—which we observe as fluctuations in superionized line-strengths, profiles, and displacements—and in location of H α envelope, but not in episodic frequency; there, the difference is strong. But then we further push the PN and novae to the quasi-thermal photosphere class by noting that at all phases other than that of episodic-ejection, each appears to have the $\sim 10^3$ km/s steady mass-flow, characteristic of Be developed emission phases, in the superionized region: i.e., upper-corona and pre-decelerated postcorona. To the best of our present knowledge—which lacks details on the Be-shell phase—we can apparently represent the Be stars at all phases by the sequential model of Chapter 4 (but see below). The novae appear to exhibit a simple expansion, with decelerating collision very far from the star, as measured by the appearance of the forbidden coronal lines late in the outburst evolution. We do not know whether the PN measure the location at which a nova-like decelerating collision occurs; or whether the H α nebula measures the present location of a Be-type, close-in, encounter which has propagated outward to its present location, because no other episodic outburst occurred. In any event, all ordinary novae, and most PN, exhibit a hot blue photosphere of the central star; so we conclude that outside the actual episodic-ejection phase, there is not much visual veiling by the exophotosphere. In the farUV, we see essentially chromosphere-corona.

A better assessment should come from comparing the gross model of the variable-mass-flux atmospheric sequence, derived from Be and Be-similar stars, to more-frequently-variable cataclysmic stars: the recurrent and dwarf novae, which blend into the symbiotic stars. We put their contribution into focus by returning to one possible association of mass-flux activity in Be stars to photospheric phenomena. Recall that our gross, empirical model of the Be exophotosphere found the H α envelope to be transparent in the PaC (visual), marginally-opaque in the BaC (near- and far-UV), and strongly-opaque in the LyC. Only in the latest, coolest, Be stars is there a possible ambiguity between lines produced in H α envelope and lower-chromosphere; such distinction is a problem in the T Tauri stars. So a major problem lies in the statistical result that in the visual (PaC), Be stars are significantly-brighter than B-normal—as much as one visual magnitude. The T Tauri show the effect, but considerably smaller. So either the H α envelope has a very much greater visual opacity than our empirical analysis produced, which seems hard to introduce, or we must expect significant photospheric changes accompanying those phase-changes defined by the H α -emission strength. Keeping our interpretation of these latter as resulting from mass-flux variability, we should have to consider that the suggested photospheric changes are associated with such mass-flux variability. Current, highly-preliminary, simultaneous studies of luminosity variation in the visual and farUV continua of a few Be stars appear to find that the two continua vary in the same sense—they increase together (Doazan and Barylak, 1984). Speculatively, these data—combined with the H α envelope diagnostics—suggest a slow rise in photospheric radius with increased mass-flux activity. At the moment, such suggestion is more conjecture than well-substantiated fact. It does, however, accord with the secular behavior, during times of increasing H α -emission, summarized for γ Cas and 59 Cyg in Chapter 3 and by Doazan (1982). Again, simultaneous observations at $\lambda < 910\text{\AA}$ are needed.

Then the phase-variations of the recurrent novae and the dwarf novae, summarized in Chapter 3, contribute to putting into focus the problem just summarized. First, we cannot forget that all the cataclysmic stars were first recognized because of their significantly-large variations in the visual continuum. By contrast to the pulsating-variables, where the major luminosity variations come from those of the effective photospheric temperature, the major cataclysmic variations in luminosity appear to come from variation in effective photospheric radius. The clearest illustration lies in our discussion of Pottasch’s caricatured, fluorescing-screen, model of ordinary novae. In the early stages,

the total radiative output remains unchanged; the rise in visual luminosity, and reddening-shift toward later spectral classes, accompanies the increase in shell-radius and RE-degradation from the far-blue spectral regions. There is no dissipation of the ejected-shell's aerodynamic energy in these early stages—not until the far-distant collisions that produce the distant H α envelope and LSE discussed above. This increased visual luminosity, later of farUV luminosity (cf Fig. 3-4) is the primary variability in luminosity and spectrum for these low-frequency, large-amplitude episodic ejections of ordinary novae—no matter what their cause. The secondary changes in luminosity and spectrum correspond to the far-distant collision which produces H α envelope and LSE—possibly collisions with the steady mass-flow, earlier episodic debris, ISM, or whatever.

Then, in the same way, we note the primary, recurrent, smaller-amplitude, photospheric-shell ejection in recurrent novae. But we should also recall the very significant, 3-year study of T Cor Bor by Cassatella, et al. (1982)—which exhibited strong farUV (BaC) variability over this period without accompanying, significant, visual (PaC) variability. At quiescence, the short-wavelength farUV spectrum was typical cool-star: flat continuum, superionized lines in emission. Over the cycle of this secondary kind of mass-flux activity, the same spectral region developed a hotter-star resemblance: continuum increasing toward the blue, tendency toward some superionized lines being in absorption. The primary, abrupt, outburst of this recurrent nova is the nova-like one of increased visual luminosity corresponding to increased photospheric area. The secondary, protracted, activity, slowly increasing over about a year, produced a hot shell, transparent in the visual, opaque in this short-wavelength farUV. Then, in summarizing dwarf-novae behavior, we noted their three apparent phases: quiescence—a cool-star farUV appearance; outbursts—few-day duration, at 10-day intervals; and super-outbursts—10-day duration, at 100-day intervals. All these show strong individuality, up to factors of 10 variation about these stated values, while maintaining the relative existence of the three phases. And, at maximum mass-flux activity, this spectral region resembles a hot-star: continuum strongly increasing toward the blue, both absorption and P Cyg superionized line-profiles.

So all these cataclysmic objects exhibit these two kinds of phenomena—each, presumably associated with a mass out-flow: one, an increase in photospheric area producing the visible continuum, so visual luminosity increase, and also sometimes farUV, with possible phase-lag; the other, an increase in opacity and emissivity of hot exospheric regions, presumably chromospheric-coronal, which are transparent to the visual. This latter is reflected in just those secondary outbursts of the recurrent novae described above. One must distinguish which is primary and which secondary for the dwarf-novae—high-frequency bursts, lower-frequency outbursts, the latter having the larger amplitude. So, presumably, we associate the longer-period outbursts with the continuation of the “primary” sequence from novae through recurrent novae. These two kinds of outbursts are neither necessarily related nor dissociated: such remains to be established. A primary question is whether either is more likely to occur near a “peak” in the other. It seems more certain that the two must interact; and possibly, they interact within themselves. Such should correspond to the production of H α envelope, and the whole LSE, as described previously. So the primary addition of the cataclysmic objects to the atmospheric patterns, and sequences, of the Be and Be-similar stars, lies in this variability of pre-LSE: the photosphere, chromosphere, and corona. The WR and Sun typified one atmospheric sequential pattern: grossly time-independent radial sequence of photosphere-chromosphere-corona; largely-invisible LSE, except for the several WR objects showing distant nebulae. The Be typified that sequence exhibiting an LSE, and those variations in farUV line-spectrum exhibiting the mass-flux variability that produce the LSE, which includes a quasi-thermal photosphere as its lowest-lying member. The cataclysmic objects remove the quasi-thermal character of the photosphere by permitting it velocities that are sufficiently large and impulsively-initiated to cause an abrupt change in visual continuum. The symbiotic stars remain a kaleidoscopic bridge between cataclysmic and Be-type sequences; exhibiting the symbiotic richness in observational appearance that results from such richness in distinctive regions comprising the sequence.

Then we see the significance of the slow rise in Be visual luminosity. It represents one extreme of the cataclysmic “abrupt” change in visual luminosity by an abruptly-ejected-shell photosphere. The Be-type represents the limit of a very slow, subthermal, ejection—at a very small \dot{M} , compared with the cataclysmic values. It also represents the unambiguous observational dominance by the secondary mass-flux activity; which produces a distant LSE for ordinary novae and PN, and near LSE for Be and Be-similar stars. The primary shell-ejection was ultra-velocity abrupt

and short-lived episodic for the ordinary novae; and the secondary mass-flow is represented by the “quiet” continuous outflow, which reaches some 10^3 km/s. The primary shell-ejection—we retain “primary” to denote that which affects the visual continuum—of the Be-type is at subthermal velocity; a slow upward motion in the rising Be-phase. The secondary mass-flow “activity,” which exists over extended periods of time—unlike the ordinary novae, but progressively like recurrent and dwarf novae—consists of the episodic outbursts, of small amplitude, which are that mass-flux variability which produces the LSE. Those major mass-flow fluctuations of this secondary variety occur largely in the high-velocity component, as we saw—thus, observably, in the pre-decelerated postcorona. We did, however, note current observations showing, for some stars (e.g., θ Cr B, 59 Cyg), at some phases, strong decrease of superionized line intensity in both low- and high-velocity components. Such behavior resembles that of the cataclysmic stars, which we ascribed to chromospheric changes. Clearly, while we associated both primary and secondary behavior, in all these stars, with mass-flow characteristics, we must admit the possibility of associated variability in nonradiative energy flux not transporting mass. The problem is to distinguish between the variability, and effects, of these two fluxes. We return to the problem in Section B.

Summarizing, we resolve the problem of the slow increase in visual luminosity of the Be—and T Tauri and other Be-similar—stars by identifying two phenomena of mass-flow, and luminosity and spectral variability; and identifying these with a similar two kinds of phenomena in cataclysmic stars. While these two phenomena are undoubtedly associated, the empirical and thermodynamic details of such association are not yet clear. What is important to note is the evolution of the relative importance of the two phenomena, with respect to observed photospheric and exophotospheric variability and individuality—in luminosity, in velocity, and in location of radiating surface-layer or region. It is obvious that any velocity fluctuation in the slow outward photospheric motion in Be stars can amplify outward into the atmosphere, and self-interact, as discussed in Chapter 4. It is equally obvious that spherically-ejected photospheres, having $U > q$, already exhibit a $(r^2 U)^{-1}$ rather than HE density distribution; thus any HE character of the chromosphere, and any transthermal character of the lower-corona, are suppressed, as they apparently are for the WR stars. This leaves the primary characteristic of a chromosphere-corona to be a nonradiative heating, in these sequences which do not have a quasi-thermal photosphere. Whether such heating demands a nonradiative energy flux not transporting mass, or comes from velocity gradients in this superthermic flow producing an aerodynamic, non-radiative, energy dissipation remains to be settled.

B. SPHERICALLY-PULSATING PHOTOSPHERES

Above, we have thus far identified three gross varieties of atmospheric sequences. These all result from the replacement of the single-region atmosphere, a static thermal photosphere, of the speculative standard model, fixed by the properties of the radiative flux, by some sequence of distinctive atmospheric regions. The properties of the several sequences depend upon the independent existence, variability, and individuality of at least three fluxes: radiative-energy, nonradiative-energy, and mass. The simplest gross sequence yet identified is found in stars exhibiting effectively-constant values for all three fluxes: a quasi-thermal photosphere; a chromosphere-corona where a non-radiative heating and an acceleration through thermal, superthermal, superescape velocities occurs; and a nondecelerated postcorona, where some acceleration may occur, and there is a slow cooling. The Sun is a prototype, low-mass-loss example. The WR objects are a somewhat ambiguous example of a high-mass-loss variety. The ambiguity arises in the question whether we actually observe a photosphere, or whether one indeed exists; in order that we may be self-consistent in describing such O VI as superionized. There is further ambiguity in whether those WR objects showing a distant H α nebula may be a transition to the second gross sequential variety; and whether those central stars of PN identified as WR-objects may represent the same kind of transition-variety. The second gross sequence has been identified in stars exhibiting at least a variable mass-flux. It replaces the nondecelerated postcorona of the first sequence by a decelerated postcorona, followed by the regions of the LSE. Its simplest form of a single variety of mass-flux variability—characterized by variability in frequency and amplitude—may not exist; the slow secular rise, then eventual fall, of visual luminosity in the Be, and T Tauri, stars raises the question. The third gross variety of sequence may include the second as a limiting case. Here, one has two distinguishing characteristics. Simplest, is that

the photosphere may be nonthermal, with arbitrarily-large velocities at some epochs or phases. More elaborate, is the identification of two varieties of mass-flow or mass-ejection: one, with large opacity and arbitrary velocity at the photospheric level, so that it is already identified in significant visual luminosity variability; the other, identified by luminosity and spectral variability outside the visual, usually at least in the farUV. The relative observational prominence, and thermodynamic significance, of these two varieties of mass-flow show progressive differences between various types of stars—indeed, such differences are undoubtedly what define the several types. This third gross sequence also exhibits the regions, and phenomena, of an LSE; again variable, and individual.

As stressed, these three gross sequences arise from the properties of the mass-flow from the star: the basic characteristic of an open thermodynamic system. The characteristics of the observed mass-flows, and associated phenomena, are such as to require a nonthermal character for at least the immediate subatmospheric regions of the star; so we have a (nonthermal, open) character for subatmosphere, atmosphere, and local environment. Such mass-ejection from the star is hardly a recent idea; the ambiguity is between the historical idea of a mass-ejection as fundamental, with any nonradiative heating being secondary; and the idea in more recent years of a nonradiative heating producing atmospheric regions from which matter can escape thermally—the heating being large enough to produce superescape thermal velocities of the gas as a whole, not of just a few particles on the tail of a thermal velocity distribution. The favored heating mechanism of the hot-coronal approach has been dissipation from a system of progressive waves, ultimately arising from the instability of the hydrogen convection zone in the subatmosphere. But such also is the source of spherical-pulsations in the cooler stars: the cepheids, long-period variables, etc. as discussed in Chapter 3. And Schwarzschild's contribution to Eddington's original picture of such pulsation was to note that such pulsations must eventually become progressive waves, which must eventually steepen enough to form shock-waves, and thus dissipate nonradiative energy. Thus both Sun and cepheid should produce a chromosphere: the first from stochastic heating, without favored phase; the latter, presumably phase-dependent. And this is what the observations abstracted in Chapter 3 show: the continuous presence of chromospheric indicators—e.g., Ca II H and K emission cores—in stars with no spherical pulsational variability; the phase-dependent existence of Ca II, and indeed H α , in spherically-pulsating stars. To a first approximation, this picture of chromospheric production from wave-generation and dissipation, either stochastic or spherically-symmetric, seems self-consistent in distinguishing between these two gross types of chromospheric-coronal sub-sequences: essentially-constant, or variable; exemplified by Sun and cepheid-type stars, respectively. So, this identification of chromospheric-coronal variability introduces at least a fourth gross atmospheric sequence, whose postcoronal character is yet unspecified.

For perspective, we return to the mass-flux distinction between the first two gross types of atmospheric regional sequences: which really focuses on the LSE sub-sequence; again exemplified by Sun and Be-similar stars, respectively. The perspective comes from recognizing that those B-stars which never, or very rarely, show the Be-phase effectively fall into the type-1 sequential category, Sun-like except in size of mass-flux. As discussed in Chapter 4, the general stellar photosphere is unstable against a perturbation consisting of a small radial outflow; it amplifies to produce such a type-1 gross atmospheric sequence if there is a nonradiative heating in the upper-photosphere and chromosphere-corona. Thus, for sufficiently-small mass-flux, one could imagine that some stars in this type-1 category have a mass-flow whose origin is such a small, possibly stochastic, radial-velocity perturbation. To obtain the much larger mass-flux characterizing other stars in this type-1 category, one needs something more than such a small-perturbation origin of the photospheric mass-flow. And certainly, to produce the postcoronal variability, and especially the photospheric variability, one needs an organized origin for the photospheric velocity field which results in the mass-flux. Paradoxically, the more organized the origin of the photospheric velocity field, the more suppressed is the ultra-velocity delivery of the mass-loss to the ISM; thus also, the kinetic energy delivered to the ISM. That decrease in kinetic energy resulting from the postcoronal deceleration is, of course, delivered to the LSE via the deceleration process.

Applying the same considerations to the nonradiative energy dissipation in chromosphere-corona by those oscillations/pulsations generated in the hydrogen convection zone, we see that a stochastic heating of at least the lower-chromosphere suffices to maintain the quasi-steady appearance of the conventional, cool-star, chromospheric

indicators like Ca II and Mg II. Extending such heating to the upper-chromosphere, and lower- and upper-corona suffices to maintain both the quasi-steady, broader superionization, X-ray emission, and the continuous mass-flux. But just as that organized motion which introduces a variable mass-flux inhibits—i.e., decelerates—it in the LSE, so the organized motion of spherical-pulsation inhibits—i.e., temporarily suppresses—at least the low-chromospheric indicators of Ca II, sometimes the high-chromospheric indicator of Mg II. We recall that in the cepheids, Ca II H and K emission cores appear only just after luminosity minimum, and last the longer, the longer the pulsation period; they do not appear at all in stars with periods less than some 4 days. We also recall that the Mg II emission cores persist over a greater fraction of the cycle than do the Ca II, in a given star. Apparently, that kind of “oscillatory” activity which provides a greater nonthermal systematic velocity of the photosphere pushes farther out in the atmosphere the regions of nonradiative heating, when the motion is a mass-propagation rather than simply a wave-propagation. This accords with our use of mass-flow as setting an upper height limit at beginning of nonradiative heating. This general behavior accords with that found for the novae. And we note that the phase of Ca II emission—the phase of nonradiative heating—is when the material falls inward, not when it expands. It is the differential motion of compression which induces a mechanical heating. Either the simple ejection-expansion of the novae, or that part of the pulsation before the wave has steepened into a shock, propagate a mass-flux without dissipation. We elaborate in Volume II.

As abstracted from Whitney’s discussion of wave-steepening, as sketched in the Willson-Hill LPV modeling, and as illustrated by the Burger-de Jager observations/model of the β Cep stars, all in Chapter 3, one must admit a wide range of variety in the exophospheres of these pulsating stars as a function of photospheric pulsation period and its initial velocity-profile. The range in such profile, observationally, across the whole variety of pulsating variables is from almost impulsive to leisurely pulsation. It is similar to that range in “primary” photospheric mass-flow, or photospheric shell-ejection, discussed in Section A. Indeed, the similarity is marked. The basic distinction is between a clearly identifiable periodic phenomenon in the pulsation, and the no-well-defined time-scales of the existing cycles for the shell-ejection.

III. ABSTRACTED SUMMARY OF GROSS DISTINCTIVE RADIAL SEQUENCES OF DISTINCTIVE ATMOSPHERIC REGIONS

Our objective in this Chapter 5 is to identify, and characterize observationally and thermodynamically, gross distinctive radial sequences of distinctive atmospheric regions—not to infer why they exist; that is the goal of Chapter 6. Nonetheless, we cannot ignore those associations—possibly correlations—between distinguishing characteristics of the sequences and thermodynamic properties of the stars in which they appear. Moreover, since a major objective is to decide whether the star must be described as an unrestricted (open, nonthermal) thermodynamic system, or can be considered only as a slightly-perturbed (closed, thermal) system, we cannot ignore this choice between thermal perturbation and nonthermal state in our empirical-theoretical identification of sequences and properties. Then we can succinctly summarize the sequences we have identified.

We continually put all such identifications into perspective relative to the standard-atmospheric sequence consisting only of photospheric subregions: those across which there is only the evolution from LTE-LOS, through LTE-R, to thermal nonLTE, in distribution functions for photons and internal energy states of particles. All non-thermal storage and propagation, hence their evolution across the atmosphere, are forbidden; there is no variability, and no individuality among stars having the same (chemical-composition, gravity, radiative flux). Any time-dependence must come from evolution of internal structure. There are no fluxes of nonradiative energy or mass.

The simplest gross sequence which we have identified exhibits a chromospheric-coronal subsequence of non-radiatively heated, ionized/excited, thermally-distended regions; these overlap, and underlie, a subsequence of regions which are mass-flow distended. Such an atmospheric sequence provides to the parental ISM a radiative-flux, which is higher-energy than the photospheric one, and a mass-flux, which is superthermic-velocity relative to the coronal T_e . The coronal properties require an associated mass-flux; the mass-flux properties require a nonradiative heating. Under thermal standard models, the ionization zones of at least H and He, possibly of other sufficiently-abundant elements,

are unstable against the production of nonradiative energy fluxes. The thermal-model atmospheric structure is unstable against the production of a mass-flow which, under a nonradiative heating, can become a mass-flux from the star. The basic question is whether, for some stars in which this type-1 sequence appears reasonably adequate to describe the observational picture, the sizes and effects of such stochastically-produced nonradiative-energy and mass fluxes suffice to represent the details of the observations. Because the flux-generation is stochastic, variability, and any major individuality, seem excluded. Again, observational and thermodynamic consistency must be the ultimate judge of the adequacy of this type-1 sequence to fully describe at least some stars.

The type-2 sequence which we have identified seems demanded to describe those stars showing an H α emission envelope, and other features which we describe as an LSE. Its basic characteristic is a mass-flux variability, which appears in a wide variety of frequencies and amplitudes. Its major perturbation is in replacing the nondecelerated postcorona of type-1 by a decelerated, and rapidly cooled, postcorona, plus the other LSE regions. An unrestricted postcoronal variability and individuality are admitted. A nonstochastic driving of a mass-flux from the photosphere appears required, but we describe the photosphere as quasi-thermal, implying that the variable mass-flux is, at all phases, subthermal in the photosphere. We are not sure whether this type is an idealized limit of type-3 following, or whether it actually suffices to describe some stars.

Our type-3 sequence differs from type-2 in admitting two grossly different kinds of nonstochastically-originating mass-flux. One may be of the kind admitted in type-2: quasi-thermal photospheric properties; optically-opaque mainly outside the visual spectrum. The second kind of variable mass-flux may be impulsive in character, and have arbitrarily large velocities, in the photosphere: it may be a photospheric shell-ejection, as exhibited in a variety of stars exhibiting this type atmospheric sequence. It shares the type-2 character of having a decelerated postcorona and an LSE; which are highly variable and individualistic.

Our type-4 sequence distinguishes itself by departing from the possibility of a wholly stochastic origin for the nonradiative energy flux. This departure can also exist for the sequences types-2 and -3; but a stochastic origin for such energy-flux could be adequate for them. It cannot be, for this type-4. The nonradiative energy flux represents a nonthermal, organized motion. To date, some aspects of the cepheid-like pulsations as initiated by thermal instability of the H–He ionization zone, under random perturbations, seem reasonably self-consistent in representing visual luminosity. The mass-flux aspects, and the spectral appearance in the farUV, remain open to question. An outstanding need is to represent the concurrent features of chromospheric and mass-flux variability, and admit that individuality arising in the existence of some stars in the instability strip which do not show these pulsational features. So, this type-4 sequence, while identified, is hardly well-characterized, at the moment: both observationally and thermodynamically. Observationally, we are curious about the similarity between the Be-type spectrum shown at several phases in the farUV, and the behavior of the cataclysmic stars in this respect. Thermodynamically, we are curious about the possibility of incorporating the mass-flux, and spectral-appearance, variability into the current pulsational models of cepheids, via the several pulsating-piston, hence impulsive, representations. We seek a bridge between shell-ejection and spherically-pulsating photospheres—and their exophotospheric sequences.

Page intentionally left blank

Page intentionally left blank

INFERENCE ON THE THERMODYNAMIC CHARACTERISTICS OF A STAR FROM THE OBSERVED DISTINCTIVE RADIAL SEQUENCES OF THE DISTINCTIVE ATMOSPHERIC REGIONS COMPRISING THAT STELLAR ATMOSPHERE

I. SUMMARY-PERSPECTIVE

Chapter 2 surveyed what a speculative-theoretician would predict for the structure of a stellar atmosphere, if he were convinced—a priori, without verifying his intuition by diagnosing observations other than very grossly—that the star must be a (closed, thermal) thermodynamic system, after some initial period of collapse from the ISM. Its atmosphere would be a nonlinear thermal transition region between a quasi-Equilibrium stellar interior and a nonlinearly nonEquilibrium ISM, any instabilities being linear. The range of thermal energies in the atmosphere would not be large; and their level would be measured by the blackbody equivalent of the energy in the visual spectral continuum. Any incompleteness in modeling all this would simply reflect the modeler's as-yet incomplete knowledge of nonlinear, thermal, nonEquilibrium thermodynamics. To adopt such a (closed, thermal) modeling, even as a first approximation, one must exclude from consideration about half the well-studied stars, including the brightest ones and the Sun, and most observations outside the visual spectral range.

Chapter 3 surveyed the stars' testimony on the adequacy of such intuition, focusing on those which have most strongly protested, which have in consequence been labeled "peculiar." Modern spatial observations show that evidence from much larger numbers of stars protesting this (closed, thermal) categorization has been veiled by the Earth's atmosphere. They were labeled normal because they were only incompletely observed. Thermodynamically self-consistent diagnostics of all this material show that the atmospheres of the stars themselves have sometimes veiled peculiarity: the actual large range in thermal energy level within one star's atmosphere, and the variety of nonthermal effects producing such range. Rather than a single, thermally quasi-homogeneous, photospheric region, Chapter 3 exhibits the stellar atmosphere as consisting of a wide variety of distinctive atmospheric regions: some, whose thermal energy much exceeds that of the visual radiation field; some, whose thermal energy falls considerably below it. The range of nonthermal phenomena, associated with such thermal range, is equally large: within a given atmosphere, outflow velocities can range from very-low subthermic to ultra-superthermic. Phenomena ranging from thermal X-rays to dust, in the same atmosphere, for a variety of kinds of photospheres, are observed. The striking contrast between real and speculative stars does not lie simply in the presence of some nonphotospheric region, and the observational peculiarity it produces; it lies in the presence of *multiple* nonphotospheric regions, and the symbiotic appearance their varied presence and character produces. Stellar binarity, and higher multiplicity of components, is widespread. But the observed existence of such multiple, thermodynamically strongly different, atmospheric regions in single stars demonstrates that multiple-stars, each with only a photosphere, is hardly the preferable alternative in modeling the symbiotic spectra of stars in which there is marginal other implication of binarity. Rather, these data suggest that one use symbiotic aspects to infer details of regional structures of stellar atmospheres—and then ask what produces them.

Chapter 4 surveyed those types of distinctive atmospheric regions comprising the stellar atmosphere, which we have presently sufficient observational material and thermodynamic insight to identify. Not all types of such distinctive regions appear at all times in all stars to the same observational prominence. Indeed, some types of regions have not been observed at all, in some stars, at some epochs. By contrast, under the standard speculative atmospheric model, all stars exhibit, at all epochs, the same regional structure: viz, a photosphere that has always the same kinds of subregions; and such idealized stars are classified according to their photospheric appearance. Real-world stars differ. For each of these, the atmosphere appears, at a given epoch, as one of several gross types of distinctive sequences of the above distinctive regions. Each type of sequence—i.e., each type of atmosphere—is empirically-thermodynamically characterized by the particular types of regions which appear in that sequence—i.e., appear as the atmosphere. One sees observational variety among the stars exhibiting that type of sequence—i.e., exhibiting that type of atmospheric structure—at that particular epoch, according to the particular variety of each type region comprising the sequence. Clearly, the observations must cover the complete spectral range; otherwise, the presence or absence of some particular type of region in the sequence, at that epoch, will be unknown; and one may err in identifying the type sequence that is present, at that epoch. That is, one may err in inferring the particular atmospheric structure characterizing that particular star at that particular epoch, if one does not have simultaneous coverage of its complete spectrum, and if one is obliged to proceed wholly empirically in his diagnostics. Thus the striking contrast between real and speculative stars does not lie simply in the real star's ability to produce a multiple variety of types of distinctive, exophotospheric regions. It lies equally in the real star's ability to *not* produce some of these particular types—never, or at some epochs. We note that these atmospheric sequences exist in distinctive types, not simply as random ensembles of regions; and sequences are specified by presence or absence of particular types of regions. Thus, the star's ability to produce, or not produce, some types of regions—hence some types of atmospheric structural pattern—at some epoch, implies that the production reflects an organized, nonthermal thermodynamic structure for that region forming the lower boundary of the atmosphere, rather than simply reflecting disorganized, stochastic, fluctuations about a thermal—or even quasi-thermal—configuration. Whether this subatmospheric configuration forms boundary values for a storage mode extending, or initial values for a propagation mode ejecting, or source for the variety of fluxes entering, into the stellar atmosphere is not the critical point. It is that this lower boundary environment is organized, nonthermal, and dynamic; rather than being simply thermal, producing fluctuations—possibly stochastic; and exists for a wide variety of stars, all across the HR diagram. So, in parallel to delineating the variety of atmospheric structural patterns, an ultimate objective must also be to infer from such atmospheric patterns what are the subatmospheric nonthermal configurations that produce them.

Chapter 5 surveyed those types of distinctive sequences of distinctive atmospheric regions—i.e., those distinctive types, or patterns, of atmospheric structure—which we have thus far identified. A given type is not restricted to a kind of star, or a given MK class, or even to a particular region of the HR plane. Thus, observationally, the parameters of classical photospheric taxonomy—visual spectrum, and either visual luminosity or gravity—are inadequate to classify or predict the type of atmospheric structural pattern a given star will satisfy, at a particular epoch. Empirically-thermodynamically, this inadequacy arises in the observed universal presence of nonradiative-energy and mass-fluxes, and the independent variability of these and the radiative flux, in actual stars. The two-dimensional HR diagram representation of stellar atmospheres is inadequate; its use suppresses their actual multi-dimensional character. By contracting the equations, standard atmospheric modeling—on whose validity classical photospheric taxonomy rests—imposes that the two nonradiative fluxes be negligibly small, and that the radiative flux only vary over evolutionary times. Empirically-theroretically, we saw that the various types of sequences of regions—i.e., of types of atmospheric structure—rest primarily upon kinds of variability of the several fluxes. Variety within a given type of atmospheric regional sequence—i.e., atmospheric structural pattern—arises in differences in size of each of the fluxes; and possibly in size of gravity, rotation, primaeval magnetic field, etc. Possibly, the influence of these latter may enter primarily in conditioning the variety of nonthermal storage and propagation modes actually present in a given star. Thus the striking contrast between real and speculative stars does not lie simply in the real star's ability to produce, or not produce, a multiple variety of distinctive atmospheric regions arranged in a variety of ordered radial sequences. It lies equally in the real star's need—throughout its evolutionary life of concentration from the ISM—to

structure at least its atmospheric and subatmospheric regions into some varieties of organized, nonthermal configurations, which exhibit some kinds of time-dependence that are neither evolutionary-secular nor random fluctuations. So the star must be allowed to have a nonthermal structure in at least its atmosphere and immediate subatmosphere. Its particular variety, in a given star at a given epoch, reflects heavily in the character of a time-dependent mass-flux from the star. Thus, generally, we must allow the star to be an (open, nonthermal) thermodynamic system. And, modeling of the atmosphere cannot be divorced from modeling of at least the immediate subatmosphere. Specifying the energy generation, the mass, the chemical composition, and the visually-defined radius do not suffice to specify the atmosphere exhibited by real-world stars, at least to our present understanding of the configurations assumed by (open, nonthermal) systems.

So, empirically-theoretically, we must try to classify, diagnose, and model an atmospheric structure of a real-star that is much richer than that of the standard model, and depends upon more parameters. It is richer, a priori, because we must admit that the star is an (open, nonthermal) system, which includes as a special variety a (closed, thermal) system. It is observationally richer in the sense displayed by the distinctive regions of Chapter 4, by the regional sequences of Chapter 5, and by that symbiotic appearance resulting from the multi-regional structure and its time-dependence. It is provocatively-richer in its implications on the existence of a richer variety of internal structure, for at least some regions, than is currently included in thermal internal models and evolution. Moreover, our discussion of the importance of time-dependent mass-loss, and its relation to nonthermal storage modes, invalidates a discussion of stellar evolution under a mass-loss which consists simply of thermal evaporation from the extreme outer atmosphere. It is not so much the precise values of the mass-loss which are important; but the nonthermal structure which underlies them, which the values and time-dependence of the mass-loss reflect. In the standard model of the thermal photosphere and interior, the star needs only return an energy flux to the ISM during its evolutionary concentration; and all that energy flux is contained in the radiative flux. But the real star must return both a mass and an energy flux to the ISM during its evolutionary concentration; and the energy flux must be both radiative and non-radiative. Then the stellar atmospheric and subatmospheric structure must be consistent with, and diagnostically reflect, that process of concentration+energy-liberation translating into at least these three fluxes. In the standard model, the radiative flux is both the sole diagnostic tool and the thermodynamic conditioner of atmospheric energy and mass distributions, for given gravity. In the real star, all these other three fluxes participate in the diagnostics, and the atmospheric conditioning.

So, in parallel to that richer atmospheric structure which we just begin to classify, diagnose, and model free from imposed preconception, there lies an equally richer uncertainty in the theoretical formulation, then solution, of its mathematical representation. One assembles it empirically-theoretically, free from preconception. We want to be very sure that we ignore no physical effects, nor terms in equations, which may be significant only in some regions but whose effects are pervasive. An example is the viscosity in the boundary layer at the moving sphere's surface, which causes separation of the flow from the surface everywhere to the rear of a certain point, with viscosity being negligible everywhere away from the surface (cf Figs. 4-1 to 4-6). Another example is the neglect of source-sink terms in the source-function, simply because they are much smaller than the scattering term; or a neglect of the distinction between the photoionization and collisional source-sink terms; reflected in the divergence of T_e and T_{ex} in Fig. 2-3, and diagnostic ambiguity. Overall, one cannot apply those standard-atmosphere contractions which suppress the independent existence, and time-dependence, of nonradiative energy and mass fluxes. We cannot neglect those terms in eq. (3.C) whose presence permits the thermal and escape points to differ, thus do not suppress the lower-corona. We cannot neglect those terms whose absence permits a radiative acceleration to produce an asymptotic velocity depending only on gravity, and suppresses any nonradiative heating. We cannot neglect those terms producing the LSE.

At the moment, given the observational material in Chapters 3, 4, and 5, we see that our knowledge of, and insight into, all the problems of classification, diagnostics, and modeling are hardly complete. The simplest illustration lies in the current controversy on whether the mass-flux is a parameter predictable from other fluxes, or must be independently specified by the subatmospheric conditions. I think the material collected in this monograph demonstrates the latter, and the resulting implications on atmospheric and subatmospheric taxonomy, diagnostics, and

modeling. If correct, we either need much more empirical material on the time-dependence of the several fluxes, or one proceeds simply speculatively. In Chapter 4, I tried to establish algorithms for proceeding as far as one can go nonspeculatively; but they are hardly very extensive. Clearly, a wholly-theoretical approach must begin with determining the subatmospheric nonthermal structure, in order to specify the values, and time-dependence, of the several fluxes. This represents a joint project between atmospheric and interior theoreticians; thus far, none have tried to explore it. The situation provokes my reply to Mihalas' 1977 dismissal of much excitement in future stellar atmospheric studies. The stellar atmosphere—and its neighbor, the subatmosphere—are far from mature fields; they should be on the frontiers of current research; they will undoubtedly provide many surprises in the future. Noting the observational similarity between the “cool, low-velocity, local environmental H and Fe II” spectra of the Be-similar stars, and the Seyfert galaxies, one such surprise may well focus on the way one approaches “subatmospheric” structure of the nuclei of the latter, guided by results from the former, to understand “atmospheres.”

So, at the moment, it seems most practical to adopt the orientation of these Chapters 3, 4, and 5 to put into focus precisely which empirical-theoretical studies can clarify specific aspects of the atmospheric-structural problem. We do this; considering taxonomic, diagnostic, and modeling aspects in that order. Our guiding focus remains that of this chapter's title: *inferences on thermodynamic characteristics of the star*. Until we are certain on details of these thermodynamic characteristics, we are uncertain about what we are trying to model. A general (open, nonthermal) system is as yet too broad a category for wholly-theoretical studies, just as (closed, thermal) is too narrow a category to represent the observations.

II. TAXONOMIC CONSIDERATIONS

So long as we continue stellar classification studies under the assumption that (quality, quantity) of the radiation flux—i.e., spectral and luminosity types—suffice to specify a star, we continue the illusion that the standard model suffices to describe the atmosphere. Then, the goal of such taxonomic studies continues to be *an application of the standard model*: to the galactic distribution of stars presumed to be in the same evolutionary phase—i.e., having the same MK class; to the differential occurrence and distribution of stars with abundance differences—i.e., spectroscopic anomalies within an MK class; to the apparent relation between kinematical and astrophysical properties of stars; etc. So long as one does not admit nonradiative energy-flux, mass-flux, variability pattern in all fluxes, and possibly conditions of origin, as classification parameters parallel to the radiative flux and gravity—one continues to obtain only a “two-dimensional projection” of the multi-dimensional specification of “physically-alike” stars, and their relation to cosmology.

Thus my viewpoint here is that contemporary stellar taxonomy must begin with the Fontenelle orientation: it must first seek to define what are “physically-alike” stars, from both individual and statistical studies; then proceed to statistical studies of the cosmological properties of such like stars. Our discussions in Chapters 3, 4, and 5 give at least preliminary definitions of “like” stellar atmospheres; and they give some idea of the occurrence of “thermodynamically-alike” stars across the HR plane. “Thermodynamically-alike” has two levels: first, all stars appear to be (open, nonthermal) systems; second, there appear to be a variety of different atmospheric structural patterns, which reflect a variety of at least subatmospheric conditions. So, to the first level, *all* stars appear to be alike. To the second level, we introduce that kind of criterion of like stars which (closed, thermal) models imposed: all like stars have the same atmospheric structural pattern. “Physically-alike” represents the objective of the MK classes: like stars have the same atmospheric structural pattern, but in addition they have the same values for all the thermodynamic parameters of thermodynamic fluxes and their variability pattern, the same time-history if that turns out to be critical, the same mass and gravity, magnetic field, etc. Whether such “physically-alike” stars exist remains to be explored. So the goals of what should be a contemporary taxonomy are to explore stellar “aliqueness” to each of these three levels—and then the cosmology of such stars, to each level. At the third level, we see we join that common preoccupation with the biologists mentioned in the Foreword: are there indeed Platonian prototype stars, or are all stars individual at this most detailed level?

But I have continually stressed that we have identified distinctive atmospheric regions, and sequences of regions—thus atmospheric structural patterns—only up to the limit of our present empirical-theoretical knowledge. We must admit that these categories can be enlarged, or reduced, tomorrow, by new data. At the moment, we have no global thermodynamic framework which gives us confidence that our delineation is in any way definitive. So, the above taxonomic investigations must be viewed as maybe refining—at least verifying—our definitions of alikeness, in its several degrees. I make this more explicit, in forecasting programs for this contemporary taxonomy.

A. CLASSIFICATION ACCORDING TO PHOTOSPHERIC CHARACTERISTICS

The original goal of stellar taxonomy was to distinguish types of *stars*. It rapidly became a classification of *stellar atmospheres*; essentially, of *stellar photospheres* as fluorescing screens, for visual spectrophotometry. The range in variety focused on the radiative flux: on the change in values of two thermodynamic parameters—total stellar energy produced, stellar radius. Our present focus includes this one on the thermal radiative properties of the photosphere, but also includes four others: all nonthermal; all excluded by the standard model; all are no longer peculiar, just representative of different subatmospheric conditions, which we want to infer. The most striking broad division of photospheres is into grossly nonthermal and quasi-thermal: the cataclysmic and pulsating stars emphasize the first. What we need is a systematic classification of this nonthermal category, especially of the phase-relations between visual and nonvisual kinematic, and time-dependent, features. This is critical for establishing the kind of boundary conditions we need; to distinguish between pulsation and impulsive-piston modeling. The β Ceph-type studies by Burger and de Jager; the modeling by Willson and Hill; these are the specific examples on which we need broader data to proceed. One needs statistical results, to establish what range of such border-line alternative, across the HR diagram, exists; to obtain insight into possible subatmospheric cause, and the range in variety of atmospheres which results.

A second broad division of photospheres grades smoothly into the first. It distinguishes those photospheres associated, and not associated, with transmitting a variable nonradiative energy flux. It appears that all photospheres, at some epoch, transmit a nonradiative energy flux. We have stressed the progression between the maybe-stochastic, high-order nonradial, oscillations in solar-like atmospheres which provide a continuous source of nonradiative heating; through the phase-dependent nonradiative heating of the ordered, spherical-pulsations of cepheid-like atmospheres; to the classical novae, exhibiting a shell-ejection which evolves as simple, nondissipative, expansion for a large radial distance. Individually, one would like to delineate the intermediate varieties of this progression. Statistically, one searches distribution of types in relation to any other stellar and cosmological properties.

The third broad division of photospheres raises the same question as does the second division, but relative to the mass-flux. It focuses on those stars which do, and those which do not, exhibit some variety of LSE. We are interested both in the variety of LSE as well as their presence. Re the former, the distinction between emission-phases, and shell-phases, in all varieties of stars is something which must be broadly explored: again, both individually and statistically. The distinction between the classical, Struve, use of shell; and the one we have also used in discussing ionization shells and multiple velocity components; must be better delineated: individually and statistically. It is true of all these categories that only visual studies, unlinked to simultaneous studies in other spectral regions, are frustratingly-incomplete. But this is especially true in delineating the transition between chromosphere-corona and cool, LSE shells.

Finally, the fourth kind of distinction between varieties of photospheres associates closely to the preceding, and exemplifies the gradualness property: photospheres which are, and those which are not, significantly veiled by the exophotospheric regions. Gradualness stands out, because from Chapter 3 we have seen the different degrees to which such veiling is acknowledged, or is neglected. Kuhl's T Tauri studies, in which he shifted the usual taxonomic region to include the nearIR and H α , stand out. They shift the "normal" T Tauri star to a K-type photosphere rather than that earlier-believed, closer to F–G. Such a result focuses also on the problem we have stressed of the "quiet-phase" spectral type of the cataclysmic stars—and also of the cepheids. Is the quiet phase, radiative-energy characterized, photosphere "red" or "blue"? The latter is associated with the central stars of PN, folklorically-originating in the ejection of the outer layers of a red giant. It is also associated with the quiet, nonepisodic-ejection phases of

ordinary novae. "Red" is associated with the quiet phases of these cataclysmic stars with episodes more frequent than the "l-ejection" novae and PN. But we also see "B, Be-star, blue-star" characteristics of quiet phases of some cepheids, some dwarf-novae. We should expect "red"-phases of stars heavily enveloped by an LSE, independently of their photospheric properties; we would however like to know what these are. Probably, the greatest service a contemporary taxonomy could accomplish is precisely that which was the objective of historical taxonomy: delineate the photospheric, radiative-flux, characteristics of the star. But, such delineation must be done in full consciousness of its veiling-phase observational dependence; and in full openness to investigate, not to prejudge, how much of the "symbiotic" change in spectrum between quiet and active phases comes from multiple-star, and from multi-regional atmosphere, characteristics.

B. CLASSIFICATION ACCORDING TO EXOPHOTOSPHERIC CHARACTERISTICS

The basic difference between this and classification according to photospheric characteristics rests on the exophotosphere being fundamentally discordant with standard modeling. So, there is no possibility of adopting classical taxonomy, especially based on MK classes. We have already discussed the properties of peculiarity in visual and non-visual spectral regions, and their relations to exophotospheric structure; so we need not repeat a list of characteristic parameters to be used in statistical/classification studies. And, we have discussed the additional reinforcement of stellar peculiarity which new observing regions, such as the X-rays, give. One cannot predict, or even classify, exophotospheric characteristics simply from photospheric taxonomy. Like photospheric, and visual spectral, taxonomy, exophotospheric and nonvisual is a physical as well as statistical taxonomy. Its basic goal is to search and establish what are "like" stars, to the several levels of likeness. Only then can we ask for statistical, and cosmological, properties of groups of like stars.

III. DIAGNOSTIC CONSIDERATIONS

In the context of stellar atmospheres, diagnostic studies have two aspects. One is that upon which we have mainly focused in this book: a gross diagnosis of the variety of thermodynamic fluxes from a star to infer the gross regional structure of a stellar atmosphere, and the individuality of that structure among various stars. A second variety of diagnostic studies focuses on applying the gross results of the first to details of particular stars. The utility of the standard model was that the first kind of diagnostic study was unnecessary: one presumed the atmospheric structure to be known; one focused on the second kind of study; its elaboration consisted of computing more numerically-detailed models. The results of such computations, applied to observations, presumably gave the composition and evolutionary phase of that star. Unfortunately, there were exhibited the peculiarities and anomalies upon which we have focused, which put into question the results obtained by focusing only upon the second kind of diagnostic studies. Abundance-differences, random nonthermal velocities, nonLTE effects were confused. Thermal instabilities, atmospheric structural uncertainties, and binarity were equally confused. Finally, the weight of evidence convinced all observers, and some speculative model-builders, that the first aspect of atmospheric diagnostics could no longer be ignored in applying the second aspect. The only question is how completely one sets aside diagnostics of the second kind, until one translates the results of gross diagnostics of the first kind into individual modeling. The Chapter 1 remarks are appropriate: no one waits for perfection.

My viewpoint is that at the moment, we should not give much weight to other than gross diagnostics of individual stars for their individual atmospheric structural pattern, until we have more detailed results from such diagnostics. Let me take a specific example, comparative diagnostics of ζ Oph, τ Sco, γ Cas. All these stars are about BO V: the first and last are Oe and Be, respectively. τ Sco exhibits no emission lines in the visual; negligible variability; and was the prototype B star for classical diagnostics, of the second kind, at the height of classical modeling, under the scheme of Unsold's masterful book (1938), which launched the education of many of us. Modern observations show, equally in all these stars, superionized lines up through O VI, and thermal X-rays; so all have chromospheres-coronae. All farUV superionized lines, in all the stars, are much broader than thermal; there are highly individual blue-shifts of these lines, as discussed in Chapter 3. So all these stars show significant mass-fluxes; the values quoted

by various authors overlap, among these stars, from the farUV data. But ζ Oph and γ Cas show H α -emission lines, and strong variability in shifts and components of the farUV lines, not shown by τ Sco. So the first two stars have an H α -emission envelope, and an LSE; τ Sco does not. The differential X-ray strengths confirm this diagnosis. But the mass-flux variability patterns differ strongly between ζ Oph and γ Cas. ζ Oph has the greater short-term variability; but shows lesser relation between H α and farUV variability. On the basis of its harder X-ray pattern, γ Cas has been called binary; there is no other confirming evidence for such. Clearly, we have grossly diagnosed the differential atmospheric structural patterns of these three stars, according to the distinct characters of regions and sequences set up in Chapters 4 and 5, about as far as we can go at the moment. We can try to make detailed distributions of U , n_{H} , T_e and then compute details of ionization distribution; an essential prerequisite is evaluation of the several time-scales over which changes in these distributions occur. At the moment, it hardly seems productive; our main focus lies on trying, observationally, to establish just what these variability patterns are, and how they are linked to variability in the several fluxes—to even gross degree. One can repeat all these details, and conclusions, for the wide variety of stars now under study. Detailed proto-patterns have not yet emerged.

Thus, diagnostically, it seems that our goals, at the moment, should be mapping out gross structure, to the above level, for a variety of stars, following the kinds of regions and sequences thus far established. Parallel to the taxonomic studies, one tries, then, to characterize each star, on which sufficient details exist, according to the following diagnostic scheme.

A. CHARACTERISTICS OF PHOTOSPHERE

- (1) Its character of quasi-thermal or nonthermal, according to whether there have been epochs of $U(\text{photosphere}) \cong q$; and the characteristics of $U(r, t)$ in the photosphere according to systematic-outflow, oscillatory, ejective, or only small-amplitude random.
- (2) The history of luminosity-variability, and of inferred veiling effects by the exophotosphere on that part of the spectrum produced in the photosphere. One needs time-history studies to try to distinguish veiling effects of the LSE and the ISM. Symbiotic variability studies exhibit the same.
- (3) The relation of such effects as rotation, primaeval magnetic fields, etc. to storage modes in photosphere and subatmosphere—as inferred empirically-theoretically. The additional role of magnetic fields as transport-link between storage modes, like rotation, and chromospheric-coronal dissipation. At the moment, one should emphasize association over causality; trends, over correlations.

B. CHARACTERISTICS OF CHROMOSPHERE-CORONA

- (1) Its character of quasi-steady or variable; and the associated attempts to characterize the nonradiative heating source between quasi-stochastic and variable. Attempt to obtain detailed, time-dependent characteristics of the non-radiative heating.
- (2) The size of the mass-flux in that particular chromosphere-corona; hence beginning heights of chromosphere, lower-corona, upper-corona. Devise ways, including laboratory, to study the character of the transthermic flow in the lower-corona; and the effect on it of variability in both nonradiative heating and mass-flux.
- (3) The differential location of the escape-point; can it occur in a cooled post-corona; possibly in a never-very-hot corona?
- (4) The details of the post-thermal acceleration. Detailed study of that radiative acceleration resulting from chromosphere-corona presence; as a function of total C-C opacity, and size of source-function, in the farUV but especially at $\lambda < \text{LyC}$.

C. CHARACTERISTICS OF THE NONDECELERATED POSTCORONA

- (1) Distinction between stars exhibiting such to very great distances, such as Sun and many WR stars; and those terminating it far away, but still close enough to qualify as producing an LSE.

(2) The ionization/excitation state of such stars as a function of distance.

(2.a) In the lowest atmospheric regions, photospheric and subphotospheric as WR vs. Sun.

(2.b) In the outer regions, exemplified by the WR behavior. The contrast between the classical PN distribution of ionization; that of the novae; and that of the WR. Then, the perturbation introduced by the current, $\sim 10^3$ km/s), continuous flow in PN and novae.

(3) Exploring whether the absence of visual, low-ionization emission indicators such as H α , Fe II is indeed a general criterion for the absence of such postcoronal deceleration; hence, the absence of an LSE. Extending the Be–B star distinction to those sg which do, and those which do not, exhibit such H α -emission and variability should be productive, when detailed.

D. CHARACTERISTICS OF THE DECELERATED POSTCORONA

(1) More careful, and extensive, delineation of the various types of stars showing such deceleration, and the resulting LSE, is essential. We have grossly labeled them Be-similar, because of the combined aspects of H α -emission and variability; then used the cataclysmic stars to exhibit the two gross aspects of variability in mass-flux which seem to exist; then stressed the symbiotic stars as exhibiting the richest change in relative regional prominence. Photospheric consistency, as well as other, needs exploration.

(2) Much more detailed exploration of the various alternatives introduced by the relative mixtures of the episodic and continuous mass-flux variability. The difference in kinematic geometry between the Be-emission and Be-shell phases needs to be very much clarified: observationally, pictorially. Especially, the sometimes-precursor role of shell-production in marking the end of bright Be-phases needs exploration.

(3) All details of the shock(s) associated with the deceleration need exploration, especially diagnostically. A possible linkage of this second $T_e(\text{max})$ to the double gaussian representation of X-ray fluxes needs study. The rapid cooling which must be associated with such strong shocks demands careful instrumental considerations, for such diagnostics. Observational comparison of the Be and ordinary-novae extremes, for location of such shocks, should be productive. We have stressed the presence in novae, absence in Be stars, of the forbidden coronal lines—indicative of low-density and large emitting volumes in the region where they arise. This comparison closes on the questions raised above of stars where the postcoronal deceleration occurs far from the star itself.

(4) More basically, we must explore details of the distinction between sg and MS-e stars, and between B-absorption and Be-emission phases; as exemplified by the Bsg types Ia and Ib, and between τ Sco and (γ Cas, ζ Oph, 59 Cyg). The data are rich because the stars are bright; what lacks is sufficient simultaneous observations covering X-ray through radio regions.

(5) An absolutely crucial question is that stressed by Fig. 3-33, the value of $U(\text{max})$ in a given star, at a given epoch. Its actual value is the resultant of three factors: (i) the value of the post-thermal acceleration to the escape point—if it is radiative, then the value of the chromospheric-coronal radiation field, determined by the amount of nonradiative heating and the size of the mass-flux; (ii) the distance over which the deceleration operates, fixed by the time-history of the mass-flux variability that controls where the decelerating collision begins; (iii) the time-evolution of that collision-region. The observed value of $U(\text{max})$ is fixed by its actual value; by the atmospheric density where U reaches $U(\text{max})$, a low value inhibiting observation; by any LSE veiling, which can mask its observability. I emphasize: this question is absolutely crucial for estimating the kinetic-energy flux in the pre-LSE regions of the atmosphere; and the density-gradient within the LSE, hence the diagnosis of farIR and radio data.

E. CHARACTERISTICS OF THE LOCAL-STELLAR-ENVIRONMENT

(1) Above, we stressed the need for careful exploration of the range of stellar types showing a postcoronal deceleration of the mass-flow, hence an LSE. We need the same careful exploration of the phenomena attributed to an LSE.

(1.a) Phenomena of H α -emission; H α shell profiles; and Fe II, etc. shell profiles are unambiguous in defining an LSE. So are low-ionization/excitation forbidden lines. So are dust signatures.

(1.b) The prevalence of veiling by exophotospheric regions, to some degree, becomes more recognized. A separation of chromospheric-coronal veiling from that by the LSE is not difficult in the line-spectrum; nor is it in X-rays. $U(r)$ can be as important as $T_e(r)$ in diagnosing $F(\lambda)$ in the farUV and IR.

(1.c) There is nothing more thought-provoking than to find those narrow, undisplaced, lines of C IV used as ISM reference lines suddenly changing their depth and equivalent width by a factor of two, as 59 Cyg continues its evolution from B-abs phase to strong Be-emission. If, indeed, these pseudo-ISM lines are actually produced in the Be atmosphere rather than in the ISM, their location must be interior to the LSE. They are, indeed, pseudo-, not local-stellar environment. They represent an effect of the chromosphere-corona, either precorona or just in the postcoronal deceleration before sufficient cooling occurs to reach the LSE-proper. A decision between the alternatives is essential for diagnosing the complete superionized line-components.

IV. MODELING ASPECTS

One is ready to compute detailed models when he can specify precisely the detailed thermodynamic characteristics of the star and the equations, together with boundary and/or initial value conditions, which suffice to describe this thermodynamics. Generally, the equations are simplified or contracted in particular regions; but such simplification must be justified. At the moment, our empirical/theoretical analysis has established that all stars must be considered as (open, nonthermal) systems, which return fluxes of energy and mass to the ISM as they evolve toward greater concentration, and more organized structure, than the ISM has. If the system were Equilibrium, or linearly nonEquilibrium, at each stage, such evolution toward more organized concentration would violate the Second Law of Equilibrium Thermodynamics. However, the system is nonlinearly nonEquilibrium at each stage, especially in the transition regions between star and ISM; so entropy cannot be defined; and the evolution toward greater, organized, concentration violates nothing. We simply must be sure that the equations, and boundary or initial value conditions, reflect at each stage this nonlinearly nonEquilibrium structure and return of independent fluxes of mass and energy to the ISM; otherwise, the concentration-evolution, and stellar structure, is thermodynamically inconsistent.

Then we have seen that the equations must predict and describe the production of such mass and energy fluxes, and their action in producing the several distinctive regions and sequences of distinctive regions, which accomplish the transition from star to ISM, and which we observe and diagnose as the stellar atmosphere. The character of these fluxes, and the boundary or initial value conditions at the base of the atmosphere, are produced by the star as a whole—effectively its subatmospheric structure, taking into account the atmosphere as its outer transition layer. Thus, to actually predict flux-character and conditions at the atmosphere—subatmosphere interface, we would need to solve those equations describing an (open, nonthermal) structure for the immediate subatmosphere, possibly the whole interior. I have not seen even preliminary attempts at such, which include the transition region of the atmosphere as an upper boundary.

The classical, thermal, linear nonEquilibrium approach to stellar structure simplified the problem by divorcing interior and atmospheric solutions: the effect of the interior was to produce a radiative flux incident on the atmosphere; a subatmospheric outer radius; a gravity. The plane-parallel approximation to the thin atmosphere so generated needs only the radiative flux and gravity. Modern perturbation on this thermal system admits the nonthermal energy fluxes produced by the thermal instability of the hydrogen-helium ionization zones; but includes no generation of mass-fluxes linked to subatmospheric thermodynamic state.

We set aside linear modeling as uninteresting. Then we see that a corresponding approximation to modeling, by iteratively-separating interior and atmosphere solutions, can proceed at three levels, taking into account the material in Chapters 3, 4, and 5—which requires the existence of thermodynamically-similar regions, regional-sequences, and fluxes all across the HR plane.

At the least-structured level, we have seen that ionization-zones of abundant elements are unstable against the production of nonradiative energy fluxes, which propagate upward, eventually become nonlinear and dissipate, heating the atmosphere. We have also seen that all photospheres, in which radiation-pressure does not exceed gravity, are unstable against the production of an outward mass-flow. Thus, such a stochastic quasi-thermal photosphere and

subphotosphere can produce a heated mass-flux, which ends in mass-loss from the star. We can produce that regional sequence which terminates in a nondecelerated postcorona. All the necessary equations are in Chapter 4. There are two problems in the approach. First, there is no way to specify the amplitudes of nonradiative-energy and mass-fluxes, simply from that existence of instabilities shown by a linear stability analysis. The problem is well-discussed in the references of Chapter 3 on pulsational instability. Its presence is equally clear in our Chapter 4 discussion of the mass-flow instability. The original, acoustic-wave production of nonradiative energy for coronal heating in the Sun was based on linearized computations which break down under significant amplitudes for the generating mechanism. Second, we have already discussed those methods which try to remedy the inadequacy of specifying amplitudes from the generation mechanism for the instabilities. These are the approaches which try to use atmospheric conditions, divorced from the generation mechanism, to impose amplitudes. Parker's approach explicitly depends on an amplitude-specified nonradiative energy flux generation; and implicitly depends on the instability of the atmosphere against an outward mass-flow of unspecified amplitude. His imposed condition of identity of thermal and escape points then imposes a mass-flux amplitude. We have discussed its inadequacies; it sets only a lower-limit on the mass-flux. Thus, we can generate, and model, the outward evolution of a mass-flux, producing the simplest atmospheric regional sequence—*except* that we have no precise amplitudes for nonradiative energy and mass fluxes. By arbitrarily imposing these amplitudes, we make the model quantitative—and eliminate the need for such things as the Parker condition—but it is still basically stochastic in origin. It is not capable, physically, of introducing either variability—in energy or mass fluxes—or, in consequence, atmospheric sequences other than the simplest. It is also very marginal whether, even allowing for the chromospheric-coronal radiation field, it can cover the observed range from Sun to WR stars.

At an intermediate-structured level, one can replace the stochastic noise, or high-order nonradial pulsations, generation in the ionization zones by generating a spherical pulsation, according to the Cox and the Christy discussions referred to in Chapter 3. These nonlinear treatments result in a pulsation amplitude; but they do not include the transition-region consistency of a mass-loss. If one adjoins something like the Willson-Hill approach, one can—as abstracted there—produce a mass-flux whose properties depend on the pulsation properties. But self-consistency between the two sets of computations can only come iteratively. The amplitudes of the pulsation obtained under, e.g., the Christy approach result from that amplitude-limiting dissipation coming from radiative properties; chromospheric-coronal nonradiative dissipation, and mass-loss, are not included. Effectively for that reason, the Willson-Hill approach, and others like it abstracted in Chapter 3, replace the actual pulsation by a piston. As stressed, the problem is self-consistency; but under the approach, a choice of piston characteristics can introduce a variability, and individuality. Also, one can cover the whole range from strict periodicity to impulsive heating and ejection. In abstract, the basic origin of the nonthermal heating and mass-flow is still a thermal instability, in the ionization zone. One has simply devised amplitude-limiting, algorithmic processes for introducing, iteratively, amplitudes for these fluxes. A self-consistency among the iterations has yet to be attempted.

At the third level, one recognizes that if one really seeks nonthermal storage modes, instability-investigation of thermal storage modes is necessarily incomplete. One reduced the second level to specifying the properties of a piston, which forms the base of the atmosphere. One asks self-consistency of such properties by iteration with the subatmospheric instability. One could equally try to iterate self-consistency with a nonthermal configuration of the subatmosphere. Clearly, this is where the future lies. Our algorithms in preceding chapters essentially reduce to treating the outward evolution of the fluxes, and atmospheric regions, produced by such specification of piston properties. We have seen that they can represent the distinctive regions, and sequences of regions, provided the properties of the pistons are fixed observationally. So, at the moment, we can at most construct empirical, not theoretical, models. We can only focus on consistency, not cause. But, given the general presence of “peculiarity” under our present sophistication of causal modeling, this present, empirical, level is not bad, to satisfy curiosity of *what*, even if not yet *why*.

Let me summarize those aspects of atmospheric modeling which we can do at the moment, with some expectation that they have something to do with real stars, as we observe them. Wholly empirically-descriptively, we have summarized how we can identify the presence of certain distinctive atmospheric regions, arranged in one of several

types of distinctive sequences, in a particular star at a particular epoch: *if* we have sufficiently-broad spectral and temporal observational coverage. We have introduced various algorithmic approximations which produce gross estimates of U , T_e , n_H in at least many of these regions, for some types of sequences—i.e., some types of atmospheric structural patterns. Primarily, our algorithms suffice to treat those sequences including a quasi-thermal photosphere, where we can begin the model with something like the thermal photospheres modeled in Chapter 2, adjoining a mass-flux whose photospheric velocity is too small to perturb RE and HE, and a nonradiative energy flux which the photosphere only transmits. One major problem lies in understanding how to characterize the nonradiative flux other than wholly speculatively, hence arbitrarily-broad in possibilities. A second major problem lies in understanding how to represent $U(r)$ beyond the thermal point, especially beyond the escape point. A radiative acceleration seems the most promising one, in view of the similarity of $U(\max)$ across the HR diagram when we allow for the various obscuring features. However, the chromospheric-coronal radiation field must be included, and its uncertainty in value matches that in the nonradiative flux and LSE veiling. Then, in passing from nondecelerated to decelerated postcoronae, in this quasi-thermal photospheric sequence, we need a guide to some representation of mass-flux variability other than, again, proceeding wholly speculatively. The range of individuality among the Oe and Be stars exhibits how tantalizingly-close we are to seeing rough-patterns of such time-dependence, and how frustratingly-far we are in terms of being given sufficient observing time to complete such patterns in stars which are bright enough to be well-followed. The basic bottle-neck, of course, is the too-general belief that one-observation-inspiration, followed by computer-simulation, can somehow replace telescope-, and laboratory-, dedication. But until it is unclogged, a purely-theoretical modeling remains speculative, even for this simplest case. Present inadequacy in thermal photospheric modeling, which forms the beginning of this kind of exophotospheric modeling, has been summarized in Chapter 2.

It remains to construct similar algorithmic approaches to infer rough values of $U(r)$, $T_e(r)$, and $n_H(r)$ in those sequences where the photospheric members are not quasi-thermal. I cited the Pottasch-type models for impulsive-ejection photospheres; the Willson-Hill, for pulsating; simply as examples with which one might start. Clearly, these examples must be tied more intimately to the farUV data which do exist, and the X-ray and farIR + radio which begin to become extensive but have not been used in such modeling, in the sense of exploiting the symbiotic aspects.

The fascinating aspect, in such modeling, is of course those sequences—possibly those atmospheric regions—and atmospheric structural patterns which we have *not* identified. I think, however, from the theoretical-thermodynamic aspect, we have identified the major characterization of a star and its atmosphere: its being an (open, nonthermal) thermodynamic system, which is capable of a wide variety of configurations, diagnosable and classifiable by the variety of fluxes, including at least radiative and nonradiative energy, and mass—probably hydromagnetic. To say that we need to know the specific nonthermal configuration of atmosphere and subatmosphere for a complete modeling is insufficient; we need to know how to set about gaining such knowledge. It's a hope, rather than a certainty, that such flux-diagnostics will specify these subatmospheric modes. We'll see how it progresses with the current intensive efforts on the solar subphotospheric, photospheric, and chromospheric pulsational-mode studies; and attempts at intensive efforts on the Be-star exophotospheric modes.

Page intentionally left blank

Page intentionally left blank

APPENDIX

A. MANNER OF DESCRIPTION OF A CONCENTRATION OF MATTER AND ENERGY:

We interpret a star as a quasiEquilibrium, evolving, local concentration of matter and energy in an environmental medium that is nonlinearly nonEquilibrium and parental. The medium is locally unstable against concentration, both because of gravitation and because of the nonEquilibrium occupation numbers of energy and matter states for its constituent particles, which gives it the “parental” character: *exothermic under concentration*. But globally, the medium is in a quasi*-statistically-steady-state, with an evolution whose time-scale is much larger than the evolutionary time-scale of the star. *Equilibrium* means *Thermodynamic Equilibrium*, as defined in the following Section B and in Volume 2; *quasiEquilibrium*, as defined in Section B and in Volume 2, requires, *locally*, Equilibrium statistical distribution functions for microscopic energy states (statistical individual states for photons and particles) in the *interior*, greatly-predominating, part of the concentration. Because such Equilibrium distribution functions arise from detailed-balance in local microscopic interactions between particles and photons, we explicitly assume that the overwhelming part of a stellar concentration of matter and energy can be described by configurations whose properties depend strongly on such local interactions—the more strongly, the more interior the point considered. An extreme example of a contrary kind of configuration is one where individual particles move under the gravitational field of the concentration as a whole, with only weak perturbations of such orbits by local interactions between individual particles; and where the internal energy state of the particle is fixed by the radiation field of the concentration as a whole, only weakly-modified by local collisional excitation of internal energy states. Such a contrary configuration *may* occur in the extreme outer stellar atmosphere, or in parts of the interstellar medium near a star.

We define a configuration to be *thermally-controlled* when its *local* state is everywhere wholly determined by local, uncorrelated, microscopic interactions between particles and photons: we define in this situation the modes of storage of matter and energy to be *wholly thermal*. The limiting example of such a thermal configuration is the isolated, homogeneous concentration in an Equilibrium state, on which the only boundary condition is its *isolation*. When, on the contrary, the local configuration and the local storage modes also depend upon *correlated* interactions between particles and photons, under the influence of nonlocal macroscopic fields and boundary conditions, the concentration is defined to have also *nonthermal* modes of storage of matter and energy, and the configuration is not thermally-controlled. In this case, it *may* be possible to describe the *local* state of the configuration by a combination of: (A) *a set of statistical distribution functions for microscopic quantities*, that gives (A.i) the location and (A.ii) the statistical occupation-numbers of the local microscopic states of matter and energy; and (B) *a thermodynamic specification of a set of macroscopic states of matter and energy* that gives (B.i) the local modes of storage and (B.ii) the local amplitudes of storage. The former, (A), are called thermal; the latter, (B), are called nonthermal.[†]

*quasi-: because it is itself slowly evolving in its role as the “atmosphere” of the next-larger-concentration—the galaxy—in the hierarchy of concentrations that form the set of objects in the universe.

[†]e.g., nonthermal kinetic energy modes such as pulsation, convection; nonthermal macromolecular modes such as proteins.

Such a combined statistical and thermodynamical description must give these micro- and macro-scopic states of matter and energy as functions of position, time, and of the particular concentration and environment. Thus a proper set of boundary conditions specifying the transition between concentration and environment is essential. In this situation, we infer and measure structure and evolution of the concentration by means of the nonzero space-fluxes between concentration and environment (which includes the observer). Such space-fluxes arise, essentially, by: the departure from a homogeneous spatial distribution of statistical, Equilibrium, microscopic, distribution functions (thermal diffusive fluxes); the departure from Equilibrium forms for these statistical distribution functions (non-linear thermal fluxes); and by the existence of thermodynamic, macroscopic, nonthermal, storage modes (non-thermal fluxes).

I stress the distinction between, and the necessity for the combined use of: a *statistical* description of local, microscopic, thermal storage modes; and a *thermodynamic* specification of local, macroscopic, nonthermal storage modes as a part of a global *thermodynamic* specification of the distribution over the whole concentration of those state parameters which specify each of these storage modes, by means of the proper boundary conditions on the concentration-environment transition. *Statistical* description and *thermodynamic* specification are equivalent *only* in the degenerate Equilibrium configuration, where the statistical distribution functions have a universal form independent of matter and energy stored, and where the three macroscopic storage parameters of total mass, total energy, total volume suffice to specify microscopic occupation numbers or macroscopic thermodynamic state, the two being equivalent, there being no nonthermal storage modes. Only in this Equilibrium configuration does the expression "statistical thermodynamics" have meaning. In all other configurations, we must distinguish carefully between *thermodynamic* and *statistical*, including also the distinction between these and *stochastic*:

By a *thermodynamic* description of an *object*, we mean a description of the *whole object*, viewed as an entity, complete with a set of boundary conditions that describe the transition-interaction between object and its environment. A *local* thermodynamic description of a part, or a region, of the object can only be presented as a part of the thermodynamic description of the whole object: one must choose carefully the boundary-transition conditions to link whole and part. To attempt a thermodynamic description whose objective is to isolate some part of the object from the object as a whole can only lead to anomaly. One example would be an attempt to describe structure and function of the foot of an animal in isolation from the animal. Another example lies in the first attempts, by Emden, to model stars as *isolated* gas-spheres, having neither internal energy sources, nor fluxes to the environment. No matter that the structure of the deep interior differs by only small factors—in temperature, pressure, density—from more complete models: the representation of those parts of the star which we observe had no relation to reality. The same negative result holds for models which a priori and arbitrarily suppress thermodynamic nonthermal modes, whose presence would lead to significant nonthermal mass-fluxes, in favor of imposing strictly thermal modes, which lead to only insignificant (observationally) mass-fluxes, and thus anomaly between model and observations.

By a *statistical* description of particles and photons by microscopic distribution functions, we mean a *local* set of such distribution functions, whose forms and parameters depend both upon local particle and photon interactions, *and* upon the *local* values of "fields" of possibly nonlocal origin (e.g., gravity, radiation). Hopefully, to specify such statistical distribution functions, one can find a set of parameters less numerous than those required to simply tabulate, numerically, each microscopic energy level and statistical occupation number. Then we carefully distinguish between the values of these "distribution-function parameters" (DFP), and the range in values for energy states and occupation numbers permitted by the distribution functions for given values of their "DFP."

Statistical, for distribution functions, refers simply to the range in values of energy states and occupation numbers—relative to their isolated single-particle values, under given values for the DFP. For example, a gaussian statistical distribution function for thermal velocities gives us a certain "breadth and distribution of amplitude" of (statistical) atomic absorption coefficient because of Doppler effect alone. But such statistical distribution functions do not exhibit random variations in space and time coming from the microscopic nature of the particles and photons to which they refer: there is no "stochastic" behavior.

A *stochastic* function is generally defined as a *randomly-varying* function: one whose value is fixed by probability considerations quite apart from the problem of interest. The classic example is Brownian motion: where one studies the trajectory of a micro-object in some solution, subject to both exterior fields and to the random-thermal collisions by the particles in the medium. Another, better, example, is the motion of a star under the galactic gravitational field, perturbed by random gravitational encounters with other stars, these chance encounters originating from a random distribution of stellar orbits.

Thus we must carefully distinguish between local range and amplitude of thermal energy states coming from the *statistical* superposition of the properties of the local concentration of particles, and any *stochastic* behavior of the DFP, of whatever origin.

In summary: the basis of the frequent identification of *whole-object thermodynamics* with *local statistical physics* lies in the identification of *Equilibrium* thermodynamics with *Equilibrium* statistical physics; in the degenerate Equilibrium configuration of homogeneity and isolation. To identify thermodynamics with Equilibrium thermodynamics is to infinitesimalize the range of its scope. Interaction between either different systems, or inhomogeneous parts of one system, are not considered in Equilibrium thermodynamics: only the combination of different (homogeneous) Equilibrium systems into one larger (homogeneous) Equilibrium system. The properties of such combinations have been vulgarized into the so-called “laws of thermodynamics:” actually, of *Equilibrium* thermodynamics, not thermodynamics in its broad sense, to which the famed “irreversible trend toward *disorganization*” of the Second Law is inapplicable. On the contrary, our present interests lie in just the trend toward *greater organization*, which characterizes the *evolution* of a star from its parental medium (and, in precisely the same way, *evolution* and *Evolution* of biological systems). And in precisely this question of irreversibility, we must distinguish between pseudo-stochastic explanations such as “a process appears irreversible (or reversible) according as the initial state recurs in long (or short) time relative to that during which the process is studied,”* and an actual irreversibility corresponding to degradation of nonthermal modes into thermal (Chapters 2 and 3). (cf Volume 2.)

B. LANGUAGE AND TERMINOLOGY:

The state of a concentration of matter and energy—which we sometimes call the *ensemble* or the *system*—is the totality of all the statistical distribution functions and thermodynamic storage modes which are necessary to describe that concentration. The *state-parameters* are then those parameters necessary and sufficient to specify these distribution functions and storage modes: the *location* of energy and matter modes, and their *populations* or *amplitudes*. Clearly, there may be a number of equivalent sets of state-parameters; we are always seeking the minimal sets, simply for convenience. If the concentration is indeed isolated and homogeneous, we can discuss the state of the concentration as a whole; otherwise, we discuss the *local* (in space, in time) state. We see that the parameters specifying the occupation numbers and amplitudes of the states of matter and energy can themselves be state-parameters; we usually hope that a lesser set suffices. In addition, we recognize that while single-particle states in a diffuse concentration are usually known a priori, sometimes in the more general case the states themselves may be functions of the configuration; so that in a broad sense, the state-parameters must also include those necessary to specify what are the states of matter and energy. In any given context, we must be careful to specify in which sense “state-parameter” is used: to specify location, or population/amplitude, of states. There is a further, but slight, ambiguity in distinguishing the state of a single particle from the state of the concentration; but the distinction is usually quite clear, at least if the following is kept in mind.

So we now delineate certain limiting kinds of configurations: first, on *location* of states; second, on *occupation numbers* of states. We always use an astrophysical situation as specific example; but generalization is direct.

(1) *Location* of states:

By *matter-state* we mean the chemical element or elementary particle. The *location* of state is the kind of particle: the *occupation number*, their *concentration* (chemical abundance, in astrophysics). Then we define:

High-density astrophysics is that domain where the *matter-states* of the ensemble are functions of the configuration.

*cf the discussion by Chandrasekhar and von Neumann, from which this remark is quoted (1943).

High-energy astrophysics is that domain where *occupation numbers* of *matter states* are functions of the configuration.

Low-density, low-energy astrophysics is that domain where neither the matter-states, nor their occupation numbers, are functions of the configuration, both being a priori specified. The stellar atmosphere and the stellar environment fall into this domain.

By *energy-state* we mean the combination of internal energy states for a single particle, its kinetic energy, energy modes of the ensemble as a whole and energy in any externally-applied fields. Then we define:

Single-particle astrophysics is that domain where the microscopic energy states themselves are not functions of the configuration.

Many-body effects refer to changes in single-particle energy levels induced by the presence of other particles; rigorously, the energy levels of the system as a whole should be computed, not those of the single-particles.

Gaseous astrophysics is that domain where it suffices, to some “adequate” degree of approximation, to compute any departure from single-particle energy states as a perturbation by many-body effects. Macroscopic energy states however characterize the gas as a whole. The atmosphere and its environment *usually* fall into this category; an exception is the presence of dust particles.

Solid-liquid astrophysics is that domain where the microscopic energy states characterize (some part of) the ensemble (locally) as a whole.

(2) *Occupation numbers* of states (and limitation on the fluxes which may affect their values):

By adiabatic isolation of two energy or matter states (either of a single particle or of an ensemble) from each other, we mean no flux of energy or matter between the states. By adiabatic isolation of two ensembles from each other, we mean no direct fluxes of energy or matter between them. Any mutually-compensating gain or loss of energy within the ensemble composed of the two ensembles must be associated with *change in position* of the “walls” enclosing them. An *adiabatic wall* is the manner, or instrument, by which such isolation is effected. Any other kind of wall is called a *diabatic* wall. A particular kind of diabatic wall that permits an energy, but not a matter, flux is called a *diathermic* wall.

By a *steady-state* configuration, we mean that the state of an ensemble which can be described wholly by macroscopic state parameters—locally or as a whole—does not change in time. By *statistically-steady-state*, we mean that the state of the ensemble requires at least some microscopic state-parameters, and that the time-averages of the various occupation numbers of all states—microscopic and macroscopic—do not change in time. Often times, *equilibrium* is used to describe either steady-state or statistically-steady-state; we carefully distinguish in the following between *Equilibrium*, *equilibrium*, and steady-state or statistically-steady-state.

By a *Thermodynamic Equilibrium*, or *Equilibrium*, configuration of an ensemble, we mean that the ensemble: (i) is adiabatically isolated from the rest of the Universe and can be described wholly by a set of macroscopic state-parameters, called the *Thermodynamic Equilibrium (TE)* set of state-parameters; (ii) is in a steady-state; (iii) is homogeneous with respect to the location and populations of local matter and energy states, which are wholly thermal.

By a *local TE* configuration, we mean that there exist a set of TE-state-parameters which suffice to describe *all* local microscopic distribution functions, and that these distribution functions have, locally, the same functional forms that they would have if the local conditions were homogeneous throughout the ensemble. We denote this configuration by “locTE” or “extreme LTE.”

By adiabatic macroscopic distribution functions, hence adiabatic nonthermal modes of concentration, or storage, for matter and energy, we mean those which do not introduce a departure from locTE microscopic distribution functions.

By a *linear* nonEquilibrium configuration, we mean: that *most* microscopic distribution functions have forms which are independent of the local fluxes of matter and energy, and are locally described by TE state-parameters; all fluxes within the ensemble are *linear*—which means that state-fluxes between microscopic states can be neglected, state-fluxes between macro- and micro-scopic distribution functions can be described by macroscopic parameters alone, and each space-flux can be represented as the space-gradient of some macroscopic parameter; those macroscopic state-parameters needed in addition to the thermodynamic Equilibrium ones are determined by the non-thermal storage modes required to describe the concentration—if no such additional macroscopic state-parameters are needed, we say the storage modes are only *thermal*.

By quasi-adiabatic macroscopic distribution functions, and storage modes, we mean those which do not introduce a departure from a linear nonEquilibrium configuration.

By a quasi-Equilibrium concentration we mean: at any moment, we can compute, to some adequate degree of approximation, its configuration as though it did not change in time; that for all parts of the concentration, *except* for some transition-zone to the environment, the configuration is linear nonEquilibrium, except for some limited set of microscopic distribution functions whose very slow evolution is exothermic. This last set of distribution functions we refer to as “frozen-in.”

We conclude empirically, for the astrophysical situation—and we conjecture, for the biological situation—that possibly, apart from an initial phase (gravitational condensation for astrophysics), it is the evolution of these frozen-in degrees of freedom which conditions the evolution of astronomical concentrations, hence the “local” evolution of the Universe.

By a *nonlinear* nonEquilibrium configuration, we mean: that the above linear conditions are not satisfied; in the extreme limit, wholly microscopic state-parameters are required, local fluxes are comparable in size with local concentration or storage, and local fluctuation in such distribution functions (in space, in time) are comparable to the storage quantities. Hopefully, we do not often need to treat this extreme limit.

By the transition-zone between a quasiEquilibrium concentration and the ambient medium within which it arose, we mean that outer part of the concentration where the local state evolves, in space, from linear nonEquilibrium to whatever is the statistically-steady-state configuration of the ambient medium. It is of course not necessary that every concentration be quasiEquilibrium nor that every medium be locally statistically-steady-state; so not every concentration has a transition-zone in the defined sense. So, the idea of a transition-zone as we use it here must be extended, eventually. The same applies, of course, to a concentration introduced into an “alien” medium—e.g., a solid ablating because of its high-velocity motion through a gas can have one kind of a “transition-zone.” The “boundary” between certain organic substances and their environment (“skin”) provides an interesting conjectural example. In the present book, however, we restrict attention to the transition-zone defined above.

Page intentionally left blank

Page intentionally left blank

REFERENCES

- Abbott, D. C., 1978, *Astrophys. J.*, **225**, 893.
- Abbott, D. C., 1980, *Astrophys. J.*, **242**, 1183.
- Abbott, D. C., 1982a, *Proc. IAU Symp. No. 99*, ed. C. de Loore and A. J. Willis (Dordrecht, Holland: Reidel), p. 185.
- Abbott, D. C., 1982b, *Astrophys. J.*, **263**, 723.
- Abbott, D. C., Biegging, J. H., and Churchwell, E., 1981, *Astrophys. J.*, **250**, 645.
- Allen, D. A., 1980, *Mon. Not. Roy. Astron. Soc.*, **192**, 521.
- Aller, L. H., 1943, *Astrophys. J.*, **97**, 135.
- Aller, L. H., 1953, 1st ed., 1963, 2nd ed., *The Atmospheres of the Sun and Stars* (New York: Ronald Press Co.).
- Aller, L. H., 1956, *Gaseous Nebulae* (London: Chapman and Hall).
- Aller, L. H., 1983, *The Planetary Nebulae*, in preparation.
- Altamore, A., Baratta, G. B., Cassatella, A., Friedjung, M., Giangrande, A., Ricciardi, O., and Viotti, R., 1981, *Astrophys. J.*, **245**, 630.
- Arp, H. C., 1956, *Astron. J.*, **61**, 15.
- Athay, R. G., 1961, in *Physics of the Solar Chromosphere*, R. N. Thomas and R. G. Athay (New York: John Wiley Co./Interscience Pub.).
- Athay, R. G., 1970, *Astrophys. J.*, **161**, 713.
- Athay, R., 1972, *Radiation Transport in Spectral Lines* (Dordrecht, Holland: Reidel).
- Athay, R., 1976, *The Solar Chromosphere and Corona: Quiet Sun* (Dordrecht, Holland: Reidel).
- Athay, R. G., Billings, D. E., Evans, J. W., and Roberts, W. O., 1954, *Astrophys. J.*, **120**, 94.
- Athay, R. G., Menzel, D. H., Pecker, J. C., and Thomas, R. N., 1955, *Astrophys. J.*, Supp. 1, 505.
- Athay, R., and Skumanich, A., 1967, *Ann. Astrophys.*, **30**, 669.
- Athay, R., and Skumanich, A., 1969, *Astrophys. J.*, **155**, 273.
- Athay, R. G., and Thomas, R. N., 1956a, *Astrophys. J.*, **123**, 299, 309.
- Athay, R. G., and Thomas, R. N., 1956b, *Astrophys. J.*, **124**, 586.
- Athay, R. G., and Thomas, R. N., 1957a, *Astrophys. J.*, **125**, 788.
- Athay, R. G., and Thomas, R. N., 1957b, *Astrophys. J.*, **125**, 804.
- Athay, R. G., and Thomas, R. N., 1958, *Astrophys. J.*, **127**, 96.
- Auer, L., and Mihalas, D., 1969a, *Astrophys. J.*, **156**, 157.
- Auer, L., and Mihalas, D., 1969b, *Astrophys. J.*, **156**, 681.
- Auer, L., and Mihalas, D., 1969c, *Astrophys. J.*, **158**, 641.
- Auer, L., and Mihalas, D., 1970, *Mon. Not. Roy. Astron. Soc.*, **149**, 65.
- Baker, J., and Menzel, D. H., 1938, *Astrophys. J.*, **88**, 52.
- Baker, J. G., Menzel, D. H., and Aller, L. H., 1938, *Astrophys. J.*, **88**, 422.
- Baliunas, S. L., Hartman, L., and Dupree, A. K., 1981, in *The First Two Years of IUE*, NASA CP-2171, p. 325.

- Bappu, M. K. V., and Sahade, J., ed. 1973, in *Wolf Rayet and High Temperature Stars, Proc. IAU Symp. No. 49* (Dordrecht, Holland: Reidel).
- Barker, P. K., 1979, Ph. D. Dissertation (Boulder: University of Colorado).
- Barlow, M. J., 1982, in *Wolf Rayet Stars, Observations, Physics, Evolution, Proc. IAU Symp. No. 99*, ed. C. de Loore and A. J. Willis (Dordrecht, Holland: Reidel), p. 149.
- Barlow, M. J., Blades, J. C., and Hummer, D. G., 1980, *Astrophys. J. (Letters)*, **241**, L27.
- Barlow, N. J., and Cohen, M., 1977, *Astrophys. J.*, **213**, 737.
- Beals, C. S., 1929, *Mon. Not. Roy. Astron. Soc.*, **90**, 202.
- Beals, C. S., 1930, *Pub. Dom. Astr. Obs.*, **4**, 294.
- Beals, C. S., 1938, *Colloque International d'Astrophysique*, College de France, Proc. Hermann et Cie 1941, Actualités Scientifiques et Industrielles, No. 901.
- Beals, C. S., 1951, *Pub. Dom. Astrophys. Obs. Victoria*, **9**, 1.
- Benvenuti, P., and Perinotto, M., 1980, in *The Second European IUE Conference*, ESA SP-157, p. 187.
- Bertout, C., 1982, in *The Third European IUE Conference*, ESA SP-176, p. 89.
- Bertout, C., and Thum, C., 1980, *Astron. Astrophys.*, **107**, 368.
- Biermann, L., 1946, *Naturwiss*, **33**, 118.
- Bijaoui, A., and Doazan, V., 1979, *Astron. Astrophys.*, **73**, 285.
- Blair, W. P., Stencel, R. E., Shaviv, G., and Feibelman, W. A., 1981, *Astron. Astrophys.*, **99**, 73.
- Blanco, C., Bruca, L., Catalano, S., and Marilli, E., 1982a, *Astron. Astrophys.*, **115**, 280.
- Blanco, C., Bruca, L., Catalano S., and Marilli, E., 1982b, in *The Third European IUE Conference*, ESA SP-176, p. 117.
- Blanco, C., Catalano, S., and Marilli, E., 1980, in *The Second European IUE Conference*, ESA SP-157, p. 63.
- Böhm K. H., 1960, in *Stellar Atmospheres*, ed. J. Greenstein (Chicago: University Chicago Press).
- Böhm-Vitense, E., 1954, *Z. Astrophys.*, **34**, 209.
- Böhm-Vitense, E., 1955, *Z. Astrophys.*, **36**, 145.
- Böhm-Vitense, E., and Dettmann, T., 1980, *Astrophys. J.*, **236**, 560.
- Boyartchuk, A. A., 1968, *Soviet Astr., A. J.*, **11**, 818.
- Brandt, J. C., 1970, *Introduction to the Solar Wind* (San Francisco: W. H. Freeman and Co.).
- Brown, A., Jordan, C., and Wilson, R., 1979, in *The First Year of IUE*, ed. A. J. Willis (London: University College London), p. 232.
- Burger, M., and de Jager, C., 1980, in *The Second European IUE Conference*, ESA SP-157, p. 47.
- Burger, M., de Jager, C., and Van den Oord, G. H. J., 1981, in *The Pulsating B Stars*, ed. GEVON and C. Sterken (Nice: Obs. Pub.), p. 181.
- Burgers, J. M., and Thomas, R. N., ed., 1957, in *Third Symp. on Cosmical Gas Dynamics, Proc. IAU Symp. No. 8, Rev. Mod. Phys.*, **30**, 905.
- Caccin, B., and Rigutti, M., ed., 1978, *Proc. of the 6th Course of the Advanced School of Astronomy "E Majorana"*, Erice 1976, *Mem. Soc. Astron. Italiana*, **48**.
- Cannon, C. J., 1983, *Textbook on Radiative Transfer* (Cambridge University Press), in press.
- Cannon, C. J., Thomas, R. N., 1975, in *20 Colloq. Int. Astrophys.*, (Liège, Belgium: Université de Liège), p. 231.
- Cannon, C. J., and Thomas R. N., 1977, *Astrophys. J.*, **211**, 910.
- Capriotti, E. R., 1978, in *Planetary Nebulae, Observation and Theory, Proc. IAU Symp. No. 76*, ed. Y. Terzian (Dordrecht, Holland: Reidel), p. 263.
- Cassatella, A., Clavel, J., Gilra, D., Reimers, D., and Stickland, D. J., 1980, in *The Second European IUE Conference*, ESA SP-157, p. 233.
- Cassatella, A., Patriarchi, P., Selvelli, P. L., Bianchi, L., Cacciari, C., Heck, A., Perryman, M., and Wamsteker, W., 1982, in *The Third European IUE Conference*, ESA SP-176, p. 229.

- Cassinelli, J. P., 1979, *Ann. Rev. Astron. Astrophys.*, **17**, 275.
- Cassinelli, J. P., and Abbott, D. C., 1981, in *The First Two Years of IUE*, NASA CP-2171, p. 127.
- Cassinelli, J. P., and Mac Gregor, K. B., 1983, in *Stellar Chromospheres, Coronae and Winds*, preprint.
- Cassinelli, J. P., Mathis, J. S., and Savage, B. D., 1981, *Science*, **212**, 1497.
- Castor, J. I., 1979, in *Mass Loss and Evolution of O Stars*, *Proc. IAU Symp. No. 83*, ed. P. S. Conti and C. de Loore, (Dordrecht, Holland: Reidel), p. 175.
- Castor, J. I., Abbott, D. C., and Klein, R. I., 1975, *Astrophys. J.*, **195**, 157.
- Castor, J. I., and Lamers, H. J. G. L. M., 1979, *Astrophys. J. Supplement*, **39**, 481.
- Cayrel, R., 1963, *C. R. Acad. Sci.*, Paris, **257**, 3309.
- Chamberlain, J., 1961, *Astrophys. J.*, **133**, 675.
- Chandrasekhar, S., 1934, *Mon. Not. Roy. Astron. Soc.*, **94**, 14, 522, 726.
- Chandrasekhar, S., 1958, *Astrophys. J.* **128**, 114.
- Chandrasekhar, S., 1960, *Radiative Transfer* (New York: Dover).
- Chandrasekhar, S., and Breen, F. H., 1946, *Astrophys. J.*, **104**, 430.
- Chandrasekhar, S., and Munch, G., 1946, *Astrophys. J.*, **104**, 446.
- Chapman, R. D., 1981, *Astrophys. J.*, **248**, 1043.
- Charters, A. C., and Thomas, R. N., 1945, *J. Aero. Sci.*, **12**, 468.
- Chavarría-K, C., 1981, *Astron. Astrophys.*, **101**, 105.
- Chiosi, C., and Stalio, R., (ed., 1981, *Effects of Mass Loss on Stellar Evolution*, *Proc. IAU Colloq. No. 59*, (Dordrecht, Holland: Reidel).
- Cillié, G. G., and Menzel, D. H., 1935, *Harvard Obs. Circ.*, No. 410.
- Cillié, G. G., Menzel, D. H., 1937, *Astrophys. J.*, **85**, 88.
- Cohen, M., 1980, *Mon. Not. Roy. Astron. Soc.*, **191**, 499.
- Cohen, M., Bieging, J. H., and Schwartz, P. R., 1982, *Astrophys. J.*, **253**, 707.
- Cohen, M., and Kuhl, L. V., 1979, *Astrophys. J., Supplement*, **41**, 743.
- Cohen, M., and Vogel, S. N., 1978, *Mon. Not. Roy. Astron. Soc.*, **185**, 47.
- Collins, G. W., 1970, in *Stellar Rotation*, *Proc. IAU Colloq. No. 4*, ed., A. Stettebak (Dordrecht, Holland: Reidel), p. 107.
- Collins, G. W., 1974, *Astrophys. J.*, **191**, 157.
- Conti, P. S., 1978, *Astron. Astrophys.*, **63**, 225.
- Conti, P. S., 1981, *Proc. IAU Colloq. No. 59*, ed. C. Chiosi and R. Stalio (Dordrecht, Holland: Reidel), p. 1.
- Conti, P. S., 1982, in *The Wolf-Rayet Stars*, *Proc. IAU Symp. No. 99*, ed. C. de Loore and A. J. Willis, (Dordrecht, Holland: Reidel), p. 1.
- Conti, P. S., and de Loore, C., ed., 1979, *Mass Loss and Evolution of O-type Stars*, *Proc. IAU Symp. No. 83*, (Dordrecht, Holland: Reidel).
- Conti, P. S., and Garmany, C. D., 1981, *Astrophys. J.*, **238**, 190.
- Conti, P. S., and Massey, P., 1981, *Astrophys. J.*, **249**, 471.
- Conti, P. S., Massey, P., and Garmany, C. D., 1982, preprint.
- Conti, P. S., and Underhill, A. B., 1985, *The O and WR Stars*, *Monograph Series on Nonthermal Phenomena in Stellar Atmospheres*, NASA-SP, in preparation.
- Cordova, F. A., and Mason, K. O., 1982, *Astrophys. J.*, **260**, 716.
- Cram, L. E., 1979, *Astrophys. J.*, **234**, 949.
- Cram, L. E., Giampapa, M. S., and Imhoff, C. L., 1980, *Astrophys. J.*, **238**, 905.
- Cram, L. E., Keil, S. L., and Ulmschneider, P., 1979, *Astrophys. J.*, **234**, 768.

- Cram, L. E., and Kuhi, L. V., 1984, in *Stellar Atmospheres, Monograph Series on Nonthermal Phenomena*, NASA-CNRS, to be published.
- Cox, J. P., 1965, in *The Fifth Symp. on Cosmical Gas Dynamics, IAU Symp. No. 28*, ed R. N. Thomas, (New York: Academic Press, (1967)), p. 8.
- Cox, J. P., 1980, *Theory of Stellar Pulsation*, (Princeton: Princeton University Press).
- Darius, J., Giddings, J. R., and Wilson, R., 1979, *The First Year of IUE*, NASA-ESA-SRC, p. 363.
- de Jager, C., 1958, *Mem. Soc. Roy. Sci.* (Liège, Belgium: Université de Liège), Ser. IV (20) 172.
- de Jager, C., 1980, *The Brightest Stars* (Dordrecht, Holland: Reidel).
- Deubner, F. L., 1981, in *The Sun as a Star, Monograph Series on Nonthermal Phenomena in Stellar Atmospheres*, ed. S. D. Jordan, NASA SP-450, p. 65.
- Deutsch, A. J., 1956, *Astrophys. J.*, **123**, 210.
- Deutsch, A. J., 1960, in *Stellar Atmospheres: Stars and Stellar Systems, Vol. VI*, ed. J. Greenstein (Chicago: University of Chicago Press), p. 543.
- Deutsch, A. J., 1961, in *The Fourth Symp. on Cosmical Gas Dynamics, Aerodynamic Phenomena in Stellar Atmospheres, IAU Symp. No. 12*, ed. R.N. Thomas, Varenna 1961, p. 238.
- Doazan, V., 1982, in *The B Stars With and Without Emission Lines, Monograph Series on Nonthermal Phenomena in Stellar Atmospheres*, ed. A. B. Underhill and V. Doazan, NASA SP-456.
- Doazan, V., 1983, private communication.
- Doazan, V., and Barylak, M., 1984, to be published.
- Doazan, V., Franco, M., Rusconi, G., Sedmak, G., and Stalio, R., 1983b, *Astron. Astrophys.*, in press.
- Doazan, V., Franco, M. L., Stalio, R., and Thomas, R. N., 1981, in *The Be Stars, IAU Symp. No. 98*, ed. M. Jaschek and H. Groth (Dordrecht, Holland: Reidel), p. 319.
- Doazan, V., Harmanec, P., Koubsky, P., Krpata, J., and Zdarsky, F., 1982a, *Astron. Astrophys. Supplement*, **50**, 481.
- Doazan, V., Harmanec, P., Koubsky, P., Krpata, J., and Zdarsky, F., 1982b, *Astron. Astrophys.*, **115**, 138.
- Doazan, V., Kuhi, L. V., and Thomas, R. N., 1980, *Astrophys. J. (Letters)*, **235**, L20.
- Doazan, V., Kuhi, L. V., Marlborough, J. M., Snow, T. P., and Thomas, R. N., 1980, in *The Second European IUE Conference*, ESA SP-157, p. 151.
- Doazan, V., Morossi, C., Stalio, R., Thomas, R. N., and Willis, A., 1983a, *Astron. Astrophys.*, in press.
- Doazan, V., and Thomas, R. N., 1982a, in *The Third European IUE Conference*, ESA SP-176, p. 287.
- Doazan, V., and Thomas, R. N., 1982b, in *The B Stars With and Without Emission Lines*, ed. A. B. Underhill and V. Doazan, NASA SP-456.
- Duerbeck, H. W., Klare, G., Krautter, J., Wolf, B., Seitter, W. C., and Wargau, W., 1980, in *The Second European IUE Conference*, ESA SP-157, p. 91.
- Dulcina-Hacyan, D., Andriolat, Y., Audouze, J., Friedjung, M., Gordon, C., and Rocca-Volmerange, B., 1980, in *The Second European IUE Conference*, ESA SP-157, p. 87.
- Dumont, S., and Heidmann, N., 1973, *Astron. Astrophys.*, **27**, 273.
- Dumont, S., Heidmann, N., Kuhi, L. V., and Thomas, R. N., 1973, *Astron. Astrophys.*, **29**, 199.
- Dupree, A. K., Black, J. H., Davis, R. J., Hartmann, L., and Raymond, J. C., 1979, in *The First Year of IUE*, ed. A. J. Willis (London: University College London), p. 217.
- Dyck, H. M., Simon, T., and Zuckerman, B., 1982, *Astrophys. J. (Letters)*, **255**, L103.
- Eddington, A., 1918, *Mon. Not. Roy. Astron. Soc.*, **79**, 2, 177.
- Eddington, A., 1926, *The Internal-Constitution of the Stars* (Cambridge, England: Cambridge University Press).
- Edlen, B., 1943, *Z Astrophys.*, **22**, 30.
- Edwards, S., 1979, *Pub. Astron. Soc. Pacific*, **91**, 329.
- Eichendorf, W., Reipurth, B., Caccin, B., Russo, G., and Sollazzo, C., 1982, in *The Third European IUE Conference*, ESA SP-176, p. 129.

- Elsasser, W. M., 1966, *Atom and Organism* (Princeton: Princeton University Press).
- Elsasser, W. M., 1975, *The Chief Abstractions of Biology* (North Holland and American Elsevier Publ.)
- Emden, R., 1907, *Gaskugeln* (Leipzig and Berlin: B. G. Teubner).
- Evans, T. L., 1968, *Mon. Not. Roy. Astron. Soc.*, **141**, 109.
- Evans, T. L., 1982, *Mon. Not. Roy. Astron. Soc.*, **199**, 925.
- Faraggiana, R., and Hack, M., 1981, in *The Second European IUE Conference*, ESA SP-157, p. 223.
- Feautrier, P., 1968, *Ann. Ap.*, **31**, 257.
- Feibelman, W. A., 1982, *Astrophys. J.*, **258**, 548.
- Feigelson, E., and DeCampli, W., 1981, *Astrophys. J. (Letters)*, **243**, L89.
- Fernie, J. D., 1980, *Astron. Astrophys.*, **87**, 227.
- Fischel, D., Lesh, J. R., and Sparks, W. M., ed., 1980, *Current Problems in Stellar Pulsation Instabilities*, NASA TM-80625.
- Fitzpatrick, E. L., Savage, B. D., and Sitko, M. L., 1982, *Astrophys. J.*, **256**, 578.
- Gahm, G. F., 1979, *IAU Report Commission 27*.
- Gahm, G. F., 1981, *The Universe at Ultraviolet Wavelengths, in The First Two Years of IUE*, NASA CP-2171, p. 105.
- Gallegher, J. S., and Starrfield, S. G., 1976, *Mon. Not. Roy. Astron. Soc.*, **176**, 53.
- Gallegher, J. S., and Starrfield, S. G., 1978, *Ann. Rev. Astron. Astrophys.*, **16**, 171.
- Garmany, C. D., 1983, in *Observational Basis for Stellar Atmosphere Velocity Fields*, ed. R. Stalio (Obs. Trieste Pub. 1983).
- Garmany, C. D., and Conti, P. S., 1982, in *The Wolf-Rayet Stars, IAU Symp. No. 99*, ed. C. de Loore and A. J. Willis (Dordrecht, Holland: Reidel), p. 105.
- Garrison, L. M., 1978, *Astrophys. J.*, **224**, 535.
- Garrison, L. M., and Anderson, C. M., 1977, *Astrophys. J.*, **218**, 438.
- Gauzit, J., 1955, *Ann. d'Ap.*, **18**, 354.
- Gebbie, K. B., and Steinitz, R., 1974, *Astrophys. J.*, **188**, 399.
- Gebbie, K. B., and Thomas, R. N., ed., 1968a, *The Wolf-Rayet Stars*, NBS SP-307.
- Gebbie, K. B., and Thomas, R. N., 1968b, *Astrophys. J.*, **154**, 271, 285.
- Gebbie, K. B., and Thomas, R. N., 1970, *Astrophys. J.*, **161**, 229.
- Gebbie, K. B., and Thomas, R. N., 1971, *Astrophys. J.*, **168**, 461.
- Geltman, S., 1962, *Astrophys. J.*, **136**, 935.
- Gerasimovic, B. P., 1934, *Mon. Not. Roy. Astron. Soc.*, **94**, 737.
- GEVON and Sterken, C., 1981, *Proc. of the Workshop on Pulsating B Stars* (Nice Obs. Pub.).
- Giampapa, M. S., Calvet, N., Imhoff, C. L., and Kuhi, L. V., 1981, *Astrophys. J.*, **251**, 113.
- Glansdorff, P., and Prigogine, I., 1977, *Structure, Stabilité, et Fluctuations* (Paris: Masson).
- Goldberg, L., 1939, *Astrophys. J.*, **89**, 623.
- Goldberg, L., 1957, *Astrophys. J.*, **126**, 318.
- Goldberg, L., Hege, E. K., Hubbard, E. N., Strittmatter, P. A., and Cocke, W. J., 1982, *Workshop on Cool Stars, Stellar Systems and the Sun*, ed. M. S. Giampapa, L. Golub, Smithsonian Astrophys. Obs. SP 392, p. 131.
- Gordon, K. C., and Kron, G. E., 1943, *Astrophys. J.*, **97**, 311.
- Gray, D. F., and Linsky, J. L., ed., 1980, *Stellar Turbulence, IAU Colloq. No. 51*, Lecture Notes in Physics, Vol. 114 (Berlin: Springer-Verlag).
- Greenstein, J., ed., 1960, *Stellar Atmospheres* (Chicago: University of Chicago Press).
- Groth, H. G., 1957, *Zs. f. Ap.*, **43**, 185.

- Gulliver, A. F., 1977, *Astrophys. J. Supplement*, **35**, 441.
- Gurzadyan, G. A., 1970, *Planetary Nebulae*, (Dordrecht, Holland: Reidel), ed. D. G., Hummer.
- Habing, H., ed., 1970, *Sixth Symp. on Cosmical Gas Dynamics, Interstellar Gas Dynamics, IAU Symp. No. 39* (Dordrecht, Holland: Reidel).
- Hamann, W. R., 1981, *Astron. Astrophys.*, **93**, 353.
- Hamann, W. R., Gruschinske, J., Kudritzki, R. P., and Simon, K. P., 1981, *Astron. Astrophys.*, **104**, 249.
- Hammer, R., 1982a, *Astrophys. J.*, **259**, 767.
- Hammer, R., 1982b, *Astrophys. J.*, **259**, 779.
- Harrington, J. P., 1969, *Astrophys. J.*, **156**, 903.
- Harrington, J. P., 1970, *Astrophys. J.*, **162**, 913.
- Harrington, J. P., 1982, in *Advances in U.V. Astronomy: Four Years of IUE Research*, NASA CP-2238, p. 610.
- Hartmann, L., 1982, *Astrophys. J. Supplement*, **48**, 109.
- Hartmann, L., Dupree, A. K., and Raymond, J. C., 1980, *Astrophys. J. (Letters)*, **236**, L143.
- Hartmann, L., Dupree, A. K., and Raymond, J. C., 1981, *Astrophys. J.*, **246**, 193.
- Hartmann, L., and Mac Gregor, K. B., 1980, *Astrophys. J.*, **242**, 260.
- Harwit, M., 1981, *Physics Today*, **34**, 172.
- Hassal, B. J. M., Pringle, J. E., Wade, R. A., and Whelan, J. A. J., 1982, in *The Third European IUE Conference*, ESA SP-176, p. 179.
- Hearn, A. G., 1972, *Astron. Astrophys.*, **19**, 417.
- Hearn, A. G., 1973, *Astron. Astrophys.*, **23**, 97.
- Hearn, A. G., 1982, *Astron. Astrophys.*, **116**, 296.
- Hearn, A. G., and Vardavas, A. M., 1981, *Astron. Astrophys.*, **98**, 230, 241, 246.
- Heidman, N., and Thomas, R. N., 1980, *Astron. Astrophys.*, **87**, 36.
- Herbig, G., 1952, *Cont. Dominion Ap. Obs.*, **27**, 347.
- Herbig, G. H., 1960, *Astrophys. J. Supplement*, **4**, 337.
- Herbig, G. H., 1962, *Adv. Astron. and Astrophys.*, **1**, 47.
- Herbig, G. H., 1969, *16th Intl. Astrophysical Symp.* (Liège, Belgium: Université de Liège).
- Herbig, G. H., 1977, *Astrophys. J.*, **214**, 747.
- Hill, S. J., 1972, *Astrophys. J.*, **178**, 793.
- Hoyle, F., and Wilson, D. C., 1958, *Astrophys. J.*, **128**, 604.
- Hutchings, J. B., 1979, *Astrophys. J.*, **233**, 913.
- Hutchings, J. B., and von Rudolff, I. R., 1980, *Astrophys. J.*, **238**, 909.
- Jaschek, M., and Groth, H., ed., 1982, *The Be Stars, IAU Symp. No. 98*, (Dordrecht, Holland: Reidel).
- Jaschek, M., and Groth, H., ed., 1982, *The Be Stars*, Jaschek, C., 1980, *Astron. Astrophys. Supplement*, **42**, 103.
- Jefferies, J. T., 1968, *Spectral Line Formation* (Waltham, Massachusetts: Blaisdell).
- Jefferies, J., and Pottasch, S., 1959, *Ann. Astrophys.*, **22**, 318.
- Jefferies, J., and Thomas, R. N., 1958, *Astrophys. J.*, **127**, 667.
- Jockers, K., 1970, *Astron. Astrophys.*, **6**, 219.
- Jordan, C., de Ferraz, M. C., and Brown, A., 1982, in *The Third European IUE Conference*, ESA SP-176, p. 83.
- Jordan, S. D., ed., 1981, *The Sun as a Star, Monograph Series on Nonthermal Phenomena in Stellar Atmospheres*, NASA SP-450.
- Jordan, S. D., and Avrett, E. H., 1973, *Stellar Chromospheres*, NASA SP-317, Washington, D.C.
- Joy, A. H., 1945, *Astrophys. J.*, **102**, 168.
- Kitchin, C. R., 1982, *Early Type Emission-Line Stars* (Bristol: Helger).

- Klare, G., Krautter, J., Wolf, B., Stahl, O., Vogt, N., Wargau, W., and Rahe, J., 1982, *Astron. Astrophys.*, **113**, 76.
- Klinglesmith, D. A., 1971, *Models of Stellar Atmospheres*, NASA SP-3065.
- Kondo, Y., Modisette, J. L., Dufour, R. J., and Whaley, R. S., 1976, *Astrophys. J.*, **206**, 163.
- Kondo, Y., Morgan, T. H., and Modisette, J. L., 1977, *Pub. Astron. Soc. Pacific*, **89**, 675.
- Kopal, Z., 1946, *Astrophys. J.*, **103**, 310.
- Kopal, Z., and Shapley, M. B., 1946, *Astrophys. J.*, **104**, 160.
- Kourganoff, V., and Busbridge, I. W., 1952, *Basic Methods in Transfer Problems, Radiative Equilibrium and Neutron Diffusion* (Oxford: Clarendon Press).
- Kraft, R. P., 1958, *Astrophys. J.*, **127**, 625.
- Kraft, R. P., 1962, *Astrophys. J.*, **135**, 408.
- Kraft, R. P., 1964, *Astrophys. J.*, **139**, 457.
- Kraft, R. P., 1965a, *Astrophys. J.*, **142**, 681.
- Kraft, R. P., 1965b, in *The Fifth Symp. on Cosmical Gas Dynamics, IAU Symp. No. 28*, ed. R. N. Thomas (New York: Academic Press (1967)).
- Krautter, J., and Bastian, U., 1980, *Astron. Astrophys.*, **88**, L6.
- Krautter, J., Klare, G., Wolf, B., Duerbeck, H. W., Rahe, J., Vogt, N., and Wargau, W., 1981, *Astron. Astrophys.*, **102**, 337.
- Krook, M., 1955, *Astrophys. J.*, **122**, 488.
- Kudritski, R. P., Simon, K. P., Hamann, W. R., 1982, *Astron. Astrophys.*, **118**, 245.
- Kuhi, L. V., 1964, *Astrophys. J.*, **140**, 1409.
- Kuhi, L. V., 1968, in *The Wolf Rayet Stars*, ed. K. B. Gebbie and R. N. Thomas, NBS SP-307, 125.
- Kuhi, L. V., 1973, in *The Wolf Rayet and High-Temperature Stars, Proc. IAU Symp. No. 49*, ed. M. K. V. Bappu and J. Sahade (Dordrecht, Holland: Reidel).
- Kuhi, L. V., 1982, in *The Observational Basis of Stellar Velocity Fields, Trieste Workshop*, ed. R. Stalio (Obs. Trieste Pub. 1983).
- Kuhi, L. V., 1984, in Cram and Kuhi, 1984.
- Kurucz, R. L., 1979, *Astrophys. J. Supplement*, **40**, 1.
- Kwok, S., 1980, *J. Roy. Astron. Soc. Canada*, **74**, 216.
- Kwok, S., 1981, in *Effects of Mass Loss on Stellar Evolution, IAU Colloq. No. 59*, ed. C. Chiosi and R. Stalio (Dordrecht, Holland: Reidel), p. 347.
- Kwok, S., 1982a, *Astrophys. J.*, **258**, 280.
- Kwok, S., 1982b, *Sky and Telescope*, **63**, 449.
- Kwok, S., Purton, C. R., Fitzgerald, P. M., 1978, *Astrophys. J. (Letters)*, **219**, L125.
- La Dous, C., 1983, *Astron. Astrophys.*, in press.
- Lambert, D. L., and Pagel, B. E. J., 1968, *Mon. Not. Roy. Astron. Soc.*, **141**, 299.
- Lamers, H. J. G. L. M., 1980, *The First Two Years of IUE Conference*, NASA CP-2171, p. 93.
- Lamers, H. J. G. L. M., 1981, *Astrophys. J.*, **245**, 593.
- Lamers, H. J. G. L. M., Gathier, R., and Snow, T. P., 1982, *Astrophys. J.*, **258**, 186.
- Lamers, H. J. G. L. M., and Rogerson, J. B., 1975, *Nature*, **256**, 19.
- Lamers, H. J. G. L. M., and Rogerson, J. B., 1978, *Astron. Astrophys.*, **66**, 417.
- Lamers, H. J. G. L. M., and Snow, T. P., 1978, *Astrophys. J.*, **219**, 504.
- Landini, M., and Monignori-Fossi, B. C., 1973, *Astron. Astrophys.*, **25**, 9.
- Larson, R. B., 1972, *Mon. Not. Roy. Astron. Soc.*, **157**, 121.
- Ledoux, P., and Walraven, Th., 1958, in *Hb. D. Physik*, ed. S. Flugge (Berlin: Springer-Verlag) **51**, 353.
- Leibacher, J., 1981, in *The Sun as a Star, Monograph Series on Nonthermal Phenomena in Stellar Atmospheres*, ed. S. D. Jordan, NASA SP-450.

- Leibacher, J. W., and Stein, R. F., 1981, in *The Sun as a Star, Monograph Series on Nonthermal Phenomena in Stellar Atmospheres*, ed. S. D. Jordan, NASA SP-450, p. 263, 289.
- Lesh, J. R., 1968, *Astrophys. J. Supplement*, 17, 371.
- Lesh, J. R., 1981, in *Pulsating B Stars*, ed. GEVON and Sterken (Obs. Nice Pub.).
- Lesh, J. R., and Karp, A. H., 1977, *Veroff. Remeis. Sternw. Bamberg*, 11, 625.
- Limber, D. N., 1964, *Astrophys. J.*, 140, 1391.
- Limber, D. N., 1967, *Astrophys. J.*, 148, 141.
- Limber, D. N., 1969, *Astrophys. J.*, 157, 785.
- Linsky, J. L., 1977, in *The Solar Output and its Variations*, ed. O. R. White (Boulder: Colorado University Press), p. 477.
- Linsky, J. L., 1980, *Ann. Rev. Astron. Astrophys.*, 18, 439.
- Linsky, J. L., 1981, in *Solar Phenomena in Stars and Stellar Systems*, ed. R. M. Bonnet and A. K. Dupree, (Dordrecht, Holland: Reidel), p. 99.
- Linsky, J. L., and Avrett, E. H., 1970, *Pub. Astron. Soc. Pacific*, 82, 169.
- Linsky, J. L., and Haisch, B. M., 1979, *Astrophys. J. (Letters)*, 229, L27.
- Lloyds Evans, T., see Evans T. L.
- Lucy, L. B., 1982, *Astrophys. J.*, 255, 278, 286.
- Lucy, L. B., and Solomon, P. M., 1970, *Astrophys. J.*, 159, 879.
- Lucy, L. B., and White, R. L., 1980, *Astrophys. J.*, 241, 300.
- Lutz, J. H., 1978, in *Planetary Nebulae, Observations and Theory, IAU Symp. No. 76*, ed. Y. Terzian (Dordrecht, Holland: Reidel), p. 185.
- Machado, M. E., Avrett, E. H., Vernazza, J. E., and Noyes, R. W., 1980, *Astrophys. J.*, 242, 336.
- Madore, B., 1977, *Mon. Not. Roy. Astron. Soc.*, 178, 50.
- Madore, B., and Fernie, J. D., 1980, *Pub. Astron. Soc. Pacific*, 92, 315.
- Malina, R., Bowyer, S., and Basri, G., *Astrophys. J.*, 262, 717.
- Malle, L., 1982, Interview in Paris Herald Tribune.
- Mammano, A., and Ciatti, F., 1975, *Astron. Astrophys.*, 39, 405.
- Mariska, J. T., Doschek, G. A., and Feldman, U., 1980, *Astrophys. J.*, (Letters), 238, L87.
- Mariska, J. T., and Withbroe, G. L., 1978, *Solar Physics*, 60, 67.
- Marlborough, J. M., 1969, *Astrophys. J.*, 156, 135.
- Marlborough, J. M., 1970, *Astrophys. J.*, 159, 575.
- Marlborough, J. M., 1976, in *Be and Shell Stars, IAU Symp. No. 70*, ed. A. Slettebak (Dordrecht, Holland: Reidel), p. 335.
- Marlborough, J. M., and Snow, T. P., 1976, in *Be and Shell Stars, IAU Symp. No. 70*, ed. A. Slettebak (Dordrecht, Holland: Reidel), p. 179.
- Marlborough, J. M., Snow, T. P., and Slettebak, A., 1978, *Astrophys. J.*, 224, 157.
- Massey, P., Conti, P. S., and Niemela, V. S., 1981, *Astrophys. J.*, 246, 145.
- Mattei, J. A., 1978, *J. Roy. Astron. Soc. Canada*, 72, 61.
- Mayr, E., 1978, *Scientific American*, 239, 46, and Lectures at College de France, 1978.
- McCrea, W. H., 1929, *Mon. Not. Roy. Astron. Soc.*, 89, 718.
- McLaughlin, D. B., 1931, *Pub. Obs. Univ. Michigan*, 4, 198.
- McLaughlin, D. B., 1943, *Pub. Michigan Obs.*, Vol. 8, p. 187.
- McLaughlin, D. B., 1960, *Stars and Stellar Systems, VI, Stellar Atmospheres*, ed. J. L. Greenstein (Chicago: University of Chicago Press), p. 585.
- Mc Math, R. R., Mohler, O. C., Pierce, A. K., and Goldberg, L., 1956, *Astrophys. J.*, 124, 1.

- Menzel, D. H., 1929, *Pub. Astron. Soc. Pacific*, 41, 344.
- Menzel, D. H., 1937, *Astrophys. J.*, 85, 330.
- Menzel, D. H., 1947, A. Cressy Morrison Prize I, New York Academy of Sciences.
- Menzel, D. H., and Cillié, G. G., 1937, *Astrophys. J.*, 85, 88.
- Menzel, D. H., and Pekeris, C. L., 1935, *Mon. Not. Roy. Astron. Soc.*, 96, 77.
- Merrill, P. W., 1933, *Astrophys. J.*, 77, 44.
- Merrill, P. W., and Burwell, C. G., 1933, *Astrophys. J.*, 98, 153.
- Mewe, R., 1979, *Space Sci. Rev.*, 24, 101.
- Michalitsianos, A. G., Kafatos, M., and Hobbs, R. W., 1980, *Astrophys. J.*, 241, 774.
- Mihalas, D., 1970, *Stellar Atmospheres*, 1st ed., 1978, 2nd ed. (San Francisco: W. H. Freeman and Co.).
- Mihalas, D., 1974, Warner Prize Lecture, *Astron. J.*, 79, 1111.
- Mihalas, D., and Luecke, W., 1971, *Mon. Not. Roy. Astron. Soc.*, 153, 229.
- Milne, E. A., 1930, *Handbuch der Astrophysik*, Vol. 3, Chap. II (Berlin: Springer-Verlag).
- Miyamoto, S., 1947a, *Mem. Astrophys. Japan*, 1, 8.
- Miyamoto, S., 1947b, *Mem. College Sci. Kyoto University*, 25, 31.
- Miyamoto, S., 1949, *Jap. Astron.*, 1, 17.
- Miyamoto, S., 1950, *Astrophys. J.*, 113, 181.
- Miyamoto, S., 1952, *Pub. Astron. Soc. Japan*, 4, 1, 28.
- Miyamoto, S., 1953, *Z. Astrophys.*, 31, 282.
- Miyamoto, S., 1954a, *Pub. Astron. Soc. Japan*, 5, 142.
- Miyamoto, S., 1954b, *Pub. Astron. Soc. Japan*, 6, 103.
- Miyamoto, S., 1955, *Pub. Astron. Soc. Japan*, 7, 27.
- Miyamoto, S., 1958, *Pub. Astron. Soc. Japan*, 9, 146.
- Morton, D. C., 1967, *Astrophys. J.*, 147, 1017.
- Morton, D. C., and Widing, K. G., 1961, *Astrophys. J.*, 133, 596.
- Münch, G., 1950, *Astrophys. J.*, 112, 266.
- Nakada, M. P., Chapman, R. D., Neupert, W. M., and Thomas, R. J., 1976, *Sol. Phys.*, 47, 611.
- Newkirk, G., 1967, *Ann. Rev. Astron. Astrophys.*, 5, 213.
- Nicolis, G., and Prigogine, I., 1977, *Self-Organization in Non-Equilibrium Systems* (New York: John Wiley Co./Interscience).
- Niemela, V. S., 1973, *Pub. Astron. Soc. Pacific*, 85, 220.
- Noyes, R. W., and Kalkofen, W., 1971, *Solar Physics*, 15, 120.
- Nussbaumer, H., Schmutz, W., Smith, L. J., and Willis, A. J., 1982, *Astron. Astrophys. Supplement*, 47, 257.
- O'Dell, C. R., 1963, *Astrophys. J.*, 138, 1018.
- Oliversen, N. A., and Anderson, C. M., 1983, in *The Nature of Symbiotic Stars, IAU Colloq. No. 95*, ed. M. Friedjung and R. Viotti (Dordrecht, Holland: Reidel), p. 71.
- Osterbrock, D. E., 1964, *Ann. Rev. Astron. Astrophys.*, 2, 95.
- Osterbrock, D. E., 1974, *Astrophysics of Gaseous Nebulae* (San Francisco: Freeman).
- Osterbrock, D. E., and O'Dell, C. R., ed., 1968, *Planetary Nebulae, IAU Symp. No. 34* (Dordrecht, Holland: Reidel).
- Oxenius, J., 1970, *Naturforsch.*, 25a, 1302.
- Pallavacini, R., Golub, L., Rosner, R., Vaiana, S., Ayres, T., and Linsky, J. L., 1981, *Astrophys. J.*, 248, 279.
- Panagia, N., and Felli, M., 1975, *Astron. Astrophys.*, 39, 1.
- Pannekoek, A., 1930, *Mon. Not. Roy. Astron. Soc.*, 91, 139.
- Pannekoek, A., 1946, *Physica*, 12, 761.

- Paris Colloq. on Novae, *Wolf Rayet and P Cygni-Stars*, 1938, Conferences du College de France, 901 (Paris Hermann Pub. (1941)).
- Parker, E. N., 1958, *Astrophys. J.*, **128**, 664.
- Parker, E. N., 1963, *Interplanetary Dynamical Processes* (New York: John Wiley Co./Interscience).
- Parker, E. N., 1981, *Astrophys. J.*, **251**, 266.
- Parsons, S. B., 1980, *Astrophys. J.*, **239**, 555.
- Payne-Gaposchkin, C. H., 1930, *The Stars of High Luminosity* (New York: McGraw-Hill).
- Payne-Gaposchkin, C. H., 1957, *The Galactic Novae* (Amsterdam).
- Payne-Gaposchkin, C. H., 1977, *Astron. J.*, **82**, 665.
- Payne-Gaposchkin, C. H., 1978, *Ann. Rev. Astron. Astrophys.*, **16**, 1.
- Payne-Gaposchkin, C. H., and Gaposchkin, S., 1938, *Variable Stars, Harvard Observatory Monograph No. 5*, Cambridge, Massachusetts.
- Pecker, J. C., 1956, *Ann. Astrophys.*, **22**, 499 et seq.
- Peimbert, M., 1981, in *Physical Processes in Red Giants, Proc. of the 2nd Workshop of the Advanced School of Astronomy*, Erice, ed. I. Iben, Jr., and A. Renzini (Dordrecht, Holland: Reidel), p. 409.
- Perinotto, M., and Benvenuti, P., 1981, *Astron. Astrophys.*, **101**, 88.
- Perinotto, M., Benvenuti, P., and Cacciari, C., 1981, in *Effects of Mass Loss on Stellar Evolution, IAU Colloq. No. 59*, ed. C. Chiosi and R. Stalio (Dordrecht, Holland: Reidel), p. 45.
- Perinotto, M., Benvenuti, P., and Cerruti-Sola, M., 1982, *Astron. Astrophys.*, **108**, 314.
- Peters, G. J., 1976, in *Be and Shell Stars, Proc. IAU Symp. No. 70*, ed. A. Slettebak (Dordrecht, Holland: Reidel), p. 209.
- Peters, G. J., 1979, *Astrophys. J. Supplement*, **39**, 175.
- Peters, G. J., 1982, in *Advances in Ultraviolet Astronomy: Four Years of IUE Research*, NASA CP-2238, p. 575.
- Plaskett, H. H., 1928, *Pub. Dom. Astrophys. Obs. Victoria*, **4**, 119.
- Poeckert, R., 1980, *Pub. Dom. Astrophys. Obs.*, **15**, 357.
- Poeckert, R., 1982, in *The Be Stars, IAU Symp. No. 98*, ed. M. Jaschek and H. Groth (Dordrecht, Holland: Reidel), p. 453.
- Poeckert, R., and Duric, N., 1980, *Pub. Dom. Astrophys. Obs.*, **XV (7)**, 327.
- Poeckert R., and Marlborough, J. M., 1978a, *Astrophys. J.*, **220**, 940.
- Poeckert, R., and Marlborough, J. M., 1978b, *Astrophys. J. Supplement*, **38**, 229.
- Pottasch, S., 1958, *Bull. Astron. Neth.*, **14**, 29.
- Pottasch, S., 1959a, *Ann. Astrophys.*, **22**, p. 297.
- Pottasch, S., 1959b, *Ann. Astrophys.*, **22**, p. 310.
- Pottasch, S. R., 1983, *Planetary Nebulae*, in preparation.
- Pottasch, S. R., and Thomas, R. N., 1959, *Astrophys. J.*, **130**, 941.
- Pottasch, S. R., and Thomas, R. N., 1960, *Astrophys. J.*, **132**, 195.
- Prandtl, L., 1904, *Phys. Zs.*, **5**, 599.
- Preston, G. W., Smak, J., and Paczynski, B., 1965, *Astrophys. J. Supplement*, **12**, 99.
- Prigogine, I., 1965, *Introduction to the Thermodynamics of Irreversible Processes* (New York: John Wiley Co./Interscience, 2nd ed.).
- Querci, F., and Querci, M., 1979, Lectures, Summer School, Aussois, France.
- Querci, F., Querci, M., and Johnson, H. R., ed., 1984, *The M-Type Stars, Monograph Series on Nonthermal Phenomena in Stellar Atmospheres*, NASA SP, to be published.
- Redman, R. O., 1942, *Mon. Not. Roy. Astron. Soc.*, **102**, 134, 140.
- Reimers, D., 1973, *Astron. Astrophys.*, **24**, 79.

- Reimers, D., 1975, in *Problems in Stellar Atmospheres and Envelopes*, ed. B. Baschek (Berlin: Springer-Verlag), p. 229.
- Reimers, D., 1977a, *Astron. Astrophys.*, **54**, 485.
- Reimers, D., 1977b, *Astron. Astrophys.*, **57**, 395.
- Reimers, D., 1977c, *Astron. Astrophys.*, **61**, 217.
- Reimers, D., 1980, in *The Second IUE European Conference*, ESA SP-157, p. xxxiii.
- Renzini, A., 1981, in *Physical Processes in Red Giants*, Erice, 1980, ed. I. Iben, Jr., and A. Renzini (Dordrecht, Holland: Reidel), p. 431.
- Renzini, A., Cacciari, C., Ulmschneider, P., and Schmitz, F., 1977, *Astron. Astrophys.*, **61**, 39.
- Roberts, W. O., 1945, *Astrophys. J.*, **101**, 136.
- Robinson, E. L., 1976, *Ann. Rev. Astron. Astrophys.*, **14**, 119.
- Rosner, R., and Vaiana, G. S., 1979, in *Proc. of the Intl. School of Astrophys.*, ed. G. Sette and R. Giacconi (Erice).
- Rosseland, S., 1929, *Astrophys. J.*, **63**, 218.
- Rudkjøbing, M., 1947, *Pub. Mind. Medd. Kobenhavens Obs.*, No. 145.
- Russo, G., Sollazzo, C., and Coppola, M., 1981, *Astron. Astrophys.*, **102**, 20.
- Sahade, G., 1960, in *Stars and Stellar Systems, Vol VI, Stellar Atmospheres*, ed. J. L. Greenstein, (Chicago: University of Chicago Press).
- Sahade, G., 1976, *Mem. Soc. Roy. Sci.*, **IX** (Liège, Belgium: Université de Liège), p. 303.
- Sahade, G., 1980, in *The Wolf-Rayet Stars, College de France Lectures*, College de France Publication.
- Sahade, G., and Zorec, J., 1981, *Mem. Soc. Astron. Italiana*, **52**, 23.
- Saiko, M., 1970, *Pub. Astron. Soc. Japan*, **22**, 455.
- Saitko, K., 1970, *Ann. Tokyo Astron. Obs.*, **12**, Serie 2, 53.
- Scharmer, G. B., 1976, *Astron. Astrophys.*, **53**, 341.
- Schatzman, E., 1950, *Ann. Astrophys.*, **13**, 384.
- Schmelteko pf, A. E., Fehsenfeld, F., and Ferguson, E., 1967, *Astrophys. J. (Letters)*, **148**, L155.
- Schmidt, E. G., and Parsons, S. B., 1982, *Astrophys. J. Supplement*, **48**, 185.
- Schneeberger, T. J., Worden, S. P., and Wilkerson, M. S., 1979, *Astrophys. J. Supplement*, **41**, 369.
- Schwarzschild, M., 1938a, *Z. Astrophys.*, **15**, 14.
- Schwarzschild, M., 1938b, *Harv. Obs. Circ.*, 429.
- Schwarzschild, M., 1938c, *Harv. Obs. Circ.*, 431.
- Schwarzschild, M., 1948, *Astrophys. J.*, **107**, 1.
- Shapley, H., 1914, *Astrophys. J.*, **40**, 448.
- Shaw, J. F., Mitchner, M., and Kruger, C. H., 1970, *Phys. Fluids*, **13**, 339.
- Shoub, E., 1977, *Astrophys. J. Supplement*, **34**, 259.
- Simon, R., 1963, *J. Quant. Spectrosc. and Rad. Transf.*, **3**, 1.
- Sitko, M. L., and Savage, B. D., 1980, *Astrophys. J.*, **237**, 82.
- Slettebak, A., 1976, in *Be and Shell Stars, Proc. IAU Symp. No. 70*, ed. A. Slettebak (Dordrecht, Holland: Reidel), p. 123.
- Slettebak, A., 1979, *Space Sci. Rev.*, **23**, 541.
- Slettebak, A., and Reynolds, R. C., 1978, *Astrophys. J. Supplement*, **38**, 205.
- Smak, J., 1966, *Ann. Rev. Astron. Astrophys.*, **4**, 19.
- Smith, M. A., 1981, in *Pulsating B Stars*, ed. GEVON and Sterken (Nice Obs. Pub.), p. 317.
- Smith, M. A., and Karp, A. H., 1978, *Astrophys. J.*, **219**, 522.
- Snow, T. P., 1981, *Astrophys. J.*, **251**, 139.
- Snow, T. P., and Marlborough, J. M., 1976, *Astrophys. J. (Letters)*, **203**, L87.

- Snow, T. P., and Morton, D. C., 1976, *Astrophys. J. Supplement*, **32**, 429.
- Snow, T. P., Peters, G. J., and Mathieu, R. D., 1979, *Astrophys. J. Supplement*, **39**, 359.
- Sobolev, V. V., 1960, in *The Moving Envelopes of Stars* (Cambridge: Harvard University Press).
- Sofia, S., ed., 1980, *Proc. NASA Workshop on Variations of the Solar Constant*, NASA CP-2191.
- Spitzer, L., 1949, in *The Atmospheres of the Earth and Planets*, ed. G. P. Kuiper (Chicago: University of Chicago Press).
- Stalio, R., ed., 1982, *Trieste Workshop on Observational Basis of Stellar Velocity Fields* (Obs. Trieste Pub. 1983).
- Starrfield, S., Sparks, W. M., and Truran, J. W., 1976, in *Structure and Evolution of Close Binary Systems*, *IAU Symp. No. 73*, ed. Eggleton et al. (Dordrecht, Holland: Reidel), p. 155.
- Stencel, R. E., Kondo, V., Bernat, A. P., and McCluskey, G. E., 1979, *Astrophys. J.*, **233**, 621.
- Stickland, D. J., Penn, C. J., Seaton, M. J., Snijders, M. A. J., and Storey, P. J., 1981, *Mon. Not. Roy Astron. Soc.*, **197**, 107.
- Stromgren, B., 1935, *Z. für Astrophys.*, **10**, 237.
- Struve, O., 1931, *Astrophys. J.*, **73**, 94.
- Struve, O., 1942, *Astrophys. J.*, **95**, 134.
- Struve, O., and Elvey, C. T., 1934, *Astrophys. J.*, **79**, 409.
- Struve, O., and Swings, P., 1932, *Astrophys. J.*, **75**, 161.
- Surdej, J., and Heck, A., 1982, *Astron. Astrophys.*, **116**, 80.
- Terzian, Y., ed., 1978, *Planetary Nebulae, Observations and Theory* (Dordrecht, Holland: Reidel).
- Thomas, R. N., 1947, *Astrophys. J.*, **106**, 482.
- Thomas, R. N., 1948a, "Superthermic Phenomena in Stellar Atmospheres," Paper I, *Astrophys. J.*, **108**, 130.
- Thomas, R. N., 1948b, *Astrophys. J.*, **108**, 142.
- Thomas, R. N., 1949, *Astrophys. J.*, **109**, 500.
- Thomas, R. N., 1950a, *Astrophys. J.*, **111**, 165.
- Thomas, R. N., 1950b, *Astrophys. J.*, **112**, 337.
- Thomas, R. N., 1950c, *Astrophys. J.*, **112**, 343.
- Thomas, R. N., 1957, *Astrophys. J.*, **125**, 260.
- Thomas, R. N., 1961a, in *Physics of the Solar Chromosphere*, R. N. Thomas and R. G. Athay (New York: John Wiley Co./Interscience Pub.).
- Thomas, R. N., ed., 1961b, *Fourth Symp. on Cosmical Gas Dynamics, Aerodynamic Phenomena in Stellar Atmospheres*, *IAU Symp. No. 12*, Bologna, N. Zanichelli.
- Thomas, R. N., 1965, *Some Aspects of NonEquilibrium Thermodynamics in the Presence of a Radiation Field* (Boulder: University of Colorado Press).
- Thomas, R. N., ed., 1967, *Fifth Symp. on Cosmical Gas Dynamics, Aerodynamic Phenomena in Stellar Atmospheres*, *IAU Symp. No. 28* (New York: Academic Press London).
- Thomas, R. N., 1968, in Gebbie, K. B., and Thomas, R. N., 1968a, in *The Wolf-Rayet Stars*.
- Thomas, R. N., 1973, *Astron. Astrophys.*, **29**, 297.
- Thomas, R. N., 1976, in Caccin and Rigutti, 1978, pp. 339, 579.
- Thomas, R. N., 1977, *Foundations of Physics*, **7**, 137.
- Thomas, R. N., 1982, *Astrophys. J.*, **263**, 870.
- Thomas, R. N., and Athay, R. G., 1961, *Physics of the Solar Chromosphere* (New York: John Wiley Co./Interscience Pub.).
- Thomas, R. N., and Zirker, J. B., 1961a, *Astrophys. J.*, **133**, 588.
- Thomas, R. N., and Zirker, J. B., 1961b, *Astrophys. J.*, **134**, 733.
- Thomas, R. N., and Zirker, J. B., 1961c, *Astrophys. J.*, **134**, 740.
- Tjin A Dje, H. R. E., and The, P. E., 1982, in *The Third European IUE Conference*, ESA SP-176, p. 113.

- Traving, G., 1980, *Stellar Turbulence*, IAU Colloq. No. 51, ed. D. A. Gray and J. F. Linsky, Lecture Notes in Physics, Vol. 114 (Berlin: Springer-Verlag), p. 172.
- Trieste Workshop, 1982, *Observational Basis for Velocity Fields in Stellar Atmospheres*, ed. R. Stalio, Trieste Obs. Pub. (1983).
- Trieste Workshop, 1983, *Effects of Variable Mass Loss on Stellar Environment*, ed. R. Stalio, Trieste Obs. Pub. (1984).
- Ulmschneider, P., 1979, *Space Sci. Rev.*, 24, 71.
- Ulrich, R. K., and Knapp, G. R., 1979, *Astrophys. J. (Letters)*, 230, L99.
- Underhill, A. B., 1982, in *The B Stars With and Without Emission Lines*, ed. A. B. Underhill and V. Doazan, NASA SP-456, Washington, D.C.
- Underhill, A. B., and Doazan, V., ed. 1982, *The B Stars With and Without Emission-Lines, Monograph Series on Nonthermal Phenomena in Stellar Atmospheres*, NASA SP-456, Washington, D.C.
- Unsold, A., 1930, *Z. Astrophys.*, 1, 138.
- Unsold, A., 1938, 1st edition, 1955, 2nd edition, *Physik der Sternatmosphären* (Berlin: Springer-Verlag).
- Unsold, A., 1952, *Zs. f. Naturforsch.*, 7a, p. 121.
- Vaiana, G. S., Cassinelli, J. P., Fabbiano, G., Giacconi, R., Golub, L., Gorenstein, P., Haisch, B. M., Harnden, F. R., Johnson, H. M., Linsky, J. L., Maxson, C. W., Mewe, R., Rosner, R., Seward, F., Topka, K., and Zwaan, C., 1981, *Astrophys. J.*, 245, 163.
- Vaiana, G. S., and Rosner, R., 1978, *Ann. Rev. Astron. Astrophys.*, 16, 393.
- Van de Hulst, H. C., 1953, in *The Sun*, ed. G. P. Kuiper (Chicago: University of Chicago Press).
- Van Regemorter, H., 1962, *Astrophys. J.*, 136, 906.
- Vernazza, J. E., Avrett, E. H., and Loeser, R., 1976, *Astrophys. J. Supplement*, 30, 1.
- Vernazza, J. E., Avrett, E. H., and Loeser, R., 1981, *Astrophys. J. Supplement*, 45, 635.
- Vernazza, J. E., and Reeves, E. M., 1978, *Astrophys. J. Supplement*, 37, 485.
- Viotti, R., 1980, *Informally Circulated Report on Z And and Symbiotic Stars*.
- Vogel, S. N., and Kuhl, L. V., 1981, *Astrophys. J.*, 245, 960.
- Walborn, N. R., 1974, *Astrophys. J. (Letters)*, 191, L95.
- Walborn, N. R., 1981, *Astrophys. J. (Letters)*, 243, L37.
- Walter, F., Charles, P., and Bowyer, S., 1980, in *The Cool Stars, Stellar Systems and The Sun*, ed. A. K. Dupree, Smithsonian Astrophys. Obs. Special Report No. 389, p. 35.
- Walter, F., and Kuhl, L. V., 1981, *Astrophys. J.*, 250, 254.
- Weyman, R., 1962, *Astrophys. J.*, 136, 476.
- Whelan, J. A. J., 1981, in *The Second European IUE Conference*, ESA SP-157, p. xxxix.
- Whipple, F. L., 1938, Harvard Bull. No. 908.
- White, N. E., Swank, J. H., Holt, S. S., and Parmar, A. N., 1982, *Astrophys. J.*, 263, 277.
- Whitney, C. A., 1955, *Ann. Astrophys.*, 18, 375.
- Whitney, C. A., 1956, *Ann. Astrophys.*, 19, 34, 142.
- Whitney, C. A., 1965, in *The Fifth Symp. on Cosmical Gas Dynamics, Aerodynamic Phenomena in Stellar Atmospheres*, ed. R. N. Thomas (London, New York: Academic Press (1967)).
- Wildt, R., 1939, *Astrophys. J.*, 89, 295.
- Willis, A. J., 1980, in *The Second European IUE Conference*, ESA SP-157, p. iL.
- Willis, A. J., 1981, *Effects of Mass Loss on Stellar Evolution*, IAU Colloq. No. 59, ed. C. Chiosi and R. Stalio (Dordrecht, Holland: Reidel), p. 27.
- Willis, A. J., 1982, in *Wolf-Rayet Stars, Observations, Physics Evolution*, IAU Symposium No. 99, ed. C. de Loore and A. J. Willis (Dordrecht, Holland: Reidel), p. 87.
- Willis, A. J., 1983, in *Observational Basis for Stellar Atmospheric Velocity Fields*, Trieste Workshop, ed. R. Stalio, Obs. Trieste Pub.

- Willis, A. J., and Wilson, R., 1978, *Mon. Not. Roy. Astron. Soc.*, **182**, 559.
- Willson, L. A., 1976, *Astrophys. J.*, **205**, 172.
- Willson, L. A., and Hill, S. J., 1979, *Astrophys. J.*, **228**, 854.
- Wilson, O. C., 1950, *Astrophys. J.*, **111**, 279.
- Wilson, O. C., 1950, *Astrophys. J.*, **117**, 264.
- Wilson, O. C., 1957, *Astrophys. J.*, **126**, 525.
- Wilson, O. C., 1960, *Astrophys. J.*, **132**, 136.
- Wilson, O. C., and Abt, H., 1954, *Astrophys. J. Supplement*, **1**, 1.
- Wilson, O. C., and Bappu, M. K. V., 1957, *Astrophys. J.*, **125**, 661.
- Wing, R. F., 1980, in *Current Problems in Stellar Pulsation Instabilities*, ed. D. Fischel, J. R. Lesh, and W. M. Sparks, NASA TM-80625, p. 533.
- Withbroe, G. L., and Noyes, R. W., 1977, *Ann. Rev. Astron. Astrophys.*, **15**, 363.
- Wood, P. R., 1979, *Astrophys. J.*, **227**, 220.
- Wood, R., 1980, in *Current Problems in Stellar Pulsation Instabilities*, ed. D. Fischel, J. R. Lesh, and W. M. Sparks, NASA TM-80625, p. 611.
- Woolley, R. V. D. R., and Allen, C. W., 1948, *Mon. Not. Roy. Astron. Soc.*, **108**, 292.
- Woolley, R. V. D. R., and Allen, C. W., 1950, *Mon. Not. Roy. Astron. Soc.*, **110**, 358.
- Wright, K. O., 1970, in *Vistas in Astronomy*, **12**, 147.
- Zirin, H., 1976, *Astrophys. J.*, **208**, 414.
- Zirker, J. B., 1956, Thesis, Harvard University.
- Zirker, J. B., 1958, *Astrophys. J.*, **127**, 680.
- Zirker, J. B., 1981, in *The Sun as a Star, Monograph Series on Nonthermal Phenomena in Stellar Atmospheres*, ed. S. Jordan, NASA SP-45, p. 135.
- Zirker, J. B., 1983, in *Observational Basis for Stellar Velocity Fields*, Trieste Workshop, ed. R. Stalio, Obs. Trieste Pub.
- Zirker, J. B., and Thomas, R. N., 1961a, *Astrophys. J.*, **133**, 588.
- Zirker, J. B., and Thomas, R. N., 1961b, *Astrophys. J.*, **134**, 733.
- Zirker, J. B., and Thomas, R. N., 1961c, *Astrophys. J.*, **134**, 740.

INDEX

- acceleration
 - radiative 256 *et seq*, 300, 306
- accretion 3–18
- activity 118
- anomaly 3–18, 115–263
- atmospheric instability 291 *et seq*
- atmospheric modeling (*see also* model atmosphere)
 - empirical-theoretical 3–18, 115–263, 279–343, 341
 - speculative-theoretical 3–113
- atmospheric region (*see also* chromosphere, corona, local-stellar-environment, photosphere, post-coronal domain)
 - chromosphere-corona 285
 - distinctive atmospheric regions 274, 279–322, 323–324
 - distinctive sequences of regions 274, 323–331
 - local-environment 312, 318
 - photospheric 283
 - post-coronal domain 309
- Balmer
 - continuum 193
 - emission-line (*see also* H α emission envelope) 151 *et seq*
- Be-similar stars 173 *et seq*, 176, 182, 185, 325–326, 329
- Be stars 146, 173 *et seq*, 325
- binary
 - eclipsing 207–230
 - mass-transfer 135, 139, 145
 - symbiotic alternative to multi-regional structure 132, 135, 143, 148, 184, 196, 197 *et seq*, 333
- Boltzmann equation 28
- cataclysmic stars 122–149, 326
 - several types of mass-flux variability 327
- chromosphere 208, 280, 285, 324
- chromosphere-corona 339
- circumstellar (*see* local-environment)
- collision-dominated source-sink terms 76 *et seq*
- continuous spectrum modeling (*see also* model atmospheres) 19–113
- corona
 - lower 216, 287
 - upper 299
- decelerated post-corona 182, 195, 310, 339
- density
 - distribution 48, 202, 213, 219–220, 223
- dust signatures 182, 195
- eclipse-probing of extended atmospheres 207–230, 207, 223, 226
- ejected-shell photospheres (*see* photospheres)
- ejection 136 *et seq*
- emission
 - from scattering 78
 - lines-profiles 153 *et seq*
 - lines-stars 116, 120, 149 *et seq*
 - lines-variety 151, 153
 - peculiarity 149, 151
- energy
 - hydromagnetic 119
 - mechanical 140, 197
 - non-radiative 119, 140, 163, 239
- equilibrium (*see* Appendix)
 - hydrostatic 23, 47, 202
 - quasi- (*see* Appendix)
 - radiative 23, 47
 - thermodynamics 7 (*see also* Appendix)

- equivalent 2-level atom 76
- escape-point 296, 307, 310 (Table 4-3)
- evolution
 - Evolution vs evolution xiv–xv
- excitation
 - super-excitation 236
- extended atmospheres
 - class of peculiar stars 116, 120, 177, 202–230
 - definition 202
- flux
 - defined 25–29
 - hydromagnetic
 - from thermal models 36
 - mass
 - thermal-diffusive 39, 115
 - non-radiative 249–263
 - non-thermal (*see also* mass, nonradiative, hydro-magnetic) 334
 - radiative (*see also* effective-temperature) 37
 - space 28, 71
 - state 29, 71
 - time-dependence 33, 122, 334
- gradualness 121, 178
- H α emission-envelope 173 *et seq.*, 312, 324–325
 - definition of emission-line stars by 149, 173
- H–R diagram 22 (Figure 2-2), 125 (Figure 3-1)
- hot-coronal mass-loss 9, 258 *et seq.*, 298
- individuality 121, 178, 191, 197
- infra-red
 - excess 182–183
- intermediate state-parameters 29
- ISM
 - parental character 3–18
- linear nonequilibrium (*see also* Appendix), 53–54 *et seq.*
- line-blanketing 108 *et seq.*
- local-stellar-environment 183, 194, 312, 318, 339
- locally-opaque-situation 79, 237
- local-thermodynamic-equilibrium
 - matter only 19, 59
 - matter and radiation, linear nonequilibrium 19, 50, 53–54 *et seq.*
- luminosity
 - defining effective-temperature 41
 - excess for Be and T Tauri stars 191, 326
 - relative to mass-flux kinetic energy 263 (Table 3-11)
 - variability 122–149
- Lyman-continuum excess 215
- magnetic activity 118
- mass-flow
 - continuous vs episodic 327–328
 - perturbation on HE 219, 287 *et seq.*
- mass-flux (*see also* variability)
 - episodic vs continuous 143, 144, 178, 189
 - individuality 173–185
 - time-dependence 310, 324–326
- mass-loss (*see also* mass-flow and mass-flux) 17, 141, 165
 - variable 176, 310, 324
- mass-ejection 140, 161
- model atmosphere
 - classical 56, 59
 - closed, thermal 49, 59, 115
 - empirical-theoretical xvi, 16–18, 279–343
 - gray
 - LTE columnar 51
 - LTE spherical 54
 - LTE-R 59
 - multi, LTE-R 65
 - nonLTE 83
 - H $^{-}$ quasi-LTE-R 85
 - multi, nonLTE radiative dominated 103 *et seq.*
 - neoclassical 71, 83
 - plane-parallel 22
 - speculative-theoretical 4–11, 19–113
 - standard (*see also* closed, thermal) 40
- monochromatic radiative equilibrium 51
- nondecelerated post-corona 309, 339
- normal stars
 - ambiguity
 - in Sg I 149
 - in WR 150
 - definition 116, 149

- nonLTE
 - linear 8, 19–113 (*see also* Appendix)
 - nonlinear 8, 19–113 (*see also* Appendix)
 - thermal, equivalently statistical-equilibrium 17
- nonthermal storage modes, xv, 7, 334, (*see also* Appendix)
- opacity-induced LTE = LOS 79
- Parker condition, equality of thermal and escape points 298
- peculiar stars
 - definition 17, 116
- peculiarity, types of 116, 119
 - basis for modeling 117, 119
- photosphere 198, 339
 - ejected-shell 283, 325–326
 - quasi-thermal 283, 323
 - spherically-pulsating 283, 325, 328
- planetary-nebulae
 - as far-out H α shell 7, 3–72 *et seq*
 - data 3–72 *et seq*
 - example of radiative-control of nonLTE 75
 - proto-PN 142
- post-coronal domain 312
- pulsating variables 124 *et seq*
- radiative
 - acceleration 256 *et seq*, 300, 306
 - chromospheric-coronal 302 *et seq*
 - equilibrium (*see* equilibrium) 23, 47
- rotational-correlation with
 - mass-loss 184
 - superionization 184
 - x-rays 194, 245–246
- rotationally-induced instability 177, 183
- scattering-domination of source-function 76
- shell
 - Be stars 146, 153
 - novae 136 *et seq*
 - nova-like 141
- shock 127–128
- source-sink terms in source-function 76 *et seq*
- spectral lines
 - P Cygni 153, 253
 - sub-ionized 173–185
 - super-ionized, 230–249
- spherically-pulsating photosphere (*see* photospheres)
- stars
 - quasi-equilibrium 9
- star types (*see* 125 (Figure 3-1))
 - Beta Cephei 124, 126, 131, 133
 - Cepheids 124, 126, 128
 - (closed, thermal) 118, 333
 - long-period variables (Mira) xv, 124, 126, 127, 133
 - novae, 134 *et seq*, 140
 - (open, nonthermal) xv, 118, 333
 - P Cyg 146
 - RR Lyr 126, 128
 - T Tauri 153, 155, 163, 190 *et seq*, 326
 - Wolf-Rayet (WR) stars and phenomenon 165 *et seq*
 - W Virginis 128–129
- sub-ionization (*see also* ionization) 116, 120, 176, 184
- sun, exophotospheric peculiarities of
 - lower chromosphere 208
 - lower corona 216
- super-excitation 236
- super-ionization (*see also* ionization) 116, 120, 129, 131, 165–166, 179, 182, 193, 230, 241
- super-thermic velocities 116, 120, 165–166, 230, 249 *et seq*, 252
- symbiotic
 - character 186, 189, 196 *et seq*, 198, 324, 333
 - star 116, 120, 136, 189, 196 *et seq*, 324–325
- taxonomy
 - classical xiv, 334
 - modern exophotospheric 338
 - modern photospheric 337
 - nonvisual xiv
 - time-dependent xiii
- temperature
 - distribution 213, 219
 - effective 41
 - radiative-quality dominated 92 *et seq*

temperature-control bracket 101
classical-boundary 23, 52, 64, 68

thermal
definition (*see* Appendix)
models (*see* model atmospheres)
storage modes A-1–A-5

thermal-point 296, 299 (Table 4-2)

transition-region
between chromosphere and corona 218–219,
233, 296, 299 (Table 4-2)
between photosphere and chromosphere 284–
285, 287 (Table 4-1), 323

transition-zone between star and ISM

trans-thermal flow
defined 288
defining lower-corona 294–295
instability of 294–295

turbulence 129, 262

variable star classes 116, 120, 122
cataclysmic 127, 134 *et seq*
pulsational 124 *et seq*
spectrum 127, 146 *et seq*, 191

velocity – systematic
atmospheric deceleration 182, 195, 310, 339
atmospheric maximum value 252 (Figure 3-33),
306
distribution 48
sub-thermal in photosphere 291
superescape flow 249 *et seq*, 300
superthermal flow 249 *et seq*, 300
transthermal flow in lower-corona 288, 294

velocity – turbulent (*see* turbulence)

wind (*see* mass-flow).

x-ray
correlation with extended atmosphere 179, 194
correlation with rotation 194, 245–246

AUTHOR'S ADDRESSES

Richard N. Thomas

*Laboratoire d'Astrophysique Theorique
Collège de France – CNRS
Institut d'Astrophysique
98 bis, Boulevard Arago
75014 Paris
FRANCE*

*135 Timber Lane
Pine Brook Hills
Boulder, Colorado 80302*

*Solar-Stellar Program
Sacramento Peak Observatory
Sunspot, New Mexico 88349*

*Osservatorio Astronomico
Via G. B. Tiepolo 11
I 34131 Trieste
ITALY*

National Aeronautics and
Space Administration

Washington, D.C.
20546

Official Business

Penalty for Private Use, \$300

SPECIAL FOURTH CLASS MAIL
BOOK

Postage and Fees Paid
National Aeronautics and
Space Administration
NASA-451



NASA

POSTMASTER: If Undeliverable (Section 158
Postal Manual) Do Not Return
